

CALTECH Biology Annual Report 2004

Legend for the front cover illustration

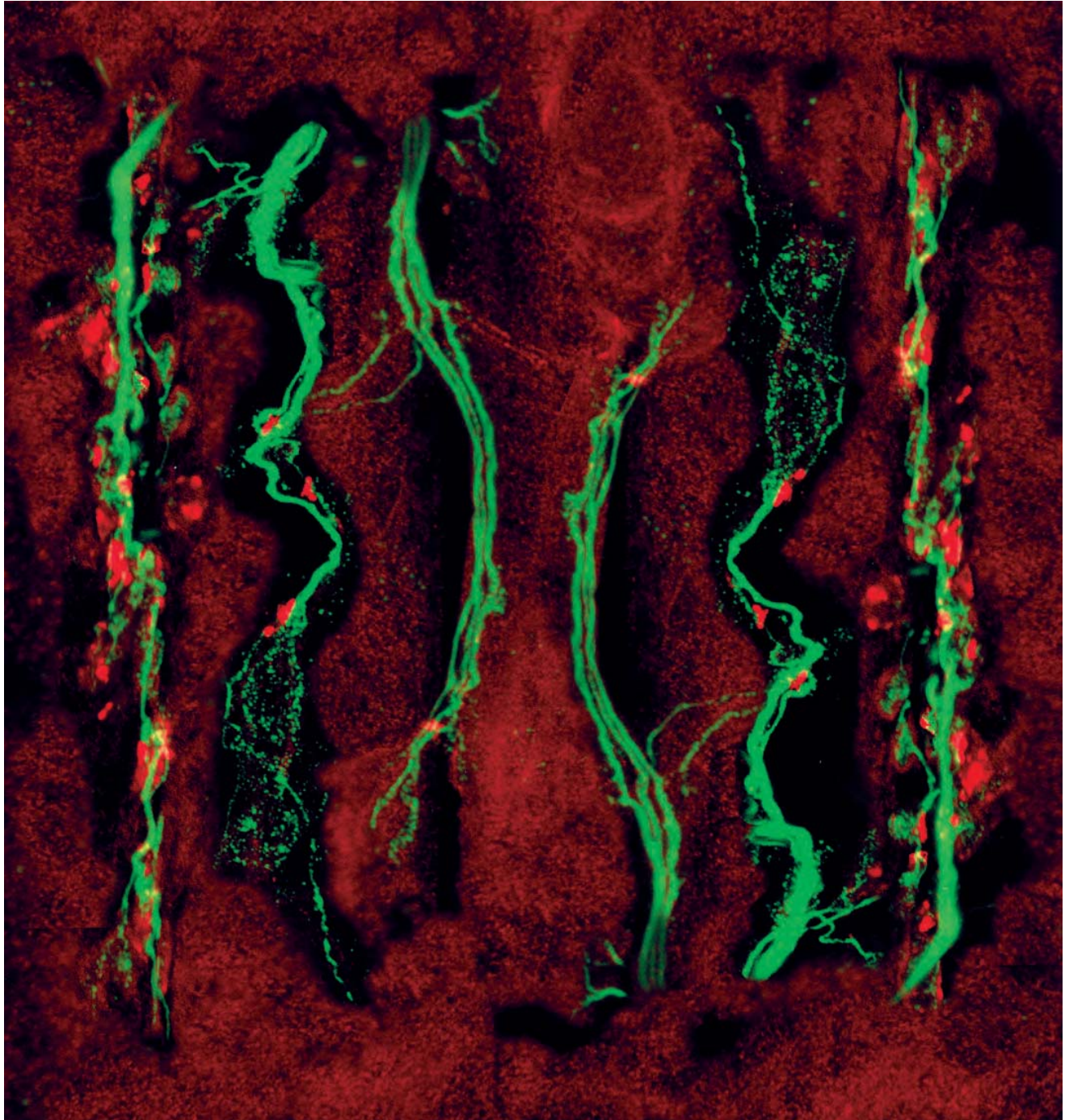
Andrew J. Ewald - (Scott E. Fraser Laboratory)

An early frog embryo, imaged at high-resolution using surface imaging microscopy, a novel technique first applied to developmental biology in the Biological Imaging Center at Caltech (Ewald *et al.*, *Dev. Dynamics*, 2002). In this neurula stage embryo, the archenteron (large cavity) has formed and the blastopore has closed, thus completing the major goals of gastrulation. Recent work from the Fraser Lab has studied the molecular control of archenteron formation and blastopore closure and demonstrated that both processes require non-canonical Wnt signaling, acting through Dishevelled (Ewald *et al.*, *Development*, in press). Quantitative analytical techniques, also developed in the Fraser Lab, were applied to demonstrate that the cellular events of gastrulation are dissociable, and therefore providing a possible explanation for the observed diversity of gastrulation mechanisms among amphibians.

Legend for the back cover illustration

Edward Coles – (Marianne Bronner-Fraser Laboratory)

Whole-mount immunohistochemistry of an E11 mouse embryo with anti- α -tubulinIII (Tuj1) – an early marker of differentiating neurons. This projected z series was imaged using a Zeiss confocal microscope (Beckman Imaging Center).



Negative regulation of synaptic eIF4E by postsynaptic Pumilio

Image by Violana Nesterova, Kai Zinn and Kaushiki Menon

The cover shows accumulation of postsynaptic eIF4E aggregates (red) adjacent to a presynaptic microtubule marker (green), at *Drosophila* neuromuscular junctions (NMJs). The picture is an inverted mirror image of different neuromuscular junctions, oriented longitudinally. In our paper we examine the synaptic function of a translational repressor, Pumilio at *Drosophila* NMJs. eIF4E, is upregulated in Pumilio mutants (represented by NMJs with many eIF4E aggregates in the image) and is rescued by postsynaptic Pumilio expression (represented by NMJs with fewer eIF4E aggregates in the image). Genetic epistasis and *in vitro* binding experiments indicate Pumilio regulates synaptic function by controlling translation factor eIF4E expression.

Division of Biology

California Institute of Technology

Pasadena, CA

**Annual Report
2003 - 2004**

BIOLOGY - 2004

Yolanda Duron, Annual Report Coordinator

Research Reports

Biological research summarized in this report covers the time period from June, 2003, through July, 2004. The annual report is not intended to serve as an official forum, since some portions of the research listed in this report have not yet been published. When referring to an individual abstract(s), special permission must be obtained from the investigator.

References to published papers cited throughout the report are listed at the end of each individual research report.

TABLE OF CONTENTS

INTRODUCTION

INSTRUCTION AND RESEARCH STAFF	13
ADMINISTRATIVE STAFF	21

MOLECULAR, CELLULAR, AND INTEGRATIVE NEUROSCIENCE

JOHN M. ALLMAN, PH.D.

Summary.....	25
1. A functional magnetic resonance imaging study of humor	25
2. History influences financial choice	25
3. The scaling of frontal cortex in primates and carnivores	25
4. The Von Economo spindle neurons are morphologically distinct from pyramidal neurons	26
5. The role of the frontoinsular cortex in social cognition	26
Publications	26

RICHARD A. ANDERSEN, PH.D.

Summary.....	27
6. Macaque supplementary eye fields neurons exhibit task-specific spatial tuning	28
7. Re-learning spatial representations via Bayesian estimation.....	28
8. Translation speed compensation in area MSTd	28
9. Efficacy and adaptation in parietal local field potentials used in a brain machine interface for cursor control.....	29
10. Decoding trajectories in real-time from posterior parietal cortex	29
11. Cognitive control signals for neural prosthetics.....	29
12. Perceptual bias in V1 neuronal responses to ambiguous three-dimensional objects.....	29
13. Network activity in posterior parietal cortex during decision-making for reaches	30
14. Motor imagery activates human parietal reach region.....	30
15. Parietal reach activity during planned obstacle avoidance	30
Publications	31

DAVID J. ANDERSON, PH.D.

Summary.....	32
16. Lim homeodomain proteins mark hypothalamic and amygdaloid circuits that are involved in the expressions of innate behaviors	33
17. Delineating the neuronal to glial transition in the developing spinal cord.....	34
18. The amygdala central nucleus in innate vs. conditioned fear.....	34
19. Identifying genes and neural correlates underlying an innate avoidance behavior in Drosophila	34
20. Olig gene targets in CNS glial cell fate determination	35
21. Modeling "emotional" behavior in Drosophila.....	35
22. Molecular approach to studying the neuronal circuits of innate fear	35
23. GDF7-expressing roof-plate cells mark a sensory-restricted neural crest population.....	36
24. In vivo studies of the development of the vascular and nervous system.....	36
25. Molecular mechanism underlying neurogenic capacity	36
26. EphrinB2 in peripheral endothelial cells is essential for the proper embryonic vessel development	37
27. An innate avoidance behavior is dictated by a specific olfactory circuit in Drosophila	37
28. Axonal tracers targeted to the MrgD locus reveal that nociceptive (pain-sensing) information is carried by molecularly distinct and parallel neuronal circuitry.....	38
Publications	38

SEYMOUR BENZER, PH.D.

Summary 39

29. Genetics and circuitry of nociception 39

30. Circuit analysis of an innate avoidance behavior in *Drosophila* 40

31. Isolation and characterization of mutations that cause obesity and excessive feeding in *Drosophila* 40

32. Genetic and pathological analysis of oxygen toxicity in *Drosophila* 40

33. The role of Apolipoprotein D in normal and pathological aging in *Drosophila* 41

34. Enhancement of *Drosophila* longevity by exogenous bacteria 41

35. Peptide modulators of Methuselah, a G protein-coupled receptor associated with extended lifespan 41

36. Lifespan extension of *Drosophila* by reduction of polyamines 41

37. A screen for mutants that modulate lifespan upon nutritional changes in *Drosophila* 42

38. A longevity mutant involving the pentose phosphate pathway 42

39. Identifying the tissue responsible for the female longevity bias in *Drosophila* 42

Publications 42-43

MARY B. KENNEDY, PH.D.

Summary 44

40. Role of synGAP in spine maturation 45

41. A role for synGAP in regulating neuronal apoptosis 45

42. Signal transduction in SynGAP mutant mice 45

43. Activation of Ca²⁺/calmodulin-dependent protein kinase II (CaMKII) by concentrations of Ca²⁺ and calmodulin present in vivo 45

44. Activation of CaMKII by calmodulin mutants with specific Ca²⁺-binding sites removed 46

45. Quantitative model of calcium-binding to calmodulin in spines 46

46. Phosphorylation of synGAP by CaM kinase II does not inhibit its activity 46

Publications 47

CHRISTOF KOCH, PH.D.

Summary 48

47. Intrinsic subthreshold noise in cultured hippocampal neurons 49

48. Subthreshold voltage noise of rat neocortical pyramidal neurons 49

49. Backpropagating action potentials in dendrites with stochastic ion channels 49

50. A learning rule for local synaptic interactions between excitation and shunting inhibition 49

51. Modeling extracellular electrical stimulation of unmyelinated axons by symmetric bipolar current pulses 50

52. A synaptic mechanism for computing the maximum of two inputs 50

53. Model of extracellular potential illustrates factors contributing to the waveform of single unit recordings in vivo 50

54. Unsupervised spike detection and sorting with wavelets and super-paramagnetic clustering 51

55. Invariant visual representation by single neurons in the human brain 51

56. Single-trial event-related potentials with wavelet denoising 51

57. Towards real-time unsupervised spike sorting via template matching 51

58. Selectivity of local field potentials in the human brain 52

59. A detection theory account of change detection 52

60. Humans segregate and integrate auditory and visual signals in a statistically optimal fashion 52

61. Neural mechanisms underlying temporal aspects of conscious visual perception 52

62. Face adaptation is reduced by binocular suppression 53

63. Neural correlates of preattentive face-gender discrimination 53

64. Visual awareness and the neural correlate of orientation selective adaptation 53

65. Absence of visual awareness does not affect the formation of negative afterimages 54

66. Non-local cortical interactions help determine where to look in natural scenes 54

67. What do we see when we glance at a scene? 55

68. Biasing the percept of ambiguous visual stimuli 55

69. Binding "hardwired" vs. "arbitrary" feature conjunctions 55

70. The attentional requirements of face recognition 56

71. Clutter effects in visual search: Human psychophysics 56

72. Continuous flash suppression 57

73. Awareness in fear conditioning 57

74. Prefrontal activity covaries with explicit knowledge of CS/US contingency in human aversive conditioning 57

75.	Detection and tracking of objects in underwater video	58
76.	Is bottom-up attention useful for object recognition?	58
77.	On the usefulness of attention for object recognition	58
78.	Unsupervised learning and control provide ambient intelligence to smart buildings.....	58
	Publications	59

MASAKAZU KONISHI, PH.D.

	Summary.....	60
79.	Nucleus Uvaeformis controls auditory responsiveness of HVC in the zebra finch song system.....	60
80.	Running cross-correlation in the owl's nucleus laminaris	60
81.	Frequency convergence in the auditory thalamus of the owl	61
82.	Robustness of multiplicative processes in auditory spatial tuning.....	61
83.	Miniature microdrive for chronic recording in barn owls	61
	Publications	61

GILLES LAURENT, PH.D.

	Summary.....	62
84.	Intensity versus identity coding in the locust olfactory system.....	62
85.	Olfactory memory and physiology of the dorsal paired medial neurons of <i>Drosophila</i>	62
86.	Combined two-photon laser scanning microscopy and electrophysiological recording in insect brain.....	62
87.	Adaptive odor processing in the honeybee.....	63
88.	Ensemble processing of odor sequences and overlaps in the locust antennal lobe	63
89.	Associative memory and olfactory representation.....	64
90.	Cytoarchitecture of an insect olfactory system	64
91.	Characterization of odor-evoked dynamics in the insect antennal lobe.....	64
92.	Functional connectivity between antennal lobe projection neurons and mushroom body Kenyon cells in the locust	64
93.	Two-photon imaging with genetically expressed calcium sensors in the <i>Drosophila</i> brain.....	65
94.	Nonlinear changes in neuronal ensemble responses evoked by varying odor ratios in mixtures	65
95.	Search for connectivity patterns	66
	Publications	66

HENRY A. LESTER, PH.D.

	Summary.....	67
96.	Using physical chemistry to differentiate nicotinic from cholinergic agonists at the nicotinic acetylcholine receptor	67
97.	Tyrosine residues that control binding and gating in the 5-HT ₃ receptor revealed by unnatural amino acid mutagenesis.....	68
98.	The ligand-binding site of serotonin in the MOD-1 receptor	68
99.	Temporal control of protein phosphorylation with caged amino acids.....	68
100.	Probing the muscarinic type-2 acetylcholine receptor binding site through incorporation of unnatural amino acids.....	69
101.	Improving nonsense suppression by suppressing eRF-1 with siRNA.....	69
102.	Incorporation of unnatural amino acids into NMDA receptors expressed in mammalian cells	69
103.	Synthesis of cysteine-S-methoxycoumarin (Cys(MC)): An additional fluorescent unnatural amino acid candidate for nonsense suppression methodology.....	70
104.	Single-cell electroporation of CHO-K1 cells with YPF cDNA.....	70
105.	Micro-electroporation of HEK 293 cells with the human ether-a-go-go related gene hERG1A subunit	70
106.	A fluorophore attached to nicotinic acetylcholine receptor β M2 detects productive binding of agonist to the $\alpha\delta$ site.....	71
107.	Fluorescent mapping of conformational dynamics in nicotinic receptors	71
108.	FRET analysis of molecular motion at the channel gate in nicotinic receptors.....	72
109.	FRET studies of cross-inhibition between P2X and nicotinic channels	72
110.	Mechanisms of nicotine-induced functional upregulation of α 4-containing nicotinic receptors	72
111.	Fluorescently-tagged α 4 nicotinic receptor knock-in mice	73
112.	The ANDFLE mutations do not enhance Ca ²⁺ block of α 4 β 2 neuronal nicotinic receptors	73
113.	Nicotine activation of α 4* receptors is sufficient for reward, tolerance and sensitization	73
114.	Functional expression studies of α 4-containing nicotinic receptors with a Leu9'Ala gain of function mutation	74

115.	Enhanced expression of L9'S mutant nAChR in adult mice increases the loss of midbrain dopaminergic neurons	74
116.	Enhanced expression of L9'S mutant nAChR in adult mice using transgenic expression of inducible cre	74
117.	Use of hypersensitive $\alpha 4$ mice to study the role of $\alpha 4$ in the hippocampus.....	75
118.	Preparation of constructs for $\beta 2$ ADFLE mutations and $\beta 2$ -XFP fusion proteins.....	75
119.	RGS9-deficient mice show abnormal involuntary movements following application of dopamine agonists.....	75
120.	Interaction of the $\alpha 7$ acetylcholine receptor with the Alzheimer's amyloid peptide.....	76
121.	Investigating trafficking and mis-trafficking of fluorescently-labeled GABA transporter, mGAT-1	76
122.	Visualization of mGAT1 incorporation in boutons using total internal reflection fluorescence microscopy	77
123.	Postsynaptic mechanisms are essential for forskolin-induced potentiation of synaptic transmission	77
124.	On-resin assembly of a linkerless lanthanide(III)-based luminescence label and its application to the total synthesis of site specifically labeled mechanosensitive channels.....	77
125.	Studies on the voltage dependence of the mechanosensitive channel of small conductance (MscS).....	78
126.	Gating transitions in bacterial ion channels measured at 3 μ s resolution	78
	Publications	79

PAUL H. PATTERSON, PH.D.

	Summary.....	80
127.	Maternal influenza infection is likely to alter fetal brain development indirectly: The virus is not detected in the fetus	80
128.	Maternal viral infection and mental illness: Gene expression changes in the brains of adult offspring.....	80
129.	The maternal inflammatory response and its effects on the neurodevelopment and behavior of the offspring	81
130.	Production of maternal and fetal cytokines in response to influenza infection or administration of synthetic dsRNA.....	81
131.	The effect of maternal influenza infection on neurobehavioral development of the offspring.....	81
132.	Patterns of brain activity in the adult offspring of mice born to influenza-infected mothers.....	82
133.	Do cytokines mediate the effects of maternal infection on fetal brain development?.....	82
134.	Effects of LIF on adult neural stem cells in normal and APP23 mice	82
135.	Leukemia inhibitory factor and senile plaques in Alzheimer's mice.....	82
136.	Using leukemia inhibitory factor (LIF) to prevent secondary cell death after spinal cord injury	82
137.	The role of leukemia inhibitory factor in the regulation of the response to seizure	83
138.	Single chain antibodies to dissect the biological functions of mutant huntingtin.....	83
139.	Interaction of mutant huntingtin with the NF- κ B pathway	83
140.	Anti-Htt antibodies as possible therapeutics for Huntington's disease	84
141.	The effect of behavioral stress on immune surveillance and melanoma progression	84
	Publications	84-85

ERIN M. SCHUMAN, PH.D.

	Summary.....	86
142.	Dendritic spine motility: Analysis and experiments.....	86
143.	The mechanism of neuronal activity-dependent regulation of surface N-cadherin internalization	86
144.	Miniature synaptic events regulate local protein synthesis in dendrites of hippocampal neurons.....	87
145.	Functions of Pumilio in the development and synaptic plasticity of hippocampal neurons	87
146.	The structural basis for an allele-specific deficit in regulated secretion of brain-derived neurotrophic factor (BDNF) at hippocampal synapses	87
147.	Visualization of cadherin-cadherin association in living cells.....	88
148.	A novel approach for the identification of locally synthesized proteins in neuronal dendrites	88
149.	Dopaminergic stimulation of local protein synthesis activates silent synapses.....	89
150.	Synaptic plasticity and the ubiquitin-proteasome system (UPS).....	89
151.	A proteasome-sensitive connection between PSD-95 and GluR1 endocytosis	89
152.	The direct entorhinal cortical input to area CA1 of the hippocampus is required for the consolidation of a long-term spatial memory	90
153.	Single-unit neural correlates of visual recognition memory in the human hippocampus-amygdala complex.....	90
	Publications	90

SHINSUKE SHIMOJO, PH.D.

Summary.....	91
154. Perceptual-binding and persistent pre-attentive surface segregation	91
155. Perceptual alternation induced by visual transients	92
156. How early does the brain "know" what it likes? Evidence from pupilometry.....	92
157. Orienting behavior robustly contributes to preference decision-making.....	92
158. Gaze, decision processes and cortical activation: A joint eye tracking/EEG study.....	93
159. Steady state misbinding of color and motion.....	93
160. Transcranial magnetic stimulation reveals the content of post-perceptual visual processing.....	93
161. Human parietal cortex remaps cue-priming effect across saccades: Cortical location and dynamics assessed by transcranial magnetic stimulation.....	94
162. Significant audio-visual interaction for spatially congruent stimuli	94
163. Development of multisensory spatial integration and perception in humans	95
Publications	95

ATHANASSIOS G. SIAPAS, PH.D.

Summary.....	96
164. Cortical phase-locking to hippocampal theta oscillations	96
165. Cortico-hippocampal interactions during slow-wave sleep.....	96
Publications	97

KAI G. ZINN, PH.D.

Summary.....	98
166. Searching for RPTP substrates.....	99
167. Syndecan is a candidate ligand for the Drosophila RPTP Dlar.....	100
168. Identification of genes involved in axon guidance and synaptogenesis by transgenic RNAi.....	100
169. Characterization of receptor tyrosine phosphatase DPTP4E.....	100
170. Genetic analysis of neural layer formation of the mushroom body, an olfactory learning and memory center, in Drosophila.....	101
171. The translational repressor Pumilio regulates presynaptic morphology and controls postsynaptic accumulation of translation factor eIF-4E	101
172. Role of fog in embryonic axon guidance in Drosophila.....	101
173. Assaying Pumilio for prion-like behavior	102
174. Drosophila Spastin regulates synaptic microtubule networks.....	102
175. What is the role of Drosophila beached in nervous system development?	102
Publications	103

STRUCTURAL, MOLECULAR AND CELL BIOLOGY**GIUSEPPE ATTARDI, PH.D.**

Summary.....	107
176. A novel major D-loop replication origin reveals a new mode of human mtDNA synthesis.....	107
177. Further characterization of the mtDNA replication origins.....	108
178. Regulation of human mtDNA transcription: Study of the role of mTERF in controlling the rRNA synthesis.....	108
179. Molecular characterization of a functional variant of mTERF and the practical application for the investigation of the mTERF function.....	109
180. Investigation of proteins interacting with sites of the human mtDNA main control region specifically targeted by an aging-dependent accumulation of mutations.....	109
181. C150T human mitochondrial DNA mutation analysis	110
182. Hypersensitivity of the outer mitochondrial membrane to digitonin in the early stages of apoptosis.....	110
183. Increased sensitivity to apoptosis in complex I mutant	111
184. Characterization of mitofusins differentially expressed in various human cell lines and tissues: Implications for mitochondrial organization	112
Publications	112

DAVID BALTIMORE, PH.D.

Summary	113
185. Interaction of the NF- κ B transcription factor with the κ B DNA binding sites in the HIV-1 LTR.....	113
186. Specificity of transcriptional activation in the NF- κ B/Rel protein family.....	113
187. The role of NF- κ B in cell growth and transformation.....	114
188. Engineering immunity via instructive immunotherapy	114
189. Wnt signaling in the nervous system.....	114
190. Dynamics of LPS-stimulated activation of NF- κ B.....	115
191. Development of chimeric mouse model with fully functional human immune system	115
192. NF- κ B role in the cellular UV response.....	115
Publications	116

PAMELA J. BJORKMAN, PH.D.

Summary.....	117
193. Characterization of FcRn-mediated transport pathways via confocal microscopy	119
194. Electron tomography of intracellular vesicles containing FcRn-IgG complexes in the small intestine of neonatal rats and in FcRn-expressing MDCK cells	119
195. Assay for ligand-induced dimerization of FcRn	120
196. Three-dimensional EM studies of IgG transport and cell adhesion	120
197. Characterization of the chicken yolk sac IgY receptor.....	120
198. Crystal structure of a dimeric IgA-binding fragment of the human polymeric immunoglobulin receptor	121
199. Structural studies of a herpes simplex virus immunoglobulin G receptor	121
200. Structural studies of a pheromone receptor-associated MHC class Ib molecule.....	121
201. Structural and functional studies of MHC class I homologs in HCMV.....	121
202. Crystallographic studies of the complexes of murine immunoreceptor NKG2D and its ligands RAE-1 β and H60	122
203. Crystallographic studies of ligand binding by Zn- α 2-glycoprotein.....	122
204. HFE and transferrin directly compete for transferrin receptor in solution and at the cell surface.....	122
205. A hydrophobic patch on transferrin receptor regulates the iron-release properties of receptor-bound transferrin.....	122
206. Structural and biophysical studies of transferrin receptor 2	123
207. Structural studies of prostate-specific membrane antigen	123
208. Biochemical and structural studies of ferroportin	123
209. Crystal structure of a secreted insect ferritin reveals a symmetrical arrangement of heavy and light chains	124
210. Conformational studies of Huntingtin Exon 1 by fluorescence energy transfer.....	124
211. Structural and binding studies of anti-poly-Gln scFvs bound to Huntingtin Exon 1	124
Publications	125

CHARLES J. BROKAW, PH.D.

Summary.....	126
212. Symmetry breaking in models of nodal cilia.....	126

JUDITH L. CAMPBELL, PH.D.

Summary.....	127
213. Identification of mutations synthetically lethal with dna2-1 and dna2-2 mutants	127
214. Global interaction network involving DNA2.....	128
215. Magnetospirillum magnetotacticum has four paralogs of the ftsZ gene	128
216. Aging cells show a global stress and DNA damage response	128
217. Biochemical characterization of Pol σ and its interaction with Pol ϵ	129
218. Trf4 and Tfr5 are nuclear proteins that associate preferentially with origins of replication in S-phase cells	129
219. Overproduction of the replication initiation protein Cdc6 inhibits the metaphase to anaphase transition	129
220. Mechanism of and model for Cdc6 inhibition of mitosis	130
221. Interaction between Saccharomyces cerevisiae DNA polymerases epsilon and sigma	131
222. Analysis of mutations in potential Mec1 phosphorylation sites.....	131
223. Conserved genes associated with controlled magnetite mineralization in bacteria.....	131
224. Evidence that yeast SGS1, DNA2, RRM3, SRS2, and FOB1 interact to maintain rDNA stability.....	132
Publications	132

DAVID C. CHAN, PH.D.

Summary.....	133
225. Protective effects of mitochondrial fusion on cell function and mouse development.....	134
226. Structure-function analysis of murine Mfn1 and Mfn2	134
227. Functional analysis of Mfn2 mutations in Charcot-Marie-Tooth disease.....	135
228. Structural study of mitochondrial fusion by mitofusin complexes	135
229. Proteomic identification of novel factors involved in mitochondrial fusion and fission	135
230. Analysis of homotypic and heterotypic interactions between murine Mfn1HR2 and Mfn2HR2.....	135
231. Analysis of HIV-1 gp41 mutants.....	136
Publications	136

RAYMOND J. DESHAIES, PH.D.

Summary.....	137
232. p97 regulation via interaction with a variety of p47-related co-factors	138
233. Structural studies of the 19S proteasome regulatory particle	139
234. Nedd8 protein modification, the COP9 signalosome and SCF	139
235. Role of ubiquitin-activating enzyme in ubiquitin-dependent degradation.....	139
236. Using MudPIT to characterize components of the proteasome pathway in yeast	140
237. Determining the function of the six ATPases in the 19S subunit of the proteasome	140
238. The roles of ubiquitin-mediated proteolysis in transcription.....	140
239. Control of mitotic exit in <i>S. cerevisiae</i>	141
240. Analysis of proteasome substrate specificity by mass spectrometry.....	141
241. Regulation of <i>Saccharomyces cerevisiae</i> Cdc14	141
242. Mechanisms of multiubiquitin chain synthesis by Cdc34	142
243. Targeting cancer-promoting proteins for ubiquitination and degradation	142
244. Determining the requirements for proteolysis by purified 26S proteasomes.....	142
Publications	142-143

WILLIAM G. DUNPHY, PH.D.

Summary.....	144
245. Positive regulation of Wee1 by Chk1 and 14-3-3 proteins.....	144
246. Requirement for Atr in phosphorylation of Chk1 and cell cycle regulation in response to DNA replication blocks and UV-damaged DNA in <i>Xenopus</i> egg extracts.....	145
247. Claspin, a novel protein required for the activation of Chk1 during a DNA replication checkpoint response in <i>Xenopus</i> egg extracts.....	145
248. Repeated phosphopeptide motifs in Claspin mediate the regulated binding of Chk1	145
249. Claspin, a Chk1-regulatory protein, monitors DNA replication on chromatin independently of RPA, ATR, and Rad17	145
250. <i>Xenopus</i> Drf1, a regulator of Cdc7, accumulates on chromatin in a checkpoint-regulated manner during an S-phase arrest	145
251. Phosphorylated Claspin interacts with a phosphate-binding site in the kinase domain of Chk1 during ATR-mediated activation	146
252. Adaptation of a DNA replication checkpoint response depends upon inactivation of Claspin by the Polo-like kinase.....	146
253. Absence of BLM leads to accumulation of chromosomal DNA breaks during both unperturbed and disrupted S-phases	146
254. Mcm2 is a direct substrate of ATM and ATR during DNA damage and DNA replication checkpoint responses	146
Publications	147

GRANT J. JENSEN, PH.D.

Summary.....	148
255. Comparison of helium and nitrogen as cryogens for tomography of purified protein complexes.....	148
256. Reducing charging effects at helium temperatures	149
257. Development of dual-axis cryoelectron tomography.....	149
258. Tomography of HIV at various stages of maturation	149
259. Cryoelectron tomography of a minimal cell, <i>Mesoplasma florum</i>	149
260. Electron tomography of <i>Mycoplasma genitalium</i>	150
261. Electron tomography of <i>E. coli</i>	150

262.	Electron tomography of a model cell demonstrating asymmetric cell division, <i>Caulobacter crescentus</i>	150
263.	Identification of large macromolecular complexes with cryoelectron tomograms of whole cells	151
264.	Spatially-explicit models of whole cells.....	151
265.	Peach, an efficient distributed computational system.....	152
266.	Near-atomic resolution protein structure determination without crystals.....	152
267.	Computer simulations of image formation and three-dimensional reconstruction.....	152

STEPHEN L. MAYO, PH.D.

	Summary.....	154
268.	Exploration of the neutral sequence space between pairs of proteins.....	154
269.	Evaluating a force field via fixed composition sequence design calculations.....	154
270.	Designing a high affinity peptide for TRAF6.....	155
271.	Improvement of protein design algorithms by incorporating dynamic backbone motions.....	155
272.	Design and testing of engineered IgG antibodies with increased in vivo half-lives.....	155
273.	Determining the crystal structure of a fully redesigned helical protein	156
274.	Computational design and experimental characterization of de novo protein dimers.....	156
275.	Computationally designed chorismate mutase active site variants	156
276.	Computational design of a novel enzyme for catalysis of a pericyclic reaction.....	157
277.	Computational design of a novel aldolase.....	157
278.	In silico prediction of metallo- β -lactamases with improved catalytic efficiency.....	157
279.	Computational design of a novel enzyme to catalyze a kinetic resolution	158
280.	Water-soluble membrane proteins by computational design.....	158
281.	Computational design of Ca^{2+} -deficient calmodulin: Interactions with protein kinase II.....	158
282.	Improved continuum electrostatic solvation for protein design	159
283.	Force field development for protein design.....	159
	Publications	159-160

JAMES H. STRAUSS, PH.D.

	Summary.....	161
284.	Flexibility of the yellow fever virus E protein	161
285.	The function of flavivirus E protein in virus assembly.....	162
286.	Production and in vitro reactivation of immature yellow fever virus particles containing prM	162
287.	RNA replication and viral assembly of chimeras between yellow fever virus and dengue 2 virus.....	162
288.	Capsid chimeras between YF and DEN	163
289.	Generation of alphaviruses containing uncleaved pE2 glycoprotein	164
290.	Antisera against YF helicase and DEN capsid protein	164
291.	Expression and purification of alpha virus non-structural and structural proteins	164
	Publications	164

ALEXANDER VARSHAVSKY, PH.D.

	Summary.....	165
292.	Mechanistic and functional studies of N-terminal arginylation	166
293.	Mechanistic, structural, and functional studies of bacterial Leu/Phe-tRNA-protein transferases	167
294.	Female lethality and apoptosis of spermatocytes in mice lacking the UBR2 ubiquitin ligase of the N-end rule pathway.....	168
295.	Construction and analysis of mouse strains lacking the UBR3 ubiquitin ligase	168
296.	Quantitative analyses of interactions between components of the N-end rule pathway and their substrates or effectors	169
297.	Phosphorylation of UBR1: Its regulation and functions.....	169
298.	RECQL4, mutated in the Rothmund-Thomson and RAPADILINO syndromes, interacts with ubiquitin ligases UBR1 and UBR2 of the N-end rule pathway	169
299.	Spalog and sequelog: Neutral terms for spatial and sequence similarity.....	170
	Publications	171

DEVELOPMENTAL AND REGULATORY BIOLOGY

JOSÉ ALBEROLA-ILA, PH.D.

Summary.....	175
300. Lck directs CD4/CD8 lineage commitment	175
300a. Alterations in Lck activity can change cell fate determination	175
300b. Development of a tunable Lck system to directly test purely quantitative vs. kinetic models of lineage commitment	176
301. Role of GATA-3 in CD4/CD8 lineage commitment	176
301a. GATA-3 is important for CD4/CD8 development.....	176
301b. Signals that control GATA-3 expression in the thymus	177
301c. Structure-function analysis of the GATA-3 domains important for CD4 lineage commitment	177
302. Novel genes involved in CD4/CD8 lineage commitment.....	177
303. Ras/MAPK pathway and the control of positive selection	178
303a. MAPK is not the only Ras effector involved in positive selection	178
303b. Analysis of Ras effector mutants	178
303c. Using microarrays to dissect the genetic networks that control positive selection downstream Ras	179
303d. Ksr is required to link Ras to the MAPK cascade during positive selection	179
303e. Development of ERK activity sensors to monitor MAPK activation	179
303f. Does the Ras/MAPK cascade play a role in CD4/CD8 determination?.....	180
304. PI3-K controls thymic exit.....	180
305. Role of Notch during the DN to DP transition.....	181
Publications	181

MARIANNE BRONNER-FRASER, PH.D.

Summary.....	182
306. A novel chicken spalt gene expressed in branchial arches reduces neurogenic potential of the cranial neural crest	182
307. Cancerous stem cells can arise from pediatric brain tumors	182
308. Id gene expression in amphioxus and lamprey highlights the role of genetic cooption during neural crest evolution	183
309. Combined intrinsic and extrinsic influences pattern cranial neural crest migration and pharyngeal arch 183 morphogenesis in axolotl	183
310. Graded potential of neural crest to form cornea, sensory neurons and cartilage along the rostrocaudal axis.....	183
311. Segregation of lens and olfactory precursors from a common territory.....	184
312. Developmental origins and evolution of jaws: New interpretation of "maxillary" and "mandibular"	184
313. Discover of genes involved in placode formation.....	184
Publications	184-185

ERIC H. DAVIDSON, PH.D.

Summary.....	186
314. Computational analysis of the emerging sea urchin genome sequence	189
315. The conservation of cis-regulatory information in lower deuterostomes	189
316. A microsatellite-based physical map of the purple sea urchin genome	189
317. Understanding gene regulation through motif analysis	190
318. A genome-wide survey of sea urchin transcription factors	190
319. Transcriptional control of the sea urchin brachyury gene	191
320. cis-Regulation of Spgcm.....	191
321. cis-Regulatory analysis of SpWnt8	192
322. cis-Regulatory analysis of SpFoxb	192
323. Transposition of the "regulatory module"—from the study of the negative modules in the Endo16192 promoter	192
324. Identified, proving and cloning UI, a protein involved in the sea urchin developmental regulatory gene network	193
325. Develop a high-throughput way to identify the interrelationship between regulatory modules and finding the non-conserved repression modules in the Otx locus.....	193
326. Trans-specification of primary mesenchyme cells through genetic rewiring of the mesoderm specification network.....	194

327.	<i>cis</i> -Regulatory analysis of the sea urchin delta gene	195
328.	A <i>cis</i> -regulatory analysis of SpGata-e.....	195
329.	Constitution of transcription complexes at the C-element of sm50 gene.....	195
330.	Understanding the transcriptional control of cyIIa	196
331.	<i>cis</i> -Regulation of the early and late forms of SpKrox1	196
332.	Delta expression in starfish and sea urchin embryo after 500 my divergence.....	197
333.	Regulatory gene network evolution: A comparison of endomesoderm specification in starfish and sea urchins.....	197
334.	Regulatory aspects of sea urchin biomineralization.....	198
335.	Discovery of a Precambrian bilaterian microfossil	198
	Publications	199-200

MICHAEL H. DICKINSON, PH.D.

	Summary.....	201
336.	Neural control of hummingbird flight	201
337.	Analysis of odor localization in walking <i>Drosophila</i>	201
338.	Kinematics and steering-muscle control of saccades in flying <i>Drosophila</i>	202
339.	Biomechanics and neurobiology of flight initiation in <i>Drosophila</i>	202
340.	Odor localization in flying <i>Drosophila</i>	203
341.	Modular displays for rapid development of programmable visual stimuli	204
342.	Vision as a compensatory mechanism for disturbance rejection in upwind flight	204
343.	Visual-olfactory sensory fusion in fruit flies.....	205
344.	Advanced numerical simulation model of free flight behavior in insects.....	206
345.	Ethological studies on resource-emigration in <i>Drosophila</i>	207
346.	Aerodynamics of forward flight in <i>Drosophila</i>	208
	Publications	208

MICHAEL ELOWITZ, PH.D.

	Summary.....	209
347.	Gene regulation at the single cell level.....	209
348.	Probabilistic decision-making in <i>Bacillus subtilis</i> starvation response.....	209
349.	Synthetic transcriptional network motifs.....	209
350.	Framework for the construction of synthetic transcriptional networks.....	210
	Publications	210

SCOTT E. FRASER, PH.D.

	Summary.....	211
351.	Cranial neural crest migration in the avian embryo.....	212
352.	Organization and development of genetically-defined olfactory glomeruli	213
353.	Becoming a new neuron in the adult olfactory bulb	213
354.	Imaging the enteric nervous system in development and in disease	213
355.	Planar cell polarity signaling controls orientation of oriented cell divisions during zebrafish gastrulation.....	214
356.	Convergent extension and <i>Xenopus</i> gastrulation: Convergent extension is required for blastopore closure, archenteron elongation and archenteron inflation, but is dispensable for mesoderm internalization.....	214
357.	Quantitative imaging of the sea urchin genetic regulatory network.....	214
358.	Assessing the role of microvascular blood flow during mammalian development	215
359.	Circulating blood island-derived cells contribute to vasculogenesis in the embryo proper	215
360.	In toto imaging of zebrafish development.....	216
361.	Automatic registration of 3D time-periodic confocal images	216
362.	Analysis of intracellular non-viral vector motion using correlation spectroscopy	217
363.	Biofunctionalization of self-assembled monolayers on Au substrates.....	217
364.	Biofunctionalized nano-electromechanical systems (BioNEMS)	218
365.	Applications of terahertz imaging to medical diagnostics.....	218
366.	MRI of quail embryogenesis.....	221
367.	3D time-lapse analysis of early <i>Xenopus</i> development using μ MRI	221
368.	Enzyme responsive MRI contrast agents for cancer imaging	222
369.	Contrast enhanced magnetic resonance microscopy of diffusion anisotropy in biological tissues.....	222
370.	In vivo assessment of brain function in transgenic mice using manganese enhanced MRI	223

371.	Fast imaging at high fields with intermolecular multiple quantum coherences	225
372.	Design and development of RF micro-surface coil for NMR microscopy	226
373.	Neuronal circuitry by magnetic resonance imaging in living animals.....	227
	Publications	230-231

BRUCE A. HAY, PH.D.

	Summary.....	232
374.	Yeast and fly-based screens for proteases that can cleave in a transmembrane environment.....	232
375.	Gene activation screens for cell death regulators: MicroRNAs, small non-coding RNAs, define a new family of cell death regulator	233
376.	IAPs, cell death and ubiquitination.....	233
377.	Identification of DIAP1-interacting proteins	233
378.	How does Drosophila activate caspase-dependent cell death?	233
379.	Bruce, cell death, caspases and spermatogenesis.....	234
380.	Maintaining tissue size: The role of death-induced compensatory proliferation.....	235
381.	Autophagic cell death, caspase inhibition in <i>C. elegans</i> , and the echinus mutant.....	235
	Publications	235

ELLIOT M. MEYEROWITZ, PH.D.

	Summary.....	236
382.	A gene expression map for Arabidopsis flower development.....	236
383.	Cell behavior and gene expression dynamics in SAMs.....	237
384.	Transient perturbation of signaling and meristem maintenance.....	237
385.	Regulation of WUSCHEL expression and WUSCHEL activity.....	238
386.	Analysis of post-transcriptional regulation of MODIFIER OF B FUNCTION	238
387.	Identifying genes involved in leaf identity as downstream transcriptional targets of JAGGED 238 and investigating upstream regulators.....	238
388.	Improving an in vivo experimental system for studying Arabidopsis meristem development	239
389.	In vivo manipulation of Arabidopsis gene expression at the cellular level	239
390.	Auxin and phyllotaxis	239
391.	Spatio-temporal dynamics of primordial gene expression, growth and signaling.....	240
392.	Microarray analysis of auxin induced genes	240
393.	HANABA TARANU is a GATA transcription factor that regulates shoot apical meristem and flower development in Arabidopsis	241
394.	Interactions between HAN and CUC proteins in setting up organ boundaries in Arabidopsis	241
395.	Probing the cellular function and downstream targets of HANABA TARANU, a GATA transcription factor essential for Arabidopsis development.....	241
396.	Functional analysis of two close homologs of HANABA TARANU in Arabidopsis development	242
397.	A semidominant mutation of HANABA TARANU causes fasciated shoot apical meristem in Arabidopsis.....	242
398.	The homeotic protein AGAMOUS controls microsporogenesis by regulation of SPOROCTELESS.....	243
399.	Downstream functions of the homeotic protein AGAMOUS during stamen development.....	243
400.	Evolutionarily function of homeotic gene AG during stamen development	243
401.	cis-Element analysis of the AGT2ATH gene, a putative target of AGAMOUS involved in polarity establishment in Arabidopsis carpels.....	244
402.	Systematic analyses of transcriptional networks during reproductive organ development in Arabidopsis.....	244
403.	Genome-wide binding site analysis of AG by chromatin immunoprecipitation (ChIP) in Arabidopsis	245
404.	Exploring floral organ number patterning.....	245
405.	Identifying genetic partners of PAN	246
406.	Identification of LFY and AP1 downstream genes in Arabidopsis using microarrays	246
407.	Looking for genes involved in the AP1 pathway.....	247
408.	EEP1 microRNA regulates organ number during flower development in Arabidopsis thaliana.....	247
409.	Identification of additional factors in the EEP1 microRNA regulated pathway of organ boundary 247 formation in Arabidopsis thaliana	247
410.	A family of putative mechanosensitive ion channels in Arabidopsis thaliana	248
	Publications	248-249

ELLEN V. ROTHENBERG, PH.D.

Summary.....	250
411. Transcriptional changes induced by Notch signaling and a transcriptional and kinetic analysis of B- and T-cell development.....	251
412. Notch target genes and their roles in T-cell development.....	251
413. Using retroviral expression of siRNAs to test the requirement for GATA-3 at the DN3 stage of thymopoiesis.....	252
414. A developmentally regulated upper limit for GATA-3 activity in T-lineage differentiation.....	252
415. Functional analysis of the hematopoiesis-specific transcription factor PU.1 in the development of T lymphocytes.....	253
416. Subversion of T-lineage commitment by PU.1 in a clonal cell line system.....	253
417. Identifying the potential regulatory elements controlling PU.1 expression.....	254
418. Functional characterization of PU.1 regulatory elements.....	254
419. A regulatory "parts list" for early T-cell development.....	255
420. Genes upregulated specifically in pro-T cells as compared to pre-myeloid cells.....	255
421. Genes upregulated in pro-T cells as compared to pro-B cells.....	256
422. Exploring the state-space of transcriptional regulatory networks.....	256
423. Evolution of transcriptional regulatory ensembles that support lymphocyte development.....	257
424. Developmental potentials of early thymocyte subsets.....	257
425. Deranged early T-cell development in immunodeficient strains of non-obese diabetic mice.....	258
426. Genetic mapping of the pre-T cell checkpoint breakthrough in NOD-scid/scid mice.....	258
427. Preferential expression of an IL-2 regulatory sequence transgene in TCR $\gamma\delta$ and NKT cells.....	258
428. Epigenetic marking of the IL-2 locus without transcription in IL-2-inducible T-lineage cells.....	259
Publications.....	260

MELVIN I. SIMON, PH.D.

Summary.....	261
429. Molecular Biology Laboratory of the Alliance for Cellular Signaling (AfCS): RNAi project.....	261
430. Molecular Biology Laboratory of the Alliance for Cellular Signaling (AfCS): cDNA cloning projects.....	262
431. Molecular Biology Laboratory of the Alliance for Cellular Signaling (AfCS): Yeast two-hybrid project.....	262
432. Inhibition of gene expression in the macrophage-like cell line RAW264.7.....	263
433. Transcriptional ligand screen of mouse B cell and macrophage reveals signaling pathways.....	263
434. Isotype-specific roles of G β subunits in chemokine-dependent cellular responses.....	264
435. Identification of retinal ganglion cell subset-specific genes.....	264
Publications.....	264-265

PAUL W. STERNBERG, PH.D.

Summary.....	266
436. A physiological role for EGFR signaling in <i>C. elegans</i> growth.....	267
437. The <i>Caenorhabditis elegans</i> fos family member Ce-fos, promotes cell invasive behavior.....	267
438. Frizzled and Ryk pathways function in parallel to control P7.p lineage orientation in the <i>C. elegans</i> vulva.....	268
439. The role of cam-1 in <i>C. elegans</i> vulval development.....	268
440. Cell fate patterning and/or differentiation in 2 $^{\circ}$ vulval lineages.....	268
441. Heterochronic transcription factor lin-29 and coordination of vulval morphogenesis.....	268
442. Role of Wnt and Notch signaling and Hox gene in the patterning of <i>C. elegans</i> hook sensillum competence group.....	269
443. Spicule development and signal transduction specificity.....	269
444. Male linker cell migration.....	269
445. WormBase, database of <i>Caenorhabditis</i> genomes, genetics and biology.....	270
446. WormBook - An online review of <i>C. elegans</i> biology.....	270
447. Predicting genetic interactions by multi-source data integration.....	270
448. Experimental annotation of <i>C. elegans</i> and <i>C. briggsae</i> genomes by the TEC-RED technique.....	270
449. cis-Regulatory sequence analysis in <i>Caenorhabditis sensu stricto</i> versus <i>sensu lato</i>	271
450. Pipeline for cis-regulatory sequence annotation.....	271
451. Functional analysis of EGL-30-mediated signaling in <i>C. elegans</i>	272
452. Sperm transfer during male mating behavior.....	272
453. Control of locomotory behavior in <i>C. elegans</i> male mating.....	272

454.	Comparative analyses of ASH-mediated behaviors.....	273
455.	An automated system for measuring parameters of nematode sinusoidal movement.....	273
456.	Nematode sinusoidal movement: Theory and experiment	274
457.	Quantitative analyses of nematode locomotion on different food sources	274
458.	Beneficial and pathogenic interactions in the nematode gut: One bacterium, two interactions.....	274
459.	Engineering <i>C. elegans</i> cells.....	274
	Publications	275

BARBARA J. WOLD, PH.D.

	Summary.....	276
460.	Analysis of transcriptional protein complexes via MudPIT mass spectrometry	277
461.	Developing genomic DNA as a comprehensive cohybridization standard for use in microarray gene expression measurements	277
462.	Defining myogenic determination and differentiation on a whole-genome scale	278
463.	Characterization of pediatric sarcomas by microarray-based gene expression studies.....	278
464.	Gene expression and metabolic organization in <i>Shewanella oneidensis</i> biofilms.....	279
465.	Comparative sequence analysis in vertebrate genomes: Seqcomp, and MUSSA	280
466.	Identifying and testing candidate regulatory regions for genes of the myogenic regulatory circuit.....	280
467.	CompClust: A computational framework for machine learning and data mining.....	280
468.	Comparison of clustering algorithms for use in large-scale gene expression analysis.....	281
469.	Role of a homeogene, <i>msx-1</i> , in adult muscle regeneration	281
470.	Expression profiling of stem cell lines	282
471.	A new method for assaying gene expression	282
472.	Computational analysis of Pho4 binding site presence, in vivo Pho4 binding, and phosphate dependent gene expression.....	283
473.	The Sigmoid pathway modeling system.....	283
474.	Comparative genomics for somite development regulatory element identification	284
475.	Optimization of the sequence comparison algorithm by the core match method.....	284
476.	Regulation of messenger RNA translation during skeletal muscle differentiation.....	284
477.	Transcriptome changes in rat skeletal muscle in response to simulated microgravity.....	285
478.	Automation of genome-wide and cross-genome cis-regulatory element identification and assessment using Cistematic.....	285
479.	Multigenome-scale analysis of cis-regulatory elements for specific transcription factors	286
480.	An analysis of the relationship of zinc finger structure in mammalian transcription factors and of their preferred binding sites	286
	Publications	287

FACILITIES	289
-------------------------	-----

GRADUATES	301
------------------------	-----

FINANCIAL SUPPORT	307
--------------------------------	-----

INDEX	311
--------------------	-----

Introduction

100, 75, 50 and 25 Years Ago

100 Years Ago: 1904

Although the name California Institute of Technology was not used until 1920, and the Division of Biology was not started until 1928, there were biologists at Throop Polytechnic Institute, an earlier name for what is now Caltech. In 1904, Joseph Grinnell, the most distinguished of them, joined the faculty. He was an 1897 graduate of Throop, went to Stanford for graduate work, then joined the Throop faculty as Instructor in Natural Science in 1904. By 1906, he was Professor of Biology, but left Throop in 1908 to become the Director of the Museum of Comparative Zoology and Professor at U.C. Berkeley. He is considered the first important west coast mammalogist; in 1924, he first published the concept of the ecological niche. Grinnell Mountain in the San Bernardino range is named for him.

75 Years Ago: 1929

1929 marked the first graduation of a Biology Division Ph.D. student at Caltech. The student was Albert Tyler, with a thesis entitled "Experimental production of double embryos." He was a student in the laboratory of Professor T.H. Morgan, the Division Chair. After his graduation he stayed in the Division, first as instructor, and then through the ranks to professor, remaining until his death in 1968.

50 Years Ago: Biology 1954 at the California Institute of Technology

"Approximately a hundred academic staff members were responsible for the research, teaching and other activities of the Division of Biology in its twenty-seventh year of existence. Research problems ranged all the way from the chemistry of Los Angeles smog to investigations of the integrative mechanisms of the cerebrum..."

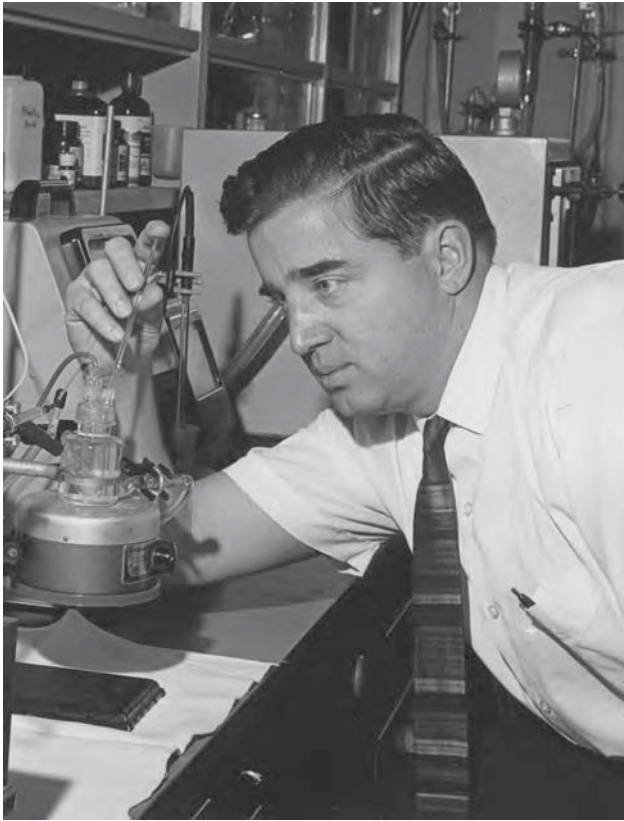
Two Visiting Professors, Dr. Barbara McClintock of the Carnegie Institution of Washington, Cold Spring Harbor, New York, and Dr. John B. Buck of the National Institutes of Health contributed in important ways to the teaching program of the Division. In graduate genetics, Dr. McClintock gave a series of approximately 20 lectures, based largely on her own work in cytogenetics of maize...

An important addition to the faculty of the Division was made in the appointment of Dr. Roger W. Sperry as Professor of Psychobiology...

A significant step in the development of the Chemistry-Biology program at the Institute was the start of construction of the new \$1,500,000 Norman W. Church Laboratory for Chemical Biology..."

25 Years Ago: Caltech Biology Annual Report 1979

"The abstract by Hobby et al., that follows is probably the last that will appear in the Biology Annual Report on our attempts to simulate the results obtained on the surface of Mars by the Carbon Assimilation experiment. The Viking findings, which implied a small synthesis of organic matter from atmospheric carbon, were very surprising... The reaction was too thermostable to be considered biological; other Viking data also make it extremely unlikely that Mars is a habitat of life." From the abstract of Professor Norman H. Horowitz.



Professor of Biology, William J. Dreyer, died April 23, 2004 after a long illness.

A native of Kalamazoo, Michigan, Dreyer earned his B.A. degree at Reed College in 1952 and his Ph.D. in biochemistry at the University of Washington in 1956. After graduating, he worked as a research biochemist at the National Heart Institute and the National Institute of Arthritis and Metabolic Diseases before joining Caltech.

Dreyer was perhaps best known for developing an automated sequencer that allowed researchers to quickly determine the order of amino acids in a protein, an instrument that helped to launch the field of biotechnology. He also proposed in the 1960s that genes could be "reshuffled" to provide additional information for the formation of proteins. At first controversial, the theory came into prominence after it was confirmed by other researchers.

At a Society for Biomolecular Screening conference last year, Caltech alum Leroy Hood credited Dreyer for mentoring his early career, teaching him to think conceptually, and introducing him to "the exhilaration of rapidly paced molecular immunology." Dreyer always emphasized two principles, he added: "Always practice biology at the leading edge" and "if you really want to change biology, develop new technology for pushing back the frontiers of biological knowledge."

Dreyer authored a number of journal articles and held many patents, including one for an immunological reagent and radioimmunoassay and two for poly-acrylate beads that he developed with two colleagues.

An avid pilot since 1960, Bill often flew to Baja California and around the western United States and British Columbia. He once remarked that his taste for flying his Cessna P210 at 15,000 feet—high for a small plane but low for commercial aircraft—was "an allegory for my tastes in scientific research. I like to work where research isn't too competitive and crowded—to move beyond the current mob scene, even if the place where I end up is lonely."

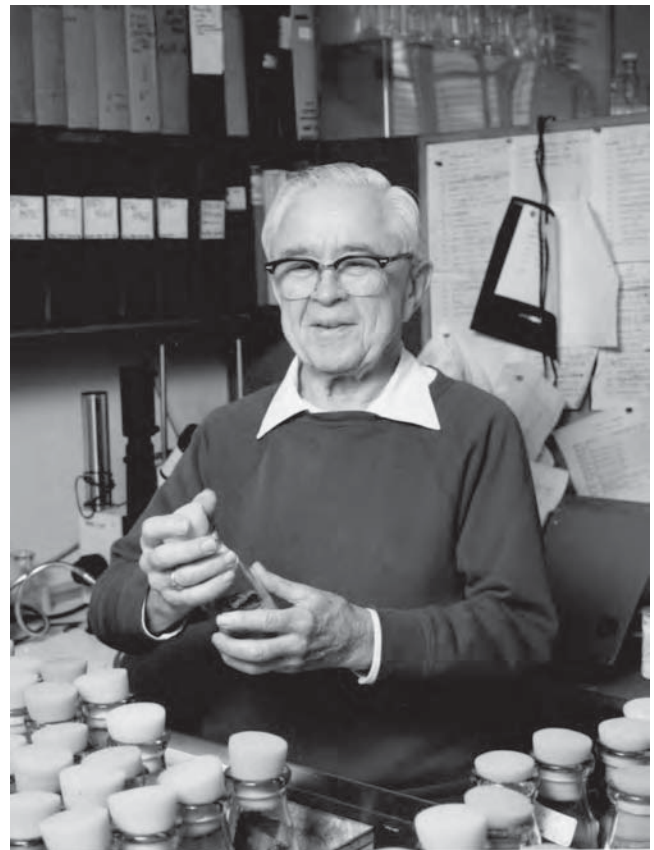
Thomas Hunt Morgan Professor of Biology, Edward Lewis, Emeritus, died July 21, 2004 after a long battle with cancer.

Born May 20, 1918, in Wilkes-Barre, Pennsylvania, Lewis as an adolescent became interested in the genetics of the fruit fly, *Drosophila melanogaster*, which was already being touted as an excellent animal for research by Caltech's Thomas Hunt Morgan. Lewis performed genetics experiments on *Drosophila* while just a freshman in high school, and after taking a bachelor's degree in 1939 at the University of Minnesota, came to Caltech for a doctorate and remained at the Institute for the rest of his life, save for four years in the U.S. Army Air Force during World War II, when he worked as a meteorologist.

A member of the California Institute of Technology faculty since 1946, Lewis spent his life working on the genetics of the fruit fly, with special attention to the fundamental ways in which the genes relate to embryonic development. The work had profound implications for a basic understanding of the genetic regulation of development in humans.

In a book published on Lewis earlier this year, author and longtime collaborator Howard Lipshitz wrote that Lewis's scientific research was "the bridge linking experimental genetics as conducted in the first half of the 20th century, and the powerful molecular genetic approaches that revolutionized the field in its last quarter." Lipshitz also lauded Lewis's much less widely known work on the understanding of radiation and cancer, and the closely related issues concerning nuclear-weapons testing policy.

In a campus article appearing in 1957, Lewis described his success in causing the flies to develop with four wings (they normally have two). "We now have a working model for picturing the genetic control of development," he said. His prognostication was correct, and nearly four decades later the Nobel Committee, in awarding Lewis the Nobel Prize in physiology or medicine in 1995, cited his triumph in identifying and classifying "a small number of genes that are of key importance in determining the body plan and the formation of body segments." The Nobel Committee also lauded Lewis for his discovery of "how genes were arranged in the same order on the chromosomes as the body segments they controlled.



HONORS and Awards - 2004



Meyerowitz

Smith

Schuman

W. Bryan Smith is the winner of the Ferguson Award for the 2003-2004 academic year. This award goes to the student who is judged by the faculty to have produced the best Ph.D. thesis over the past year. Dr. Smith performed his graduate studies in the laboratory of Professor Erin Schuman.

His thesis work focused on mechanisms governing the spatial specificity of neuronal communication. A single neuron in the brain may contain as many as ten thousand synaptic connections, small groups of which are independently regulated. For example, the strength of some synapses may increase in response to a given stimulus, while synapses nearby remain unchanged. One of the requirements for long-lasting changes in synaptic strength is that the neuron must produce new proteins. If, as traditionally believed, all protein synthesis occurs in the cell body, neurons must ship the proteins great distances, and with a high degree of specificity. A more plausible approach would be for neurons to produce the proteins locally, near the synaptic sites where they are needed. Prior to Dr. Smith's work, such local, dendritic protein synthesis had not been clearly demonstrated. Using a green fluorescent protein (GFP) reporter in a series of imaging experiments, Dr. Smith provided definitive, visual proof that isolated dendrites of hippocampal neurons are capable of protein synthesis. His work further showed that dopamine, an important neuromodulator, can directly affect synaptic strength in a local protein synthesis-dependent manner.

PROFESSORIAL AWARDS 2004

James G. Boswell Professor of Neuroscience, Richard A. Andersen, received a NASA Tech Brief Award for a novel implantable cortical neuroprosthesis device. He was elected by the neuroscientists of the American Association for the Advancement of Science to serve on the Nominating Committee for Neuroscience from 2004-2007. He has been invited to give a Special Lecture at the Society for Neuroscience Meeting this year and has also been invited to be a visiting professor at the College de France, giving four lectures next year.

James G. Boswell Professor of Neuroscience, Seymour Benzer, was the recipient of the Bower Award and Prize for brain research, Franklin Institute, Philadelphia; was presented with the Peter Gruber Foundation Award for Neuroscience, San Diego, CA; and the Gairdner International Award for Medical Research, Toronto, Canada.

Max Delbrück Professor of Biology, Pamela Bjorkman, received the following honors and awards: The Dan H. Campbell Memorial Lecture, Midwinter Conference of Immunologists; Southwestern Medical Foundation Distinguished Visiting Professor Honoring Women in Science and Medicine, University of Texas at Southwestern; Keynote Speaker, 12th International Congress of Immunology; Max Delbrück Professor of Biology.

Albert Billings Ruddock Professor of Biology, Marianne Bronner-Fraser, was the recipient of the following honors and awards: Scientific Advisory Board—March of Dimes, 2004-present; Joint Genome Center Sequencing Review Committee, 2004-present; Harvey Lecturer, Rockefeller University, 2004; NHGRI Comparative Genome Evolution Review Committee, 2004.

Associate Professor of Biology, Raymond J. Deshaies, was appointed to the Defense Sciences Study Group of the Institute for Defense Analysis, and was named Distinguished Lecturer, Cornell University.

Assistant Professor of Biology and Applied Physics, Michael Elowitz, was the recipient of a Searle Fellowship.

Assistant Professor of Biology, Grant J. Jensen was named a Searle Scholar.

Bing Professor of Behavioral Biology, Masakazu Konishi, was awarded the Gerard Prize, from the Society for Neuroscience; the Edward M. Scolnick Prize in Neuroscience from McGovern Institute, MIT; the Lewis S. Rosenstiel Award for Distinguished Work in Basic Medical Sciences, Brandeis University; and the Karl Spencer Lashley Award from the American Philosophical Society.

Professor of Biology, Stephen L. Mayo, was elected as a member of the National Academy of Sciences.

George W. Beadle Professor of Biology and Division Chair, Elliot Meyerowitz, gave a plenary lecture at the XIX International Congress of Genetics in Melbourne, Australia in July, 2003; and was the Duke Distinguished Lecturer at Duke University in February, 2004. He has been selected as a Phi Beta Kappa Visiting Lecturer for the years 2004-2006. In May 2004, he was elected a Foreign Member of the Royal Society.

Professor of Biology, Paul H. Patterson, was named Distinguished Visiting Professor by the Institute of Psychiatry, King's College, London.

Professor of Biology, Ellen Rothenberg, was awarded the 2003-2004 Biology Undergraduate Student Advisory Committee Award for Excellence in Teaching.

Howard and Gwen Laurie Smits Professor of Cell Biology Alexander Varshavsky has received the 2005 Stein and Moore Award from the Protein Society. He shared this award with Dr. Avram Hershko (Technion, Haifa, Israel). In 2004, Varshavsky gave the Hofmann Lecture at the University of Pittsburgh.

The Biology Division hosted the following Wiersma Visiting Faculty in the last year:

December 3, 2003

Harvey Karten

Department of Neuroscience, UCSD

"Lettvin's bug detector – Evolution and neuromorphic engineering: Holding the visual hierarchy map upside down"

January 14, 2004

Marina Picciotto

Department of Psychology, Yale University School of Medicine

"Protein kinase and protein phosphatase machinery at synapses"

March 10, 2004

Thomas Schwarz

Children's Hospital, Harvard University

"Cellular traffic in the fly: Motors and membrane targeting"

June 3, 2004

Cynthia Kenyon

Hillblom Center for the Biology of Aging, Department of Biochemistry & Biophysics, UCSF

"From worms to mammals: The regulation of lifespan by insulin/IGF signaling"

In 2004, special named lectures were presented:

NORMAN DAVIDSON LECTURE – MARCH 29, 2004

Michael Snyder

Department of Molecular, Cellular & Developmental Biology, Yale University

"Global analysis of genomes and proteomes"

KROC LECTURES

February 9, 2004

Jules Hoffman

Institut de Biologie Moleculaire, CNRS

"Recognition and signaling in the immune response of *Drosophila*"

April 5, 2004

Matthew Scott

Departments of Biology & Genetics, Stanford University School of Medicine

"Genomic approaches to mesoderm development"

WEIGLE LECTURE – MAY 17, 2004

Stanley Korsmeyer

Dana-Farber Cancer Institute, Boston, Harvard University

"Gateways to apoptosis"

HOROWITZ LECTURES – October 13, 2003

Paul Berg

Cahill Professor of Biochemistry, Emeritus, Stanford University School of Medicine

"One gene-one enzyme: A genomic perspective"

John Doebley

Genetics Department, University of Wisconsin

"The domestication of maize"

Maxine Singer

President Emeritus, Carnegie Institute of Washington

"The public fact of genetics"

LEWIS SYMPOSIUM, FEBRUARY 4, 2004

Howard Lipshitz

Divisions of Endocrinology & Genetics, The Hospital for Sick Children

"From fruit flies to fallout: Ed Lewis and his science"

TYLER LECTURE

April 4, 2004

Joan Massague

Department of Cellular Biology, Memorial Sloan-Kettering Cancer Center

"Organ-specific metastasis genes and functions"



Photos from Keck Symposium on November 17, 2003



Above, more photos from Keck Symposium on November 17, 2003



Photos from Mitochondrial DNA in Health, Disease and Aging, a Symposium in Honor of Giuseppe Attardi on December 3, 2003 at the University of North Carolina

Biology Division Staff

Instruction and Research

Administrative

Instruction and Research Staff Division of Biology

Elliot M. Meyerowitz, Chairman, Division of Biology
Pamela J. Bjorkman, Executive Officer for Biology
Erin M. Schuman, Executive Officer for Neurobiology

Professors Emeriti

John N. Abelson, Ph.D.
George Beadle Professor of Biology

Seymour Benzer, Ph.D., D.Sc.h.c. Crafoord Laureate
James G. Boswell Professor of Neuroscience (Active)

Charles J. Brokaw, Ph.D., Biology

John J. Hopfield, Ph.D.
Roscoe G. Dickinson Professor of Chemistry and Biology

Norman H. Horowitz, Ph.D., Biology

Edward B. Lewis, Ph.D. Nobel Laureate
Thomas Hunt Morgan Professor of Biology

Ray D. Owen, Ph.D., Sc.D.h.c., Biology (Active)

Senior Research Associate Emeritus

Roy J. Britten, Ph.D.
Distinguished Carnegie Senior Research Associate in Biology, Emeritus

Professors

John M. Allman, Ph.D.
Frank P. Hixon Professor of Neurobiology

Richard A. Andersen, Ph.D.
James G. Boswell Professor of Neuroscience

David J. Anderson, Ph.D.¹
Roger W. Sperry Professor of Biology

Giuseppe Attardi, Ph.D., M.D.
Grace C. Steele Professor of Molecular Biology

David Baltimore, Ph.D.,
Nobel Laureate, Biology

Pamela J. Bjorkman, Ph.D.¹
Max Delbrück Professor of Biology

Marianne Bronner-Fraser, Ph.D.
Albert Billings Ruddock Professor of Biology

Judith L. Campbell, Ph.D.
Chemistry and Biology

Eric H. Davidson, Ph.D.
Norman Chandler Professor of Cell Biology

Michael H. Dickinson, Ph.D.
Esther M. and Abe M. Zarem Professor of Bioengineering

William G. Dunphy, Ph.D.¹
Biology

Scott E. Fraser, Ph.D.
Anna L. Rosen Professor of Biology

Mary B. Kennedy, Ph.D.
The Alan and Lenabelle Davis Professor of Biology

Christof Koch, Ph.D.
The Lois and Victor Troendle Professor of Cognitive and Behavioral Biology and Professor of Computation and Neural Systems

Masakazu Konishi, Ph.D.
Bing Professor of Behavioral Biology

Gilles Laurent, Ph.D., D.V.M.
Lawrence A. Hanson Jr. Professor of Biology and
Computation and Neural Systems

Henry A. Lester, Ph.D.
Bren Professor of Biology

Stephen L. Mayo, Ph.D.¹
Biology and Chemistry

Elliot M. Meyerowitz, Ph.D.
George W. Beadle Professor of Biology
Chair, Biology Department

Paul H. Patterson, Ph.D.
Biology

Jean-Paul Revel, Ph.D.²
Albert Billings Ruddock Professor of Biology
Dean of Students

Ellen V. Rothenberg, Ph.D.
Biology

Shinsuke Shimojo, Ph.D.
Biology

Melvin I. Simon, Ph.D.
Anne P. and Benjamin F. Biaggini Professor of Biological
Sciences

Paul W. Sternberg, Ph.D.¹
Thomas Hunt Morgan Professor of Biology

James H. Strauss, Ph.D.
Ethel Wilson Bowles and Robert Bowles Professor of
Biology

Alexander J. Varshavsky, Ph.D.
Howard and Gwen Laurie Smits Professor of Cell Biology

Barbara J. Wold, Ph.D.
Bren Professor of Molecular Biology

Kai Zinn, Ph.D.
Biology

¹Joint appointment with Howard Hughes Medical Institute
²Undergraduate Student Advisor

Associate Professors

Raymond J. Deshaies, Ph.D.¹
Biology

Bruce A. Hay, Ph.D.
Biology

Erin M. Schuman, Ph.D.¹
Biology

¹Joint appointment with Howard Hughes Medical Institute

Assistant Professors

José Alberola-Ila, M.D., Ph.D.
Biology

Grant J. Jensen, Ph.D.
Biology

David C. Chan, M.D., Ph.D.
Biology
Bren Scholar

Athanasios G. Siapas, Ph.D.
Computation and Neural Systems
Bren Scholar

Michael Elowitz, Ph.D.
Biology and Applied Physics
Bren Scholar

Lecturers

David S. Koos, Ph.D.
Jane E. Mendel, Ph.D.
James R. Pierce, M.D.
Stewart Scherer, M.D.

DIVISION OF BIOLOGY

SENIOR RESEARCH ASSOCIATES

R. Andrew Cameron, Ph.D.
 Anne Chomyn, Ph.D.
 Iain D.C. Fraser, Ph.D.
 Akiko Kumagai, Ph.D.
 Jane E. Mendel, Ph.D.
 Jose Luis Riechmann, Ph.D.
 Ellen G. Strauss, Ph.D.

SENIOR RESEARCH FELLOWS

Christopher A. Buneo, Ph.D.
 Martin Garcia-Castro, Ph.D.
 Petr Hájek, Ph.D.
 Gabriela Hernandez-Hoyos, Ph.D.
 Toshiro Ito, Ph.D.
 Joanna L. Jankowsky, Ph.D.

Ali Khoshnan, Ph.D.
 David W. McCauley, Ph.D.
 Mollie K. Meffert, M.D., Ph.D.
 Paola Oliveri, Ph.D.
 Jose L. Peña, M.D.
 Anthony P. West, Jr., Ph.D.

FACULTY ASSOCIATE

Alice S. Huang, Ph.D.

MOORE DISTINGUISHED SCHOLARS

Carl O. Pabo, Ph.D.
 Markus Meister, Ph.D.

VISITING PROFESSOR

Joseph Bogen, Ph.D.

VISITING ASSOCIATES

Elaine L. Bearer, Ph.D.
 Hamid Bolouri, Ph.D.
 William L. Caton III, Ph.D.
 Tobias Delbrück, Ph.D.
 Igor Fineman, M.D.
 Leroy Hood, M.D., Ph.D., D.Sc.h.c, D.h.c.
 Shih-Chii Liu, Ph.D.
 Angelique Y. Louie, Ph.D.

Eric Mjolsness, Ph.D.
 Johannes Schwarz, M.D.
 Neil Segil, Ph.D.
 Ladan Shams, Ph.D.
 Sandra B. Sharp, Ph.D.
 Gary M. Wessel, Ph.D.
 John C. Wood, M.D., Ph.D.

MEMBER OF BECKMAN INSTITUTE

Russell E. Jacobs, Ph.D.

MEMBERS OF THE PROFESSIONAL STAFF

Eugene Akutagawa, B.S.
 Janet F. Baer, D.V.M.
 Gary R. Belford, Ph.D.
 Lillian E. Bertani, Ph.D.
 Martin E. Budd, Ph.D.
 Sangdun Choi, Ph.D.
 Bruce Cohen, Ph.D.
 Rochelle A. Diamond, B.A.
 Mary Dickinson, Ph.D.
 Pamela Eversole-Cire, Ph.D.
 Gary M. Hathaway, Ph.D.
 Suzanna J. Horvath, Ph.D.

Cesar G. Labarca, Ph.D.
 Ker-hwa (Susan) Tung Ou, M.S.
 Shirley Pease, B.Sc.
 Piotr Polaczek, Ph.D.
 Andrew J. Ransick, Ph.D.
 Hiroaki Shizuya, M.D., Ph.D.
 Peter Siegel, Ph.D.
 Peter Snow, Ph.D.
 Julian Michael Tyszka, Ph.D.
 Chiou-Hwa Yuh, Ph.D.
 Zie Zhou, Ph.D.

SENIOR POSTDOCTORAL SCHOLARS

Elizabeth Haswell, Ph.D.
 Helen McBride, Ph.D.
 Tom Taghon, Ph.D.
 Carol C. Tydell, D.V.M.
 Frank Wellmer, Ph.D.

POSTDOCTORAL SCHOLARS

Satoko Adachi, Ph.D.
 Bader Al-Anzi, Ph.D.
 Gabriela Alexandru, Ph.D.

Catherine C. Baker, Ph.D.
 Martin L. Basch, Ph.D.
 Sylvian Bauer, Ph.D.
 Bryan David Beel, Ph.D.
 Marlene Biller, Ph.D.
 Hemant S. Bokil, Ph.D.
 Mark P. Boldin, Ph.D.
 Christopher Brower, Ph.D.
 Marina Brozovic, Ph.D.
 Marina Brozovic, Ph.D.
 Ted J. Brummel, Ph.D.

Holly J. Carlisle, Ph.D.
 Rafael Casellas, Ph.D.
 David F. Chang, Ph.D.
 Mark A. Changizi, Ph.D.
 Chun-Hong Chen, Ph.D.
 Hsiuchen Chen, Ph.D.
 Jing Chen, Ph.D.
 Lili Chen, Ph.D.
 Jae Hyoung Cho, Ph.D.
 Mee Hyang Choi, Ph.D.
 Pritsana Chomchan, Ph.D.
 Todd A. Ciche, Ph.D.
 Daniel John Clayton, Ph.D.
 Edward G. Coles, Ph.D.
 Jason David Connolly, Ph.D.
 Brian Corneil, Ph.D.
 Markus W. Covert, Ph.D.

Karin Crowhurst, Ph.D.
 He Cui, Ph.D.

Pradeep Das, Ph.D.
 Mindy I. Davis, Ph.D.
 Maria Elena de Bellard, Ph.D.
 Benjamin Deneen, Ph.D.
 Benjamin Deverman, Ph.D.
 Kamran Diba, Ph.D.
 Mohammed Dibas, Ph.D.
 Daniela Dieterich, Ph.D.
 Xinzhong Dong, D.¹
 Robert A. Drewell, Ph.D.
 Annick Dubois, Ph.D.

Andrew J. Ewald, Ph.D.
 Maxellende Ezin, Ph.D.

Carlos I. Fonck, Ph.D.
 A. Nicole Fox, Ph.D.
 Yasuko Funabiki, Ph.D.
 Elizabeth-Sharon Fung, Ph.D.

Limor Gabay, Ph.D.
 Alexander M. Gail, Ph.D.
 Laura S. Gammill, Ph.D.
 Feng Gao, Ph.D.
 Lisa R. Girard, Ph.D.
 Venugopala R. Gonehal, Ph.D.
 Emmanuelle Graciet, Ph.D.
 Bradley E. Greger, Ph.D.
 Lingjie Gu, Ph.D.
 Huatao Guo, Ph.D.

Chih-Ju Han, Ph.D.
 Sang-Kyou Han, Ph.D.
 Bridget M. Hanser, Ph.D.
 Shengli Hao, Ph.D.
 Wulf Eckhard Haubensak, Ph.D.
 Ryusuke Hayashi, Ph.D.
 Yuichiro Hayashi, Ph.D.
 Wanzhong He, Ph.D.
 Yongning He, Ph.D.
 Marcus G.B. Heisler, Ph.D.
 Andrew B. Herr, Ph.D.
 Veronica F. Hinmann, Ph.D.
 Kristina Holmberg, Ph.D.
 Rong-gui Hu, Ph.D.
 Byung Joon Hwang, Ph.D.¹
 Cheol-Sang Hwang, Ph.D.
 Jong-Ik Hwang, Ph.D.

Cristina Valeria Iancu, Ph.D.
 Takao Inoue, Ph.D.

Mili Jeon, Ph.D.
 Seong-Yun Jeong, Ph.D.¹
 Changan Jiang, Ph.D.¹
 Henrik Johnsson, Ph.D.

Igor Kagan, Ph.D.
 Pankaj Kapahi, Ph.D.
 Jan Piotr Karbowski, Ph.D.
 Mihoko Kato, Ph.D.
 Yun Kee, Ph.D.
 Bradley J. Kerr, Ph.D.
 Eugenia Khorosheva, Ph.D.

Soo-Mi Kim, Ph.D.¹
 Gary L. Kleiger, Ph.D.
 Anne K. Knecht, Ph.D.
 Irene Knuesel, Ph.D.
 Reinhard Koester, Ph.D.
 David Koos, Ph.D.
 Takumi Koshiba, Ph.D.
 Alexander Kraskov, Ph.D.
 Nicole J. Kubat, Ph.D.
 Mitsuhiko Kurusu, Ph.D.

Micheline N. Laurent, Ph.D.
 Tim Lebestky, Ph.D.
 Joon Lee, Ph.D.¹
 Vivian Lee, Ph.D.
 John F. Leite, Ph.D.
 Walter Lerchner, Ph.D.
 Pingwei Li, Ph.D.
 Wenhui Li, Ph.D.
 Michael Liebling, Ph.D.
 J. Russell Lipford, Ph.D.
 Jeffrey A. Long, Ph.D.
 Sally Lowell, Ph.D.
 Wange Lu, Ph.D.
 Agnes Lukaszewicz, Ph.D.
 Peter Y. Lwigale, Ph.D.

Whee Ky Ma, Ph.D.
 Sacha A. Malin, Ph.D.
 Pasquale Manzerra, Ph.D.
 Edoardo Marcora, Ph.D.
 Melanie S. Martin, Ph.D.
 Miguel Martin-Hernandez, Ph.D.
 Thibault Mayor, Ph.D.
 Kathryn L. McCabe, Ph.D.
 Sean Megason, Ph.D.
 Daniel K. Meulemans, Ph.D.
 Takuya Minokawa, Ph.D.
 Dane A. Mohl, Ph.D.
 Laurent Moreaux, Ph.D.
 Fraser J. Moss, Ph.D.
 Yoh-Suke Mukouyama, Ph.D.¹
 Hans-Michael Muller, Ph.D.
 Israel Muro, Ph.D.
 Sam Musallan, Ph.D.

Zoltan Nadasdy, Ph.D.
 Raad Nashmi, Ph.D.

Peter Oelschlaeger, Ph.D.
 Colm O'Tuathaigh, Ph.D.
 Jeong S. Oh, Ph.D.
 Richard A. Olson, Ph.D.
 Kenji Orimoto, M.D., Ph.D.¹
 Ochan Otim, Ph.D.

Rigo Pantoja, Ph.D.
 Cyrus Papan, Ph.D.
 Rachel S. Papan, Ph.D.
 Sungmin Park-Lee, Ph.D.
 Gentry M. Patrick, Ph.D.
 Robia G. Pautler, Ph.D.
 Bijan Pesaran, Ph.D.
 Mathew D. Petroski, Ph.D.
 Joseph J. Plecs, Ph.D.¹
 Joel Pomerantz, Ph.D.
 Konstantin Pyatkov, Ph.D.

Xian-Feng Qin, Ph.D.
 Rodrigo Q. Quiroga, Ph.D.

Anuradha B. Ratnaparkhi, Ph.D.
 Daniel Rizzuto, Ph.D.
 Nivalda Rodriguez-Pinguet, Ph.D.
 Orma Rosenthal, Ph.D.
 Benjamin D. Rubin, Ph.D.

Melissa Saenz, Ph.D.
 Alok J. Saldanha, Ph.D.
 Tatjana Sauka-Spengler, Ph.D.
 Gary C. Schindelman, Ph.D.
 Deirdre D. Scripture-Adams, Ph.D.
 Sharad J. Shanbhag, Ph.D.
 David R. Sherwood, Ph.D.
 Nina T. Sherwood, Ph.D.
 Bhavin Sheth, Ph.D.
 Julia Shifman, Ph.D.
 Kum-Joo Shin, Ph.D.
 Patrick Sieber, Ph.D.
 Timur Shutenko, Ph.D.
 William Bryan Smith, Ph.D.
 Irina Sokolova, Ph.D.
 Elizabeth R. Sprague, Ph.D.
 Jagan Srinivasan, Ph.D.¹
 Gurol M. Suel, Ph.D.
 Greg Seong-Bae Suh, Ph.D.
 Michael A. Sutton, Ph.D.

Konstantin D. Taganov, Ph.D.
 Chin-Yin Tai, Ph.D.
 Andrew R. Tapper, Ph.D.
 Elizabeth B. Torres, Ph.D.
 W. Daniel Tracey Jr., Ph.D.
 Thomas P. Treynor, Ph.D.
 Qiang Tu, Ph.D.
 Glenn C. Turner, Ph.D.

Cheryl Van Buskirk, Ph.D.

David W. Walker, Ph.D.
 Horng-Dar Wang, Ph.D.
 Lorraine R. Washburn, Ph.D.
 Dai Watanabe, M.D., Ph.D.
 Angela Weiss, Ph.D.
 Allyson Whittaker, Ph.D.
 Patrick Wilken, Ph.D.
 Brian A. Williams, Ph.D.
 Rachel I. Wilson, Ph.D.
 Elizabeth R. Wright, Ph.D.
 Shau-Ming Wu, Ph.D.

Zan-Xian Xia, Ph.D.
 Peizhang Xu, Ph.D.
 Xian-Zhong Xu, Ph.D.
 Zhenming Xu, Ph.D.

Cain Hoi Yam, Ph.D.
 Zhiru Yang, Ph.D.¹
 Hae Yong Yoo, Ph.D.¹
 Soon Ji Yoo, Ph.D.
 Hao Yu, Ph.D.
 Mary Yui, Ph.D.

Jin Zhang, Ph.D.
 Yuanxiang Zhao, Ph.D.
 Weiwei Zhong, Ph.D.
 Jianmin Zhou, Ph.D.
 Lisa Taneyhill-Ziemer, Ph.D.
 Mark J. Zylka, Ph.D.

¹Joint appointment with Howard Hughes Medical Institute

Visitors

Alejandro Bäcker, Ph.D.
 Libera Berghella, B.S.
 Fumiko Maeda, Ph.D., M.D.
 Rex A. Moats, Ph.D.
 Nicola Raule, B.S.
 Armando Miguel Remondes, B.S.
 Jason C. Tsai, M.D.

Biology Graduate Students

Meghan Adams
Oscar Alvizo²
Xavier Ambroggio
Ramzi Azzam

Magdalena Bak
Catherine Baker
Susannah Barbee
Martin Basch
Helen Holly Beale
John Bender
Jordan Benjamin
Kyle Bernheim
Rajan Bhattacharyya¹
Sujata Bhattacharyya
Baris Bingol
Kiowa Bower
Bede Broome
C. Titus Brown
Seth Budick
Charles Bugg²
Eliot Bush

Michael Campos¹
Ronald M. Carter
Gil Carvalho
Stijn Cassenaer
Eun Jung Choi
Gloria Choi
Gestur B. Christianson¹
Gregory Cope²
Jeffrey Copeland
Robert S. Cox III
Laura Croal

Chiraj Dalal²
Sagar Damle
Tristan De Buysscher¹
Scott Detmer
Mary Devlin²
Christopher Dionne

Jessica Edwards
Jonathan Erickson³

Alexander Farley
Shabnam S. Farivar
Jolene Fernandes
William Ford¹

Nazli Ghaboosi
Anthony Giannetti²
Hilary Glidden¹
Carl S. Gold¹

Daniel Gold
Ying Gong²
Sean Gordon²
Noah Gourlie²
Johannes Graumann
Harry Green
Erik Griffin
Ming Gu¹

Christopher Hart
Houman Hemmati
Gregory Henderson
Anne Hergarden
Gilberto Hernandez
Christian Hochstim
Alex Holub¹
Geoffrey Hom²
Jean Huang
Po-ssu Huang²
Jun Ryul Huh

Princess Imouhueda³
Hiroshi Ito
Asha Iyer

Vivek Jayaraman¹

Jennifer Keefe²
Jongmin Kim
Jane Khudyakov²
Rajan Kulkarni²
Steven Kuntz²

Christopher Lacenere
Kirsten Lassila²
Brian Lee
Pei Yun Lee
Isabella Lesur²
Thomas H.C. Leung
Ben Lin
Lilyn Liu
Carolina Livi
Carole Lu
Tinh N. Luong

Angie Mah²
Davin Malasarn
Stefan Materna²
Ofer Mazor¹
Daniella Meeker¹
Andrew Medina-Marino

Daniel Meulemans
Anna K. Mitros¹
Sarina Mohanty²
Jennifer Montgomery
Farshad Moradi¹
Eric Mosser
Julien Muffat
Grant H. Mulliken¹
Gavin Murphy²

Patricia Neil¹
Matthew Nelson¹
Dirk Neumann¹
Dylan Nieman¹

Elizabeth Ottesen

Maria Papadopoulou
Yao-Chun Peng
Javier Perez-Orive¹
Robert J. Peters¹
Alexa Price-Whelan

Juan Ramirez-Lugo
Lavanya Reddy¹
Leila Reddy¹
Clara Reis²
Michael Reiser¹
Julian Revie²
Roger Revilla²
Adrian Rice²
Ted Ririe
Alice Robie
Tobias Rosen
Ueli Rutishauser¹

Kathleen Sakamoto, M.D.
Anna Salazar
Jennifer Sanders
Shu Ping Seah
Premal Shah²
Kai Shen¹
Huazhang Shen
Celia Shiau
Dong Hun Shin
Claudiu Simion
Jasper Simon
Eric Slimko¹

Stephen E.P. Smith
W. Bryan Smith
Amber Southwell

Tracy Teal¹
Devin Tesar
Naotsugu Tsuchiya¹

Luis Vazquez
Dirk Walther¹
Luigi Warren
Karli Watson
Karen Wawrousek²
Jeffrey Wiezorek, M.D.
Casimir Wierzynski¹
Ashley Wright
Daw-An Wu

Xinan Xiu²

Lili Yang
Hui Yu

Mark Zarnegar
Brian Zid
Eric Zollars²

¹Computational and Neural Systems

²Division of Biochemistry

³Bioengineering

Biology Research and Laboratory Staff – 2004

Stephanie L. Adams
 Jennifer M. Alex, A.A.
 Mary Alvarez
 Armando Amaya
 Jennifer Ambroggio, B.A., M.S.
 Gabriel Amore, Ph.D.
 Kristen Andersen
 Michael Andersen
 Caprece Anderson
 Lilia Añonuevo
 Igor Antoshechkin, Ph.D.
 David Arce
 Alexandra Arias, B.S.
 Elena Armand, M.D.
 Cirila Arteaga
 Jenny Arvizu
 Mary Ary

Esther Bae, B.A.
 Carlzen Balagot
 Darcy Ballister
 Meyer Barembaum, Ph.D.
 Guillermina Barragan
 Carol Bastiani, Ph.D.
 Ruben Bayon, B.S.
 Christie Beel, B.A.
 Gary Belford
 Kevin Berney, A.B.
 Ted Biondi, B.S.
 John Bleech, B.A.
 Benoit Boulat, Ph.D.
 Natasha Bouey
 Ana Lydia Bowman
 Boris Breznán, Ph.D.
 Lakshimi Bugga, M.S.
 Gentian Buzi, M.S.

Ana Campos
 Yun Cao
 Cynthia Carlson, B.A.
 John B. Carpenter, B.S.
 Pilar Carrillo, B.S.
 Gavin Chan
 Juancarlos Chan, B.S.
 Jung Sook Chang, B.S.
 Jules Chen
 Sherwin Chen, B.S.
 Wen Chen, Ph.D.
 Evelyn Cheung
 Dasgupta Chiranjib
 Tsz-Yeung Chiu, B.S.
 Sangdun Choi
 Suk Hen Chow
 Sonia Collazo, M.S.
 Ana Colon, A.A.
 Robin Condie
 Stephanie Cornelison, B.S.

Christopher Cronin, B.S., M.E.

Susan Dao, B.A.
 Robin Deis
 John de la Cueva
 Silva Delker
 John Demodena, B.S.
 Andrey Demyanenko, Ph.D.
 Tatyana Demyanenko, Ph.D.
 Elisa Denny, B.A.
 Purnima Deshpande, M.S.
 Kavitha Dhandapani
 Prabha Dias, Ph.D.
 Rhonda Digusto, B.A.
 Hongyu Ding
 Ping Dong, M.D.
 Andrew Dowsett, Ph.D.
 Leslie Dunipace, M.A.
 Janet Dyste, A.A.

Jean Edens

Maria Farkas, B.A.
 Steven M. Flaherty, B.S.
 Mary D. Flowers, M.A.
 Michael Fontenetto
 Paige Fraser

Jessica Gamboa
 Arnavz Garda, B.Sc.
 Maggie Garrison, B.S.
 Jahlionais Gaston
 Cheryl Gause
 Shahla Gharib, Ph.D.
 Leach Gilera-Rorrer, B.S.
 Michael P. Goard
 Sidra G. Golwala
 Martha Gomez
 Abel Gonzalez
 Constanza Gonzalez
 Kenneth Goodrich
 Blanca Granados
 Hernan Granados
 Rachel Gray
 Lingjie Gu
 Joaquin Gutierrez
 Richele Gwartz, B.S.

Yvonne Hadju-Cronin
 Julie Hahn, B.S.
 Atiya Hakeem, Ph.D.
 Kathleen Hamilton
 Parvin Hartsteen
 Argelia Helguero, B.S.
 Martha L. Henderson, M.S.
 Carlos M. Hernandez
 Bernard Heymann, Ph.D.

Christine Hickler
 Kristina Hilands
 Timothy Hiltner, M.S.
 Craig Hokanson
 David Horvath
 Qu Huang
 Kathryn Huey-Tubman, M.S.

Aleksandra Illicheva
 Nahoko Iwata

Cynthia Jones
 Matthew Jones

Joon Kang
 Valerie Karplus
 Joyce Kato, B.S.
 Aura Keeter
 Carolyn Kelsch
 Bruce Kennedy, M.S.
 Eimear Kenny, B.S., M.Sc.
 Jiseo Ki, M.S.
 Jong Woo Kim
 Brandon King
 Ranjana Kishore, Ph.D.
 Christine Kivork
 Jan Ko, B.S.
 Patrick F. Koen
 Shi-Ying Kou, M.D.
 Stephanie Kovalchik
 David Kremers
 Steven Kwoh, B.S.

Russell Lansford, Ph.D.
 Santiago Laparra
 Nicholas Lawrence, M.A.
 Patrick Leahy, B.S., (KML)
 Kwan F. Lee
 Raymond Lee, Ph.D.
 Sun Young Lee, M.S.
 Vivian M. Lee
 Daniela Leopoldt
 Catherine Lin, M.S.
 Ian J. Lipsky
 Christine Lisnock, B.S.
 Jamie Liu, B.S.
 Linda Llamas
 Li-Ching Lo, M.S.
 Thomas Lo, Jr., B.S.
 Harrison Luu
 Ana Marie Lust, B.A.
 Lloyd Lytle, B.S.

Josephine Macenka, B.S.
 N. Vanessa Maldonado, B.S.
 Valeria Mancino, M.S.
 Gina Mancuso, B.A.

Blanca Mariona
 Aurora Marquina
 Steven R. Marsh, B.A.
 Lea Martel
 Melanie Martin
 Monica Martinez, B.S.
 Jorge Mata
 Jose Mata
 David R. Mathog, Ph.D.
 Sarah Lynn May
 Doreen McDowell, M.S.
 Sheri McKinney, B.S.
 Gladys Medina
 Rodolfo Mendez
 Kaushiki Menon, Ph.D.
 Edriss Merchant, B.S.
 Anca Mihalas
 Dylan Morris
 Jennifer Mortenson, B.S.
 Gabriella Mosconi
 Gustavo Muñoz, B.A.
 Jesse Muñoz, A.A.
 Mary Ann Muñoz
 Marta Murphy, B.A.
 Mala Murthy

Cecilia Nakamura
 Inderjit Nangiana, M.S.
 Paliakavanai Narasimhan, Ph.D.
 Violana Nesterova, M.S.
 Lisa Newhouse
 Albert T.-Q. Nguyen, B.S.

Robert Oania
 Shannon O'Dell
 Carolyn Ohno, Ph.D.
 Nick Oldark
 Corey Olsen, B.S.
 Elizabeth Olson, B.A., A.S.
 Blanca Ortega

Dolores Page, B.A.
 Rashmi Pant, Ph.D.
 John Papsys, B.S.
 Ji Young Park
 Kelsie Weaver Pejsa, B.S.
 Maria Perez-Perrara, M.S.
 Myra Perez
 Barbara Perry
 Andrei Petcherski, Ph.D.
 Rosetta Pillow, A.A.
 Timur Pogodin, M.D.

Parlene Puig

John Racs, B.S.
 Carrie Ann Randle
 Anitha Rao, M.S.
 Vijaya Rao, M.S.
 Alana Rathbun
 Erika Reyes
 Jane Rigg, B.A.
 Maral Robinson, B.S.
 Carole Robles
 Monica Rodriguez-Torres
 Maria del Mar Roldan-Ortiz, B.S.
 Floreen Rooks, B.A.
 Maria Rosales
 Alan Rosenstein, M.S.
 Alison Ross, B.A.
 Donaldo Ruano-Campos
 Seth Ruffins, Ph.D.
 Felicia Rusnak, B.S.

Lorena Sandoval
 Eric Santiestevan, A.B.
 Leah T. Santat
 Mirna Santos
 Nephi Santos, A.S.
 Viveca Sapin, B.S.
 Leslie T. Schenker, B.S.
 Erich Schwarz, Ph.D.
 Viktor Shcherbatyuk, Ph.D.
 Jun Sheng, Ph.D.
 Bhavin Sheth
 Limin Shi, M.S., Ph.D.
 Daphne Shimoda
 Mitzi Shpak, B.S.
 Peter Siegel, Ph.D.
 Juan Silva, B.S.
 John Silverlake, B.S.
 Jeffrey Smith
 Geoffrey Smith, B.S.
 Kayla Smith, B.S.
 Diane Solis, B.S.
 Lauren Somma, B.A., R.N., C.D.E.
 Ingrid Soto
 Amber Steele
 Randall Story, Ph.D. (KML)
 Michael Suh
 Kannika Supanyo
 Jayne Sutton

Johanna Tan-Cabugao
 Nicole Tetreault, B.S.

Deanna Thomas, B.A.
 Leonard M. Thomas, Ph.D.
 Noreen Tiangco, B.S.
 William Tivol, Ph.D.
 Diane Trout, B.S.
 Julian M. Tyszka, Ph.D.

Kimberly M. Van Auken
 Laurent Van Trigt, M.S.
 Vanessa Vargas
 Candace Vavra, A.A.
 Luis Vega
 Roberto Vega
 Rati Verma, Ph.D.

Estelle Wall
 Chi Wang, M.A.
 Jue Jade Wang, M.S.
 Qinghua Wang, B.A.
 Christopher Waters
 Erin Watkin
 Holli Weld, B.S.
 Floriano Welison
 Amanda Whipple
 Gwen Williams, A.S., A.G.
 Jon B. Williams
 Johnny Williams, (KML)
 Darryl Willick
 Charles Winters
 Jane Wyllie, M.S.

Vicky Yamamoto
 Thasneem Yao, M.B.A.
 Carolina Young
 Jonathan Young
 Rosalind Young, M.S.
 Chang-Jun Yu, Ph.D.
 Hong Yu, M.S.
 Qiu Yuan
 Chiou-Hwa Yuh, Ph.D.
 Gina Yun, B.A.
 Miki Yun, B.A.

Joelle Zavzavadjian, M.S.
 Rosario Zedan
 Xiaowei Zhang, M.S.
 Jie Zhou
 Shu Zhen Zhou
 Xiaocui Zhu, Ph.D.
 Ute Zimmerman, M.S.

Administrative Staff

Mike Miranda, Administrator
 Laura Rodriguez, Assistant to Chairman

Accounting

Carole Worra

Computer Facility

Vincent Ma
 Scott Norton
 Tom Tubman

Graduate Student Program

Elizabeth M. Ayala

Grants

Carol Irwin

Instrument Repair Shop

Anthony Solyom

Laboratory Animal Care Administration

Janet F. Baer, Director
 Claire Lindsell, Assistant Veterinarian
 Cynthia Tognazzini, Facilities Operations Manager
 Peggy Blue
 Michael Burt

Machine Shop

Leroy Lamb

Personnel

Mary Marsh

Research Fellow Program

Gwenda Murdock

Stockroom and Supplies

William F. Lease, Supervisor
 Giao K. Do
 Jesse E. Flores
 Jose Gonzales
 Pat Perrone

Word Processing Facility

Stephanie A. Canada, Supervisor
 Yolanda Duron

Beckman Institute

Roxanne Carlisle, Grants
 Laurinda Truong, Personnel
 Manny de la Torre, Receiving

The Mabel and Arnold Beckman Laboratories of Behavioral Biology

Janie Morales-Castro, Grants
 Sandra Koceski, Personnel/Accounting
 Patricia Mindorff, Special Projects

Michael P. Walsh, Supervisor, Electronics Shop
 Tim Heitzman, Electronics Shop

Braun Laboratories in Memory of Carl F and Winifred H Braun

Mabel Chik, Grants

Broad Center for the Biological Sciences

Samantha J. Westcott, Grants
 Janie Malone, Personnel
 Andreas Feuerabendt, Receiving

William G. Kerckhoff Marine Laboratory

Randall West

Molecular, Cellular and Integrative Neuroscience

John M. Allman, Ph.D.
Richard A. Andersen, Ph.D.
David J. Anderson, Ph.D.
Seymour Benzer, Ph.D., D.Sc.h.c.
Mary B. Kennedy, Ph.D.
Christof Koch, Ph.D.
Masakazu Konishi, Ph.D.
Gilles Laurent, Ph.D., D.V.M.
Henry A. Lester, Ph.D.
Paul H. Patterson, Ph.D.
Erin M. Schuman, Ph.D.
Shinsuko Shimojo, Ph.D.
Thanassios G. Siapas, Ph.D.
Kai G. Zinn, Ph.D.

Hixon Professor of Neurobiology: John M. Allman
 Graduate Students: Eliot C. Bush, Karli Watson
 Research and Laboratory Staff: Atiya Hakeem,
 Stephanie Kovalchik, Nicole Tetreault

Support: The work described in the following research reports has been supported by:

W.M. Keck Foundation
 Moore Foundation
 Packard Foundation
 Swartz Foundation

Summary: We are focusing on the evolution and functions of the frontal lobe and particularly on a distinctive class of neurons located in fronto-insular (FI) and anterior cingulate cortex (ACC), the Von Economo spindle cells, which are found in African apes and humans, and probably comprise a phylogenetic specialization with this clade. We are also investigating through functional magnetic resonance imaging, the neural activity associated with humor, which involves the areas containing these specialized neurons. Humor involves the quick intuitive judgment that a certain situation is discordant with expectation. We are also investigating financial decision-making behavior under uncertain conditions. Our study indicates that such decisions are heavily influenced by prior outcomes in risky choices. Since both FI and ACC are active during risky decisions and financial loss and may initiate changes in choices, we suspect that this influence on behavior may involve circuitry within these areas. Overall, we think that the Von Economo spindle neurons may be part of the neural substrate for quick, intuitive decisions in complex situations.

1. A functional magnetic resonance imaging study of humor

Karli Watson, Ben Matthews*, John Allman

To complement these anatomical studies, we are also using event-related fMRI to probe the functionality of the spindle cell regions. We scanned normal subjects in a 3 T Siemens Trio system while they observed a series of line drawings and rated each for funniness. This allowed us to compare brain activation states associated with humor, while controlling for the visual and interpretive processing associated with viewing line drawings. As reported previously, we found that funny versus unfunny cartoons activate regions of the basal ganglia and brainstem.¹ These regions are associated with the ascending dopaminergic pathway and probably underlie the hedonic aspects of humor. In addition to past studies, however, we also found that humor activates a distributed frontal network that includes the frontal pole and the two spindle cell-containing regions, anterior cingulate cortex and fronto-insular (FI) cortex. We suggest that these frontal regions underlie the detection and subsequent reconciliation of incongruity that is required to evoke the subjective sensation of humor.

In addition to employing the standard method of analysis using general linear models (SPM2), we are using

independent component analysis (ICA) to look at variations in the BOLD signal. ICA has the advantage of being data driven, as opposed to hypothesis driven, which is conducive to the discovery of unexpected results. To date, separation of our data into independent components have revealed a number of spatially distinct signals associated with the humor paradigm. Striate and extra-striate activation are separated into different components, as are motor, FI, frontal pole, and temporal lobe activation. Differences in activation profiles for the various components may allow us to observe the interactions among these regions.

*Undergraduate, Caltech

Reference

Mobbs, D., Greicius, M.D., Abdel-Azim, E., Menon, V. and Reiss, A.L. (2003) *Neuron* 40(5):1041-1048.

2. History influences financial choice
 Stephanie Kovalchik, John Allman

We have found a very interesting phenomenon in the gambling task that depends on the past history of gambles that influences the ability to adjust to changing risk. Subjects choose between two decks under two different conditions, Version A and Version B. In Version A, \$1 cards are interspersed with a some very negative cards, so that the subject will loose money by selecting from that deck, while the other deck contains \$0.50 cards interspersed with smaller penalties, so that they subject will gain money be selecting from \$0.50 deck. In Version B, the \$1 cards have smaller penalties so that the subject will gain more money selecting cards from it versus the \$0.50 deck. After 60 card selections, the deck reward structure is reversed for both versions, but the subject is not told this, and the subject makes another 60 selections. We found that in Version B, young subjects have a much harder time adjusting to the change in reward than in Version A. Thus, it was difficult for young subjects to adjust to the fact that the predominately higher value cards are associated with greater loss, when this was not the initial condition for the series. The initial caution elicited by Version A in which the subjects learned to forego the \$1 cards seemed to help them to adjust to the subsequent change in reward structure. Elderly subjects do not show this overconfident effect for Version A exhibited by younger subjects. These effect of prior risk experience may serve as a useful means to probe the functioning of anterior cingulate and orbitofrontal cortical mechanisms for mediating financial choice.

3. The scaling of frontal cortex in primates and carnivores

E.C. Bush, J.M. Allman

Size has a profound effect on the structure of the brain. Many brain structures scale allometrically, that is, their relative size changes systematically as a function of brain size. Here we use independent contrasts analysis to examine the scaling of frontal cortex in 43 species of mammals including 25 primates and 15 carnivores. We

find evidence for significant differences in scaling between primates and carnivores. Primate frontal cortex hyperscales relative to the rest of neocortex and the rest of the brain. The slope of frontal cortex contrasts is 1.18 (95% confidence interval, 1.06-1.30) for primates, which is significantly greater than isometric. It is also significantly greater than the carnivore

4. The Von Economo spindle neurons are morphologically distinct from pyramidal neurons

Karli Watson, John Allman

We developed a morphometric probe that allows us to quantify characteristics that differentiate the Von Economo spindle cells from other neurons. Using binary images of nissl-stained human tissue sections, we used Image J to determine the first and second moments of various soma types. Graphing the feret length (longest edge-to-edge measurement across the soma), the y-skew, and major-to-minor axis ratio of each cell reveals a clear separation between the pyramidal and spindle cell populations. Future application of this probe will allow us to unambiguously categorize spindle cells, and may be useful for separating of other classes of neurons, as well.

5. The role of the frontoinsular cortex in social cognition

Corinna Zygourakis¹, Ralph Adolphs², John Allman

The spindle cells are large bipolar neurons unique to hominoid primates that have recently been mapped to the frontoinsular cortex (FI) brain region. Several neuro-imaging studies collectively suggest that the spindle cell area in FI and adjacent cortex is responsive to "social intention" in the form of angry faces, feelings of guilt, violations of social norms, empathy, and cooperation. We therefore hypothesize that FI lesions (that destroy the FI spindle cells) may hinder subjects' ability to detect expressions of social intention, particularly in the form of shame, guilt, embarrassment, and empathy. To test our hypothesis, we develop a set of film clips that depict the social emotions of shame, guilt, embarrassment, and empathy, as well as the primary emotions (happiness, sadness, fear, anger, surprise, disgust). Normal and FI lesion subjects view the film clips and answer questions pertaining to the emotional content of the stimuli. Skin-conductance and heart rate monitoring is also performed while subjects view the clips. Statistical analysis of data from FI lesion subjects and normal subjects enables us to map the range of emotional responses in the FI brain region. Results indicate significant deficiencies in the lesion patients' recognition of the social emotions, but not the primary emotions, as compared to the normal subjects. Thus, it appears that the FI is part of the neural circuitry that interprets social intention.

¹Undergraduate, Caltech

²HSS Professor, Caltech

Publications

- Bush, E.C. and Allman, J.M. (2003) The scaling of white matter to gray matter in cerebellum and neocortex. *Brain Behav. Evol.* 61:1-5.
- Bush, E.C. and Allman, J.M. (2004) The scaling of frontal cortex in primates and carnivores. *Proc. Natl. Acad. Sci. USA* 101:3962-3966.
- Bush, E.C., Simons, E.L., Dubowitz, D.J. and Allman, J.M. (2004) Endocranial volume and optic foramen size in *Parapithecus grangeri*. In: *Anthropoid Origins*, Ross C. (ed.), Kluwer/Plenum, New York pp. 603-614.
- Kovalchik, S., Camerer, C., Grether, D., Plott, C. and Allman, J.M. (2004) Aging and decision-making: A comparison between neurologically healthy elderly and young individuals. *J. Econ. Behav. Organiz.* In press.
- Sherwood, C.C., Lee, P.W., Rivara, C.B., Holloway, R.L., Gilissen, E.P., Simmons, R.M., Hakeem, A., Allman, J.M., Erwin, J.M. and Hof, P.R. (2003) Evolution of specialized pyramidal neurons in primate visual and motor cortex. *Brain Behav. Evol.* 61:28-44.
- Tetreault, N., Hakeem, A. and Allman, J.M. (2004) Retinal ganglion cell size and distribution in prosimian primates. In: *Anthropoid Origins*, C. Ross (ed), Kluwer/Plenum, New York, pp. 449-461.

James G. Boswell Professor of Neuroscience:
 Richard A. Andersen
 Visiting Associates: William L. Caton, Igor Fineman,
 Mel Goodale, Partha Mitra
 Member of the Professional Staff: Boris Breznen
 Senior Research Fellows: Hans Scherberger
 Research Fellows: Marina Brozovic, Chris Buneo, Jorge
 Cham¹, Jason Connolly, Brian Corneil, He Cui, Alexander
 Gail, Bradley Greger, Igor Kagan, Sam Musallam, Zoltan
 Nadasdy, Zoran Nenadic¹, Bijan Pesaran, Rodrigo Quian
 Quiroga, Dan Rizzuto, Elizabeth Torres, Shau-Ming Wu
 Graduate Students: Kyle Bernheim, Rajan
 Bhattacharyya, Eddie Branchaud¹, Michael Campos, Hilary
 Glidden, Brian Lee, Daniella Meeker, Grant Mulliken,
 Matthew Nelson
 Research and Laboratory Staff: Kristen Andersen,
 Frances De Guzman, Aleksandra Ilcheva, Lea Martel,
 Kelsie Pejsa, Viktor Shcherbatyuk, Tessa Yao
¹Mechanical Engineering, Caltech

Support: The work described in the following research reports has been supported by:

Christopher Reeves Foundation
 Defense Advance Research Project Agency (DARPA)
 Department of the Navy, Office of Naval Research
 (ONR)
 Howard Hughes Medical Institute (HHMI)
 Human Frontiers Scientific Program
 James G. Boswell Professor of Neuroscience
 McKnight Endowment Fund for Neuroscience
 National Institutes of Health (USPHS)
 National Science Foundation
 Pasadena Neurological Fellowship
 Sloan Foundation
 Swartz Foundation

Summary: Neural mechanisms for visual-motor integration, spatial perception and motion perception. While the concept of artificial intelligence has received a great deal of attention in the popular press, the actual determination of the neural basis of intelligence and behavior has proven to be a very difficult problem for neuroscientists. Our behaviors are dictated by our intentions, but we have only recently begun to understand how the brain forms intentions to act. The posterior parietal cortex is situated between the sensory and the movement regions of the cerebral cortex and serves as a bridge from sensation to action. We have found that an anatomical map of intentions exists within this area, with one part devoted to planning eye movements and another part to planning arm movements. The action plans in the arm movement area exist in a cognitive form, specifying the goal of the intended movement rather than particular signals to various muscle groups.

One project in the lab is to develop a cognitive-based neural prosthesis for paralyzed patients. This prosthetic system is designed to record the electrical activity of nerve cells in the posterior parietal cortex of paralyzed patients, interpret the patients' intentions from these neural signals using computer algorithms, and convert the "decoded" intentions into electrical control

signals to operate external devices such as a robot arm, autonomous vehicle or a computer.

Recent attempts to develop neural prosthetics by other labs has focused on decoding intended hand trajectories from motor cortical neurons. We have concentrated on higher-level signals related to the goals of movements. Using healthy monkeys with implanted arrays of electrodes we recorded neural activity related to the intended goals of the animals and used this signal to position cursors on a computer screen without the animals emitting any behaviors. Their performance in this task improved over a period of weeks. Expected value signals related to fluid preference, or the expected magnitude or probability of reward were also decoded simultaneously with the intended goal. For neural prosthetic applications, the goal signals can be used to operate computers, robots and vehicles, while the expected value signals can be used to continuously monitor a paralyzed patient's preferences and motivation.

Our laboratory also examines the coordinate frames of spatial maps in cortical areas of the parietal cortex coding movement intentions. Recently, we have discovered that plans to reach are coded in the coordinates of the eye. This is particularly interesting finding because it means the reach plan at this stage is still rather primitive, coding the plan in a visual coordinate frame rather than the fine details of torques and forces for making the movement. We have also discovered that when the animal plans a limb movement to a sound, this movement is still coded in the coordinates of the eye. This finding indicates that vision predominates in terms of spatial programming of movements in primates.

Another major effort of our lab is to examine the neural basis of motion perception. One series of experiments is determining how optic flow signals and efference copy signals regarding eye movements are combined in order to perceive the direction of heading during self-motion. These experiments are helping us understand how we navigate as we move through the world. A second line of investigation asks how motion information is used to construct the three-dimensional shape of objects. We asked monkeys to tell us which way they perceived an ambiguous object rotating. We found an area of the brain where the neural activity changed according to what the monkey perceived, even though he was always seeing the same stimulus. In other experiments we have been examining how we rotate mental images of objects in our minds, so-called mental rotation. In the posterior parietal cortex we find that these rotations are made in a retinal coordinate frame, and not an object based coordinate frame, and the mental image of the object rotates through this retinotopic map.

We have successfully performed functional magnetic resonance imaging (fMRI) experiments in awake, behaving monkeys. This development is important since this type of experiment is done routinely in humans and monitors the changes in blood flow during different cognitive and motor tasks. However, a direct correlation of brain activity with blood flow cannot be achieved in humans, but can in monkeys. Thus, the correlation of cellular recording and functional MRI activation in monkeys will provide us with a better understanding of the

many experiments currently being performed in humans. A 4.7 Tesla vertical magnet for monkey imaging has recently been installed in the new imaging center in the Broad building. We will use this magnet, combined with neural recordings, to examine the correlation between neural activity and fMRI signals.

6. Macaque supplementary eye fields neurons exhibit task-specific spatial tuning
B. Breznen, M. Campos, R.A. Andersen

We recorded from 86 neurons in the supplementary eye fields (SEF) of one macaque monkey during two tasks. We first mapped neurons' two-dimensional receptive field (RF) in a memory saccade task. Then we used the same grid of targets to probe the RF in an object-based saccade task. In this task, we first cued left or right side of an isosceles triangle and then re-positioned it so that the previously cued side of the triangle was spatially aligned with one of the targets on the grid. Only 44% of the cells tuned in the memory saccade task maintained the location of the RF in the object task. The majority of the tuned cells either lost the tuning (36%) or changed the location of the RF (20%). For the cells that kept the spatial tuning we further analyzed it in different contexts i.e., we compared the tuning for the targets located on the left vs. right side of the object as well as for different object orientations. Only a small fraction of the cells kept the spatial tuning in all contexts (7%), for the rest the tuning was present only in some contexts. In addition to spatial tuning, SEF cells also carried information about the target side of the object (57% of all cells) and the orientation of the object on the screen (22%). This information was usually superimposed in the spatial RF in a form of a gain field: 72% of the tuned cells were gain field modulated. We also found a small number of cells (16% of all cells) that encoded exclusively the object-centered location of the target. Our results show that SEF neurons encode spatial information in a task-specific way i.e., the same cell exhibits different spatial tuning depending on the task. These results are in contrast with our results from the lateral intraparietal area (LIP), where 84% of the cells maintain their spatial RF in both tasks. This may reflect the functional difference of the two areas: whereas area LIP is involved in spatial transformations underlying saccades, area SEF encodes abstract task-specific associations.

7. Re-learning spatial representations via Bayesian estimation
M. Brozovic, R.A. Andersen

We are studying how neurons in the posterior parietal cortex (PPC) adjust their tuning curves as they learn a new spatial mapping within their reference frame. In general, parietal neurons have a preferred direction when planning for eye or reach movements. For example, a neuron in the parietal reach region (PRR) might have the highest firing rate when planning to execute a 45-degree reach (up and right) towards a visual target. We are interested in how the tuning curve changes when an offset is introduced into the visual feedback for the hand-target position.

A two-layer network with non-linear transfer functions was designed to perform reach movements toward visual targets. The desired output of the network was obtained using a Bayesian regression (MacKay, 1995). The model assumed a simple Gaussian prior distribution defined by hyper-parameter alpha. In addition the likelihood function that described the Gaussian noise in the target data was characterized by a hyper-parameter beta. Network training was achieved by minimizing the error function and updating the values of the hyper-parameters.

In the second stage of network training, we introduced an offset in the target data while using the previously established probability hyper-parameters as the starting point. The effect of relearning on the representations of space in the hidden units was examined. The preliminary results show that in order to accommodate the new spatial mapping, the tuning curves shift, as well as scale with respect to their priors.

Support contributed by: NEI and the Sloan-Swartz Center at Caltech.

8. Translation speed compensation in area MSTd
B. Lee, B. Pesaran, Z. Nadasdy, R.A. Andersen

MSTd is involved in the computation of heading direction from the focus of expansion (FOE) of the visual image. We previously found that MSTd neurons adjust their focus tuning curves to compensate for shifts in the FOE produced by eye rotation (Bradley et al., 1996). In addition, we found this compensation adjusts for pursuit speed (Shenoy et al., 2001). The shift in the FOE during pursuit eye movements is also affected by the speed of translation. Slower translation causes a larger shift in the FOE than faster translation. To investigate whether MSTd neurons adjust their focus tuning curves to compensate for varying simulated translation speeds, we recorded extracellular responses from MSTd neurons in a Rhesus monkey (*Macaca mulatta*) performing pursuit eye movements across displays of varying translation speeds. We found that for a given eye pursuit speed, seven of ten focus-tuned MSTd neurons show a larger shift in their tuning curves for slow translation speeds and a smaller shift for fast translations speeds. These shifts align the focus-tuning curve with the true heading and not with the retinal position of the FOE. Since the eye is pursuing at the same rate for varying translation speeds, this indicates that retinal signals related to translation are used to adjust the amount of compensation in MSTd. In a simulated pursuit task, the gaze was fixed while the display was swept across the visual field to create the same retinal image as in the real pursuit task. We found that many MSTd neurons also shift their tuning curves towards the actual heading direction instead of aligning with the retinal image. However the shift in the focus-tuning curve in this simulated condition is not as great as in the real eye pursuit condition. These results indicate that the combination of extra-retinal signals from eye pursuit movements and retinal cues related to translation speed is used by MSTd to represent heading direction.

Support contributed by: NEI, J.G. Boswell Professorship, and the HHMI Pre-Doctoral Fellowship.

9. Efficacy and adaptation in parietal local field potentials used in a brain machine interface for cursor control

D. Meeker, R.A. Andersen

Previous studies have indicated that spikes can effectively be used as control signals for abstract effectors in a brain machine interface (BMI). In this study, local field potentials (LFPs) from a macaque were used to control a BMI in a binary cursor-positioning task. Recordings were made serially from 24 sites in parietal reach region (PRR) while the monkey performed a delayed reach to eight targets. The two targets with the largest mahalanobis distance between the power spectral densities (PSDs) were selected for use in the binary task, and in order to establish baseline signal levels, the reach task was repeated a minimum of 20 times in each of these two directions. Using the PSDs from the preceding reach trials to inform the prediction, a cursor was then introduced which, providing sufficient certainty (>0.85) in the maximum-likelihood estimate of the target location, would become visible at the predicted target location after the delay period. In this closed-loop brain control task, the average performance of the BMI for each site was 71.5 10.2% correct; 16% lower than the average performance of a spike-controlled BMI performing the same task, with PRR signals. However, performance of the BMI did show a trend of improvement, with 7/24 sites showing significant improvement and steady baseline performance by the last 50 cursor trials in the experiment, and one showing a significant decrease in performance. The average improvement in those sites was 6.3%. Additionally, the mahalanobis distance between targets after the introduction of the cursor increased on average by 20.15; 14/24 sites increased distance and 4/24 decreased. The remaining sites did not change. These changes may be related to a rapid adaptation and improvement in performance seen with a spike-controlled BCI used for the same task, and may reflect a global signal involved in the incentive valance of the different phases of the task.

Support contributed by: DARPA and NEI.

10. Decoding trajectories in real-time from posterior parietal cortex

G.H. Mulliken¹, S. Musallam¹, R.A. Andersen

Recently, we successfully decoded movement intentions using delay activity recorded from neural ensembles in posterior parietal cortex (PPC). Here, we show that movement trajectories can also be decoded using neural activity from PPC. Single-unit and multi-unit activity were simultaneously recorded from 96 microwire electrodes implanted in the medial intraparietal sulcus (MIP) and Area 5 of one rhesus monkey. Experimental sessions were divided into a training segment and a closed-loop brain control segment. During the training segment, the monkey fixated a central cue and used a joystick to guide a 4 mm diameter (0.45 degrees) cursor to a 2 cm target located 11 cm (12.5 degrees) from the fixation point. The monkey was rewarded whenever the cursor was within 1.5 cm of the target for at least 100 ms. After approximately 600 training trials, a linear model of absolute cursor position was constructed. The effective degrees of freedom of the model were controlled using ridge regression.

During the brain control segment, the monkey fixated a central cue while the position of the cursor was determined by the model prediction, independent of joystick position. Cursor position was updated every 100 ms until either the target was reached, a break of fixation occurred or 10 s elapsed. Performance during brain control trials was $>70\%$ for eight targets. The median time-to-target for successful trials was 875 ms. Off-line analysis of motor-error tuning suggests that PPC encodes both trajectory representation and a cognitive, goal-oriented representation of the impending movement. Decoding intent using motor-error could be important when rapidly predicting large amplitude movements.

¹Computation and Neural Systems, California Institute of Technology

Support contributed by: NEI, DARPA, and the Boswell Foundation.

11. Cognitive control signals for neural prosthetics
S. Musallam, B.D. Corneil, B. Greger, H. Scherberger, R.A. Andersen

An important question in neuroprosthetic research is what parameters can be decoded and used for prosthetic applications. We explored whether cognitive activity not directly related to visual input or motor output can be used as prosthetic control signals. We recorded signals related to movement intention during a brain control task in which signals were recorded from the parietal cortex of three monkeys, decoded with a computer algorithm, and used to position cursors on a computer screen. The intended goals and also the value of the reward the animals expected to receive at the end of each trial were decoded from the recordings. The monkeys' performance in this task improved over weeks. Intentional signals extracted from recordings that lasted for as little as 200 ms led to performance significantly above chance. Using cognitive signals, we can predict the reward preference (juice or water) of the animal and the expected magnitude and probability of reward. Similar to the parietal cortex, the goal of the planned movement could also be decoded in the brain control task using recordings from the dorsal premotor cortex. These results indicate that brain activity related to cognitive variables extracted from a small number of neurons can be a viable source of signals for the fast control of a neural prosthetic. The goal signals can be used to operate computers, robots and vehicles, while the decision variables can be used to continuously monitor a paralyzed patient's preferences and motivation.

This work was supported by: DARPA, NEI, HFSP, ONR, Christopher Reeves Foundation, and the Boswell Foundation.

12. Perceptual bias in V1 neuronal responses to ambiguous three-dimensional objects

Z. Nadasdy, B. Pesaran, M. Saenz, C. Koch*, R.A. Andersen

We studied spike responses of V1 superficial layer neurons in a perceptual decision task. A rhesus monkey was trained to hold fixation during presentations of a three-dimensional (structure-from-motion) object and to make a perceptual decision in an alternative forced choice paradigm while recording single cell activity. The disparity of

constituent dots was varied from trial-to-trial to render perceptually ambiguous or unambiguous objects. Neurons with disparity and direction tuning were selected. We estimated the probability with which the firing rate of a given V1 neuron would allow an ideal observer to predict the monkey's perceptual choice in the task. Neuronal responses to zero-disparity (ambiguous) objects were sorted according to the perceptual decision and the choice probability was determined for each neuron (Britten et al., 1996). Based on the sample of 110 neurons the distribution of firing rate discriminability indices showed a significant bias from zero ($p < 0.01$) starting at ~500 ms after the stimulus onset. The choice probability was significantly different from by chance for 20% of the cells and generally correlated with the perceptual report. The long latency of the perceptual bias suggests that a subpopulation of V1 neurons receive feedbacks from higher visual cortical areas including MT/MST.

*Professor, Division of Biology, Caltech

Support contributed by: NEI and the J.G. Boswell Professorship.

13. Network activity in posterior parietal cortex during decision-making for reaches

B. Pesaran, R.A. Andersen

To study the development of reach plans in PPC under more natural conditions, we trained two monkeys to perform a task in which they were allowed to choose where to look and where to reach. Monkeys were presented with three identical reach targets one of which resulted in a reward. The reward target was assigned randomly each trial and they made reaches to search for the reward until they found it. We chronically implanted multielectrode arrays in the medial bank of the intraparietal sulcus (mIPS; 64 electrodes) and area 5 (A5; 32 electrodes) in each of two monkeys and we recorded spiking, local field potential (LFP) activity and eye position as they performed the task. To characterize the selection and planning process before the first reach we used a predictive framework in which the monkeys' choice was predicted from neural activity and we compared these choice probabilities from spiking and LFP activity in each cortical area. Spiking and LFP activity in both mIPS and A5 showed strong spatial tuning for the reach direction but had different temporal dynamics. Spike rate in both areas and LFP activity in A5 became significantly tuned just prior to reaching while LFP activity in the mIPS was spatially tuned earlier during the delay period. Decoding spike activity, we found reach direction (1 of 8) could be most accurately decoded at reach onset (mIPS:97%; A5:84%). This declined to chance 400 ms before the reach. Decoding LFP activity, we found reach direction (1 of 8) could also be most accurately decoded at reach onset (mIPS:90%; A5:95%). Surprisingly, LFP activity in mIPS predicted the reach choice up to 300 ms earlier than LFP activity in A5 or spiking activity in either area. In summary, we find LFP activity in mIPS predicts the reach choice earlier than recorded spiking suggesting this area may receive top-down inputs before computing the visual-motor transformation or that intra-cortical activity is initiated very early in mIPS.

Support contributed by: NIH, DARPA, and the J.G. Boswell Professorship.

14. Motor imagery activates human parietal reach region

D.S. Rizzuto, H.K. Glidden, I. Fineman*, R.A. Andersen

Motor planning signals, including movement goal location, have been recorded from macaque parietal reach region (PRR). Creating a brain-machine interface using motor planning signals from the human homologue of PRR could help paralyzed and locked-in patients regain mobility and/or the ability to communicate. Before such a device can be implanted, however, the precise location of human PRR must be uniquely determined for each patient. This requires a task that elicits PRR activity in the absence of movement. Using functional imaging in normal subjects we found that, compared to visual fixation, imagined pointing elicits the same pattern of activation as real pointing. Studying seven right-handed subjects in a blocked-design point/imagined-point/fixation task we found that every subject exhibited activation along the medial bank of the left (contralateral) intraparietal sulcus, including the human homologue of PRR, as well as bilateral activation of motor cortices. In addition, four of the subjects exhibited increased bilateral dorso-lateral prefrontal (DLPFC) activity, while an additional two subjects exhibited increased DLPFC activity on either the left or right side. These findings offer the possibility of using functional imaging to guide the implantation of a cortical prosthetic into the PRR of paralyzed and/or locked-in patients.

*Department of Neurosurgery, Huntington Memorial Hospital, Pasadena, CA

Support contributed by: DARPA, NEI, ONR, and the Boswell Foundation.

15. Parietal reach activity during planned obstacle avoidance

E.B. Torres, C.A. Buneo, R.A. Andersen

The generation of goal-directed motions requires transforming perceptual goals into motor actions. A feed-forward neural network implementation of a recent computational theory (Torres, 2001) performs this transformation in an intermediate geometric stage that simulates actions by separating motion in space and time. This action-simulation process results in two learning periods: a geometric one, (optimization in space) and an 'automatic' one, (optimization in time). We are currently exploring the role of the posterior parietal cortex (PPC) in obstacle avoidance using a task that imposes a separation (in time) between geometric and automatic learning. While fixating straight ahead, two rhesus monkeys performed center-out reaches to 10-14 targets (10-15 repetitions/target) in an instructed delay-reaching task. Movements were performed in three alternating blocks: a block with no obstacles (R1), an obstacle block (OBR), and a second no obstacle block (R2). In both animals, hand trajectories (obtained from electromagnetic sensors) reflected the formation of new geometric strategies during OBR: hand paths were substantially more curved for movements near the obstacle than in either R1 or R2.

Though curved, these hand paths were highly consistent throughout OBR while the temporal aspects of the movements were initially highly variable but became progressively more regular. Consistent with the changes in planned geometric paths between blocks, most cells (~80%) showed a strong effect of the obstacle during the delay period (two-way ANOVA on target location and obstacle condition, $p < 0.05$). In addition, 50% of the neurons showed a significant change in firing rate in late OBR compared to early OBR (2-way ANOVA, $p < 0.05$), consistent with changes in the temporal aspects of the movements. These data suggest that delay period activity in the PPC reflects geometric aspects of reach trajectories and may reflect temporal aspects of pending movements as well.

Support contributed by: NEI, DARPA, J.G. Boswell, Sloan, and the Swartz Foundations.

Publications

- Andersen, R.A. and Buneo, C.A. (2003) Sensory-motor integration in the posterior parietal cortex: Specific, intermediate, and network properties. In: *The Parietal Lobes*. A. Segal, R.A. Andersen, H.O. Freund, and D.D. Spencer, (eds.), Lippincott, Williams & Wilkins, Philadelphia, PA pp. 159-178.
- Andersen, R.A., Batista, A.P., Snyder, L.H., Buneo, C.A. and Cohen, Y.E. (2004) Programming to look and reach in the posterior parietal cortex. In: *The New Cognitive Neuroscience 3rd edition*, M.S. Gazzaniga, (ed.), MIT Press, Cambridge, MA. In press.
- Andersen, R.A., Burdick, J.W., Musallam, S., Cham, J.G., (2004) Cognitive neural prosthetics. *Trends Cog. Sci.* In press.
- Andersen, R.A., Burdick, J.W., Musallam, S., Scherberger, H., Pesaran, B., Meeker, D., Corneil, B.D., Fineman, I., Nenadic, Z., Branchaud, E., Cham, J.G., Greger, B., Tai, Y.C. and Morjarradi, M.M. (2004) Recording advances for neural prosthetics. *IEEE Eng. Med. & Biol.* 26:1532-1535.
- Andersen, R.A., Musallam, S. and Pesaran, B. (2004) Selecting signals for a brain-machine interface. *Curr. Op. Neurobiol.* In press.
- Buneo, C.A., Jarvis, M.R., Batista, A.P. and Andersen, R.A. (2003) Properties of spike train spectra in two parietal reach areas. *Exp. Brain Res.* 153:134-139.
- Cham, J.G., Branchaud, E., Nenadic, Z., Andersen, R.A. and Burdick, J.W. (2004) A semi-chronic motorized microdrive and control algorithm for autonomously isolating and maintaining optimal extracellular action potentials. *J. Neurophysiol.* In press.
- Cohen, Y.E. and Andersen, R.A. (2004) Multimodal spatial representations in the primate parietal lobe. In: *Crossmodal Space and Crossmodal Attention*, J. Driver and C. Spence (eds.), Oxford University Press, Oxford, UK, pp 99-122.
- Cohen, Y.E. and Andersen, R.A. (2004) Multimodal representations of space in the posterior parietal cortex. In: *Handbook of Multisensory Integration*, G. Calvert, C. Spence, and B. Stein, (eds.), MIT Press, Cambridge, MA pp. 463-479.
- Connolly, J.D., Andersen, R.A. and Goodale, M.A. (2003) FMRI evidence for a 'parietal reach region' in the human brain. *Exp. Brain Res.* 153:140-145.
- Corneil, B.D. and Andersen, R.A. (2004) Dorsal neck muscle vibration induces upward shifts in the endpoints of memory-guided saccades in monkeys. *J. Neurophysiol.* 92:553-566.
- Mojarradi, M., Binkley, D., Blalock, B., Andersen, R., Ulshoefer, N., Johnson, T. and Del Castillo, L. (2003) A miniaturized neuroprosthesis suitable for implants into the brain. *IEEE Transactions on Neural Systems and Rehabilitation Engineering* 11:1534-4320.
- Musallam, S., Corneil, B.D., Greger, B., Scherberger, H. and Andersen, R.A. (2004) Cognitive control signals for neural prosthetics. *Science* 305:258-262.
- Nishida, S., Motoyoshi, I., Andersen, R.A. and Shimojo, S. (2003) Gaze modulation of visual aftereffects. *Vision Res.* 43:639-649.
- Scherberger H., Fineman, I., Musallam, S., Dubowitz, D.J., Bernheim, K.A., Pesaran, B., Corneil, B.D., Gillikin, B. and Andersen, R.A. (2003) Magnetic resonance image-guided implantation of chronic recording electrodes in the macaque intraparietal sulcus. *J. Neurosci. Meth.* 130:1-8.
- Scherberger, H. and Andersen, R.A. (2003) Sensorimotor transformation in the posterior parietal cortex. In: *The Visual Neurosciences*, L. Chalupa and J.S. Werner, (eds.), MIT Press, Cambridge, MA, pp. 1324-1336.
- Scherberger, H., Goodale, M.A. and Andersen, R.A. (2003) Target selection for reaching and saccades share a similar behavioral reference frame in the macaque. *J. Neurophysiol.* 89:1456-1466.
- Shenoy, K.V., Meeker, D., Cao, S., Kureshi, S.A., Pesaran B., Buneo C.A., Batista A.P., Mitra P.P., Burdick J.W. and Andersen R.A. (2003) Neural prosthetic control signals from plan activity. *NeuroReport* 14:591-597.

Roger W. Sperry Professor of Biology: David J. Anderson

Research Fellows: Benjamin Deneen, Xinzhong Dong, Wulf Eckhard Haubensak, Tim Lebestky, Walter Lerchner, Yosuke Mukoyama, Kenji Orimoto, Gregory S.B. Suh, Mark Zylka

Graduate Students: Gloria Choi, Anne Hergarden, Christian Hochstim, Donghun Shin

Research and Laboratory Staff: Jung Sook Chang, Liching Lo, Gina Mancuso, Monica Martinez, Gabriele Mosconi, Myra Perez, Laurent Van Trigt

Support: The work described in the following reports has been supported by:

- American Cancer Society
- Howard Hughes Medical Institute
- Human Frontier Science Program
- Jane Coffin Childs Memorial Fund for Medical Research
- Merck
- National Heart, Lung and Blood Institute
- National Institute of Neurological Diseases and Stroke
- National Institute of Mental Health
- National Institutes of Health
- Pritzker Neurogenesis Research Consortium

Summary: We are studying the development of neural stem cells, and interactions between developing nerves and blood vessels. We have also begun to study the neural circuitry for innate fear, in both flies and mice.

Stem cells are primitive, undifferentiated cells that have the capacity both to reproduce themselves (self-renew) and to differentiate into specialized cell types, such as neurons or muscle cells. A fundamental problem in neural development is to understand how the stem cells of the nervous system produce all the different types of cells composing the adult brain. These include different subtypes of neurons and of non-neuronal cells called glia. Our approach is to isolate neural stem and progenitor cells, characterize their developmental capacities, and identify some of the molecules and genes that control their differentiation from outside and inside the cell. Our principal accomplishments in recent years have been: (1) the direct isolation of neural stem cells from uncultured tissue and the development of an *in vivo* transplantation assay for these cells; (2) the identification and functional analysis of "master genes" that control neuronal differentiation; and (3) the identification and functional analysis of a new family of related master genes that sequentially control neurogenesis and gliogenesis. We have also pursued studies in the field of angiogenesis, stemming from our discovery that arteries and veins are molecularly distinct from the earliest stages of blood vessel formation.

Isolation and characterization of neural stem cells

A fundamental issue in neural stem cell biology is to understand how many different kinds of neurons and glia a single stem cell can produce. We have developed procedures to identify and isolate neural crest stem cells

directly from uncultured tissue, based on their selective labeling by antibodies that bind specific proteins on the cell's surface. Using these markers, we can use fluorescence-activated cell sorting to purify the stem cells away from the other, unwanted cell types. We can then examine the differentiation capacities of these stem cells by challenging them with various differentiation signals in petri dishes or in host embryos.

In petri dishes, for example, we can ask how the stem cells choose among their different fates: neuron, glia or smooth muscle. Are these decisions made on "autopilot," according to some internal genetic program, or do they depend on the cell's local external environment? We found that the cells choose their fate according to their environment, and we identified several specific proteins, or growth factors, that, when added to the culture medium, push the stem cells to select a given differentiated fate from their menu of options. Some factors promote neuronal differentiation, others promote glial differentiation, and still others promote smooth muscle differentiation.

Master genes for neuronal and glial differentiation

We have identified several master switch genes for the neuronal fate. Expression of these genes in stem cells is sufficient to drive their differentiation to neurons. Are there similar master switch genes for the glial fate? Recently, we identified the Olig genes, a new family of genes that are sufficient to drive the differentiation of stem cells to oligodendrocytes, the myelin-forming glia of the central nervous system. Independent work from the laboratory of Thomas Jessell (HHMI, Columbia University College of Physicians and Surgeons) has shown that Olig genes can promote differentiation of motor neurons at earlier stages of development. More recently, we have shown that deletion of the Olig genes in mice prevents differentiation of both motor neurons and oligodendrocytes. This loss reflects a fate-conversion event, rather than simply a failure of differentiation. Spinal cord precursors lacking Olig genes generate certain kinds of interneurons and astrocytes (another type of glial cell), rather than motor neurons and oligodendrocytes. Thus, Olig genes seem to link the choice between two alternative subtypes of neuron to the choice between two alternative subtypes of glia.

Novel receptors for pain-sensing neurons

Sensory neurons, which derive from the neural crest, innervate the skin and mediate responses to touch, pressure, heat, cold, and painful stimuli. In the course of identifying new marker genes for these neurons, we discovered a large family of novel genes, called Mrgs, that encode receptors expressed on the cell surface. The Mrgs appear to be expressed by sensory neurons and no other cell type in the body. Although the exact molecules recognized by these "orphan" receptors is not yet known, they appear to be able to bind neuropeptides, short proteins that can modulate neuronal function. An exciting possibility is that the MRGS modulate pain sensitivity, in

which case they could prove useful as targets for new analgesic drugs.

Identity specification and patterning of developing arteries and veins

Several years ago, we discovered serendipitously that arteries and veins are molecularly distinct, and that bidirectional interactions between these two types of blood vessels are essential for proper circulatory system development. We have now exploited our ability to distinguish arteries and veins molecularly to investigate when and how these differences arise during development. Using these tools, we have recently discovered that in developing skin, the branching pattern of arteries, but not veins, is aligned with that of peripheral nerves. In the absence of nerve fibers, arteries fail to differentiate properly. Moreover, mutations that change the branching pattern of the nerves change that of arteries as well. These data suggest that signals from the nerve are required for proper arterial differentiation in the skin, and that the branching pattern of peripheral nerves provides a "template" to pattern the branching of arterial blood vessels.

Neural circuits for innate fear in mice and flies

In a new initiative, we have developed a novel experimental system to study the neural circuits that control behavioral responses to innately fearful stimuli. We have identified unimodal sensory stimuli that can elicit different fear behaviors (flight or freezing) in laboratory mice, depending on the context and/or prior experience of the animals. We are using quantitative immediate early gene expression analysis to map, with single-cell resolution, the brain regions that are active in these different behaviors. Efforts to identify genes expressed in these regions, both constitutively and in an activity-dependent manner, are also underway, using oligonucleotide microarrays and laser-capture microdissection. Identification of molecular markers for brain regions associated with emotional behaviors should permit us to determine the function of these regions, by creating transgenic animals in which the activity of neurons in these regions can be reversibly silenced (using techniques being developed in Professor Henry Lester's laboratory), as well as, to map their connectivity. These studies should better define the neural substrates of subjective emotional states, and ultimately may aid in a clearer understanding of the pathophysiological basis of affective disorders in humans, such as anxiety and depression.

In parallel with these studies in mice, we have initiated conceptually similar experiments in the fruitfly, *Drosophila melanogaster*. Our goal is to identify simple and robust innate behaviors, and then perform unbiased "anatomical" and genetic screens to map the neuronal circuits and identify the genes that control these behaviors. This dual approach will provide an opportunity to integrate molecular genetic and circuit-level approaches to understanding how genes influence behavior. The

"anatomical" screen exploits the availability of "enhancer trap" lines in which the yeast transactivator protein GAL4 is expressed in specific subsets of neurons, and a conditional (temperature-sensitive) neuronal silencer gene that prevents synaptic transmission. Currently we have developed assays for an innate avoidance response triggered by a conspecific putative alarm pheromone (fly "fear"), as well as, for arousal intensity and hedonic valence, two important axes underlying emotional states in humans.

Grants from the National Institutes of Health and the Pritzker Foundation supported portions of this work.

16. Lim homeodomain proteins mark hypothalamic and amygdaloid circuits that are involved in the expressions of innate behaviors
Gloria B. Choi, David J. Anderson

We are interested in innate behaviors, and more specifically, we are trying to understand how the circuits in the brain controlling these innate behaviors form during development.

Numerous functional studies have demonstrated that different nuclei in two brain regions, the amygdala and hypothalamus, are involved in the expression of either reproductive or defensive behaviors. More interestingly, the projections from the medial amygdala to various hypothalamic nuclei are topographically organized in such a way that the circuitry critical for the expression of reproductive behaviors largely remains segregated from that controlling the behavioral output of defense.

By doing an expression screen and microarray analysis, we found a LIM homeodomain transcription factor, *Lhx6*, to be expressed in the medial amygdala posterior dorsal (MeApd), a reproductive nucleus of the medial amygdala. We have shown that *Lhx6* marks a population of neurons in MeApd that projects only to the reproductive, but not to the defensive, hypothalamic nuclei by analyzing *Lhx6*-PLAP knock-in mice and by performing retrograde labeling experiments.

The medial amygdala is a major projection field of the accessory olfactory bulb, which transmits pheromonal information from the vomeronasal organ. In this context, we have also demonstrated that *Lhx6*-expressing neurons in MeApd respond only to reproductive chemosensory signals, but not to defensive ones.

Thus, *Lhx6* expression marks neurons in MeApd that respond to reproductive chemosensory cues and that project to hypothalamic nuclei that control the behavioral output for reproduction. We are in the process of the making conditional knock-outs of *Lhx6* in order to study whether *Lhx6* expression is necessary for setting up the specific and topographically organized circuit from MeApd to the various reproductive nuclei in the hypothalamus.

Reference

Zhou, Q., Choi, G. and Anderson, D.J. (2001) *Neuron* 31(5):791-807.

17. Delineating the neuronal to glial transition in the developing spinal cord

Benjamin Deneen, David J. Anderson

Development of the nervous system (CNS) is dependent upon the appropriate spatial and temporal generation of the three main neural cell types: neurons, oligodendrocytes, and astrocytes. While the spatial dorsal-ventral combinatorial code responsible for the differing neuronal cell types generated in the ventricular zone has been deciphered, the mechanisms governing the temporal switch from neuronal to glial generation remain elusive. The goal of this study is to identify genes that control the transition from neurogenesis to gliogenesis.

As a model for this developmental transition we chose to utilize Olig-expressing cells, because the Olig genes are specifically expressed in the pMN domain of the developing spinal cord during both neurogenic and gliogenic phases of development. In this study we utilized an Olig2/GFP transgenic mouse in order to prospectively isolate Olig2-expressing cells via FACS analysis from embryonic spinal cord across this developmental interval (E9.5 through E12.5) in 24 hr increments. Using these methods of cell isolation, we have been able collect sufficient numbers of cells from each timepoint to generate cRNA probes to hybridize to Affymetrix microarrays.

We have analyzed the expression profiles of genes that demonstrate a three-fold change in expression between E9.5 and E12.5, and found that these genes cluster in eight distinct groups. Among the 36,000 genes queried, approximately 90 candidate transcription factors were identified amongst these eight distinct clusters. Based on the kinetics of gene expression one can make predictions of gene function for example, genes that increase in expression over the time-interval are likely to promote the transition to gliogenesis, while genes that decrease over the time-interval are likely to inhibit this transition. As a means of functionally analyzing these genes we have chosen to utilize electroporation into the embryonic chick neural tube because: 1) there does not exist a mouse culture system that can faithfully recapitulate the sequential generation of first neurons, then glia; and 2) chick neural development closely resembles that of the mouse and provides an *in vivo* system in which to examine the function of these genes.

18. The amygdala central nucleus in innate vs. conditioned fear

Wulf Haubensak, David Anderson

Fear is a central emotion underlying defensive behaviors across species, and in turn, represents a human emotion that can be addressed in experimentally tractable model systems. A prerequisite for any mechanistic understanding of its neuronal basis is to identify the neuronal circuits mediating fear-related behaviors.

Numerous studies have pointed to a central role of medial temporal lobe structures, particularly the amygdala, in various forms of fear. Typically, these structure-function relationships have been obtained by mapping patterns of neuronal activity accompanying fear-associated

behaviors, and functionally validating these correlations by surgical lesions. However, these methods are not suitable to investigate single neuronal circuits with cellular resolution. This is especially important when it comes to assign function to the anatomical subregions of the amygdala. The amygdala central nucleus (CeA) plays a crucial role in conditioned fear. However, its function in innate fear and the differences in the neuronal basis of innate and conditioned fear, remain to be elucidated.

Here, we explore a comprehensive strategy using gene expression patterns to identify and functionally characterize specific neuronal circuits, allowing to refine these structure-function relationships with higher precision. We use a combination of genes specific for neurons within the CeA to direct, in genetically-modified mice, the expression of genetically-encoded trans-synaptic tracers (wheat germ agglutinin and the c-terminal fragment of tetanus toxin) selectively to these cells to map their circuitry. Similarly, we express inducible genetically-encoded neuronal silencers (e.g., invertebrate chloride channels that can be activated by drug administration; Slimko et al., 2002), in the same cells to silence the circuit in a temporal defined manner in behavioral paradigms for conditioned (measuring freezing in tone/foot-shock conditioned mice), and innate fear (measuring ultrasound induced freezing in foot-shock sensitized mice; Mongeau et al., 2003). Using stimuli of the same modality in both paradigms, eventual differences can be directly traced back to a differential processing of the two forms of fear at the level of the CeA.

19. Identifying genes and neural correlates underlying an innate avoidance behavior in **Drosophila**

Anne Hergarden, David Anderson

The neural control of behavior is not well understood. In order to tackle this problem, we will begin by examining a simple and robust behavior. *Drosophila* adults avoid low concentrations of carbon dioxide. This avoidance behavior is mediated by a single type of olfactory receptor neurons which express the putative gustatory receptor GR21A. This dedication of a few neurons to the perception of a single odorant molecule leads us to the question of whether there is a simple circuit underlying the carbon dioxide avoidance behavior. I am interested in identifying additional neural substrates involved in carbon dioxide avoidance. To this end, I am reversibly silencing subregions of the fly brain by crossing brain-specific Gal4 lines to UAS-Shibire^{ts} (Kitamoto, 2001) and testing the progeny for deficits in carbon dioxide avoidance. I will use secondary assays including locomotor and general olfactory assays to ensure the specificity of the behavior and I will use a UAS-reporter line to identify the expression pattern. I am also using various transneuronal tracing techniques to identify the secondary neurons involved in carbon dioxide detection as well as, their processes. Finally, I am screening single gene mutant collections in order to identify genes which modulate this avoidance behavior.

20. Olig gene targets in CNS glial cell fate determination

Christian Hochstim, David Anderson

We are interested in how progenitors in the nervous system give rise to various types of mature neurons and glia. The two major types of glial cells in the central nervous system are oligodendrocytes and astrocytes. They are generated following neurogenesis from spatially restricted domains of the ventricular zone. We are interested in the genetic determinants controlling the decision of progenitors to adopt an oligodendrocyte or astrocyte fate. At the stage of gliogenesis, the bHLH transcription factors Olig1 and Olig2 are specifically expressed in the oligodendrocyte lineage and Olig2 is essential for oligodendrocyte generation in the spinal cord. Furthermore, lineage tracing in the Olig1,2 $-/-$ homozygous mutant spinal cord using an Olig2-GFP knockin allele reveals GFP⁺ cells generate astrocytes, a fate transformation in the absence of Olig expression. In an attempt to identify Olig target genes involved in this fate specification, we have performed a screen where GFP⁺ oligodendrocyte (+/-) and astrocyte (-/-) precursors were FACS isolated and their mRNA expression profiles were compared using Affymetrix mouse genome cDNA microarrays. We are currently confirming the differential expression of candidate genes by in situ hybridization on tissue sections of Olig1,2 +/- and Olig1,2 $-/-$ spinal cord, as well as, functionally characterizing candidate genes with interesting in situ expression. Our candidates include novel astrocyte genes (markers), as well as, transcription factors which are putative fate regulators.

21. Modeling "emotional" behavior in **Drosophila**

Tim Lebestky, David J. Anderson

Emotional behaviors in humans convey a positive or negative response to a stimulus, and this response is manifest in discrete, highly conspicuous ways, such as stereotyped facial expressions and physiological arousal. Although *Drosophila* do not present the richness of human emotions in their behavior, they may share fundamental molecular similarities that could allow us to dissect the way that neural circuits function to provide graded responses in intensity, as measured both qualitatively and quantitatively. To this end, we are developing automated, high-resolution behavioral assays that will allow a reproducible characterization of graded behavioral responses to negatively valenced stimuli, for high-throughput genetic screens. One such assay follows the startle effects on locomotion and escape behaviors in response to a series of air-puffs, delivered at regular intervals. We observe a reproducible escalation of locomotor activity and jump-response behaviors as a function of time and puff number. By initially screening through mutants and collections of flies that are conditionally silenced at specific circuits (Gal4-UAS system), we hope to delineate the molecular mechanisms and neural circuits involved in the generation and modulation of such emotive responses.

Similar to mammals, *Drosophila* utilizes biogenic amines as neurotransmitters for normal neuronal function and behavior. A serotonin transporter, dSERT, with significant functional homology to the mammalian SERT family has been cloned and physiologically characterized in-vitro (Demchyshyn et al., 1994); however, there is no genetic analysis of this, or any other aminergic transporter in-vivo. Given the importance of this molecular family and the successful advancement of in-vivo RNAi techniques in *Drosophila*, we are currently developing techniques to look at gain and loss-of-function conditions in a spatially and temporally-regulated manner in adult flies. It is our hope that by tightly controlling the gene dosage and induction level of the RNAi, we may observe quantifiable phenotypic differences in behaviors that may give insights into how molecular thresholds influence the escalation or decline of distinct internal states in adult animals.

22. Molecular approach to studying the neuronal circuits of innate fear

Walter Lerchner, Laurent van Trigt, David J. Anderson

Fear is perhaps the most conserved emotion in our evolution. The ability to associate certain situations with fear is absolutely essential to avoid dangerous situations. However, in our complex society it is possible that the same mechanisms can lead to stress and anxiety disorders. In particular a traumatic event can lead to unspecific fear that alters the behavior in subsequent situations.

Our lab has established a behavioral procedure in which mice are exposed to an aversive ultrasound in their home environment. Naive animals respond to the sound with flight responses, i.e., active defense behavior. However, mice that were previously exposed to a series of foot-shocks respond to the ultrasound with freezing (absence of movement, i.e., passive defense response) in addition to a reduced amount of flight responses. Subsequent studies have carefully mapped differential neuronal activation in the central nervous system during and following ultra-sound exposure in these two groups.

This project aims to take this effort a step further by applying molecular biology to better understand the neuronal circuits underlying this change in behavior. We identified several genes with restricted expression in areas predicted to play important roles in the circuit. We have isolated promoters of some of these genes in order to generate BAC transgenic and knock-in mice that will express axonal reporters and silencing cassettes. None of the genes identified show expression solely in the areas of interest. Thus, the cassettes are designed to allow spatial and temporal specificity using the promoters of two genes with overlapping expression.

One of the genes identified encodes a yet uncharacterized protein with homology to the urokinase plasminogen activator receptor. It is expressed in several areas implicated in emotional processes, which makes this gene particularly suited for manipulation of the circuit.

We created BAC transgenes and targeted mutations into the start of the open reading frame of the gene in order to silence subpopulations of neurons expressing it. The spatial specificity of the silencing will be provided by BAC transgenic mice using genes with overlapping expression patterns. In addition we are studying the function of its protein *in vitro*.

23. GDF7-expressing roof-plate cells mark a sensory-restricted neural crest population
Liching Lo, David J. Anderson

Little is known about the timing, location, and mechanisms of the sensory and autonomic lineage segregation during neural crest development. Although single-cell lineage tracing experiments reveal some multipotent or lineage-restricted populations, we do not know whether such variation is stochastic or pre-determined, due to lack of markers. The roof plate is required for proper development of some dorsal interneurons. GDF7 is a member of the BMP family and is expressed exclusively in the roof plate. Previously, we have used a Cre-recombinase-based-fate-mapping approach to show that Ngn2-expressing neural crest cells are biased toward a sensory fate. However, since Ngn2 is expressed by migrating neural crest cells, as well as by some pre-migratory dorsal neural tube cells, we could not determine when and where the bias occurs. In this study, we used GDF7-Cre fate mapping to further address if early specification of sensory fate can occur prior to emigration. We found that GDF7-expressing roof-plate cells are strongly biased toward a sensory, but not neuronal, fate. Since GDF7 is expressed exclusively in the neural tube, this is the first evidence that pre-migratory neural crest cells are restricted to certain neuronal subtype fates (autonomic vs. sensory). The roof plate is also a source of signaling molecules, such as Wnts and BMPs. Previously, we have shown by *in vitro* culture that high concentrations of BMP2 promotes autonomic, while low BMP2 concentrations promotes sensory, differentiation. Using the same *in vitro* culture system, we found that GDF7 does not promote autonomic neuronal differentiation at any concentration tested. These data suggest that GDF7 may promote sensory lineage commitment. Taken together, those data indicate that the GDF7-expressing roof-plate is not only a source of fate-restricted neural crest cells but is also a source of signals for this restriction.

24. **In vivo** studies of the development of the vascular and nervous system

Yosuke Mukoyama, David Anderson

Blood vessels and peripheral nerves branch together, and neurogenesis occurs close to blood vessels in the hippocampus and subventricular zone in the brain. However, their functional relationship remains poorly understood. Recently, we have shown that the pattern of arterial branching is determined by that of the nerve in the embryonic limb skin. Moreover, the fact that nerves secrete vascular endothelial growth factor (VEGF), which stimulates arterial differentiation *in vitro*, suggests that

nerves may function to induce arteries, but not veins through VEGF. We are currently investigating VEGF involvement *in vivo* by examining conditional VEGF knockout mice that completely lack VEGF expression in peripheral nerves. The mutants show severe defects in arterial differentiation in the limb skin. This observation is consistent with our *in vitro* studies, suggesting that VEGF-A is involved in arterial differentiation.

In vivo mechanisms controlling differentiation and self-renewal of neural stem cells in the peripheral and central nervous system (PNS and CNS) remain unclear. We are currently establishing *in vivo* approaches to address these questions using mouse-chick chimeras. Since we have isolated PNS stem cells (neural crest stem cells) and have identified molecules that determine their differentiation fates *in vitro*, *in vivo* function of the molecules will be tested by transplanting cultured neural crest stem cells in which gain- and loss-of-function are manipulated. We are also establishing direct transplantation of prospectively isolated CNS progenitors into chick spinal cord, to address their differentiation capacities. The expression of bHLH transcription factor Olig2 marks population(s) in the ventricular zone spinal cord that generate motor neurons (MNs) in the earlier stage and oligodendrocytes (Oligos) in the later stage. We are interested in the cellular mechanisms controlling the transition from neurogenesis to gliogenesis occurs. Freshly isolated Olig2⁺ cells from E9.5 (a stage for MNs) or E13.5 (a stage for Oligos) mouse spinal cord have been directly transplanted into the chick spinal cord, and their neurogenic and gliogenic potentials tested. This direct transplantation allows us to ask fundamental questions about whether there is a common precursor/stem cell to MNs and Oligos in the spinal cord.

25. Molecular mechanism underlying neurogenic capacity

Kenji Orimoto, David J. Anderson

Neural crest stem cells (NCSCs) can differentiate into autonomic neurons, Schwann cells and myofibroblasts in response to BMP2, GGF2/Notch ligands, and BMP2/TGF- β s, respectively. Accordingly, NCSCs possess neurogenic, gliogenic, and myofibroblastogenic capacities, as well as self-renewal capacity. When NCSCs are treated with Notch ligands for 24 hr, they completely lose their ability to differentiate into neurons, even in the presence of BMP2, while they still maintain the abilities to differentiate into Schwann cells and myofibroblasts under the appropriate instructive cues.

Mash1 plays a pivotal role in induction of autonomic neurons initiated by BMP2. Potential candidates for neurogenic capacity are defined as genes that are present in NCSCs, and promote Mash1-mediated neurogenesis triggered by BMP2. Since the robust induction of Mash1 by BMP2 is greatly reduced when NCSCs are pre-treated by Notch ligands, neurogenic capacity could be inactivated by Notch signaling. It is presumed that there is cross talk between the BMP and Notch signaling cascades. To get a better understanding of

molecular mechanism of differentiation of autonomic neurons, Affymetrix microarray analysis was conducted to compare gene expression profiles of Notch-activated NCSCs and corresponding the control NCSCs.

The data are currently being analyzed using multiple statistical platforms, including Affymetrix MAS and Rosseta Resolver systems. To validate the difference in expression of identified genes, quantitative RT-PCR assays will be performed using the original RNA sources. To test the functional involvement of candidate genes in cell fate regulation, gain-of-function and loss-of-function (RNAi system) assays will be conducted using lentivirus-mediated gene expression system. To examine the spatio-temporal regulation of expression, *in situ* hybridization will be employed.

The genes identified as gene clusters enriched in stem cells are further analyzed to see whether they are functionally involved in Mash1 induction and neuronal differentiation initiated by BMP2. The genes identified as clusters enriched in non-neuronal progenitors could be downstream targets directly affected by the Notch signaling cascade, as well as early markers for Schwann cell progenitors.

26. EphrinB2 in peripheral endothelial cells is essential for the proper embryonic vessel development

Donghun Shin, David J. Anderson

EphrinB2 conventional knockout and endothelial-specific knockout mice show the same angiogenesis defects during embryonic development. EphrinB2 is expressed in heart endocardial cells as well as in peripheral endothelial cells, and both mutants show heart defects as well as peripheral angiogenesis defects in head, trunk and yolk sac. It is not clear whether the peripheral angiogenesis defects in the mutant reflect a local requirement for ephrinB2 signaling, or rather may be secondary to the heart defects.

We generated a novel Cre line by inserting an EGFP-Cre fusion construct into a novel gene that is expressed in peripheral arterial endothelial cells, but not in endocardial cells. Using this Cre line and a conditional ephrinB2 allele, we have deleted ephrinB2 in peripheral endothelial cells but not in heart endocardial cells. Half of the conditional ephrinB2 mutants show severe angiogenesis defects as well as, heart defects at E9.5 and other conditional mutants show the angiogenesis defects in yolk sac without heart defects at E10.5. This difference may stem from variation in Cre activity which we observed in Cre:Rosa26R double heterozygous embryos by β -gal expression pattern. By careful analysis in the heart, we found out that the novel Cre line has Cre activity in outflow tract endocardial cells, although it does not have activity in atria and ventricular endocardial cells. Therefore, we are not sure whether the severe heart defects and the angiogenesis defects seen in the conditional mutants at E9.5 are caused by ephrinB2 deletion in peripheral endothelial cells, or by deletion in heart outflow tract endocardial cells. To address this issue, we are

trying to delete ephrinB2 in heart outflow tract endocardial cells, but not in peripheral endothelial cells, using other Cre lines active only in heart outflow tract endocardial cells. However, data from the conditional mutants having angiogenesis defects without the heart defects at E10.5 suggest that the peripheral angiogenesis defects in ephrinB2 mutants may not be secondary to the heart defects. These data support a local role for ephrinB2 in the angiogenic remodeling of the peripheral vasculature during embryonic development.

27. An innate avoidance behavior is dictated by a specific olfactory circuit in **Drosophila**

Greg S.B. Suh, Allan Wong*, Anne Hergarden, Jing Wang*, Seymour Benzer, Richard Axel*, David J. Anderson

We have developed a novel behavioral paradigm for an innate avoidance response in *Drosophila*. This paradigm involves avoidance of a putative "alarm" substance (AS) emitted by flies subjected to stress. Responder flies were given a choice in a T-maze between a fresh tube and a conditioned tube in which a set of emitter flies was previously traumatized. Most responders choose the fresh tube; Performance Index typically falls between 95 and 80 under optimal conditions. Gas chromatograph/mass spectrometry and respirometer analyses indicated that CO₂ is a component of the AS. Flies exhibit avoidance responses to CO₂ in a dosage-dependent manner. We next sought to functionally map olfactory circuits mediating avoidance response to CO₂. Flies in which a genetically-encoded, calcium-responsive indicator (GCaMP) was expressed throughout the antenna lobe revealed that a single pair of the ventral-most glomeruli, known as V, are activated by CO₂. Moreover, functional inactivation of the GR21D1+ sensory neurons which project to the V glomerulus using UAS-Shibire^{ts} (see below) was sufficient to abolish the avoidance response to CO₂. We have independently mapped groups of neurons essential for the avoidance response to the AS by carrying out an unbiased neuronal inactivation screen using the Gal4 x UAS-Shibire^{ts} system. Flies bearing a Gal4 enhancer trap and a UAS-Shibire^{ts} were assayed in the behavior paradigm at the non-permissive temperature (30°C) and were compared to their performance at the permissive temperature (21°C). We have screened ~250 Gal4 enhancer trap lines and identified five lines defective in this assay, but retained normal olfactory responses to various odorants and locomotive activities. In one of the five lines, c761, the avoidance response to CO₂ is also defective at the non-permissive temperature and the Gal4 is expressed in the V glomerulus, innervated by GR21D1+ neurons. The Gal4 of c761 is expressed in a larger population of neurons in the antenna compared to GR21D1+ neurons, which is consistent with the fact that c761 bearing UAS-Shits failed to respond to both CO₂ and the AS.

*Columbia University

28. Axonal tracers targeted to the **MrgD** locus reveal that nociceptive (pain-sensing) information is carried by molecularly distinct and parallel neuronal circuitry

Mark J. Zylka, David J. Anderson

We recently identified a large family of G protein-coupled receptors, called Mas-Related Genes (Mrgs). Several of these genes are expressed in subsets of small-diameter nociceptive (pain-sensing) neurons. To determine what role these genes and sensory circuits play in pain signaling, we generated several MrgD knock-out mouse lines where the coding region of MrgD was replaced with EGFP-F (farnesylated EGFP) or hPLAP (human placental alkaline phosphatase) axonal markers and the doxycycline-inducible transcription factor rtTA-M2. By studying axonal projections in these animals, we found that MrgD⁺ neurons terminate exclusively in the epidermis as free-nerve endings. MrgD⁺ neurons do not innervate any other known targets of nociceptive neurons such as hair follicles, blood vessels, or visceral organs. MrgD⁺ fibers comprise 70% of the free-nerve endings in the epidermis, with CGRP⁺ fibers representing the remaining 30%. Centrally, MrgD⁺ and CGRP⁺ fibers terminate in adjacent but non-overlapping lamina in the spinal cord. These neuroanatomical studies indicate that cutaneous nociceptive stimuli are conveyed by two molecularly distinct and parallel pain circuits. Currently, we are using the knocked-in copy of rtTA, in combination with TRE-driven transgenes, to inducibly silence and/or ablate the circuitry defined by MrgD expression. These selective molecular and cellular manipulations will permit us to uncover the functional and behavioral significance for parallel cutaneous pain circuitry in mammals.

Publications

- Gabay, L., Lowell, S., Rubin, L.L. and Anderson, D.J. (2003) De-regulation of dorso-ventral patterning by Fgf confers tri-lineage differentiation capacity on CNS stem cells in vitro. *Neuron* 40:485-499.
- Han, C.J., O'Tuathaigh, C.M., Van Trigt, L., Quinn, J., Fanselow, M.S., Mongeau, R., Koch, C. and Anderson, D.J. (2003) Trace but not delay fear conditioning requires attention and the anterior cingulate cortex. *PNAS* 100:13087-13092.
- Lo, L.C., Zirlinger, M., Zhou, Q., Choi, G. and Anderson, D.J. (2004) The logic of neural cell lineage restriction: Neurogenesis revisited. In: *Stem Cells the Nervous System: Functional and Clinical Implication*, Fred Gage, ed., Springer-Verlag, Berlin, Heidelberg, pp. 25-41.
- Zirlinger, M. and Anderson, D.J. (2003) Molecular dissection of the amygdala and its relevance to autism. *Genes, Brain Behav.* 5:282-294.
- Zylka, M.J., Dong, X., Southwell, A.L. and Anderson, D.J. (2003) Atypical expansion in mice of the sensory neuron-specific Mrg G protein-coupled receptor family. *Proc. Natl. Acad. Sci. USA* 100:10043-10048.

James G. Boswell Professor of Neuroscience, Emeritus (Active): Seymour Benzer
 Visiting Associate: Carol A. Miller
 Postdoctoral Fellows: Bader Al-Anzi, Ted Brummel, Pankaj Kapahi, W. Dan Tracey Jr., David W. Walker, Horng-Dar Wang
 Research and Laboratory Staff: Stephanie Cornelison, Nick Lawrence, Viveca Sapin, John Silverlake, Ching-Hua Wei, Rosalind Young
 Graduate Students: Gil Carvalho, Julien Muffat, Brian Zid

Support: The work described in the following research reports has been supported by:

American Federation for Aging Research
 The James G. Boswell Foundation
 Bristol-Myers Squibb
 Ellison Medical Foundation
 Life Science Research Foundation
 McKnight Foundation
 National Institutes of Health, USPHS
 National Science Foundation
 Retina Research Foundation

Summary: Our group uses *Drosophila* as a model system in which to identify and characterize genes involved in behavior, aging, and neurodegeneration. The high degree of homology between the fly and human genomes forms the basis of a strategy for understanding the corresponding human genes. Three behavioral paradigms are currently under investigation. One is a model of nociception that bears much resemblance to human pain, with mutants such as painless representing an entry into a molecular genetic analysis of this phenomenon. The second is an alarm response, in which flies subjected to vibration emit an odor that induces avoidance by other flies, which is being studied in collaboration with Professor David Anderson's group. The third is a genetic analysis of appetite and obesity.

To study the genetics of aging, we use a single-gene approach to screen for mutants with enhanced longevity, and analyze the functions of the genes involved. For instance, the mutant, *methuselah*, extends the average lifespan of *Drosophila* by some 30%, and also provides increased resistance to different stresses.

The *methuselah* protein is related to G protein-coupled receptors of the secretin receptor family, and has a unique N-terminal ectodomains. In collaboration with Professor Bjorkman's group, the crystal structure of the ectodomains was solved at 2.3 Å resolution. The structure represents one of only a few available three-dimensional structures of GPCRs. It reveals a folding topology likely to be conserved in Mth-related proteins, and contains a potential ligand-binding site in the form of a shallow interdomain groove with a solvent-exposed tryptophan, the only tryptophan residue in the ectodomains. Antagonists that reduce the effective activity of the receptor would be expected to mimic the defect in *methuselah*, thus possibly extending lifespan. In collaboration with Professor

Richard Roberts' group, a library of peptides was generated, from which a subset was selected that show very high binding affinity to Mth protein. In collaboration with Dr. Anthony West, of the Bjorkman group, we have produced monoclonal antibodies to the protein, and expression of *mth* in cultured cells shows localization of the protein at the cell membrane. We are using such cultures, along with the small peptides as putative ligands, to test for G-protein activation in a suitable reporter system.

Exposure of flies to 100% oxygen causes early death, and we have found that an early-induced event is local disruption of mitochondrial structure in the form of internal "swirls." These also accumulate in normal aging, and their formation can be suppressed by mutations in the *methuselah* gene. Other mutants, such as *hyperswirl*, are unusually sensitive to oxygen, and display large numbers of swirls. Analysis of such mutants may provide clues to primary mechanisms of oxidation damage.

Dietary caloric restriction extends lifespan in various organisms, and we are investigating that phenomenon in *Drosophila*, as well as the role of steroid hormones and bacterial flora. We have developed biomarkers to monitor the progress of aging during lifetime, and have shown that lifespan can be extended by simple feeding of a drug which alters the balance of induction and repression of different sets of genes.

29. Genetics and circuitry of nociception W. Dan Tracey, Seymour Benzer

We have recently described a paradigm for studying nociception in *Drosophila*. In response to the touch of a probe heated above 38°C, *Drosophila* larvae produce a stereotypical rolling behavior, unlike the simple avoidance response to an unheated probe. In a genetic screen for mutants defective in this noxious heat response, we identified the painless gene. This year, we have begun to characterize the properties of other mutants identified in the screen. For example, one mutant lacks fine filopodial projections on a subset of multidendritic neurons. In addition, we have performed a new screen with the goal of identifying the brain circuitry required for *Drosophila* nociception. In this screen, a collection of some 400 neuronal GAL4 driver lines were crossed to a line (UAS-Shi^{ts}) that causes GAL4-dependent, temperature-inducible neuronal inactivation. At the non-permissive temperature, neuronal subsets expressing the GAL4 driver become inactivated due to the dominant action of the Shi^{ts} gene. The larval progeny were raised to non-permissive temperature, then tested with a noxious heat probe for the rolling response. From this screen, we identified 30 lines that do not show the rolling response at the non-permissive temperature. The patterns of expression of these lines in the larval nervous system will be investigated to identify the circuitry that controls the rolling response.

30. Circuit analysis of an innate avoidance behavior in **Drosophila**

Greg S. Suh¹, Allan Wong², Anne Hergarden¹, Richard Axe², Seymour Benzer, David J. Anderson³

We have developed a novel behavioral paradigm for an innate avoidance response in *Drosophila*. This paradigm involves avoidance of a substance emitted by flies subjected to stress, called *Drosophila* Stressed Odorant (dSO). Responder flies are given a choice in a T-maze between a fresh tube and a conditioned tube in which a set of emitter flies was previously traumatized. Most responders choose the fresh tube; the performance index typically falls between 85 and 95% under optimal conditions. Gas chromatograph/mass spectrometry and respirometer analysis indicated that CO₂ is a component of dSO, and flies exhibit avoidance response to CO₂ in a dosage-dependent manner. We next sought to functionally map olfactory circuits mediating the avoidance response to CO₂. Flies in which a genetically-encoded, calcium-responsive indicator (GCaMP) was expressed throughout the antennal lobe revealed that a single pair of the ventral-most glomeruli, known as V, are activated by CO₂. Moreover, functional inactivation of the GR21A+ sensory neurons which project to the V glomerulus, using UAS-Shi^{ts} was sufficient to abolish the avoidance response to CO₂. We have independently mapped groups of neurons essential for the avoidance response to dSO by carrying out an unbiased neuronal inactivation screen using the Gal4/UAS-Shi^{ts} system. Flies bearing a Gal4 enhancer trap and UAS-Shi^{ts} were assayed in the behavior paradigm at a non-permissive temperature (30°C), compared to their performance at a permissive temperature (21°C). We have screened ~250 Gal4 enhancer trap lines and identified five lines defective in this assay, but retain normal olfactory responses to various odorants and normal locomotive activity. In one of the five lines, c761, the avoidance response to CO₂ is also defective at the non-permissive temperature. In that strain, Gal4 is expressed in the V glomerulus, which is innervated by GR21A+ neurons. The Gal4 of c761 is expressed in the antenna in a larger population of neurons than the GR21A+ neurons, consistent with the fact that c761 bearing UAS-Shi^{ts} failed to respond to either CO₂ or dSO.

¹Columbia University

²Biology Graduate Student, Caltech

³Biology Professor, Caltech

31. Isolation and characterization of mutations that cause obesity and excessive feeding in **Drosophila**

Bader F. Al-Anzi, Seymour Benzer

There is a strong correlation between fat content and the ability of a fly to resist starvation. One, therefore, can select for mutant obese flies based on their ability to resist starvation. Potentially obese flies should survive while all others die, making it possible to screen thousands of mutagenized flies in a relatively short time. Approximately 22,000 mutagenized males were tested, out

of which 36 males passed the first starvation trial and were used to establish mutant lines. To date, eight of those lines exhibit bona fide starvation resistance that is associated with an increase in their lipid content. Histological studies have also shown that this increase in the lipid content is associated with an increase in both fat cell size and number in those mutants as compared to wild type.

Many behavioral and metabolic abnormalities, such as excessive feeding, low activity level, and metabolic shift towards fatty acid synthesis, can cause obesity. We are using behavioral and biochemical assays to determine the underlying defects that are responsible for the obese mutant phenotypes. These include feeding rate, metabolic rate, level of activity, fat cell count, and level of de novo fatty acid synthesis.

The use of *Drosophila* in obesity research may help determine whether appetite and body weight regulation have underlying biological mechanisms that have been conserved throughout the Metazoa, as has been shown to be the case for genes that regulate such behavioral phenomena as learning and the circadian clock.

32. Genetic and pathological analysis of oxygen toxicity in **Drosophila**

David W. Walker, Seymour Benzer

Mitochondrial dysfunction and reactive oxygen species have been implicated in aging and in a wide range of age-related diseases. Identifying primary events that result from acute oxidative stress may provide targets for therapeutic interventions to minimize aging. Previously, we reported a striking initial pattern of mitochondrial degeneration in the flight muscle under conditions of oxygen stress or aging: the cristae within individual mitochondria become locally rearranged, in a "swirl." We have further characterized the phenomenon and demonstrated that, under hyperoxia, cytochrome c undergoes a conformational change manifested by display of an otherwise hidden epitope. The conformational change is correlated with widespread apoptotic cell death in the flight muscle, as revealed by in situ TUNEL labeling.

We are currently focusing our attention on the pathological consequences of mitochondrial dysfunction in the *Drosophila* central nervous system. In a genetic screen, we isolated the mutant hyperswirl (hys), which is dramatically short-lived and displays a striking mitochondrial pathology. To determine whether mitochondrial decay in hys results in neurodegeneration, the brains of hys flies were examined by toluidine blue staining of semithin plastic sections for light microscopy. hyperswirl mutant brains develop vacuoles in the medulla and lamina. To determine whether brain degeneration in hys proceeds through an apoptotic mechanism, brains from hys and age-matched controls were subjected to TUNEL staining. A dramatic increase in TUNEL-positive nuclei was observed in the brains of 10-day-old adult hys mutants relative to age-matched controls, suggesting that mitochondrial dysfunction may result in cell death through an apoptotic mechanism. We are using a range of

antibodies to identify the neuronal subtype that undergoes degeneration in hyperswirl. At the same time, we are testing the ability of other genes to protect against apoptotic cell death in hys and in normal flies exposed to hyperoxia.

33. The role of Apolipoprotein D in normal and pathological aging in **Drosophila**

Julien A. Muffat, David W. Walker, Seymour Benzer

Human Apolipoprotein D (hApoD) is upregulated 350% in the CSF of patients with Alzheimer's disease. The protein appears to be secreted by astrocytes and other reactive glial cells, and is recruited to sites of neuronal injury and amyloid deposition. As ApoD and its homologs are small hydrophilic molecules capable of carrying a single hydrophobic ligand (such as cholesterol), they may play a role in neuronal maintenance and survival, either by carrying trophic factors or essential building blocks of cell membranes.

Drosophila Glial Lazarillo (Glaz) shares 40% of its protein sequence with hApoD. Preliminary results of in situ hybridization in adult *Drosophila* indicate that thoracic muscles and the nervous system are the main organs expressing Glaz. We have shown that 10-fold overexpression of the Glaz gene, using the UAS/GAL4 bipartite system, results in 30% longer lifespan for *Drosophila*. This overexpression also enhances stress resistance, as assessed by starvation, desiccation, heat shock or hyperoxia. Such flies also contain 20% less fat than controls. By the use of various tissue-specific driver lines, we observed that overexpression in vertical muscles and parts of the nervous system is sufficient to produce the beneficial effects.

34. Enhancement of **Drosophila** longevity by exogenous bacteria

Ted Brummel, Alisa Ching¹, Laurent Seroude², Anne F. Simon³, Seymour Benzer

We have discovered that the presence of bacteria during the first week of *Drosophila* adult life can enhance longevity. Analysis of this effect in a panel of long-lived mutants revealed a range of responses. Most behaved in a manner similar to wild-type flies. However, the long-lived ecdysone receptor mutant, *EcR^{v559fs}* was found to be little affected by the presence of bacteria. A second long-lived strain, DJ817, showed an exaggerated benefit. Since the presence of bacteria might alter nutrition, we measured food intake in the presence and absence of bacteria, but observed no differences.

Late in life, bacteria were found to accelerate mortality. To understand how bacteria modulate the various stages of lifespan, we are using a biochemical approach aimed at identifying specific molecules that may positively impact longevity, combined with conventional microbiological methods to determine the bacterial composition within *Drosophila* cultures.

¹Grad Student, Caltech

²Queens University Kingston, Ontario, Canada

³UCLA, Brain Research Institute, Los Angeles, CA

35. Peptide modulators of Methuselah, a G protein-coupled receptor associated with extended lifespan

William W. Ja¹, Anthony P. West², Pamela J. Bjorkman³, Seymour Benzer, Richard W. Roberts⁴

Mutation in the methuselah (*mth*) gene results in a 30% increase in average lifespan and enhanced resistance to a variety of stresses, including starvation and hyperoxia. *Mth* is a G protein-coupled receptor (7 transmembrane structure) with an ~25-kDa, N-terminal ectodomain. Previously, using mRNA display of large random libraries, our laboratory isolated peptides that bind the *Mth* ectodomain. These peptides demonstrated high affinity to the ectodomain, with dissociation constants from 15 to 60 nM. A low-resolution crystal structure of a *Mth* ectodomain:peptide complex revealed that the peptide binds at a putative interaction site between the extracellular loops and the ectodomains of *Mth*. As GPCR signaling is generally transduced through movements of the transmembrane domains, the structural data suggest that the peptides could act as modulators of *Mth* signaling.

Recently, Cvejic et al. (2004) published the discovery of Stunted, a natural agonist for *Mth*; a eukaryotic cell line stably expressing *Mth* was used in a calcium-signaling assay to isolate agonists from fractionated fly lysates. Using this assay, we have determined that a number of our in vitro selected peptides act as antagonists of the *Mth* signaling by Stunted. The most potent peptides exhibit submicromolar IC₅₀ values. The application of these peptides toward the synthetic extension of *Drosophila* lifespan is currently being tested.

¹Graduate Student, Chemistry, Caltech

²Postdoctoral Scholar, Bjorkman Lab, Caltech

³Professor of Biology, Caltech

⁴Assistant Professor of Chemistry, Caltech

Reference

Cvejic, S., Zhu, Z., Felice, S.J., Berman, Y. and Huang, X.Y. (2004) *Nat. Cell Biol.* 6:540-546.

36. Lifespan extension of **Drosophila** by reduction of polyamines

Brian M. Zid, Pankaj Kapahi, Seymour Benzer

Polyamines are small, ubiquitous polycations that are essential for normal growth. We discovered two defects in spermidine synthase, an enzyme in the polyamine biosynthetic pathway, that have increased lifespan in *Drosophila*. Ornithine decarboxylase (ODC), which is upregulated in many types of cancer, is the rate-limiting enzyme in the polyamine biosynthetic pathway. We have found that overexpression of gutfeeling, the *Drosophila* homolog of antizyme, an ODC inhibitor, also increases lifespan, and the long-lived mutants showed lower polyamine levels.

Polyamine levels were also found to be lower with dietary restriction and reduction of flux through the growth-promoting nutrient sensing TOR pathway. Tissues

from dietary-restricted mice also showed reduced polyamines, indicating an evolutionarily conserved mechanism in which polyamines may be a link between dietary restriction and nutrient-sensing growth pathways.

37. A screen for mutants that modulate lifespan upon nutritional changes in **Drosophila**

Pankaj Kapahi, Gil Carvalho, Seymour Benzer

Reduction of calories to 30-40% less than consumed ad libitum by rodents increases both maximum and mean lifespan by >50%. Dietary restriction (DR) has been shown to extend lifespan in various species, including *C. elegans*, *D. melanogaster*, *S. cerevisiae*, and *Mus musculus*. On the other hand, overnutrition in humans is linked with Type II diabetes, cardiovascular and neurodegenerative diseases, some cancers, and increased mortality rate. In order to understand the genetic factors that modulate lifespan, we undertook a screen for *Drosophila* mutants that are hypersensitive to a rich diet.

We found that reduction of the concentration of yeast extract in the fly food produces an effect on lifespan similar to that seen in rodents upon caloric restriction. We set up food with varied levels of yeast extract, keeping constant other diet components (5% sucrose, 0.5% agar, and 8% cornmeal). "Overnutrition" is defined as 5% or greater yeast extract (hiY). We find a dose-dependent increase in body size with increase in yeast extract. As in the mouse experiments, we also see an accompanying decrease in reproduction, measured by the number of eggs laid per female. These results agree with the hypothesis that there is a tradeoff between somatic maintenance and reproduction, which may arise due to competitive allocation of nutrients.

We discovered that, on hiY (but not on lowY), certain mutant fly strains failed to develop to adulthood. We have named these mutants creosote (ceo), after Mr. Creosote, a character in Monty Python's 'The Meaning of Life,' who explodes upon overeating. This provides a sensitive paradigm in which to screen for drugs and genes that suppress the toxic effects of overnutrition. Among P-element insertion lines, we have isolated five such strains, which fall into at least two complementation groups. To examine the effects on adult lifespan of these mutations, we raised ceo homozygotes to adulthood on 1% yeast extract food, then placed them on hiY. They suffered over 70% decrease in lifespan, whereas on 1% yeast extract food, their lifespans were only slightly less than the normal. Characterization of the genes involved is in progress.

38. A longevity mutant involving the pentose phosphate pathway

Hornig-Dar Wang, Seymour Benzer

An EP mutant EP(2)2456, isolated by screening for resistance to both oxidative stress (paraquat) and starvation, displayed extended lifespan at 25°C. Both phenotypes are recessive; the heterozygote lacks both the stress resistance and life extension. To eliminate possible effects of genetic background, the mutant was outcrossed

ten times with control *w¹¹¹⁸* flies, and a homozygous EP line was established. The outcrossed EP line retained the phenotypes of stress resistance and life extension. Plasmid rescue of the outcrossed EP mutant revealed that there was only one EP element, and that it remained in the original insertion site. RT-PCR and Northern blotting indicated reduced expression of the ribose-5-phosphate isomerase (*rpi*) gene near the EP insertion. The enzyme is involved in the pentose phosphate pathway of glucose metabolism. We generated P-element excision lines, and some showed decreased expression of *rpi*. We are in the process of checking whether those with lowered *rpi* expression have enhanced stress resistance and increased lifespan. Flies transgenic for RNAi of *rpi* will be tested to confirm the phenotypes. We measured food intake for the long-lived EP mutant and *w¹¹¹⁸* controls, and found them to be very similar, indicating that caloric restriction does not account for the life extension of the mutant. Further characterization of the EP line is in process.

39. Identifying the tissue responsible for the female longevity bias in **Drosophila**

David W. Walker, Seymour Benzer

In most animal species, including humans, the female is longer lived. In the United States, the mean life expectancy of women is almost seven years greater than for men. The underlying mechanisms governing the female survival advantage remain unknown. To examine which tissues are involved, we generated male flies with different regional patterns tissue feminization, using the transformer gene, the product of which is known to feminize cells in a dominant and autonomous fashion. The system involves two transgenic lines, one being a UAS-transformer line in which the female version of the sex determination gene transformer (*tra*) is placed under the control of the upstream activating sequence (UAS) of the yeast transcription factor GAL4, the second being a GAL4 line which expresses GAL4 in a tissue-specific pattern.

Using a panel of enhancer trap lines with different patterns of Gal4 expression, we examined the longevity of males expressing transformer in various tissues. Some of the partially transformed males lived as much as 18% longer than control flies heterozygous for UAS-*tra* or the GAL4 enhancer trap. We are characterizing the precise patterns of expression to identify those tissues that are critical for this lifespan extension.

Publications

Brummel, T., Ching, A., Seroude, L., Simon, A.F. and Benzer, S. (2004) *Drosophila* lifespan enhancement by endogenous bacteria. Proc. Natl. Acad. Sci. USA. In press.

Kapahi, P., Zid, B.M., Harper, T., Koslover, D., Sapin, V. and Benzer, S. (2004) Regulation of lifespan in *Drosophila* by modulation of genes in the TOR signaling pathway. Curr. Biol. 14:885-890.

- Suh, G.S.B., Wong, A.M., Hergarden, A.C., Wang, J.W., Simon, A.F., Benzer, S., Axel, R. and Anderson, D.J. (2004) A single population of olfactory sensory neurons mediates an innate avoidance behavior in *Drosophila*. *Nature*. In press.
- Walker, D.W. and Benzer, S. (2004) Mitochondrial "swirls" induced by oxygen stress and in the *Drosophila* mutant "hyperswirl." *Proc. Natl. Acad. Sci. USA* 101:10290-10296.
- Wang, H.-D., Kazemi-Esfarjani, P. and Benzer, S. (2004) Multiple stress analysis for isolation of *Drosophila* longevity genes. *Proc. Natl. Acad. Sci. USA* 101:12610-12615.

Allen and Lenabelle Davis Professor of Biology: Mary B. Kennedy

Associate Researcher: Leslie T. Schenker

Assistant Researcher: Alan Rosenstein

Senior Postdoctoral Scholars: Pat Manzerra

Postdoctoral Scholars: Holly Carlisle, Mee-Hyang Choi, Eugenia Khorosheva, Irene Knuesel, Edoardo Marcora, Jeong Oh, Luis Vázquez, Lori Washburn

Graduate Students: Holly Beale, William Ford¹, Tinh Luong, Andrew Medina-Marino, Stefan Mihalas², Celia Shiau³

Research and Laboratory Staff: Abigail Elliot⁴, Cheryl Gause, Margaret Hainline⁵

¹Graduate Student, CNS, Caltech

²Graduate Student in Physics, Caltech

³Rotation Student, Biology Program

⁴SURF, Caltech

⁵SURF, Grinnell College

Support: The work described in the following research reports has been supported by:

The Allen and Lenabelle Davis Professorship of Biology

French Foundation for Alzheimer's Research

Human Frontiers Science Program

National Institutes of Health

Summary: The Kennedy lab studies molecular mechanisms of synaptic regulation in the central nervous system. Memories are stored in the brain through long-lasting changes in the strength of synapses between neurons. These changes are triggered when the synapses are used to perceive the object or event being remembered. Regulation of synaptic strength may also underlie mood changes and is important for minute-by-minute information processing. Some neurotransmitters, such as glutamate and acetylcholine, which activate ligand-gated ion channels, can also initiate long-lasting biochemical changes that change synaptic strength. Excitatory synapses contain signaling protein complexes at the postsynaptic membrane, within a structure called the postsynaptic density (PSD). We are interested in the structure and functional organization of these signaling complexes and their roles in synaptic plasticity.

We have used cell biological, microchemical and molecular genetic methods to identify the protein components of the PSD fraction purified from brain (Kennedy, 1997, 2000). These include the scaffold molecule PSD-95; the NR2B subunit of the NMDA-type glutamate receptor; Ca²⁺/calmodulin-dependent protein kinase II (CaM kinase II); a Ras GTPase-activating protein called synGAP; a putative adhesion molecule, densin-180; a myosin motor termed myosin V or "dilute myosin"; and a septin molecule, cdc10. By now, most of the major proteins in the PSD fraction have been identified. In addition, sequencing and assembly of the human and mouse genomes are nearly finished, providing us with a complete "parts list" for signaling complexes. This is an exciting time, because we can turn our attention to the task

of understanding how proteins are organized at the synapse and how they function together as a signaling machine.

One important synaptic signaling complex assembles around the cytosolic tail of the NMDA receptor. This complex includes many of the proteins that we found in the postsynaptic density. Activation of the NMDA receptor leads to influx of calcium and activation of CaM kinase II. It is well known that disruption of the CaMKII gene leads to derangement of synaptic regulation. CaMKII can phosphorylate the protein synGAP, and may regulate its location or activity at synapses, but the function of synGAP is unknown. We used homologous recombination in embryonic stem cells to create mutant mice in which the synGAP protein is deleted, and have used the mutant mice to establish some of the influences of synGAP on brain development and function.

In conjunction with our biochemical and cell biological experiments, we are using computer simulations and measurements of rapid kinetics to study the kinetics and interactions of signaling pathways in the tiny postsynaptic spine. The complex signaling machinery at the synapse integrates a variety of signaling influences and determines the "set-point" of synaptic strength at individual synapses. Many important signaling reactions are triggered by calcium influx into the postsynaptic spine, and result in phosphorylation of proteins, eventually leading to changes in synaptic strength. We have initiated a collaboration with scientists at the Salk Institute to build computer simulations of the flux of protein phosphorylation events in spines in the hippocampus. We will use the program MCell to implement stochastic simulation methods that model the position and behavior of immobilized signaling molecules within the spine. We will formulate our quantitative understanding of each protein and reaction in a signaling scheme, and assemble these into a complex kinetic simulation in MCell. We will then generate testable predictions about the flow of protein phosphorylation events in excitatory spines and dendrites, under conditions of calcium influx that cause changes in synaptic strength. Our ultimate goal is to create simulations that will illuminate our understanding of biochemical information coding at different types of synapses in the brain. Predictions arising from the simulations will be tested experimentally by measuring the time-course and spatial distribution of phosphorylation of CaMKII and other phosphorylated synaptic molecules under a variety of physiological conditions. This effort will lay the groundwork for understanding the behavior of highly interconnected signaling pathways at the synapse.

References

Kennedy, M.B. (1997) *Trends Neurosci.* 20:264-268.

Kennedy, M.B. (2000) *Science* 290:750-754.

40. Role of synGAP in spine maturation

Luis E. Vázquez, Margaret Hainline

This year we found that synapse formation and spine maturation are accelerated by ~2 days in neurons cultured from mice in which synGAP has been deleted by homologous recombination (synGAP ko's). In the mutant cultures, spines are well developed by day 10 in vitro (10 DIV); whereas in wild-type cultures, dendritic filopodia have not yet developed into spines. This knockout phenotype can be rescued (i.e., spine maturation reversed) by introduction of recombinant wild-type synGAP on day 9 in vitro. In contrast, mutation of either of two of synGAP's functional domains renders it unable to rescue this phenotype. SynGAP contains a GTPase-activating domain (GAP) that can inactivate Ras, and a terminal (T/SXV) domain that binds to PSD-95 holding it in the NMDA receptor complex. Introduction of synGAP with a mutation in the GAP domain or a deletion of the (T/SXV) domain into synGAP ko neurons does not rescue the knockout phenotype, indicating that both domains play a role in control of spine maturation. Since the T/SXV domain serves to localize synGAP close to PSD-95 and the NMDAR, this result suggests that both loss of GAP activity and mislocalization of synGAP within the spine microdomain can result in deregulated Ras activity.

41. A role for synGAP in regulating neuronal apoptosis

Irene Knuesel, Abigail Elliot

SynGAP may play an important role in coupling NMDA-type glutamate receptor activation to signaling pathways downstream of Ras. Mice with a homozygous deletion of synGAP die in the first few days after birth. Therefore, to study the functions of synGAP, we used the cre/loxP recombination system to produce conditional mutants in which synGAP is eliminated during the first three weeks after birth. In these mice, loss of synGAP can be detected after ~ one week, and its magnitude is variable. The resulting phenotypes fall into two groups. Mutant mice in which the level of synGAP protein is reduced to 20–25 % of wild type die at 2–3 weeks old. Mice in which the levels remain higher than ~40% of the wild type level survive and remain healthy. In all of these mice, however, an abnormally high number of neurons in hippocampus and cortex undergo apoptosis as detected by caspase-3 activation. The level of caspase-3 activation in neurons correlates inversely with the level of synGAP protein measured at 2 and 8 weeks after birth, indicating that neuronal apoptosis is enhanced by reduction of synGAP. These data show that synGAP plays a role in regulation of the onset of apoptotic neuronal death.

42. Signal transduction in SynGAP mutant mice

Pat Manzerra

SynGAP is a synaptic Ras GTPase-activating (GAP) protein identified in our lab, which is enriched in the postsynaptic density fraction prepared from rat forebrain. SynGAP is associated with the NMDA receptor complex through its interaction with PSD-95. We have

hypothesized that, by catalyzing inactivation of Ras, synGAP down regulates NMDA receptor-mediated signaling, in particular, the Ras-mediated activation of ERK/MAP kinase. To gain more insight into the functions of synGAP in vivo, our lab used homologous recombination to generate mice in which the gene encoding synGAP is deleted. Although the homozygous mutant mice die a few days after birth, primary neuronal cultures prepared from cortex and hippocampus of the mutants live in culture as long as wild-type neurons. We found that the initiation and magnitude of ERK activation is unaltered following the stimulation of NMDARs in neurons cultured from SynGAP mutants compared to those cultured from wild-type litter mate controls. However, activation of ERK is prolonged following stimulation of NMDARs in the synGAP mutants. Currently, we are comparing Ras-mediated signaling through other receptors in mutant cultures to determine the receptor signaling specificity of synGAP function.

In addition, given the role of synGAP in regulating NMDA receptor-mediated signaling, we also investigated the possibility of an effect of the synGAP mutation in in vitro models of pathological neuronal cell death. We found that synGAP mutant cultures are less susceptible than wild-type cultures to cell death initiated by over stimulation of NMDA receptors, but not to cell death initiated by over stimulation of AMPA-type glutamate receptors. These studies support the hypothesis that synGAP is a key molecule regulating NMDA receptor-mediated signaling through Ras, and cell death.

43. Activation of Ca²⁺/calmodulin-dependent protein kinase II (CaMKII) by concentrations of Ca²⁺ and calmodulin present **in vivo**
Mee-Hyang Choi, Vladan Lucic*

In preparation for the construction of simulations of postsynaptic signal transduction through the NMDA receptor, we are investigating activation of CaMKII by Ca²⁺ and calmodulin at concentrations in the range that are likely to be encountered in postsynaptic spines at or near the postsynaptic density. This year we used fluorescence-binding and enzymatic assays to show that, as predicted by physical chemical considerations, the apparent affinity of calmodulin for Ca²⁺ is increased dramatically in the presence of its target protein, CaMKII. For example, in the presence of .28 μM CaMKII and 12 μM calmodulin, activation and autophosphorylation of CaMKII can be initiated by addition of as little as .35 μM-free Ca²⁺, a concentration well below the range of K_D's for binding of Ca²⁺ to calmodulin in the absence of target proteins. The cooperativity of Ca²⁺-binding induced by the presence of CaMKII, at the concentrations described above, results in a steep Ca²⁺ activating curve with half maximal activation at ~0.5 μM Ca²⁺ and maximal activation at ~3 μM. Thus, activation of CaMKII is likely to occur in the spine at much lower effective Ca²⁺ concentrations than previously believed.

*Present address: Max Planck Institute for Biochemistry, Munich, Germany

44. Activation of CaMKII by calmodulin mutants with specific Ca^{2+} -binding sites removed
Mee-Hyang Choi, Julia Shifman*, Stefan Mihalas

As Ca^{2+} enters the postsynaptic spine, each molecule of calmodulin (CaM) binds Ca^{2+} ions stochastically. Calculations indicate that most of the free CaM will bind up to two Ca^{2+} ions at its carboxyl end that has two binding sites with a higher affinity for Ca^{2+} than the two sites located at the N-terminus. Under conditions present in the spine, only a small proportion of free CaM will have all four Ca^{2+} -binding sites filled. The existence of a cooperative effect on Ca^{2+} -binding in the presence of the target protein CaMKII (see abstract 43) implies that CaM with less than four Ca^{2+} bound has a significant affinity for CaMKII. In order to appropriately simulate the competition for Ca^{2+} -bound CaM that occurs among different target proteins following influx of Ca^{2+} into the spine, we need to know the binding constants for binding of CaM to CaMKII when two Ca^{2+} are bound at the C-terminal sites on CaM, and at the N-terminal sites. In collaboration with the Mayo lab, we used state-of-the-art protein design methods to develop two mutant CaMs that bind Ca^{2+} only at the N terminus (CaM-2N) or only at the C terminus (CaM-2C), retaining the closed, apo- structure at the mutated terminus. Both of these mutants can bind to and activate CaMKII when Ca^{2+} is present, although they require higher concentrations of both Ca^{2+} and CaM than WT. We tested a range of conditions similar to those present in spines (3-10 μM mutant CaM, and 1-10 μM -free Ca^{2+}). We observed activation of CaMKII under these conditions by both mutants, although, as expected, CaM-2C activated CaMKII at lower concentrations of both Ca^{2+} and CaM than did CaM-2N.

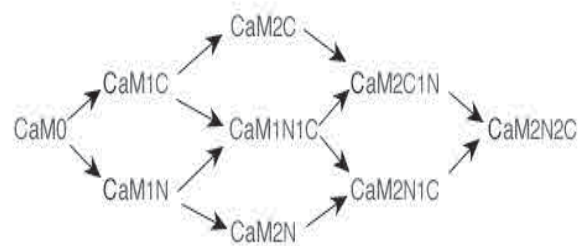
*Steve Mayo Laboratory, Caltech

45. Quantitative model of calcium binding to calmodulin in spines
Stefan Mihalas

To begin to explore how CaM can differentially activate Ca^{2+} -triggered cascades we have constructed a model of Ca^{2+} binding to CaM under conditions thought to exist in postsynaptic spines. We constructed a simple model of Ca^{2+} dynamics in a spine incorporating the Ca^{2+} buffering characteristics measured by Sabatini et al. (2002) Neuron 33:439. This model generates Ca^{2+} microdomains in the spine in which the concentration of Ca^{2+} varies with time and distance from the postsynaptic density during depolarization of the membrane. We are interested in modeling binding of Ca^{2+} to CaM, which has two higher affinity Ca^{2+} -binding sites at its carboxyl end, and two lower affinity sites at its amino-terminal end. Successive binding of Ca^{2+} to each binding site occurs as diagrammed in Fig. 1. From the four-measured macroscopic affinity constants of Ca^{2+} for CaM and from equilibrium equations describing the 12 binding sequences shown below, we calculated the microscopic affinity constants of Ca^{2+} for each individual binding site on CaM. We can use these affinities to calculate the proportions of $\text{CaM}_{c,n}$ (where $c=0-2$, $n=0-2$ bound Ca^{2+} ions at the C and N termini of

CaM, respectively) at given concentrations of Ca^{2+} and CaM. When we use the measured macroscopic constants for free CaM as the starting point, the $\text{CaM}_{2,0}$ species predominates through most of the range of concentrations of Ca^{2+} in spines, with the fully bound species $\text{CaM}_{2,2}$ becoming significant only at the highest Ca^{2+} concentrations. However, the presence of Ca^{2+} /CaM-dependent protein kinase II (CaMKII) increases the apparent affinities of CaM for Ca^{2+} . Therefore, we devised a strategy to determine the range of concentrations of each $\text{CaM}_{c,n}$ bound to CaMKII at given Ca^{2+} concentrations, and to determine how the presence of CaMKII influences the apparent affinities of CaM for Ca^{2+} . We use published values of macroscopic off rates for unbinding of Ca^{2+} from CaM in the presence and absence of CaMKII to calculate an estimated range of microscopic on and off rates of Ca^{2+} binding to CaM when it is bound to CaMKII. We then use similar methods to calculate a range of microscopic on and off rates for binding of $\text{CaM}_{c,n}$ to CaMKII from the equations for thermodynamic equilibrium of the Ca^{2+} /CaM/CaMKII system. Our goal is to add a model of CaMKII activation into these simulations so that we can test predictions of the combined models. We are presently experimentally determining parameters that we need to accomplish this goal.

Figure 1: Successive binding of Ca^{2+} to C-terminal and N-terminal sites on calmodulin.



46. Phosphorylation of synGAP by CaM kinase II does not inhibit its activity
Jeong Oh

Our lab previously reported that phosphorylation of synGAP by CaM kinase II inhibits its GTPase-activating activity (1). This year we found that synGAP activity is, in fact, not directly inhibited by phosphorylation by CaM kinase II. The experiments presented in the previous paper involved two successive enzymatic reactions. In the first, synGAP in the postsynaptic density was prephosphorylated by CaM kinase II in the presence of Ca^{2+} , calmodulin, and 0.1 mM ATP. Phosphorylated PSD fractions were then assayed for ras GTPase activating activity (GAP activity). Pyrophosphate, a potent inhibitor of phosphatases in the PSD fraction, was added to the GAP assay to preserve the phosphorylation state of synGAP. Because of a fault in the design of the experiments, controls were not included in which both ATP and pyrophosphate were present in GAP

assays containing nonphosphorylated synGAP. We have now found that the combination of residual ATP (30 μ M) from the prephosphorylation reaction and 6 mM sodium pyrophosphate is sufficient to inhibit the GAP activity of synGAP. No additional inhibition is produced by phosphorylation of synGAP by CaM kinase II. The error was reinforced by an experiment shown in the paper that indicated inhibition of synGAP activity was blocked when inhibiting antibodies against CaM kinase II were included during the prephosphorylation reaction. We cannot reproduce blockade of synGAP inhibition by these antibodies. We published a correction (2) and indicated that the paper would be more appropriately titled "A synaptic Ras-GTPase activating protein phosphorylated by CaM kinase II."

References

- (1) Chen, H.-J., Rojas-Soto, M., Oguni, A. and Kennedy, M.B. (1998) *Neuron* 20:895-904.
- (2) Oh, J.S., Chen, H.-J., Rojas-Soto, M., Oguni, A. and Kennedy, M.B. (2002) *Neuron* 33:151.

Publications

- Jeng, J., Manzerra, P. and Kennedy, M.B. Densin-180 is a transmembrane protein. Submitted for publication.
- Knuesel, I., Elliot, A., Chen, H.-J., Mansuy, I.M. and Kennedy, M.B. A role for synGAP in regulation of neuronal apoptosis. Submitted for publication.
- Oh, J.S., Manzerra, P. and Kennedy, M.B. (2004) Regulation of the neuron-specific Ras GTPase activating protein, synGAP, by Ca^{2+} /calmodulin-dependent protein kinase II. *J. Biol. Chem.* 279:17960-17988.
- Vázquez, L.E., Chen, H.-J., Sokolova, I. and Kennedy, M.B. SynGAP regulates spine formation. In press.

Professor of Biology and Engineering and Applied Science: Christof Koch

Visiting Professor: Joseph Bogen

Research Fellows: Kamran Diba, Fred Hamker, C.J. Han, Alexander Kraskov, Whee Ky Ma, Colm O'Tuathaigh, Rodrigo Quian Quiroga, Melissa Saenz, Rufin Van Rullen, Patrick Wilken

Graduate Students: Ronald McKell Carter, Carl Gold, Constanze Hofstoetter, Asha Iyer, Ania Mitros, Chunhui Mo, Farshad Moradi, Robert Peters, Lavanya Reddy, Leila Reddy, Naotsugu Tsuchiya, Dirk Walther

Research and Laboratory Staff: Alex Bäcker*, Philippe P. Brieu, David Kewley, Shannon Moreen O'Dell, Candace Vavra

*Visiting Scientist, Sandia National Laboratories, Albuquerque, NM

Support: The work described in the following research reports has been supported by:

DARPA

Engineering Research Center for Neuromorphic Systems (NSF)

William T. Gimbel Discovery Fund in Neuroscience

Keck Foundation

Mettler Fund for Autism

Mind Science Foundation

The Gordon and Betty Moore Foundation

National Geospatial Intelligence Agency

National Institutes of Health

National Institutes of Mental Health

National Science Foundation

Office of Naval Research

Sandia National Laboratories

Sloan Foundation

Swartz Foundation

Summary: Research in the laboratory of Professor Christof Koch focuses on three areas: (1) biophysics of computation in single neurons; (2) understanding visual selective attention and visual consciousness at the neuronal, behavioral and computational levels; and (3) studying the role of attention, working memory and awareness in associative fear conditioning in humans and mice. For more details and all publications, see <http://www.klab.caltech.edu>.

Research carried out in our group as part of a program called "Biophysics of Computation" studies how the biophysics, synaptic architecture, and dendritic architecture of individual neurons subserve information processing. This research has been summarized in a textbook, *Biophysics of Computation: Information Processing in Single Neurons*, by C. Koch and published by Oxford University Press in 1999. To what extent do neuronal noise sources (thermal noise, channel noise, noise due to synaptic background firing, and so on) limit signal detection or signal reconstruction at the level of individual neurons? What are the biophysical mechanisms underlying neuronal computations? How do neurons multiply? How complex are single nerve cells? What is

the code used to transmit this information? Analytical work, backed up by detailed computer simulations of nerve cells based on electrophysiological data from our experimental collaborators at the Hebrew University in Jerusalem (Idan Segev and Yosef Yarom) and elsewhere, is used to generate experimentally verifiable predictions. With Guyri Buzsaki at Rutgers, we are investigating the relationship between extra- and intracellular spike waveforms and with Tomaso Poggio at MIT we are identifying ways in which single neurons can implement specific neuronal operations, such as the MAX operation. We continue to analyze the variability, and selectivity of single- and multi-unit firing activity and local field potentials from recordings in the medial temporal and frontal lobes in human patients and in monkey's visual cortex.

Understanding complex information-processing tasks, in particular the action of selective, visual attention (both saliency-driven bottom-up as well as task-dependent, top-down forms) requires a firm grasp of how the problems can be solved at the "computational" level, and how the resulting algorithms can be implemented by the known architecture of the visual cortex and associated subcortical areas. We use analytical methods, coupled with detailed computer simulations of the appropriate circuitry in the primate visual system, to study how these neuronal networks control selective visual attention and gaze and how they give rise to motion perception, object discrimination and detection (in collaboration with Tomaso Poggio at MIT and Laurent Itti at USC). The resulting algorithms are being applied to problems in image analysis and machine vision. Researchers in our laboratory study visual perception in the presence and (near)-absence of selective visual attention, as well as our ability to classify and distinguish two-dimensional visual patterns using psychophysical techniques in normal subjects. We are complementing these studies using noninvasive fMRI imaging (with our 3.4 T scanner) under the identical stimulus protocols to investigate such questions as object recognition with and without spatial selective attention, as well as orientation and face-specific adaptation. Our laboratory continues to collaborate with Itzhak Fried at UCLA in recording single units from multiple electrodes in the medial temporal cortex of awake patients during visual perception, recognition and change detection.

We continue to collaborate with Francis Crick (Salk) to develop a neurobiological framework to understand how subjective feelings (in particular, conscious visual perception) can arise in the mammalian forebrain. This two decade-long research program has found its way into a book for a general scientific audience, *The Quest for Consciousness: A Neurobiological Approach*, by C. Koch and published by Roberts and Company in 2004. In order to make experimentally verifiable progress on the mind-brain problem, it will be critical to interfere deliberately, transiently, rapidly and reversibly with groups of genetically identifiable forebrain neurons in experimental animals. In collaboration with

David Anderson (Caltech), Henry Lester (Caltech) and Michael Fanselow (UCLA), we have developed an associative fear-conditioning paradigm in both mice and normal human subjects. We are investigating the role of working memory, attention and awareness in acquiring delay versus trace conditioning in both species and in identifying their underlying neuronal representations, with a particular focus on the anterior cingulate cortex (with Ray Dolan's group at University College in London).

47. Intrinsic subthreshold noise in cultured hippocampal neurons

Kamran Diba, Henry Lester*, Christof Koch

Ion channels open and close stochastically. The fluctuation of these channels represents an intrinsic source of noise that affects the input-output properties of the neuron. We combined whole-cell measurements with biophysical modeling to characterize the intrinsic stochastic and electrical properties of single neurons as observed at the soma. We measured current and voltage noise in 18-day post-embryonic cultured neurons from the rat hippocampus, at various sub- and near-threshold holding potentials in the presence of synaptic blockers. The observed current noise increased with depolarization, as ion channels were activated, and its spectrum demonstrated generalized $1/f$ behavior. Exposure to TTX removed a significant contribution from Na channels to the noise spectrum, particularly at depolarized potentials, and the resulting spectrum was now dominated by a single Lorentzian ($1/f^2$) component. By replacing the intracellular K^+ with Cs^+ , we demonstrated that a major portion of the observed noise was due to K^+ channels. We compared the measured power spectral densities to a 1-D cable model of channel fluctuations based on Markov kinetics. We found that a somatic compartment, in combination with a single equivalent cylinder, described the effective geometry from the viewpoint of the soma. Four distinct channel populations were distributed in the membrane and modeled as Lorentzian current noise sources. Using the NEURON simulation program, we summed up the contributions from the spatially distributed current noise sources and calculated the total voltage and current noise. Our quantitative model reproduces important voltage- and frequency-dependent features of the data, accounting for the $1/f$ behavior, as well as the effects of various blockers.

*Professor of Biology, California Institute of Technology

48. Subthreshold voltage noise of rat neocortical pyramidal neurons

Gilad Jacobson*, Kamran Diba, Anat Yaron-Jakoubovitch*, Yasmin Oz*, Christof Koch, Idan Segev*, Yosef Yarom*

Neurons are noisy elements. Noise arises from both intrinsic and extrinsic sources, and manifests itself as fluctuations in the membrane potential. These fluctuations limit the accuracy of a neuron's output but have also been suggested to have a computational role under various scenarios. Here we present a detailed study of voltage

amplitude and spectrum at the soma of layer IV-V pyramidal neurons of the rat neocortex in slice preparation. We focus on the contribution of synapses and Na^+ conductance to the voltage noise and demonstrate that voltage noise increases non-linearly as the cell depolarises (from 0.4 mV SD at -75 mV to 1.2 mV SD at -55 mV). The increase in voltage noise was accompanied by an increase in the cell impedance, due to voltage-dependence of Na^+ conductance (the negative slope conductance at the subthreshold voltage regime). This impedance increase accounts for about 70% of the voltage noise increase. The increase in voltage noise and impedance is restricted to the low-frequency range (0.2-2 Hz) in the presence of synaptic activity. Synaptic noise dominates the high-frequency range (> 5 Hz), having little effect on the cell impedance in our preparation. The results imply that ion channel noise has a significant contribution to membrane voltage fluctuations at the subthreshold voltage range, and that Na^+ conductance plays a key role in determining the amplitude of this noise by acting as a voltage-dependent amplifier of low-frequency transients.

*The Interdisciplinary Center for Neural Computation, The Hebrew University, Jerusalem 91904, Israel

49. Backpropagating action potentials in dendrites with stochastic ion channels

Kamran Diba, Christof Koch, Idan Segev*

Stochastic ion channels are a source of variability for signal transmission in neuronal membranes. The thermal environment of neurons results in randomly occurring changes in the conformation of gating proteins. This stochasticity can potentially limit the faithfulness and reproducibility of electrical signal transmission through the membrane. In this paper we numerically simulate the effects of stochastic ion channels on the backpropagation of action potentials into the dendrites of a reconstructed layer 5 pyramidal neuron. We find that in most instances, there is little variation in timing or amplitude for a single backpropagating action potential. However, for trains of action potentials, variable backpropagation can occur. Additionally, we report that dendritic Ca^{2+} spike generation can be susceptible to channel variability.

*The Interdisciplinary Center for Neural Computation, The Hebrew University, Jerusalem 91904, Israel

50. A learning rule for local synaptic interactions between excitation and shunting inhibition

Chun-Hui Mo, Ming Gu, Christof Koch

The basic requirement for direction selectivity is a non-linear interaction between two different inputs in space-time. In some models, the interaction is hypothesized to occur between excitation and inhibition of the shunting type in the neuron's dendritic tree. How can the required spatial specificity be acquired in an unsupervised manner? We here propose an activity-based, local learning model that can account for direction selectivity in visual cortex based on such a local veto operation and that depends on synaptically-induced changes in intracellular calcium concentration. Our

biophysical simulations suggest that a model cell with our learning algorithm can develop direction selectivity organically after unsupervised training. The learning rule is also applicable to a neuron with multiple direction selective subunits, and to a pair of cells with opposite direction selectivities and is stable under different starting conditions, delays and velocities.

51. Modeling extracellular electrical stimulation of unmyelinated axons by symmetric bipolar current pulses

Roberto Valerio, Christof Koch

The overall research question is a biophysical one. To understand at the quantitative level, the effect that a symmetric bipolar current pulse, delivered through an extracellular electrode, has on the firing properties of unmyelinated axons embedded into a resistive medium. Surprisingly, this question has never been addressed using a biophysical detailed model. It is, however, of increasing interest to both the clinical as well as the neuroscience community, as direct neuronal stimulation with such electrodes is increasingly being used to move from mere correlation to causation. Theoretical models of neural excitation are essential for the interpretation of experimental studies of the nervous system and provide a quantitative method for the design of electrodes and stimulus paradigms for functional electrical stimulation. One of the main questions to answer is over what electrical current range can such cortical microstimulation trigger spikes? To investigate this, we used the single cell simulator NEURON as well as Matlab code. After modeling the axonal membrane with the standard Hodgkin-Huxley membrane patch model, we computed the minimum extracellular electrode current needed to get an action potential in an infinite axon for different values of three parameters under study. In particular, we studied the functional dependency of the minimum electrode current from axon diameter, electrode-axon distance and stimulus pulse width. The underlying three-variable function turned out to be approximately separable in the first two variables, and its essential behavior can be captured by a potential function of simple rational and polynomial expressions. As far as we know, ours is the first attempt to characterize in a systematic way the excitation thresholds of unmyelinated nerve fibers when symmetric bipolar current pulses are applied extracellularly. Given the high interests in these results, this project should lead to a significant scientific publication.

52. A synaptic mechanism for computing the maximum of two inputs

Ulf Knoblich, Christof Koch

The MAX function has been postulated to play an important role in object recognition in visual cortex (Riesenhuber and Poggio 1999). It is thought to be essential in order to achieve selectivity and invariance found in complex cells in visual cortex. Recently, evidence for the presence of single cells which compute a soft-MAX

operation has been found in cat primary visual cortex (LampI et al., 2004).

We investigated a model of a synaptic mechanism to perform this computation utilizing both excitatory and inhibitory synaptic conductances for each input. We assume that each input gives rise to an excitatory as well as an inhibitory postsynaptic potential which is created through an interneuron. Due to the nonlinear response properties of the interneuron, the ratio of excitatory to inhibitory input increases with increasing input. This causes the membrane potential to saturate at different levels at the postsynaptic site.

Combining two of these inputs results in a membrane potential that closely resembles the potential induced by the larger of the two inputs ("soft-MAX") because of the local interaction of the excitatory and inhibitory inputs.

This model provides a good fit for the intracellular measurements in a population of complex cells found in cat primary visual cortex. According to the model, saturation occurs at the synapse but not in the cell's soma. This prediction should be easily testable and will guide future experiments.

Reference

LampI, I., Ferster, D., Poggio, T. and Riesenhuber, M. (2004) *J. Neurophysiol.*

Riesenhuber, M. and Poggio, T. (1999) *Nat. Neurosci.* 1019-1025.

53. Model of extracellular potential illustrates factors contributing to the waveform of single unit recordings **in vivo**

C. Gold, D. Henze*, G. Buzsaki*, Christof Koch

We use the Line Source Approximation (Holt and Koch, 1999) to model the extracellular voltage waveform shape and magnitude resulting from the spiking activity of individual neurons. We compare simultaneous intracellular and extracellular recordings of CA1 neurons recorded in vivo (Henze et al., 2000) with model predictions for the same cells reconstructed and simulated with compartmental models. The model includes ionic channel properties and densities based on data collected in studies of CA1 pyramidal cells in vitro (Ina, Ik, Id, Ic, Ia, Im, lahp, In, Il, Ir, It, Ih), along with passive membrane properties that incorporate a detailed spine distribution. We tuned the parameters of the channel model in order to match the simulation to the recordings for all pyramidal cells for which complete histology was available (N=8). The model illustrates how the different components of the membrane current combine to create the variety of features seen in single unit recordings, as well as the role played by the position of the recording electrode with respect to the cell.

*Center for Molecular and Behavior Neuroscience, Rutgers University

Reference

Holt, G.R. and Koch, C. (1999) *J. Neurosci.* 6:169-184.

Henze, D.A., Borhegyi, Z., Csicsvari, J., Mamiya, A., Harris, K.D. and Buzaki, G. (2000) *J. Neurophysiol.* 390-400.

54. Unsupervised spike detection and sorting with wavelets and super-paramagnetic clustering
R. Quian Quiroga, Z. Nadasdy, Y. Ben-Shaul*

This study introduces a new method for detecting and sorting spikes from multi-unit recordings. The method combines the wavelet transform, which localizes distinctive spike features, with super-paramagnetic clustering, which allows automatic classification of the data without assumptions such as low variance or Gaussian distributions. Moreover, an improved method for setting amplitude thresholds for spike detection is proposed. We describe several criteria for implementation that render the algorithm unsupervised and fast. The algorithm is compared to other conventional methods using several simulated data sets whose characteristics closely resemble those of in vivo recordings. For these data sets we found that the proposed algorithm outperformed conventional methods.

*ICNC, The Hebrew University, Jerusalem, Israel

55. Invariant visual representation by single neurons in the human brain
R. Quian Quiroga, L. Reddy, G. Kreiman¹, C. Koch, I. Fried²

We can easily recognize a person or object even if shown from different angles or under strikingly different conditions. How neurons in the brain are capable of achieving this invariant representation is still unclear and has led to different hypotheses, mainly based on theoretical arguments. In this study we address this question by analyzing the responses of neurons in the human medial temporal lobe to different presentations of several individuals and objects. Using a recently proposed spike sorting, we extracted single-unit and multi-unit activity from intracranial recordings in the temporal lobe of epileptic patients candidates who are candidates for surgery. From a total of 64 micro-wires, usually located in the hippocampal structure and adjacent areas, it was possible to isolate between 40 and 80 simultaneously recorded units per experiment. For each patient, we first analyzed single- and multi-unit responses to presentations of about 100 different pictures, comprising famous and non-famous people, animals, landmarks, objects, etc. We selected those images for which at least one unit showed a significant response and in subsequent experimental sessions, we presented different views of those individuals or objects. We observed highly selective neurons that were activated by different presentations of a single individual or object, with very few or no responses to the other presentations. Noteworthy, these responses were in many cases limited to bursts of 5 to 10 spikes in a very limited time range. These results point towards a sparse and invariant representation of individuals by neurons in the human temporal lobe.

¹Massachusetts Institute of Technology

²UCLA Medical School, Department of Neurosurgery

56. Single-trial event-related potentials with wavelet denoising
R. Quian Quiroga, H. Garcia*

The application of a recently proposed denoising implementation for obtaining event-related potentials at the single-trial level is shown. We study its performance in simulated data as well as in visual and auditory event-related potentials. For the simulated data, the method gives a significantly better reconstruction of the single-trial event-related responses in comparison with the original data and also in comparison with a reconstruction based on conventional Wiener filtering. Moreover, with wavelet denoising we obtain a significantly better estimation of the amplitudes and latencies of the simulated ERPs.

For the real data, the method clearly improves the visualization of both visual and auditory single-trial event-related potentials. This allows the calculation of better averages, as well as the study of systematic or unsystematic variations between trials. Since the method is fast and parameter free, it could complement the conventional analysis of event-related potentials.

*Raul Carrea Institute for Neurological Research, FLENI. Montaneses 2325. 1428 - Buenos Aires, Argentina

57. Towards real-time unsupervised spike sorting via template matching

Casimir Wierzynski, R. Quian Quiroga

The extraction and segregation of spiking activity from recordings of extracellular potentials is a longstanding problem in electrophysiology [1]. Quian Quiroga et al., have recently demonstrated [2] a novel and effective strategy using wavelet coefficients and super-paramagnetic clustering (SPC) [3] for unsupervised spike sorting. In this work we investigated techniques for adapting this algorithm for use in real-time applications. To this end, we devised a template-matching scheme that first uses SPC to form templates for each category of spike in a training phase, then classifies new spikes by matching them to the nearest template. We compared six combinations of spike features sets (time and wavelet domain) and distance metrics (Euclidean, Mahalanobis, and nearest neighbor) according to their accuracy on simulated spike data and their computational load. We found combination of features sets and distance metrics such that this template matching is nearly as accurate as SPC and several orders of magnitude faster. Such schemes could therefore be useful in real-time spike sorting applications involving hundreds of simultaneous channels or in embedded systems.

References

- [1] Lewicki, M.S. (1998) *Network: Computation in Neural Systems* 9(4):R53-R78.
- [2] Quian Quiroga, R., Nadasdy, Z. and Ben-Shaul, Y. *Neural Computation*. In press.
- [3] Blatt, M., Wiseman, S. and Domany, E. (1996) *Phys. Rev. Lett.* 76:3251-3254.

58. Selectivity of local field potentials in the human brain
Alexander Kraskov, Rodrigo Quian Quiroga, Christof Koch, Itzhak Fried*

We started to investigate local field potentials in the human temporal medial lobe. The recordings are done from the brain of epileptic patients in collaboration with Dr. Itzhak Fried, UCLA. The main goal of this project is to characterize the selectivity of the LFP's to different image categories (e.g., photos of faces versus pictures of landmark buildings) or to individual images and to study the relationship between the selectivity of single and multi units and the LFPs. That is, if we record from a neuron that shows great selectivity of faces or even to the face of a single individual, will the LFP recorded from the same electrode also show such selectivity or a different one? This would be important for practical purposes since recording LFPs is much easier and more robust to electrode movement than picking up spiking activity from a single neuron. Stimulus selectivity in the LFP would also reveal spatial clustering of neurons, that is, the fact that neurons with similar stimulus selectivity (e.g., to faces) cluster in space.

We are interested in extracting specific information from the LFPs and therefore we choose continuous wavelet transform method to explore time and frequency structure of LFPs. This method allows us to consider selectivity in individual frequency bands (standard electroencephalographic frequency bands δ , θ , α , β , γ) and in different time intervals (well known peaks of evoked responses).

We started from the analysis of power spectrum that looks quite smooth and has a $1/f^\alpha$ appearance with average α about 1.9. Moreover, in many electrodes we found significant oscillations in different frequency bands (e.g., θ , α).

As a preliminary result we found selectivity to animal category in the electrodes that were also selective according to single and multi units.

*UCLA Medical School, Department of Neurosurgery

59. A detection theory account of change detection
Patrick Wilken*, Wei Ji Ma

Previous studies have suggested that visual short-term memory (VSTM) has a storage limit of approximately four items. However, the type of high-threshold model (HTM) used to derive this estimate is based on a number of unattractive assumptions, and has been criticized in other experimental paradigms (e.g., visual search). Here we report findings from nine experiments in which VSTM for color, spatial frequency and orientation was modeled using a signal detection theory (SDT) approach. In Experiments 1-6, two arrays composed of multiple stimulus elements were presented for 100 ms with a 1500 ms ISI. Observers were asked to report in a yes/no fashion whether there was any difference between the first and second arrays, and to rate their confidence in their response on a 1-4 scale. In Experiments 1-3 only one stimulus element difference

could occur ($T = 1$) while set size was varied. In Experiments 4-6, set size was fixed while the number of stimuli that might change was varied ($T = 1, 2, 3, 4$). Three general models were tested against the ROCs generated by the six experiments. In addition to the HTM, two SDT models were tried: one assuming summation of signals prior to a decision, the other using a max rule. In Experiments 7-9 observers were asked to directly report the relevant feature attribute of a stimulus presented 1500 ms previously, from an array of varying set size. Overall the results suggest that observers encode stimuli independently and in parallel, and that performance is limited by internal noise, which is a function of set size.

*Otto von Guericke Universität, Fakultät für Naturwissenschaften, Universitätplatz 2, D-39106 Magdeburg, Germany

60. Humans segregate and integrate auditory and visual signals in a statistically optimal fashion
Ladan Shams*, Wei Ji Ma

Like most animals, humans are endowed with multiple sensory modalities. This attribute poses the nervous system, at any instant, with the eminent problem of estimating which sensory signals have been caused by the same source and should be integrated, and which have been caused by different sources and should be segregated. We report that the rule used by the nervous system for combining and segregating auditory and visual signals is statistically optimal. These results provide the first unifying account for the entire spectrum of cue combination, ranging from no integration, to partial interactions, to complete fusion. Our findings also show that a well-known auditory-visual illusion is indeed an epiphenomenon of this general, statistically optimal strategy.

*Department of Psychology, University of California, Los Angeles, CA

61. Neural mechanisms underlying temporal aspects of conscious visual perception
Wei Ji Ma, Fred Hamker*, Christof Koch

The purpose of this project has been to study fundamental aspects of the time course of visual perception using computational models. In particular, we focused on the phenomenology of feature inheritance, a form of backward masking in which a target stimulus bequeaths a property to a later mask stimulus. This illusion, and its variations, can elucidate why the brain does not always perceive the time course of events in accordance with physical reality, and which neural mechanisms may underlie it.

Our answer to this question is that the brain engages in a form of hypothesis testing, in which input is tested against a template, i.e., an expectation of what the input will be like. When no template is present, it is created from the input, but in an inert fashion. In this way, the target feature – in our model the orientation of a briefly flashed bar – can influence the mask feature. We arrive at this conclusion by carefully examining the different

parameter domains in the illusion. For some parameter values, temporal integration of the stimuli occurs, leading to the percept of a superposition of the two. For others, the percept is feature inheritance. Finally, in the limit of long durations, perception should reflect the physical course of events veridically. These conditions, plus known aspects of perception, such as a threshold on neural activity before a stimulus can be perceived, constrain our model. We model hypothesis testing through a multiplicative interaction, in which the population activity pattern corresponding to the template gets multiplied cell by cell (that is, orientation by orientation) with the bottom-up activity. We argue that this does not necessarily involve feedback into early visual areas; previous authors had claimed such feedback to be pivotal.

*Allgemeine Psychologie, Psychologisches Institut II, Westf. Wilhelms-Universität, Fliednerstrasse 21, 48149 Münster, Germany

62. Face adaptation is reduced by binocular suppression

Farshad Moradi, Christof Koch, Shinsuke Shimojo*

When two dissimilar images are presented to corresponding regions of each eye, one image suppresses the other one from visual awareness. Binocular-suppression has little effect on the build-up of several visual aftereffects (tilt aftereffect, translational motion aftereffect, grating adaptation). Thus, invisible stimuli can penetrate some level of cortical visual processing. However, the global motion aftereffect is reduced in magnitude by rivalry suppression. Here, we used configural adaptation to images of human faces to investigate whether high-level aftereffects are suppressed by rivalry. Human fMRI and monkey electrophysiological studies demonstrate that rivalry modulates activity in cortical areas involved in processing faces and objects, although there is evidence from human fMRI that perceptually invisible images still can affect those areas. Participants were trained to identify four individuals. Different identity strengths were created by morphing the original stimuli with an average face. We demonstrated that four seconds of adaptation in the non-dominant eye significantly shifts the psychometric function. Suppression was induced during adaptation by presenting a moving pattern to the dominant eye. Observers monitored the visibility of the face by holding a key down. When the adapting face was perceptually suppressed for less than 3 sec, the aftereffect was comparable in magnitude to the control condition. However, when the adaptor was invisible for more than 3 sec, there was no shift in the psychometric function ($p < 0.01$). This indicates that the neural mechanisms underlying configural adaptation to faces depend, at least in part, on perceptual awareness.

*Professor of Biology, Caltech

63. Neural correlates of preattentive face-gender discrimination

Leila Reddy, Farshad Moradi, Christof Koch

Recently, fMRI studies have reported that activity in the Fusiform Face Area (FFA) is reduced or eliminated in the absence of attention. In these studies, an "attended" condition (where subjects make a behavioral report on face images) is compared to an "unattended" condition where another task is performed and the faces are behaviorally irrelevant. It is unclear, however, how activity correlates with behavioral performance (since there is no required performance for unattended faces), and thus if the observed decrease in activity is purely due to the lack of top-down attention or if it is explained by the behavioral irrelevance of the faces. Recently, using a dual-task paradigm, we showed that the attentional cost associated with face-gender discrimination is minimal. When subjects reported the gender of a peripherally presented face while performing an attentionally engaging task at fixation, their performance suffered but little compared to when attention was available. In this condition, minimal attentional resources are available to the peripheral face, but it remains behaviorally relevant. Thus we are in a position to determine how neural activity varies with behavioral performance and attentional modulation. We use fMRI to examine the effects of attention on brain activation using the dual-task paradigm. Preliminary results show that FFA activity is mostly unaffected by whether subjects perform the face task alone (peripheral-task condition) or in conjunction with the central task (dual-task condition). Interestingly, the activity is decreased in the "central-task" condition when the faces are still present but are behaviorally irrelevant. This latter result is consistent with previous reports: neural activity is affected by the behavioral relevance of stimuli. In addition, however, the fact that FFA activity is maintained in the dual-task condition indicates that attentional manipulation per se leaves both performance and neural activity unaffected.

64. Visual awareness and the neural correlate of orientation selective adaptation

Constanze Hofstoetter*, Farshad Moradi, Christof Koch

We used fMRI to investigate orientation selective adaptation (OSA) in visual cortex and its correlation with visual awareness. Psychophysical studies have demonstrated that OSA does not require visual awareness, and hence it presumably originates in early visual areas. Seven participants viewed high-contrast grating patterns in a 3T scanner (EPI, TR=2s, TE=30ms). The visual display was divided into seven regions (co-centric rings covering the upper visual field). Corresponding retinotopic maps for each ring were determined using separate localizers (two runs) for each participant in the occipital lobe. Each ring was composed of a grating (of either 45 or 135 deg stripes, random width 0.1-2 deg) which flickered at 2.5 Hz and flipped its orientation every 30-50s (10 runs*6 flips/ring). Participants were asked to monitor the rings

and report those that flipped. On average, they missed the change in orientation in more than half of the trials due to crowding and flickering that masked changes in orientation, in particular for the peripheral rings. When correctly reported, the change in orientation was accompanied by a small but highly significant increase in BOLD signal ($0.15 \pm 0.02\%$, $p < 1.2e-8$). This increase may reflect the transient associated with the change in orientation, or it may signal that a subpopulation of neurons that are not adapted is being stimulated. However, when the observers failed to notice the change in orientation, there was no increase in activity ($0.007 \pm 0.02\%$). In the few trials that the location of the change was misperceived, there was a significant increase in the activity at the reported location. These findings indicate that the increase in BOLD activity in early visual cortex can reflect the consciously perceived change, a signal presumably originating in higher stages. These results imply that attention and awareness are important confounding factors in fMRI adaptation studies.

¹Institute of Neuroinformatics, ETH/University of Zurich, Zurich, Switzerland

65. Absence of visual awareness does not affect the formation of negative afterimages
Constanze Hofstoetter*, Christof Koch, Daniel C. Kiper*

Researchers set out only recently to tackle the neural correlates of consciousness (NCC) by scientific means. One promising strategy has been to study conditions during which a visual stimulus is present, but observers fail to perceive it. The key question is what type of information processing occurs in the absence of visual awareness. Investigating this issue allows us to gain insight into those sites that mediate conscious visual perception.

Visual aftereffects, i.e., visual traces observed after prolonged exposure to an adapting stimulus, offer a powerful tool to approach this question. Various techniques have been employed to investigate if aftereffects can be induced by perceptually invisible stimuli. Here we present a novel technique exploiting the phenomenon of motion-induced blindness (MIB; Bonneh et al., 2001). In MIB, salient target stimuli become intermittently perceptually suppressed when superimposed on a moving background. We aimed to determine whether suppression of a visual stimulus by MIB has any effect on the strength and duration of the negative afterimage it induces.

Subjects had to report on their perception of two moderate-intensity yellow squares during the adaptation phase. Subsequently, they were asked to rate the intensity and persistence of the negative afterimages that were induced by these adapting stimuli. In MIB trials, the yellow squares were presented superimposed on a cloud of moving blue dots and thereby became intermittently perceptually invisible. In "playback" trials no moving background was present, but the squares were physically

removed mimicking the subjects' local percept in the previous MIB trial.

Our results show that the persistence and intensity of negative afterimages are determined entirely by the physical, not the perceptual exposure to an adapting stimulus. This implies that visual awareness of the adapting stimulus is not required for the generation of afterimages. Therefore, the neural substrate responsible for the formation of negative afterimages must precede that supporting visual awareness for these stimuli. This finding is consistent with assigning the formation of afterimages solely to low-level processes, such as the adaptation of cells in the retina and LGN. Our results strengthen the hypothesis that neural activity early in the visual system is not sufficient for conscious perception. They also demonstrate that the NCC occur at distinct stages in the visual hierarchy.

*Institute of Neuroinformatics, ETH/University of Zurich, Zurich, Switzerland

Reference

Bonneh, Y.S., Cooperman, A. and Sagi, D. (2001) *Nature* 411:798-801.

66. Non-local cortical interactions help determine where to look in natural scenes
Robert J. Peters, Asha Iyer, Laurent Itti*, Christof Koch

Recent research (Parkhurst et al., *Vis. Res.* 2002) showed that a model of bottom-up visual attention can account in part for the spatial positions of locations fixated by humans while free-viewing complex natural and artificial scenes. That study used a definition of salience based on local detectors with coarse global surround inhibition. Here, we use a similar framework to investigate the roles of a variety of non-linear interactions known to exist in the visual cortex, and of eccentricity-dependent processing. For each of these, we added a component to the salience model, including richer interactions among orientation-tuned units, both at spatial short-range (for clutter reduction) and long-range (for contour facilitation), and a detailed model of eccentricity-dependent changes in visual processing. Subjects free-viewed naturalistic and artificial images while their eye movements were recorded, and the resulting fixation locations were compared with the models' predicted salience maps. We found that the proposed interactions indeed play a significant role in the spatiotemporal deployment of attention in natural scenes; about half of the observed inter-subject variance can be explained by these different models. This suggests that attentional guidance does not depend solely on local visual features, but must also include the effects of non-local interactions. As models of these interactions become more accurate in predicting behaviorally relevant salient locations, they become useful to a range of applications in computer vision and human-machine interface design.

*USC

Reference

Parkhurst, D., Law, K. and Niebur, E. (2002) *Vis. Res.* 42:107-123.

67. What do we see when we glance at a scene?

Asha Iyer, Fei Fei Li¹, Pietro Perona²

What exactly do we see when we glance at a scene? And does what we see change as the glance becomes longer? We asked naïve subjects to report what they saw in briefly presented photographs. Our subjects received no specific information as to the content of each stimulus, and were asked to report what they saw in free-form text. Thus, our paradigm differs from previous studies where subjects were either cued before a stimulus was presented, and/or were probed with multiple-choice questions. Our experiment consisted of two stages. First a group of 22 native English-speaking subjects were shown 100 novel gray-scale photographs foveally. The photographs contained a broad sample of indoor and outdoor real-life scenarios. Each presentation time was chosen at random from a set of seven possible times (from 27 ms to 500 ms). A perceptual mask followed each photograph immediately. After each presentation subjects reported what they had just seen as completely as possible. In the second stage, another group of sophisticated individuals who were not aware of the goals of the experiment were instructed to score each of the descriptions produced by the subjects in the first stage. Individual scores pertained to specific attributes, representing different categories of content. For example, scores were ascribed for attributes such as edges, contours, shapes, colored patches (reflecting sensory data); urban, rural, forest, ocean, household rooms, etc. (reflecting scene-related information); furniture, vehicles, trees, rocks, roads, bridges, etc. (reflecting inanimate object-related information); mammals, birds, aquatic life, presence/gender/identity of people, etc. (reflecting animate object-related information); these were a small subset of the attributes assessed. We find that sensory data is reported before object recognition or scene identification. Object- and scene-related information was reported with a similar timecourse. The presence of animals and people were reported early, often with display times below 50 ms. Scene recognition and slightly coarser than entry-level object categorization were accurately performed within 100 ms.

¹Graduate Student, Electrical Engineering, Caltech

²Professor, Electrical Engineering, Caltech

References

Biederman, I., Mezzanote, R.J. and Rabinowitz, J.C. (1982) *Cogn. Psychol.* 14:143-177.

Hollingworth, A. and Henderson, J.M. (1998) *J. Exp. Psychol.* 127(4):398-415.

68. Biasing the percept of ambiguous visual stimuli

Melissa Saenz, Christof Koch

Ambiguous visual stimuli evoke unstable percepts that spontaneously alternate between different interpretations over time. In a recent report (Leopold et al., 2002) this percept was stabilized, even frozen, onto a particular interpretation when the ambiguous stimulus was presented intermittently rather than continuously. Here we report that intermittent viewing can also destabilize an ambiguous percept - reliably inducing a perceptual reversal with every stimulus onset. The ambiguous figure used here was a structure-from-motion rotating cylinder presented 5 deg in the periphery. This 2-D pattern of moving dots yields a strong percept of a 3-D cylinder whose direction of rotation spontaneously reverses between two opposing interpretations (in this case, up or down) during continuous viewing. The cylinder stimulus was shown for on-times of 1 sec separated by blank-times in which only the fixation point was present. The duration of the blank-time (0, 200, 400, 800, 1600, or 3200 ms) was varied in separate blocks. After blank-times of 200ms the percept typically reversed with every stimulus onset, while for gap times of 3200 ms the percept was more likely to stay the same (replicating the previously reported freezing effect). For intermediate blank-times, there was a smooth transition between the "reversing" and "freezing" phenomena. This pattern was highly consistent across subjects (n=10) and also occurred when the stimulus was presented foveally. The phenomena may thus reveal the involvement of two different visual memory systems operating over different time scales. Further experiments revealed that both the reversing and freezing effects can be evoked even when the stimulus changes location (moving to the opposite visual hemifield) with each onset. This suggests that perceptual reversals are not driven simply by local sites of motion adaptation, but may reflect competition between global object interpretations.

References

Leopold, D.A., Wilke, M., Maier, A. and Logothetis, N.K. (2002) *Nature Neurosci.* (2002) 5:605-609.

69. Binding "hardwired" vs. "arbitrary" feature conjunctions

Rufin VanRullen

Binding is often referred to as the process by which basic features of an object are conjoined within the focus of attention to allow recognition. We have previously argued, however, that certain high-level "objects" can be recognized outside the focus of attention. We proposed that binding exists, in fact, under two forms. The visual system heavily relies on 'hardwired' binding whereby relevant objects and feature conjunctions are selectively coded by dedicated neuronal populations (e.g., faces, animals, color-orientation conjunctions). Attention is not required for this form of binding, but must sometimes be engaged to resolve spatial competition within a receptive field. Without such 'hardwired'

selectivities, binding of arbitrary feature conjunctions can still occur but necessitates attention (e.g., bisected two-color disks, randomly rotated letters). Here we verify that the first postulated form of binding ('hardwired') is indeed preattentive, but only parallel when stimuli are reasonably separated: under dual-task conditions where full attention is unavailable, a single peripheral animal, face or color-orientation conjunction can be recognized, but will suffer from the addition of a second distracting stimulus (natural scene, face, etc.), only if it is placed in the vicinity of the target stimulus. In other words, the 'hardwired binding' problem might be receptive-field specific. This is confirmed by a second experiment in which two simultaneous masked stimuli must be compared. The SOA is chosen so that a similar stimulus in isolation is easily identified. With animal vs. non-animal scenes, human faces or color-orientation conjunctions, this comparison task can be performed with well separated but not with neighboring stimuli. In contrast, bisected disks or randomly rotated letters cannot be compared even at large spatial separations (see Figure). Thus, while 'arbitrary' binding always requires attention, 'hardwired' binding only does when receptive field competition occurs.

References

- VanRullen, R. (2003) *J. Physiol. (Paris)* 97:207-213.
 VanRullen, R. and Dong, T. (2003) *Vis. Res.* 43(21):2191-2196.
 VanRullen, R., Reddy, L. and Koch, C. (2004) *J. Cog. Neurosci.* 16(1):4-14.

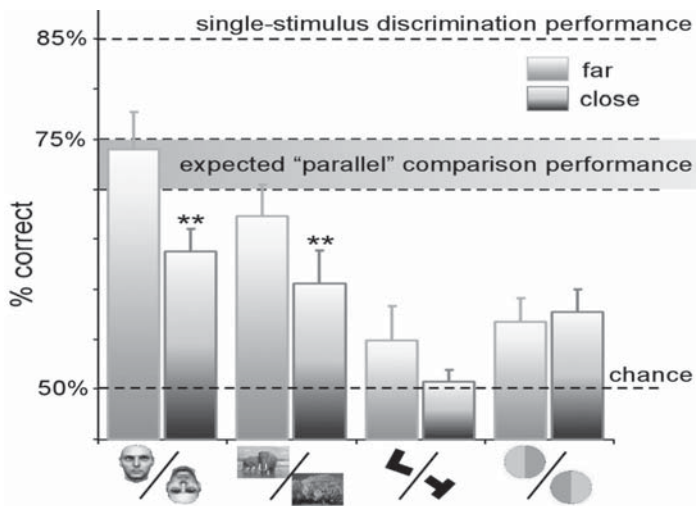


Figure: Performance of the comparison task for four different visual discriminations (upright vs. inverted faces, animal vs. non-animal scenes, rotated L vs. T, bisected disks), and two stimulus separations ('far,' 'close'). The 'synthetic' stimuli on the right cannot be discriminated in parallel, whatever the inter-stimulus separation. On the other hand, the 'natural' discriminations on the left are easily performed with well-separated stimuli, but suffer a 'local binding problem' when the stimuli to be compared lie too close.

70. The attentional requirements of face recognition

Lavanya Reddy, Christof Koch, Pietro Perona*

The attentional requirements of a face recognition task were investigated using two paradigms. With the dual-task paradigm, we found that subjects were able to recognize famous faces remarkably well even in the near-absence of attention. A recent study has demonstrated the existence of neuronal populations selective to particular faces: perhaps the existence of these selectivities is what allows face recognition to occur in the absence of attention. On the contrary, the same face recognition task in the Rapid Serial Visual Presentation (RSVP) method led to an "attentional blink." The apparent contradiction in the two sets of results suggests that the two paradigms might be testing different kinds of attention: this lays a foundation for further investigation of the differences between spatial and temporal modes of attention.

*Professor, Electrical Engineering, Caltech

Reference

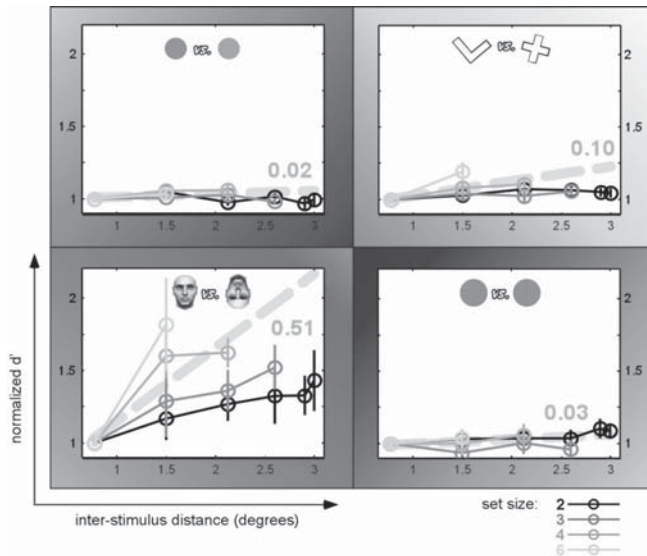
- Reddy, L., VanRullen, R. and Koch, C. Manuscript submitted.
 VanRullen, R., Reddy, L. and Koch, C. (2004) *J. Cog. Neurosci.* 16(1):4-14.

71. Clutter effects in visual search: Human psychophysics

Lavanya Reddy, Rufin VanRullen, Christof Koch

Recent experiments from the Koch lab have revealed that categorization of an isolated natural scene or object could be performed in the near absence of attention (Li et al., 2002; Reddy et al., 2004). Surprisingly, the same tasks were performed poorly in visual search conditions where a target must be detected among multiple distractors. We have proposed that for these natural scenes and objects, parallel visual search performance – the hallmark of preattentive processing – might be impaired by receptive fields clutter (VanRullen et al., 2004). To demonstrate this, we used a modification of the visual search paradigm in which we varied parametrically the set size (number of elements presented) and the inter-stimulus distance (an inverse measure of clutter). We found that, only in the case of a task involving natural target objects (face photographs), decreasing clutter could yield significant performance improvements in visual search (in fact, sensitivity was found to increase by more than 50% for each 1° increase in inter-stimulus distance). This result is a significant first step in bridging the gap between attentional requirements recorded on isolated stimuli (dual-task) and those estimated from cluttered displays (visual search). Further, it provides a human psychophysics counterpart to the electrophysiological experiments of DiCarlo, investigating clutter effects in visual cortex.

Figure 1. In four different tasks, representing the various possible outcomes of visual search and dual-task experiments, we varied parametrically the set size (number of elements presented) and the amount of clutter (as assessed by the inter-stimulus distance). For only one of these tasks (upright vs. inverted faces) does decreasing clutter lead to a dramatic improvement in visual search performance. This result is a critical step to understanding why natural objects can be processed preattentively when presented in isolation (e.g., dual-task) but not in cluttered displays (e.g., visual search).



72. Continuous flash suppression Naotsugu Tsuchiya, Christof Koch

Visual illusions that produce perceptual suppression despite constant retinal input, such as binocular rivalry (BR) or flash suppression (FS), are potent tools to study the neural correlates of consciousness. However, the duration and timing of perceptual suppression in BR are difficult to control, and FS attains only short duration of suppression, too short to produce aftereffect. Furthermore, FS requires pre-adapting period, which makes it impossible to use in studies that require complete perceptual unawareness. Here, we introduce Continuous Flash Suppression (CFS). With CFS, we can control the timing of suppression and suppress stimuli for long duration (> several minutes) without subjects noticing the suppressed stimuli at all. We used several categories of figures (Gabor patches and angry faces) as suppressed stimuli and other categories as continuously changing dominant stimuli (Gabor patches of different orientations, random textures consisted of small color rectangles, gray or color neutral faces, scrambled faces). Both stimuli were presented at the fovea (10x10 deg, with a stereoscope, 50 cm from the display). The dominance duration of suppressed stimuli during a 60s trial was the observation variable. As the contrast and saliency of suppressed stimuli decreases, dominance duration of the suppressed figure decreases. As suppressed stimuli are low-pass filtered, the dominance of the suppressed figure decreases. ISI between dominant stimuli is crucial; in general, short

ISI (<1 sec) produces strong and prolonged suppression. Under a wide range of parameters, a stimulus that usually dominates about 30s in a 60s BR trial can be suppressed completely (i.e., 0s dominance in 60s trial). We report a classical human fear conditioning study that utilized CFS. Subjects could report their on-going subjective visibility of figures during 2s stimuli presentation, while they tried to associate electrical shocks with angry face stimuli that were completely masked by CFS.

73. Awareness in fear conditioning Naotsugu Tsuchiya, McKell Carter, Christof Koch

We studied the relationship between the degree of human fear conditioning using skin conductance response and the degree of CS-US contingency awareness using on-line report of shock expectancy. Our protocol was similar to that in Carter et al., (2003) unless specified. We compared the relationship between delay (n=8) and trace group (n=7) using a differential conditioning protocol. Subjects had to indicate their shock expectancy by moving their eyes along an axis on the monitor. In the trace group, the correlation coefficient r was 0.81 ($p < 0.05$), while r was 0.47 ($p > 0.2$) in delay. Thus, trace conditioning demonstrates a significant dependence on awareness while delay conditioning does not. We also used a within-subject paradigm, where trace/delay differential conditioning was employed within a single experiment. Using three auditory CSs, we confirmed our previous results: $r = 0.64$ ($p < 0.03$) in trace while $r = 0.18$ ($p > 0.5$) in delay (n=12 for each). We then tried to replicate unconscious fear conditioning with fear-relevant CSs, hypothesizing that unconscious conditioning would be stronger in delay because it was less dependent on awareness. To have enough time to monitor on-line awareness via key press, we presented a fear-relevant CS in one eye, while showing to the other eye neutral images that were replaced every 100 ms for 2 seconds. This 10 Hz flickering stimulus reliably suppressed the contralateral stimulus from awareness, acting as a "continuous flash suppression." None of the 13 subjects became aware of the contingency (on-line expectancy $p > 0.2$) or noticed the presence of the suppressed fear-relevant CS at any of 78 trials (verbal report). Under these conditions showing no on-line expectancy or no perception of fear-relevant CS picture, no delay conditioning ($p > 0.2$) was observed.

Reference

Carter, R.M., Hofstoetter, C., Tsuchiya, N. and Koch, C. (2003) Proc. Natl. Acad. Sci. USA 100:1399-1404.

74. Prefrontal activity covaries with explicit knowledge of CS/US contingency in human aversive conditioning Ronald McKell Carter

We sought to address the neural representation of explicit and implicit knowledge. Our experimental approach involved using BOLD fMRI to ascertain the neural substrate underlying contingency awareness during

delay and trace human aversive conditioning. Four abstract images were randomly assigned to one of four trial types: delay CS+, trace CS+, or one of two unpaired baseline stimuli (CS-) during concurrent aversive delay and trace conditioning. CS+ trials were reinforced with a mild electric shock (US) 50% of the time. Forty-four slice tilted axial images were acquired using a 3T head-only scanner. Subjects were asked to indicate their shock expectancy by pressing one of three buttons (shock, unsure or no shock). Skin conductance (SC) and expectancy responses for each trial were then used as parametric regressors of conditioning. Analyses of fourteen subjects were conducted as the conjunction of trace and delay conditioning and reinforced and non-reinforced trials. Results comparing hemodynamic activity for CS+ > CS- trials replicate the majority of activity demonstrated by human fMRI studies of aversive conditioning. Bilateral middle frontal gyrus (DLPFC) BOLD responses were correlated with accurate online shock expectancy to differing degrees that reflected the subject's ability to accurately describe the CS/US relationship using a second assessment of explicit knowledge (post-experimental questionnaire). These results are consistent with previous imaging work in the related areas of cognitive re-assessment and working memory. Para-hippocampal and amygdala BOLD responses correlated with the amplitude of normalized skin conductance responses on each trial in a manner reflecting the strength of conditioning (as measured by the average CS+,CS- skin conductance response difference).

75. Detection and tracking of objects in underwater video

D. Walther, D.R. Edgington*, C. Koch

For oceanographic research, remotely operated underwater vehicles (ROVs) routinely record several hours of video material each day. Manual processing of such large amounts of video has become a major bottleneck for scientific research based on this data. We have developed an automated system that detects and tracks objects that are of potential interest for human video annotators. By pre-selecting salient targets for track initiation using a selective attention algorithm, we reduce the complexity of multi-target tracking, in particular of the assignment problem. Detection of low-contrast translucent targets is difficult due to variable lighting conditions and the presence of ubiquitous noise from high-contrast organic debris ("marine snow") particles. We describe the methods we developed to overcome these issues and report our results of processing ROV video data.

*Monterey Bay Aquarium Research Institute

Reference

IEEE International Conference on Computer Vision and Pattern Recognition (2004) 1:544-549.

76. Is bottom-up attention useful for object recognition?

U. Rutishauser, D. Walther, C. Koch, P. Perona*

A key problem in learning multiple objects from unlabeled images is that it is a priori impossible to tell which part of the image corresponds to each individual object, and which part is irrelevant clutter which is not associated to the objects. We investigate empirically to what extent pure bottom-up attention can extract useful information about the location, size and shape of objects from images and demonstrate how this information can be utilized to enable unsupervised learning of objects from unlabeled images. Our experiments demonstrate that the proposed approach to using bottom-up attention is indeed useful for a variety of applications.

*Professor, Electrical Engineering, Caltech

Reference

IEEE International Conference on Computer Vision and Pattern Recognition (2004) 2:37-44.

77. On the usefulness of attention for object recognition

Dirk Walther, Ueli Rutishauser, Christof Koch, Pietro Perona*

Today's object recognition systems have become very good at learning and recognizing isolated objects or objects in images with little clutter. However, unsupervised learning and recognition in highly cluttered scenes or in scenes with multiple objects are still problematic. Faced with the same issue, the brain employs selective visual attention to select relevant parts of the image and to serialize the perception of individual objects. In this paper we demonstrate the use of a computational model of bottom-up visual attention for object recognition in machine vision. By comparing the performance of David Lowe's recognition algorithm with and without attention, we quantify the usefulness of attention for learning and recognizing multiple objects from complex scenes, and for learning and recognizing objects in scenes with large amounts of clutter.

*Professor, Electrical Engineering, Caltech

Reference

2nd International Workshop on Attention and Performance in Computational Vision 2004 (2004) 1:96-103.

78. Unsupervised learning and control provide ambient intelligence to smart buildings

U. Rutishauser, J. Trindler, R. Douglas

Buildings are changing their nature from static structures of bricks and mortar to dynamic work and living environments that actively support and assist their inhabitants. These new buildings are expected to behave intelligently. Engineering such a system poses a number of challenges. Decisions must be made in near-real time. The system must have a way to interact with its users to obtain feedback. On the other hand, it should not intrude

on the user. In this article we particularly highlight the problem from a machine-learning perspective.

Reference

The Neuromorphic Engineer (2004) 1:3-4.

Publications

Carter, R.M., Hofstoetter, C., Tsuchiya, N. and Koch, C. (2003) Working memory and fear conditioning. *Proc. Natl. Acad. Sci.* 100:1299-1404.

Crick, F. and Koch, C. (2004) What are the neuronal correlates of consciousness? In: *Problems in Systems Neuroscience*, L. van Hemmen and T.J. Sejnowski, eds., Oxford University Press, New York, NY. In press.

Crick, F.C. and Koch, C. (2004) Consciousness, the neural correlates of. In: *The Oxford Companion to the Mind*, 2nd edition, R.L. Gregory and O.L. Zangwill, eds. In press.

Crick, F. and Koch, C. (2003) A framework for consciousness. *Nature Neurosci.* 6:119-127.

Crick, F.C., Koch, C. Kreiman, G. and Fried, I. (2004) Consciousness and neurosurgery. *Neurosurgery* 55:273-282.

Edgington, D., Walther, D., Salamy, K.A., Risi, M., Sherlock, R.E. and Koch, C. (2003) Automated event detection in underwater video. In: *MTS/IEEE Oceans 2003*, San Diego, CA.

Gabbiani, F., Krapp, H.G., Hatsopoulos, N., Mo, C., Koch, C. and Laurent, G. (2004) Multiplication and stimulus invariance in a looming-sensitive neuron. *J. Physiol.* In press.

Gold, C. and Sollich, P. (2004) Model selection for support vector machines. *Neurocomputing.* In press.

Hamker, F.H. (2003) The reentry hypothesis: Linking eye movements to visual perception. *J of Vision* 3: 808-316.

Hamker, F.H. (2004) Predictions of a model of spatial attention using sum- and max-pooling functions. *Neurocomputation.* In press.

Han, C.J., O'Tuathaigh, C.M., van Trigt, L., Quinn, J.J., Faselow, M.S., Mongeau, R., Koch, C. and Anderson, D.J. (2003) Trace but not delay fear conditioning requires attention and the anterior cingulate cortex. *Proc. Natl. Acad. Sci. USA* 100:13087-13092.

Han, C.J., O'Tuathaigh, C.M. and Koch, C. (2004) A practical assay for attention in mice. In: *Cognitive Neuroscience of Attention*, Posner, M.I., ed., Guilford Press, New York. pp. 294-312.

Herzog, M.H., Parish, L., Koch, C. and Fahle, M. (2003) Fusion of competing features is not serial. *Vis. Res.* 43:1951-1960.

Hofstoetter, C., Koch, C. and Kiper, D. (2004) Absence of visual awareness does not affect the formation of negative afterimages. *Consci. Cognition.* In press.

Koch, C. (2004) *The Quest for Consciousness: A Neurobiological Approach.* Roberts and Company, Publishers, Boulder, CO.

Koch, C. (2004) Qualia. *Curr. Biol.* 14(13):R496.

Koch, C. and Crick, F.C. (2004) The Neuronal Basis of Visual Consciousness. In: *The Visual Neurosciences.*

L. Chalupa and J.S. Werner, eds., MIT Press, Cambridge, Massachusetts, pp. 1682-1692. 2004.

Koch, C. and Crick, F.C. (2004) The neuronal basis of visual consciousness. In: *The Visual Neurosciences*, L. Chalupa and J.S. Werner, eds., MIT Press, Cambridge, MA.

Li, F.F., VanRullen, R., Koch, C. and Perona, P. (2004) Why does natural scene categorization require little attention? Exploring attentional requirements for natural and synthetic stimuli. *Visual Cognition.* In press.

Ma, W.J., Hamker, F. and Koch, C. (2004) Neural mechanisms underlying temporal aspects of conscious visual perception. In: *The First Half Second: The Microgenesis and Temporal Dynamics of Unconscious and Conscious Visual Processes.* H. Ogmen and B.G. Breitmeyer, MIT Press. In press.

Mo, C-H., Gu, M. and Koch, C. (2004) A learning rule for local synaptic interactions between excitation and shunting inhibition. *Neural Comput.* In press.

Peters, R.J., Gabbiani, F., and Koch, C. (2003) Human visual object categorization can be described by models with low memory capacity. *Vis. Res.* 43:2265-2280.

Reddy, L., Wilken, P. and Koch, C. (2004) Face-gender discrimination is possible in the near-absence of attention. *J. of Vision* 4:106-117.

Rutishauser, U., Walther, D., Koch, C. and Perona, P. (2004) Is attention useful for object recognition? *IEEE International Conference on Computer Vision and Pattern Recognition II*, 37-44.

VanRullen, R. and Koch, C. (2003) Visual selective behavior can be triggered by a feed-forward process. *J. Cogn Neurosci.* 15:209-217.

VanRullen, R. and Koch, C. (2003) Competition and selection during visual processing of natural scenes and objects. *J. of Vision* 3:75-85.

VanRullen, R. and Koch, C. (2003) Is perception discrete or continuous? *Trends Cogn. Sci.* 7:207-213.

VanRullen, R. and Koch, C. (2004) Visual attention and visual awareness. In: *Handbook of Clinical Neurophysiology*, G. Celesia, ed., Elsevier Press. In press.

VanRullen, R., Reddy, L. and Koch, C. (2004) Visual search and dual-tasks reveal two distinct attentional resources. *J. Cogn. Neurosci.* 16:4-14.

Walther, D., Edgington, D., Salamy, K.A., Risi, M., Sherlock, R.E. and Koch, C. (2003) Automated video analysis for oceanographic research. In: *IEEE International Conference on Computer Vision and Pattern Recognition (CVPR 03)*, Madison, WI.

Walther, D., Edgington, D.R., Koch, C. (2004) Detection and tracking of objects in underwater video. *IEEE International Conference on Computer Vision and Pattern Recognition I*, 544-549.

Walther, D., Rutishauser, U., Koch, C. and Perona, P. (2004) On the usefulness of attention for object recognition. *2nd Workshop on Attention and Performance in Computational Vision at the European Conference for Computer Vision*, 96-103.

Bing Professor of Behavioral Biology: Masakazu Konishi
 Member of the Professional Staff: Eugene Akutagawa
 Senior Research Fellow: José Luis Peña
 Research Fellow: Theresa Nick
 Postdoctoral Scholars: Yuichiro Hayashi, Sharad Shanbhag, Dai Watanabe
 Research and Laboratory: Maria Lucia Pérez
 Graduate Student: Bjorn Christianson

Support: The work described in the following research reports has been supported by:

Bing Professor Research Pool
 National Institute of Mental Health
 National Institute on Deafness and Other Communication Disorders

Summary: Our group has become small after the departure of six members during the last two years. Kazuo and Yasuko Funabiki returned to Kyoto University and Yuichiro Hayashi joined Kazuo as an assistant. Teresa Nick is now an assistant professor at the University of Minnesota and Anthony Leonardo is a postdoctoral fellow in the laboratory of Markus Meister at Harvard. Anthony has received a Helen Hay Whitney Fellowship and also a Young Investigator Award from the International Society for Neuroethology. Ben Arthur is a postdoctoral fellow in the laboratory of Ron Hoy at Cornell University.

Our research projects on songbirds and owls continue. Postdoctoral fellow Dai Watanabe, an expert in both molecular biology and neurobiology, and Gene Akutagawa work on the mechanisms of central auditory gating. Gene's expertise in histology has revealed new connections between the song control system and other parts of the brain. These connections may explain the relationships between sleep and neuronal responses to the bird's own song. In zebra finches, neurons within the song control system respond to the birds' own song only when the bird is asleep or under anesthesia.

We have four people working on the owl's auditory system. Space-specific neurons in the owl's midbrain respond selectively to sound coming from a particular direction, because they are tuned to specific combinations of interaural time and level differences, which define the owl's auditory space. We previously showed that the space-specific neuron multiplies postsynaptic potentials from the time and level processing pathways. Jose Luis Peña now finds that the rule of multiplication applies even when the input from the time pathway is greatly reduced. Bjorn Christianson and Jose are working on another mathematical process that the owl's brain performs. Lucia and Jose are finding basic physiological differences between the auditory pathway that goes to a terminal in the midbrain and the one that goes to the thalamus in the owl. They find few neurons that satisfy the definition of space-specific responses in the thalamus. Sharad Shanbhag has been assembling and testing a new electrode-drive system for recording from the behaving owl.

79. Nucleus Uvaeformis controls auditory responsiveness of HVC in the zebra finch song system
 Yuichiro Hayashi

Songbirds learn their vocalizations in their early-stage of life. Neurons of the vocal motor pathway of songbirds convey neural signals for song production and respond to auditory stimuli only when the bird is silent, asleep or under anesthesia. This behavioral state-dependent modulation or gating has been observed in nucleus HVC and its efferent target RA. We have recently shown that auditory response of Nif, a major source of auditory input to HVC, is also modulated by behavioral state. This result indicates that Nif relays the behavioral state-dependent change of auditory responses of other nuclei in the vocal motor pathway. One candidate controlling this modulation (gating) is thalamic nucleus Uvaeformis (Uva) that projects to both Nif and HVC. To understand how this gating of auditory responses occurs, we tested whether stimulation of Uva affects HVC activity or not. Electrical stimulation of Uva in the anesthetized bird completely inhibited both ongoing and auditory activity in HVC. Interestingly, the inhibition caused by single brief (100 ms) stimulation of Uva lasted ~1 min, and then the spontaneous and auditory activity of HVC gradually recovered. The result supports the idea that Uva controls the gating of auditory activity in the vocal motor pathway.

80. Running cross-correlation in the owl's nucleus laminaris
 Gestur Bjorn Christianson, José Luis Peña

The response of nucleus laminaris neurons of barn owls is tuned to interaural time difference (ITD). These and similar neurons in mammals are thought to perform a running (local) cross-correlation between neural signals encoding binaural auditory stimuli. However, the theoretical significance of the local nature of this computation has never been fully examined. We derived an analytic expression of the running cross-correlation of arbitrary stimuli in terms of the Fourier series, and tested the predictions of this theory.

Laminaris neurons respond in a phase ambiguous manner, where ITDs separated by integer multiples of the period of the stimulating frequency elicit similar responses. When a broadband noise stimulus is used, the response is similarly ambiguous for ITDs close to the characteristic delay (CD) of the neuron. However, as the difference between the ITD and the CD increases, the rate of response gradually declines and the frequency of oscillation of the ITD curve drifts. The existence, time-scale, and magnitude of this effect are consistent with the predictions of the running cross-correlation model, which attribute it entirely to the effective frequency tuning of the neuron. The relationship between the ITD tuning and the effective frequency tuning of the neurons was studied using both iso-intensity frequency stimulation and reverse correlation techniques. Frequency tuning properties could

be derived entirely by the ITD curves of the neurons, and vice versa.

81. Frequency convergence in the auditory thalamus of the owl

María Lucía Pérez, José Luis Peña

The owl's forebrain and optic tectum contain "space-specific neurons" that are selective for the direction of sound propagation. Their spatial receptive fields result from the sensitivity to combinations of interaural time (ITD) and intensity differences across frequency. The neural pathways that lead to the thalamic and tectal representation of auditory space are separate, before receptive fields tuned to a unique and restricted area of space are synthesized. The first nuclei of these pathways are the nucleus ovoidalis (OV) and the external nucleus of the inferior colliculus (ICx), respectively. Both receive projections from the lateral shell of the inferior colliculus (ICIs) but are not interconnected. Whereas the map of auditory space of ICx has been extensively studied, little is known about how auditory spatial cues are combined in single neurons of the thalamic pathway.

We examined how OV neurons responded to ITDs in different frequency bands. Of the neurons tuned to ITD (n=194), those broadly tuned to frequency (n=94) responded preferentially to only one value of ITD, when the stimulus was broadband. However, their selectivity to ITD as measured with tones varied for different frequencies, in contrast to space-specific neurons of the tectal pathway. Although the owl's brain can encode time at high frequencies, some OV neurons showed ITD sensitivity restricted to the low frequency bands. We used tracers to identify the ICIs neurons that project to the forebrain and tectal pathways. Dextran-amine tracers were injected in OV and ICx. Brain sections were examined with a confocal microscope. No double-labeled cells were found in ICIs.

Our electrophysiological findings suggest that the integration of frequency and ITD by space-specific neurons is different in the two pathways. The anatomical tracing indicates that ICx and OV receive projections from different midbrain neurons.

82. Robustness of multiplicative processes in auditory spatial tuning

José Luis Peña, Masakazu Konishi

The space-neurons of the owl's external nucleus of the inferior colliculus are selective for the direction of sound sources. They are tuned to particular pairs of interaural time (ITD) and level (ILD) differences, which define the horizontal and vertical coordinates of auditory space, respectively. Mathematical analyses show that the amplitude of postsynaptic potentials in these neurons is a product of two components that vary with either ITD or ILD. The study of how this computation works for different input levels requires an independent control of the input. Since the owl's auditory system uses a process similar to cross-correlation for detection of ITD, addition of random noise to correlated signals reduces the output of

the ITD processing pathway. By varying the degree of binaural correlation we could accurately and reversibly change the amplitude of the ITD component of postsynaptic potentials in the space-specific neurons. Multiplication worked for the entire range of postsynaptic potentials created by manipulation of ITD.

83. Miniature microdrive for chronic recording in barn owls

Sharad Shanbhag

The barn owl is an ideal model system for studying the behavioral and neural mechanisms of auditory localization. Over the past 30 years, much work has been done to characterize this behavior as well as understand the neural mechanisms of auditory localization. However, most studies have been performed on owls that are either restrained or anesthetized. In order to better understand the neurophysiology of auditory localization during behavior, we have developed a miniature motorized microdrive system to enable recording of neurons from awake, behaving owls. The assembled microdrive is a cylinder 10 mm in diameter and 22 mm high. Each of three miniature DC brushless motors (Micro Position Systems, Biel-Bienne, Switzerland) is coupled to a threaded drive shaft using miniature gears with a 1:1 ratio. Rotation of the drive shafts causes linear motion of the electrodes carried by shuttles threaded onto the drive shafts. A modified Sutter MP-285 motor controller (Sutter Instruments, Novato, CA) is used to drive the motors and allows positioning of the electrode in 5 μ m steps. Maximum travel distance for each electrode is 14 mm that allows recording from deeper midbrain and brainstem auditory structures of the owl. The assembled drive with motors, electrodes and connectors weighs 10 g, well within the carrying capability of the owl. Electrodes may be replaced by removing the top cap and driving the shuttles up and out of the drive, eliminating the need to remove the microdrive from the animal if the drive is chronically implanted in the owl. In addition to our use in owls, the drive is also suitable for use in larger rodents and other vertebrate species.

Special thanks to Susumu Kitamura and the J. Morita Company for fabricating the drive and drive components.

Publications

Funabiki, Y. and Konishi, M. (2003) Long memory in song learning by zebra finches. *J. Neurosci.* 23:6928-6935.

Arthur, J.B. (2004) Sensitivity to spectral interaural intensity difference cues in space-specific neurons of the barn owl. *J. Comp. Physiol. A* 190:91-104.

Konishi, M. (2004) The role of auditory feedback in birdsong. *Ann. NY Acad. Sci.* 1016:463-476.

Lawrence A. Hanson Jr. Professor of Biology and Computation and Neural Systems: Gilles Laurent
 Moore Fellow: Markus Meister
 Postdoctoral Scholars: Laurent Moreaux, Ben Rubin, Glenn Turner, Rachel I. Wilson
 Graduate Students: Bede M. Broome, Stijn Cassenaer, Sarah (Shabnam) Farivar, Vivek Jayaraman, Ron Jortner, Ofer Mazor, Maria Papadopoulou, Javier Perez-Orive, Renaud Richard, Kai Shen, Mattias Westman, Valentin Zhigulin

Supported: The work described in the following research reports has been supported by:

Helen Hay Whitney Foundation
 W.M. Keck Foundation
 Lawrence A. Hanson Jr. Professorship of Biology
 National Institute of Mental Health
 National Institute on Deafness and Other Communication Disorders
 National Institutes of Health
 National Science Foundation
 Swartz Foundation

Summary: We are interested in information coding in the brain and in the design principles of circuits involved in processing sensory information. We are particularly interested in understanding the role of time, synchronization and oscillations in information coding and in relating the biophysical properties of neurons and synapses to the function of the networks in which they are embedded. We therefore study the cellular, synaptic and network aspects of neural processing. We focused our research this year on the olfactory system of insects (antennal lobes and mushroom bodies, circuits analogous to the vertebrate olfactory bulbs and anterior/posterior piriform cortices), using locusts, *Drosophila* and honeybees as primary model systems. Our work combines experimental (behavioral, electro-physiological and two-photon imaging), and modeling techniques and aims at understanding functional aspects of brain circuits design and the rules of information coding used by the nervous system.

84. Intensity versus identity coding in the locust olfactory system

Vivek Jayaraman, Mark Stopfer

We examined the encoding and decoding of odor identity and intensity by neurons in the first and second relays of the olfactory system of the locust, the antennal lobe and the mushroom body, respectively. Changes in odorant concentration led to changes in the firing patterns of individual antennal lobe projection neurons (PNs), similar to those caused by changes in odor identity, thus potentially confounding representations for identity and concentration. However, when these time-varying responses were examined across many PNs, concentration-specific patterns clustered by odor identity, resolving the apparent confound. The principal neurons in the mushroom body – Kenyon cells (KCs) – had very sparse

identity-specific responses with varying degrees of concentration invariance. The tuning of KCs to identity and concentration and the patterning of their responses are consistent with piecewise decoding of their PN inputs over oscillation-cycle length epochs.

References

Stopfer, M., Jayaraman, V. and Laurent, G. (2003) *Neuron* 39:991-1004.

85. Olfactory memory and physiology of the dorsal paired medial neurons of *Drosophila*

Glenn C. Turner, Rachel I. Wilson, Gilles Laurent

We are investigating the changes in neural representations that accompany learning and memory in *Drosophila*, using electrophysiological and behavioral approaches. Flies can learn to associate a particular odor with a reinforcer such as footshock or bitter taste. Retention of this olfactory memory may require the activity of the Dorsal Paired Medial (DPM) neurons (Waddell et al., 2000), a pair of bilaterally symmetric cells that innervate the mushroom body, a structure known to be involved in olfactory memory in insects. DPM activity is thought to be required for enduring changes of synaptic output strength from the intrinsic mushroom body neurons (Kenyon cells) onto postsynaptic targets called a/b/g-lobe neurons. These changes are presumed to cause behavioral avoidance of odors paired with the reinforcer.

To determine what might activate DPM during learning, we examined DPM responses to olfactory and gustatory stimuli. We observe both odor- and taste-evoked excitatory responses. Whole-cell patch-clamp recordings from the DPM cell body indicate it is a non-spiking neuron that responds to odors and tastes with graded potentials comprising a rapid initial depolarization and a more prolonged decay. The olfactory responses do not appear to depend on the hedonic quality of the odor: DPM responds to all odors tested, including odors that are attractive and those that are aversive to naive flies. Because DPM arborizes in the mushroom body, its responses may be used to monitor collective KC output. To determine whether learning alters DPM activity, we are examining responses in flies trained to associate a specific odor with footshock using the T-maze apparatus. Our goal is to assess whether persistent activity in DPM and/or a measurable potentiation of input synapses to DPM are evoked by this behavioral learning paradigm.

Reference

Waddell, S. et al. (2000) *Cell* 103:805-813.

86. Combined two-photon laser scanning microscopy and electrophysiological recording in insect brain

Laurent Moreaux, Gilles Laurent

We are investigating the correspondence between neuronal activity (spike time series and sub-threshold synaptic signals) and intracellular molecular calcium signals in *Drosophila* central olfactory neurons by

combining *in vivo* intracellular electrophysiological recording and calcium imaging by two-photon laser scanning microscopy. The goal is to understand the encoding and representation of odors in the early olfactory system (antennal lobe) and more precisely to understand the mismatch between previous calcium imaging data obtained by the Axel and Misenböck labs and the electrophysiological data obtained by the Laurent lab. The calcium imaging data indicate that antennal lobe output is identical to afferent input; the antennal lobe is proposed to act as a simple relay. By contrast, physiological data indicate that antennal lobe output is distributed in space and in time, and thus, profoundly transformed in this network. We should be able to elucidate this question by examining the degree of correlation between calcium signals (using a fluorescent intracellular calcium indicator) and afferent input and spikes from the output neurons of the antennal lobe (using whole-cell recording). Our preliminary results seem to indicate that calcium imaging represents both afferent synaptic input and spike output from the principal neurons; this could be due to the high calcium permeability of central nACh receptors and to the dominance of this mode of calcium entry over voltage-gated channels activated by action potentials.

87. Adaptive odor processing in the honeybee
Benjamin Rubin

One of the primary goals of systems neuroscience is to understand how the brain encodes and processes information about the world and uses it to produce adaptive behaviors. To achieve this goal, we have chosen to study the honeybee olfactory system, since both the anatomy and physiology of the olfactory system, as well as behaviors guided by the olfactory system, are well characterized and amenable to experimentation. In the honeybee as in other insects, odors are transduced by receptor neurons that are located in the antennae and project to the antennal lobes (ALs). In the ALs, different odors are represented by overlapping but distinct spatiotemporal activity patterns. Stimulated AL projection neurons undergo relatively slow periods of excitation and inhibition and also tend to oscillate synchronously on a faster timescale, and as a result, each odor activates a dynamic ensemble of active neurons whose membership is updated at each cycle of the 20-30 Hz oscillations (Stopfer et al., 1997). We are currently using tetrodes to record from ensembles of AL neurons in order to assess the population responses to a set of related odors.

Recordings from putative single units reveal spontaneous and odor-induced activity that is comparable to intracellularly recorded antennal lobe neuronal activity. These recordings will be used to test whether the population responses to different odors diverge over time as they do in the zebrafish, a finding that has been hypothesized to reflect processing adapted to facilitating accurate discrimination among similar odors (Friedrich and Laurent, 2001). The recordings are also being conducted in conjunction with ongoing proboscis extension response conditioning experiments, in which

honeybees are trained to form an association between an odor and a sucrose reward. While imaging experiments have shown that responses to the rewarded odor are selectively enhanced following learning (Faber et al., 1999), it remains unclear how the dynamic responses of populations of individually recorded AL neurons will have changed. These experiments will be used to test the hypothesis that AL responses adapt to reflect the behavioral relevance of odors; in other words, that the population responses to similarly conditioned (i.e., two rewarded) odors will converge more (or diverge less) than the responses to odors differentially conditioned (i.e., one rewarded and one unrewarded) odors.

References

- Friedrich, R.W. and Laurent, G. (2001) *Science* 291:889-894.
Stopfer, M., Bhagavan, S., Smith, B.H. and Laurent, G. (1997) *Nature* 390:70-74.

88. Ensemble processing of odor sequences and overlaps in the locust antennal lobe

Bede Broome, Vivek Jayaraman, Gilles Laurent

Odors evoke complex sequences of activity in antennal lobe projection neurons (PNs), the insect analogs of mitral/tufted cells. These PN activity patterns evolve over hundreds of milliseconds, are consistent from trial to trial, and contain information about odor identity and concentration. However, in natural settings, olfactory systems are often confronted with the task of identifying odor blends or multiple odorants that are received in short temporal succession. How does stimulus history affect the PN ensemble response, and how do PNs encode temporally overlapping patterns of odor input? To address these questions, we presented two odors at 12 different time delays relative to one another, while recording extracellular multi-single-unit activity from ensembles of up to 25 PNs and the local field potential elicited by PNs in a downstream processing center, the mushroom body. We observed that ensemble PN responses, as seen in correlations and visualized using locally linear embedding, capture properties of odor sequence stimuli not seen in individual PN responses. Using multiple discriminant analysis, we were able to classify PN ensemble response vectors at individual time points and reveal the time scales at which PN representations evolve to match stimulus changes. PN representations were classified as the binary mixture only in certain overlap periods, and matched those of the second odor presented only for some initial conditions. We predict that these conditions would also be relevant for the insect's perception of odor sequences.

References

- Perez-Orive, J., Mazor, O., Turner, G.C. et al. (2002) *Science* 297(5580):359-365.
Stopfer M., Jayaraman, V. and Laurent, G. (2003) *Neuron* 39(6):991-1004.

89. Associative memory and olfactory representation

S. Cassenaer, G. Laurent

An identified honeybee neuron, VUMmx1, appears to encode the reward stimulus in conditioning experiments (Hammer, 1993). VUMmx1 endogenously responds to sucrose, and activating the cell during odorant presentation subsequently gives rise to proboscis extension in response to the odorant alone. VUMmx1 projects to the antennal lobe (AL), the mushroom body (MB) and the lateral protocerebral lobe, and injection of the VUMmx1 transmitter octopamine in the AL and MB can also replace sucrose as the unconditioned stimulus (Hammer and Menzel, 1998). One interpretation of these behavioral experiments is that olfactory representations in the AL and MB could be changed by newly formed associations between odors and sucrose stimuli mediated by VUMmx1.

Neurons analogous to VUMmx1 that project to the AL and to the MB have been identified in the locust as well (Braunig, 1991). We characterize how olfactory representations in the locust are affected by pairing odorant presentation with direct activation of these cells or with injection of octopamine.

References

Braunig, P. (1991) *Phil. Trans. Royal Soc. London Series B-Biol. Sci.* 332:221-240.

Hammer, M. (1993) *Nature* 366:59-63.

Hammer, M. and Menzel, R. (1998) *Learning & Memory* 5:146-156.

90. Cytoarchitecture of an insect olfactory system

Sarah Farivar, Gilles Laurent

The insect mushroom body (MB) receives and processes olfactory information. The MB is a highly conserved structure, found in all but a few insect species and has been shown to be a relevant area in learning and memory of olfactory information. The functional properties of the intrinsic cells of the MB, the Kenyon cells (KCs), has been extensively studied and their integrative properties are starting to be understood. To help decipher their role in odor processing, we are studying the morphology of these cells, in an effort to map the ways in which these cells sample information from the upstream olfactory relay, the antennal lobe. Using data from electrophysiology and intracellular dye fills of both KCs and the projection neurons of the antennal lobe, we are characterizing these cells based on their own morphology, the morphology of the underlying structures, and the cells' connectivity to one another. We have thus far identified previously undescribed MB features and divisions and also identified some specific KCs within those regions.

91. Characterization of odor-evoked dynamics in the insect antennal lobe

Ofer Mazor, Gilles Laurent

The antennal lobe (AL) is the first site of olfactory processing in the locust brain. It contains two main neuron types: inhibitory local neurons (LNs) and

excitatory projection neurons (PNs), which form the only output. The AL responds to a 1 sec odor stimulation with a dynamic pattern of activity that includes a 20-30 Hz global oscillatory response combined with slower patterns of excitation and inhibition (100s of msec long) in PNs. These slower dynamics are neuron- and odor-specific.

We used silicon probes to record the simultaneous extracellular responses of 5-20 PNs to "square" odor pulses. We find that for long odor pulses (6-10 sec) the slow dynamics in PNs are strongest in the first 2 sec after odor onset and again just after odor offset (N=246 PN-odor pairs). For the remainder of the odor presentation, each PN reaches a steady firing rate that differs from odor to odor and is typically different from its baseline rate.

PNs synapse directly onto Kenyon cells (KCs). Extracellular recordings from KCs under the same conditions reveal strong odor-specific responses during the periods of onset and offset dynamics, and weaker responses while the PN responses were more stable. This suggests that the dynamic portions of the PN responses are better suited to driving KC activity.

Currently, we are studying the PN population onset response in light of what we already understand about the transfer of information from PNs to Kcs (1). Specifically, we are interested in quantifying the trial-to-trial variability in population firing patterns, as well as the speed at which the population response changes over the course of a single trial. We are also delivering odor pulses of different durations to test how the offset dynamics depend on odor duration, and how they interact with the onset response in a short (300-1000 ms) odor pulse.

Reference

(1) Perez-Orive, J., Mazor, O., Turner, G.C., Cassenaer, S., Wilson, R.I. and Laurent, G. (2002) *Science* 297:359-365.

92. Functional connectivity between antennal lobe projection neurons and mushroom body Kenyon cells in the locust

Ron A. Jortner, Gilles Laurent

The antennal lobe (AL), the first relay of the locust olfactory system, is a network of ca. 1000 excitatory (PN) and inhibitory (LN) neurons, which generates odor-evoked oscillatory firing encoding odor identity and concentration. The mushroom body (MB), the next relay in the system, consists of ca. 50,000 Kenyon cells (KC), which encode odor information using sparse, precisely timed firing. While it is anatomically and physiologically well established that PNs synapse onto KCs, much remains unknown about the properties of individual connections and the statistics of connectivity. Understanding these properties would contribute to our understanding of the transformation in neural coding schemes between the AL and the MB.

In this study, we examine the functional connectivity between PNs and KCs using electrophysiological tools. We simultaneously record the membrane potential of a single KC using an intracellular

electrode and action potentials of multiple single-unit PNs using tetrodes. We then compute the correlations between the PN firing and the KC membrane potential (spike-triggered averaging) during spontaneous activity. Using this approach, we have been able to find PN-KC pairs where the KC shows an average membrane potential deflection immediately following the PN action potential, indicative of a synaptic connection between them. These putative EPSPs had an average amplitude of 65 ± 30 microvolts (mean \pm SD), and a delay of 6.2 ± 2 milliseconds from the PN spike, in accordance with the previously measured conductance delay of PN axons. The EPSPs could usually not be seen in the raw KC traces, due to background activity. We are presently working to quantify the connectivity distribution between the PN and KC populations.

93. Two-photon imaging with genetically expressed calcium sensors in the **Drosophila** brain

Vivek Jayaraman

We are trying to understand the neurophysiological basis of a recently developed system of imaging with genetically-expressed calcium sensors in the *Drosophila* brain. The expression of the sensor, a calcium-sensitive fluorescent protein named G-CaMP (1), can be restricted to genetically-defined populations of neurons, which are then imaged using a laser scanning two-photon microscope (2,3). Interpreting the images of brain activity produced using such methods is however, problematic. For example, one group using G-CaMP in the antennal lobe has suggested that projection neurons (PNs) are rather narrowly tuned to odors, and that their responses directly reflect the uniglomerular input they receive from their olfactory sensory neurons (OSNs) (2). This is in contrast to work in the Laurent lab suggesting that PNs are more broadly tuned, consistent with a transformation of OSN input by the antennal lobe circuitry (4). A different group using G-CaMP expressed in Kenyon cells has claimed that odors evoke sparse, stereotyped and spatially-restricted responses in the mushroom body of flies (3). This finding is consistent with locust electrophysiological data from the Laurent lab (5). In both sets of imaging experiments, however, it is unclear what electrophysiological signal the imaging signal being measured corresponds to. It is conceivable that the sparseness and narrow tuning seen in these imaging experiments is a result of the relatively high threshold of activation of G-CaMP. It could also be that the calcium transients being imaged correspond more to synaptic input than the opening of voltage-dependent calcium channels, making the correlation of imaging signal with neuronal spiking highly nonlinear.

In our experiments, we will simultaneously image G-CaMP expressing neurons and record their physiology using intracellular and cell-attached techniques. This will allow us to establish the correlation between physiology and G-CaMP signal. We are also interested in the potential changes in the G-CaMP fly's behavior and G-CaMP-expressing neuron's activity that might be

produced by the presence of a sensor that likely affects calcium buffering in the cell. To investigate this issue, we are doing behavioral and electrophysiological experiments comparing wild-type flies to G-CaMP-expressing flies. Assuming that flies expressing G-CaMP do not show any abnormalities in behavior or in neuronal physiology, and once we have a clear understanding of the electrophysiological underpinnings of the G-CaMP signal, we plan to use the sensor to help understand odor-evoked responses of populations of neurons in the early areas of the fly olfactory system.

References

1. Nakai, J., Ohkura, M. and Imoto, K. (2001) *Nature Biotechnol.* 19:137-141.
2. Wang, J.W., Wong, A.M., Flores, J., Vosshall, L.B. and Axel, R. (2003) *Cell* 112:271-282.
3. Wang, Y., Guo, H.-F., Pologruto, T.A., Hannan, F., Hakker, I., Svoboda, K. and Zhong, Y. (2004) *J. Neurosci.* 24:6507-6514.
4. Wilson, R.I., Turner, G.T. and Laurent, G. (2004) *Science* 303:366-370.
5. Perez-Orive, J., Mazor, O., Turner, G.T., Cassenaer, S., Wilson, R.I. and Laurent, G. (2002) *Science* 297:359-365.

94. Nonlinear changes in neuronal ensemble responses evoked by varying odor ratios in mixtures

Kai Shen, Gilles Laurent

Odor perception is largely synthetic. It involves the formation of unique representations from which the components cannot be easily segmented. In their natural habitat, animals usually experience odor mixtures (e.g., flower fragrances). It is thus likely that neural representations of odor mixtures involve nonlinear interactions, such that the representation of a mixture is not a simple combination of the representation of its components. While this notion is supported by observations both at the level of olfactory receptor neurons and in behavioral studies, its mechanisms are only beginning to be explored experimentally in the olfactory brain. We examined the encoding and decoding of odor components within mixtures by neurons in the antennal lobe and the mushroom body, first and second relays, respectively, of the locust olfactory system. We recorded the multi-single-unit activity of ensembles of projection neurons, (PNs), the principal cells of the antennal lobe, and Kenyon cells, (KCs), the intrinsic cells of the mushroom body, while presenting 2-, 3-, and 4- mixtures of monomolecular odors. We examined the change in PN ensemble responses as we systematically varied the ratio of concentrations of the different components of the mixture. Applying principal component analysis for dimensionality reduction of the PN ensemble spatiotemporal response patterns, we observed that responses to different mixtures formed distinct clusters and varied in a nonlinear manner with odor ratio. While using locally linear embedding to visualize the time-varying

dynamics of the PN ensemble, we also found that at certain ratios, the response trajectories changed abruptly from being more similar to the representation of one odor component to another. Finally, we examined the degree to which these transformations were mirrored in the responses of the targets of the PNs in the mushroom body, the KCs.

95. Search for connectivity patterns
Maria Papadopoulou

The organization of the flow of information in the insect olfactory system is fairly well understood: odorant receptors are expressed in the olfactory receptor neurons (ORNs) in the antenna, which connect to projection neurons (PNs) in the antennal lobe (AL); these cells in turn project to Kenyon cells (KCs) in the mushroom body (MB) and cells in the lateral horn (LH). However, the precise cell-to-cell connectivity from one stage of the circuit to the next has not yet been determined. This information is, however, important for a better understanding of the computations involved in olfactory processing.

An interesting aspect of the locust olfactory system is the transformation between representations in AL and MB. PNs in the AL have more broadly tuned odor responses than KCs in the MB that are far more selective; essentially, we see a transformation from a dense representation in the AL to a sparse one in the MB (1,2). Olfactory memories are stored in the MB; a sparse code could reduce overlap between individual odor representations and facilitate memory formation and retrieval (2). Critical to an understanding of how this sparseness is achieved is the convergence ratio between PNs and KCs, and the synaptic weights of PN-KC connections (3). Labeling connected pairs of PNs and KCs would allow us to perform simultaneous electrophysiological recordings and address the latter issue.

Tracing individual pathways could also help resolve the connections of PNs with LH neurons. One group has shown that PNs innervating the same glomerulus in the fly system have similar axonal projection patterns in the LH (4), arguing for a topographic map from the AL to the LH. Labeling connected PNs and LH neurons would help determine if, indeed, that is the case.

In an effort to address the above questions, we use a tracer, biotinylated dextran amine (BDA), which crosses synapses predominantly in the anterograde direction. BDA is a transynaptic tracer that is used extensively as an anterograde tracer in other model organisms (rat, mouse, chick embryo), but has not hitherto been used in insects. The general approach we take is to inject the tracer in the locust antenna, where it would be taken up by the ORNs and label connected PNs and higher order neurons. Another transynaptic tracer under consideration is wheat germ agglutinin (WGA). Here, the advantage lies in the fact that it can be genetically engineered in the fly and could therefore, be selectively

expressed under the promoter of a neuron expressing a specific odorant receptor.

Once the basic labeling mechanism works, we plan to use a fluorescently-tagged tracer to identify pairs of synaptically-connected cells for simultaneous electrophysiological recordings.

References

1. Perez-Orive, J., Mazor, O., Turner, G.T., Cassenaer, S., Wilson, R.I. and Laurent, G. (2002) *Science* 297:359-365.
2. Laurent, G. (2002) *Nat. Rev. Neurosci.* 11:884-895.
3. Huerta, R., Nowotny, T., Garcia-Sanchez, M., Abarbanel, H.D. and Rabinovich, M.I. (2004) *Neural Comput.* 8:1601-1640.
4. Wong, A.M, Wang, J.W. and Axel, R. (2002) *Cell* 109:229-241.

Publications

- Friedrich, R.W., Habermann, C.J. and Laurent, G. (2004) Multiplexing using synchrony in the zebrafish olfactory bulb. *Nature Neurosci.* 7(8):862-871.
- Perez-Orive, J., Bazhenov, M. and Laurent, G. (2004) Intrinsic and circuit properties favor coincidence detection for decoding oscillatory input. *J. Neurosci.* 24(26):6037-6047.
- Friedrich, R.W. and Laurent, G. (2004) Dynamics of olfactory bulb input and output activity during odor stimulation in zebrafish. *J. Neurophysiol.* 91(6):2658-2669.
- Wilson, R.I. Turner, G.C. and Laurent, G. (2004) Transformation of olfactory representations in the *Drosophila* antennal lobe. *Science* 303(5656):366-370.

Bren Professor of Biology: Henry A. Lester
 George Grant Hoag Professor of Chemistry: Dennis Dougherty¹

Visiting Associate: Johannes Schwarz

Members of the Professional Staff: Bruce Cohen, Cesar Labarca

Associate Biologist: Purnima Deshpande

Postdoctoral Fellows: Daniel Clayton, David Dahan¹, Mohammed Dibas, Carlos Fonck, Joanna Jankowsky, John Leite, Fraser Moss, Raad Nashmi, Rigo Pantoja, Nivalda Rodrigues-Pinguet, Irina Sokolova, Andrew Tapper

Graduate Students: Darren Beene¹, Kiowa Bower, Amanda Cashin¹, Princess Imoukhuede, Lori Lee¹, Kathryn McMenimen¹, Sarah Monahan¹, Tingwei Mu¹, E. James Petersson¹, Erik Rodriguez¹, George Shapovalov², Eric Slimko, Steve Spronk¹, Michael Torrice¹, Joanne (Xinan) Xiu, Niki Zacharias¹

Rotating Graduate Student: William Ford

Research and Laboratory Staff: Pamela Fong, Kathleen Hamilton, Steven Kwoh, Rain Lynham, Sheri McKinney

SURF Students: Jose Munoz, Lydia Ng

Volunteers: Stephanie Huang, Sigrid Schwarz

¹Division of Chemistry and Chemical Engineering, California Institute of Technology

²Division of Physics, Mathematics and Astronomy, California Institute of Technology

Support: The work described in the following research report has been supported by:

Bren Chair

California Tobacco-Related Disease Research Program

Elizabeth Ross Fellowship

Keck Foundation

Moore Foundation

National Institute of Drug Abuse

National Institute of General Medical Science

National Institute of Mental Health

National Institute of Neurological Diseases and Stroke

National Parkinson Foundation

Summary: We continue our work on ion channels, receptors, and transporters. We have continued to analyze several strains of knock-in mice generated in our laboratory for two ligand-gated channels, the nicotinic $\alpha 4$ receptor and the serotonin 5-HT₃ receptor. The nicotinic receptor work is enhanced by a promising new strain, Leu9'Ala. This work has generated interesting insights into nicotine addiction, neurodegenerative disease, and epilepsy. Strains that contain GFP tags on their nicotinic receptors, and that duplicate mutations underlying human epilepsies, are under construction. The epilepsy mutations in nicotinic receptors are also under study in oocyte expression systems. We have also started to explore the possible role of the $\alpha 7$ nicotinic receptor in Alzheimer's disease, again using mouse models. The hypersensitive 5-HT₃ receptor knock-in mice have generated insights into murine urologic syndrome.

Our work on selective silencing of mammalian neurons has generated a promising set of techniques and

reagents based on ligand-activated chloride channels. We are now developing "proof of concept" transgenic mouse strains.

We continue our joint work with the Dougherty group, in Caltech's Chemistry Division, on aspects of ion channel structure-function. We have brought novel techniques to these studies, including mass spectrometry and fluorescence. We work on unnatural amino-acid mutagenesis. We have now studied the cation- π interaction that helps agonists bind to several cys-loop receptors. We have now extended unnatural amino-acid incorporation to mammalian cells.

With the Dougherty group and with Neurion Pharmaceuticals in Pasadena, we have started to analyze the binding of blocking drugs to the hERG potassium channel, also using unnatural amino acid mutagenesis. The channel is important because it underlies many instances of drug-induced long-QT syndrome. We are also beginning unnatural amino acid experiment on G protein-coupled receptors.

We collaborate with both Dougherty and Doug Rees, also in the Chemistry Division, on bacterial ion channels of known atomic-scale structure. We gathered data at bandwidths more than an order of magnitude greater than usual; but some gating transitions are still too fast to measure. We are seeking the origin of voltage sensitivity in the MscS channel.

Our work continues on quantitative aspects of transporter function, primarily measured with fluorescence and with knock-in mice. We are using fluorescence to analyze the mobility of GABA transporters. As an interesting side benefit of the GABA transporter knock-in mouse, we have generated and analyzed a knockout mouse for the same molecule.

The late Norman Davidson led a subgroup working on aspects of synaptic plasticity, particularly those that depend on A kinase stimulation. Members of this subgroup are now analyzing their data and preparing papers for publication.

Our group's home page has additional up-to-date information, images, and notices of positions. It's at <http://www.cco.caltech.edu/~lester>.

96. Using physical chemistry to differentiate nicotinic from cholinergic agonists at the nicotinic acetylcholine receptor

Amanda L. Cashin^{*}, E. James Petersson^{*}, Henry A. Lester, Dennis A. Dougherty^{*}

Membrane receptors constitute the majority of pharmaceutical targets, but a paucity of high resolution structural data inhibits efforts to produce detailed insights into drug-receptor interactions. For the nicotinic acetylcholine receptor (nAChR), crystal structures of the ACh binding protein (AChBP) have proved useful, but the functional relevance of the interactions suggested by these structures must still be determined. We show that a physical chemistry approach, combining high precision chemical manipulations of the receptor with quantum mechanical calculations, can make these determinations.

In particular, we establish that two agonists – nicotine (Nic) and ACh – use different noncovalent binding interactions to activate the nAChR. ACh uses a cation- π interaction to Trp α 149, while Nic employs a hydrogen bond to a backbone carbonyl in the same region of the agonist binding site. The highly potent nicotine analogue epibatidine (Epi) achieves its high potency by taking advantage of both the cation- π interaction and the backbone hydrogen bond. In addition, modeling suggests that an unconventional aromatic C-H \cdots O=C hydrogen bond further augments the binding of Epi. These studies illustrate the subtleties and complexities of the interactions between drugs and membrane receptors and establish a paradigm for obtaining detailed structural information.

[†]Division of Chemistry and Chemical Engineering, Caltech

97. Tyrosine residues that control binding and gating in the 5-HT₃ receptor revealed by unnatural amino acid mutagenesis

Darren L. Beene¹, Kerry L. Price², Dennis A. Dougherty¹, Sarah C.R. Lummis²

The mechanism by which agonist binding triggers pore opening in ligand-gated ion channels is poorly understood. We have used unnatural amino acid mutagenesis to introduce subtle changes to the side chains of tyrosine residues (Tyr141, Tyr143, Tyr153 and Tyr234), which dominates the 5-HT₃ receptor-binding site. Heterologous expression in oocytes, combined with radioligand binding data and a model of 5-HT computationally docked into the binding site, has allowed us to determine which of these residues are responsible for binding and/or gating. We have shown that Tyr 143 forms a hydrogen bond that is essential for receptor gating but does not affect binding, while a hydrogen bond formed by Tyr153 is involved in both binding and gating of the receptor. The aromatic group of Tyr234 is essential for binding and gating, while its hydroxyl does not affect binding but plays a steric role in receptor gating. Tyr141 is not involved in agonist binding or receptor gating, but is important for antagonist interactions. These data, combined with a new model of the non-liganded 5-HT₃ receptor, lead to a mechanistic explanation of the interactions that initiate the conformational change leading to channel opening. Thus, we propose that the entry of 5-HT into the binding pocket causes displacement of Tyr143 and Tyr153, and results in the formation of new hydrogen and other bonds; these provide both the torsional force and the energy required to trigger the conformational change leading to channel opening. Similar rearrangements may trigger gating in all Cys-loop receptors.

¹Division of Chemistry and Chemical Engineering, Caltech

²Department of Biochemistry, U. Cambridge, Tennis Court Road, Cambridge, CB2 1GA

98. The ligand-binding site of serotonin in the MOD-1 receptor

Tingwei Mu^{*}, Dennis A. Dougherty^{*}

We continued to study the ligand binding sites for the neurotransmitter serotonin (5-HT) in the MOD-1 receptor of *C. elegans*. Previously we identified that the primary ammonium group of serotonin makes a strong cation- π interaction with Trp 226 of MOD-1. To further confirm this idea, the unnatural tethered agonists approach was performed at position 180 and 226. The tethered agonists would simulate the effect of the agonists, and the ion channel would be spontaneously open after the incorporation, which could be blocked by the channel blocker. The tethered agonists of Tyr-O-3-P and Tyr-O-3-Q were incorporated into the positions of 180 and 226, and picrotoxin was used as the channel blocker to test the tethered agonist efficiency. Tyr-O-3-P at position 226 gave the highest efficiency, suggesting that the primary ammonium group of serotonin was near position 226. Recently the crystal structure of acetylcholine binding protein (AChBP) was determined, which is homologous to the extracellular domain of the Cys-loop superfamily. Therefore, we applied homology modeling to build the extracellular domain of MOD-1 by using AChBP as the template. HierDock was used to predict the binding site of serotonin into MOD-1. The canonical cation- π interaction between serotonin and Trp 226 was demonstrated. The primary ammonium group of serotonin was sandwiched between the aromatic side chains of Tyr 180 and Trp 226, and it formed a hydrogen bond with the main chain carbonyl group of Tyr 180. Two novel hydrogen bonds between the hydroxyl group of serotonin and Asn 223 and between the indolic amino group of serotonin and Gln 228 were also identified from the docking result. This is the first vivid binding pattern of serotonin in the MOD-1 receptor. Currently we are developing the method of the combination of the unnatural amino acid mutagenesis and the different agonist effects to test the docking model.

^{*}Division of Chemistry and Chemical Engineering, Caltech

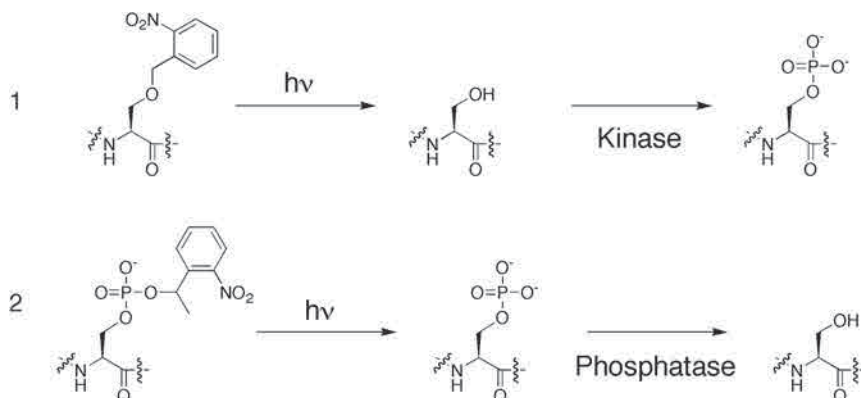
99. Temporal control of protein phosphorylation with caged amino acids

E.J. Petersson^{*}, D.A. Dougherty^{*}, H.A. Lester

Phosphorylation of serine, threonine, and tyrosine residues is a ubiquitous and dynamic post-translational protein modification that results in a wide variety of alterations in protein function. Traditionally, changes in phosphorylation have been controlled by applying drugs to upregulate kinases or downregulate phosphatases. However, these methods are inherently limited by the rate of the phosphorylated protein's interaction with the regulatory proteins. This prevents any precise kinetic analysis of the downstream effects of phosphorylation. We have established a set of caged amino acids that can be photolyzed to turn on kinase or phosphatase activity site specifically with ms/s time resolution. In a "proof-of-principle" experiment, we have incorporated 1 and 2 into full-length mVASP protein and shown that we can control

the phosphorylation state of the protein at S153 by decaging.

*Division of Chemistry and Chemical Engineering, Caltech



100. Probing the muscarinic type-2 acetylcholine receptor binding site through incorporation of unnatural amino acids

Michael M. Torrice*, Dennis A. Dougherty*

The G-protein-coupled receptor (GPCR) family of transmembrane proteins is a target for many pharmaceuticals. The muscarinic type-2 acetylcholine receptor (M₂AChR) belongs to the aminergic class of family A GPCRs. Previous work in this group on the nicotinic acetylcholine receptor has shown that the cationic acetylcholine (ACh) was bound through a cation- π interaction with a conserved Trp residue. Studies on the M₂AChR binding site will focus on understanding the roles of conserved anionic and aromatic residues in binding cationic amine ligands.

Incorporation of unnatural amino acids into the M₂AChR will allow for chemical-scale studies of the receptor binding site. A series of fluorinated Trp amino acids will be incorporated at W6.48 and W7.40 to probe the existence of a cation- π interaction. The unnatural amino acid, nitro-alanine (NO₂-Ala), will be synthesized and incorporated at D3.32 to probe electrostatic interactions between receptor and ligand, as suggested in the literature. NO₂-Ala is isosteric to Asp, but lacks a net-negative charge. Preliminary studies incorporating 5, 7-difluoro Trp (F₂W) at the conserved aromatic residues. W6.48 and W7.40, have shown that W7.40 is the possible site of a cation- π interaction between M₂AChR and ACh.

*Division of Chemistry and Chemical Engineering, California Institute of Technology

101. Improving nonsense suppression by suppressing eRF-1 with siRNA

Joanne Xiu¹, Dennis A. Dougherty²

Introducing unnatural amino acids into proteins by nonsense suppression has proven to be an effective and powerful tool to study protein structure-function relationships on the chemical scale. This strategy has greatly facilitated structure-function studies of a series of membrane-bound ion channels. This project reported

attempts to increase nonsense suppression efficiency in *Xenopus laevis* oocytes and human embryonic kidney (HEK) cells using RNA interference to target eukaryotic release factor 1 (eRF1). Multiple 21-nt chemically synthesized small interfering RNA molecules targeting different positions of either *Xenopus* eRF1 or human eRF1 were introduced into oocytes or HEK cells, respectively. The changes of eRF1 mRNA level of both cell lines were monitored by reverse transcription PCR (RT-PCR or RNA PCR). In *Xenopus* oocytes, the expression of mouse muscle nAChR produced in a nonsense suppression experiment was monitored using two-electrode voltage clamp electrophysiology. In HEK cells, the expression of EGFP produced by nonsense suppression was observed by fluorescent microscopy. Preliminary results demonstrate degrading eRF1 by RNAi to be a promising strategy to improve nonsense suppression efficiency, particularly in HEK cells.

¹Graduate Student, Biochem. & Mol. Biochem., Caltech

²Division of Chemistry and Chemical Engineering, Caltech

102. Incorporation of unnatural amino acids into NMDA receptors expressed in mammalian cells

Kiowa S. Bower*, Dennis A. Dougherty*

Methods have been developed to successfully incorporate unnatural amino acids into channels expressed in mammalian cells (Monahan et al., 2003). We plan to develop these methods further and use them to study the function of NMDA receptors in mammalian cells. We will to assess the effectiveness of our method for the study of NMDA receptors using unnatural amino acids already in our possession to alter the Mg²⁺ block properties of the receptor. Changes in the Mg²⁺ IC₅₀ will be measured to assess the effect of these unnatural amino acids. If successful, we will examine aspects of ligand binding and gating in the NMDA receptor.

¹Division of Chemistry and Chemical Engineering, Caltech

Reference

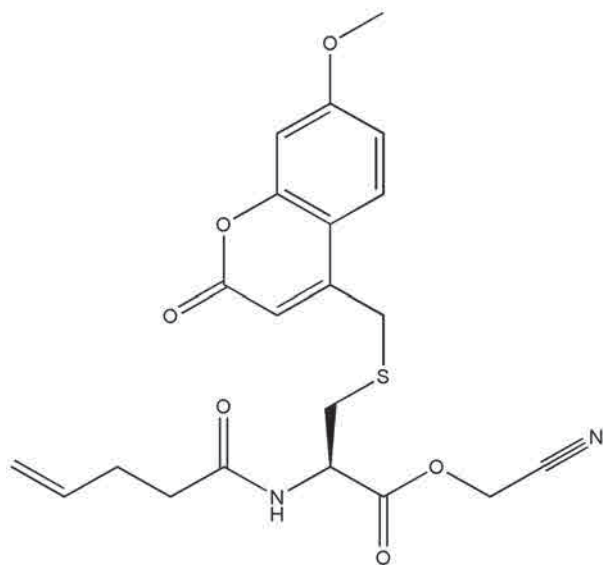
Monahan, S.L., Lester, H.A. and Dougherty, D.A. (2003) *Chem. Biol.* 10:573-580.

103. Synthesis of cysteine-**S**-methoxycoumarin (Cys(MC)): An additional fluorescent unnatural amino acid candidate for nonsense suppression methodology

Rigo Pantoja, E. James Petersson*

A new fluorescent unnatural amino acid candidate is being added to our repertoire. The synthesis of 4PO-cysteine-methoxycoumarin cyanomethyl ester (4PO-Cys(MC)-OCH₂CN) is complete. 4PO-Cys(MC)-OCH₂CN is suitable for coupling to 5'-phospho-2-deoxycytidylyl-(3',5')-adenosine (dCA), which we will then ligate to the THG73 suppressor tRNA. Coupling reactions between Cys(MC) and dCA have been carried out. Successful coupling has been observed by UV absorption spectroscopy which yields a 260 nm/345 nm ratio of 2.2. Upon further confirmation of the unnatural amino acid-dCA product with high resolution mass spectrometry we will ligate it to the tRNA. Then, the 4PO-Cys(MC)-tRNA species will be utilized with nonsense suppression methodology to incorporate Cys(MC) into the Lue47 site of Shaker K⁺ ion channel. The Shaker K⁺ ion channel is homotetramer, thus, four Cys(MC) should be incorporated per ion channel. Incorporating four fluorescent unnatural amino acids per channel will afford us a relatively high fluorescence signal which is necessary since suppressed protein expression levels can be orders of magnitude lower than standard heterologous expression levels. The voltage-dependent Shaker K⁺ ion channel has been characterized extensively by our group and others, making it an attractive candidate for characterizing fluorescent unnatural amino acids.

*Division of Chemistry, Caltech



104. Single-cell electroporation of CHO-K1 cells with YFP cDNA
Rigo Pantoja

Single-cell electroporation (SCE) is potentially an ideal technology for unnatural amino acid mutagenesis. While transient many-cell electroporation techniques have significantly advanced the application of unnatural amino acid mutagenesis of ion-channels expressed in mammalian cells, 5 μ L of precious reagents are still required for each transfection event, and often only a single cell from each dish is used per electrophysiology experiment (Monahan et al., 2003). SCE requires only nanoliters for electroporating several dozen cells in a session, effectively using 100 times less material. In an effort to determine the feasibility of SCE for unnatural amino acid mutagenesis we have carried out preliminary work. This was made possible by using a patch-clamp microscope set-up. The power supply used was a factory beta-unit Axoporation lent to us by Axon Instruments (Foster City, CA). The Axoporation is a stand-alone unit with programmable voltage-pulse stimulus protocols and real-time pipette current and resistance readouts prior to and during electroporation. Therefore, electroporation parameters can be quickly optimized for varying reagents and cell types. Thus, we used the Axoporation to independently electroporate fluorescein dye and YFP cDNA into CHO-K1 cells. The specific voltage pulse protocol consisted of a pulse train with a pulse amplitude of -7.5 V and 1 ms duration. The pulse train was applied for a total time of 1.5 sec at a 200 Hz frequency. The parameters selected are similar to those reported in the literature. Fluorescence microscopic inspection of the dye in the cells was performed immediately, whereas YFP expression could be confirmed 12 hours after stimulus. YFP expression was also inspected 48 hours after electroporation, and approximately 66 % (n = 24) of the cells yielded YFP fluorescence. We will next turn our attention to determining whether SCE can be used to transfect the required reagents for unnatural amino acid mutagenesis.

105. Micro-electroporation of HEK 293 cells with the human **ether-a-go-go** related gene hERG1A subunit
Fraser J. Moss

Improper function of the human ether-a-go-go related K⁺ channel (hERG1, KCNH2) prolongs the cardiac action potential, resulting in long-QT syndrome. hERG dysfunction can be caused by congenital mutations that prevent proper insertion of the channel into the cell membrane, as well as by certain prescription drugs (e.g., terfenadine, cisapride, moxifloxacin) that block the hERG channel as a side effect of their therapeutic action. We are investigating these causes of hERG dysfunction through unnatural amino acid (UAA) mutagenesis that specifically targets residues underlying drug blockade or trafficking defects. We are assessing hERG activity in mammalian expression systems rather than *Xenopus* oocytes, because test substances can accumulate in the oocyte yolk,

resulting in significant variability and error in potency estimates. Furthermore, oocytes are maintained at 18°C, and temperatures below 37°C have been shown to rescue trafficking defects in some hERG mutants. As a prelude to studies with UAAs, we have successfully expanded the use of micro-electroporation as described by Monahan et al. (2003) to transiently transfect HEK 293 cells with the hERG1A subunit. Four 120 V pulses of 50 ms duration are sufficient to transfect 2.5 µg of wild-type hERG1A cDNA. Optimizing the technique to transfect cDNA expands the Monahan method which utilized mRNA. Distinctive hERG1A currents are detected by whole-cell patch clamp electrophysiology 48-72 h after transfection. Ongoing experiments will demonstrate that microporation can co-transfect a hERG1A amber mutant and suppressor tRNA aminoacylated with the natural residue to rescue the wild-type phenotype. Simultaneously, we will demonstrate that microporation can deliver unnaturally aminoacylated tRNAs to suppress hERG1A amber mutants. Additionally, we are developing new tRNA suppressor molecules derived from the human serine amber suppressor (HSAS) tRNA. We have demonstrated that by removing or inverting the HSAS variable arm we have developed orthogonal tRNAs to suppress amber codons in ion channel subunit mRNA when they are chemically aminoacylated. We hypothesize that the mammalian origin of these tRNAs may help improve suppression efficiency in mammalian cells.

Reference

Monahan, S.L., Lester, H.A. and Dougherty, D.A. (2003) *Chem. Biol.* 10:573-580.

106. A fluorophore attached to nicotinic acetylcholine receptor **βM2** detects productive binding of agonist to the **αδ** site
David S. Dahan¹, Mohammed I. Dibas, E. James Petersson¹, Vincent C. Auyeung, Baron Chanda², Francisco Bezanilla², Dennis A. Dougherty¹
To study conformational transitions at the muscle nicotinic acetylcholine (ACh) receptor (nAChR), a rhodamine fluorophore was tethered to a Cys sidechain introduced at the β19' position in the M2 region of the nAChR expressed in *Xenopus* oocytes. This procedure led to only minor changes in receptor function. During agonist application, fluorescence increased by ($\Delta F/F$) ~10%; and the emission peak shifted to lower wavelengths, indicating a more hydrophobic environment for the fluorophore. The dose-response relations for ΔF agreed well with those for epibatidine-induced currents, but were shifted ~100-fold to the left of those for ACh-induced currents. Because (i) epibatidine binds more tightly to the $\alpha\gamma$ binding site than to the $\alpha\delta$ site and (ii) ACh binds with reverse site selectivity, these data suggest that ΔF monitors an event linked to binding specifically at the $\alpha\delta$ subunit interface. In experiments with flash-applied agonists, the earliest detectable ΔF occurs within ms, i.e., during activation. At low [ACh] ($\leq 10 \mu\text{M}$), a phase of ΔF

occurs with the same time constant as desensitization, presumably monitoring an increased population of agonist-bound receptors. However recovery from ΔF is complete before the slowest phase of recovery from desensitization (time constant ~250 s), showing that one or more desensitized states have fluorescence like that of the resting channel. That conformational transitions at the $\alpha\delta$ -binding site are not tightly coupled to channel activation, suggests that sequential rather than fully concerted transitions occur during receptor gating. Thus, time-resolved fluorescence changes provide a powerful probe of nAChR conformational changes.

¹Division of Chemistry and Chemical Engineering, Caltech
²Department of Physiology and Department of Anesthesiology, David Geffen School of Medicine, University of California, Los Angeles

107. Fluorescent mapping of conformational dynamics in nicotinic receptors
Mohammed I. Dibas

The mechanism that couples agonist binding and channel gating in the nicotinic receptors is still unknown. However, recent studies hypothesized that agonist binding induces series of conformational changes leading several loops of the N-terminus domain to interact with the TM2/TM3 loop and gate the channel. Using simultaneous fluorescent and voltage clamp technique, we will explore the conformational dynamics and associated environmental changes induced by agonist binding. We performed individual cysteine substitutions on several residues in the N-terminus domain of the muscle nicotinic α_1 and β_1 subunits {Loop2 (α_1 V43, α_1 E45, β_1 E45), Loop 5 (α_1 A96, α_1 D97, α_1 G98), Loop 7 (α_1 F135, α_1 F137), Loop β 8/9 (α_1 F170, α_1 G174, α_1 W176), Pre-TM1 domain (α_1 Q208, α_1 R209, α_1 L210, β_1 R219, β_1 R220, β_1 K221)}. Additionally, we mutated individual residues in the TM2/TM3 loop of the α_1 subunit (α_1 S248, α_1 S249, α_1 A250, α_1 C*Ins 250, α_1 V251, α_1 C*Ins252, α_1 P252, α_1 L253, α_1 G255) to cysteine. Using two-electrode voltage clamp (TEVC) electrophysiology, we will characterize the functional effect of cysteine substitution in the muscle nicotinic receptors. Based on the structural data available in the literature, all cysteines introduced in the N-terminus and the TM2/TM3 domains should be accessible in the absence and presence of agonist. We will test the accessibility of these cysteine residues to the fluorescent dye sulforhodamine methanethiosulfonate (MTSR) and thereafter we will conduct simultaneous voltage and fluorescent measurements on labeled oocytes injected with the cysteine mutants. Our goal is to determine the nature of conformational changes induced by agonist binding within loops 2, 5, 7 and 9, the Pre-TM1 domain and the TM2-TM3 loop.

108. FRET analysis of molecular motion at the channel gate in nicotinic receptors
Mohammed I. Dibas

Recent structural studies hypothesized that the TM2 domains, which form the channel gate in nicotinic receptors, may rotate in response to agonist binding. Using fluorescence resonance energy transfer (FRET), we will measure the intersubunit distance changes in the TM2 domains during gating and desensitization. We initially measured FRET signals between GFP (green fluorescent protein) genetically engineered into the γ subunit TM3-TM4 loop and sulforhodamine methanethiosulfonate (MTSR) tethered to the 19' residue in the β subunit TM2 domain. In preliminary studies, oocytes expressing $\alpha\beta_{(A19'C-MTSR)}\gamma_{GFP}$ receptors showed a 1.5 % decrease in GFP (donor) fluorescence in the presence of MTSR (acceptor) during agonist application. In the absence of MTSR during agonist application, we observed a slight increase in GFP fluorescence. Therefore, our initial studies suggest that the decrease in GFP fluorescence is due to energy transfer to MTSR during agonist exposure. More importantly, our FRET studies suggest that the 19' residue may rotate in response to agonist binding. Future FRET experiments will focus on determining the FRET angular dependence on θ , the angle between the transition moments of GFP (donor) inserted into the γ subunit TM3-TM4 loop and MTSR (acceptor) tethered to several residues in the β subunit TM2 domain (15', 17' and 19'). Subsequent studies will focus on studying FRET signals between γ -GFP and MTSR attached to the TM2 domains of other subunits.

109. FRET studies of cross-inhibition between P2X and nicotinic channels

Raad Nashmi, James Fisher*, David N. Bowser*, Baljit S. Khakh*

ATP-gated P2X channels and ACh-gated nicotinic channels exhibit functional interactions when expressed either in heterologous coexpression systems or at endogenous levels in neurons: co-activation of both channel types results in responses that are smaller than the predicted sum of the individual components. This lack of summation is termed cross-inhibition. We have now extended previous work on cross-inhibition to P2X₂ and $\alpha 4\beta 2$ nicotinic channels, and used electrophysiology, fluorescence resonance energy transfer (FRET) and total internal reflection fluorescence (TIRF) microscopy between CFP and YFP-tagged channels to probe mechanisms. Co-activation resulted in currents that deviated from the predicted current by $38.9 \pm 4.3\%$, and this and other electrophysiological properties were consistent with occlusion of the nicotinic component. We measured FRET efficiency (e) of $34 \pm 6\%$ for P2X₂ channels labelled on their C termini with CFP and YFP, and $24 \pm 3\%$ for $\alpha 4\beta 2$ channels labelled with CFP ($\beta 2$) and YFP ($\alpha 4$) within the M3-M4 intracellular loop (Nashmi et al., 2003). We measured strong FRET between CFP or YFP labelled P2X₂ and $\alpha 4\beta 2$ channels when the cognate acceptor or

donor fluorophore was on the $\beta 2$ subunit ($e = 23 \pm 6$ and $26 \pm 3\%$), but weak or no FRET between P2X₂ and $\alpha 4\beta 2$ channels when the acceptor ($e=10\%$) or donor ($e=0\%$) fluorophores were on the $\alpha 4$ subunit. These data suggest a closer spatial relationship between the C-terminal tails of P2X₂ subunits and the M3-M4 loops of $\beta 2$ subunits, than between P2X₂ C termini and the M3-M4 loops of $\alpha 4$ subunits. The relationship between this apparent spatial arrangement and cross-inhibition will be considered, along with detailed analysis of FRET between P2X₂ and $\alpha 4\beta 2$ nicotinic channels in HEK293 cells and cultured neurons.

Support: MRC, EMBO, HFSP, TRDRP, NIH (NS-11756)

*MRC Laboratory of Molecular Biology, Cambridge, CB2 2QH

110. Mechanisms of nicotine-induced functional upregulation of $\alpha 4$ -containing nicotinic receptors

Raad Nashmi, Sheri McKinney, Cesar Labarca, Purnima Deshpande

Chronic levels of nicotine exposure as found in smokers or in experimental rodents administered nicotine results in elevated levels of nicotinic acetylcholine receptors (nAChRs). However, mRNA levels of a variety of nicotinic receptors, including $\alpha 4$ and $\beta 2$, remain unchanged in the CNS. A decrease in turnover rate or increased assembly of nAChRs may be the principal cause of upregulation. It is unclear how nicotine mediates this effect; therefore, we study the signaling pathways responsible for nicotinic receptor upregulation. Transfection of wild-type ventral midbrain neurons (1-2 weeks in culture) with fluorescently-tagged $\alpha 4$ and $\beta 2$ nAChR subunits ($\alpha 4$ -YFP and $\beta 2$ -CFP) displayed increased receptor expression in dendrites 24 hr following $1 \mu M$ nicotine incubation. There was also increased Förster resonance energy transfer (FRET) between $\alpha 4$ -YFP $\beta 2$ -CFP subunits in the soma of nicotine-treated neurons as compared to controls, indicating increased receptor assembly. In addition, fura-2 measurements were done on ventral midbrain neurons (21 d in culture) from E14 WT mice or from knock-in mice heterozygous for the Leu9'Ala (L9'A) mutation in the $\alpha 4$ nAChR subunit, which confers nicotine hypersensitivity. Nicotine dose-response relations showed that the L9'A neurons have a lower EC_{50} (0.12 vs $4.9 \mu M$) and a ~four fold larger response than WT neurons. Nicotine was applied to L9'A neuronal cultures for 3 d at 10 nM, which selectively activated only $\alpha 4$ (L9'A) containing receptors. There was a significant increase in ACh ($100 \mu M$ for 2 sec) mediated Ca^{2+} influx in nicotine treated neurons ($181 \pm 23\%$ of influx in control cultures). The PKC inhibitor bisindolymaleimide I (500 nM), chronically coapplied with nicotine, partially prevented this increased Ca^{2+} influx (to $140 \pm 37\%$). We plan to examine the contribution of other signaling pathways in the upregulation of nicotinic receptors by pharmacological inhibition of specific kinases during nicotine incubation. In conclusion, chronic nicotine resulted in increased functional Ca^{2+} influx through $\alpha 4$

containing receptors, and this may be mediated, in part, through activation of the PKC signaling pathway.

111. Fluorescently-tagged $\alpha 4$ nicotinic receptor knock-in mice
Raad Nashmi, Purnima Deshpande, Cesar Labarca, Julian Revie

In order to examine the localization patterns of $\alpha 4$ nicotinic acetylcholine receptor (nAChR) subunits in the CNS we fused fluorescent proteins to the M3-M4 intracellular loop of the $\alpha 4$ nAChR subunit. We have tested the cDNA of this construct in transfected midbrain neurons and HEK 293T cells and obtained near normal functional expression, ACh pharmacological sensitivity and subcellular targeting. We produced analogous fluorescently-labeled $\alpha 4$ nAChR genomic targeting constructs and made significant progress in producing three lines of knock-in mice. We generated the following genomic targeting constructs: $\alpha 4$ -YFP, $\alpha 4$ L9'A-YFP, and $\alpha 4$ -CFP. Recently, chimera pups were born from the $\alpha 4$ -YFP and $\alpha 4$ -CFP lines. Blastocyst injections for the nicotine hypersensitive $\alpha 4$ L9'A-YFP line are planned.

Using quantitative fluorescence microscopy we will examine the localization of $\alpha 4$ nAChRs in the CNS. We will initially perform immunohistochemistry using an antibody against the $\alpha 4$ nicotinic receptor subunit in wild type, $\alpha 4$ -YFP, $\alpha 4$ L9'A-YFP, $\alpha 4$ -CFP, and $\alpha 4$ knock-out (negative control). We will examine whether the localization patterns between WT and the fluorescently-tagged $\alpha 4$ knock-ins are similar and the expression levels are comparable. Expression levels will also be examined with Western blots. Developmental expression patterns of $\alpha 4$ -YFP, $\alpha 4$ -CFP and $\alpha 4$ L9'A-YFP will be examined at E10, E15, E20, P1, P10, P20, and P60.

We will examine changes in $\alpha 4$ expression and assembly with chronic nicotine throughout the CNS. Osmotic pumps delivering nicotine at 4 mg/kg/hr or saline (controls) will be implanted subcutaneously in knock-in mice. Mouse brains will be sectioned (at days 0, 1, 2, 4, and 8) and examined using laser scanning confocal microscopy for altered expression levels and subcellular targeting. Fluorescence resonance energy transfer (FRET) will be performed in ($\alpha 4$ -YFP)($\alpha 4$ -CFP) mice receiving either nicotine or saline to examine whether nicotine alters subunit assembly of nicotinic receptors. In conclusion, we hope that the findings of this study will allow an accurate temporal and spatial mapping of $\alpha 4$ nicotinic receptor expression in the CNS and the effects of chronic nicotine exposure.

112. The ANDFLE mutations do not enhance Ca^{2+} block of $\alpha 4\beta 2$ neuronal nicotinic receptors
Nivalda O. Rodrigues-Pinguet, Thierry J. Pinguet*, Bruce N. Cohen

We previously showed that rat homologs ($\alpha 4$ S252F, $\alpha 4$ +L264, $\alpha 4$ S256L, $\beta 2$ V262L, $\beta 2$ V262M) of five nicotinic mutations linked to autosomal dominant nocturnal frontal lobe epilepsy (ANDFLE) inhibit Ca^{2+}

potentiation of the $\alpha 4\beta 2$ acetylcholine (ACh) response. To study the molecular mechanism underlying this inhibition, we co-expressed these mutations with one in the amino-terminal domain $\alpha 4$ (E180Q) that eliminates the positive allosteric effects of Ca^{2+} . If the ANDFLE mutations inhibit Ca^{2+} potentiation by enhancing $\alpha 4\beta 2$ Ca^{2+} block, then Ca^{2+} should block the $\alpha 4$ (E180Q):ANDFLE double mutant ACh response more than it blocks the $\alpha 4$ (E180Q) single mutant ACh response. Consistent with this hypothesis, 2 mM Ca^{2+} reduced the peak $\alpha 4$ (E180Q) $\beta 2$ 1 mM ACh response by $10 \pm 1\%$ ($n = 4$) and, the $\alpha 4$ (E180Q:+L264) $\beta 2$ and $\alpha 4$ (E180Q) $\beta 2$ (V262M) responses by $50 \pm 2\%$ ($n = 4$), an enhancement of block consistent with the effects of the corresponding single ANDFLE mutations on $\alpha 4\beta 2$ Ca^{2+} potentiation. In contrast, 2 mM Ca^{2+} did not inhibit the $\alpha 4$ (E180Q:S252F) $\beta 2$ 1 mM ACh response and it reduced the $\alpha 4$ (E180Q:S256L) $\beta 2$ response by only $10 \pm 4\%$ ($n = 8$). Hence, these two ANDFLE mutations inhibit Ca^{2+} potentiation by interfering with the positive allosteric effects of Ca^{2+} . Finally, 2 mM Ca^{2+} reduced the $\alpha 4$ (E180Q) $\beta 2$ (V262L) 1 mM ACh response by $30 \pm 5\%$ ($n = 6$), too small an enhancement of block to account for the effects of the corresponding single ANDFLE mutation on $\alpha 4\beta 2$ Ca^{2+} potentiation. Thus, either (1) the different ANDFLE mutations inhibit $\alpha 4\beta 2$ Ca^{2+} potentiation by two different molecular mechanisms or, (2) they all inhibit $\alpha 4\beta 2$ Ca^{2+} potentiation by interfering with the positive allosteric effects of Ca^{2+} but the $\alpha 4$ +L264, $\beta 2$ V262L, and $\beta 2$ V262M mutations interact additionally with the $\alpha 4$ (E180Q) mutation to convert Ca^{2+} into a negative allosteric modulator.

*Luxtera, Inc, Carlsbad, CA, USA

113. Nicotine activation of $\alpha 4^*$ receptors is sufficient for reward, tolerance and sensitization

Andrew R. Tapper, Sheri L. McKinney, Raad Nashmi, Johannes Schwarz¹, Purnima Deshpande, Cesar Labarca, Paul Whiteaker², Michael J. Marks², Allan C. Collins²

The identity of nicotinic receptor subtypes sufficient to elicit both the acute and chronic effects of nicotine associated with dependence is unknown. Exon 5 of the mouse $\alpha 4$ nicotinic receptor gene was replaced with an altered exon harboring a single codon mutation, Leu9'Ala in the pore forming M2 domain, rendering $\alpha 4^*$ receptors hypersensitive to nicotine. At nicotine concentrations lower than those effective on wild-type neurons, mutant midbrain neurons are excited in cultures and in slices; and chronic exposure (3-4 d) to low-dose nicotine upregulates nicotine responses in midbrain cultures. Conditioned nicotine-induced reinforcement behavior occurs in hypersensitive animals at doses 50-fold lower than the optimal doses for wild-type animals. In addition, nicotine-induced temperature effects are attenuated after several single daily low-dose i.p.

injections, indicating the development of tolerance. Daily low-dose nicotine injections also produce sensitization of locomotor behavior. Thus, low-dose nicotine administration to the $\alpha 4^*$ -hypersensitive cells and animals mimics experiments with a hypothetical perfect $\alpha 4^*$ -selective agonist, but with the precise pharmacodynamics of nicotine itself; and nicotine activation of $\alpha 4^*$ receptors is sufficient for reward, tolerance, and sensitization.

¹Department of Neurology, University of Leipzig, 04103, Germany

²Institute of Behavioral Genetics, University of Colorado, Boulder, CO 80309

114. Functional expression studies of $\alpha 4$ -containing nicotinic receptors with a Leu9'Ala gain of function mutation

Carlos Fonck, Michael Marks*, Paul Whiteaker*, Cesar Labarca, Raad Nashmi, Sheri McKinney, Nivalda Rodrigues-Pinguet, Bruce Cohen, Allan C. Collins*

The most important nicotinic acetylcholine receptor subtype, in terms of agonist sensitivity, abundance and widespread brain distribution, appears to be the one formed by $\alpha 4$ coassembled with $\beta 2$ subunits. We have generated knock-in mice containing a Leu9'Ala mutation in the $\alpha 4$ subunit of nicotinic receptors, which increases receptor sensitivity to agonists such as nicotine and acetylcholine (ACh). In addition to studying the behavior of the L9'A mice, we are also interested in understanding the mechanisms that control the functional expression of these hypersensitive receptors. To further characterize the mutation, nicotine and/or ACh responses were measured in: a) voltage-clamped *Xenopus* oocytes expressing mouse $\alpha 4\beta 2$ and $\alpha 4\beta 2$ receptors; b) thalamic primary cell cultures obtained from heterozygous (het) and homozygous (hom) L9'A mouse embryos; and c) synaptosomes made from cortex and thalamus of het and hom L9'A mice. In oocytes, the EC₅₀s of the nicotine and ACh concentration-response relationships showed a 30-fold decrease in L9'A compared to WT receptors. At saturating concentrations of nicotine, the maximal mutant and WT nicotine responses were similar. Fura 2-loaded cell cultures derived from L9'A embryos were ~15-25 times more sensitive to nicotine- and ACh-induced increases in intracellular Ca²⁺ compared to WT. L9'A cells also displayed a 4-fold larger Fura 2 response than WT cells at saturating nicotine concentrations. Synaptosomes made from L9'A thalamus and cortex were 5-10 times more sensitive in the ACh-induced ⁸⁶Rb⁺ efflux assay compared to WT. At saturating ACh concentrations, interestingly, synaptosomes obtained from hom L9'A mice had a marked reduction (70 %) in ⁸⁶Rb⁺ efflux compared to WT. In conclusion, hypersensitive $\alpha 4$ L9'A-containing receptors are expressed in L9'A mice but factors such as host cell type, developmental stage, and/or subcellular distribution appear to affect the level of functional L9'A expression.

*Institute of Behavioral Genetics, University of Colorado, Boulder, CO 80309

115. Enhanced expression of L9'S mutant nAChR in adult mice increases the loss of midbrain dopaminergic neurons

Johannes Schwarz¹, Sigrid C. Schwarz¹, Oliver Dorigo², Alexandra Stuetzer¹, Cesar Labarca, Purnima Deshpande, Jose S. Gil², Arnold J. Berk², Henry A. Lester

Knock-in mice expressing hypersensitive L9'S $\alpha 4$ nicotinic receptors (nAChR) display dominant neonatal lethality and a dopaminergic deficit in embryonic midbrain. Heterozygous L9'S mice that retain the neomycin selection cassette express low levels of the mutant allele and are viable and fertile. Analyses of adult brains of these surviving heterozygous mice also show mild deficits of dopaminergic neurons but rather increased than decreased spontaneous locomotion.

We removed the neomycin cassette in adult animals via helper-dependent adenovirus (HDA)-mediated cre recombination. Locomotion was altered before and after amphetamine application in L9'S HDA-cre injected animals, while there was no effect in L9'S HDA-control or littermate wild-type (WT) mice injected with either virus. Immunocytochemical analyses revealed a marked loss of dopaminergic neurons in L9'S HDA-cre injected mice compared to controls. 20-33 days post-injection there was expression of YFP in many neurons and few glial cells at the injection site.

HAD-mediated gene transfer into the midbrain induced sufficient functional expression of cre in dopaminergic neurons to allow for postnatal recombination and a subsequent increase of L9'S mutant nAChR expression, which led to cholinergic toxicity of dopaminergic neurons.

¹Department of Neurology, University of Leipzig, Liebigstr. 22a, 04316 Leipzig, Germany

²Molecular Biology Institute and Department of Microbiology, Immunology and Molecular Genetics, University of California, Los Angeles, CA 90095, USA

116. Enhanced expression of L9'S mutant nAChR in adult mice using transgenic expression of inducible cre

Johannes Schwarz¹, Sabine Gehre¹, Cesar Labarca, Henry A. Lester

Knock-in mice expressing hypersensitive L9'S $\alpha 4$ nicotinic receptors (nAChR) display dominant neonatal lethality and a dopaminergic deficit in embryonic midbrain. Heterozygous L9'S mice that retain the neomycin selection cassette express low levels of the mutant allele and are viable and fertile. Adult excision of the neomycin cassette induces a Parkinsonian phenotype and dramatic degeneration of substantia nigra dopaminergic neurons.

We have constructed a transgenic mouse that expresses cre fused to a mutated ligand-binding domain of the estrogen receptor. When a synthetic agonist binds to

this receptor, cre can enter the nucleus and mediate cre-dependent recombination. Expression of this cre-ERT2 gene is restricted to catecholaminergic neurons via control of a 9 kb fragment of the rat tyrosine-hydroxylase promoter.

Several positive founder mice have been identified. Expression of the transgene has been identified using PCR and RT-PCR. Currently transgenic mice are mated with heterozygous L9'S mice and young adult mice are being treated with the synthetic estrogen receptor agonist tamoxifen. Spontaneous locomotor behavior and the number of dopaminergic neurons in substantia nigra will be assessed shortly.

We hope that these double transgenic mice represent a useful animal model to test treatment strategies aimed at protecting dopaminergic neurons from excitotoxic degeneration.

¹Department of Neurology, University of Leipzig, Liebigstr. 22a, 04316 Leipzig, Germany

117. Use of hypersensitive $\alpha 4$ mice to study the role of $\alpha 4$ in the hippocampus

Irina V. Sokolova

Heterozygous Leu9'Ala knock-in mice expressing hypersensitive nicotinic acetylcholine receptors (nAChR) $\alpha 4$ subunits were used to study the effect of nicotine on neuronal membrane currents. In patch-clamp experiments using coronal brain slices, perfusion with nicotine (1 μ M) on the background of MLA (10 nM) induced a long-lasting increase of the frequency of spontaneous IPSCs by $51 \pm 30\%$ of baseline (15 min after nicotine washout) in about half of CA1 pyramidal neurons. This effect of nicotine in Leu9'Ala mice was comparable to that in the wild-type mice ($33 \pm 8\%$ increase of baseline IPSC frequency 15 min after nicotine washout). Perfusion with nicotine on the background of MLA (10 nM) did not affect the holding currents of the voltage-clamped CA1 pyramidal neurons and stratum radiatum (SR) interneurons. Local application of nicotine over neuronal cell bodies (using a glass micropipette and a Picospritzer) also produce no effect on the holding currents in these types of hippocampal neurons as well (six experiments on each type of neurons).

However, in about half of the stratum lacunosum moleculare (SLM) interneurons in Leu9'Ala, but not in the wild type, preparations local application of nicotine produced a negative deflection of the holding membrane current. The nicotine-induced current resulted from a direct effect of nicotine on $\alpha 4$ -containing nAChRs, since it was not blocked by the glutamate receptor antagonist kynurenic acid (2 mM), GABA_A receptor antagonists picrotoxin (100 μ M) and gabazine (20 μ M) and glycine receptor antagonist strychnine (2 μ M), but was completely and reversibly blocked by DH β E (2 μ M). Maximum response to nicotine was observed at concentrations of nicotine ≥ 10 μ M and constituted 102 ± 18 pA. At concentrations < 10 μ M, responses to nicotine declined proportionately to nicotine concentration (50 ± 6 pA at 5

μ M and 26 ± 8 pA at 2 μ M nicotine). Morphological studies of nicotine-responsive interneurons suggested a possible role they might play in modulation of pyramidal neuron excitability and hippocampal population oscillations.

118. Preparation of constructs for $\beta 2$ ADFLE mutations and $\beta 2$ -XFP fusion proteins

Cesar Labarca, Raad Nashmi, Purnima Deshpande

These constructs were prepared for generation of knock-in mice by homologous recombination in ES cells.

ADNFLE mutations: A 6.3 kb fragment of 129SvJ $\beta 2$ genomic DNA (from Jim Boulter) containing exon 5 was extended at the 3' end with a 3.7 kb fragment prepared by PCR from 129 SvJ ES cell genomic DNA. The 10 kb fragment was inserted into the EcoRI-KpnI site of pKO Scrambler V907 vector (Lexicon-Genetics). The V22'L and V22'M mutations were introduced by site directed mutagenesis using the Quick Change protocol (Stratagene). A neomycin resistance cassette flanked by loxP sites was inserted 176 bp downstream from exon 5 for positive selection. A diphtheria toxin A chain cassette was inserted in the RsrII site of pKO to provide negative selection. Arms of homology on both sides of the mutation are about 4 kb.

XFP fusion proteins: The same 10 kb fragment of $\beta 2$ genomic DNA in pKO, with the neomycin resistance and diphtheria toxin selection cassettes, was used to prepare these constructs. CFP with an upstream c-myc tag was introduced in frame into the PpuMI restriction site, which is in the M3-M4 intracellular loop of $\beta 2$, at aminoacid position 381. YFP with an upstream HA epitope tag was introduced in frame into the PpuMI site. Insertion of the fluorescent protein at that position does not seem to affect the function of the receptor. Fluorescently-tagged AChR receptors containing yellow (YFP) and cyan (CFP) fluorescent proteins incorporated into that site resemble wild-type receptors in maximal responses to ACh, dose-response relations, ACh-induced Ca²⁺ influx, and somatic and dendritic distribution when expressed in human embryonic kidney (HEK) 293T cells and cultured midbrain neurons.

Reference

Nashmi et al. (2003) J. Neurosci. 17:11554-11567.

119. RGS9-deficient mice show abnormal involuntary movements following application of dopamine agonists

Jana Ebert¹, Petra Seyffarth¹, Maja Jungnitsch¹, Melvin I. Simon, Henry A. Lester, Johannes Schwarz¹

Drug-induced abnormal involuntary movements (AIM) can cause considerable dysfunction in patients with Parkinson's disease receiving levodopa treatment or patients receiving neuroleptic therapy. The pathophysiology of these movement disorders is to a large extent unclear. Alterations of striatal dopamine-

D2-receptors (DRD2) signaling very likely contribute to their pathogenesis since both agonists and antagonists of DRD2 can cause drug-induced AIM. Regulator of G-protein signaling 9 (RGS9) is expressed in the brain exclusively in medium spiny striatal projection neurons and belongs to the family of G α GTPase accelerating proteins increasing the OFF kinetic of DRD2 signaling. We have previously shown that reserpinized- or haloperidol-treated RGS9-deficient mice show profound AIM when challenged with quinpirole or apomorphine.

In this study we investigated the frequency and severity of AIM following various doses of apomorphine, quinpirole, SKF 38393 or levodopa in untreated and haloperidol-treated RGS9-deficient mice and their wild-type littermates. We showed that RGS9-deficient animals without pretreatment with dopamine-depleting or DRD2-blocking agents displayed significantly more dystonic posturing and jerky limp movements compared to their wild-type littermates after application of high doses of quinpirole or apomorphine. Following pretreatment with haloperidol these differences were more pronounced. The DRD1 agonist SKF 38393 did not elicit abnormal behavior or differences in behavior between genotypes, confirming that RGS9 selectively dampens DRD2 signaling.

We conclude that physiological expression of RGS9 is necessary for motor control following stimulation of DRD2. Alterations in expression of this gene could provide a molecular explanation and a novel drug target for drug-induced AIM.

¹Department of Neurology, University of Leipzig, Germany

120. Interaction of the α 7 acetylcholine receptor with the Alzheimer's amyloid peptide

Joanna Jankowsky

Several reports in the recent literature have revealed a potential interaction between the amyloid- β peptide (A β) of Alzheimer's disease and the α 7 nicotinic acetylcholine receptor. The reports suggest that the A β peptide, found as aggregates throughout the brains of patients with Alzheimer's disease, can bind to and inhibit the activity of the α 7 ion channel. The relative importance of this interaction in the pathogenesis of Alzheimer's disease is not yet known, however, the abundance of the α 7 receptor in the forebrain and its ability to modulate the strength of synaptic transmission in multiple neurotransmitter systems suggest that any decrease in α 7 activity could have a large impact on neuronal function.

We have begun to investigate the interaction of A β with the α 7 receptor using several different approaches. Initially, we have used *Xenopus* oocytes to express the α 7 receptor in vitro and examine the conditions required for the reported A β interaction. Specifically, we would like to address whether the receptor sensitivity crosses species (human-mouse), whether it is dependent on the aggregation state of the peptide, and whether external calcium plays any role in the α 7 response to A β .

An alternative approach we have begun towards understanding the role of this interaction in Alzheimer's disease will use genetically engineered mice to study the rate of amyloid aggregation and neuronal loss in animals that either lack the α 7 receptor (knock-out) or which express a (knock-in) hypersensitive mutation. The α 7 null and hypersensitive strains will be crossed to transgenic animals that express a mutated form of amyloid precursor protein (APP). These APP transgenic mice overproduce the A β peptide and develop an aging-associated amyloid pathology much like the human patients. The matings to the α 7 strains can take several generations to complete, after which mice with the desired genotype need to be aged for up to nine months. The second generation of crosses is already underway and offspring with the needed genotypes are now being identified.

121. Investigating trafficking and mis-trafficking of fluorescently-labeled GABA transporter, mGAT-1

Fraser J. Moss, Joanna L. Jankowsky

We intend to understand the density, intracellular processing, PDZ interactions, trafficking, and possible dimerization of the GABA transporter mGAT1, by studying knock-in mice carrying fusions between mGAT1 and fluorescent proteins. Our laboratory has already generated an mGAT1-GFP strain and described its use to identify GABAergic interneurons in both tissue sections and in culture and to quantify the membrane density of mGAT1 protein in presynaptic boutons. Unfortunately, biochemistry determined most of the GFP-tagged GAT1 protein did not actually insert into the neuronal membrane like the wild-type animals, but resided within the cytoplasm 100 Å below of the membrane surface. Re-examination of our construct determined that fusing GFP to the C-terminal of mGAT1 probably masked motifs important for the delivery of the mGAT-1 molecule into the plasma membrane, in particular the last three amino acids that resemble a class II PDZ-interacting domain. We therefore, generated a new set of fluorescent constructs that added the C-terminal of the human GAT1 after the fluorophore. The lengths of added hGAT1 C-terminal varied from 3 to 45 residues, the goal being to identify the minimum number needed to restore wild-type trafficking. [³H]-GABA uptake assays were performed on mouse neuroblastoma N2a cells transiently transfected with each construct. We found that uptake by fluorescently-labeled mGAT1 is restored to wild-type levels by the addition of the 8 h GAT1 C-terminal residues. Intriguingly, addition of the 15 to 28 C-terminal residues allowed greater uptake than wild-type mGAT1, while addition of 45 residues has the same diminished function as our original knock-in fusion protein. These data indicate that although the last eight amino acids are important for driving membrane insertion of mGAT1, other regulatory elements in the GAT1 C-terminus also modulate mGAT1 GABA uptake in vitro. Future work will further characterize the +8 mGAT1 fusion proteins and generate the next iterations of fluorescent mGAT1 knock-in mice.

122. Visualization of mGAT1 incorporation in boutons using total internal reflection fluorescence microscopy
Princess Imoukhuede

This project aims to understand the density, intracellular processing, trafficking, and possible dimerization of the GABA transporter mGAT1. To this end, our model system is cerebellar cultures from knock-in mice carrying fusions between mGAT1 and fluorescent proteins (XFP, where G = green; C, cyan; Y, yellow). In collaboration with Dr. Robert Chow of the University of Southern California, we are testing the hypothesis that GAT1 is carried on unique vesicles. Such vesicles will be characterized by watching fusion events and quantifying the amount of mGAT1 molecules within vesicles using evanescent wave-total internal reflection fluorescence (TIR-FM) microscopy. EF/TIR-FM is best used to detect movements of fluorescently-labeled molecules within ~100 nm of the cell surface. We performed a systematic series of preliminary experiments to find a substrate that allows the membrane to approach the glass slide within 100 nm. Once cell-substrate conditions were optimized we turned our attention to perform imaging studies. We induce trafficking events by applying a translocation cocktail to the cell imaging media and use TIR-FM to monitor the resulting vesicle movement on and off the membrane. Next, we will use cultures at various ages, post-plating, in order to monitor pre- and post-vesicle fusion.

123. Postsynaptic mechanisms are essential for forskolin-induced potentiation of synaptic transmission

Irina V. Sokolova, Norman Davidson

It has been demonstrated that stimulation of protein kinase A (PKA) results in an enhancement of synaptic transmission in the hippocampus and other brain areas. Although postsynaptic AMPA-specific glutamate receptors are among potential PKA targets, analysis of electrophysiological experiments using classical quantal analysis attributes the effect of PKA activation to presynaptic mechanisms. To further investigate mechanisms of the PKA-mediated potentiation of synaptic transmission we used rat hippocampal embryonic cultures. Paired recordings under the perforated patch demonstrated that treatment with forskolin for 15 min produced long-lasting potentiation of evoked EPSCs (eEPSCs) mediated by the cAMP/PKA pathway. eEPSC amplitudes increased to 240 ± 10 % of baseline after 15 min of forskolin treatment (early potentiation). eEPSCs declined upon forskolin washout but stabilized at a potentiated level about 10 min after the start of washout. Potentiation remained for at least 85 min after forskolin washout and constituted 152 ± 7 % of baseline (late potentiation). Disruption of presynaptic processes with the whole-cell and internal solution containing PKA inhibitor peptide did not affect early potentiation in all five experiments. Late potentiation persisted in three of five experiments with the presynaptic neuron under the whole-cell configuration. In

contrast, postsynaptic whole-cell recording impaired early potentiation and abolished late potentiation. The enhancement of miniature current frequency produced by forskolin in the perforated patch configuration was attenuated when recorded using the whole-cell configuration. When the effect of dendritic filtering of mEPSCs was minimized by using low-density neuronal cultures, forskolin also induced an increase of mEPSC amplitudes in the perforated patch, but not in the whole-cell, experiments. As demonstrated with Western blot, forskolin treatment produced phosphorylation of the AMPA receptor subunit GluR1 at Ser 845, an amino acid residue specifically targeted by PKA. Potentiation of eEPSCs was not activity dependent and persisted under non-stimulated conditions. NMDA receptor blockade did not abolish forskolin-induced potentiation. In summary, we demonstrated that forskolin-induced potentiation of eEPSCs was mediated by postsynaptic mechanisms, which includes phosphorylation of AMPA receptors at the site targeted by PKA.

124. On-resin assembly of a linkerless lanthanide(III)-based luminescence label and its application to the total synthesis of site specifically labeled mechanosensitive channels
Daniel Clayton, Christian F.W. Becker¹, George Shapovalov², Gerd G. Kochendoerfer¹

Lanthanide(III)-based chelates are used increasingly for spectroscopy applications, in particular Luminescence Resonance Energy Transfer (LRET), due to the unique long-lived luminescence properties of the chelated ions. LRET is a type of luminescence assay where a lanthanide donor (Tb^{3+} or Eu^{3+}) transfers energy to an organic fluorescent acceptor in a distance-dependent manner, thus yielding static or dynamic distance information. For the purpose of using an LRET approach to study the structure and function of mechanosensitive channels, a synthesis strategy for the on-resin assembly of luminescent lanthanide chelates from commercially available compounds was developed. Advantages of this novel approach include the absence of spacers between the metal ion and the attachment site, and compatibility with typical chemical protein synthesis protection schemes. Methoxycoumarin-labeled lysine and tris(t-butyl)-DOTA were consecutively coupled with high efficiency to a free amino group in otherwise fully protected peptide segments using standard peptide synthesis methods. Addition of stoichiometric amounts of Tb^{3+} to the modified, cleaved and purified peptides yielded the desired lanthanide chelate. To assess the luminescent properties of the resulting protein constructs after reconstitution into a TFE/water mixture (4:1) the methoxycoumarin ring of the label was excited at 336 nm resulting in an emission spectrum typical of Tb^{3+} with a luminescence lifetime of 0.67 ms. Incorporation of this label into a chemically-synthesized, full-length mechanosensitive channel of large conductance (MscL) of *E. coli* and subsequent reconstitution into vesicles resulted in a functional mechanosensitive channel of comparable conductance to

the wild-type channel. However, this channel required increased suction to gate and exhibited more flickery activity at the fully open state than observed previously for recombinant or biotinylated synthetic Ec-MscL. The location of the probe close to the backbone of this protein may provide precise information about conformational changes during channel opening from LRET studies.

¹Gryphon Therapeutics, 600 Gateway Blvd., South San Francisco, USA

²Division of Biology and Division of Physics, Math, and Astronomy, California Institute of Technology

125. Studies on the voltage dependence of the mechanosensitive channel of small conductance (MscS)

Lori W. Lee, Steven A. Spronk, Dennis A. Dougherty

The mechanosensitive channel of small conductance (MscS) acts as a safety valve for cells under osmotic stress by responding to stretching of the cell membrane. It is characterized by a conductance of 1 nS. Gating of MscS is also voltage modulated. The molecular basis of its voltage sensitivity remains elusive, but the crystal structure of MscS from the Rees group suggests that several arginines may play a role. We aim to determine the role of these arginines, specifically arginine 46, in voltage sensitivity using mutational analysis coupled with molecular dynamics simulations. Single-channel electrophysiological analysis of the Arg46Ala mutant of *E. coli* MscS is under way. Furthermore, Arg46Ala-MscS does not exhibit voltage desensitization/inactivation as seen with wild-type *E. coli* MscS. Molecular dynamics simulations suggest that Arg46 mutants are insensitive to voltage. They suggest that wild-type MscS behaves differently in the presence or absence of a voltage, but Arg46Ala-MscS does not. Our experimental and computation results may test the hypothesis that arginine 46 plays a role in the voltage sensitivity of *E. coli* MscS.

126. Gating transitions in bacterial ion channels measured at 3 μ s resolution

George Shapovalov^{*}, Henry A. Lester

Ion channels of high conductance (>200 pS) are widespread among prokaryotes and eukaryotes. Two examples, the *E. coli* mechanosensitive ion channels Ec-MscS and Ec-MscL, pass currents of 125 - 300 pA. To resolve temporal details of conductance transitions, a patch-clamp setup was optimized for low-noise recordings at a time resolution of 3 μ s (10-20 times faster than usual). Analyses of the high-resolution recordings confirm that Ec-MscL visits many subconductance states and show that most of the intersubstate transitions occur more slowly than the effective resolution of 3 μ s. There is a clear trend toward longer transition times for the larger transitions. In Ec-MscS recordings, the majority of the observed full-conductance transitions are also composite. We detected a short-lived (~20 μ s) Ec-MscS substate at 2/3 of full conductance; transitions between 2/3 and full conductance did not show fine structure and had a timecourse limited

by the achieved resolution. Opening and closing transitions in MscS are symmetrical and are not preceded or followed by smaller, rapid currents ("anticipations" or "regrets"). Compared with other, lower-conductance channels, these measurements may detect unusually early states in the transitions from fully closed to fully open. Increased temporal resolution at the single-molecule level reveals that some elementary steps of structural transitions are composite and follow several alternative pathways, while others still escape resolution. High-bandwidth, low-noise single-channel measurements may provide details about state transitions in other high-conductance channels; and similar procedures may also be applied to channel- and nanopore-based single-molecule DNA measurements.

^{*}Division of Biology and Division of Physics, Math, and Astronomy, California Institute of Technology

Publications

Beene, D.L., Price, K.L., Lester, H.A., Dougherty, D.A. and Lummis, S.C.R. (2004) Tyrosine residues that control binding and gating in the 5-HT₃ receptor revealed by unnatural amino acid mutagenesis. *J. Neurosci.* In press.

Bhattacharya, A., Dang, H., Zhu, Q.-M., Schnegelsberg, B., RoZengurt, N., Cain, G., Prantil, R., Vorp, D.A., Guy, N., Julius, D., Lester, H.A., Ford, A.P.D.W. and Cockayne, D.A. (2004) Uropathic observations in mice expressing a constitutively active point mutation in the 5-HT_{3A} subunit. *J. Neurosci.* 24:5537-5548.

Christian, F.W. Becker, D.C., Shapovalov, G., Lester, H.A. and Kochendoerfer, G.G. (2004) On-resin assembly of a linkerless lanthanide(III)-based luminescence label and its application to the total synthesis of site-specifically labeled mechanosensitive channels *Bioconjugate Chemistry.* In press.

Clayton, D., Shapovalov, G., Maurer, J.A., Dougherty, D.A., Lester, H.A. and Kochendoerfer, G. (2004) Total chemical synthesis and electrophysiological characterization of mechanosensitive channels from *Escherichia coli* and *Mycobacterium tuberculosis*. *PNAS* 101:4764-4769.

Dahan, D., Dibas, D.I., Petersson, E.J., Auyeung, V.C., Chanda, B., F. Bezanilla, F., Dougherty, D.A. and Lester, H.A. (2004) A fluorophore attached to nicotinic acetylcholine receptor β M2 detects transitions of the $\alpha\delta$ agonist binding site. *PNAS* 27:10195-10200.

Diba, K., Lester, H.A., Koch, C. (2004) Intrinsic noise in cultured hippocampal neurons: Experiment and modeling. *J. Neurosci.* In press.

- Gutman, G.A., Chandy, K.G., Adelman, J.P., Aiyar, J., Bayliss, D.A., Clapham, D.E., Covarriubias, M., Desir, G.V., Furuichi, K., Ganetzky, B., Garcia, M.L., Grissmer, S., Jan, L.Y., Karschin, A., Kim, D., Kuperschmidt, S., Kurachi, Y., Lazdunski, M., Lesage, F., Lester, H.A., McKinnon, D., Nichols, C.G., O'Kelly, I., Robbins, J., Robertson, G.A., Rudy, B., Sanguinetti, M., Seino, S., Stuehmer, W., Tamkun, M.M., Vandenberg, C.A., Wei, A., Wulff, H. and Wymore, R.S. (2003) International Union of Pharmacology, XLI. Compendium of voltage-gated ion channels: Potassium channels. *Pharmacol Rev.* 55:583-586.
- Kovoor, A., Seyffarth, P., Ebert, J., Barghshoon, S., Chen, C.-K., Schwarz, S., Axelrod, J.D., Simon, M.I., Lester, H.A. and Schwarz, J. (2004) The DEP domain and the role of RGS9 in drug-induced dyskinesia. Submitted for publication.
- Lester, H.A., Dibas, M.I., Dahan, D.S., Leite, J.F. and Dougherty, D.A. (2004) Cys-loop receptors: New twists and turns. *Trends Neurosci.* 6:329-336.
- Nashmi, R., Dickinson, M.E., McKinney, S., Jareb, M., Labarca, C., Fraser, S.E. and Lester, H.A. (2003) Assembly of $\alpha 4\beta 2$ nicotinic acetylcholine receptors assessed with functional fluorescently labeled subunits: Effects of localization, trafficking, and nicotine-induced upregulation in clonal mammalian cells and in cultured midbrain neurons. *J. Neurosci.* 23:11554-11567.
- Orb, S., Wieacker, J., Labarca, C., Fonck, C., Seyffarth, P., Lester, H.A. Schwarz, J. (2004) Knock-in mice with Leu9'Ser $\alpha 4$ nicotinic receptors: substantia nigra dopaminergic neurons are hypersensitive to agonist and are lost postnatally. *Physiological Genomics* 18:299-307.
- Owens, J.C., Balogh, S.A., McClure-Begley, T.D., Butt, C.M., Labarca, C., Lester, H.A., Picciotto, M.R., Wehner, J.M. and Collins, A.C. (2003) $\alpha 4\beta 2^*$ nicotinic acetylcholine receptors modulate the effects of ethanol and nicotine on the acoustic startle response targets for both nicotine and ethanol. *Alcoholism: Clin. Exp. Res.* 27:1867-1875.
- Shapovalov, G. and Lester, H.A. (2004) Gating transitions in bacterial ion channels measured at 3 μ s resolution. *J. Gen. Physiol.* 124:151-161.
- Storch, A., Lester, H.A., Boehm, B.O. and Schwarz, J. (2003) Functional characterization of dopaminergic neurons derived from rodent mesencephalic progenitor cells. *J. Chem. Neuro. Anat.* 2:133-142.
- Tapper, A.R., McKinney, S.S., Nashmi, R., Schwarz, J., Deshpande, P., Labarca, C., Whiteaker, P., Marks, M.J., Collins, A.C. and Lester, H.A. (2004) Nicotine activation of $\alpha 4^*$ receptors is sufficient for reward, tolerance and sensitization. *Science.* In press.

Professor: Paul H. Patterson
 Visiting Professor: Ming-ji Fann
 Senior Research Fellow: Ali Khoshnan
 Research Fellows: Sylvian Bauer, Benjamin Deverman, Kristina Holmberg, Bradley Kerr, Natalia Malkova
 Graduate Students: Walter Bugg, Jennifer Montgomery, Stephen Smith, Amber Southwell
 Research and Laboratory Staff: Jan Ko, Viviana Gradinaru¹, Jennifer Li¹, Doreen McDowell, Limin Shi, Nora Tu¹, Andrea Vasconcellos¹, Erin Watkin, Wendy Xu¹
¹Undergraduate student, Caltech

Support: The work described in the following research reports has been supported by:

Cline Neuroscience Discovery Grant
 Cure Autism Now Foundation
 Ginger and Ted Jenkins
 Hereditary Disease Foundation
 HiQ Foundation
 McGrath Foundation
 McKnight Neuroscience of Brain Disorders Award
 National Institute of Mental Health
 National Institute of Neurological Disease and Stroke
 Roman Reed Spinal Cord Injury Research Fund of California
 Stanley Medical Research Institute

Summary: Much of the research in this laboratory involves the study of interactions between the nervous and immune systems. Using knockout (KO) mice and over-expression in vivo with viral vectors, we are exploring the role of neuropoietic cytokines in PNS and CNS injury and repair, Alzheimer's disease and inflammation. Also in the context of neuroimmune interactions, we are investigating a mouse model of mental illness based on the known risk factor of maternal influenza infection. We are also testing potential therapies for Huntington's disease (HD), using intracellular expression of antibodies, and manipulating NF κ B activity. An additional project involves the study of the mechanism of behavioral stress and melanoma tumor progression.

Cytokines are diffusible, intercellular messengers that were originally studied in the immune system. Our group contributed to the discovery of a new family that we have termed the neuropoietic cytokines, because of their action in both the nervous and hematopoietic/immune systems. We have demonstrated that one of these cytokines, leukemia inhibitory factor (LIF), can coordinate the neuronal, glial and immune reactions to injury. Using both delivery of LIF in vivo and examination of the consequences of knocking out the LIF gene in mice, we find that this cytokine has a powerful regulatory effect on the inflammatory cascade, both within and outside the nervous system. Moreover, LIF can regulate neurogenesis following injury. We find that LIF is a critical regulator of astrocyte and microglial activation following stroke, seizure or trauma, and this cytokine also regulates inflammatory cell infiltration, neuronal and oligodendrocyte death, gene

expression, as well as the production of new neurons from stem cells following injury. These results highlight LIF as an important therapeutic target. We are also examining the role of LIF in a transgenic mouse model of Alzheimer's disease to determine its effects on inflammation and cell proliferation, as well as on plaque formation and removal.

Cytokine involvement in a new model of mental illness is also being investigated. This mouse model is based on findings that maternal viral infection can increase the likelihood of schizophrenia or autism in the offspring. We are using behavioral, neuropathological, molecular and brain imaging methods to investigate the effects of maternal influenza infection on fetal brain development and how this leads to altered behavior in adult offspring.

We are utilizing intracellular antibody expression to block the toxicity of mutant huntingtin (Htt), the protein that causes HD. We have produced single chain antibodies (scFvs) that bind to various domains of Htt, and these can either exacerbate or alleviate Htt toxicity in cultured cells, acute brain slices, and in a *Drosophila* HD model. Work has begun on delivering these scFvs in mouse models of HD. We have also implicated the NF κ B signaling pathway in the pathogenesis of HD, and identified several steps in this signaling cascade as potential therapeutic targets.

127. Maternal influenza infection is likely to alter fetal brain development indirectly: The virus is not detected in the fetus
 Limin Shi, Nora Tu, Paul H. Patterson

Epidemiological studies have shown that maternal infection can increase the risk for mental illness in the offspring. In a mouse model of maternal respiratory infection with influenza virus, the adult offspring display striking behavioral, pharmacological and histological abnormalities. Although influenza primarily infects the respiratory system, there are reports of viral mRNA and protein in the fetus of infected pregnant animals. To determine the extent of viral spread following maternal respiratory infection in our mice, we used RT-PCR to assay various maternal and fetal tissues for the influenza mRNAs Na, NS2, NuP and MP. While maternal lungs exhibit uniformly very strong signals, maternal blood and placenta are only rarely positive, while fetal brains are negative for these viral RNAs. This evidence suggests that the effects of maternal infection on fetal brain development are indirect, probably involving the maternal inflammatory response.

128. Maternal viral infection and mental illness: Gene expression changes in the brains of adult offspring
 Benjamin E. Deverman, Limin Shi, Paul H. Patterson, Jeff Gregg¹

Schizophrenia and autism are complex developmental disorders that are influenced by both genetic and environmental factors. A number of studies indicate that maternal respiratory viral infection increases the incidence of schizophrenia and autism in the offspring.

To understand how maternal infection affects neurodevelopment, we infect pregnant mice with influenza virus and assess the offspring for behavioral and neuropathological abnormalities. In previous studies, we have reported that the adult offspring of infected mothers display a number of behavioral abnormalities that are consistent with mental illness. In order to obtain an unbiased overview of the molecular changes that may underlie these behavioral abnormalities, we are using Affymetrix arrays to compare gene expression in several brain regions taken from the adult offspring of mothers exposed to influenza during pregnancy as well as control offspring. Preliminary results identify several alterations in gene expression that are consistent with those observed in microarray experiments performed on RNA from the postmortem brains of schizophrenic patients, as well as a number of interesting changes not previously reported. In addition, several of the changes involve genes that have been linked to susceptibility to schizophrenia. We are now confirming our findings using quantitative, real-time RT-PCR, in situ hybridization, and/or immunostaining. Findings from this study may aid in our understanding of how genes and environmental factors such as maternal infection interact to alter neurodevelopment in a manner that leads to mental illness.

¹MIND Institute, U.C. Davis

129. The maternal inflammatory response and its effects on the neurodevelopment and behavior of the offspring

Benjamin E. Deverman, Paul H. Patterson

Adult mice born to mothers infected with influenza virus at E9.5 (mid-gestation) have abnormalities in behavior and brain histology that are consistent with those seen in patients with schizophrenia or autism. These abnormalities are likely caused by the maternal inflammatory response to the viral infection as we find that the offspring of mothers injected at E9.5 with poly(I:C), a synthetic dsRNA that elicits an inflammatory response similar to viral infection, exhibit pre-pulse inhibition deficits similar to those observed in the offspring of influenza-infected mothers. Furthermore, using sensitive RT-PCR techniques, we have been unable to detect evidence of direct viral infection of the fetus. To better understand the mechanism by which the maternal inflammatory response can influence neurodevelopment, we are injecting poly(I:C) into pregnant mice at different times during gestation. Because the onset of the cytokine response to poly(I:C) is much more rapid and the duration of the response is shorter than the response to influenza inoculation, we are using poly(I:C) as a tool to dissect the critical time periods during which the fetal brain is most sensitive to activation of the maternal inflammatory response. Specifically, we are looking for correlations between the timing of the cytokine response and the presence of the behavioral and neuropathological abnormalities we observe in the offspring of influenza-infected mice.

130. Production of maternal and fetal cytokines in response to influenza infection or administration of synthetic dsRNA
Wendy Xu¹, Benjamin E. Deverman, Stephen Smith, Paul H. Patterson

Significant epidemiological evidence suggests that there is an increased incidence of schizophrenia and autism in the offspring of women exposed to respiratory viral infection during particular times during pregnancy. In a mouse model based on these findings, the adult offspring of mothers exposed to influenza during pregnancy exhibit several behavioral and neuropathological abnormalities that are consistent with those observed in schizophrenia and autism. Moreover, at least one of these abnormalities is also seen in the adult offspring of mothers injected with poly(I:C), a dsRNA that elicits an inflammatory response similar to that induced by influenza infection. The inflammatory response to viral infection is mediated by the numerous cytokines, many of which could have profound effects on fetal brain development. Therefore, we are measuring cytokine induction during the inflammatory response to influenza virus and poly(I:C) in both maternal and fetal tissues in an effort to determine which cytokines may be responsible for the behavioral and neuropathological abnormalities. We are assessing cytokine levels in the fetal brain, the placenta, and in the maternal serum and lungs using RT-PCR, ELISA and multiplex methods.

¹Caltech undergraduate student

131. The effect of maternal influenza infection on neurobehavioral development of the offspring
Natalia Malkova, Paul H. Patterson

On the basis of epidemiological evidence indicating that maternal influenza infection leads to an increased risk of schizophrenia and autism in the offspring, a mouse model has been developed in which the pregnant mother receives a respiratory infection of human influenza virus at mid-gestation. At birth, the offspring display no signs of encephalopathy or direct viral infection. They do, however, display neuropathology at birth and in adulthood, including reduction in neocortical and hippocampal thickness, pyramidal cell atrophy and reduced levels of reelin. To assess how this model relates to autism, the early behavioral development of pups born to influenza-infected mothers is being studied. One assay involves the repeated ultrasonic vocalizations that are observed when infants are separated from their mothers or social companions. This early vocalization response is strongly conserved in evolution as an affective and communicative display, most likely because of its survival value in eliciting maternal search and retrieval responses, nursing and caretaking. We are also utilizing a mother-recognition test to assess the affinity of pups born to infected mothers for their mothers versus other lactating females.

132. Patterns of brain activity in the adult offspring of mice born to influenza-infected mothers
Natalia Malkova, Ming-Ji Fann, Paul H. Patterson

There is suggestive evidence that brain circuitry is altered in the schizophrenic brain. Imaging studies have also highlighted abnormalities in the responses of the brains of autistic subjects to various sensory stimuli. We have begun a project to investigate the brain circuitry in our mouse model of mental illness. The approach is to map the patterns of activation induced by various sensory stimuli in the brains of adult mice born to infected mothers. These patterns can then be compared to those of mice born to normal mothers, who do not display the abnormal behaviors or neuropathology observed in the mice born to infected mothers. Mapping global neuronal activity is being done histologically using antibodies against a number of immediate early gene proteins and members of MAP kinase pathways. Early results indicate that selective brain areas respond strongly to the sensory stimulation provided in the acoustic startle response test. It will also be of interest to compare the responses of the control and experimental mice to dopaminergic and glutaminergic drugs, as these transmitter systems are the focus of most of the pharmacological studies of schizophrenia.

133. Do cytokines mediate the effects of maternal infection on fetal brain development?
Stephen Smith, Jennifer Li¹, Limin Shi, Paul H. Patterson

Influenza respiratory infection of pregnant mice causes behavioral abnormalities in their offspring consistent with those seen in schizophrenia and autism. We also have evidence that these changes in fetal brain development are due to the maternal anti-viral response rather than to direct viral infection of the fetus. We are testing the hypothesis that certain cytokines produced by the mother are responsible for altering fetal brain development. The approach is to: (i) determine which cytokines are induced in the maternal circulation by respiratory infection; (ii) attempt to mimic the effects of infection by injecting these cytokines in non-infected pregnant mice; and (iii) block the effects of maternal infection on the offspring by injecting pregnant mice with anti-cytokine antibodies or use pregnant cytokine knockout mice. One of the prominent cytokines upregulated by infection is interleukin-6 (IL-6). Preliminary evidence indicates that maternal injection of IL-6 leads to adult offspring with deficits in prepulse inhibition.

¹Caltech undergraduate student

134. Effects of LIF on adult neural stem cells in normal and APP23 mice
Sylvian Bauer, Paul H. Patterson

In the adult brain, newly generated neurons are incorporated in the olfactory bulb (OB) and the subgranular zone of the hippocampus. This neurogenesis can be modulated in vivo by exogenous growth factors,

which can promote neuronal replacement after injury. We have previously shown that leukemia inhibitory factor (LIF) is necessary in vivo for the lesion-induced proliferation of neuronal progenitors that regenerate olfactory sensory neurons in the adult mouse (Bauer et al., 2003, *J. Neurosci.* 23:1792-1803). We are now asking if LIF regulates neurogenesis in the normal adult brain and in the context of a chronic neurodegenerative condition, using APP23 mice, a model of Alzheimer's disease. Adult C57Bl/6J and APP23 mice received a single intracerebroventricular injection of recombinant adenovirus expressing either LIF or LacZ. Bromodeoxyuridine (BrdU) was then injected i.p. once daily (100 mg/kg) for seven days, and the animals were perfused two weeks after the first BrdU injection. Our results thus far show that adenoviral delivery of LIF strongly represses neurogenesis in the SVZ-OB system by reducing cell proliferation and neuronal differentiation in the SVZ, while increasing the formation of astrocytes. In contrast, cell proliferation is increased in the cortex and periventricular areas, where more newly generated astrocytes are detected. In addition, a strong induction of brain inflammation is seen in mice injected with the LIF adenovirus, suggesting that the majority of proliferating cells could be microglia. The extent of neurogenesis in the hippocampus is currently under investigation.

135. Leukemia inhibitory factor and senile plaques in Alzheimer's mice
Andrea Vasconcellos¹, Sylvian Bauer

Plaques containing amyloid- β (A β) peptide are a key feature of Alzheimer's disease (AD) neuropathology. AD also involves an inflammatory response mediated by activated microglia, which have phagocytic function and release cytokines. Here we examine the effect of leukemia inhibitory factor (LIF), a cytokine up-regulated in AD brains, on plaque size and density in the brains of transgenic mice expressing a mutant form of amyloid precursor protein (APP) that causes AD in humans. These transgenic APP mice (APP23) were treated with exogenous LIF through the delivery of a recombinant adenovirus vector (LIF-AdV) to the cerebral ventricles. Control mice were injected with an adenovirus coding for the gene LacZ (LacZ-AdV). Staining for A β in the frontal cortex of APP mice reveals a decreased amyloid burden in LIF-treated brains. Quantification of amyloid burden in the cortex and hippocampus at various times after adenovirus injection will help elucidate the action of LIF. In addition, we are investigating the role of LIF in the AD inflammation in these APP mice.

¹Caltech undergraduate student

136. Using leukemia inhibitory factor (LIF) to prevent secondary cell death after spinal cord injury
Bradley J. Kerr, Paul H. Patterson

Injury to the mammalian spinal cord is accompanied by a delayed, secondary wave of oligodendrocyte apoptosis that arises several days after the

initial injury. This apoptosis occurs in white matter tracts undergoing Wallerian degeneration distant to the injury epicenter. Delayed oligodendrocyte death represents a significant clinical impediment for recovery from spinal cord injury as it may contribute to lesion expansion, chronic demyelination and impairment of axonal conductance in pathways spared from the initial damage. One treatment strategy is to deliver trophic factors to the injured spinal cord to support oligodendrocyte survival. A strong candidate to support oligodendrocyte survival after spinal cord injury is the pleiotropic cytokine, leukemia inhibitory factor (LIF). In vitro, LIF potentiates the differentiation and survival of oligodendrocyte precursors, and can also prevent oligodendrocyte apoptosis in response to growth factor removal or in response to cytotoxic challenge such as the addition of interferon- γ . More recently, in vivo studies have demonstrated that LIF is effective in preventing oligodendrocyte death in a mouse model of multiple sclerosis, Experimental autoimmune encephalomyelitis (EAE). We, therefore, asked whether systemic delivery of LIF could ameliorate oligodendrocyte death in a mouse model of spinal cord injury. We find that daily administration of LIF inhibits apoptosis and promotes oligodendrocyte survival after spinal cord injury. Interestingly, however, this effect does not appear to be mediated by a direct action of LIF on oligodendrocytes but rather via microglia/macrophages, which results in augmented expression of another trophic factor capable of supporting oligodendrocytes survival, insulin-like growth factor 1 (IGF-1).

137. The role of leukemia inhibitory factor in the regulation of the response to seizure
Kristina H. Holmberg

Our group previously found that the cytokine leukemia inhibitory factor (LIF) is induced in astrocytes in response to seizure. I have used pilocarpine to induce seizure in LIF knockout (KO) mice to test the hypothesis that LIF regulates astrocyte, microglial and neuropeptide responses to seizure in the hippocampus. Compared to wild type (WT), the LIF KO mouse displays reduced astrocyte and microglial activation following seizure. Moreover, LIF KO mice show dramatically altered neuropeptide Y (NPY) expression in response to seizure. There is also a sexual dimorphism in the responses of the LIF KO mice. Small differences are seen in the seizure responses between WT and LIF KO in expression of NPY receptor and brain-derived neurotrophic factor as well. However, galanin, known to increase following seizure, shows only minor differences between WT and KO mice. Thus, LIF is required for normal glial responses to seizure and, as in the peripheral nervous system, LIF regulates the expression of certain CNS neuropeptides in vivo.

138. Single chain antibodies to dissect the biological functions of mutant huntingtin
Ali Khoshnhan, Jan Ko, Viviana Gradianaru¹, Paul H. Patterson

Huntington's Disease (HD) is caused by expansion of a polyglutamine stretch in the N-terminus of the protein, huntingtin (Htt). Expression of this mutant Htt results in selective death of neurons in the striatum and the cortex. Large nuclear aggregates and amyloid-like complexes containing Htt are observed in post-mortem tissues. Elucidating the mechanism of neuronal dysfunction caused by mutant Htt and devising molecular strategies for blocking its toxic effects are the goals of this project. We generated eight monoclonal antibodies (mAbs) that recognize the expanded polyglutamine (polyQ) domain, the polyproline (polyP) domains, or the C-terminus of exon-1 of Htt (HDx-1). We have cloned the complementary DNAs of the antigen binding regions of several of these mAbs and have assembled recombinant single chain antibodies (scFvs). Intracellular expression of the MW7 scFv targeted to the polyP domains of Htt reduces cell death caused by expression of mutant Htt in cultured cells, in brain slices and in a *Drosophila* HD model. In contrast, expression of two scFvs recognizing the polyQ domain exacerbates mutant Htt toxicity. Studies are in progress to explore the therapeutic potential of MW7 in a mouse HD model. Anti-polyQ scFvs are being used as reagents to understand the molecular mechanism of Htt aggregation.

¹Caltech undergraduate student

139. Interaction of mutant huntingtin with the NF- κ B pathway

Ali Khoshnhan, Erin Watkin, Jan Ko

Transcriptional dysregulation by mutant huntingtin (Htt) protein has been implicated in the pathogenesis of Huntington's disease (HD). We have found that mutant Htt activates NF- κ B pathway. Mutant Htt physically associates with IKK γ , a regulatory component of the I κ B kinase complex (IKK). In cultured cells, this interaction results in the activation of IKK, leading to the phosphorylation and degradation of the inhibitory protein I κ B α . These findings have in vivo relevance, as striatal extracts from HD transgenic mice have higher levels of IKK than extracts from control mice, and activated NF- κ B is found in the nucleus of striatal and cortical neurons in the HD mice. Binding to IKK γ is mediated by the expanded poly-glutamine stretch in mutant Htt, and is augmented by the proline-rich motifs of Htt. Expression of IKK γ promotes mutant Htt aggregation and nuclear localization. Conversely, a N-terminally truncated form of IKK γ , which interferes with IKK activity, blocks Htt-induced NF- κ B activation and reduces the toxicity of mutant Htt in cell culture and in an acute brain slice model of HD. Toxicity is also inhibited by expression of a mutant F-box deleted E-3 ubiquitin ligase, (Δ F- β TRCP), which specifically blocks degradation of I κ B inhibitory proteins. Thus, aberrant interaction of mutant

Htt with IKK γ , and subsequent NF- κ B activation, may be important for HD pathology. Studies are in progress to understand the interplay between mutant Htt protein, the IKK complex and signaling pathways that are influenced by these interactions.

140. Anti-Htt antibodies as possible therapeutics for Huntington's disease

Amber L. Southwell, Ali Khoshnan, Paul H. Patterson

Huntington's disease (HD) is a progressive neurodegenerative disorder characterized by chorea, dementia and selective degeneration of striatal neurons. The autosomal dominant mutation responsible for HD is an expansion of a CAG repeat coding for polyglutamine in exon 1 of the huntingtin (Htt) protein. Our group has generated single chain monoclonal antibodies that bind Htt and can be expressed intracellularly (intrabodies). The MW1 and two intrabodies, directed against expanded polyglutamine, increase mutant Htt-induced aggregation and cell toxicity in culture. MW7, an intrabody directed at a pair of polyproline stretches in Htt, decreases mutant Htt-induced aggregation and cell death. This effect has been demonstrated in cell culture, acute brain slices (with Peter Reinhart at Duke), and in a *Drosophila* model of HD (with George Jackson at UCLA). The therapeutic potential of MW7 will next be tested in a mouse model of HD. An inducible MW7 transgenic mouse will be generated using the tet-off system. This mouse can then be crossed to the R6/2 mouse HD model. Region-specific tTA transgenic mice can eventually be used to determine the importance of MW7 treatment in specific brain areas. Temporal control of MW7 expression with doxycycline can be used to compare treatment in pre- and post-symptomatic mice. Once temporal and brain regional information is available, adult HD mice can be treated with MW7 using gene therapy. We have generated an adeno-associated viral vector coding for MW7 and IRES-GFP. This virus will be injected into the striatum, cortex or ventricles of pre- and post-symptomatic mice. The mice will then be tested for changes in their behavioral and histological phenotypes. We will also test protein transduction as a therapeutic option. We have generated an expression vector coding for MW7 fused to pep-1, a protein transduction domain. This fusion protein will be injected intracranially or systemically in pre- and post-symptomatic mice. The mice will then be tested for changes in their behavioral and histological phenotypes. Insights acquired through these experiments may contribute to the generation of therapeutics for HD.

141. The effect of behavioral stress on immune surveillance and melanoma progression

Jennifer Montgomery, Paul H. Patterson

We are investigating the relationship between stress, the immune system and melanoma tumor progression. We have found that a paradigm of alternating rotational stress, restraint and cold-water swimming raises the stress hormone corticosterone while avoiding

habituation. In these FVB and C57BL/6 mice, corticosterone-binding globulin does not change with stress, indicating that the increased corticosterone in the experimental animals is free to activate the hypothalamic-pituitary-adrenal axis. In addition, we have assayed the cytokines IL-1 β , TNF- α , IL-6 and IFN- γ , as they have been implicated in the stress response as well as in melanoma growth in culture. We find no changes in the serum concentrations of these cytokines, and so are currently investigating the levels of these cytokines in the hypothalamus, spleen and liver. The same stress protocol is also being applied to a new mouse model of melanoma that is based on the genetics of human tumors. In this transgenic model, cutaneous melanoma occurs spontaneously at a predictable time point, allowing us to study the disease in situ as it naturally progresses. We are monitoring the timing of tumor onset and cytokine levels in mice that undergo behavioral stress and comparing them to control mice that remain unstressed. In addition, we are investigating the effect of this stress protocol on subcutaneously implanted melanoma tumors. We are also beginning experiments that use systemic injection of synthetic glucocorticoids in place of behavioral stress.

Publications

- Armstrong, B.D., Hu, Z., Abad, C., Yamamoto, M., Rodriguez, W.I., Cheng, J., Tam, J., Gomariz, R.P. Patterson, P.H. and Waschek J.A. (2004) Lymphocyte regulation of neuropeptide gene expression following neuronal injury. *J. Neurosci. Res.* 74:240-247.
- Bauer, S., Han, J., Rasika, S., Mauduit, C., Jourdan, F., Benahmed, M., Moyse, E. and Patterson, P.H. (2003) Leukemia inhibitory factor induction is a key signal of lesion-triggered neurogenesis in the adult mouse olfactory epithelium. *J. Neurosci.* 23:1792-1803.
- Kerr, B.J. and Patterson, P.H. (2004) Potent pro-inflammatory actions of leukemia inhibitory factor (LIF) in the spinal cord of the adult mouse. *Exper. Neurol.* 188:391-407.
- Khoshnan, A., Ko, J., Watkin, E.E., Paige, L.A., Reinhart, P.H. and Patterson, P.H. (2004) Activation of the I κ -B kinase complex and NF- κ B contributes to mutant huntingtin neurotoxicity. *J. Neurosci.* 24:7999-8008.
- Khoshnan, A., Ou, S., Ko, J. and Patterson, P.H. (2004) Antibodies against huntingtin: Production and screening of monoclonal and single chain recombinant forms. In: *Methods in Molecular Biology*, vol. 277: Triplet Repeat Protocols, M. Kohwi, ed., Human Press, Totowa, NJ., pp. 87-102.
- Pichel, J.G., Fernandez-Moreno, C., Vicario-Abejon, C., Testillano, P.S., Patterson, P.H. and de Pablo, F (2003) Developmental cooperation of LIF and IGF-1 in mice is tissue-specific and essential for lung maturation involving the transcription factors Sp3 and TTG-1. *Mech. Dev.* 120:349-361.
- Shi, L., Fatemi, S.H., Sidwell, R.W. and Patterson, P.H. (2003) Maternal influenza infection causes behavioral and pharmacological changes in the offspring. *J. Neurosci.* 23:297-302.

- Shi, L, Tu, N. and Patterson, P.H. (2004) Maternal influenza infection is likely to alter fetal brain development indirectly: The virus is not detected in the fetus. *Inter. J. Dev. Neurosci.* In press.
- Watanabe, Y., Hashimoto, S., Kakita, A., Takahashi, H., Ko, J., Mizuno, M., Someya, T., Patterson, P.H. and Nawa, H. (2004) Neonatal impact of leukemia inhibitory factor on neurobehavioral development in rats. *Neurosci. Res.* 48:345-353.

Associate Professor: Erin M. Schuman
 Visiting Associate: Adam Mamelak¹
 Postdoctoral Fellows: Daniela Dieterich, Changan Jiang,
 Gentry Patrick, Michael Sutton, Chin-Yin Tai
 Graduate Students: Baris Bingol, Jessica Edwards, Noah
 Gourlie, Eric Mosser, Shreesh Mysore, Armando Miguel
 Remondes², W. Bryan Smith, Ueli Rutishauser
 Technical Staff: Michael Goard, Holli Weld
 Administrative Staff: Ana Maria Lust, Alana Rathbun
 Undergraduate Students: Melinda Owens³, Nick Wall³
¹Huntington Memorial Hospital, City of Hope
²Graduate student, Instituto Gulbenkian de Ciênciã,
 Oeiras, Portugal
³Undergraduate students, Division of Biology, California
 Institute of Technology

Support: The work described in the following research
 reports has been supported by:

Amgen
 ERC - NSF
 The German Academy of Natural Scientists Leopoldina
 Gimbel Discovery Fund
 Howard Hughes Medical Institute
 Huntington Hospital Research Institute
 Instituto Gulbenkian de Ciênciã
 National Institutes of Health, USPHS
 National Institute of Mental Health

Summary: Synapses, the points of contact and
 communication between neurons, can vary in their size,
 strength and number. These differences in synapses and
 their ability to change throughout the lifetime of the animal
 contributes to our ability to learn and remember. We are
 interested in how synapses are modified at the cellular and
 molecular level. We are also interested in how neuronal
 circuits change when synapses change their properties.
 We conduct all of our studies in the hippocampus, a
 structure known to be important for memory in both
 humans and animals. We use molecular biology,
 electrophysiology and imaging to address the questions
 detailed below.

A major focus of the lab concerns the cell
 biological mechanisms that govern modifications at
 individual synaptic sites. In particular, we are interested
 in the idea that dendritic protein synthesis and degradation
 may contribute to synaptic plasticity. We are also
 interested in mRNA and protein trafficking during synaptic
 plasticity.

We are also examining the role of the cadherins
 family of cell adhesion molecules in synaptic plasticity.
 Several labs have shown that cadherins are localized to
 synapses in the hippocampus. Earlier, we demonstrated
 that function-blocking cadherin antibodies or peptides can
 prevent long-term potentiation, without interfering with
 basal synaptic transmission. We hypothesize that cadherin
 bonds may be sensitive to local fluxes in extracellular
 calcium imposed by action potential activity. We are now
 examining the molecular mechanisms by which cadherins
 influence synaptic strength and the involvement of

cadherins in the formation and maintenance of synapses,
 using fluorescence resonance energy transfer and
 endocytosis assays

142. Dendritic spine motility: Analysis and experiments

Shreesh P. Mysore, Michael A. Sutton

Dendritic spine motility has recently received
 significant attention in neuroscience research. It has been
 shown to be influenced by several molecular pathways and
 is correlated with synaptic activity, sensory input
 manipulations, and LTP induction. However, in most
 cases, changes in motility are reported in subsets of
 imaged spines by identifying gross changes in
 morphology. There is thus a need to develop a systematic
 scheme to analyze the motility of large numbers of spines,
 across different treatment conditions, and in an unbiased
 manner. This will enable the use of spine motility as an
 assay system between treatments, and facilitate
 investigations into motility mechanisms. We are
 developing an analysis scheme to rigorously quantify
 morphological dynamics in large sets of spines. We
 measure spine characteristics along the dimensions of size,
 shape, and position, and use these to define motility
 measures. We then track motility at two time scales - slow
 and fast - and thereby investigate the morphological
 behavior of spines under different conditions. This scheme
 has been validated using time-lapse fluorescence
 microscopy experiments in cultured hippocampal neurons
 with treatments that produce known effects (e.g., blocking
 motility with the actin-disrupting agent Cytochalasin D).
 We are currently using the scheme to investigate the roles
 of spontaneous neurotransmitter release, and also of cell-
 adhesion molecules in the regulation of motility.

143. The mechanism of neuronal activity-dependent regulation of surface N-cadherin internalization

Chin-Yin Tai

The cadherins are a family of Ca²⁺-dependent
 cell-cell adhesion molecules found at neuronal synapses
 and cellular junctions. Structural studies of several
 cadherin proteins show that they form zipper-like homo-
 oligomers via their extracellular domains. N-cadherin, a
 member of the classic cadherin family is highly expressed
 in brain and localized at synaptic contacts. Synaptic
 plasticity is often associated with morphological changes
 at the old synaptic contacts, as well as formation of new
 contacts, raising the possibility that cadherin turnover
 plays an important role in regulating these events.
 However, little is known about the spatial and temporal
 dynamics of surface cadherin turnover at the synapse. I
 have embarked on a series of biochemical and microscopic
 experiments to address this issue.

I have determined the kinetics of N-cadherin
 internalization and recycling by surface biotinylation
 experiments in cultured hippocampal neurons, and have
 found N-cadherin undergoes a rapid shuttling in and out of
 the plasma membrane. Within one hour, the majority of

surface N-cadherin is internalized, and within 10 minutes, almost all the internalized N-cadherin is back to the surface. Recently, N-cadherin has been found to co-purify with the N-methyl-D-aspartate (NMDA) receptor supercomplex, suggesting a role for the NMDA receptor-mediated activities in the regulation of N-cadherin turnover.

Indeed, when neurons are briefly treated with NMDA (20 μ M, 3 min), a NMDA receptor agonist, the rate of N-cadherin internalization is dramatically reduced. In addition, when the NMDA receptor is blocked by the antagonist APV, the rate of N-cadherin internalization returns to the non-treated level. In the future, I will determine the specificity of this NMDA receptor-dependent regulation and perform antibody live-labeling experiments to address the spatial control of N-cadherin internalization.

144. Miniature synaptic events regulate local protein synthesis in dendrites of hippocampal neurons

Michael Sutton, Nick Wall

Although it is now well established that neuronal dendrites are capable of mRNA translation, the signals that regulate dendritic protein synthesis are still largely unknown. We have demonstrated that, in the context of chronic activity blockade, miniature synaptic events (mEPSPs) potently regulate protein synthesis in the dendrites of cultured hippocampal neurons. Using a GFP-based protein synthesis reporter (a Sindbis viral vector in which the coding sequence for a destabilized, myristoylated GFP is flanked by the 5' and 3' UTR of α -CAMKII) in combination with time-lapse confocal microscopy, we examined dendritic protein synthesis from 9-12 hr after chronic activity blockade (1 μ M TTX). When the impact of mEPSPs are chronically blocked by the glutamate receptor antagonists CNQX and APV (TTX+Block), an increase in reporter synthesis in both proximal and distal dendrites is observed (relative to controls). When mEPSPs are permitted (TTX alone), however, a marked decrease in protein synthesis is observed in both of these compartments. Acute application of CNQX and APV (+TTX) 9 hr after pre-incubation in TTX alone produces a rapid increase in reporter synthesis in both proximal and distal dendrites, suggesting that in the absence of evoked synaptic transmission, mEPSPs tonically inhibit dendritic protein synthesis. Similarly, blocking spontaneous vesicle release with botulinium toxin A (BoNT/A; 100 nM) when cells were pre-treated chronically (7 hr) with TTX alone also stimulated dendritic translation, providing parallel evidence that mEPSPs tonically inhibit dendritic protein synthesis. Finally, the acute effects of BoNT/A were occluded by chronic mini blockade (TTX+Block), suggesting that the increase in dendritic protein synthesis observed in each case derives from blocking mEPSPs. These results reveal a previously unknown role for miniature synaptic events in regulating dendritic protein synthesis in neurons. The spatial resolution and

mechanisms of translational regulation by mEPSPs are currently being investigated.

145. Functions of Pumilio in the development and synaptic plasticity of hippocampal neurons

Changan Jiang

Pumilio is the founding member of the Puf-family of translational repressors. In *Drosophila*, it represses the translation of target mRNAs by binding to their 3'-untranslated regions (3'-UTR) and recruiting two other co-repressors, Nanos and Brain-tumor. Recent studies showed that *Drosophila* pumilio mutants have defects in dendrite morphogenesis and long-term memory, suggesting that it functions in neuronal development and synaptic plasticity. To study the functions of pumilio in mammalian neurons, we have cloned rat pumilio homologues, rPum1 and rPum2. Northern blot analysis shows both pumilios are expressed in rat hippocampal neurons, with rPum2 as the dominant form. Immunostaining of cultured hippocampal neurons revealed that Pumilios are mainly present in the RNA granules, suggesting that it may play a role in the packaging and targeting of dendrite-localized mRNAs. Suppression of rPum2 expression by siRNA leads to a dramatic decrease of dendritic spine density, while overexpression of rPum2 increases spine density. These results suggest that rPum2 plays an important role in spine formation and/or maintenance. Currently, we are examining whether rPum2 performs this function by transporting spine development-related mRNAs and whether it is essential for neuronal activity-induced morphological changes of spines.

146. The structural basis for an allele-specific deficit in regulated secretion of brain-derived neurotrophic factor (BDNF) at hippocampal synapses

Noah M. Gourlie

BDNF rapidly enhances synaptic transmission when secreted at hippocampal synapses in response to activity. However, a genetic variant (G196A, Val66Met) of BDNF in primates is secreted at significantly lower levels than its wild-type counterpart. Human population studies by others indicate associations between this variant (Met66-) of BDNF and obsessive-compulsive disorder, anorexia nervosa, bulimia nervosa, and specific deficiencies in memory. The current study aims to determine which molecular interactions along the regulated secretory pathway are altered by the single amino acid substitution, and how their alteration may impair secretion.

Secondary structural calculations and specificity considerations identified subtilisin-kexin isozyme 1/site 1 protease (SKI-1/S1P) as a promising target molecule for investigation. To assess the necessity of proBDNF cleavage by SKI-1 for regulated secretion, an uncleavable mutant (R54A, Val66) of proBDNF was generated. Collaboratively with Changan Jiang, I am employing lentiviral delivery constructs to observe, by confocal microscopy, the differential trafficking of three distinct

proBDNF proteins at near-endogenous expression levels: Val66-, Met66-, and R54A-proBDNF, each appended with Venus yellow fluorescent protein.

Furthermore, an altered affinity of Met66-proBDNF for the SKI-1 protease relative to Val66-proBDNF may manifest differential competitive effects on the processing of SKI-1's other substrates: the sterol regulatory element binding proteins (SREBPs), prosomatostatin, and the endoplasmic reticulum stress factor, ATF6. To examine this possibility, the SREBP-initiated cholesterol biosynthesis pathway of hippocampal neurons is being tested during lentiviral expression of either Val66- or Met66-proBDNF, by assaying the cells' recovery from cholesterol depletion.

147. Visualization of cadherin-cadherin association in living cells
Eric Mosser

Classic cadherins, in particular N- and E-cadherins, are expressed and localized at synaptic sites of the adult rat hippocampus and involved in LTP. Cadherins exhibit Ca^{2+} -dependent adhesion: the removal of Ca^{2+} from the extracellular solution results in a loss of adhesion. Thus, it is possible that changes in extracellular Ca^{2+} associated with synaptic activity may alter cadherin-cadherin interactions. We are attempting to visualize cadherin-cadherin associations at cell-cell junctions with the eventual goal of monitoring hippocampal synapses during synaptic activity. This will enable us to determine if synaptic activity and plasticity affects cadherin dynamics and synaptic structures. To visualize cadherins in living cells, we have utilized a transposon-mediated random GFP insertion technique to create E-cadherin constructs with ECFP or EYFP variants inserted on a flexible linker at various sites on the extracellular domain in mouse L cells. ECFP can act as a fluorescence resonance energy transfer (FRET) donor for EYFP and FRET will be used to visualize the 'trans' homophilic interactions between cadherins on adjacent cells in co-cultures, or the 'cis' interactions between cadherins on cells expressing both FRET donor and acceptor cadherin constructs. We have demonstrated FRET between ECFP- and EYFP-labeled cadherins in HEK 293 cells transiently expressing both donor and acceptor constructs. We have created stable lines of L cells (which are known to express no or very low levels of endogenous cadherins) expressing either the ECFP- or EYFP-cadherin fusions. Viral vectors will be prepared for expression of these constructs in neurons. Cadherin containing one GFP variant will be expressed in presynaptic neurons, while cadherin containing the other GFP variant will be expressed in postsynaptic neurons. FRET will then be used to detect these exogenous cadherins and their homophilic interactions between pre- and postsynaptic cells in differing conditions. In particular, we will examine the effects of synaptic activity and varying extracellular calcium concentrations on cadherin-cadherin dynamics. Surprisingly little is known about the cadherin homophilic interaction; hopefully this approach will not only allow us to learn something about

cadherin's role in the synapse but also shed some light on the basic nature of this interaction.

148. A novel approach for the identification of locally synthesized proteins in neuronal dendrites

Daniela C. Dieterich*, A. James Link¹, David A. Tirrell², Johannes Graumann³, Geoff Smith³

Activity-dependent local protein synthesis in dendrites is required for different forms of long-lasting plasticity, like long-term potentiation or depression (LTP or LTD). Many components of the translational machinery can be found in postsynaptic density fractions and are localized beneath postsynaptic sites on dendrites. However, only a limited number of dendritically translated proteins have been identified so far, like the microtubule-associated protein 2 or the α subunit of the Ca^{2+} /calmodulin-dependent protein kinase II. Here we describe a novel approach to isolate and identify the translation products in neuronal dendrites, as well as to determine the quantitative translational capability of dendrites upon synaptic stimulation. The identification of further dendritically synthesized proteins according to different stimuli promises to offer a more thorough understanding of synaptic plasticity at the molecular level. To isolate and identify dendritically synthesized proteins we use a new and unique protein tagging technique in combination with multidimensional chromatography mass spectrometry, known as MudPIT.

The protein tagging is based on a copper-catalyzed azide-alkyne ligation using the azide-group bearing non-canonical amino acid azidohomoalanine (AHA) and a biotinylated alkyne-ligand. AHA serves as a surrogate for methionine during protein synthesis, thereby delivering new chemical functionality to these proteins. Protein-incorporated AHA can subsequently be biotinylated by treatment with biotin-PEO-propargylamide, a tris(triazolyl)amine ligand and CuBr. Thus, the biotinylated proteins can be purified for subsequent mass spectrometry analysis by avidin chromatography. To exclude any contamination with somatically synthesized proteins, newly synthesized proteins from either rat brain synaptoneurosomes or isolated dendrites of hippocampal cultures will be analyzed. Synaptoneurosomes are a biochemical fraction enriched with translation-active synaptic terminals, but devoid of somata and nuclei. Isolated dendrites will be obtained from a special culture system using polycarbonate nets to separate dendrites from cell bodies.

In a series of pilot experiments we have shown, that AHA can be incorporated into newly synthesized proteins of cultured hippocampal neurons (div 12-14). In control experiments where AHA was replaced with methionine, no biotinylated proteins were recovered following avidin chromatography. In a first tandem mass spectrometry analysis of avidin-purified proteins from AHA-treated whole-cell lysates of neuronal cultures more than 200 proteins could be identified. Next steps will involve the generation of new biotinylated alkyne-tags,

which allow for either a specific proteolytic cleavage of avidin-bound proteins or a second biotin-independent purification to enhance the specificity of this technique.

³Supported by the German Academy for Natural Scientists LEOPOLDINA (BMBF-LPD9901/8-95)

¹Division of Chemistry and Chemical Engineering, Caltech

²Professor, Division of Chemistry and Chemical Engineering, Caltech

³Raymond J. Deshaies Lab, Biology Division, Caltech

149. Dopaminergic stimulation of local protein synthesis activates silent synapses

W. Bryan Smith, Shelley R. Starck¹, Richard W. Roberts², Erin M. Schuman

Dopamine is an important modulator of neuronal function, critically involved in such diverse behavioral phenomena as motivation, addiction, Parkinson's disease, and schizophrenia. While the effects of dopamine in addiction and pathology have been the focus of intense investigation, the mechanisms underlying the dopaminergic modulation of glutamatergic synaptic plasticity are poorly understood. Recent experiments implicate the dopaminergic pathway in a variety of learning and memory tasks, including spatial memory in rats, operant conditioning in *Aplysia*, and working memory in primates.

In the hippocampus, dopaminergic signaling acting via the cAMP-PKA pathway is thought to play a key role in protein synthesis-dependent forms of synaptic plasticity. The molecular mechanisms by which dopamine influences synaptic function, however, are not well understood. Using a green fluorescent protein (GFP)-based reporter of translation, as well as a fluorescein-conjugated puromycin molecule as reporter of endogenous protein synthesis, we have shown that dopamine D1/D5 receptor activation stimulates local protein synthesis in the dendrites of cultured hippocampal neurons. Furthermore, we identify the GluR1 subunit of AMPA receptors as one protein upregulated by dopamine receptor activation. In addition to enhancing GluR1 synthesis, dopamine receptor agonists increase the incorporation of surface GluR1 at synaptic sites. The insertion of new GluRs is accompanied by an increase in the frequency, but not the amplitude, of miniature synaptic events. Interestingly, both effects (the increased surface GluR1 and increased mini frequency) are blocked by inhibitors of protein synthesis, as well as an NMDA receptor antagonist. Together, these data suggest a local protein synthesis-dependent activation of previously silent synapses as a result of dopamine receptor stimulation.

¹Graduate Student, Chemistry, Caltech

²Assistant Professor, Chemistry, Caltech

150. Synaptic plasticity and the ubiquitin-proteasome system (UPS)

G.N. Patrick

The availability of proteins likely plays an important role in synaptic function and plasticity. Protein synthesis has been clearly shown to play a role in synaptic plasticity; however, little is known about the potential role of ubiquitin-mediated protein degradation. We have recently shown that acute proteasome activity is required for agonist-mediated internalization of AMPAR in hippocampal neurons. Our recent endeavors have been to characterize the temporal and spatial requirements for proteasome activity in hippocampal neurons. Using time-lapse confocal microscopy and a degradation reporter where ubiquitin is fused to green fluorescent protein (GFP) through an N-terminal ubiquitin fusion domain (UFD) linkage, we have followed the activity of the proteasome in a temporal and spatial manner as monitored by GFP fluorescence. Biochemical analysis in COS7 and hippocampal neurons has shown that the degradation reporter is not only recognized and degraded by the proteasome, it is also competent for ubiquitination. Agonist of glutamate receptors stimulate the degradation of the reporter. In contrast, inhibitors of the proteasome block the degradation of this reporter. In addition, the degradation and/or accumulation of the reporter at synapses are evident in our live-imaging and post-hoc immuno-labeling with synaptic markers. These studies are intended to provide spatial and temporal information on how the ubiquitin-proteasome system might regulate the development, maturation, and continued remodeling of mammalian synapses.

151. A proteasome-sensitive connection between PSD-95 and GluR1 endocytosis

Baris Bingol

Synaptic transmission at excitatory synapses can be regulated by changing the number of synaptic glutamate receptors (GluRs) through endocytosis and exocytosis. The endocytosis of GluRs has recently been shown to require the activity of the ubiquitin proteasome system (UPS): proteasome inhibitors or dominant-negative forms of ubiquitin block the ligand-stimulated internalization of GluRs. We have examined whether PSD-95 is a potential target of the UPS. Following neurotransmitter stimulation, PSD-95 levels are negatively correlated with the magnitude of internalized GluR1 in individual neurons. Neurotransmitter stimulation also results in a proteasome-dependent decrease in dendritic PSD-95. Consistent with the idea that PSD-95 degradation is important for GluR internalization, overexpression of PSD-95 can inhibit neurotransmitter-stimulated GluR1 endocytosis. If PSD-95 is a direct target for proteasomal degradation, then the polyubiquitination of PSD-95 is expected. Using experimental conditions that favor the detection of polyubiquitination, however, no ubiquitination of PSD-95 was detected. These results suggest that the indirect regulation of PSD-95 levels by the proteasome contributes to ligand-stimulated GluR endocytosis.

152. The direct entorhinal cortical input to area CA1 of the hippocampus is required for the consolidation of a long-term spatial memory
Miguel Remondes

The hippocampus and its associated medial temporal lobe structures are required for the formation, consolidation and retrieval of episodic memories. Most theories of hippocampal-dependent memories invoke an interplay between the hippocampus and the cortex, although the nature and identity of the cortical inputs are poorly understood. Using selective electrolytic lesions, we examined the role of the direct entorhinal projection (temporoammonic-TA) to hippocampal area CA1 in short- and long-term spatial memory in the Morris water maze. As shown by others animals that received complete hippocampal lesions prior to training exhibited impaired short-term memory for the target quadrant in the maze. Animals that received restricted TA lesions, however, showed no deficit in short-term memory; their performance was indistinguishable from sham-lesioned controls. When tested four weeks after training, sham-lesioned animals exhibited long-term memory for the target; in contrast, the TA-lesioned animals no longer showed significant target quadrant preference. The establishment of many long-lasting memories requires a process called consolidation, which involves the exchange of information between the cortex and hippocampus. The disruption of long-term memory by the TA lesion could reflect a requirement for TA input for the acquisition of long-term memory, or, alternatively, could reflect a requirement for TA-conveyed cortical input for the consolidation of long-term spatial memory. To distinguish between these two possibilities, we trained animals, verified the acquisition and retention of spatial memory after a 24 hr delay period, and then subjected a subset of these trained animals to TA lesions. TA animals still exhibited a deficit in their ability to identify the target quadrant when examined four weeks later. Animals for which the TA lesion was delayed by three weeks, however, showed significant preference for the target quadrant, indicating that the memory had already been adequately consolidated at the time of the lesion. These results indicate that, following learning, ongoing cortical input conveyed by the TA path is required to consolidate long-term spatial memory.

153. Single-unit neural correlates of visual recognition memory in the human hippocampus-amygdala complex
Ueli Rutishauser, Adam Mamelak

The hippocampus has long been implicated in memory encoding; its role in retrieval and recognition, however, is unclear. Neurons coding for familiarity and novelty are thought to be an important part of memory retrieval. We investigated the properties of human medial temporal lobe (MTL) neurons using in vivo recordings from intracranial depth electrodes implanted in epilepsy surgery patients. Specifically, we investigated: i) whether MTL neurons respond to visual stimuli; and ii) whether

neuronal activity predicts novelty/familiarity. To accomplish this, we developed a technique for recording and separating large numbers of single cells from the extracellular signal that we record while we ask patients to perform visual psychophysical experiments. We are able to cleanly separate a large number of simultaneously recorded single cells. This allows us to correlate behavior with single-unit neuronal activity. We find three largely distinct sub-populations of neurons that have one of the following properties: i) respond to visual stimuli (are visually responsive); ii) signal novelty; or iii) signal familiarity. On average, 30 percent of human hippocampal neurons clearly signal novelty or familiarity, while only about 10 percent are visually responsive. Most visually responsive neurons do not indicate novelty/familiarity of the stimulus. We further find two encoding strategies: some neurons encode novelty with a significant firing rate increase, whereas others encode novelty with a significant firing rate decrease. These findings suggest that the human MTL is involved in the processing of visual stimuli. Contrary to previous functional MRI studies, these findings suggest that the human hippocampus is part of the visual recognition memory system.

Publications

- Bingol, B. and Schuman, E.M. (2004) A proteasome-sensitive connection between PSD-95 and GluR1 endocytosis. *J. Neuropharmacol.* In press.
- Murase, S. and Schuman, E.M. (2003) Cadherins and synaptic plasticity: Activity-dependent cyclin-dependent kinase 5 regulation of synaptic beta-catenin-cadherin interactions. *Philos. Trans. Royal Soc.* 358:749-756.
- Patrick, G.N., Bingol, B., Weld, H.A. and Schuman, E.M. (2003) Ubiquitin-mediated proteasome activity is required for agonist-induced endocytosis of GluRs. *Curr. Biol.* Published online 10/20/03, 13:2073-2081.
- Remondes, M. and Schuman, E.M. (2003) Properties of early- and late-phase LTP at temporoammonic-CA1 synapses. *Learning & Memory* 10:247-252.
- Remondes, M. and Schuman, E.M. The direct entorhinal cortical input to area CA1 of the hippocampus is required for the consolidation of a long-term spatial memory. *Nature.* In press.
- Smith, W.B., Starck, S.R., Roberts, R.W. and Schuman, E.M. Dopaminergic stimulation of local protein synthesis enhances surface expression of GluR1 and synaptic transmission in hippocampal neurons. Submitted.
- Steward, O. and Schuman, E.M. (2003) Compartmentalized synthesis and degradation of proteins in neurons. *Neuron* 40:347-359.
- Sutton, M.A., Aakalu, G.N., Wall, N. and Schuman, E.M. (2004) Miniature synaptic events regulate local protein synthesis in the dendrites of hippocampal neurons. *Science* 304:1979-1983.

Professor: Shinsuke Shimojo
 Visiting Associates: Lynne E. Bernstein, Ladan Shams, Masataka Watanabe
 Visitor: Fumiko Maeda
 Postdoctoral Scholars: Joydeep Bhattacharya, Mark A. Changizi, Christine Chee-Ruiter, Ryusuke Hayashi, Bhavin Sheth
 Graduate Students: Patricia Neil, Dylan Nieman, Claudiu Simion, Daw-An Wu
 Undergraduate Students: Neda Afsarmanish, Alice Lin, Yen-Ru (Elinor) Lin, Benjamin Matthews
 Research and Laboratory Staff: Susan Dao, Parlene Puig

Support: The work described in the following research reports has been supported by:

Human Frontier Science Program
 National Institutes of Health
 National Science Foundation

Summary: We continue to examine the dynamic/adaptive nature of human visual perception – including its crossmodal, representational, sensory-motor, developmental, emotional, and neurophysiological aspects. Using a variety of methods including eye tracking, EEG, fMRI and MEG, we also examine how exactly peripheral sensory stimuli, neural activity in the sensory cortex, and the mental experience of perception are related to each other.

(1) We continue to focus on various visual situations with perceptual ambiguity in order to dissociate between stimulus-driven and "mentally constructed" aspects of perception. For instance, we have shown that a visual transient tends to lead to a flip between bistable percepts. In another study, we showed evidence of steady-state feature misbinding, where color and motion are misbound in the visual periphery due to strong binding in the fovea. This is to our knowledge the first solid evidence of stable feature misbinding even with attention and against knowledge. These findings help us to understand how the brain integrates different visual inputs/clues to attain stable perceptual interpretation of the world.

(2) Following our earlier work indicating that dynamic gaze shift (and perhaps orienting response in general) is a somatic precursor of conscious preference judgment, we extended the analyses in two directions. First, we analyzed pupillary responses while the subject was engaged in the same two-alternative, forced-choice preference task on faces. As a result, while gaze shift was selectively correlated with their subsequent preference judgment, pupillary response tended to be correlated more generally with their attention. This finding is quite opposite to the conventional knowledge about these two types of bodily responses. Second, we measured ERPs while the subject was engaged in the same preference task, and found that there is strong coherence of neuronal activity localized in the left lateral-medial frontal lobe and limited in the lower gamma range of frequency.

(3) We continue our work applying TMS (Transcranial Magnetic Stimulation) to the visual cortex of alert normal subjects, to reveal neural mechanisms underlying conscious visual perceptual experience. In the latest study, we have demonstrated that after one has seen a flashed visual object, administration of dual-pulse TMS to the occipital cortex causes portions of the object to be seen again. We surmise that neurons which were previously activated by visual stimuli are more excitable by TMS, possibly due to residual neural activity. This paradigm has turned out to provide a unique opportunity to assess how exactly the visual cortical activity brings about the content of our perceptual experience. In yet another study using TMS, we have provided the first evidence for causal relationship between neural activity of PPC (the posterior parietal cortex) and the coordinate transformation that is necessary to maintain visual constancy across saccadic eye movements.

(4) We continue our effort to understand auditory-visual integration in both adults and in infants. In adult ERP study, we found a surprisingly early (<150 ms from the onset of A-V stimuli) evidence of non-linear interaction between these two sensory modalities, which is consistent with behavioral reaction-time data. In infants, we provided a systematic full-set data, for the first time in the field, of how auditory, visual, and auditory-visual processing develop in the first year of life. Against commonsensical notion, we found surprisingly rich and complicated patterns of interaction between the modalities in the early period of human life.

154. Perceptual-binding and persistent pre-attentive surface segregation

Farshad Moradi, Shinsuke Shimojo

Visual input is segregated in the brain into subsystems that process different attributes such as motion and color. At the same time, visual information is perceptually segregated into objects and surfaces. Here we demonstrate that perceptual segregation of visual entities based on a transparency cue precedes and affects perceptual binding of attributes.

Adding an irrelevant transparency cue paradoxically improved the pairing of color and motion for rapidly alternating surfaces. Attributes are registered over the temporal window defined by the perceptual persistence of segregation, resulting in asynchrony in binding. Attention is necessary for correct registration of attributes in the presence of ambiguity.

Reference

Moradi, F. and Shimojo, J. Vision Res. In press.

155. Perceptual alternation induced by visual transients

R. Kanai*, Farshad Moradi, Shinsuke Shimojo, F.A.J. Verstraten*

When our visual system is confronted with ambiguous stimuli, the perceptual interpretation spontaneously alternates between the competing incompatible interpretations. The timing of such perceptual alternations is highly stochastic and the underlying neural mechanisms are poorly understood. Here, we show that perceptual alternations can be triggered by a transient stimulus presented nearby. The induction was tested for four types of bistable stimuli: structure-from-motion, binocular rivalry, Necker cube, and ambiguous apparent motion. While underlying mechanisms may vary among them, a transient flash induced time-locked perceptual alternations in all cases. The effect showed a clear dependency on the adaptation to the dominant percept prior to the presentation of a flash.

These perceptual alternations show many similarities to perceptual disappearances induced by transient stimuli (Kanai and Kamitani, 2003; Moradi and Shimojo, 2004). Mechanisms linking these two transient induced phenomena are discussed.

*U. Utrecht, The Netherlands

Reference

Kanai, R., Moradi, F., Shimojo, S. and Verstraten, F.A.J. Perception. In press.

156. How early does the brain "know" what it likes? Evidence from pupillometry

Claudiu Simion, Shinsuke Shimojo

It has been reported that pupil size is positively correlated with stimulus attractiveness. While it is a well-known effect which makes some professional poker players wear eye shades when they play, little is known about the temporal dynamics of this reflexive reaction.

We analyzed the pupil size of observers while they were inspecting pair of stimuli for the purpose of making two-alternative forced-choice decisions about them. They had to indicate which face was more attractive (face-like), which face was rounder (face-round), which face was less attractive (face-dislike) or which of two Fourier-descriptor generated shapes was more attractive (Fourier-like). The trials were terminated by the observers' choice. Meanwhile, we measured the pupil size using the EyeLink2 system.

We compared the change in pupil area (averaged over fixations) when observers moved their gaze from their subsequent choice to the non-choice stimulus, when they switched from non-choice to choice, and when they made adjacent fixation on the same stimulus. In the face-like and Fourier-like conditions, the pupil size significantly increased from non-choice to choice, while there was no change in size in the opposite direction. In the face-round task we found no significant change in any direction, while in the face-dislike task we found the opposite result, a size

increase only when switching from choice (disliked) to non-choice (liked).

We have shown recently that the brain needs the assist of the orienting system to make a decision of preference (gaze cascade effect, Shimojo, et al., 2003). There, an increasing gaze bias towards choice was revealed as early as 1 sec before decision in all conditions, reflecting the contribution of the orienting behavior to the decision making process. However, pupillary responses may be an even better indicator of preference, because unlike the gaze bias, they are correlated with attractiveness regardless of task.

157. Orienting behavior robustly contributes to preference decision-making

Shinsuke Shimojo, Claudiu Simion

We have revealed a "gaze cascade effect" (Shimojo, et al., 2003) as an illustration of the mechanism of preference decision-making. It refers to a tendency of gaze being gradually biased towards choice, interpreted as indicating a contribution of the orienting behavior to preference decisions. The present study tests the robustness and generality of the effect and interpretation in two particular conditions.

First, observers were shown the same face pairs twice, with an inter-session delay of one day and had to decide which face was more attractive. Approximately 80% of all the decisions were identical from one session to the next. We show a gaze cascade effect in both sessions and in the reversed decision trials when analyzed separately. We confirm thus that the gaze cascade accompanies the decision process even when implicit or explicit memory of a past decision exists, suggesting that preference formation, not memory consolidation, needs the assist of gaze for functioning.

Second, we evaluate the contribution of the orienting behavior to preference decisions by minimizing the cognitive input. Observers chose the more attractive face in a pair while only being able to see through a small gaze-contingent window, thus visualizing at most one facial feature at a time, with no configural information. If the cascade effect was the result of an early attractiveness bias in the face pairs, this task should not show it at all. Instead, we found a cascade effect of similar size, but four times longer (earlier onset) than when observers could see the whole face. This confirms that the smaller the cognitive input in a preference decision, the larger the assist of the orienting behavior in making a choice.

Altogether, the results are consistent with our model, in which cognitive and orienting inputs feed into a decision module and are integrated over time until the signal passes a "consciousness threshold" for the decision to be made.

158. Gaze, decision processes and cortical activation: A joint eye tracking/EEG study
Claudiu Simion, Joydeep Bhattacharya*, Shinsuke Shimojo

Using eye tracking, we reported (VSS02) a gaze bias towards choice in several 2AFC tasks involving human faces and abstract shapes. The gaze bias translated in a progressive increase in the likelihood that the future choice is inspected, culminating with a significant (>80%) bias prior to decision; this bias, termed the "gaze cascade effect" was incorporated in a model where orienting behavior (gaze) plays an active role in preferential decisions.

We investigated the neural basis of such decision processes by simultaneous recordings of multivariate EEG signals and eye tracking, while subjects inspected pairs of faces or abstract shapes. Four separate conditions were considered, where subjects had to decide: 1) Which face was more attractive; 2) which face was less attractive; 3) which face was rounder; and 4) which shape was more attractive. A passive-viewing condition was included, where subjects inspected faces with for future recognition. Wavelet-based time-frequency analysis revealed the dynamics of middle and high frequency band (14-70 Hz) activity. Significant increases from pre-stimulus intervals were found in the gamma frequency band (>30 Hz) in prefrontal regions; this effect was mostly pronounced in the last second before decision. Stronger gamma band neural responses were found in the face attractiveness task, compared to the other 2AFC tasks, whereas minimal increase during the passive condition was noted. Moreover, left hemispheric lateralization was found in the last 400 ms before decision in the face attractiveness task. Contrarily, activity in the beta and gamma frequency bands decreased during the same time period during the "rounder" and "less attractive" tasks.

This suggests that the "more attractive" task is functionally distinct from the other two tasks, maybe because it naturally links orienting and liking, while the others involve top-down suppression and control.

*Current address: Austrian Academy of Sciences, Vienna, Austria

159. Steady state misbinding of color and motion
Daw-an Wu, Shinsuke Shimojo

When you see a red ball rolling across the floor, the ball's redness, roundness and motion appear to be unified and inseparably bound together as features of the ball. But neurophysiological evidence indicates that visual features such as color, shape and motion are processed in separate regions of the brain. Theoretically, this may pose a "binding problem" for the brain, which must re-assemble the separate feature information to produce the unified perceptions we experience in everyday life. Previous investigations of the binding of basic visual features required the use of stimuli with brief presentation times or rapidly changing features to induce errors or inefficiencies. The confounds of memory, expectation and task strategy have led some to contend that the binding problem does

not actually exist. We present a misbinding illusion which persists despite continuous and attentive viewing. This illusion solidifies the evidence for the existence of a binding problem, and induces individually identifiable instances of misbinding suitable for neurophysiological investigation.

The illusion is seen in stimuli containing two sheets of random dots, where one sheet is moving up and one is moving down. The sheets contain dots of two colors such that the central and peripheral portions of the stimuli combine color and motion in opposite fashions. On the upward-moving sheet, dots in the center are red and dots in the periphery are green. On the downward-moving sheet, dots in the center are green and dots in the periphery are red. (online demo available on the Shimojo Lab website, <http://neuro.caltech.edu>). Observers gazing at the center of the display perceive peripheral dots erroneously: they "bind" color and motion in the wrong combination. The entire display therefore appears to be covered by a sheet of red dots that are moving upwards and a sheet of green dots that are moving downwards.

Reference

Wu, D.A., Kanai, R. and Shimojo, S. (2004) *Nature* 429:262.

160. Transcranial magnetic stimulation reveals the content of post-perceptual visual processing
Daw-an Wu, Shinsuke Shimojo

We have found that after one has seen a flashed visual object, administration of dual-pulse TMS to the occipital cortex causes portions of the object to be seen again. Furthermore, after one watches a flash-lag display, perceiving the position of the flash erroneously, subsequent TMS causes the flash to be seen again, but in the correct position (Wu and Shimojo, VSS '02). We surmise that neurons that were previously activated by visual stimuli are more excitable with respect to TMS, possibly due to residual neural activity. Here we use TMS to reveal the visual content of unknown neural activity, building a spatio-temporal map of post-perceptual visual processing. We find that signals in the intensity and color channels have different rates of decay, and can be independently activated by TMS, causing the signals to be artificially segregated and merged.

Exp. 1) We flashed full-screen colored spatial frequency gratings followed by TMS after a delay; varying grating orientation, delay, and stimulator coil position. Subjects outlined the region in which they saw the grating re-appear, and then adjusted the display's brightness and color saturation to match their percept; verbal comments were tape-recorded. Subjects saw distinct regions that contained the colored grating, solid color, or uncolored gratings, often all in the same trial. As the delay between visual stimulus and TMS increases, the elicited percept declines both in brightness and size. However, the effect is still present beyond 2 sec. Regions drawn were elongated parallel to the gratings. Moving the coil caused

the regions to expand or shrink, but did not shift their centers systematically.

Exp. 2) We flashed full-screen monochromatic gratings followed by full-screen homogeneous color flashes, followed by TMS; varying orientation and delays. Subjects reported that patches of solid color and monochrome grating would be elicited by TMS. Where they overlapped, they would appear overlaid or transparent. Under certain conditions, the luminance grating and color percepts would merge, and a colored grating would be seen.

161. Human parietal cortex remaps cue-priming effect across saccades: Cortical location and dynamics assessed by transcranial magnetic stimulation

Ryusuke Hayashi, Richard Andersen*, Shinsuke Shimojo

Some coordinate transformation from the retinotopic (RET) frame to a non-retinotopic frame is necessary to keep our visuospatial perception constant across eye movements (we will group all non-RET frames as environmental (ENV)). Here, we applied dual-pulse transcranial magnetic stimulation (TMS) to the posterior parietal cortex (PPC) in healthy human observers to disrupt the coordinate transformation process during cue-primed tasks involving saccadic eye movements. We assessed the cue-priming effect by measuring reaction time (RT) to a target after external cue presentation. Observers were required to move their eyes in the interval between cue and target and to judge whether the same-colored target was left or right by pressing buttons. By comparing RTs between the two conditions, (1) the target presented at the ENV same/RET different location relative to the cue location; and (2) the target presented at the ENV different/RET same location, one can determine whether priming mainly affects either the RET or the ENV coordinate systems. The results of the behavior without TMS show that priming is yoked to the ENV frame rather than the RET frame. We then TMS the PPC during the same tasks, testing nine parietal scalp sites, two saccade directions (left and right) and three TMS timings (0 ms, 100 ms and 200 ms after the saccade onset) to investigate the spatio-temporal aspects of the process. We found that TMS delivered to the right PPC at 100 ms after the onset of a leftward saccade effectively causes the priming to shift reference frame from the ENV frame to the RET frame, indicating that the locus of priming is represented in the RET coordinate and updated with eye movements to fit with the ENV coordinate. The activity of a particular PPC area at a specific time is therefore vital for integrating the eye signal with the RET representation of primed location. The most effective TMS location to disrupt the remapping process may correspond to the human homolog of the monkey LIP.

*Professor, Division of Biology, Caltech

162. Significant audio-visual interaction for spatially congruent stimuli

Patricia Neil¹, Aman Chawla^{2,3}, Joydeep Bhattacharya^{3,4}, Shinsuke Shimojo

Studies on auditory and visual interactions encompass a wide range of tasks and methodologies (electrophysiology, functional imaging, psychophysics), sometimes resulting in seemingly conflicting conclusions. Direct comparison of results from different experimental paradigms can be difficult when the stimuli, tasks, and analytical approaches differ from study to study. Animal studies have shown that spatially and temporally congruent visual and auditory stimuli produce an enhanced neural response in multisensory neurons of the superior colliculus, whereas incongruent stimuli produce either suppression or no change in neuronal response. A similar behavioral response has been found in humans, where congruent visual and auditory stimuli produce reduced response latencies in target localization. Attempts to localize where in the brain congruent and incongruent multisensory interactions occur have largely focused on the roles of temporal properties and arbitrary or learned connections, such as linguistic properties. In this study, we investigate the role of spatial congruency in multisensory interaction in adult human subjects (n=11) using both multi-channel EEG signal recordings and saccade analysis. The auditory stimuli were short bursts of white noise; visual stimuli were single vertical lines of three red LEDs. The auditory and visual stimuli were presented either separately or synchronously at the same or different spatial location. Subjects were required to identify the spatial location of the target by directing their gaze. The audio-visual interaction was studied by comparing the sum of the visual and auditory event-related-potential (ERP) responses to audiovisual ERPs. The results revealed strong audio-visual interaction with earliest onset latency of 150 ms for spatially congruent stimuli but no such consistent audio-visual interaction was found for spatially incongruent stimuli. Although a multitude of cortical regions showed temporally sustained interaction, the earliest effect was found in anterior frontal regions that might influence the posterior sensory-specific areas by possible feedback projections. These results, altogether, demonstrate that the spatial coincidence can significantly modulate the neuronal information processing in the modality-specific regions in the human brain, thus mediating multi-sensory interaction, an essential requirement for a unitary behavioral response.

¹Computation & Neural Systems, Caltech

²Department of Electrical & Computer Eng., Cornell University, Ithaca, NY, USA

³Division of Biology, Caltech, Pasadena, CA, USA

⁴Comm. for Scientific Visualization, Austrian Academy of Sciences, Vienna, Austria

163. Development of multisensory spatial integration and perception in humans
Patricia A. Neil¹, Christine Chee-Ruiter, Christian Scheier, David J. Lewkowicz², Shinsuke Shimojo

Previous studies have shown that adults respond faster and more reliably to bimodal compared to unimodal localization cues. The current study investigated for the first time the development of audiovisual (AV) integration in spatial localization behavior in infants 1-10 months of age. We observed infants' head and eye movements in response to auditory, visual, or both kinds of stimuli presented either 25 or 45 degrees to the right or left of midline. We found that infants younger than four months of age responded similarly to unimodal and bimodal stimuli. Although older infants were found to respond faster to bimodal stimuli than to auditory stimuli for certain eccentricities and ages, the fastest bimodal response latencies were not reliably different from visual response latencies at the same eccentricities. As such, we found no behavioral confirmation that the nonlinear cross-modal integration found in adults is present in infants under 10 months of age. This finding is consistent with neurophysiological findings from multisensory sites in the superior colliculus of infant monkeys showing that multisensory enhancement of responsiveness is not present at birth but emerges later in life. Finally, we found age-dependent position and modality effects on response latency.

¹Computation & Neural Systems, Caltech

²Florida Atlantic University, USA

Publications

- Bhattacharya, J., Watanabe, K. and Shimojo, S. (2004) Nonlinear dynamics of evoked neuromagnetic responses signifies potential defensive mechanisms against photosensitivity. *Int. J. Bifurcation & Chaos*. In press.
- Fujisaki, W., Shimojo, S., Kashino, M. and Nishida, S. (2004) Recalibration of audiovisual simultaneity. *Nature Neurosci.* 7:773-778.
- Kanai R., Sheth, B.R. and Shimojo, S. Stopping the motion and sleuthing the flash-lag effect: Spatial uncertainty is the key to perceptual mislocalization. *Vis. Res.* In press.
- Moradi, F. and Shimojo, S. Perceptual-binding and persistent pre-attentive surface segregation. *Vis. Res.* In press.
- Moradi, F. and Shimojo, S. (2004). Suppressive effect of sustained low-contrast adaptation followed by transient high-contrast on peripheral target detection. *Vis. Res.* 44:449-460.
- Nakamura, S. and Shimojo, S. (2003) Sustained deviation of gaze direction can affect "inverted vection" induced by the foreground motion. *Vis. Res.* 43:745-749.
- Nijhawan, R., Watanabe, K., Khurana, B. et al. (2004) Compensation of neural delays in visual-motor behaviour: No evidence for shorter afferent delays for visual motion. *Visual Cognit.* 11:275-298.

- Nishida, S., Motoyoshi, I., Andersen, R.A. et al. (2003) Gaze modulation of visual aftereffects. *Vis. Res.* 43:639-649.
- Scheier, C., Lewkowicz, D.J. and Shimojo, S. (2003) Sound induces perceptual reorganization of an ambiguous motion display in human infants. *Dev. Sci.* 6:233-241.
- Scheier, C., Lewkowicz, D.J. and Shimojo, S. (2003) To bounce or not to bounce? A reply to Slater. *Dev. Sci.* 6:243-244.
- Sheth, B.R. and Shimojo, S. (2004) Sound-aided recovery from and persistence against filling-in. *Vis. Res.* 44:1907-1917.
- Sheth, B.R. and Shimojo, S. (2004) Extrinsic cues suppress the encoding of intrinsic cues. *J. Cog. Neurosci.* 16:339-350.
- Sheth, B.R. and Shimojo, S. (2003) Signal strength determines the nature of the relationship between perception and working memory. *J. Cog. Neurosci.* 15:173-184.
- Shimojo, S., Simion, C. and Shimojo, E. et al. (2003) Gaze bias both reflects and influences preference. *Nature Neurosci.* 6:1317-1322.
- Watanabe, K., Sato, T.R. and Shimojo, S. (2003) Perceived shifts of flashed stimuli by visible and invisible object motion. *Perception* 32:545-559.
- Wu, D.A., Kanai, R. and Shimojo, S. (2004) Steady-state misbinding of colour and motion. *Nature* 429:262-262.

Conference Abstracts

- Hayashi, R., Andersen, R.A. and Shimojo, S. (2004) Abstract 91-Human parietal cortex remaps cue-priming effect across saccades: Cortical location and dynamics assessed by transcranial magnetic stimulation. *Vision Sciences Society.*
- Moradi, F. and Shimojo, S. (2004) Abstract 125-Surface segregation and the time-course of feature binding. *Vision Sciences Society.*
- Neil, P. and Chaula, A. et al. (2004) Significant audio-visual interaction for spatially congruent stimuli. *Vision Sciences Society.*
- Shimojo, S. and Simion, C. (2004) Abstract 103-Orienting behavior robustly contributes to preference decision-making. *Vision Sciences Society.*
- Simion, C. and Shimojo, S. (2004) Abstract 91-How early does the brain "know" what it likes? Evidence from pupilometry. *Vision Sciences Society.*
- Watanabe, M., Maeda, F. and Shimojo, S. (2004) Abstract 189-Bidirectional transfer of motion aftereffect between vision and audition. *Vision Sciences Society.*
- Wu, D-A. and Shimojo, S. (2004) Abstract 40-Transcranial magnetic stimulation (TMS) reveals the content of post-perceptual visual processing. *Vision Sciences Society.*

Assistant Professor: Athanassios G. Siapas
 Research Associate: Evgueniy Lubenov
 Graduate Students: Ming Gu, Hiroshi Ito, Jason Rolfe,
 Casimir Wierzynski

Support: The work described in the following research report has been supported by:

Alfred P. Sloan Foundation
 Bren Foundation
 James S. McDonnell Foundation
 The William T. Gimbel Discovery Fund in Neuroscience

Summary: Our research focuses on the study of information processing across networks of neurons, with emphasis on the neuronal mechanisms that underlie learning and memory formation. Many lines of evidence suggest that the process of memory formation occurs by gradual integration of recently learned information into distributed cortical networks through the interactions between cortical and hippocampal circuits. However, the direct experimental investigation of these interactions has been difficult since, until recently, simultaneous chronic recordings from large numbers of well-isolated single neurons were not technically feasible. These experiments became possible with the advent of the technique of chronic multi-area tetrode recordings in freely behaving rodents. Using this technique we monitor the simultaneous activity of large numbers of cortical and hippocampal cells during the acquisition and performance of memory tasks, as well as during the sleep periods preceding and following experience.

Tracking neuronal activity across different behavioral and brain states is important as memory formation is believed to occur over several stages, with the encoding of mnemonic information in hippocampal networks occurring during active exploratory behavior, and the gradual consolidation of memories in neocortical sites occurring under the influence of hippocampal activity during off-line periods, such as sleep. Consistent with this idea, brain activity during these different brain states is drastically different, with each state marked by a characteristic combination of network oscillations.

Our research efforts concentrate on analyzing the structure of cortico-hippocampal interactions in the different brain states and on characterizing how this structure is modulated by behavior, how it evolves throughout the learning process, and what it reflects about the intrinsic organization of memory processing at the level of networks of neurons. Our efforts also focus on studying the role of sleep in memory consolidation by characterizing the structure and experience-specific changes of cortico-hippocampal patterns in different stages of sleep. Our experimental work is complemented by theoretical studies of network models and the development of tools for the analysis of multi-neuronal data.

164. Cortical phase-locking to hippocampal theta oscillations

Evgueniy Lubenov, Thanos Siapas

During awake behavior hippocampal activity is marked by the presence of pronounced 4-10 Hz LFP oscillations known as theta oscillations.¹ It has been known that the firing of hippocampal neurons preferentially occurs during particular phases of the theta rhythm, an effect known as theta phase-locking.^{2,3,4} We showed that the firing of prefrontal cortical cells is also phase-locked to the hippocampal theta rhythm, even in the absence of local cortical theta oscillations.⁵ This result is surprising because the hippocampal theta oscillations are recorded several millimeters away from the cortical recording sites, and is an example of a property in one brain area that can only be robustly analyzed in relation to electrophysiological activity in a different brain area. We developed quantitative tools that enabled us to fully establish and analyze cortical theta phase-locking properties and their non-stationarities. Our current efforts focus on characterizing how these properties are modulated by behavior. Since oscillations reflect the mode of activation of the local circuitry and impose strong order in the patterning of network activity, phase-locking may provide a powerful framework for deciphering the organization and functional role of cortico-hippocampal interactions.

References

1. Vanderwolf C.H. (1969) *Electroencephalogr. Clin. Neurophys.* 26:407-418.
2. Sinclair B.R., Seto M.G. and Bland B.H. (1982) *J. Neurophysiol.* 48:1214-1225.
3. Buzsaki G., Leung L.W.S. and Vanderwolf C.H. (1983) *Brain Res. Rev.* 6:139-171.
4. Fox S.E., Wolfson S. and Ranck J.B. (1986) *Exp. Brain Res.* 62:495-508.
5. Siapas A.G., Lubenov E.V. and Wilson M.A. In preparation.

165. Cortico-hippocampal interactions during slow-wave sleep

Evgueniy Lubenov, Ming Gu, Hiroshi Ito, Jason Rolfe, Casimir Wierzynski, Thanos Siapas

Hippocampal activity during SWS is characterized by large-amplitude irregular local field potential (LFP) fluctuations interspersed with transient fast oscillations known as ripples (~ 200 Hz).¹ In contrast to these high-frequency burst patterns in the hippocampus during SWS, neocortical activity during these periods is organized into lower-frequency oscillations^{2,3,4}, the most characteristic of which are known as sleep spindles. Spindle waves are oscillatory patterns in the 7-14 Hz frequency range that last 1-5 seconds and occur with a remarkable global coherence across thalamic and neocortical areas. We previously demonstrated that there exists a strong correlation between the onset of hippocampal ripples and neocortical spindle waves, even though these oscillatory events are characterized by very

different frequencies and durations and occur in very different brain areas.⁵ Furthermore, this relationship is reflected in the patterns of firing of cells around those events. These results suggest that cortico-hippocampal communication in SWS is not uniform across time but is structured in identifiable discrete episodes characterized by the co-occurrence of hippocampal fast oscillations and cortical slower spindle oscillations. Our current work focuses on characterizing the precise patterns of cortical and hippocampal firing around the spindle-ripple episodes, and on analyzing the relationship of these patterns to previous experience-specific activation of the same networks during awake behavior.

References

1. Buzsaki, G., Horvath, Z., Urioste, R., Hetke, J. and Wise, K. (1992) *Science* 256:1025.
2. Morison, R.S. and Dempsey, E.W. (1942) *Am. J. Physiol.* 135:281-292.
3. Steriade, M., McCormick, D.A. and Sejnowski, T.J. (1993) *Science* 262:679-685.
4. Steriade, M. (2001) *The intact and sliced brain*. MIT Press.
5. Siapas, A.G. and Wilson, M.A. (1998) *Neuron* 21:1123-1128.

Professor: Kai G. Zinn

Postdoctoral Scholars: Mili Jeon, Mitsuhiro Kurusu, Kaushiki Menon, Rachel Papan (Kraut), Anuradha Ratnaparkhi, Nina Sherwood

Graduate Students: Anna Salazar, Ashley Wright

Research and Laboratory Staff: Elena Armand, Lakshmi V. Bugga, Violana Nesterova

Support: The work described in the research reports has been supported by:

American Cancer Society

Japanese Society for the Promotion of Science (JSPS)

National Institutes of Health

National Institutes of Neurological Disorders and Stroke

Summary: Our overall focus is on the molecular mechanisms of axon guidance and synaptogenesis in *Drosophila*. Our approach combines genetics, molecular biology, biochemistry, and cell biology. We are especially interested in cell-surface and signal-transduction proteins that function in growth cones, presynaptic terminals, and their postsynaptic partners.

Receptor tyrosine phosphatases and axon guidance:

Genetics of receptor tyrosine phosphatases. In the 1990s, we showed that four receptor-linked protein tyrosine phosphatases (RPTPs) are selectively expressed on CNS axons and growth cones in the *Drosophila* embryo, and that these RPTPs regulate motor and CNS axon guidance during embryonic-development. RPTPs are likely to directly couple cell recognition via their extracellular domains to control of tyrosine phosphorylation via their cytoplasmic enzymatic domains. The extracellular regions of the fly RPTPs all contain immunoglobulin-like (Ig) and/or fibronectin type III (FN3) domains, which are usually involved in recognition of cell-surface or extracellular matrix ligands. Their cytoplasmic regions contain either one or two PTP enzymatic domains. The fly genome encodes six RPTPs.

We have performed a detailed characterization of the genetic interactions among five of the six RPTPs. We find that each growth cone guidance decision in the neuromuscular system has a requirement for a unique subset of RPTPs. In some cases the RPTPs work together, so that defects are only observed when two or more are removed. In other cases, however, phenotypes produced by removal of one RPTP are suppressed when a second RPTP is also absent. Our results provide evidence for three types of relationships among the RPTPs: partial redundancy; collaboration; and competition (Sun et al. (2001) *Mol. Cell. Neurosci.* 17:274-291) (see Ratnaparkhi abstract). We have also recently obtained mutants lacking expression of the sixth, and apparently final, RPTP, DPTP4E, and are investigating their phenotypes.

Searching for RPTP substrates. It is difficult to identify PTP substrates biochemically because PTPs usually do not display strong specificity *in vitro*. One current approach is to perform yeast two-hybrid screens with 'substrate-trap'

versions of DPTP10D, DPTP69D, and DPTP99A. We introduced a constitutively activated chicken Src tyrosine kinase into the yeast together with the PTP 'bait' constructs, in the hope that it would phosphorylate relevant substrate fusion proteins made from cDNA library plasmids. The screen should also recover non-substrate interacting proteins that may form complexes with the RPTPs *in vivo*. We have identified several classes of clones whose interactions with the substrate-trap RPTPs are dependent on coexpression of the tyrosine kinase, suggesting that they may be substrates. We are currently analyzing these further to determine which ones are likely to be of interest for the future (see Bugga abstract).

Searching for RPTP ligands, and development of a new method for identification of *Drosophila* cell-surface proteins. We have conducted several mammalian COS cell expression screens to attempt to identify ligands and/or coreceptors for the fly neural RPTPs, so far without success. This has been a major problem in the RPTP field; indeed, *in vivo* ligands for RPTPs have not been identified in any system. In order to understand how RPTPs regulate axon guidance, it is essential to know when and where they engage ligands, and how ligand-binding affects enzymatic activity and/or localization.

Our current approach to identifying ligands is based on our observation (Aloisia Schmid, unpublished; see Zinn abstract) that fusion proteins in which the extracellular domains of RPTPs are joined to human placental alkaline phosphatase (AP) can be used to stain live *Drosophila* embryos. Each of four fusion proteins (DLAR-AP, DPTP69D-AP, DPTP10D-AP, DPTP99A-AP) binds in a specific manner to the embryonic CNS. Most of the observed staining is on CNS axons. We are now screening a 'deficiency (Df) kit' of ~200 fly lines, each of which lacks a specific region of the genome, by staining homozygous Df embryos from each line with each of the fusion proteins. This method should identify the genomic regions encoding each of the RPTP ligands (see Fox abstract). We have already identified Dfs that contain genes required for DLAR-AP staining, and have tentatively defined the gene encoding the putative DLAR ligand.

We are also developing a novel method for expressing the entire repertoire of fly cell-surface proteins on the surfaces of transfected mammalian cells. Cells expressing this collection of cell-surface proteins can be screened using RPTP-AP fusion proteins in order to identify and characterize ligands. We will also generate monoclonal antibodies (mAbs) to these cell-surface proteins, and we have developed an approach which should allow us to directly clone the genes encoding the proteins recognized by these mAbs without any biochemical purification or screening of expression libraries. These genes and mAbs should be of interest in understanding axon guidance, as well as other processes that occur during fly-development.

Genes controlling axon guidance and synaptogenesis in the larval neuromuscular system. The 32 motor neurons in each hemisegment of a *Drosophila* embryo innervate 30 muscle fibers, and each motor axon extends along a stereotyped route and always targets the same fiber. Motor growth cones reach their muscle targets during late embryogenesis and then gradually mature into presynaptic terminals. These synapses continue to expand and change as the larva grows, because their strengths must be matched to the sizes of the muscle fibers they drive. The pattern of Type I neuromuscular junction (NMJ) synapses in the third instar larva is simple and highly stereotyped, with boutons restricted to specific locations on each muscle fiber.

We devised and executed a gain-of-function (GOF) screen of live larvae to find genes involved in axon guidance and synaptogenesis in this system (Kraut et al. (2001) *Current Biology* 11:417-430). Our screen identified 41 'known genes' (those with published mutant alleles) and 35 'new genes' for which high-level neuronal expression produces axonal/synaptic phenotypes. We assembled published phenotypic data on the 'known genes,' and examined larval neuromuscular LOF phenotypes for some of them ourselves. These results showed that at least 3/4 of the 'known genes' are important for nervous system development or function in wild-type flies. An analysis of homology relationships displayed by the 'known gene' and 'new gene' sets suggests that most of the 'new genes' will also have neural loss-of-function (LOF) phenotypes. The products encoded by the 76 genes identified in our screen include kinases, protein and lipid phosphatases, GTPases, guanine nucleotide exchange factors (GEFs), GTPase-activating proteins (GAPs), ATPases, cell-surface receptors, RNA-binding proteins, transcriptional regulators, and a variety of other molecules likely to be involved in protein trafficking, modification, and degradation.

We have initiated further study of a number of genes identified in the screen that are defined by existing mutations. *pumilio* (*pum*) encodes an RNA-binding protein that shuts down translation of specific mRNAs by binding to their 3' untranslated regions. We found that Pum protein is expressed in a small subset of CNS neurons, and *pum* LOF mutations alter motor axon guidance in the embryo. Pum protein is also localized to NMJs in third instar larvae, and is primarily postsynaptic. *pum* LOF larvae have NMJs that do not grow in a normal manner. Postsynaptic Pum regulates expression of a translation initiation factor, eIF-4E, which is localized to postsynaptic aggregates; thus, in *pum* mutant larvae we observe a dramatic increase in the number and size of eIF-4E aggregates. Pum protein binds directly to the 3'UTR of eIF-4E mRNA (see Menon abstract). We are also investigating aggregation of Pum protein (Salazar abstract).

Robo2 is a cell-surface protein that mediates growth-cone repulsion from sources of its ligand Slit. We find that *Robo2* overexpression alters the migration of sensory neuron cell bodies in the peripheral nervous

system (PNS), and LOF mutations in *Robo* family genes also affect PNS cell migration.

'New' genes identified by the screen, and by an earlier GOF embryonic screen conducted by Qi Sun, a former graduate student, include a number of molecules involved in protein trafficking in neurons. We have investigated two of these thus far. Spastin encodes an AAA-ATPase that is the ortholog of human spastin, a gene mutated in the disease autosomal dominant spastic hemiplegia. AAA-ATPases are a class of proteins that form multimeric complexes that regulate a variety of protein trafficking events within the cell, including vesicle sorting, protein degradation, and microtubule dynamics. There are about 30 such proteins encoded in the fly genome. We made LOF mutations in the spastin gene, and found that these produce synaptic defects. Mutant adults cannot fly or jump (see Sherwood abstract).

Beached/Blue cheese is a huge protein that is closely related to the human protein whose loss causes Chediak-Higashi syndrome, a lethal disease affecting lysosomes and related organelles (see Wright abstract #175). We are undertaking a systematic study of the 'new genes' by making transgenic RNAi lines, so that we can knock out expression of each gene in a defined set of cells (Jeon abstract).

166. Searching for RPTP substrates

Lakshmi Bugga

We are looking for proteins that interact with *Drosophila* neuronal RPTPs-10D, 69D, 99A and 52F. To attempt to achieve stable binding of the RPTPs to a tyrosine phosphorylated substrate, we have used 'substrate-trap' mutants of the RPTPs, which can bind to substrates but do not catalyze dephosphorylation, instead remaining bound to substrate in a stable complex.

To isolate RPTPs in a complex with their target substrates, we are using yeast two-hybrid system. We constructed plasmids encoding GAL4 DBD/RPTP bait proteins and introduced them into yeast together with fly cDNA libraries encoding GAL4AD-cDNA fusion proteins. We also introduced a plasmid containing a constitutively active form of chicken c-Src, driven by a constitutive yeast promoter. The bait (with or without src) and prey (cDNA) hybrid proteins are transformed into separate yeast mating strains (A and alpha) that contain three reporter genes-Adenine, Histidine, and LacZ, and also an auxotrophic marker. Positive interactions are detected by selecting on plates lacking the auxotrophic marker and screening for reporter expression.

Our screen with all four DPTPs resulted in several positive clones - about 15 genes that interact with either of the four DPTPs. We eliminated some of these genes that are either bait-independent or not specific to the interacting RPTP. We identified seven genes that interact specifically with a given DPTP, four of these genes as potential substrates based on Src dependence. Of the seven genes four are known genes - Tartan (a cell adhesion molecule expressed in embryonic CNS and PNS), Cysteine string protein (a chaperone protein expressed in larval

neuromuscular junction and adult brain), Xmas-2 (a RNA-binding protein that is involved in spermatogenesis, oogenesis and embryogenesis) and BEST:LD07122 (a DNA-binding protein). Of the three unknown genes, one is rich in proline residues and also has proline motifs which are known to bind to SH3 domains. RNA in situ with this gene showed expression in the embryonic CNS. We are currently testing these interactions in vitro by transient transfection experiments with Drosophila cell line-S2 cells and finding out the expression of rest of the unknown genes by RNA in situ, and looking for double mutant phenotypes with DPTP and tartan mutant flies.

167. **Syndecan is a candidate ligand for the Drosophila RPTP Dlar**

Nicki Fox

The structural similarity of receptor protein tyrosine phosphatases (RPTPs) to receptor tyrosine kinases (RTKs) has led to the hypothesis that ligands might also modulate receptor protein tyrosine phosphatase (RPTP) activity, as they do with RTKs. To date, most RPTPs are "orphan receptors" as their physiologically relevant ligands are unknown. The identification of ligands for RPTPs is crucial for better understanding of the exact mechanisms by which RPTP signaling affects the growth cone.

We have identified a candidate ligand, Syndecan (Sdc), for one Drosophila RPTP, Dlar. Dlar is known to affect axon guidance decisions in the embryonic neuromuscular system, as well as the visual system. Dlar is necessary for normal development, as flies null for Dlar do not survive to adulthood. While it is well established that Dlar is an important player in development, proteins that interact upstream of Dlar have not been identified.

Sdc is a heparan sulfate proteoglycan (HSPG) that consists of an extracellular core protein to which heparin sulfate side chains are attached. HSPGs have been implicated in axon guidance in other systems.

Dlar and Sdc genetically interact, as lowering Sdc levels results in an enhancement of the characteristic Dlar intersegmental nerve b (ISNb) bypass phenotype. Sdc appears to act as a ligand, rather than a co-receptor, for Dlar, which is expressed in axons. Overexpression of Sdc in the muscles, but not the neurons, causes an axon guidance phenotype. This phenotype is suppressed by removing Dlar function. We are in the process of producing recombinant Sdc for use in biochemical assays, including co-immunoprecipitations and Biacore experiments, to elucidate the biochemical properties of Dlar-Sdc interaction.

168. **Identification of genes involved in axon guidance and synaptogenesis by transgenic RNAi**

Mili Jeon, Kai Zinn

To identify genes that control axon guidance and synaptogenesis, a gain-of-function (GOF) screen was conducted in the lab. The screen identified genes whose overexpression in neurons caused abnormal development of the neuromuscular system. The screen utilized the EP

misexpression module, which consists of a P-transposable element that contains multiple copies of the UAS element linked to a basal promoter sequence. The UAS element is the recognition sequence for a yeast transcription factor GAL4. When an EP is inserted in the appropriate orientation upstream of a gene, GAL4 directs high expression of this gene by binding to the UAS elements in the EP module and initiating transcription.

The GOF strategy was chosen in order to increase the sensitivity of the screen and minimize the problem of genetic redundancy. However, because high levels of expression of genes that are not normally expressed in neurons can cause nonspecific guidance and synaptic defects, another method was necessary to identify those genes that have direct roles in these processes. To this end, we targeted a handful of genes for loss-of-function (LOF) analysis using transgenic RNAi. The genes we selected were among the 35 'new' genes identified from the screen that showed no reports of alleles in the Fly Base. We also chose these genes based on their strong GOF phenotype, expression in the wild-type nervous system by in situ hybridization, and whether these genes encoded molecules that were of interest to us.

Transgenic RNAi utilizes the GAL4-UAS transactivating system described above to express dsRNA from inverted repeat sequences. DNA constructs carrying UAS elements and inverted repeat sequences of a target gene are injected into embryos to make transgenic flies. We have generated multiple transgenic lines for seven different genes. We initiated characterization of these lines by crossing to different driver lines that will express dsRNA in neurons or muscles. Initial results show that three of the constructs show neuronal driver or muscle driver-specific lethality, one that shows lethality with both neuronal and muscle drivers, and three that show no lethality with either drivers. We are currently analyzing the embryonic and larval preparations for axon guidance and synaptogenesis defects in these crosses.

169. **Characterization of receptor tyrosine phosphatase DPTP4E**

Mili Jeon, Alice Schmid*, Kai Zinn

Among the six known receptor tyrosine phosphatases (RPTP) in the fly genome, Ptp4E is the last remaining RPTP to be characterized. Ptp4E and Ptp10D mutant animals are fully viable and do not show any detectable CNS or motor axon guidance defects. However, animals that are doubly mutant for Ptp4E and Ptp10D die during the embryonic-to-larval transition stage. These embryos when labeled with antibodies against Fas II show a disorganized CNS, where the longitudinal axons appear wavy with breaks and show invasion of one axon bundle to its neighboring tracks.

Previous detailed genetic analysis carried out in the lab revealed that Ptp10D and Ptp69D are required for proper axon guidance in the embryonic CNS. Ptp10D; Ptp69D mutants have axons that abnormally cross the midline, suggesting that these two genes are normally required for repulsion of growth cones from the midline.

The secreted protein Slit expressed in the midline glia mediates repulsion by binding to the Robo receptors in growth cones. Ptp10D and Ptp69D genetically interact with robo, slit and comm, indicating that the RPTPs signal through these genes and act as a positive regulator of Slit/Robo repulsive signaling.

We want to investigate the role of Ptp4E in the CNS by analyzing double and triple mutant combinations with Ptp10D and Ptp69D. To better characterize the guidance phenotypes, we are collaborating with Alice Schmid to label single neuroblasts with Dil, and visualize by confocal microscopy, the axon tracks of the progenitor neurons. This will allow us to characterize guidance errors at much higher resolution and will help us understand the breaks and disorganization we see in the Fas II stained CNS. In addition to genetic interaction studies, we are raising monoclonal antibodies against PTP4E. In contrast to other RPTPs that are exclusively expressed in the nervous system, in situ hybridization experiments by others showed that Ptp4E mRNA is expressed in the nervous system, as well as in the developing gut. The expression studies of Ptp4E will help us understand additional roles that Ptp4E may have during development. Finally, we also have PTP4E-AP fusion protein expressed from insect cells (Caltech Protein Expression Facility) that will allow us to detect expression of PTP4E ligands using the techniques developed in the lab.

*Eccles Institute of Human Genetics, University of Utah

170. Genetic analysis of neural layer formation of the mushroom body, an olfactory learning and memory center, in **Drosophila**

Mitsuhiro Kurusu

Topographic maps of neural circuits in the brain are very important for neural information processing. Despite of the significance of their functions, genetic mechanisms underlying the construction of topology are still unclear. The *Drosophila* mushroom body (MB), which functions as a center for olfactory learning and memory, is one of the best model system to understand the molecular mechanisms that control the sequential generation of neurons and their topological projections into layers during the development of both vertebrate and invertebrate brains.

MBs are a pair of neuropile structures, each of which is composed of four cell clusters derived from four neuroblasts. In each cell cluster, axons are arranged in birth order layers, so that newly-born neurons send their axons into the core of the peduncle and migrate toward outside as they differentiate. The molecular mechanisms underlying the construction of these topological projections of MB neurons are still unknown.

We hypothesized that candidate molecule(s) should be expressed in the younger neurons to exhibit attractive cues for follower newly-born neurons. We identified a cell adhesion protein, N-Cadherin (N-Cad), and two receptor protein tyrosine phosphatase, PTP69D and DLAR, that are specifically expressed in younger neurons. Our result demonstrate that N-Cad is essential

for the four bundles of younger neurons originated from quadruple cell clusters to converge into a single tract below the calyx forming the proximal part of the peduncle, and to form a unified core. On the other hand, PTP69D is required for correct branching at separating point and DLAR has a role in preventing MB axons from projecting beyond the brain midline. Another cell adhesion protein, Fasciclin II (Fas II), is expressed in the outer layer of mature axons but absent in the core, and is required for clonal integrity of mature neurons and layer development. This suggests that N-Cad in younger neurons and Fas II in mature neurons have distinct roles in the construction of the axon layers of the peduncle. Thus, precise regulation of the expression timing of two cell adhesion proteins is essential for the development of topological axonal layer of MB.

171. The translational repressor Pumilio regulates presynaptic morphology and controls postsynaptic accumulation of translation factor eIF-4E

Kaushiki Menon

Translational repression by *Drosophila* Pumilio (Pum) protein controls posterior patterning during embryonic development. We have shown that Pum is an important mediator of synaptic growth and plasticity at the neuromuscular junction (NMJ). Pum is localized to the postsynaptic side of the NMJ in third instar larvae, and is also expressed in larval neurons. Neuronal Pum regulates synaptic growth. In its absence, NMJ boutons are larger and fewer in number, while Pum overexpression increases bouton number and decreases bouton size. Postsynaptic Pum negatively regulates expression of the translation factor eIF-4E at the NMJ, and Pum binds selectively to the 3'UTR of eIF-4E mRNA. The GluRIIA glutamate receptor is upregulated in pum mutants and synaptic transmission is altered. These results, together with genetic epistasis studies with eIF-4E, suggest that postsynaptic Pum modulates synaptic function via direct control of eIF-4E expression.

We are currently identifying other proteins that either regulate or interact with Pum at the larval NMJ. Nanos is a zinc-finger protein that is recruited by the Pumilio-target RNA complex in the abdominal segmentation function. Preliminary evidence shows that Nanos mutants show a synaptic defect which is different from Pumilio.

172. Role of **fog** in embryonic axon guidance in **Drosophila**

Anuradha Ratnaparkhi

We have been trying to examine the role of the gene folded gastrulation (fog) in embryonic axon guidance and determine whether it interacts with the receptor tyrosine phosphatase 52F (ptp52F). To test this, we overexpressed Fog in the CNS of embryos mutant for ptp52F with the hope that the ptp52F mutation might suppress the gain-of function phenotype of Fog.

Overexpression of Fog causes ISNa motor axon defects. In addition the CNS axons also appear disorganized and are found to aberrantly cross the midline. The removal of ptp52F appears to suppress this aberrant midline crossing suggesting that ptp52F might function downstream of Fog in the CNS.

Because of its early function, fog mutant embryos fail to develop normally, making it difficult to examine the phenotype of the nervous system in these embryos. To circumvent this problem, we generated transgenic RNAi lines for fog and expressed them in the CNS using Elav-GAL4. Although the motor axons appear to project normally in most embryos, the CNS did not appear normal. A range of phenotypes was observed in which some embryos showed a normal CNS, while in others the axon bundles appeared wavy and defasciculated. This variation might reflect the variability in expression of the transgene and conditions are being tested that result in a consistent phenotype.

During gastrulation, Fog is believed to signal via a heterotrimeric G-protein called concertina (cta). To test if the same signaling pathway operates in the embryo during axon guidance, we started by examining the nervous system in cta mutants. The CNS axons in these mutants often appear wavy and a little disorganized. In addition, these mutants also show strong ISNa motor axon phenotypes where the axon either stalls or fails to branch as in the wild-type embryos.

It will be interesting to see how these different signaling molecules interact in the nervous system to regulate axon guidance.

173. Assaying Pumilio for prion-like behavior
Anna Salazar

Protein aggregation has been implicated in numerous human diseases, including prion-based encephalopathies. Prions are capable of catalyzing their own propagation in a process whereby the protein serves as a seed or template in which the WT protein becomes folded into the abnormal structure and aggregates. This process has been observed in various organisms, including yeast, in which a system has been developed to better understand prion-like behavior. In yeast, the [psi+] phenotype is caused by the aggregation of Sup35p, a translational termination factor, causing it to become inactivated. Because the aggregation of other proteins enhances the aggregation of Sup35p, this system can be used as an assay for proteins that display prion-like behavior.

Learning and memory require synapses to be able to maintain their characteristics for longer periods than the lifetimes of any proteins within the synapse. Since prion aggregates can be inherited, a prion within a synapse should be maintained indefinitely after it is induced. In addition, any new prion proteins synthesized at the synapse would become incorporated into the old aggregates. If such a protein regulated synaptic local translation, it would then be possible for a translational state to be maintained

for long periods of time by an activity-regulated conversion of the protein to a prion form.

In order to determine if nucleic acid-binding prions exist in other organisms, the *C. elegans* and *Drosophila* protein databases were analyzed to search for RNA-binding proteins with Q/N rich domains. One of the genes obtained in this search encodes Pumilio, which we have found to regulate local translation at the neuromuscular junction (see Menon abstract).

Pumilio is a translational repressor containing a Q/N-rich N-terminal domain and an RNA-binding C-terminal domain. Pum forms aggregates in certain larval genotypes.

The two Q/N rich-domains of Pumilio, the full-length protein, and several functional domains of this protein, as well as the *C. elegans* homolog are being cloned into yeast expression vectors in order to probe their ability to exhibit prion-like behavior in a well-established yeast assay.

174. **Drosophila** Spastin regulates synaptic microtubule networks
Nina Tang Sherwood

The most common form of human autosomal dominant spastic paraplegia (AD-HSP) is caused by mutations in the SPG4 (spastin) gene, which encodes an AAA ATPase. Corticospinal axons in the lumbar regions of the spinal cord degenerate in AD-HSP patients.

Loss-of-function mutations in the *Drosophila* spastin gene produce larval neuromuscular junction (NMJ) phenotypes. NMJ synaptic boutons in spastin mutants are smaller and more numerous than in wild type, and transmitter release is impaired. spastin-null adult flies have severe movement defects. They cannot fly or jump, climb poorly, and have short lifespans. Overexpression of Spastin erases the muscle microtubule network, suggesting that it is a regulator of microtubule disassembly. In spastin mutants, microtubules are depleted from the distal boutons of the NMJ.

The *Drosophila* NMJ is a glutamatergic synapse that resembles excitatory synapses in the mammalian spinal cord, so the alteration of synaptic microtubule networks that we observe in spastin mutants may be relevant to an understanding of human AD-HSP. Loss of microtubules could produce a decrease in the efficiency of anterograde or retrograde axonal transport, and this might lead to the selective degeneration of the longest corticospinal axons, as they would be most vulnerable to transport defects.

175. What is the role of **Drosophila** beached in nervous system development?
Ashley Wright, Rachel Kraut

We identified *Drosophila* beached in an overexpression screen for axon guidance and synaptogenesis defects. Overexpression of Beached causes bulges to form at synaptic branchpoints and the morphology of the synapses is altered. Dr. Kim Finley at the Salk Institute has shown that mutations in beached

(which she calls blue cheese) show progressive neurodegeneration in adult flies and lead to shortened lifespan. By larval stages we observe thickening of certain nerve bundles and synaptic abnormalities. We have also been able to identify a subset of motor neurons which die during development.

beached encodes a protein of about 3500 amino acids which contains a BEACH domain, FYVE domain, and WD40 repeats. Other members of this family of proteins have been shown to have roles in endolysosomal trafficking. One member of the family is mutated in the lethal human genetic disease Chediak-Higashi syndrome. We are working to determine the subcellular localization of Beached protein by co-localization with known markers of the endolysosomal pathway and we will look in the mutant larvae at these same markers to determine if any compartment in this pathway is altered in size or morphology. We are currently investigating how these motor neurons die by looking at trophic support via TGF- β signaling and possible involvement of the insulin-signaling pathway. We are also overexpressing cell death inhibitors in this subset of motor neurons in order to determine if these neurons are dying by apoptosis.

Publications

- Kraut, R. and Zinn, K. (2004) Roundabout 2 regulates migration of sensory neurons by signaling in trans. *Curr. Biol.* 14:1319-1329.
- Menon, K., Sanyal, S., Habara, Y., Sanchez, R., Wharton, R.P., Ramaswami, M. and Zinn, K. (2004) The translational repressor Pumilio regulates presynaptic morphology and controls postsynaptic accumulation of translation factor eIF-4E. *Neuron*. In press.
- Sherwood, N.T., Sun, Q., Xue, M., Zhang, B. and Zinn, K. (2004) *Drosophila* Spastin regulates synaptic microtubule networks and is required for normal motor function. Manuscript submitted for publication.
- Zinn, K. (2004) Dendritic tiling: New insights from genetics (Review). *Neuron*. In press.

Structural, Molecular and Cell Biology

Giuseppe Attardi, Ph.D.
David Baltimore, Ph.D.
Pamela J. Bjorkman, Ph.D.
Charles J. Brokaw, Ph.D.
Judith L. Campbell, Ph.D.
David C. Chan, Ph.D.
Raymond J. Deshaies, Ph.D.
William G. Dunphy, Ph.D.
Grant J. Jensen, Ph.D.
Stephen L. Mayo, Ph.D.
James H. Strauss, Ph.D.
Alexander Varshavsky, Ph.D.

Grace C. Steele Professor of Molecular Biology:
Giuseppe Attardi
Senior Research Associate: Anne Chomyn
Senior Research Fellow: Petr Hájek
Visitors: Katia Altomare, Nicola Raule
Postdoctoral Scholars: Jaehyoung Cho, Miguel Martin-Hernandez, Jin Zhang
Research and Laboratory Staff: Catherine Lin, Maria Roldan-Ortiz, Maria C. Rosales, Rosie Zedan

Support: The work described in the following research report has been supported by:

Ellison Foundation
National Institute on Aging
National Institutes of Health, USPHS
Passano Foundation
Grace C. Steele Professorship in Molecular Biology

Summary: This past year has seen important new developments in our laboratory in the area of mitochondrial biogenesis in human cells. The first development was the unexpected discovery of a novel major origin of mtDNA replication in the control region (D-loop region) of mtDNA from three human cell lines, as well from several immortalized human lymphocyte cell cultures. This novel origin was discovered by using a novel powerful method for identification in total cell DNA of nascent mtDNA heavy-strand chains by extension of appropriate light-strand oligodeoxynucleotide primers chosen within the D-loop sequence or 3' to this. It was subsequently confirmed by using S1 protection assays not involving in vitro experiments with the VENT DNA polymerase or PCR steps. The novel origin differs from the previously known multiple origins in its unique functional properties. In fact, nascent chains starting from this origin, at difference from those starting from the other origins, do not stop prematurely at the 3'-end of the D-loop, but proceed beyond this point as true replicating molecules. Strong evidence has been obtained that these are the main contributors to the maintenance of mtDNA under steady state conditions, while the mtDNA molecules originating at the previously known origins have an important role in the recovery after mtDNA depletion.

Another important development has been the characterization of a previously unknown mechanism involved in the control of rRNA synthesis. In particular, it has been shown that the transcription termination factor (mTERF), discovered earlier, cloned and characterized in our laboratory, which was known to control the termination of transcription of the human mtDNA rDNA transcript, has also a crucial role in the control of initiation of rDNA transcription. Pursuing our early observation that, in an in vitro transcription system, mTERF stimulates transcription of the mitochondrial rDNA, it was found that, for its stimulating activity, mTERF has to bind to the termination site, but also to the rDNA transcription initiation site. Experiments with an infrared scanning-DNA fluorescence labeling system showed that each mTERF molecule could bind in vitro up to one molecule

of transcription initiation probe and up to slightly more than one molecule of termination probe. The in vitro occurrence of this double binding was shown by the chromatin immunoprecipitation technique. The most plausible interpretation of these data is that human mitochondrial rRNA synthesis is mediated by rDNA looping. An electron microscopic analysis has confirmed the occurrence of this looping.

In the same area of research, a variant of mTERF exhibiting a much higher affinity for the transcription termination than the wild-type protein site has been isolated. This variant will be extremely useful for identifying auxiliary protein factors.

Considerable progress has also been made in our understanding of early events in the apoptotic process in mammalian cells. In particular, good evidence has been obtained supporting the hypothesis that the hypersensitivity of the outer mitochondrial membrane to digitonin, that was previously shown in our laboratory to characterize an early phase of the mitochondrial response to two apoptotic stimuli, i.e., Fas receptor-ligand interaction and staurosporine, results from oxidation events. According to this hypothesis, phospholipid fatty acids are peroxidized and subsequently eliminated by phospholipases, with the resulting lysophospholipids making the outer membrane more sensitive to digitonin.

176. A novel major D-loop replication origin reveals a new mode of human mtDNA synthesis

Nicola Raule*, Jennifer Fish*

Recently, the concept that the strand-displacement, asymmetric model for mtDNA replication (1-3) is the only or the prevalent mechanism operating in mammalian cells has been challenged. Evidence has in fact been reported as favoring the existence of a bidirectional, strand-coupled mechanism (4-6), a proposal that has raised a lively debate (7-9).

The proponents of this alternative model favor a mechanism whereby the displacement loop D-loop origins are not actually origins, but represent points of fork arrest of the bidirectional mtDNA replication initiated downstream of the D-loop. In view of this dramatic divergence of opinions concerning the role of the D-loop mtDNA replication origins, we have carried out an in-depth functional investigation of the mtDNA heavy (H)-strand replication origins in three human cell lines, HeLa, A549 and 143B.TK⁻.

This analysis has led to the discovery of a novel major origin of human mtDNA heavy(H)-strand replication in the D-loop at position 57. The nascent chains starting at this origin, in contrast to those initiated at the formerly known origins, do not terminate prematurely at the 3'-end of the D-loop, but proceed well beyond this control point, behaving as "true" replicating strands. The 57 origin is the main D-loop replication origin and is responsible for mtDNA maintenance under steady-state conditions, whereas mtDNA synthesis from the formerly identified D-loop origins plays a major role in the initial

recovery after mtDNA depletion and, possibly, in accelerating mtDNA replication in response to physiological demands. This work thus strongly supports a "maintenance mode" and an "induced mode" of mtDNA synthesis originating within the D-loop.

Both researchers contributed equally.

References

- (1) Kasamatsu, H., Robberson, D.L. and Vinograd, J. (1971) *Proc. Natl. Acad. Sci. U.S.A.* 68:2252-2257.
- (2) Robberson, D.L., Kasamatsu, H. and Vinograd, J. (1972) *Proc. Natl. Acad. Sci. U.S.A.* 69:737-741.
- (3) Clayton, D.A. (1982) *Cell* 28:693-705.
- (4) Holt, I.J., Lorimer, H.E. and Jacobs, H.T. (2000) *Cell* 100:515-524.
- (5) Yang M.Y. et al. (2002) *Cell* 111:495-505.
- (6) Bowmaker, M. et al. (2003) *J. Biol. Chem.* 278:50961-50969.
- (7) Bogenhagen, D.F. and Clayton, D.A. (2003) *Trends Biochem. Sci.* 28:357-360.
- (8) Holt, I.J. and Jacobs, H.T. (2003) *Trends Biochem. Sci.* 28:355-356.
- (9) Bogenhagen, D.F. and Clayton, D.A. (2003) *Trends Biochem. Sci.* 28:404-405.

177. Further characterization of the mtDNA replication origins

Nicola Raule, Jin Zhang

The analysis of the mitochondrial DNA (mtDNA) control region in aged subject led us to the recent discovery of a new D-loop replication origin at position 57 (see previous report) in HeLa, A549 and 143B.TK⁻ cells. This origin was at first detected with a primer extension experiment using a [5'-³²P]-labeled oligodeoxynucleotide primer according to the protocol described in Zhang et al., 2003 (1).

This discovery required further analysis to confirm it by an independent technique, and also to better understand the role of this novel origin in mtDNA replication.

An S1 protection (2-3) assay was carried by using a [5'-³²P]-labeled oligodeoxynucleotide probe. This probe was hybridized with purified mtDNA, and then digested with S1 nuclease. The products were analyzed with a polyacrylamide gel electrophoresis (PAGE) system. This completely independent experiment confirmed the presence of all the formerly known main origins of replication, as well as of the new one at position 57.

An objection that has been raised to this finding is that it might be a characteristic of cell lines, like 143B.TK⁻, A549 or HeLa cells that have been maintained in culture for a long time. So we decided to test other cell lines for the presence of the mutation. The 57 origin was in fact, detected in two different immortalized lymphocyte cell lines recently isolated (named CR681 and C223). These cell lines are as close to the in vivo conditions as we can obtain; therefore, we can conclude that the 57 origin is not an artifact of in vitro culture conditions.

These experiments provide indisputable proof of the presence of this origin of replication in human mtDNA.

References

- (1) Zhang, J., et al. (2003) *Proc. Natl. Acad. Sci. USA* 100:1116-1121.
- (2) Fernandez-Silva, P. et al. (1996) *Meth. Enzymol.* 264:129-139.
- (3) Chang, D.D. et al. (1995) *Proc. Natl. Acad. Sci. USA* 82:351-355.

178. Regulation of human mtDNA transcription: Study of the role of mTERF in controlling the rRNA synthesis

Miguel Martin-Hernandez¹, Jaehyoung Cho¹, Tony Cesare², Jack Griffith², Giuseppe Attardi

Although the so far unique mode of complete symmetrical transcription of mammalian mitochondrial DNA (mtDNA) was identified and partially characterized a long time ago (1,2), the detailed molecular mechanism of this process has started being characterized only recently. Furthermore, the regulation of mammalian mtDNA transcription is still an object of debate. In particular, as concerns the control of synthesis of the rRNAs and heavy-strand coded mRNAs, two distinct models have been proposed. According to one model, which is supported by abundant evidence from our laboratory (2), transcription of the mtDNA H-strand starts from two initiation sites within the main control region. One site (H1) produces a transcript terminating at the 3'-end of the 16S rRNA gene, which is destined to be processed, yielding the two rRNAs and the tRNA^{Phe} and tRNA^{Val}. The second site (H2) produces a polycistronic molecule, corresponding to almost the entire H-strand. According to the other model, there is a major initiation site for H-strand transcription in the H-strand promoter, which produces a transcript which can either terminate at the 3'-end of the 16S rRNA gene, producing the rRNAs, or proceed beyond this point to produce the mRNAs and tRNAs encoded downstream of the 16S rRNA gene. According to both models, termination of transcription at the 3'-end of the 16S rRNA gene involves the activity of a termination factor, mTERF, whose gene has been cloned and characterized (3). The first model, thus, assumes that control of rRNA vs. mRNA synthesis requires events occurring at both the rDNA transcription initiation and termination sites, whereas the second model assumes only events at the termination site.

An early striking observation in the analysis of mTERF, which has been recently confirmed (4), was that, in an in vitro transcription system, mTERF stimulates transcription of the mitochondrial rDNA. This finding suggested that mTERF may interact with both the termination site and the H1 initiation site, possibly causing a looping-out of the rDNA.

The aim of this work was, first of all, the confirmation of the identification and precise mapping of the two initiation sites for the human mtDNA H-strand transcription previously performed in this laboratory, and

secondly, the analysis of the role of mTERF in controlling the rDNA transcription.

In vivo and in vitro transcription experiments revealed transcripts starting at the H1 site and, in small amount, at the H2 site. Addition of mTERF specifically stimulated transcription from H1. Reconstruction experiments and mtDNA-binding assays clearly showed that, for its stimulating activity, mTERF had to bind to the termination site, and also to the H1 initiation site. Experiments carried out with an infrared scanning-DNA fluorescence labeling system revealed that each mTERF molecule could bind in vitro up to one molecule of transcription initiation probe and up to slightly more than one molecule of termination probe. The in vivo occurrence of this double binding was shown by the chromatin immunoprecipitation (CHIP) technique. The most plausible interpretation of these results is that human mitochondrial rRNA synthesis is mediated by rDNA looping. An electron microscopic analysis has indeed revealed a DNA-loop structure in the same DNA template utilized for the in vitro transcription experiments driven by mTERF.

¹Both researchers contributed equally

²University of North Carolina, Chapel Hill, NC

References

- (1) Aloni, Y. and Attardi G. (1971) *Proc. Natl. Acad. Sci. USA* 68:1757-1761.
- (2) Montoya, J., Gaines, G.L. and Attardi, G. (1983) *Cell* 42:151-159.
- (3) Fernández-Silva, P., Martínez-Azorin, F., Micol, V. and Attardi, G. (1997) *EMBO J.* 16:1066-1079.
- (4) Asin-Cayuela, J., Helm, M. and Attardi, G. (2004) *J. Biol. Chem.* 279:15670-15677.

179. Molecular characterization of a functional variant of mTERF and the practical application for the investigation of the mTERF function

Jaehyoung Cho^{*}, Miguel Martín-Hernández^{*}

We recently found and isolated several variant forms of the mTERF gene from a human HeLa cDNA library. To investigate the biological significance of these variants, we expressed the proteins with a GST tag in a bacterial expression system. Among them, one variant showed an approximately 15-fold higher mtDNA binding activity than the wild-type protein in vitro. This protein has two amino acid changes in the leucine-zipper domain. Since the recombinant wild-type mTERF expressed in any system has not shown termination activity in an in vitro transcription termination assay (1), we are presently testing whether this variant can mimic the in vivo function of mTERF in transcription termination activity. In another project, we showed mTERF simultaneously controls the termination and initiation of rDNA transcription by inducing a mtDNA loop structure. We hypothesized that another auxiliary protein factor(s) stabilizes it. To search for this protein factor, we have used several experimental approaches, including DNA affinity chromatography and

formaldehyde or UV co-crosslinking assays. In these experiments, we reproducibly observed that several proteins were co-purified with mTERF. The molecular weights of these proteins were about 55, 65 and 80 kDa. Among them, the 60-65 kDa protein may be a strong candidate for being an auxiliary protein, because in a previous report the 65 kDa mitochondrial topoisomerase I (mtTopoI) showed functional preference to the mtDNA region containing the mTERF recognition site (2). Actually topoisomerase I is well known to be an essential enzyme for nuclear DNA replication and transcription. We hypothesized that mtTopoI may release the topological constraint of supercoiled mtDNA and stabilize the loop structure at the termination site after turning on the rDNA specific transcription. We are presently testing if mtTopoI has any function for the mTERF-dependent transcription termination and re-initiation mechanism. We think that the functional variant of mTERF that we isolated will also help in the search for the auxiliary proteins. Thus, the GST-fused form can be used in a GST pull-down assay for affinity purification of a protein-DNA complex containing mTERF, mtDNA loop and auxiliary protein(s).

^{*}Both researchers contributed equally.

References

- (1) Fernández-Silva, P., Martínez-Azorin, F., Micol, V. and Attardi, G. (1997) *EMBO J.* 16:1066-1079.
- (2) Topcu, Z., Castora, F.J. (1995) *Biochem. Biophys. Acta.* (1995) 1264:377-387.

180. Investigation of proteins interacting with sites of the human mtDNA main control region specifically targeted by an aging-dependent accumulation of mutations

Jaehyoung Cho

Aging is very complicated and difficult to study in human beings. In the last decade, mitochondria and energy metabolism have been shown to have important relationships with aging and longevity (1,2). Mitochondria have their own genome and cooperate with the nuclear genome in regulating respiration, energy metabolism, and, more surprisingly, aging and longevity (1,2). The D-loop region of human mitochondrial DNA (mtDNA) harbors very crucial control sequences, such as replication origins and transcription promoters, and this control region undergoes some mutations that occur in aging-dependent manner (1,2). To investigate the molecular basis of the aging-dependent mutagenesis and its selection, we planned to identify possible protein-DNA interactions in this region. During the replication process, an early replicative mtDNA form is a long, triple helix-containing D-loop. The stability of the single-stranded portion of the D-loop may have an important role in the regulation of mtDNA copy number. Thus, we have searched for possible protein-DNA interactions in both the single-stranded DNAs (heavy and light strands) of this region. In the case of the DLP4 subregion of the D-loop region (1), which harbors major replication origins and the conserved sequence block CSB1, only the light strand showed

binding activity to several proteins in DNA mobility shift assays. We purified the proteins by ssDNA affinity chromatography, and found that these have molecular weights of 70, 55, 37, 28 and 15 kDa. Among them, the 37-kDa protein shows specific binding to a previously known origin of heavy strand replication (OH2). This OH2 region is the site of a very interesting aging-dependent mutation (C150T). Previous work in this laboratory showed that, in leukocytes from subjects of an Italian population, the homoplasmic C150T transition occurs in approximately 17% of 52 subjects 99-106 years old, but, in contrast, in only 3.4% of 117 younger individuals. Interestingly, the 37-kDa protein preferably interacts with the mutant sequence rather than with the wild-type sequence. Since 5'-end analysis of nascent heavy strands consistently revealed a new replication origin at position 149, substituting for that at 151, only in C150T mutation-carrying samples of fibroblasts or immortalized lymphocytes (1,2), the 37-kDa protein may have an important role for the selection of a remodeled replication origin. Recently, we characterized the molecular nature of this protein by LC/MS/MS (liquid chromatography and tandem mass spectrometry). The result showed that this protein is a member of the group of critical enzymes for the TCA cycle. We confirmed that the commercially available purified enzyme can also bind specifically to the OH2 region *in vitro*, and that the antibody against this protein can make a super-shifted band in a DNA mobility shift assay. Presently, we are verifying the specificity of this protein-OH2 interaction by DNase I footprinting analysis. Our data suggest the possibility that two important factors in aging, i.e., energy metabolism and mtDNA function, regulate the aging process during the lifespan.

References

- (1) Michikawa, Y., Mazzucchelli, F., Bresolin, N., Scarlato, G. and Attardi, G. (1999) *Science* 286:774-779.
- (2) Zhang, J., Asin-Cayuela, J., Fish, J., Michikawa, Y., Bonafe, M., Olivieri, F., Passarino, G., De Benedictis, G., Franceschi, C. and Attardi, G. (2003) *Proc. Natl. Acad. Sci. USA* 100:1116-1121.

181. C150T human mitochondrial DNA mutation analysis

Nicola Raule

Over the last few years a considerable amount of effort has been spent in our laboratory to study the effect of several point mutations in the main non-coding region (D-loop region) of mtDNA.

Recently, a paper from our laboratory has shown a strikingly increased frequency of a C150T mutation in the mtDNA D-loop region from centenarians and twins and from fibroblasts of aged individuals (1). The proximity of this mutation to one of the origins of replication in mtDNA has raised the question of its effects on such a delicate process as DNA replication.

To address this question, we decided to construct cybrid cell lines starting from the fusion of ρ^0 (mtDNA-less cells) and different cells carrying the specific mutation of interest. The ρ^0_{206} cell line is a derivative of the 143B.TK⁻ cell line, which has been completely depleted of mtDNA (2). The best aspect of this technique is that it eliminates most of the interference of different nuclear backgrounds, since all the transformants have near the same ρ^0_{206} nuclear background.

All attempts to obtain the fusion between ρ^0_{206} cells and fibroblasts carrying the C150T mutation have been successful. We were able to perform five fusions starting from samples of fibroblasts coming from different individuals. These fibroblasts carry the C150T mutation in different proportions.

The fibroblasts were cultured for a very short time on 3.5 cm Petri dishes before the fusion with the ρ^0_{206} cells by means of polyethyleneglycol. After the fusion, the cybrids were selected in medium containing galactose instead of glucose for two weeks, and then subcloned to obtain single-cell colonies.

Two of the fusions produced more than 20 different mutant colonies, while the other three produced over 100 wild-type colonies. All of the fusions were performed using cells carrying the C150T heteroplasmic mutation. Having several colonies from different individuals, both mutant and wild type, will allow a comparison that is expected to reveal the most important differences between the two phenotypes.

The analysis of the transformants will aim at investigating any possible effects of the mutation on mtDNA replication, as well as at testing their respiration capacity and several biochemical parameters related to the efficiency of oxidative phosphorylation.

References

- (1) Zhang, J. et al. (2003) *Proc. Natl. Acad. Sci. USA* 100:1116-1121.
- (2) King, M.P. and Attardi, G.A. (1989) *Science* 246:500-503.

182. Hypersensitivity of the outer mitochondrial membrane to digitonin in the early stages of apoptosis

Katia Altomare, Anne Chomyn*

143B osteosarcoma cells treated with the apoptosis inducer staurosporine, undergo marked changes in the outer mitochondrial membrane early in the cell death program, long before cytochrome c is released from the mitochondria in the living cell. One of these changes is an increase in the sensitivity of the outer mitochondrial membrane to the detergent digitonin. This increased sensitivity is manifested by a loss of cytochrome c *in vitro* from the mitochondria of digitonin-permeabilized cells. At the concentration of digitonin used in these experiments, control cells, i.e., those not undergoing apoptosis, retain an intact outer mitochondrial membrane and do not lose cytochrome c.

We have posited the hypothesis that the changes in the outer mitochondrial membrane result from oxidation events. More specifically, we are testing the possibility that phospholipid fatty acids are peroxidized, that these peroxidized fatty acids may be eliminated by phospholipases, and that the resulting lysophospholipids make the membrane more sensitive to digitonin. To test this hypothesis, we have overexpressed the phospholipid glutathione hydroperoxide peroxidase in our cells. Furthermore, we have tried to mimic the effects of staurosporine by using oxidants. Finally, we have tested the effect of inhibitors of phospholipase A.

Our collaborators S. Moghaddasa and E.J. Lesnefsky will analyze the lipid composition of purified mitochondria from apoptotic and non-apoptotic cells.

*In collaboration with Hirotaka Imai and Yasuhiro Nakagawa, Kitasato University, Japan and Shadi Moghaddas and Ed Lesnefsky, Case Western Reserve University, Cleveland.

183. Increased sensitivity to apoptosis in complex I mutant

Catherine Lin, Anne Chomyn*

Human cell lines carrying a pathogenic mtDNA mutation in the ND4 gene (at position 11778) undergo apoptosis induced by staurosporine much more rapidly than does a related cell line having the same nuclear background, but wild-type mtDNA (unpublished observations). The ND4 gene encodes an essential subunit of the 43-subunit complex I, the respiratory chain NADH dehydrogenase. The mutation mentioned above is the most common cause of Leber's hereditary optic neuropathy (LHON), an inherited disease that manifests itself as a sudden loss of vision.

The mutation compromises complex I activity, but does not abolish it (Hofhaus et al., 1996). An interesting feature of the NADH dehydrogenase, or NADH:ubiquinone oxido-reductase activity in mutant cells is that NADH is oxidized to NAD⁺ at a normal rate but oxygen is reduced at only 50% of the normal rate (Hofhaus et al., 1996). This apparent contradiction suggests the following interpretation: electrons transferred by the defective complex I from NADH do not always stably reduce ubiquinone, and therefore, do not always travel down the respiratory chain to oxygen. If this hypothesis is correct, then free radicals, in particular superoxide, would be expected to be generated from the inefficient reduction of ubiquinone.

We are testing the hypothesis that the increased sensitivity to apoptosis of cells carrying the ND4 LHON mutation is due to increased superoxide production in the cells. We have found that there is a slight increase in ROS (reactive oxygen species) production in mutant cells, as detected by the oxidant-sensitive fluorescent probe chloromethyl-dihydrodichlorofluorescein. We have overexpressed NDI1, the single-subunit yeast mitochondrial NADH dehydrogenase, in the mutant cells in order to determine whether the exogenous enzyme will decrease the amount of ROS production and restore

normal sensitivity to apoptosis. NDI1 gene expression has been shown to restore respiratory activity in a human mutant cell line that was completely deficient in complex I activity (Bai et al., 2001). We have found that the effects of NDI1 expression depend on the level of NDI1 expression, but that, in general, there is no correlation between the level of ROS production and the sensitivity to the apoptosis-inducing agent staurosporine.

*In collaboration with Byoung Boo Seo, Akemi, Matsuno-Yagi, Takao Yagi, Scripps Institute, La Jolla,

References

Bai, Y., Hajek, P., Chomyn, A., Chan, E., Seo, B.B., Matsuno-Yagi, A., Yagi, T. and Attardi, G. (2001) *J. Biol. Chem.* 276(42):38808-38813.

Hofhaus, G., Johns, D.R., Hurko, O., Attardi, G. and Chomyn, A. (1996) *J. Biol. Chem.* 271(22):13155-13161.

184. Characterization of mitofusins differentially expressed in various human cell lines and tissues: Implications for mitochondrial organization

Petr Hájek, Ansgar Santel¹, Margaret T. Fuller¹, Giuseppe Attardi

Mitochondria differ in size, shape and organization. They are dynamic structures that can rapidly fuse or divide. In man, mitochondrial fusion is mediated by mitofusins Mfn1 and Mfn2 and by Opa1. Mfn1 and Mfn2 are integral mitochondrial outer membrane proteins with both the large N-terminal portion, containing a GTPase domain, and the C-terminal portion projecting into the cytosol. Polyclonal antibodies against a His-tagged recombinant protein, corresponding to a large portion of the N-terminal cytosolic segment of Mfn2, and against Mfn1, have been produced in rabbits. These have provided us with powerful tools for immunoblotting and immunoprecipitation experiments. Purified antibodies against Mfn2 identified on Western blots a single band of Mfn2 and helped us to reveal that one of the previously detected isoform of Mfn2 is likely to be an unrelated protein. Mfn1 and Mfn2 protein levels were analyzed by Western blotting of whole cell lysates from various human cell lines. In these, Mfn1 and Mfn2 varied greatly in amount. Mfn2 had the highest level in HeLa S3 (suspension culture) and 143B cells, an intermediate level in HepG2 and HeLa CCL2 cells, and low level in A549 cells. Mfn1 protein was equally abundant in HepG2 and HeLa CCL2 cells, and it was reduced by ~30% in 143B and A549 cells. Although these cells exhibited striking differences in mitochondrial morphology, from a long-filament/network pattern in HeLa CCL2 cells to mostly punctate mitochondria in 143B cells, with intermediate morphology in HeLa S3 (suspension culture), HepG2 and A549 cells, surprisingly, no clear correlation between the levels of Mfn2 or Mfn1 and mitochondrial morphology was observed. Mfn2 levels varied greatly also in human tissues, with high levels in heart, kidney and testis,

intermediate level in placenta and low levels in brain, skeletal muscle, and liver.

Sequence analysis of individual clones of the RACE products from poly(A)⁺ RNA revealed an identical Mfn2 ORF in 143B, HeLa CCL2 and HeLa S3 cells, indicating the presence of only one Mfn2 mRNA species. Short [³⁵S] methionine pulse labeling of HeLa CCL2 and HeLa S3 cells, followed by immunoprecipitation under denaturing conditions and using purified anti-Mfn2 antibodies revealed two bands of different electrophoretic mobilities, one corresponding to the steady-state form of Mfn2, the other characterized by a slower electrophoretic mobility. The intensities of these bands were increased when HeLa CCL2 cells were transiently transfected with human Mfn2 cDNA, strongly suggesting that these forms are related and that the slower migrating band represents a transient form of Mfn2. In addition, the majority of Mfn2 synthesized *in vitro* from the human cDNA corresponds in electrophoretic mobility to the slower migrating, transient Mfn2 form. The slower migrating form may be either less stable or is modified to the faster migrating, steady-state form. The future investigations will be aimed at the characterization of the two Mfn2 forms, the Mfn2 interacting proteins and their relevance to mitochondrial morphology.

¹Stanford University School of Medicine, Stanford, CA

Publications

- Asin-Cayuela, J., Helm, M. and Attardi, G. (2004) A monomer-to-trimer transition of the human mitochondrial transcription termination factor (mTERF) is associated with a loss of *in vitro* activity. *J. Biol. Chem.* 279:15670-15677.
- Fish, J., Raule, N. and Attardi, G. (2004) A major D-loop replication origin for a previously unknown mode of human mtDNA synthesis. *Science*. In press.
- Greco, M., Villani, G., Mazzucchelli, F., Bresolin, N., Papa, S. and Attardi, G. (2003) Marked aging-related decline in efficiency of oxidative phosphorylation in human skin fibroblasts. *The FASEB J.* 14:1706-1708.
- Helm, M. and Attardi, G. (2004) Nuclear control of cloverleaf structure of human mitochondrial tRNA^{Lys}. *J. Mol. Biol.* 337:545-560.
- Martin-Hernandez, M., Cho, J. and Attardi, G. (2004) The human mtDNA transcription termination factor mTERF controls rRNA synthesis by simultaneously interacting with the termination and initiation sites. To be submitted.

Professor of Biology: David Baltimore
 Postdoctoral Scholars: Mark Boldin, Markus Covert,
 Huatao Guo, Shengli Hao, Wange Lu, Mollie Meffert,
 Konstantin Taganov, Jeff Wieszorek, Lili Yang
 Graduate Students: Thomas Leung
 Research Staff: Elissa Denny, Jahlionais Gaston, Anca
 Mihalas, Eric Santiestevan, Vicky Yamamoto

Support: The work described in the following research reports has been supported by:

Army Research Office (ARO)
 Association for the Cure of Cancer of the Prostate
 (CaPCURE)
 Damon-Runyon Cancer Research Foundation
 Human Frontiers Science Program Organization
 National Institutes of Health
 The Skirball Foundation

Summary: Our laboratory is involved in three major directions of research.

The first is study of the remarkable range of activity of the NF- κ B transcription factor. It activates perhaps 1000 genes in response to a wide range of stimuli. It has different physiologic roles in different cells. How one factor can be so varied in its activity is the puzzle that interests us. We are studying this at the level of DNA-protein interactions as well as signal transduction pathways. We are studying its role in normal cells and in diseases like cancer and AIDS.

The second line of work involves using gene transfer methods to reprogram the immune system. We have shown that we can design a retrovirus vector able to express cDNAs encoding both chains of the T cell receptor (TCR) protein. When mouse hematopoietic stem cells are transduced with the vector and then inoculated into irradiated mice, many of the resulting T cells express the TCR encoded by the vector. We have shown that when the TCR is able to recognize specific peptides from a tumor antigen, the animal can reject tumors carrying the antigen. We plan to extend these studies to human tumor antigens with the goal of developing a human therapy. We are also studying whether the same strategy will work for antibody gene expression by B cells with a goal of devising a new therapy for AIDS.

The third goal of the laboratory is to understand the role of the Ryk protein as a co-receptor for Wnt proteins. We have shown that Wnt interacts with both Ryk and Frizzled surface receptor proteins in a tripartite complex. We are now investigating the pathways activated by Ryk and the role of Ryk in neuronal guidance.

185. Interaction of the NF- κ B transcription factor with the κ B DNA binding sites in the HIV-1 LTR

Huatao Guo, David Baltimore
 The NF- κ B transcription factor refers to homo- and heterodimers of five gene products (p65, cRel, RelB, p50 and p52). It is a pleiotropic regulator of a large number of genes involved in many processes, such as

inflammation, immunity, apoptosis, and learning. Different NF- κ B-dependent genes may require specific homo- or heterodimers of the NF- κ B proteins. Indeed, Leung et al., found that even a single base pair change in a κ B site was able to change the specificity of the κ B site for a different NF- κ B dimer.

Soon after the finding of NF- κ B, our laboratory showed that the two κ B sites in the HIV-1 LTR play key roles in transcription of the viral genome. The two κ B sequences are identical. Consistent with their important role in HIV-1 replication, the κ B sequence is highly conserved in different HIV-1 strains. However, why the specific sequence of the κ B sites is selected remains to be answered.

We want to study how the two κ B sites in the HIV-1 LTR regulate viral transcription in response to different stimuli and why the particular κ B sequence are conserved. A lentiviral system will be used for this purpose. A portion of the HIV-1 LTR and a luciferase reporter gene were inserted in the middle of a self-inactivating lentiviral vector (Lois et al., Leung et al.). The lentivirus infects both dividing and non-dividing cells with high efficiency. This system allows us to introduce desired modification to the promoter sequence conveniently. We have changed the κ B sequence of the HIV-1 LTR to the κ B sequence of another gene promoter to test the requirement of specific κ B sequence. In addition, we are also changing the distance between the two κ B sites to test for their cooperativity. Preliminary results appear to suggest that the wild-type HIV-LTR may not present the most efficient binding.

References

Leung, T.H., Hoffmann, A. and Baltimore, D. Cell. In press.
 Lois, C., Hong, E.J., Pease, S., Brown E.J. and Baltimore, D. (2002) Science 295:868-872.

186. Specificity of transcriptional activation in the NF- κ B/Rel protein family

Thomas Leung, David Baltimore

The study of mammalian gene transcription is often complicated by the fact that multiple members of a transcription factor family recognize the same regulatory sequence. While several models have been proposed, little is known about how genes recruit specific members of transcription factor families for activation. The Nuclear Factor kappa B (NF- κ B)/Rel transcription factor family is an evolutionarily conserved gene regulation system involved in the coordination of an organism's response to infection, stress, and injury. Many different stimuli activate NF- κ B, but the transcriptional response to each stimulus is unique. Within the NF- κ B/Rel protein family, four members are involved in gene activation: p50, p52, p65, and cRel. They homo- or heterodimerize with one another to bind DNA.

Our lab has developed a genetic system to elucidate whether specific NF- κ B/Rel family members are required for gene activation in a physiological manner. Single and multiple knockouts for each member of the NF- κ B/Rel family were created, and 3T3 fibroblast cell lines were derived. Our genetic analysis with this comprehensive panel of knockout cell lines showed that NF- κ B-dependent genes have specific NF- κ B/Rel family member requirements for activation by TNF α . This finding suggested that the variety of NF- κ B/Rel dimer isoforms allows for stimulus-specific gene expression programs.

How is the requirement for specific NF- κ B/Rel family members generated? In our previous studies, no direct correlation between the sequence of DNA binding sites for NF- κ B (κ B sites) and κ B family member requirements for gene activation could be found, when we compared one gene to another. Recently, we found that although the apparent consensus sequence of κ B sites is very broad, the sites active in any one gene show remarkable evolutionary stability. This implies that the individual sequences have important characteristics and led us to examine the role of particular sequences found associated with particular genes. Using a lentivirus-based methodology for implantation of gene regulatory sequences we show that for genes with two κ B sites, both are required for activity. Swapping sites between κ B-dependent genes altered NF- κ B dimer specificity of the promoters and revealed that two κ B sites can function together as a module to regulate gene activation. Further, although the sequence of the κ B site is important for determining κ B family member specificity, rather than determining the ability of a particular dimer to bind effectively, the sequence affects which co-activators will form productive interactions with the bound κ B dimer. This suggests that binding sites may impart a specific configuration to bound transcription factors.

187. The role of NF- κ B in cell growth and transformation

Jeff Wiezorek, David Baltimore

The NF- κ B transcription factors are composed of protein homo- and heterodimers of five gene products (p65, p50, p52, c-Rel, and RelB). Diverse stimuli act through the I κ B kinases (IKKs) to promote the degradation of I κ B and allow NF- κ B translocation to the nucleus. NF- κ B activation has been implicated in several biological processes including inflammation, immunoregulation, apoptosis, and cell proliferation. Although the transforming ability of the ν -REL oncoprotein was established many years ago, recent evidence suggests other human NF- κ B family members may be important in oncogenesis. NF- κ B DNA binding activity is constitutively increased in many lymphoid and epithelial tumors. The RAS, BCR-ABL, and HER2 oncogenes and transforming viruses can activate NF- κ B. Furthermore, several genes thought to be essential to the cancer

phenotype, those controlling angiogenesis, invasion, proliferation, and metastasis, contain κ B binding sites. However, direct genetic evidence demonstrating the role of NF- κ B in transformation and cancer progression is lacking.

Our lab has generated strains of knockout mice in which one or more of the NF- κ B family members are deleted. 3T3 and primary fibroblasts of a specific genotype generated from these mice are powerful tools for dissecting NF- κ B signaling pathways. These cells and mice are being used to study different aspects of cellular senescence, transformation, and cancer progression. Furthermore, we have identified RelB as necessary for alveolar proliferation during pregnancy in a knockout model. This signaling pathway and its role in mammary transformation is under investigation. Additionally, by crossing the MMTV-cNeu transgene into NF- κ B knockout strains, the contribution of constitutive NF- κ B activity to breast cancer initiation, invasion/metastasis, and angiogenesis is being directly studied.

188. Engineering immunity via instructive immunotherapy

Lili Yang, David Baltimore

Captured in the phrase of "engineering immunity," we are interested in engineering immune system to treat cancer and other infectious diseases. Our most recent progress is the development of "instructive immunotherapy" to impart anti-tumor CD8 cytotoxic and CD4 helper T cell specificities to the mouse T cell repertoire. Genes encoding a CD8- or CD4-restricted T cell receptor were delivered into hematopoietic stem cells (HSCs) via a retroviral vector. In host mice, these HSCs generated anti-tumor T cells, which displayed a normal response to antigenic stimulation, the expected patterns of surface activation markers, and the ability to generate and maintain long-term memory. In a mouse tumor model, either cell achieved tumor suppression, and the combination yielded complete elimination of established large solid tumors. This approach offers a potential treatment for cancer and other infectious diseases.

189. Wnt signaling in the nervous system

Wange Lu, David Baltimore

Cell-cell communications play essential roles in regulating cell fate determination, cell proliferation and differentiation. The receptor tyrosine kinases are a big family of proteins involved in cell signaling. The receptor related to tyrosine kinase (Ryk) is a unique member of receptor tyrosine kinases since it contains a cryptic protein tyrosine domain. The *Drosophila* homologues of Ryk, *lionotte* and *derailed*, are involved in learning and memory and axon guidance, respectively. However the ligand of this orphan receptor has been unknown.

The extra-cellular domain of Ryk is homologous to Wnt inhibitory factor (WIF). Thus, Wnt might be the ligand of the orphan receptor Ryk. We have demonstrated that Ryk and Wnt coimmunoprecipitate. The extra-cellular

WIF domain was required for the interaction, while the intracellular domain was not required.

As Frizzleds are the canonical receptors for Wnt, we hope to know whether Ryk forms a co-receptor with Frizzled. The extra cellular domain of Frizzled-8 was fused with the human IgG Fc fragment, and was cotransfected into 293 cells with the myc-tagged Ryk extra-cellular domain and HA-tagged Wnt. Coimmunoprecipitation showed that the extra cellular domain of Frizzled can bind to Ryk and Wnt. Furthermore, overexpression of Ryk does not inhibit the Wnt/Frizzled interaction, suggesting that Ryk might form a co-receptor complex with Frizzled and Wnt.

We have also generated transgenic mice expressing siRNA to knock down the expression of endogenous Ryk. We have found that Ryk is required for axon guidance *in vivo*. Explant outgrowth assay *in vitro* suggests that Ryk is required for Wnt3a-mediated neurite outgrowth, confirming that Ryk is a functional receptor for Wnt3 α . We are now continuing analysis of Ryk function during nervous development.

190. Dynamics of LPS-stimulated activation of NF- κ B

Markus Covert

With increasing evidence that the activity of NF- κ B is important in a variety of tumors, it has become clear that determining the dynamics of such activity will be vital to understanding certain types of cancer, and could also lead to significant advances in the identification of important therapeutic targets. I propose to investigate the interactions and dynamics of the upstream signal transducing pathways that regulate NF- κ B activity under LPS and LPS-mimetic anticancer drug Taxol stimulation. Specifically, I will (1) quantitatively describe the time response to LPS and/or Taxol in terms of IKK activity, NF- κ B nuclear concentration and I κ B α gene expression in wild type as well as key knockout/knockdown MEF cell lines, (2) develop a detailed computational model incorporating the data from Aim (1) to simulate the dynamics and interactions of the MyD88-dependent and independent signaling pathways, and (3) determine whether the difference in pathway dynamics could in part explain differential gene expression between TNF α and LPS or Taxol-stimulated cells.

191. Development of chimeric mouse model with fully functional human immune system

Shengli Hao, David Baltimore

The study of the human diseases and evaluation of preclinical tests are greatly relied on the *in vivo* study of human cells and/or tissues. Because of the ethical restrictions of studies on humans, engraftment of human cells or tissues into the lab animals, particularly small lab animals, has become the primary choice to address this kind of question. The main problem to introduce human tissues and/or cells into lab animals is xenotransplantation rejection by the host. Therefore, efforts have been made over the past 30 years on animals that lack their own

functional immune system and are instead reconstituted with a human immune system. Animals such as SCID mice, RAG2 knockout mice and mice with combinatory defects, such as NOD/SCID mouse and RAG2^{null}/gc^{null} mouse, have been used. For long-term reconstitution of human hematolymphoid system, human hematopoietic stem cells are usually used for introduction into the animals. Although great progress has been achieved in recent years, however, the main problem is that the engraftment of the human hematopoietic system is still low, and the function of this system in mice is far below that of normal functions within mice or humans. Therefore, the goal of this study is to set up an ideal mouse model with a fully functional human immune system and subsequently to study the development of human hematopoietic stem cells and some related human diseases.

There are many factors that potentially determine the efficiency of engraftment, for example, the enrichment (purity) of the stem cells, the development stage of the stem cells, the route to introduce the stem cells to the host (e.g., *i.v.* or *i.p.*), the age of the host, etc. Experiments will be set up to compare the engrafting efficiency in these conditions and find the way to optimize the engrafting efficiency.

It is still a mystery how the development of the human hematopoietic system occurs during embryogenesis and in adults. This mouse model provides a unique system to address this question. We will employ gene knockout and gene overexpression techniques such as lentivirus infection to explore the key molecules that control the development of stem cells. The microenvironment (niche) of stem cells is also very important to determine whether the stem cell differentiate and maintain current state. By introducing human stromal cells, or expressing human genes in mouse stromal cell, we will address the questions such as whether niche has species specificity and identify the key regulatory molecules in the niche.

This animal model will provide an excellent platform to further study some critical human diseases such as tumors and HIV infection. It will also be ideal for the study of tumor immunotherapy and HIV vaccination, which is solely dependent on an *in vivo* animal model.

192. NF- κ B role in the cellular UV response

Konstantin Taganov, David Baltimore

Ultraviolet (UV) irradiation of mammalian cells causes the activation of several transcription factors including NF- κ B and subsequent change in transcription of many genes, collectively called UV response. NF- κ B is a dimeric protein that is activated in response to proinflammatory stimuli, infections, and physical stress and plays an integral role in many important and diverse processes, including antiapoptotic response and tumorigenesis. In resting cells, NF- κ B is sequestered in the cytoplasm via association with inhibitory proteins called inhibitors of NF- κ B (I κ B). The I κ B kinase (IKK) complex-mediated phosphorylation of the I κ B N-terminus is an important regulatory step in ubiquitin-dependent

degradation of I κ B and activation of NF- κ B. Subsequently, NF- κ B migrates to the nucleus and acts as a sequence-specific, DNA binding transcription factor.

It was suggested that UV activates cell surface receptors, such as the epidermal growth factor and TNF receptors, in ligand-independent fashion to activate mitogen-activated protein kinases leading to early (30 min~6 hr) I κ B α degradation. Even though UV mimics the action of growth factors and cytokines, it appears that ligand-induced signals and those induced by UV are processed somewhat differently and lead to distinct reactions on the IKK and I κ B. The following observations were made for UV exposure: (i) no IKK activity was detected, but the zinc-finger domain of the IKK regulatory subunit, NEMO, is essential, unlike in case of TNF- or LPS-induced NF- κ B signaling; (ii) phosphorylation of I κ B at C-terminus by CK2 leading to NF- κ B activation is a distinctive feature of early UV-response; and (iii) lack of I κ B phosphorylation at N-terminus (serines 32 and 36). The latter observation is under debate possibly due to the differences in NF- κ B activation by UV between various cell types.

There have been only limited progress in unraveling the primary targets of UV absorption and the mechanisms of NF- κ B activation in response to UV irradiation is far from being well defined. With the increasing role of NF- κ B in cancer, it is important to understand the mechanisms of its activation to stimuli relevant to tumor progression. The main goal of this study is to advance our knowledge with regard to the NF- κ B role in the cell's UV response, and investigate the regulatory network of proteins upstream of I κ B in the UV-induced signal transduction pathway leading to activation of NF- κ B by constructing a random siRNA expression library.

Publications

- Antov, A., Yang, L., Vig, M., Baltimore, D. and Van Parijs, L. (2003) Essential role for STAT5 signaling in CD25+CD4+ regulatory T cell homeostasis and the maintenance of self-tolerance. *J. Immunol.* 171:3435-3441.
- Brown, E.J. and Baltimore, D. (2003) Essential and dispensable roles of ATR in cell cycle arrest and genome maintenance. *Genes Dev.* 17:615-628.
- Hoffmann, A., Leung, T.H. and Baltimore, D. (2003) Genetic analysis of NF-kappaB/Rel transcription factors defines functional specificities. *EMBO J.* 22:5530-5539.
- Klausner, R.D., Fauci, A.S., Corey, L., Nabel, G.J., Gayle, H., Berkley, S., Haynes, B.F., Baltimore, D., Collins, C., Douglas, R.G., et al. (2003) Medicine. The need for a global HIV vaccine enterprise. *Science* 300:2036-2039.
- Leung, T.H., Hoffmann, A. and Baltimore, D. (2004) One nucleotide in a kappaB site can determine cofactor specificity for NF-kappaB dimers. *Cell* 118:453-464.
- Meffert, M.K., Chang, J.M., Wiltgen, B.J., Fanselow, M.S. and Baltimore, D. (2003) NF-kappa B functions in

synaptic signaling and behavior. *Nat. Neurosci.* 6:1072-1078.

- Porteus, M.H. and Baltimore, D. (2003) Chimeric nucleases stimulate gene targeting in human cells. *Science* 300:763.
- Porteus, M.H., Cathomen, T., Weitzman, M.D. and Baltimore, D. (2003) Efficient gene targeting mediated by adeno-associated virus and DNA double-strand breaks. *Mol. Cell Biol.* 23:3558-3565.
- Qin, X.F., An, D.S., Chen, I.S. and Baltimore, D. (2003) Inhibiting HIV-1 infection in human T cells by lentiviral-mediated delivery of small interfering RNA against CCR5. *Proc. Natl. Acad. Sci. USA* 100:183-188.
- Schatz, D.G. and Baltimore, D. (2004) Uncovering the V(D)J recombinase. *Cell* 116:S103-106, 102 p following S106.
- Zarnegar, B., He, J.Q., Oganessian, G., Hoffmann, A., Baltimore, D. and Cheng, G. (2004) Unique CD40-mediated biological program in B cell activation requires both type 1 and type 2 NF-kappaB activation pathways. *Proc. Natl. Acad. Sci. USA* 101:8108-8113.

Max Delbrück Professor of Biology: Pamela J. Bjorkman

Research Fellows: Mindy Davis, Wanzhong He, Yongning He, Pingwei Li, Rich Olson, Elizabeth Sprague, Anthony West, Jr., Zhiru (Jenny) Yang

Graduate Students: Anthony Giannetti, Agnes Hamburger, Adrian Rice, Devin Tesar

Undergraduate Students: Edward Ballister, Evelyn Cheung, Robin Deis, Yan Qi

High School Students: Darcy Ballister

Research and Laboratory Staff: Silvia Delker, Valerie Karplus, Kathryn (Beth) Huey-Tubman, Lynda Llamas, Marta Murphy, Leonard Thomas, Noreen Tiangco

Support: The work described in the following research reports has been supported by:

American Liver Foundation

(Fellowship to Mindy Davis)

Burroughs Wellcome Fund Career Awards Program

(Fellowship to Anthony West, Jr.)

Cancer Research Institute Postdoctoral Fellowship

(Fellowship to Yongning He)

Cline Neuroscience Discovery Grant

(Grant to Anthony West, Jr.)

Department of Defense, Prostate Cancer Research

(Fellowship to Mindy Davis)

Leukemia and Lymphoma Society

(Fellowship to Elizabeth Sprague)

Technology Transfer Gates Grubstake Fund

Huntington's Disease Society of America

Howard Hughes Medical Institute

Max Planck Research Award for International Cooperation

NIH

Summary: My laboratory is interested in protein-protein interactions, particularly those mediating immune recognition. We use X-ray crystallography and biochemistry to study purified proteins (Figure 1), and are beginning to include confocal and electron microscopy to examine protein complexes in cells. Some of our work focuses upon homologs and mimics of class I MHC proteins. These proteins have similar three-dimensional structures, but different functions including immune functions (IgG transport by the neonatal Fc receptor, FcRn, and evasion of the immune response by viral MHC mimics), and non-immune functions (regulation of iron or lipid metabolism by HFE and ZAG). We are also comparing the structures and functions of host and viral Fc receptors with FcRn.

Transfer of maternal IgG molecules to the fetus or infant is a mechanism by which mammalian neonates acquire humoral immunity to antigens encountered by the mother. The protein responsible for the transfer of IgG is the MHC class I-related receptor FcRn. MHC class I molecules have no reported function as immunoglobulin receptors; instead they bind and present short peptides to T cells as part of immune surveillance to detect intracellular pathogens. We solved the crystal structures of rat FcRn both alone and complexed with Fc. Our crystallographic and biochemical studies suggest that FcRn dimerizes in response to IgG binding, which may serve as a component

of a signal to initiate internalization of FcRn/IgG complexes. We also hypothesize that formation of an oligomeric ribbon of FcRn dimers on adjacent membranes bridged by IgG molecules (Figure 2) is required for FcRn function. We are now interested in understanding the roles of the FcRn dimer and the oligomeric ribbon in IgG transport. We are in the process of characterizing oligomeric ribbon formation *in vitro* using biophysical assays, and have extended these studies to real-time confocal imaging of cells undergoing FcRn-mediated transcytosis of IgG. We are also doing structure/function studies of other Fc receptors that are not MHC homologs: gE/gI, a viral Fc receptor for IgG, FcαRI, a host receptor for IgA, and the polymeric immunoglobulin receptor (pIgR), a receptor that transports dimeric IgA and polymeric IgM into secretions.

HFE is a recently discovered class I MHC homolog that is involved in the regulation of iron metabolism, an unexpected function for an MHC-related protein. HFE was discovered when its gene was found to be mutated in patients with the iron overload disease hereditary hemochromatosis. HFE has been linked to iron metabolism with the demonstration that it binds to transferrin receptor, the receptor by which cells acquire iron-loaded transferrin. We solved crystal structures of HFE alone and HFE bound to transferrin receptor. The interaction of HFE with transferrin receptor is a fascinating system to study because we can use crystal structures to answer biochemical, functional, and evolutionary questions that address how binding of HFE interferes with transferrin binding, if conformational changes in the receptor are involved in the binding of either transferrin or HFE, which part of the MHC-like HFE structure binds transferrin receptor, and how the HFE interaction with the receptor compares with interactions of ligands with MHC and MHC-like (e.g., FcRn) proteins. We are expanding our studies to include cell biological investigations of HFE and transferrin receptor intracellular trafficking in transfected cell lines using confocal microscopy and other imaging techniques.

We are also interested in other MHC homologs, including proteins encoded by viruses. Both human and murine cytomegalovirus (HCMV, MCMV) express relatives of MHC class I heavy chains, probably as part of the viral defense mechanism against the mammalian immune system. Our biochemical studies show that the HCMV homolog associates with endogenous peptides resembling those that bind to class I MHC molecules. Our current efforts focus upon defining the structure and function of these homologs in order to understand why viruses make them and how they interfere with the host immune system.

Our structural work on class I MHC homologs has elucidated new and unexpected recognition properties of the MHC fold. For FcRn and HFE, the structural and biochemical studies have revealed a similar fold and some common properties, including the assumption that both receptors "lie down" parallel to the membrane when binding ligand, and a sharp pH-dependent affinity transition near neutral pH. In the case of FcRn, we have elucidated the structural basis of its pH dependent interaction with IgG and will now focus upon cell

biological studies of intracellular trafficking, for which the pH dependent interaction is critical. The pH dependence of the HFE-TfR interaction suggested to us that intracellular trafficking studies of HFE would be interesting, so much of our future efforts on both the FcRn and HFE systems will center around probing their function in a cellular context using imaging techniques. Our functional studies

of ZAG are at an earlier stage, since a receptor for ZAG has not been identified and the mechanism by which ZAG promotes lipid degradation is unknown. We are at an even earlier stage in our studies of the viral MHC homologs, in which our primary goal will be to solve crystal structures of a viral homolog alone and complexed with its cellular receptor.

Figure 1

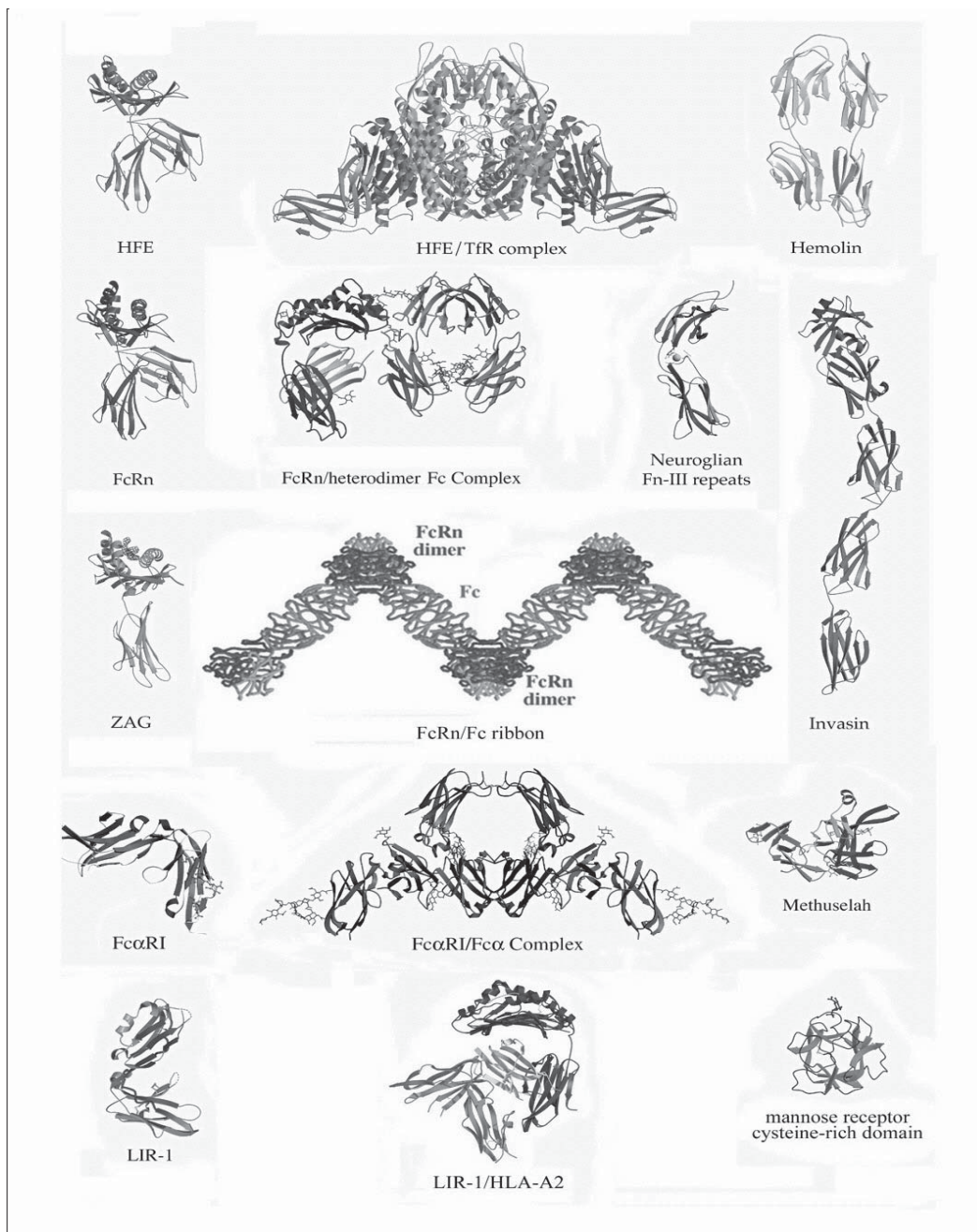
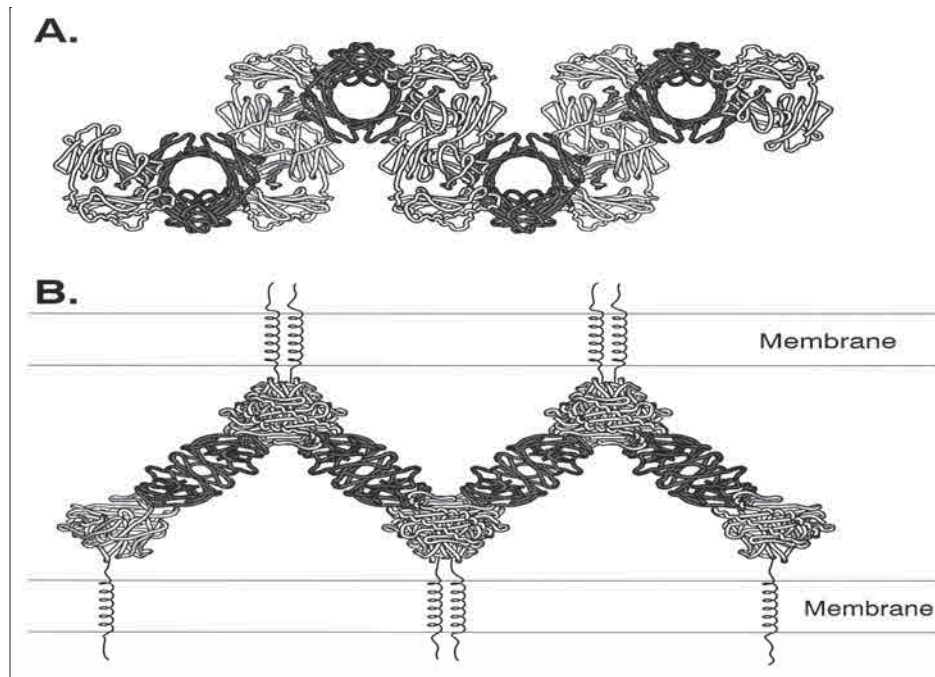


Figure 2



193. Characterization of FcRn-mediated transport pathways via confocal microscopy
Devin B. Tesar, Noreen Tiangco

Movement of specific protein molecules across epithelial cell barriers by their cognate receptors is achieved via a multivesicular transport pathway known as transcytosis. Discrete steps in the procession of a receptor-bound ligand through the transcytotic network are characterized by association with distinct subpopulations of endosomal compartments. These subpopulations of endosomes can be identified by confocal microscopy using fluorescent markers (such as transferrin) or antibodies against such markers (such as anti-Rab antibodies). We are currently working to decipher the transcytotic itinerary of FcRn in transfected MDCK cells, with or without its IgG ligand, by colocalizing FcRn and IgG with different endosomal markers. To achieve this, FcRn can be visualized by expressing a C-terminal GFP-fused form of FcRn, or by staining with an anti-FcRn monoclonal antibody that is directly conjugated to Alexa488. Rat IgG or Fc fragment can be directly labeled with fluorescent dyes (such as RITC or Cy3), and antibodies against specific endosomal markers can be viewed using secondary antibodies conjugated to a far-red dye (such as Cy5). This allows for three-color confocal analysis to determine the intracellular localization of FcRn, its ligand, and marker proteins for particular compartments at different stages within the transport process. These data can then be compared to the transport pathways of more well-characterized receptors such as the polymeric Ig receptor (pIgR) to evaluate which steps might be unique to, or particularly important during FcRn-mediated transport of IgG. Future work will focus on developing techniques for following trafficking events in live cells over the course of several minutes in real time.

194. Electron tomography of intracellular vesicles containing FcRn-IgG complexes in the small intestine of neonatal rats and in FcRn-expressing MDCK cells
Wanzhong He, Grant Jensen*, Devin B. Tesar, Noreen E. Tiangco

The neonatal Fc receptor (FcRn) transports maternal IgG across small intestinal epithelial cell barriers to provide passive immunity and serves as a protection receptor for IgG by rescuing endocytosed IgG from lysosomal degradation. In both its transport and protection roles, FcRn binds to IgG at acidic pH inside endosomes and releases IgG at the pH (7.4) of blood. Early conventional electron microscopy studies with immunoglobulin tracers provided direct evidence that the proximal small intestine of the neonatal rat selectively transports antibodies into the circulation [1]. The crystal structure of an FcRn-Fc complex revealed an oligomeric ribbon of FcRn dimers bridged by Fc molecules (Figure 2), which we propose forms inside an acidic transport vesicle. Oligomeric ribbon formation inside a vesicle is predicted to create a local region in which adjacent membranes are spaced ~200 Å apart; indeed, electron microscopy results indicated tubular vesicles are directly involved in the selective transcytosis of IgG [1]. In order to determine the configurations of FcRn-IgG complexes within different types of vesicles in an in vitro model system (FcRn-expressing MDCK cells) and in intact neonatal rat small intestines, we need a technique that will permit us to image dynamical vesicles with nanometer resolution. Electron tomography of high pressure frozen, freeze-substituted samples or frozen-hydrated thin section samples provides such a capability, and has been used to identify individual molecules at ~3 nm resolution within intact cells [2]. This technique

should allow us to derive a 3D map of transport vesicles within FcRn-expressing MDCK cells and intact small intestinal epithelial cells to ~3 nm resolution, which is sufficient for measuring the distance between adjacent membranes and possibly to identify FcRn-IgG complexes within the vesicles. We will use immunoglobulin tracers (e.g., ferritin-conjugated IgG or monofunctional nanogold-labeled Fc fragments) internalized after incubation of live cells at pH 6 to identify compartments containing FcRn-Fc complexes, then use unlabeled IgG (or unlabeled IgG mixed with a few tracers or gold markers) to determine the configurations of FcRn-IgG complexes within the vesicles and analyze dynamical events during transcytosis.

*Assistant Professor of Biology, Caltech

References

- [1] Rodewald, R. (1973) *J. Cell Biol.* 58:189-211.
 [2] He, W., Cowin, P. and Stokes, D.L. (2003) *Science* 302(5462):109-113.

195. Assay for ligand-induced dimerization of FcRn

Devin B. Tesar, Mary Dickinson*

The 6.0 Å crystal structure of FcRn complexed with wild-type Fc demonstrates the formation of an oligomeric array of FcRn dimers bridged by Fc ligands. This "oligomeric ribbon" may have functional implications in living cells. First, transport vesicles containing the oligomeric ribbon would have their opposing membrane faces brought into close (~200 Å) proximity of one another. In addition, ribbon formation would induce an ordered linear arrangement of FcRn cytoplasmic tails. The cytosolic trafficking machinery may use one or both of these features as a means of distinguishing between vesicles that contain FcRn-IgG complexes and those that contain FcRn alone or unbound IgG. Oligomeric ribbon formation would require the simultaneous occurrence of two phenomena: 1) FcRn dimerization; and 2) bridging of FcRn molecules on opposing membrane faces by Fc ligands. To test for dimerization of FcRn, either in the presence or absence of ligand, we have devised an *in vivo* assay using fluorescence resonance energy transfer (FRET). We have created chimeric FcRn molecules that either enhanced cyan fluorescent protein (ECFP) or enhanced yellow fluorescent protein (EYFP) fused that C-terminus of the cytoplasmic tail. In collaboration with Mary Dickinson and Scott Fraser at the Caltech Beckman Imaging Center, we are using laser scanning confocal microscopy in conjunction with a Zeiss LSM Meta system, capable of deconvoluting the CFP and YFP spectra, to detect energy transfer from FcRn-CFP to FcRn-YFP in stably transfected Madin Darby canine kidney (MDCK) cells, both in the presence and absence of IgG. These results will be compared to FRET measurements of engineered FcRnCFP/YFP molecules containing putative dimer-disrupting mutations. We are also testing for FRET in HLA-DR, an MHC class II molecule and an obligate heterodimer as a positive control, and, as a negative control, between FcRn-CFP and HFE-YFP. HFE is another MHC class I homolog that does not bind to IgG or interact with FcRn.

*Biological Imaging Center, Caltech

196. Three-dimensional EM studies of IgG transport and cell adhesion

Yongning He

FcRn is a cell surface receptor responsible for passive acquisition of humoral immunity in the vertebrate newborn. It also regulates IgG half-life in serum and IgG transport in different tissues. The physiological roles of FcRn rely on its pH-dependent binding interaction with IgG and its transport activity after ligand binding. Structural details concerning the mechanism of FcRn-mediated transport of IgG is relevant to therapeutic efforts to use antibodies to combat cancer and other diseases. However, serum proteins are normally taken up by vascular endothelial cells and degraded by lysosomes through a default degradation pathway, which shortens their half-lives in the blood. As the IgG protection receptor, FcRn binds IgG in acidic endosomes and escorts them back to the cell surface for the bloodstream re-entering, thereby significantly increasing its serum half-life. In our studies, FcRn molecules have been incorporated onto the surface of liposomes or lipid tubes to mimic FcRn transcytotic vesicles, then cryoEM tomography is applied to build a three-dimensional model of FcRn-IgG structure inside the vesicles. Successful completion of these studies will improve the current understanding of the IgG transport mechanism. In parallel with the FcRn studies, a similar liposome-based three-dimensional tomography study of cell adhesion molecule L1 has been performed. The homophilic adhesion activity of L1 is involved in neural and tumor cell migration and plays an important role in tumor invasion. Our current studies show that the L1-incorporated liposomes can form aggregates due to the homophilic binding activity of L1, which simulates L1-mediated cell-cell adhesion *in vivo*. Three-dimensional tomography studies will provide structural details about the mechanism of L1 homophilic recognition, hence providing valuable information for the detection and prevention of tumor migration and invasion.

197. Characterization of the chicken yolk sac IgY receptor

Anthony P. West, Jr., Andrew Herr*

In mammals, IgG is transferred from mother to young by the MHC-related receptor FcRn, which binds IgG in acidic endosomes and releases it at basic pH into blood. Maternal IgY, the avian counterpart of IgG, is transferred to embryos across yolk sac membranes. We affinity-purified the chicken yolk sac IgY receptor (FcRY) and sequenced its gene. FcRY is unrelated to MHC molecules but is a homolog of the mammalian phospholipase A₂ receptor. Analytical ultracentrifugation and truncation experiments suggest that FcRY forms a compact structure containing an IgY binding site at acidic pH, but undergoes a conformational change at basic pH that disrupts the site. FcRY is thus unrelated to mammalian FcRn in both its structure and mechanism for pH-dependent binding, illustrating distinct routes utilized by evolution to transfer antibodies.

*Present address: University of Cincinnati

198. Crystal structure of a dimeric IgA-binding fragment of the human polymeric immunoglobulin receptor

Agnes E. Hamburger, Anthony. P. West, Jr.

The polymeric immunoglobulin receptor (pIgR) is a type I transmembrane protein that delivers dimeric IgA (dIgA) and pentameric IgM to external secretions. We have solved a 1.9 Å resolution X-ray crystal structure of the N-terminal domain of human pIgR, which binds dIgA in the absence of other pIgR domains with an equilibrium dissociation constant of 300 nM. The structure of pIgR domain 1 reveals a folding topology similar to immunoglobulin variable domains, but with differences in the counterparts of the complementarity determining regions (CDRs), including a helical turn in CDR1 and a CDR3 loop that points away from the other CDRs. The unusual CDR3 loop position prevents dimerization analogous to the pairing of antibody variable heavy and variable light domains. The pIgR domain 1 structure allows interpretation of previous mutagenesis results and a structure-based comparison between pIgR and other IgA receptors.

199. Structural studies of a herpes simplex virus immunoglobulin G receptor

Elizabeth R. Sprague, W. Lance Martin¹, Robin Deis²

Herpes simplex virus type 1 (HSV-1) encodes two glycoproteins, gE and gI, which form a heterodimer on the surface of virions and infected cells. The gE-gI heterodimer has been implicated in cell-to-cell spread of virus and is a receptor for the Fc fragment of Immunoglobulin G (IgG). Previous studies localized the gE-gI binding site on human IgG to a region near the interface between the C_H2 and C_H3 domains of Fc, which also serves as the binding site for bacterial and mammalian Fc receptors. Although there are two potential gE-gI binding sites per Fc homodimer, only one gE-gI heterodimer binds per IgG in gel filtration experiments. Here we report production of recombinant human Fc molecules that contain zero, one, or two potential gE-gI binding sites and use them in analytical ultracentrifugation experiments to show that two gE-gI heterodimers can bind to each Fc. Further characterization of the gE-gI interaction with Fc reveals a sharp pH dependence of binding, with K_D values of ~340 nM and ~930 nM for the first and second binding events, respectively, at the slightly basic pH of the cell surface (pH 7.4), but undetectable binding at pH 6.0. This strongly pH-dependent interaction suggests a physiological role for gE-gI dissociation from IgG within acidic intracellular compartments, consistent with a mechanism whereby HSV promotes intracellular degradation of anti-viral antibodies.

¹Current address: Stanford University

²Caltech undergraduate student

200. Structural studies of a pheromone receptor-associated MHC class Ib molecule

Rich Olson, Kathryn Huey-Tubman

Most non-primate mammals possess a secondary olfactory system attuned to chemical signals (pheromones) secreted by conspecifics. These olfactory cues elicit a

range of reproductive and behavioral responses including synchronization of oestrus, aggression, and sex identification. Pheromones are detected by specialized G protein-coupled receptors in the vomeronasal organ (VNO), which resides at the base of the nasal cavity. The M10 family of MHC class Ib molecules has been localized exclusively to the VNO and shown to specifically interact with pheromone receptors.^{1,2} This contrasts with the typical function of class Ib proteins—the display of antigens to receptors on the surface of T cells.

We are interested in comparing the structural and functional characteristics of M10 proteins with their classical MHC Ib counterparts. Additionally, we would like to understand the role of the M10/pheromone receptor interaction in VNO function. To start, we expressed and purified a soluble construct of M10.5 using baculovirus-infected insect cells. This material exhibits a thermal denaturation profile similar to empty MHC class I molecules implying that M10.5 binds a small ligand not present during expression and purification, or, alternatively, binding to the pheromone receptor stabilizes an empty M10.5 conformation. We next crystallized and solved the structure of M10.5 confirming an open and empty peptide-binding groove, the first example of an empty class I MHC structure. We are currently working to express fragments of pheromone receptors in order to study the interaction between M10s and their cognate receptors and to look for small molecules that bind to both partners.

References

1. Ishii, T., Hirota, J. and Mombaerts, P. (2003) *Curr. Biol.* 13(5):394-400.
2. Loconto, J. et al. (2003) *Cell* 112(5):607-618.

201. Structural and functional studies of MHC class I homologs in HCMV

Zhiru (Jenny) Yang, Yan Qi

HCMV affects 70-90% of all human populations and can be life threatening to immunocompromised individuals, such as cancer, transplant, and AIDS patients. HCMV achieves its lifelong infection in host cells by adopting multiple mechanisms to evade the primed immune system, including down-regulation of host class I MHC molecules. HCMV encodes two MHC class I homologs, UL18 and UL142, which may be components of a strategy to avoid immune detection of class I MHC negative cells. UL18 is heavily glycosylated (13 potential N-linked glycosylation sites) and able to bind host-derived β2-microglobulin (the class I MHC light chain) and endogenous peptides. The host cell receptor for UL18 is LIR-1, which is most abundant in B cells, monocytes, macrophages, and dendritic cells. The UL18/LIR-1 interaction is likely to contribute to the latency and persistence of HCMV, as well as the viral evasion of host NK cell surveillance. In addition to UL18, LIR-1 also binds a broad range of host MHC class I molecules, but with an affinity that is over 1000-fold reduced compared to its affinity for UL18.¹ The structures of LIR-1 and a LIR-1/HLA-A2 complex have recently been solved in our lab.^{2,3} We are now working on the co-crystallization and structure determination of UL18 bound to LIR-1. We are also generating deglycosylated mutants of UL18 for our

crystallization trials. These studies will be extended to include a newly identified HCMV class I MHC homolog, UL142, which is present in clinical HCMV strains such as Toledo.⁴ UL142 shares about 20% amino acid sequence identity with MHC class I molecules. It could play a role in the virulence of the wild-type HCMV. Immunological, biochemical and structural studies are underway to characterize this protein. Altogether, our work on UL18 and UL142 will expand our basic understanding of the MHC class I homologs and the virus-host interaction.

[†]Undergraduate student, Caltech

References

1. Chapman, T.L., Heikema, A.P. and Bjorkman, P.J. (1999) *Immunity* 11:603-613.
2. Chapman, T.L., Heikema, A.P., West, Jr., A.P. and Bjorkman, P.J. (2000) *Immunity* 13:727-736.
3. Willcox, B.E., Thomas, L.M. and Bjorkman, P.J. (2003) *Nature Immunol.* 4:913-919.
4. Davidson, A.J. et al. (2003) *J. Gen. Virol.* 84:17-28.

202. Crystallographic studies of the complexes of murine immunoreceptor NKG2D and its ligands RAE-1 β and H60

Pingwei Li

NKG2D is an activating immunoreceptor widely expressed on NK cells, CD8⁺ T cells, $\gamma\delta$ T cells and NKT cells, which mediates immunity against tumor and microbial pathogens. The ligands for murine NKG2D include three families of MHC class I-related proteins: RAE-1, H60 and MULT1. Expression of NKG2D ligands is induced by transformation and by viral or microbial infections. NKG2D interacts with all the three families of ligands with nanomolar binding affinities. In order to understand the molecular details of the interactions of the NKG2D with these different ligands, we have crystallized complexes of mouse NKG2D with RAE-1 β and with H60.

The extracellular domains of mouse NKG2D, RAE-1 β and H60 were expressed in bacteria as inclusion bodies, refolded, and purified to homogeneity. Complexes of NKG2D with RAE-1 β or H60 were purified by gel filtration chromatography. The RAE1 β / NKG2D complex crystallizes in space group P6₁ with unit cell dimensions of a=b=58.64 Å, c=350.33 Å. There is one complex and one free RAE-1 β in the crystallographic asymmetric unit. The structure of the crystal was determined by molecular replacement and refined to a resolution of 1.95 Å. The high resolution structure allows a detailed analysis of the molecular interactions between the receptor and ligand. The H60/NKG2D complex crystallizes in space group P6₂2 with unit cell parameters of a=b=162.30 Å, c=330.64 Å. Native data to the resolution of 2.85 Å were collected and a crystallographic analysis of this complex is underway.

203. Crystallographic studies of ligand binding by Zn- α 2-glycoprotein

Silvia L. Delker¹, Anthony P. West, Jr., Lindsay McDermott², Malcolm W. Kennedy²

Zn- α 2-glycoprotein (ZAG) is a 41 kDa soluble protein that is present in most bodily fluids. The previously reported 2.8 Å crystal structure of ZAG isolated

from human serum demonstrated the structural similarity between ZAG and class I major histocompatibility complex (MHC) molecules and revealed a non-peptidic ligand in the ZAG counterpart of the MHC peptide-binding groove. We have performed additional crystallographic studies to explore the nature of the non-peptidic ligand in the ZAG groove. Comparison of the structures of several forms of recombinant ZAG, including a 1.95 Å structure derived from ZAG expressed in insect cells, suggests that the non-peptidic ligand in the current structures and in the structure of serum ZAG is a polyethylene glycol (PEG), which is present in the crystallization conditions used. Further support for PEG binding in the ZAG groove is provided by the finding that PEG displaces a fluorophore-tagged fatty acid from the ZAG binding site. From these results we hypothesize that our purified forms of ZAG do not contain a bound endogenous ligand, but that the ZAG groove is capable of binding hydrophobic molecules, which may relate to its function.

¹Present address: Department of Molecular Biology and Biochemistry, University of California, Irvine

²Division of Environmental and Evolutionary Biology, Institute of Biomedical and Life Sciences, University of Glasgow

204. HFE and transferrin directly compete for transferrin receptor in solution and at the cell surface

Anthony M. Giannetti

Transferrin receptor (TfR) is a dimeric cell surface protein that binds both the serum iron-transport protein transferrin (Fe-Tf) and HFE, the protein mutated in patients with the iron overload disorder hereditary hemochromatosis. HFE and Fe-Tf can bind simultaneously to TfR to form a ternary complex, but HFE binding to TfR lowers the apparent affinity of the Fe-Tf/TfR interaction. This apparent affinity reduction could result from direct competition between HFE and Fe-Tf for their overlapping binding sites on each TfR polypeptide chain, from negative cooperativity, or a combination of both. To explore the mechanism of the affinity reduction, we constructed a heterodimeric TfR (hdTfR) that contains mutations such that one TfR chain binds only HFE and the other binds only Fe-Tf. Binding studies using hdTfR demonstrate that TfR does not exhibit cooperativity in heterotropic ligand binding, suggesting that some or all of HFE's effects on iron homeostasis result from competition with Fe-Tf for TfR binding. Experiments using transfected cell lines demonstrate a physiological role for this competition in altering HFE trafficking patterns.

205. A hydrophobic patch on transferrin receptor regulates the iron-release properties of receptor-bound transferrin

Anthony M. Giannetti, Peter J. Halbrooks*, Anne B. Mason*

The transferrin receptor (TfR), a dimeric membrane glycoprotein, is responsible for iron uptake in most mammalian cells. At the basic pH of blood (pH 7.4), TfR binds iron-loaded transferrin (Fe-Tf) in serum,

and transports it to acidic recycling endosomes where iron is released from Fe-Tf in a TfR-facilitated process. Iron-free transferrin (apo-Tf) remains bound to TfR and is recycled to the cell surface, where apo-Tf rapidly dissociates from TfR upon exposure to the basic pH of blood. We previously demonstrated that substitution of either Trp 641 or Phe 760 in the TfR helical domain reduces TfR's binding to apo-Tf but not to Fe-Tf. Studies with a double mutant of TfR, W641A/F760A, substantiate the earlier finding by demonstrating a 300-fold weaker affinity for apo-Tf relative to wild-type TfR. To evaluate the effects of the mutations on TfR-facilitated iron release from Fe-Tf, we measured release rates at acidic pH from a monoferric form of Tf (Fe_c-Tf) alone and when bound to wild-type TfR or W641A/F760A. We find that iron release from Fe_c-Tf is 200-fold slower when it is bound to the mutant TfR than when bound to wild-type TfR. Whereas binding of Fe_c-Tf to the wild-type TfR accelerates iron release rate by 100-fold compared to free Fe_c-Tf, binding to the mutant TfR slows the iron release rate by two-fold as compared free Fe_c-Tf. These findings demonstrate that the conserved hydrophobic patch on TfR that includes W641 and F760 is required for the receptor-mediated stimulation of iron release from the C-lobe of Tf at low pH. From these data we describe a sequence of intermediate states along the pathway leading to receptor-mediated iron release.

*Department of Biochemistry, University of Vermont

206. Structural and biophysical studies of transferrin receptor 2

Valerie J. Karplus, Mindy I. Davis, Caroline A. Enns*

Transferrin receptor 2 (TfR2) is a type II membrane glycoprotein that is expressed predominantly on the surface of hepatocytes. The function of TfR2 is unknown, but the extracellular domain of human TfR2 has 45% amino acid identity to transferrin receptor 1 (TfR1), which serves as the receptor for iron-loaded transferrin (Fe-Tf). Previous surface plasmon resonance (SPR) experiments showed that TfR1 binds both Fe-Tf and the hemochromatosis protein (HFE) at the pH of the cell surface (pH=7.4). The Fe-Tf/TfR1 complex is endocytosed into acidic endosomes, where iron is released from Tf and stored in the cytoplasm in the iron storage protein ferritin. The iron-free version of Tf (apo-Tf) bound to TfR1 recycles back to the cell surface, where apo-Tf is released upon contact with the slightly basic pH of the blood. Like TfR1, TfR2 binds Fe-Tf at pH 7.4, but unlike TfR1, TfR2 does not bind HFE at basic pH. Mutations in TfR2 or HFE lead to hereditary hemochromatosis, a disease of iron overload, and thus, understanding the role of TfR2 in iron homeostasis is important. Our goal is to conduct further SPR assays to characterize binding of apo-Tf to TfR2 and to determine the crystal structure of TfR2 and TfR2 bound to Tf. We have obtained a relatively stable form of the protein's extracellular region, which we have used in preliminary SPR studies and crystallization experiments.

*Oregon Health Sciences University

207. Structural studies of prostate-specific membrane antigen

Mindy I. Davis, Melanie J. Bennett, Leonard Thomas

Prostate-specific membrane antigen (PSMA) is a 84 kDa type II transmembrane protein with carboxypeptidase activity that is expressed predominantly on the surfaces of prostate epithelial cells. PSMA hydrolyzes folate, releasing the terminal glutamate, and PSMA expressed in the brain hydrolyzes the abundant neuropeptide N-acetyl-aspartyl-glutamate, releasing glutamate as a neurotransmitter. Prostate-specific membrane antigen (PSMA) is currently used for imaging the extent of prostate cancer, and many researchers are studying PSMA for development of prostate cancer imaging agents to the extracellular region of PSMA (sPSMA).

PSMA shares ~30% amino acid sequence identity with the transferrin receptor (TfR), which binds iron-loaded transferrin and is involved in iron homeostasis. TfR contains a peptidase domain that lacks several key zinc binding ligands seen in aminopeptidases and does not bind Zn to form an active peptidase. In contrast, PSMA does not bind transferrin (as determined by surface plasmon resonance assays) and contains an active zinc peptidase domain. Our goal is to characterize the structure and function of sPSMA in order to facilitate therapeutic intervention against prostate cancer. sPSMA elutes from a size exclusion chromatography column slightly after a TfR dimer despite its higher dimeric molecular weight. Analytical ultracentrifugation was used to show that sPSMA is a compact dimer. Crystals of sPSMA expressed in baculovirus-infected insect cells were obtained last year and the structure was solved to 3.5 Å resolution by molecular replacement. Current efforts have been directed towards refinement of the model and making additional constructs to try to obtain crystals that diffract to higher resolution. In addition to the prostate cancer applications, the structure of sPSMA will provide an interesting comparison to that of TfR.

208. Biochemical and structural studies of ferroportin

Adrian E. Rice, Douglas C. Rees*

All known organisms, save two bacteria, require iron for survival. Despite its importance, iron in overabundance is toxic. In order to maintain a balance of iron levels, organisms have developed a highly specialized network of molecules designed to monitor and maintain iron homeostasis. When the fidelity of these networks is compromised, diseases such as iron deficiency and iron overload result. Mammals lack any regulated mode of iron excretion and therefore, must have highly-regulated mechanisms for controlling the acquisition of iron from the diet. The primary site of iron absorption is the duodenum of the small intestine. This process can be categorized by two phases: 1) iron uptake across the brush border into the cytoplasm of duodenal enterocytes; and 2) iron export across the basolateral membrane of these cells into the blood. Iron from the diet is reduced from Fe³⁺ to Fe²⁺ by the membrane-bound iron reductase Dcytb and is transported across the apical brush border by an integral

membrane protein called divalent metal transporter 1 (DMT1; also known as DCT1 and NRAMP2). Iron is then transported across the cell to the basolateral side where it is exported by the basolateral integral membrane iron transporter ferroportin (Fpn; also known as IREG1 and MTP1). Fpn is the only identified iron exporter in vertebrates and is an integral membrane protein containing 9-12 predicted α -helical transmembrane segments. Point mutations in Fpn lead to an autosomal dominant iron overload disease called ferroportin disease. My project aims to characterize Fpn from both a structural and biochemical standpoint. Current plans in our laboratory aim at obtaining purified recombinant Fpn for these studies.

[†]Division of Chemistry and Chemical Engineering, Caltech

209. Crystal structure of a secreted insect ferritin reveals a symmetrical arrangement of heavy and light chains

Agnes E. Hamburger, Anthony P. West, Jr.

Ferritins are iron storage proteins made of 24 subunits forming a hollow spherical shell with 432 (octahedral) symmetry. Vertebrate ferritins consist of a mixture of heavy and light chains, with the ratio of the two chains varying in different tissues. We have determined the 1.9 Å crystal structure of secreted insect ferritin from the cabbage looper/tiger moth, *Trichoplusia ni*, which reveals equal numbers of heavy and light chains arranged with 32 (tetrahedral) symmetry. The heavy chain/light chain interface has complementary features responsible for ordered assembly of the subunits, and analysis of other insect ferritin sequences suggests that 32 symmetry ferritin may be common among insects. The heavy chain contains a ferroxidase active site resembling that of vertebrate heavy chains. Each heavy chain ferroxidase site also contains a single endogenous, bound iron atom. The light chain lacks the residues that form a putative iron core nucleation site in vertebrate light chains. Instead, a possible nucleation site is observed on the inside of the light chain 3-fold pore. The structure also reveals inter- and intra-subunit disulfide bonds, most of which occur in the extended N-terminal domains unique to insect ferritins. The symmetrical arrangement of heavy and light chains and the disulfide crosslinks may reflect adaptation of insect ferritin to its role as a secreted protein.

210. Conformational studies of Huntingtin Exon 1 by fluorescence energy transfer

Kathryn Huey-Tubman, Jennifer Lee*, Jay Winkler*, Harry B. Gray*

The pathogenic mechanism in Huntington's and related neurological diseases is proposed to involve a conformational transition in expanded poly-glutamine (poly-Gln) tracts (>36 Gln). We have shown that soluble huntingtin Exon 1 fusion proteins with 16 to 46 glutamines have random coil conformations with no evidence for a global conformational change above 36 glutamines. In combination with antibody binding data, our results support a "linear lattice" model for poly-Gln, providing a new structural paradigm with implications for disease origin and drug design.¹ To test the linear lattice

model and derive information about the structure of HD Exon 1, we will use fluorescence energy transfer (FET) to examine the conformation of the HD Exon 1 proteins. For the first FET experiments, we will measure the lengths of different poly-Gln tracts by inserting donor and acceptor probes immediately before and after the glutamines. The donor and acceptor molecules should be relatively small and hydrophilic so as not to interfere with protein structure and dynamics or disrupt the amyloidogenic properties of the poly-Gln tract. We have chosen single-ring aromatic groups, N-methyl-2-aminobenzoic acid (Abz) and 3-nitrotyrosine (Y(NO₂)), as donor and acceptor. This pair has a critical Förster distance (r_0) of 31 Å allowing for characterization of distances $10 < r < 45$ Å. The Abz donor group will be attached to a cysteine introduced into HD Exon 1, and an introduced tyrosine will be nitrated by treatment with tetranitromethane to make the acceptor. Since there is no commercially available Abz probe to react with cysteine residues, Jennifer Lee has synthesized a derivative of Abz, N-methyl-2-aminobenzoate (also known as SHARK) for cysteine-selective labeling. Mutant HD Exon 1 proteins have been constructed by site-directed mutagenesis to substitute Phe 17 (the residue immediately preceding the poly-Gln tract) for tyrosine and to insert a cysteine immediately following the poly-Gln tract. Although thioredoxin itself contains two tyrosines, only one (Tyr 70) is somewhat surface exposed, as we have shown by limited nitration with the TRX-tag control protein. Using site-directed mutagenesis, we can change the positions of the donor and acceptor probes to measure distances as a function of increasing numbers of glutamines. From the resulting information, we can map the approximate conformation of the poly-Gln tract in solution and ascertain if there is a global conformational change when the number of glutamines is increased above the pathological threshold.

[†]Division of Chemistry and Chemical Engineering, Caltech

Reference

1. Bennett, M.J., Huey-Tubman, K.E., Herr, A.B., West, Jr., A.P., Ross, S.A. and Bjorkman, P.J. (2002) Proc. Natl. Acad. Sci. USA 99:11634-11639.

211. Structural and binding studies of anti-poly-Gln scFvs bound to Huntingtin Exon 1

Pingwei Li, Kathryn Huey-Tubman

The pathogenic mechanism in Huntington's and related neurological diseases is proposed to involve a conformational transition in expanded poly-glutamine (poly-Gln) tracts (>36 Gln). Soluble expanded poly-glutamine represents an intermediate state that can be targeted by therapeutics, thus we devised a method to express normal and expanded poly-glutamine in the context of huntingtin Exon 1, a portion of the Huntington disease protein sufficient to induce disease in animals. Although the pathogenic mechanism in Huntington's disease was assumed to involve a conformational transition in poly-glutamine tracts with >36 glutamines, we showed that huntingtin Exon 1 proteins with 16-46 glutamines have random-coil conformations with no evidence for a global conformational change above 36 glutamines.¹ In

combination with antibody-binding data, our results support a "linear lattice" model for poly-glutamine, in which expanded tracts have more ligand-binding sites than normal poly-glutamine. Our results predict that multivalent compounds will bind with high avidity and specificity to expanded, but not normal, poly-glutamine tracts. To test this prediction and derive potential therapeutic compounds, we have expressed monomeric and multimeric versions of the poly-Gln specific antibody MW1,² which was produced in the Patterson laboratory at Caltech. Preliminary results indicate that the multivalent forms of MW1, which are made as single chain antibody variable regions (scFvs), bind with higher apparent affinity than the monovalent version. Future plans involve solving crystal structures of poly-Gln containing polypeptides complexed with anti-poly-Gln scFvs (binding to the scFvs should stabilize the poly-Gln tract into an ordered conformation that might be crystallizable), and testing the ability of anti-poly-Gln scFvs to disrupt poly-Gln containing aggregates in transfected cells.

References

- Bennett, M.J., Huey-Tubman, K.E., Herr, A.B., West, Jr., A.P., Ross, S.A. and Bjorkman, P.J. (2002) Proc. Natl. Acad. Sci. USA 99:11634-11639.
 - Ko, J., Ou, S. and Patterson, P.H. (2001) Brain Res. Bull. 56:319-329.
- #### Publications
- Delker, S.L., West, Jr., A.P., McDermott, L., Kennedy, M.W. and Bjorkman, P.J. (2004) Crystallographic studies of ligand binding by Zn- α 2-glycoprotein. *J. Struct. Biol.* In press.
- Giannetti, A.M. and Bjorkman, P.J. (2004) HFE and transferrin directly compete for transferrin receptor in solution and at the cell surface. *J. Biol. Chem.* 279:25866-25875.
- Giannetti, A.M., Snow, P.M., Zak, O. and Bjorkman, P.J. (2003) Mechanism for multiple ligand recognition by the human transferrin receptor. *Public Library of Science (PloS)* 1:341-350.
- Hamburger, A.E., West, Jr., A.P. and Bjorkman P.J. (2004) Crystal structure of a dimeric IgA-binding fragment of the human polymeric immunoglobulin receptor. Manuscript in preparation.
- Hamburger, A.E., West, Jr., A.P. and Bjorkman P.J. (2004) Crystal structure of a secreted insect ferritin reveals a symmetrical arrangement of heavy and light chains. Manuscript in preparation.
- Herr, A.B., Ballister, E.R. and Bjorkman, P.J. (2003) Insights into IgA-mediated immune responses from the crystal structures of human Fc α RI and its complex with IgA1-Fc. *Nature* 423:614-620.
- Herr, A.H., White, C.L., Milburn, C., Wu, C. and Bjorkman, P.J. (2003) Bivalent binding of IgA1 to Fc α RI suggests a mechanism for cytokine activation of IgA phagocytosis. *J. Mol. Biol.* 327:645-657.
- Sprague, E.R., Martin, W.L. and Bjorkman, P.J. (2004) pH dependence and stoichiometry of binding to the Fc region of IgG by the herpes simplex virus Fc receptor gE-gI. *J. Biol. Chem.* 279:14184-14193.
- Vogt, T.M., Blackwell, A.D., Giannetti, A.M., West, Jr., A.P., Bjorkman, P.J. and Enns, C.A. (2003) Heterotypic interactions between TfR2 and TfR. *Blood* 101:2008-2014.
- West, Jr., A.P., Herr, A.B. and Bjorkman, P.J. (2004) The chicken yolk sac IgY receptor, a functional equivalent of the mammalian MHC-related Fc receptor, is a phospholipase A₂ receptor homolog. *Immunity* 20:601-610.
- Willcox, B.E., Thomas, L.E. and Bjorkman, P.J. (2003) Crystal structure of HLA-A2 Bound to LIR-1, a host and viral MHC receptor. *Nature Immunol.* 4:913-919.

Professor Emeritus: Charles J. Brokaw

Summary: Motor enzymes -- dyneins, kinesins, and myosins -- convert energy from ATP dephosphorylation into most of the movements performed by eukaryotic cells. We think that myosin and kinesin are reasonably well understood, although new experimental results from time to time surprise us. On the other hand, we have very little knowledge or understanding of the functioning of the axonemal dyneins that power the movements of flagella and cilia; these molecular complexes are a major challenge for the future. My current work uses computer simulation methods to explore ideas about motor enzyme function in situations ranging from experimental studies on individual motors to an intact flagellum containing tens of thousands of dyneins. Most of the simulation programs, as Macintosh applications, are available at www.cco.caltech.edu/~brokaw/software.html

212. Symmetry breaking in models of nodal cilia
Charles J. Brokaw

Our investigations of models of flagellar movement using computer simulations have primarily examined "curvature controlled" models, in which oscillation results from switching off dyneins when the curvature that they produce exceeds a preset limit. Although these models have been in existence for more than 30 years, no strong experimental evidence for control of dynein activity by curvature has appeared. Instead, oscillatory sliding in the absence of bending has been demonstrated in several experimental situations. Curvature controlled models are unable to simulate the oscillation of very short flagella, such as those produced by breaking sea urchin sperm flagella, or the cilia known as nodal cilia.

Nodal cilia are very short ($\leq 2 \mu\text{m}$) cilia found in the embryonic node on the ventral surface of early mammalian embryos. They create a right to left fluid flow that is responsible for determining the normal asymmetry of the internal organs of the mammalian body. To do this, they must consistently gyrate in a counterclockwise sense.

Development of computer programming that extends modeling of flagellar movement from two dimensions to three dimensions allows examination of three-dimensional movements such as those of nodal cilia. Planar oscillations and three-dimensional gyrations can be achieved with velocity controlled models, in which dynein activity is regulated by sliding velocity instead of by curvature. In these models, when a subset of axonemal dyneins is producing sliding in one direction, these dyneins remain on, and the antagonistic dyneins remain off, as long as the sliding velocity remains above a critical value. If this sliding is opposed by an elastic resistance, such as the bending resistance of axonemal microtubules, the sliding will eventually slow down and fall below the critical control value. The active dyneins will turn off, elastic forces will reverse the direction of sliding, and sliding in this new direction will activate the antagonistic set of dyneins. Our computer simulations show that this control

paradigm will work to generate either two- or three-dimensional oscillatory bending in short cilia.

When dyneins on one outer doublet are controlled by the sliding velocity experienced by that doublets, the system is symmetric, and the three-dimensional models can show either clockwise or counterclockwise gyration. To break this symmetry, consistent counterclockwise gyration can be achieved if the dyneins on doublet N are regulated by a mixture of the sliding velocities experienced by doublet N and N+1 (numbered in a clockwise direction, looking from the base). The challenge now is to find a realistic mechanism for achieving something like this control by an adjacent doublet.

Professor: Judith L. Campbell
 Member of the Professional Staff: Elizabeth Bertani,
 Martin Budd, Piotr Polaczek
 Research Fellows: Susanna Boronat, Shane Edwards,
 Caroline Li, Tao Wei
 Graduate Students: Isabelle Lesur, Lilyn Liu, Clara Reis

Support: The work described in the following research reports has been supported by:

Burroughs Wellcome
 Margaret Early
 NIH
 NSF
 Research Management Corporation
 TRDRP

Summary: A hallmark of cancer cells, in addition to uncontrolled proliferation, is genomic instability, which appears in the form of chromosome loss or gain, gross chromosomal rearrangements, deletions, or amplifications. The mechanisms that suppress such instability are of the utmost interest in understanding the pathogenesis of cancer. Our lab studies the components of the DNA replication apparatus that promote genomic stability, primarily using yeast genetics, biochemistry, and functional genomics.

Several years ago, Rajiv Dua in the laboratory discovered that DNA polymerase ϵ , one of four essential DNA polymerases in yeast, had not one, but two essential functions. Deletion of the polymerase domain left the cells viable because another polymerase activity could substitute. Conversely, deletion of the remaining, non-catalytic half of the protein was lethal. Shaune Edwards in the laboratory carried out a two-hybrid screen for proteins that interact with the enigmatic C-terminal region of pol ϵ in order to discover its function. She found that pol ϵ interacts with Trf5, a protein involved in establishing cohesion of sister chromatids during passage of the replication fork. She has gone on to develop evidence that the essential function of the C terminus of pol ϵ is to aid in establishing efficient sister chromatid cohesion during S phase. Another postdoctoral fellow in the laboratory, Caroline Li has characterized the Trf5 protein. She has shown that it encodes a previously unknown poly A polymerase and that it stimulates the activity of pol ϵ dramatically. Future studies are aimed at defining the mechanism by which these two proteins regulate interaction of the replisome with the cohesin complex, the glue that holds the chromosomes together, and how failure of cohesion leads to genomic instability.

At least seven human diseases characterized by cancer predisposition and/or premature aging are correlated with defects in genes encoding DNA helicases. The yeast genome contains 134 open reading frames with helicase motifs, only eight of which have been characterized. Martin Budd in our laboratory identified the first eukaryotic helicase essential for DNA replication, Dna2. He showed by interaction studies that it was a component of the machine that is required for accurate

processing of Okazaki fragments during lagging strand DNA replication. Enzymatic studies to elucidate the sequential action of the DNA polymerase, helicase, and nuclease required for this processing form an ongoing mechanistic biochemistry project in the laboratory.

Stimulated by various reports in the literature implicating Dna2 in telomere biogenesis and structure, Wonchae Choe made the interesting observation that the bulk of Dna2 is localized to telomeres and that this localization is dynamic. During G1 and G2 phases of the cell cycle, Dna2 is at telomeres. During S phase Dna2 is present on the replicating chromatin. Current studies are aimed at defining the genes that regulate the localization, including phosphorylation by the yeast ATR ortholog, Mec1. In addition to defects in replication, dna2 mutants are also very sensitive to agents that induce double strand breaks (DSBs). Osamu Imamura has shown that Dna2 is mobilized from telomeres in response to the induction of double strand breaks. He is carrying out experiments to test the model that Dna2 delocalization from telomeres is part of the signaling system that induces the DNA damage and S phase checkpoints, as has also been suggested for yKU, a protein involved in non-homologous end joining and in stabilizing telomeres.

One model of cellular aging suggests that accumulation of DNA damage leads to replicative senescence. Most endogenous damage occurs during S phase and leads to replication fork stress. At least three human diseases of premature aging or cancer predisposition - Werner, Bloom, and Rothmund-Thompson are caused by defects in helicases similar to Dna2. Martin Budd and Laura Hoopes found that dna2 mutants have a significantly reduced life span. Microarray analysis by Isabelle Lesur shows that the dna2 mutants age by the same pathway as wild-type cells; they just age faster. Interestingly, the human Bloom and Werner genes suppress the replication defect of dna2 mutants. Yeast transcriptome analysis shows that old dna2 mutants have a gene expression pattern strikingly similar to cells senescing due to telomerase defects. Future work will take advantage of the yeast system to further delineate the role of BLM and WRN proteins in mammalian cells. The work of Tao Wei in the lab suggests that instability of repetitive DNA, such as the ribosomal locus and telomeric DNA, is a major cause of genomic instability in the aging dna2 mutants.

213. Identification of mutations synthetically lethal with **dna2-1** and **dna2-2** mutants
 Martin Budd, Judith L. Campbell, Amy Tong¹, Charles Boone¹

A set of deletion mutations in *S. cerevisiae* has been constructed for all known genes (about 6200). About 5100 of these mutations are nonessential. These nonessential genes can be used for a synthetic lethal screen with a strain with a mutation in an essential gene. We have collaborated with the laboratory of Charles Boone at the University of Toronto to do a synthetic lethal screen with dna2-1 and dna2-2 mutants. We had previously

identified *rad27*, *sgs1*, *srs2*, *rrm3*, *rad52*, *est1* mutations as being synthetically lethal or sick when combined with *dna2* mutant strains. Rad27p is a nuclease that is the main player in Okazaki fragment processing. Sgs1p, Srs2p, and Rrm3p are DNA helicases involved in DNA replication, DNA repair, and the DNA checkpoint response. Sgs1p is homologous to the helicases defective in Werner Syndrome patients and Bloom Syndrome patients. Est1 protein is a subunit of telomerase the protein required to synthesize the chromosome ends. The screen has been done with *dna2-1* strains and has identified additional genes involved in DNA repair. In addition genes involved in the DNA replication checkpoint were identified. *dna2-1* is not synthetically lethal with *mec1* mutants, thus the identification of DNA replication checkpoint genes is surprising. Genes involved in DNA repair, transcriptional silencing, chromatin assembly, and the osmotic stress response are also as synthetically with *dna2-1* mutants.

¹Department of Medical Genetics and Microbiology, University of Toronto, Toronto Ontario, Canada M5S 1A8, Canada M5S 1A8

214. Global interaction network involving DNA2
Martin Budd, A. Tong, C. Boone, Judith L. Campbell

We have performed a synthetic genetic array (SGA) screen using *dna2-1* and *dna2-2* strains as queries to identify pathways requiring Dna2p. In the Synthetic Genetic Array (SGA) method a query mutant is crossed into 5000 viable mutants using a robotic technology. Double mutant spores are genetically selected and synthetic lethal or synthetic sick interactions can be scored by the absence of double mutants. This method has identified 4000 interactions among 1000 genes allowing an interaction network to be built with genes involved in cell polarity, cell wall biosynthesis, mitosis, secretion, DNA replication and DNA repair. The screen adds new evidence to our model that Dna2p is involved in OFP (Okazaki fragment processing) and establishes links to several unexpected pathways. The mutants identified in the SGA screen fall into the following functional categories: helicases involved in chromosome stability, nucleases involved in OFP, other enzymes involved in lagging strand synthesis, enzymes of DNA repair, proteins involved in both DNA replication and the replication checkpoint, proteins related to chromosomal cohesion in the rDNA, histone chaperones, histone modifying enzymes, repressors of Ty transposition, enzymes involved in the oxidative stress response, protein degradation, and polarized cell growth. Experiments based on these findings clarify the role of Dna2 in telomere biogenesis.

^{*}University of Toronto

215. **Magnetospirillum magnetotacticum** has four paralogs of the *ftsZ* gene
Vincent Auyeung¹, Peter Freddolino¹, Christopher Sung¹, Theresa Tiefenbrunn¹, Elizabeth Bertani

The product of the *ftsZ* gene of *E. coli*, a bacterial analog of tubulin, plays a structural role in bacterial cell division. In most bacteria studied so far, the gene is present in single copy and is located on the chromosome in a cluster of genes having similar function. Four sequences with a tubulin signature can be seen in the draft genome sequence of the magnetotactic organism, *Magnetospirillum magnetotacticum*. One of these is located together with other genes of similar function, as in the case with *E. coli*, but the others are scattered at different sites in the chromosome. The presence of multiple copies of *ftsZ* is not necessary simply for magnetotaxis or because of the spirillum shape, since only one copy is seen in the draft sequences of the magnetotactic organism MC-1 or the similarly-shaped *Rhodospirillum*.

An interference test was used to determine if all four paralogs of *ftsZ* are involved in cell division. The test is based on the fact that cell division of *E. coli* will be blocked if a homologous *ftsZ* gene is introduced into the organism. All four of the paralogs were obtained by PCR from *M. magnetotacticum* genomic DNA and cloned into the pMAL vector to produce *ftsZ*-MBP gene fusions. The gene fusions were each introduced into a suitable strain of *E. coli* and production of the fusion protein was induced with IPTG. Controls of vector alone or vector producing GFP-MBP had no effect on the appearance of colonies. All four of the *ftsZ* fusion proteins, however, interfered with colony formation, suggesting that indeed all four are involved in cell division.

¹Undergraduate, California Institute of Technology

216. Aging cells show a global stress and DNA damage response
Isabelle Lesur

One of the characteristics of the *dna2-1* mutant is that it is aging prematurely. The median replicative lifespan of most *S. cerevisiae* wild-type cells is about 25 generations; the maximum is about 40 generations (Jazwinski, 1993). It has recently been shown that several DNA replication mutants show drastically reduced replicative lifespan (Hoopes et al., 2002). This led to the suggestion that replication mutants represent an exaggerated case of spontaneous replication errors that occur in wild-type cells in every generation, and that cessation of cell division in both mutant and wild type is the consequence, in part, of chromosome damage occurring during DNA replication. Such a model would be consistent with the observed instability of the rDNA repeats in old cells (Sinclair, 2002). One of these DNA replication mutants is *dna2-1*. Its median lifespan is eight generations, and maximum about 15 generations, and this mutant ages in the absence of ERCs (Hoopes et al., 2002).

Our current study was designed to further define the causes of aging in wild-type yeast and of the premature

aging of the *dna2-1* strain by further defining the pathologies of old cells, both wild type and mutant. Our initial study has been to determine the genome-wide transcriptional response to progression through the lifespan using microarray analysis. In order to obtain sufficient quantities of sufficiently old cells for reproducible production of RNA and cDNAs for microarray hybridizations, we developed a method for isolating old cells based on size selection. Our results suggest that a shift toward energy storage is associated with aging. Also an extensive subset of the environmental stress response genes (ESR) were activated in the old cells, as well as genes involved in DNA repair. The response shows striking similarity to the telomerase delete response, a gene expression pattern observed in cells senescing due to deletion of the catalytic subunit of telomerase.

References

Hoopes, L., Budd, M., Choe, W., Weitao, T. and Campbell, J.L. (2002) *Mol. Cell. Biol.* 22:4136-4146.
 Jazwinski, S.M. (1993) *Genetica* 91:35-51.
 Sinclair, D.A. (2002) *Mech. Aging Dev.* 123:857-867.

217. Biochemical characterization of Pol σ and its interaction with Pol ϵ

Caroline Li, Peter Snow*, Judith L. Campbell

Our group has previously reported genetic and physical interaction of *Saccharomyces cerevisiae* Pol2 (the catalytic subunit of the essential holoenzyme DNA polymerase ϵ) with either Trf4 or Trf5. The DNA polymerase activity of Pol ϵ was dramatically stimulated in the presence of Trf4 or Trf5. Trf4 and Trf5 are part of the Pol σ gene family that is essential for the viability of *S. cerevisiae*. Trf4 and Pol2 have been reported to have DNA polymerase activity, to be involved in DNA damage repair, and to play a role in sister chromatid cohesion.

S. cerevisiae Trf4 and Trf5 were expressed and purified from insect cells. Biochemical assays revealed that Trf4 and Trf5 have limited DNA polymerase activity and poly(A) polymerase activity. The DNA polymerase activity is likely a contaminant of protein purification because when a putative active site mutant of Trf5 was made, the DNA polymerase activity remained the same as that of the wild-type protein. However, the poly(A) polymerase activity was significantly reduced in the putative active site mutant of Trf5. We are currently producing a Trf4 putative active site mutant to check for the loss of poly(A) polymerase activity. Poly(A) polymerase was observed in two proteins from *S. pombe*, Cid1 and Cid13, that are homologous to *S. cerevisiae* Pol σ . The activity is thought to be involved in gene regulation of proteins involved in the S-M checkpoint. Cid1 and Cid13 are cytoplasmic proteins, whereas Trf4 and Trf5 are found in the nucleus, so their roles may be distinct. The poly(A) polymerase activity observed was characterized and found to be maximal in the presence of manganese instead of magnesium. It is possible that the activity seen in the presence of manganese is not

physiological. We are currently pursuing the mechanism by which Trf4 and Trf5 stimulate Pol ϵ .

*Director, Protein Expression Center, Caltech

218. Trf4 and Trf5 are nuclear proteins that associate preferentially with origins of replication in S-phase cells

Shaune Edwards, Judith L. Campbell

Our group has previously reported genetic and physical interaction of *Saccharomyces cerevisiae* Pol2 (the catalytic subunit of the essential holoenzyme DNA polymerase ϵ) with both Trf4 or Trf5, two closely related and functionally redundant proteins required for DNA replication and sister chromatid cohesion. The association led to the discovery that that pol ϵ is also involved in sister chromatid cohesion. In *S. pombe*, Cid1 and Cid13, two proteins homologous to *S. cerevisiae* Trf4 and Trf5, were recently shown to be cytoplasmic poly(A) polymerases. The activity is thought to be involved in enhancing the stability of RNAs encoding proteins involved in the S-M checkpoint. Since Caroline Li in our group has found that Trf4 and Trf5 do catalyze a poly(A) polymerase reaction, albeit inefficiently, we were interested in to what extent Trf4 and Trf5 are similar to and different from the *S. pombe* homologs.

Unlike the *S. pombe* Cid1 and Cid3 proteins, we find that both Trf4 and Trf5 are nuclear proteins, though we cannot rule out some small fraction of Trf4 and Trf5 being localized to the cytoplasm. Furthermore, consistent with a role in DNA replication and in cohesion, we showed by chromatin immunoprecipitation assays that Trf4, and Trf5 colocalize in S phase, along with Pol2, the catalytic subunit of DNA polymerase ϵ , to origins of DNA replication. This work establishes that the Cid1 and Cid13 proteins in *S. pombe* are probably unrelated in function to Trf4 and Trf5. Recently, a third homolog of Trf4 and Trf5 in *S. pombe*, has been shown to have an exclusively nuclear localization, and may represent the functional Trf-homolog.

219. Overproduction of the replication initiation protein Cdc6 inhibits the metaphase to anaphase transition

Susanna Boronat, Judith L. Campbell

The replication protein Cdc6p is synthesized at the end of mitosis, binds to the chromosomally bound ORC, and in turn enables the subsequent binding of Mcm proteins at the replication origins during G1 to form pre-replicative complexes (preRCs). During late G1 phase, preRCs are activated by Clb5,6/Cdc28 and Dbf4p/Cdc7p protein kinases leading to the onset of S phase. At this stage, the preRCs are lost from origins and cannot reassemble until passage through the next mitosis, since the Clb/Cdc28 kinases block preRC formation. The levels of Cdc6p fluctuate during cell cycle: Cdc6p is synthesized at the end of mitosis, and is subject to degradation at the onset of S phase.

Cdc6p contains six potential target sites for the Cdc28 protein kinase, three at the N-terminus and three at

the C-terminus. The mutation of all these sites, a subset of them, or just one site at C-terminus (site 6), into non-phosphorylatable sites results in the stabilization of Cdc6p.

We and others have reported previously that Cdc6p ectopic expression and especially the expression of phosphorylation site mutants, produces a delay in mitosis, specifically at the metaphase to anaphase transition. We had proposed that this delay could be explained by two different, although not mutually exclusive, explanations. One possible explanation is that Cdc6p ectopic expression triggers or mimics a checkpoint that arrests cells at the metaphase to anaphase transition. We showed that no checkpoint mutants that we have tested could suppress the mitotic delay, assayed by monitoring the levels of the Pds1 protein. This result strongly suggested that Cdc6p ectopic expression is not triggering the DNA replication or the spindle checkpoint.

The second explanation would involve a direct inhibition of the APC (Anaphase Promoting Complex)/Cdc20, the complex involved in the metaphase to anaphase transition, as opposed to the alternative form of the APC, APC/Cdh1, involved in the exit of mitosis. The activation of APC/Cdc20 requires active Cdc28 kinase. Therefore, inhibition of the APC/Cdc20 could be due either to inhibition of the Cdc28 kinase or to activation of the phosphatase PP2A, known to dephosphorylate the APC, or to inhibition of both the APC and PP2A.

We have shown that Cdc6p inhibits Cdc28 kinase activity *in vitro*. However, when we analyzed the Cdc28 kinase activity, using either histone H1 or the B-subunit of the polymerase α as substrates, we did not detect a significant inhibition of Cdc28 activity. Also, some of our phosphorylation site mutants did not bind to Cdc28 and were still capable to produce a mitotic delay. These results strongly suggested that there had to be mechanism other than the direct inhibition of Cdc28p by binding to the Cdc6p.

Therefore, we investigated if activation of the PP2A phosphatase was responsible for our observations and we found that this was the case. We found that mutant yeast strains without Cdc55, one of the regulatory subunits of PP2A, did not show mitotic delay when Cdc6 phosphorylation site mutants were expressed. We showed that APC/Cdc20 function, as measured by Pds1 degradation, was restored. We also found that *cdc55* Δ restored the viability of *cdc16* strains overexpressing Cdc6 phosphorylation site mutants. We analyzed the relationship between Cdc6 and PP2A in more detail and we found that Cdc6 co-immunoprecipitated with Cdc55 and that interaction is through Cdc6 C-terminus. We also found that Cdc6 was able to interact with Cdc16, one of the APC core subunits, known to be phosphorylated to activate APC/Cdc20. The simplest and most obvious interpretation of our results was that Cdc6 interacts with PP2A through the Cdc55 regulatory subunit and this interaction results in the recruitment of PP2A to the APC, which is then dephosphorylated and deactivated.

220. Mechanism of and model for Cdc6 inhibition of mitosis

Sue Boronat, Chris Raub*, Judith L. Campbell

We are interested in understanding the mechanism of inhibition of mitosis by overproduction of Cdc6, but most importantly the biological significance of these interactions. Since the levels of Cdc6 were thought to be very low at the metaphase to anaphase transition in normal cycling cells, the fact that our results were obtained by overproduction of Cdc6 raised the question of the role, if any, of inhibition of APC/Cdc20 by Cdc6 in normal cells. We think that the answer lies in the fact that the metaphase to anaphase transition is an important node in the cell cycle upon which many regulatory systems converge.

We have proposed a model in which Cdc6 that is synthesized after anaphase, and which is present at very high levels, also serves in a normal cell cycle to fully inhibit APC/Cdc20 before Cdc20 degradation in late mitosis. In other words, we propose that the constitutive overproduction used in our experiments to date reflects a physiologically significant cell cycle specific, transient, high level of Cdc6. CDC6 transcription peaks simultaneously with CDC20 and protein synthesis occurs shortly after. Cdc6 may then interact with PP2A through the regulatory subunit Cdc55, recruit PP2A to the APC/Cdc20 and inactivate it by dephosphorylation of the core subunits. At this point, the levels of Cdc6 protein may not suffice to inhibit Clb/Cdc28, but we cannot rule out this possibility. Such inhibition would provide an additional means to inactivate APC/Cdc20, however. Later in telophase, it is possible that Cdc6 levels are high enough to inhibit Clb/Cdc28, in conjunction with Sic1, and, therefore, contribute to the activation of the APC/Cdh1 and exit of mitosis, as reported by others. Although dephosphorylation of the APC core subunits is not essential for APC/Cdh1 interaction, the fact that Cdh1 binds to an unphosphorylated APC core makes it likely that Cdc6-associated PP2A dephosphorylates the APC/Cdc20, contributing to the switch from Cdc20 to Cdh1.

We are currently working on the verification of this model. We have carried out Western blots of myc-Cdc6 expressed from its own promoter as a function of the cell cycle. The peak of myc-Cdc6 correlates with timing of Pds1 degradation, that is, it is early in mitosis and not late or in G1. Also, the levels of Cdc6 protein peak when the levels of Clb2 are still very high, an additional sign that cells are still in early mitosis. However, due to those high levels of Clb2, most probably Cdc6 is not forming pre-RCs. The profile of Cdc6 expression is, therefore, in agreement with our model.

We are also studying the effect of lack of Cdc6 during mitosis, since we expect a faster degradation of the APC/Cdc20 substrates like Pds1 and Clb5, because in the absence of Cdc6, the APC/Cdc20 would not be inactivated. Our preliminary results support our hypothesis. In a biochemical approach, we are trying to prove that endogenous levels of Cdc6 bind to Cdc55 in

anaphase and that this interaction affects APC/Cdc20 activity.

*Summer SURF Student

221. Interaction between *Saccharomyces cerevisiae* DNA polymerases epsilon and sigma
Clara C. Reis, Judith L. Campbell

Polymerase epsilon (pol ϵ) is an essential DNA polymerase required for DNA replication, repair, and the S/M checkpoint. Recently it was discovered that the essential but non-catalytic C-terminal domain of yeast DNA pol ϵ interacts both physically and genetically with pol σ , encoded by *Saccharomyces cerevisiae* TRF4 and TRF5 genes.

Mutants of both polymerases have been shown to have defects in sister chromatid cohesion. The overall goal of our studies is to explore further this interaction with respect to checkpoint response, sister chromatid cohesion, and chromosome dynamics during S phase.

If the essential functions of pol σ require interaction with pol ϵ , then one would expect pol σ and pol ϵ to be present at similar levels in the cell. The relative amounts of endogenous Pol2 subunit of pol ϵ , Trf4, and Trf5 were therefore studied in asynchronous cells, revealing that Trf4 was present in about 2.5-fold excess over Trf5, which was present at levels approximately equivalent to Pol2. We will now evaluate Dpb2 subunit of pol ϵ levels. We have also shown that the levels of the Pol2, Trf4 and Trf5 proteins are constant throughout cell cycle progression.

One possible role for this interaction is to participate in the S-phase checkpoint. Therefore, the genetic interaction between pol2 and trf4 and trf5 with respect to the checkpoint response, which leads to increase in the levels of RNR1 (ribonucleotide reductase subunit) transcription, was investigated. We found that overexpression of the RNR1 partially suppresses the ts phenotype of trf5 Δ pol2-12 and the cs phenotype trf4 Δ pol2-12, suggesting that the interaction may be part of the checkpoint signaling pathway.

Reference

Edwards, S., Li, C., Levy, D., Brown, J., Snow, P. and Campbell, J.L. (2003) *Mol. Cell. Biol.* 23:2733-2748.

222. Analysis of mutations in potential Mec1 phosphorylation sites
Martin Budd, Judith L. Campbell

Dna2 protein is involved in DNA replication and DNA repair. A proteomic screen has identified an interaction of Dna2 and Ddc2 protein. Ddc2 protein interacts with Mec1 protein, a protein kinase that is the initiating kinase for the DNA replication and DNA damage checkpoint. DNA2 protein is phosphorylated by Mec1 kinase, and is not phosphorylated by Mec1 kinase with defects in the catalytic domain. Since Mec1 regulates both the checkpoint response and the DNA repair response, the interaction with Dna2 may provide a pathway for Mec1

regulation of the DNA repair response. To identify the residues that are phosphorylated, we have initiated a collaboration with Rudi Aebersold at the Institute for Systems Analysis in Seattle. Mec1 phosphorylates SQ and TQ residues. In order to determine which possible sites might be significant, we have compared the sequence of *Saccharomyces cerevisiae* Dna2 with the protein from four other related *Saccharomyces* species to identify potential sites for Mec1 regulation. All these sites were mutated to alanine and strains containing the mutations were tested for temperature-sensitive growth, sensitivity to MMS (methyl methane sulfonate), and sensitivity to x-rays. One strain has defective growth at 37°C, and is sensitive MMS. The mutations are being combined to test for an interaction among the mutations.

223. Conserved genes associated with controlled magnetite mineralization in bacteria
Cody Z. Nash¹, L. Elizabeth Bertani, Joseph L. Kirschvink¹

The biologically controlled mineralization of magnetite (BCMM) within lipid-bilayer membranes (magnetosomes), which is the biophysical basis of magnetotactic behavior in some bacteria, appears to be under strict genetic control. In an effort to identify genes involved in this process we compared the publicly available genomes of two magnetotactic bacteria, *Magnetospirillum magnetotacticum* MS-1 and *Magnetococcus* sp. MC-1 to each other and to the NCBI protein database. Our comparison focused on finding proteins conserved, particularly between these magnetotactic bacteria. We define a conserved gene in MS-1 as a gene (i.e., gene A) which best matches some gene from MC-1, gene B, where gene B also best matches a gene from MS-1, although not necessarily gene A. Conserved genes were likewise defined for MC-1. In MS-1 and MC-1 we found 122 and 104 conserved genes respectively, showing that the two species use similar systems for BCMM. These genes appear in multiple clusters, arranged according to function suggesting that BCMM is ancestral to the α -proteobacteria instead of having been transferred laterally among the class. The conserved genes include most of the genes known to localize to the magnetosome and they also include a significant number of genes involved in functions consistent with models of magnetotaxis, including glycoprotein synthesis, redox reactions, inorganic ion transport, and signal transduction. We find support for the hypothesis that BCMM is a metabolic strategy, as well as a navigational one.

¹Division of Geological and Planetary Sciences, Caltech

224. Evidence that yeast **SGS1**, **DNA2**, **RRM3**, **SRS2**, and **FOB1** interact to maintain rDNA stability

Tao Weitao, Martin Budd, Laura L. Mays Hoopes*, Judith L. Campbell

We have proposed that faulty processing of arrested replication forks leads to increases in recombination and chromosome instability in *Saccharomyces cerevisiae* and contributes to the shortened lifespan of *dna2* mutants. Now we use the ribosomal DNA locus, which is a good model for all stages of DNA replication, to test this hypothesis. We show directly that DNA replication pausing at the ribosomal DNA replication fork barrier (RFB) is accompanied by the occurrence of double-strand breaks near the RFB. Both pausing and breakage are elevated in the early-aging, hypomorphic *dna2-2* helicase mutant. Deletion of *FOB1* suppresses the elevated pausing and DSB formation, and represses initiation at rDNA ARSs. The *dna2-2* mutation is synthetically lethal with *rrm3* or *srs2*, encoding DNA helicases involved in rDNA replication/recombination. Our current work also shows that mutations inactivating yeast RecQ helicase *Sgs1* cause the replication fork to stall and DSBs at rDNA RFB, but either the mutation in *FOB1* or an increase in *SIR2* gene dosage suppresses the fork stalling. In conclusion, the replication-associated defects in the rDNA are symbolic of similar events occurring either stochastically throughout the genome or at other regions where replication forks move slowly or stall, such as telomeres, centromeres, or replication slow zones. The data support a notion of concordant action of *Sgs1*, *Dna2*, *Sir2*, *Rrm3* and *Srs2* in pathways processing stalled replication forks and DSBs, such as those occurring at the *Fob1*-dependent RFB.

*Department of Biology and Molecular Biology, Program, Pomona College, Seaver South Laboratory, Claremont, CA 91711

Weitao, T., Budd, M. and Campbell, J.L. (2003) Evidence that yeast *SGS1*, *DNA2*, *SRS2*, and *FOB1* interact to maintain rDNA stability. *Mut. Res.* 532:157-172.

Publications

- Imamura, O. and Campbell, J.L. (2003) The human Bloom syndrome gene suppresses the DNA replication and repair defects of yeast *dna2* mutants. *Proc. Natl. Acad. Sci. USA* 100:8193-8198.
- Kao, H.I., Veeraraghavan, J., Polaczek, P., Campbell, J.L. and Bambara, R.A. (2004) On the roles of *Saccharomyces cerevisiae* *Dna2p* and *FEN1* in Okazaki fragment processing. *J. Biol. Chem.* 279:15014-15024.
- Lesur, I. and Campbell, J.L. (2004) The transcriptome of prematurely aging yeast cells is similar to that of telomerase deficient cells. *Mol. Biol. Cell* 15:1297-1312.
- Luo, K.Q., Elsasser, S., Chang, D.C. and Campbell, J.L. (2003) Regulation of the localization and stability of *Cdc6* in living yeast cells. *Biochem. Biophys. Res. Comm.* 306:851-859.
- Weitao, T., Budd, M., Hoopes, L.L.M. and Campbell, J.L. (2003) *Dna2* helicase/nuclease causes replicative fork stalling and double-strand breaks in the ribosomal DNA of *Saccharomyces cerevisiae*. *J. Biol. Chem.* 278:22513-22522.

Assistant Professor of Biology: David C. Chan
 Postdoctoral Scholars: Hsiuchen Chen, Takumi Koshiba,
 Sungmin Park-Lee
 Graduate Students: Scott Detmer, Erik E. Griffin, Tobias
 Rosen, Tara Suntoke
 Research and Laboratory Staff: Lloyd Lytle

Support: The work described in the following research reports has been supported by:

The Arnold and Mabel Beckman Foundation
 Donald Bren Foundation
 Burroughs Wellcome Fund
 Joyce Charitable Trust
 Muscular Dystrophy Association
 National Institutes of Health
 Rita Allen Foundation
 United Mitochondrial Disease Foundation

Summary: Diverse biological systems-- including viruses, cells, and organelles-- are enclosed within lipid membranes that serve to compartmentalize the systems and distinguish their contents from the environment. Under special circumstances, however, these membrane-bound systems undergo membrane fusion, in which the lipids of two compartments fuse and the internal contents ultimately mix. In general, these fusion events are multi-step processes, involving recognition of two membrane surfaces, membrane apposition, and finally, lipid and content mixing. Such membrane fusion events are central to many fundamental cellular processes, including entry of enveloped viruses into cells during infection, entry of sperm into an egg during fertilization, and fusion of organelles during protein trafficking and organelle biogenesis. Using cell biological, biophysical, and genetic approaches, our lab is studying the mechanisms through which these membrane fusion events occur.

Regulation of mitochondrial dynamics

Our major research focus is on the regulation of mitochondrial dynamics. Mitochondria are dynamic organelles that undergo cycles of homotypic fusion and fission. Such membrane fusion and fission events play important roles in controlling organelle number, subcellular distribution, morphology, and ATP production. In some cells, fusion of numerous mitochondria into a well-organized reticulum is thought to enable transmission of mitochondrial membrane potential, thereby facilitating ATP generation to active regions of the cell. In some cases, mitochondrial fusion is developmentally regulated; for example, during insect spermatogenesis, the mitochondria of immature spermatids aggregate and fuse into giant mitochondria. Such regulated mitochondrial fusion is likely required in order to accommodate the changing metabolic state of the cell.

Genetic studies have identified an essential role of mitofusin (Mfn) proteins in mitochondrial fusion. These are large GTPases that are localized to the mitochondrial outer membrane. Mammals have two homologs, terms Mfn1 and Mfn2. Mutations in Mfn2 are responsible for

Charcot-Marie-Tooth Type 2A syndrome, an inherited peripheral neuropathy. We are currently analyzing the effects of these disease mutations on mitofusin function and are developing mouse model for this disease (Scott Detmer). In addition, mutations in another protein involved in mitochondrial fusion, OPA1, are responsible for Dominant Optic Atrophy, an inherited optic neuropathy.

Although the importance of mitochondrial fusion in lower eukaryotes is well documented, its role during mammalian development remains unclear. Accordingly, we have placed a major emphasis on addressing this issue through the analysis of mice deficient in mitofusins Mfn1 and Mfn2 (Hsiuchen Chen). This work has definitively shown that mitochondrial fusion in mice requires mitofusins and has revealed an essential role of mitochondrial fusion during mouse development, particularly in formation of the placenta. In addition, our analysis leads to a model in which fusion protects mitochondrial function by enabling cooperation between mitochondria. We have also constructed mice with conditional alleles of both mitofusins and are studying their role in neuromuscular development. These studies may also lead to mouse models of human mitochondrial diseases, a diverse group of diseases characterized by defective mitochondrial function.

Genetic studies have uncovered mitofusin as a central molecule in the fusion of mitochondria, but its mechanism of action remains unknown. It may act as a truly fusogenic molecule, analogous to viral envelope proteins that directly mediate membrane fusion. Alternatively, it may act as a regulatory protein, directing assembly of a fusion machinery in a GTP-dependent manner. Our recent experiments with Mfn-null cells support the view that mitofusin is directly involved in mediating membrane fusion. We find that Mfn is required on adjacent mitochondria during membrane fusion, implying that Mfn complexes form in trans (that is, between adjacent mitochondria). In addition, we have identified a region of Mfn1 that mediates complex formation and have solved its structure by X-ray crystallography (Takumi Koshiba). These studies provide a structural understanding of how mitofusin complexes are capable of tethering mitochondria during the membrane fusion process and have implications for a wide range of intracellular membrane fusion events. We are currently performing extensive structure-function analyses of mitofusin to further address these issues (Scott Detmer, Erik Griffin, Takumi Koshiba, Sungmin Park-Lee). Finally, a complete understanding of mitochondrial dynamics will require identification of all the molecular players. We are approaching this problem through proteomic identification of molecules that interact with known proteins central to fusion and fission (Erik Griffin).

HIV entry

In a second line of research, we are continuing our investigations of membrane fusion by viral envelope proteins. A key step in the life cycle of enveloped viruses

is fusion of viral and host cell membranes. A virally-encoded glycoprotein, gp160, is responsible for mediating the entry process of HIV-1, the etiological agent of Acquired Immunodeficiency Syndrome (AIDS). The envelope precursor, gp160, is cleaved to form the subunits gp120 and gp41. gp120 directs target cell recognition, while gp41 mediates the merging of viral and cellular membranes. gp41 is composed of several distinct domains including a hydrophobic fusion peptide, two coiled-coil domains (termed N- and C-terminal helices), a membrane-spanning region, and a cytoplasmic tail.

Our current model for HIV membrane fusion invokes a series of conformational changes in the gp120/gp41 complex. Interaction between gp120 and cellular receptors liberates the gp41 fusion peptide from its native conformation and allows its insertion into the host cell membrane. A transient species termed the prehairpin intermediate is created, in which the N-terminal helices form a trimeric coiled-coil but do not interact with the C-terminal region. Subsequently, a hairpin structure is generated, in which the C-terminal helices pack in an anti-parallel manner around the trimeric N core to form a fusion-active 6-helix bundle. This N-C interaction brings the viral fusion peptide, inserted into the host-cell membrane, and the transmembrane segment, associated with the viral membrane, into close proximity. In a process that remains poorly defined, fusion of the closely apposed viral and cellular membranes follows. A mechanistic understanding of HIV membrane fusion may lead to new strategies to inhibit HIV entry into human cells.

To test this model of HIV entry, we are determining the mechanism through which peptide inhibitors prevent gp41-mediated membrane fusion. Some of these peptide inhibitors bind to fusion intermediates of gp41, and our analysis has revealed sequential steps in the fusion pathway. We are also characterizing a series of gp41 mutants that fail to fuse in order to better understand how formation of the six-helix structure leads to membrane fusion (Tara Suntok).

225. Protective effects of mitochondrial fusion on cell function and mouse development
Hsiuchen Chen

Mitochondrial dynamics involves the two opposing processes of fusion and fission. An equilibrium between the two allows for the maintenance of relatively stable morphology. In mouse embryonic fibroblasts (MEFs), for example, a tubular network of mitochondria normally predominates. If fusion is inhibited, however, unopposed fission leads to mitochondrial fragmentation. The paradox of mitochondrial dynamics is that cells invest many resources into fusion and fission, yet reducing both simultaneously also results in tubular networks. This observation suggests that fusion provides functions beyond regulation of morphology.

Using cell lines deficient in the mitochondrial fusion proteins, Mfn1, Mfn2, and OPA1, we have probed the functional consequences of losing mitochondrial

fusion. Three defects were uncovered - slower cell growth, loss of mitochondrial membrane potential, and reduction of respiratory capability. All three defects were reversible upon resumption of mitochondrial fusion. Significantly, these functional defects are consequences of lack of fusion, not fragmented mitochondrial morphology, as demonstrated by the analysis of fusion-competent but fragmented mitochondria, and fusion-deficient but tubular mitochondria.

We conclude that cells invest in mitochondrial dynamics to enable cooperation between mitochondria. Depletions of material in individual mitochondria can be replenished rapidly when membrane and content exchange occurs readily between mitochondria. Stochastic defects do not accumulate, and thus, mitochondrial fusion acts as a protective mechanism for mitochondrial and cell function.

Mitochondrial fusion is developmentally and physiologically significant. In humans, mutations in Mfn2 give rise to Charcot-Marie-Tooth disease (an inherited peripheral neuropathy), and mutations in OPA1 lead to dominant optic atrophy (an inherited optic neuropathy). Mice lacking either of the mitofusins die as embryos. To examine effects of fusion deficiencies later in life, we have created conditional knockout mice of Mfn1 and Mfn2. We bypassed the placental defect of Mfn2^{-/-} embryos by using the Meox2-Cre mice (gift of P. Soriano, FHCRC) to disrupt Mfn2 in the embryo proper without affecting extra-embryonic tissues. Preliminary studies show that Mfn2-null mice are indeed born at the expected frequency, but then die within approximately two weeks. The pups display severe runting and a near paralysis of the hind legs, reminiscent of the distal limb weakness and muscular atrophy associated with Charcot-Marie-Tooth disease. We are currently refining our analysis of these neuromuscular defects through the specific inactivation of Mfn2 in peripheral nerves.

226. Structure-function analysis of murine Mfn1 and Mfn2
Scott Detmer

Cell-based mitochondrial fusion assays (H. Chen and D. Chan) have clearly demonstrated that the mitofusin (Mfn) proteins are required for murine mitochondrial fusion. However, the mechanism through which mitofusins mediate mitochondrial membrane fusion remains unclear. To approach this issue, we are using structure-function analysis to identify critical domains in mitofusin. We have identified the GTPase domain and two heptad repeat regions as critical, and are further characterizing these regions by *in vivo* functional assays, *in vitro* interaction assays, and biophysical analysis. We have constructed Mfn1 mutants that mediate mitochondrial aggregation. This effect is dependent on heptad repeat 2 (HR2). Because Mfns are required on opposing mitochondria, and HR2 assembles into a dimeric anti-parallel coiled-coil, we propose that the clumped mitochondria are mediated by an HR2-mediated trans-complex. Such a complex could represent a tethered

intermediate that is unable to progress to full mitochondrial fusion because it lacks the GTPase domain.

227. Functional analysis of Mfn2 mutations in Charcot-Marie-Tooth disease
Scott Detmer

Recently, Zuchner et al., reported multiple Mfn2 missense mutations in the peripheral neuropathy Charcot-Marie-Tooth Type 2A, a progressive disease leading to muscular atrophy in the feet and hands of affected individuals. We are investigating the functional consequences of such mutations. When expressed in fibroblasts, the majority of the described missense mutations cause severe aggregation of all the mitochondria in the cell; this aggregation phenotype may be critical for disease progression. To extend these initial observations, we are performing structure-function analysis in fibroblast and neuronal cell lines. We are using insights from these cellular studies to guide strategies for generating mouse models of this disease.

Reference

Zuchner et al. (2004) *Nature Gen.* 36:449-451.

228. Structural study of mitochondrial fusion by mitofusin complexes

Takumi Koshiba, Scott Detmer, Hsiuchen Chen

We find that mitofusin, an integral mitochondrial outer membrane protein, is required on adjacent mitochondria to mediate fusion. This observation indicates that mitofusin complexes act in trans (that is, between adjacent mitochondria). We therefore, attempted to identify domains of mitofusin that might mediate oligomerization. We found that a carboxyl terminal heptad repeat region (HR2) of Mfn1 forms a stable oligomeric and folds into a highly helical structure. Using X-ray crystallography, we solved the structure of Mfn1 HR2 at 2.5 Å resolution. HR2 assembles into a dimeric, anti-parallel coiled coil with a highly charged surface. Significantly, the Mfn1 transmembrane segments are located at opposite ends of the 95 Å coiled coil, providing a mechanism for organelle tethering. Consistent with this proposal, truncated mitofusin, in an HR2-dependent manner, causes mitochondria to become apposed with a uniform gap. Disruption of the HR2 coiled coil by point mutations abolishes mitochondria tethering and fusion. Thus, the HR2 structure provides a structural understanding of how anti-parallel coiled coil formation can mediate organelle tethering by providing a large interaction interface while maintaining separation of the membrane anchors. These insights have implications for other intracellular membrane fusion events, which almost universally proceed through a tethering step prior to fusion.

229. Proteomic identification of novel factors involved in mitochondrial fusion and fission
Erik Griffin

To date, all mediators of mitochondrial fusion and fission have been identified genetically. Although powerful, genetic approaches are unlikely to identify genes with redundant functions or intermediate mutant phenotypes. For these reasons we are using a proteomic method, MUDPIT, being developed by Johannes Graumann in Ray Deshaies' lab to identify novel mitochondrial fusion and fission genes. MUDPIT involves affinity chromatography of an epitope-tagged protein of interest under conditions that are likely to allow copurification of binding partners. The resulting protein mixture is digested into peptides and subjected to online chromatography and mass spectrometry sequence determination. Because MUDPIT is highly sensitive and can easily identify hundreds of individual proteins in a mixture, it has great potential in identifying components of large protein complexes.

We have performed MUDPIT analysis of several proteins involved in mitochondrial dynamics. Our analysis of Fis1p, a mitochondrial protein essential for fission, has proved particularly fruitful. Fis1p is a mitochondrial transmembrane protein that mediates mitochondrial fission through its interactions with the two other fission proteins, Mdv1p and Dnm1p. We have identified a third binding partner, Caf4p, which shares sequence similarity with Mdv1p. Caf4p localizes to mitochondria, and its mutant phenotype suggests either a role in mitochondrial distribution or fission. We will distinguish between these possibilities through kinetic analysis of mitochondrial fission in a *caf4* deletion mutant and through Caf4p overexpression studies.

230. Analysis of homotypic and heterotypic interactions between murine Mfn1HR2 and Mfn2HR2

Sungmin Park-Lee

Hydrophobic heptad repeats play central roles in molecules that directly mediate membrane fusion. In both viral fusion proteins and SNARE complexes, the formation of helical bundles by hydrophobic heptad repeats serves to force two lipid bilayers together, ultimately resulting in membrane merger. Intriguingly, mitofusins also contain two prominent heptad repeats (HR1 and HR2), and we are exploring the role that these motifs play in mediating membrane fusion. Biochemical studies show that HR2 in Mfn1 and Mfn2 can form both homotypic and heterotypic complexes. Mfn1 HR2 forms an antiparallel coiled coil, as shown by X-ray crystallography (T. Koshiba).

To understand the role of the HR2 regions in mediating both homotypic and heterotypic complexes between Mfn1 and Mfn2, we are attempting to reconstitute these complexes using recombinant proteins so that they can be studied biophysically. We are currently producing recombinant versions of Mfn1 HR2 and Mfn2 HR2 and testing refolding conditions to examine complex formation.

231. Analysis of HIV-1 gp41 mutants

Tara Suntoke

To better understand the mechanism of gp41-mediated fusion, we are examining the role of the six-helix hairpin structure in the fusion pathway. Structural information about the fusion-active core reveals a largely hydrophobic interface between N- and C-terminal helices. We have created a series of mutations that are designed to reduce or prevent N-C association and thus, six-helix bundle formation. A range of hydrophobic substitutions at five different positions is being used to test the hypothesis that hairpin formation directly correlates to fusion activity. All gp41 mutants show wild-type levels of expression and precursor processing in mammalian cells, suggesting that the native structure of Env remains unaffected by the mutation. Cell-cell fusion assays reveal that mutants with bulky hydrophobic substitutions are more fusion active than those with small aliphatic substitutions. Using fluorescent dyes to monitor fusion kinetics, we find that even mutants with weak fusion phenotypes exhibit the same kinetics as wild-type envelope expressing cells.

In order to compare the stability of the six-helix bundle structures formed by each mutant, we performed a biophysical analysis of bacterially purified six-helix peptides. Helical content and thermal stability of these recombinant peptides, quantitated by circular dichroism, reveal that stability of the six-helix core correlates with hydrophobic bulk of the substitution: glycine and alanine mutants are less stable than phenylalanine substitutions at the same position. Those mutants with a more stable six-helix core structure are the same ones that exhibit greater fusogenic potential. Thus, our evidence indicates that hydrophobic contacts are important determinants of stability of the six-helix bundle structure, and that formation of this core structure directly correlates with gp41 fusion activity.

Publications

- Chen, H. and Chan, D.C. (2004) Mitochondrial dynamics in mammals. *Curr. Topics Dev. Biol.* 59:119-144.
- Karbowsky, M., Arnolt, D., Chen, H., Chan, D.C., Smith, C.L. and Youle, R.J. (2004) Quantitation of mitochondrial dynamics by photolabeling of individual organelles shows that mitochondrial fusion is blocked during the Bax activation phase of apoptosis. *J. Cell Biol.* 164:493-499.
- Koshiba, T., Detmer, S.A., Kaiser, J.T., Chen, H., McCaffery, J.M. and Chan, D.C. (2004) Structural basis of mitochondrial tethering by mitofusin complexes. *Science* 305:858-862.

Associate Professor: Raymond J. Deshaies, Ph.D.
 Research Specialist I: Rati Verma
 Research Fellows: Gabriela Alexandru, Gary Kleiger, Rusty Lipford, Thibault Mayor, Dane Mohl, Matthew Petroski, Kathy Sakamoto-UCLA STAR program
 Graduate Students: Xavier Ambroggio, Ramzi Azzam, Gregory Cope, Nazli Ghaboosi, Johannes Graumann, Angie Mah
 Research and Laboratory Staff: Robert Oania, Daphne Shimoda, Geoff Smith

Support: The work described in the following research reports has been supported by:

Damon Runyon – Walter Winchell Fund
 European Molecular Biology Organization
 Howard Hughes Medical Institute
 Jane Coffin Childs Memorial Fund
 National Institutes of Health
 Swiss National Science Foundation

Summary: The Deshaies lab works on two basic biological processes: Control of cell division, and regulation of cell function by attachment of ubiquitin or ubiquitin-like proteins to target polypeptides. We are particularly interested in how attachment of ubiquitin to proteins enables their degradation, and how this degradation is harnessed to regulate cell division.

Defective control of cell division can result in disease, as when unrestrained cell proliferation leads to cancer. Defects of the ubiquitin system can also lead to cancer, as well as neurodegenerative diseases. An understanding of how the cell division machinery and the ubiquitin system operate will thus provide insight into basic cellular processes essential to the life of eukaryotic cells, and may suggest cures for diseases that affect millions of people.

We are using biochemical, molecular, and genetic approaches in baker's yeast and mammalian cells to investigate cell proliferation and the ubiquitin system. Our long-term goal is to understand how these processes work and how they are controlled. Baker's yeast is an excellent organism for basic cell biological studies because it is easy to work with, and many studies have confirmed that yeast and animal cells use essentially identical proteins to regulate basic cellular processes.

Below, I summarize in more detail the four major areas of investigation in the lab, and provide thumbnail descriptions of all current projects.

SCF ubiquitin ligases: Mechanism, regulation, and physiology

Our prior investigations into the biochemical mechanism by which budding yeast cells transit from the G1 phase of the cell cycle to the S phase led to the discovery of the SCF ubiquitin ligases. SCF ubiquitin ligases are comprised of four subunits: Skp1, the Cullin family member Cul1 (or Cdc53), an F-box protein, and the RING-H2 domain protein Hrt1 (also known as Rbx1 or Roc1). The F-box protein serves as a receptor that docks

substrates to the catalytic core of SCF, which is comprised of the cullin and RING-H2 subunits. We have proposed that the catalytic core of SCF recruits the E2 (ubiquitin-conjugating) enzyme Cdc34, and switches on the ability of Cdc34 to transfer ubiquitin to substrate that is docked to the F-box subunit. Skp1 serves as a tether that links together the substrate-binding and catalytic modules. Interestingly, there are ~20 F-box proteins encoded in the yeast genome, and many more in metazoan genomes, suggesting that eukaryotic cells harbor many distinct SCF ubiquitin ligases, each with a unique substrate specificity. The prototype for the SCF family – SCF^{Cdc4} (where Cdc4 refers to the identity of the F-box subunit) - enables the transition from G1 phase to S phase in budding yeast by promoting the ubiquitination and degradation of the S-phase cyclin-dependent kinase inhibitor Sic1.

During the course of our studies on SCF ubiquitin ligases in animal cells, Svetlana Lyapina (now departed) discovered that SCF co-purifies with the COP9 signalosome. The COP9 signalosome (CSN) is an eight-protein assemblage that is evolutionarily related to the lid subcomplex of the 26S proteasome. CSN was originally discovered by Xing-Wang Deng and colleagues as a regulator of photomorphogenetic development in plants, and has since been implicated in a wide range of cellular and developmental processes. However, essentially nothing was known about the mechanism of action, biochemical targets, and regulation of this fascinating protein complex. Two years ago, Greg Cope reported that a novel metalloprotease active site located in the Csn5 subunit of CSN promotes cleavage of the ubiquitin-like protein Nedd8 from the Cul1 subunit of SCF. Interestingly, this active site, which we have dubbed, "JAMM" (JAb1/Mpn domain Metalloenzyme) is found in several other human proteins, including the Rpn11 subunit of the proteasome, where it serves as an essential ubiquitin isopeptidase that cleaves ubiquitin from proteins as they are being degraded by the proteasome. This finding suggests that the diverse biological activities of CSN may all relate to its ability to cleave Nedd8 from proteins such as the Cul1 subunit of SCF.

Four projects carried out in the lab over the past year build upon our discovery of the SCF family of ubiquitin ligases. Matt Petroski is investigating the biochemical mechanism by which SCF^{Cdc4} selects sites of ubiquitination in its substrates, and how it activates the ubiquitin conjugating enzyme Cdc34 to transfer ubiquitin to substrate. Rusty Lipford is investigating how SCF^{Cdc4} regulates transcription via ubiquitin-dependent degradation of transcriptional regulatory proteins. Kathleen Sakamoto's project addresses the hypothesis that tethering a protein to the F-box subunit of SCF is sufficient to activate its ubiquitination and eventual destruction. A small molecule-based approach to achieve this goal might lead to the development of a novel class of therapeutics. Finally, Greg Cope has engineered animal cells to express a point-mutated version of Csn5 in place of the wild-type protein. This will enable him to address the role of CSN

deneddylase activity in SCF regulation and cell physiology.

Mechanism of action and regulation of the 26S proteasome

Once a protein is conjugated with ubiquitin by ubiquitin ligase enzymes such as SCF, it is degraded by the 26S proteasome. The 26S proteasome is a complicated machine, with ~31 different subunits. The 26S proteasome comprises the 20S catalytic core and the 19S regulatory cap. The 20S core contains the enzyme active sites that carry out proteolysis, whereas the 19S cap controls the entry of ubiquitin-conjugated substrates into the 20S core. A major goal of the lab over the past few years has been to understand the steps in protein degradation that lie downstream of the attachment of ubiquitin by ubiquitin ligases such as SCF. How are these ubiquitinated substrates recognized by the proteasome? How are they processed for degradation? Two years ago, Rati Verma demonstrated that a critical step in the degradation of ubiquitinated substrates is the removal of the ubiquitin chain by the Rpn11 subunit of the proteasome. Rpn11 is a JAMM domain isopeptidase that resides in the lid subcomplex of the 19S cap. Over the past year, Rati has focused her efforts on understanding how ubiquitinated substrates are delivered to the 26S proteasome. She has also studied a small molecule inhibitor that blocks the delivery of substrate to the proteasome by binding to the ubiquitin chain. Meanwhile, Gary Kleiger has undertaken an analysis of the six ATPase subunits that form the 'base' subcomplex of the 19S. These ATPases are thought to govern substrate unfolding, opening of the channel into the 20S core, and translocation of substrate through this channel. Gary is taking a chemical-genetic approach to address the specific functions of these ATPases.

Proteomics

Budding yeast - with its formidable arsenal of genetic, molecular genetic, biochemical, and cell biological techniques - is an ideal system in which to develop and test new approaches in proteomics. Currently, there are three proteomic-type projects in the lab. Johannes Graumann is using a novel mass spectrometry technique - developed by John Yates at Scripps and known as "MudPIT" - to identify targets and regulators of the 26S proteasome and its substrate receptor proteins. MudPIT enables the sequencing of complex protein mixtures without the need for prior separation by SDS-PAGE, and so can identify proteins that are present at low stoichiometry, stain poorly, or are otherwise difficult to detect by conventional approaches. Thibault Mayor's project is to use MudPIT to identify the proteins that are covalently modified with ubiquitin in budding yeast. We hope to apply this method to the mapping of substrate networks for ubiquitin conjugating and deconjugating enzymes. Kathleen Sakamoto's project addresses the hypothesis that tethering a protein to the F-box subunit of SCF is sufficient to activate its ubiquitination and eventual destruction. A small molecule-based approach to achieve this goal might

lead to a general method for inactivating protein function in eukaryotic cells.

Functions of the RENT complex in cell cycle control and nucleolar biogenesis

Several years ago, Wenying Shou discovered the RENT complex, and proposed that the mitotic exit network (MEN) specifies the exit from mitosis in budding yeast by promoting disassembly of RENT. RENT is comprised of the nucleolar anchor protein Net1, the cell cycle regulatory protein phosphatase Cdc14 and the chromatin silencing protein Sir2. Cdc14 is required for the exit from mitosis, which it promotes by dephosphorylating (and thereby activating) proteins that mediate the inactivation of cyclin/CDK activity at the end of mitosis. Throughout the cell cycle, Cdc14 is confined to the nucleolus through its interaction with Net1. At the end of mitosis, the successful completion of anaphase activates the MEN signaling pathway, which disengages Cdc14 from Net1. The emancipated Cdc14 goes on to inactivate cyclin/CDK and thereby trigger the exit from mitosis. This hypothesis for how the exit from mitosis is controlled in budding yeast was dubbed 'RENT control' by Shou et al. Intriguingly, in addition to its role in cell cycle control, Net1 also mediates silencing of RNA polymerase II transcription in the nucleolus, activation of transcription by RNA polymerase I, and retention of a broad set of resident proteins within the nucleolus. The molecular mechanisms underlying the cell cycle-regulated disassembly of RENT and the role of RENT in organizing nucleolar chromatin remain largely unknown. Over the past few years, it has become apparent that RENT is disassembled by a two-step mechanism. In early anaphase, Cdc14 is released from Net1 through the actions of the Cdc14 early anaphase release (FEAR) network, whereas in late anaphase the MEN serves to sustain Cdc14 release such that its substrates are dephosphorylated and the cell exits mitosis.

Over the past year, Ramzi Azzam has established that phosphorylation of Net1 by cyclin B-Cdk complexes is a key step that underlies the release of Cdc14 from the nucleolus during early anaphase. Angie Mah has characterized the substrate specificity of protein kinase Dbf2, which is the last known component of the MEN that lies upstream of RENT. Angie hopes to use this information to understand how Dbf2 promotes the dissociation of RENT. Dane Mohl has investigated how nuclear transport may contribute to regulation of the RENT complex and exit from mitosis.

232. p97 regulation via interaction with a variety of p47-related co-factors

Gabriela M. Alexandru

The 97 kDa valosin-containing protein (p97 or VCP) is a type II AAA (ATPase associated with a variety of activities) ATPase, highly conserved from archaeobacteria to mammals. p97 plays a role in many seemingly unrelated cellular activities, such as membrane fusion, endoplasmic reticulum-associated degradation (ERAD), cell cycle regulation and protein degradation.

All of these functions involve recognition of ubiquitinated protein-substrates and, at least in some cases, their subsequent degradation by the proteasome. In its active form, p97 forms homohexameric barrel structures in which the N-termini are free to bind specific co-factors. Thus, p97 in complex with p47 is thought to regulate membrane fusion, while p97/Npl4/Ufd1 complexes are mainly required for ERAD. In an attempt to further understand the molecular basis of p97's diverse functions we have analyzed p97 immunoprecipitates from human tissue culture cells by MuDPIT mass spectrometry, searching for new p97 co-factors. This analysis revealed a whole group of previously unidentified p97-binding partners, all sharing a domain structure similar at least in part to p47. Two of them have been linked to the human diseases like atopic dermatitis and alveolar soft part sarcoma. However, the biological function for most of these proteins is largely unknown. By studying these proteins we hope to identify new p97 targets, specific for each of the above co-factors, and thereby unravel which of the many p97 functions they regulate.

233. Structural studies of the 19S proteasome regulatory particle
Xavier I. Ambroggio

Cytosolic proteins in eukaryotes are typically degraded by the 26S proteasome via the ubiquitin conjugation pathway. Degradation of ubiquitinated proteins by the proteasome is accomplished through a multi-step process in which the ubiquitin signal is recognized by the proteasome and cleaved from the substrate, the substrate is unfolded in an ATP-dependent manner, translocated through the proteasome core, and subsequently degraded. It is not clear how or in what order these activities occur. The 26S proteasome is composed of a 20S core particle and a 19S regulatory particle. The 20S core particle is a barrel-shaped structure of four stacked heptameric rings, with proteolytic active sites facing the lumen of the two central rings. Substrates are delivered to the proteolytic active sites by the 19S regulatory particle, which is composed of two distinct sub-particles, the base and lid. Six of the eight base subunits contain AAA ATPase domains and are thus thought to function like the hexameric ATPase rings that unfold proteins in other systems, such as NSF in membrane fusion and the more pertinent prokaryotic homologs, Clp protease and HslUV, that degrade misfolded proteins. Our knowledge of the lid particle is more limited than that of the base because of the lack of well-studied homologous particles. Recently, we have shown that the lid particle is responsible for the cleavage of ubiquitin chains from substrates and have determined that the domain responsible, the JAMM domain, has a metalloprotease-like active site on a cytidine deaminase fold (Ambroggio et al., 2004). Aside from Rpn11, the JAMM domain subunit, the lid contains seven other subunits whose functions are largely a mystery. To form an integrated view of 26S proteasome operation, we are currently pursuing the

atomic structures of the sub-complexes of the 19S proteasome regulatory particle.

234. Nedd8 protein modification, the COP9 signalosome and SCF

Gregory Cope

The COP9 signalosome (CSN) is a multi-subunit complex conserved from human to fission yeast *S. pombe*. This complex has been attributed to play a role in multiple processes, including photomorphogenesis in plants and cell cycle control in *S. pombe*. We have recently identified the CSN to be associated with multiple cullin proteins (termed Cul1-5) in mammalian and yeast cells (Lyapina et al. [2001] *Science* 292:1382-1385). Cullins are members of a class of E3 ubiquitin ligases that target specific substrates for ubiquitin-dependent proteolysis. One mode of regulation of cullins is through the covalent modification with the ubiquitin-like protein Nedd8. This modification increases Cul1 ubiquitin ligase activity toward substrates in vitro and is essential in the fission yeast *S. pombe*. Interestingly, we have found that CSN can promote the cleavage of the ubiquitin-like molecule Nedd8 from *S. pombe* Cul1 in vitro and in vivo. Moreover, this activity requires a putative metallo enzyme motif in Jab1/Csn5, which we term JAMM (Jab1 associated metallo motif). Through genetic and biochemical analysis, we have found that JAMM is essential for Cul1 deneddylation and acts positively on Cul1 activity in vivo [Cope et al. (2002) *Science* 298:608-611].

In an effort to more thoroughly understand the role of deneddylation of cullins in mammalian cells, we have utilized siRNA techniques to remove Csn5 from human cultured cells. We have established a human cell line from which we can inducibly deplete Csn5, and found that loss of Csn5 in human cells is lethal. Furthermore, marked changes in SCF activity and composition are found within these cells, suggesting an essential role for deneddylation in maintaining SCF integrity in vivo. We are currently attempting to characterize the mechanisms by which both neddylation and deneddylation exert their influence on SCF in vivo and in vitro.

235. Role of ubiquitin-activating enzyme in ubiquitin-dependent degradation

Nazli Ghaboosi

The ubiquitin-dependent degradation pathway begins with the activation of ubiquitin by the E1 ubiquitin-activating enzyme. The ubiquitin moiety is transferred to one of several E2 ubiquitin-conjugating enzymes and is subsequently attached to the substrate with the aid of an E3 ubiquitin ligase. The multi-ubiquitinated substrate is then targeted for degradation by the 26S proteasome through a poorly understood mechanism. It was originally thought that all substrates for the 26S proteasome must be ubiquitinated for proper targeting. However, there is convincing evidence that some proteins are targeted to the proteasome without ubiquitin modification. These ubiquitin-independent substrates call into question the necessity of ubiquitination in proteasomal targeting, as

well as the mechanism of substrate-proteasome interactions.

We would like to examine the role of ubiquitination in substrate targeting to the proteasome by identification of ubiquitin-independent substrates and ubiquitin-independent proteasome-interacting proteins. While the list of known E2s, E3s, and substrates is steadily growing, there is only one E1 enzyme in all somatic eukaryotic cell types. At the apex of this intricate network, E1 offers a unique perspective from which to address the many unanswered questions regarding proteasomal targeting.

Using random mutagenesis, we created several temperature-sensitive mutants of the essential yeast E1 gene, UBA1. We screened these mutants for stabilization of several test substrates and isolated a mutant strain, *uba1-204*, which exhibits a tightly regulated protein degradation defect. At the restrictive temperature, these cells rapidly lose all detectable ubiquitin-protein conjugates and stabilize all tested ubiquitin pathway substrates. Therefore, using this mutant it is possible to conditionally disrupt the entire downstream ubiquitination pathway. This system is being employed to determine the ubiquitin-dependence of proteasome-interacting proteins by comparing mass spectrometric profiles of affinity-purified 26S proteasomes from wild-type and *uba-204* mutant cells. In addition, E1-independent substrates are being identified using quantitative proteomics to screen for short-lived proteins that are not stabilized in the mutant cells.

236. Using MudPIT to characterize components of the proteasome pathway in yeast
Johannes Graumann

Multidimensional protein identification technology (MudPIT) is a method developed by the laboratory of John Yates at Scripps to analyze complex protein mixtures. In MudPIT, a sample is digested with protease and the resulting peptides are separated on a multidimensional capillary column that is in-line with the electrospray interface of an ion trap mass spectrometer [Link et al., 1999, *Nat. Biotechnol.* 17(7):676-682]. We recently demonstrated that this technology is sufficiently mature to be imported into a cell biology lab and applied to the proteomic characterization of multiple components of a cellular reaction pathway – i.e., pathway proteomics (Graumann et al., 2004).

Recent work in the lab (Verma et al., 2004) has revealed a novel layer of substrate specificity in the ubiquitin-proteasome system. Ubiquitinated proteins bind specific receptor proteins, which help guide the substrate to the proteasome for proteolysis. By performing MudPIT analysis of immunoprecipitates of receptor proteins and known proteasome substrates, we hope to shed light on the mechanism by which different substrates are sorted to different receptors.

237. Determining the function of the six ATPases in the 19S subunit of the proteasome
Gary Kleiger

Ubiquitin-dependent proteolysis of proteins by the proteasome is highly regulated. The 19S particle, a large protein complex containing at least 20 distinct protein subunits, regulates degradation of ubiquitinated proteins in yeast. The 19S contains six ATPases that are all essential for viability in yeast. After more than a decade since their discovery, the relevance of the ATPase activity of each of these proteins towards proteasome function is largely undetermined. The goal of this research project is to find a molecule that binds to the ATP-binding pocket of these proteins and acts as an inhibitor of ATPase activity. This will be achieved by using ATP analogues that have been modified with various alkyl groups. Only those ATP-binding proteins that have been mutated to enlarge the ATP-binding pockets will accept the ATP analogues. All other ATP-binding proteins in the cell should be unaffected, as the ATP analogue would be too big to be accommodated in the ATP-binding site. This will allow the targeting of a specific ATPase in the 19S for inhibition in both in vivo and in vitro proteasome degradation assays. Identification of an ATP analogue and corresponding ATP-binding site mutation that accepts the analogue may be useful to other researchers for studying the function of the more than 100 ATPases in yeast cells.

238. The roles of ubiquitin-mediated proteolysis in transcription
Rusty Lipford, Geoff Smith

The ubiquitin-proteasome system (UPS) plays numerous diverse roles in the regulation of transcription. We are studying the impact of the UPS on the function of yeast transcriptional activators, like Gcn4 and Gal4, which are targeted for ubiquitination and degradation. Previous studies of Gcn4 established that this activator of amino acid biosynthesis genes is a target for SCF-mediated ubiquitination and proteolysis. In addition these studies illuminated a role in Gcn4 ubiquitination for the cyclin-dependent kinase, Srb10, a component of the mediator complex of the RNA polymerase II holoenzyme. These findings suggest that the transcription machinery and, therefore, the transcription process are coupled to turnover of the activator. Most recently, we have demonstrated that inhibition of the UPS at any step (e.g., ubiquitin expression, E2 function, E3 function, or proteasome function) reduces the transcriptional activity of Gcn4 and Gal4. In fact impaired UPS function appears to prevent the association of RNA polymerase II with the promoters of target genes despite the accumulation of excess activator at these sites. These findings point to a previously unappreciated, positive role for the UPS in transcriptional activation. We are currently attempting to understand how the UPS may be facilitating the association of RNA polymerase II with activator-bound promoters. We are also interested in characterizing other transcriptional activators that are regulated by the UPS in

this manner and other mechanisms by which the UPS influences transcription.

239. Control of mitotic exit in *S. cerevisiae*

Angie Mah, Ramzi Azzam

Exit from mitosis is triggered by the loss of cyclin-dependent kinase (Cdk) activity by degradation of mitotic cyclins and accumulation of Cdk inhibitors. Cdc14 plays a critical role as it dephosphorylates, and thereby activates, the inhibitors of mitotic Cdk. Cdc14 is held in an inactive state in the nucleolus by Net1. Its release is modulated by two groups of proteins, the FEAR (Cdc Fourteen Early Anaphase Release) network and Mitotic Exit Network (MEN). The FEAR network consists of Cdc5, Spo12, Esp1 and SIK19, which control release of Cdc14 from the nucleolus during early anaphase. This release is transient, and though not essential for mitotic exit, is required for timely exit. Recent data from our group has shown that Net1 phosphorylation by Clb/Cdk is required for FEAR (Azzam et al., 2004). We are currently investigating how the FEAR network regulator Fob1 contributes to Net1 phosphorylation by CDK.

Unlike the FEAR network, the MEN is essential for mitotic exit. This regulatory group consists of Tem1, Lte1, Cdc15, Dbf2/20, Mob1 and Cdc5. MEN is required for the sustained release of Cdc14 during late anaphase. We previously demonstrated that Cdc15 directly phosphorylates and thereby activates Dbf2, another protein kinase, but only when Dbf2 is bound to Mob1 [Mah et al. (2001) Proc. Natl. Acad. Sci. 13:7325-7330].

The substrate for the Dbf2-Mob1 kinase complex remains elusive. In collaboration with Michael Yaffe's group, we have determined the optimal phosphorylation motif for Dbf2. By defining a consensus phosphorylation sequence, we hope to identify a Dbf2 substrate(s) that ultimately links the MEN pathway to its effector, Cdc14. To narrow the list of candidate substrates that contains this sequence, we have collaborated with Michael Snyder's group. Their lab has produced protein chips imprinted with the yeast proteome. By using these chips, proteins that are phosphorylated by the Dbf2-Mob1 kinase complex were detected. Combining these results with mass spectrometry data of Cdc14-interacting proteins, we hope to determine the downstream target(s) of the Dbf2-Mob1 kinase complex that mediates the effects of Dbf2 on the Cdc14-Net1 protein complex.

240 Analysis of proteasome substrate specificity by mass spectrometry

Thibault Mayor

In the cell, a large portion of protein degradation is carried out by the ubiquitin-proteasome system. Proteins to be degraded are targeted by covalent conjugation of a multi-ubiquitin chain. The multi-ubiquitin chain is formed by the attachment of ubiquitin to a lysine residue on the substrate. This is followed by the attachment of successive ubiquitins to the lysine 48 residue of the previously attached ubiquitin. Once the growing

chain contains at least four ubiquitins, it is recognized by the proteasome and the substrate can be degraded.

In the past few years, proteins that bind multi-ubiquitin chains (e.g., Rpn10, Rad23, and Dsk2) have been implicated as substrate receptors for the proteasome. In recent work, Rati Verma has shown that proteasome substrates require specific ubiquitin chain receptors to be degraded. This observation suggests that there is specificity in substrate degradation at the level of proteasome recognition. To further investigate this issue we established an affinity purification method for ubiquitin conjugates, which are then sequenced by in-line liquid chromatography/tandem mass spectrometry (LC-MS/MS). By identifying ubiquitinated proteins that accumulate in a mutant as compared to wild-type cells, we can now identify specific substrates for that particular receptor (e.g., Rpn10 substrates accumulate as ubiquitinated polypeptides in *rpn10Δ*). This approach will allow us to better understand the mechanism underlying the specificity in substrate recognition by the proteasome and will uncover the substrate proteins that are targeted to degradation by any given receptor.

241. Regulation of *Saccharomyces cerevisiae* Cdc14
Dane Mohl

Faithful inheritance of the genome requires tight control over chromosome segregation and cytokinesis. In budding yeast, two regulatory networks coordinate the activation of protein phosphatase Cdc14 with progression through anaphase in order to ensure accurate partitioning of the chromosomes.

Cdc14 is bound to Net1 and sequestered to the nucleolus in an inactive state during the majority of the cell cycle. In early anaphase, Cdc14 is briefly released from Net1 through the activity of the FEAR (Cdc fourteen early anaphase release) network. This transient release is believed to play a role in stabilizing the elongating microtubule spindle and recruiting to the nucleolus factors that are necessary for rDNA segregation. During late anaphase, the mitotic exit network (MEN) coordinates sustained release of Cdc14 with the completion of DNA segregation by monitoring the movement of a single-spindle pole body into the daughter compartment of the predivisional cell. Sustained release of Cdc14 ultimately triggers the destruction of B-type cyclins (Clb) and accumulation of Sic1, a Clb/Cdk inhibitor. These two events conspire to eliminate mitotic cyclin-Cdk activity, leading to exit from mitosis.

The focus of my work is to understand how the MEN brings about the sustained release of Cdc14 from the nucleolus. Our results suggest that both the FEAR network and MEN oppose the sequestration of Cdc14 by activating cell cycle kinases that phosphorylate members of the RENT complex and disrupt binding of Cdc14 to Net1.

242. Mechanisms of multiubiquitin chain synthesis by Cdc34

Matthew D. Petroski

The molecular mechanisms involved in synthesizing and attaching multiubiquitin chains onto targeted substrates through the combined activities of enzymes of the ubiquitin-proteasome system remain largely unknown. Using the ubiquitination of the budding yeast cyclin-dependent kinase inhibitor Sic1 by the Cdc34/SCF^{Cdc4} pathway as a model, we have developed Sic1 substrates containing a defined number of ubiquitin accepting sites that support ubiquitination of Sic1 and its subsequent degradation by the 26S proteasome in vitro and in vivo (Petroski and Deshaies, 2003). Of the 20 lysine residues scattered throughout Sic1, simultaneous mutation of six within the N-terminal region stabilizes Sic1, and adding back any single one of these lysines restores degradation. Substrates are ubiquitinated in vitro with identical kinetics regardless of whether the substrate contains a single lysine or the full complement of lysine residues. Furthermore, using antibodies specific for either mono ubiquitin or multiubiquitin chain attachments onto a substrate, we can show that a single chain is preferentially synthesized even in the presence of multiple substrate lysines. This ubiquitination appears to be highly processive as 6 to 20 ubiquitin molecules are simultaneously attached to a single acceptor site on Sic1. These chains are linked together exclusively via the lysine 48 residue of ubiquitin, suggesting an intrinsic mechanism for restricting ubiquitin lysine usage by Cdc34/SCF^{Cdc4}. Taken together, our results suggest that ubiquitin-ubiquitin attachments are kinetically favored over the initial ubiquitin-substrate attachment. Using this system, we have identified a novel mechanism that underlies the processive synthesis of ubiquitin chains by Cdc34.

243. Targeting cancer-promoting proteins for ubiquitination and degradation

Kathleen M. Sakamoto

We developed a new approach to cancer therapy that exploits the unique characteristics of the ubiquitin-dependent proteolytic system of eukaryotic cells. The goal of my project has been to identify a cell-permeable molecule that binds to the substrate-docking site of a ubiquitin ligase. By covalently linking this molecule to compounds that bind the target, we developed a novel class of drugs, ProTacs (Proteolysis Targeting Chimeric Pharmaceuticals) that trigger the destruction of proteins in cells for which there exists a small, cell-permeable ligand. We designed a ProTac that contains a peptide that binds with high affinity to the substrate-docking domain of the ubiquitin ligase SCF^{β-TRCP}. We then chemically linked the peptide to the fungal metabolite ovalicin, which binds covalently and specifically to the cellular enzyme methionine aminopeptidase-2 (MetAP-2). We demonstrated as "proof of principle" that the resulting peptide-ovalicin ProTac chimera tethers MetAP-2 to SCF^{β-TRCP}, and targets MetAP-2 for ubiquitination and degradation [Sakamoto et al. (2001) Proc. Natl. Acad. Sci.

98:8554-9]. To determine whether ProTacs could recruit different substrates to the SCF^{β-TRCP} ubiquitin ligase for ubiquitination through non-covalent interactions, we generated ProTacs containing the IκBα phosphopeptide linked to estradiol and testosterone. Both the estrogen receptor (ER) and androgen receptor (AR) have been shown to enhance growth of breast and prostate cancer, respectively. We demonstrated that ProTacs can also promote the ubiquitination and degradation of ER and AR in vitro and in vivo (Sakamoto et al., 2003). In addition, we tested a cell-permeable ProTac that contains the HIF-1 peptide linked to testosterone that targets the AR to the VHL ubiquitin ligase. Treatment of cells with the HIF-1-DHT ProTac resulted in AR degradation by the proteasome (Schneekloth et al., 2004). Future goals will focus on developing ProTacs into an effective drug for the treatment of cancer.

244. Determining the requirements for proteolysis by purified 26S proteasomes

Rati Verma, Robert Oania

Labile substrates of the 26S proteasome are earmarked for proteolysis by the covalent attachment of a multiubiquitin chain on acceptor lysines. Ubiquitinated proteins are then recruited to the 26S proteasome, where they are destroyed. We have recently shown that the multiubiquitin chain-binding proteins (MCBPs) Rad23 and Rpn10 function as receptors to recruit substrates to the proteasome (Verma et al., 2004). Under physiological conditions, the receptors display selectivity in substrate targeting, although all substrates presumably contain the universal targeting signal—a tetraubiquitin chain. We are currently investigating the molecular basis of this selectivity. Some of the hypotheses that we are entertaining to explain receptor preference are: differential subcellular localization; exact time of degradation (e.g., cell cycle timing or response to a signal); relative position of the ubiquitin chain(s) (N- or C-terminal); relative juxtaposition of ubiquitin chain(s); and structural elements within the substrate and the topology of lysine linkages within the ubiquitin chain. It is possible that receptor preference may be dictated by no single factor, but by some combination of factors. In addition, we are also investigating novel putative receptor pathways, namely those involving Cdc48, and its different interacting partners such as Shp1 and Ufd1.

Publications

- Ambroggio, X.I., Rees, D.C. and Deshaies, R.J. (2004) JAMM: A metalloprotease-like zinc site in the proteasome and signalosome. *PLoS Biol.* 2:0113-0119.
- Azzam, R., Chen, S.L., Shou, W., Mah, A.S., Alexandru, G., Nasmyth, K., Annan, R.S., Carr, S.A. and Deshaies, R.J. (2004) Phosphorylation by cyclin B-Cdk underlies release of mitotic exit. *Science* 305:516-519.
- Cope, G.A. and Deshaies, R.J. (2003) COP9 signalosome: A multifunctional regulator of SCF and other cullin-based ubiquitin ligases. *Cell* 114:663-671.

- Graumann, J., Dunipace, L.A., Seol, J.H., McDonald, W.H., Yates, J.R. III, Wold, B.J. and Deshaies, R.J. (2003) Applicability of TAP-MudPIT to pathway proteomics in yeast. *Mol. Cell. Proteo.* 3:266-237.
- Lipford, J.R. and Deshaies, R.J. (2003) Diverse roles for ubiquitin-dependent proteolysis in transcriptional activation. *Nat. Cell Biol.* 5:845-850.
- Petroski, M.D. and Deshaies, R.J. (2003) Redundant degrons ensure the rapid destruction of sic1 at the g1/s transition of the budding yeast cell cycle. *Cell Cycle* 2:410-411.
- Petroski, M.D. and Deshaies, R.J. (2003) Context of multiubiquitin chain attachment influences the rate of Sic1 degradation. *Mol. Cell* 11:1435-1444.
- Sakamoto, K.M., Kim, K.B., Verma, R., Ransick, A., Stein, B., Crews, C.M. and Deshaies, R.J. (2003) Development of PROTACs to target cancer-promoting proteins for ubiquitination and degradation. *Mol. Cell Proteo.* 2:1350-1358.
- Schneekloth, J.S. Jr., Fonseca, F.N., Koldobskiy, M., Mandal, A., Deshaies, R., Sakamoto, K. and Crews, C.M. (2004) Chemical genetic control of protein levels: Selective in vivo targeted degradation. *J. Am. Chem. Soc.* 126:3748-3754.
- Verma, R., Oania, R., Graumann, J. and Deshaies, R.J. (2004) Multiubiquitin chain receptors define a layer of substrate selectivity in the ubiquitin-proteasome system. *Cell* 118:99-110.
- Verma, R., Peter, N.R., Tochtrop, G.P., Sakamoto, K.M., D'Onofrio, M., Varadan, R., Fushman, D., Deshaies, R.J. and King, R.W. (2004) Inhibition of proteasome-dependent degradation by a small molecule that binds the ubiquitin chain. *Science*. In press.
- Wertz, I.E., O'Rourke, K.M., Zhang, Z., Dornan, D., Arnott, D., Deshaies, R.J. and Dixit, V.M. (2004) Human De-etiolated-1 regulates cJun by assembling a CUL4A ubiquitin ligase. *Science* 303:1371-1374.

Professor of Biology: William G. Dunphy
 Senior Research Associate: Akiko Kumagai
 Research Fellows: Seong-Yun Jeong, Soo-Mi Kim, Joon Lee, Wenhui Li, Hae Yong Yoo
 Graduate Students: Daniel Gold, Juan Ramirez-Lugo, Karen Wawrousek
 Research and Laboratory Staff: Esther Bae, Timur Pogodin

Support: The work described in the following research reports has been supported by:
 Howard Hughes Medical Institute
 National Institutes of Health, USPHS

Summary: In eukaryotic cells, the cyclin-dependent kinases (Cdks) control the progression of the cell cycle by regulating the accurate replication of the genome during S-phase and the faithful segregation of the chromosomes at mitosis (M-phase). The entry into these phases of the cell cycle is controlled by Cdks called S-phase promoting factor (SPF) and M-phase promoting factor (MPF). The action of these Cdks must be controlled both temporally and spatially in a very stringent manner. This strict regulation is imparted by a number of checkpoint mechanisms. For example, cells containing unreplicated DNA cannot enter mitosis due to the mobilization of the replication checkpoint. The Dunphy laboratory is engaged in the elucidation of the molecular mechanisms underlying the regulation of SPF and MPF during the cell cycle. Most of these experiments are conducted with *Xenopus* egg extracts, a system in which the entire cell cycle can be reconstituted *in vitro*.

The first member of the cyclin-dependent protein kinase family described is M-phase promoting factor (MPF), which contains the Cdc2 protein kinase and a regulatory subunit known as cyclin B. Since the identification of the molecular components of MPF, there has been rapid and extensive progress in unraveling the biochemistry of mitotic initiation. It is now well established that MPF acts by phosphorylating a myriad of structural and regulatory proteins that are involved directly in mitotic processes such as nuclear membrane disintegration, chromosome condensation, and mitotic spindle assembly. An ongoing challenge to the cell cycle field is the elucidation of how these phosphorylation reactions regulate the structural and functional properties of the various targets of MPF.

We have been most interested in how the cyclin-dependent protein kinases are regulated during the cell cycle. The principal focus of our laboratory has been on the regulatory mechanisms that govern the activation of MPF at the G2/M transition. Some immediate and long-term issues that we are tackling include:

1. What controls the timing of MPF activation so that it occurs at a defined interval following the completion of DNA replication?
2. How do various checkpoint or feedback controls influence the Cdc2/cyclin B complex?
3. What are the molecular differences between the simple biphasic cell cycle found in early embryonic cells and the more complex cell cycles that arise later in development?

More recently, we have been able to study at the molecular level some of the key events leading to the initiation of DNA replication at the G1/S transition. These events involve a cooperative interaction between the Origin Recognition Complex (ORC), the Cdc6 protein, and members of the Mcm family. These studies may ultimately help us understand how S-phase and M-phase are integrated with one another.

In principle, the regulation of cyclin-dependent kinases such as MPF could occur at any of several levels, including synthesis of the cyclin protein, association between the Cdc2 and cyclin proteins, or posttranslational modification of the Cdc2/cyclin complex. The posttranslational regulation of the Cdc2/cyclin complex is particularly important, even in early embryonic cells that manifest the simplest cell cycle programs. In recent years, many of the elaborate details of this Cdc2 modification process have been defined. For example, the binding of cyclin results in three phosphorylations of Cdc2: one at threonine 161 that is required for Cdc2 activity, and two dominantly inhibitory phosphorylations at threonine 14 and tyrosine 15. A variety of genetic and biochemical experiments have established that the inhibitory tyrosine phosphorylation of Cdc2 is an especially important mechanism of cell cycle regulation. As described in greater detail below, there is now strong evidence that the decision to enter mitosis involves considerably more than the tyrosine dephosphorylation of Cdc2. However, a thorough understanding of the kinase/phosphatase network that controls the phosphotyrosine content of Cdc2 will provide a firm foundation for understanding other facets of mitotic regulation.

Our laboratory has made substantial contributions to understanding the molecular mechanisms controlling the activation of the Cdc2 protein. For our studies, we utilize cell-free extracts from *Xenopus* eggs. Due to pioneering work in a number of the laboratories, it is now possible to re-create essentially all of the events of the cell cycle in these extracts. Consequently, it is feasible to study the molecular mechanisms of Cdc2 regulation in intricate detail with this experimental system. To facilitate these studies, we make extensive use of recombinant DNA technology to overproduce cell cycle proteins in either bacteria or baculovirus-infected insect cells. Moreover, in conjunction with our biochemical studies, we are taking advantage of the fission yeast system to exploit genetic approaches to identify novel *Xenopus* regulators of the cell cycle.

245. Positive regulation of Wee1 by Chk1 and 14-3-3 proteins
 Joon Lee, Akiko Kumagai, William G. Dunphy
 Wee1 inactivates the Cdc2-cyclin B complex during interphase by phosphorylating Cdc2 on Tyr-15. The activity of Wee1 is highly regulated during the cell cycle. In frog egg extracts, it has been established previously that *Xenopus* Wee1 (Xwee1) is present in a hypophosphorylated, active form during interphase and undergoes down-regulation by extensive phosphorylation at M-phase. We report that Xwee1 is also regulated by association with 14-3-3 proteins. Binding of 14-3-3 to Xwee1 occurs during interphase, but not M-phase, and

requires phosphorylation of Xwee1 on Ser-549. A mutant of Xwee1 (S549A) that cannot bind 14-3-3 is substantially less active than wild-type Xwee1 in its ability to phosphorylate Cdc2. This mutation also affects the intranuclear distribution of Xwee1. In cell-free kinase assays, Xchk1 phosphorylates Xwee1 on Ser-549. The results of experiments in which Xwee1, Xchk1, or both were immunodepleted from *Xenopus* egg extracts suggested that these two enzymes are involved in a common pathway in the DNA replication checkpoint response. Replacement of endogenous Xwee1 with recombinant Xwee1-S549A in egg extracts attenuated the cell cycle delay induced by addition of excess recombinant Xchk1. Taken together, these results suggest that Xchk1 and 14-3-3 proteins act together as positive regulators of Xwee1.

246. Requirement for Atr in phosphorylation of Chk1 and cell cycle regulation in response to DNA replication blocks and UV-damaged DNA in **Xenopus** egg extracts

Zijian Guo, Akiko Kumagai, Sophie X. Wang, William G. Dunphy

The checkpoint kinase Xchk1 becomes phosphorylated in *Xenopus* egg extracts in response to DNA replication blocks or UV-damaged DNA. Xchk1 is also required for the cell cycle delay that is induced by unreplicated or UV-damaged DNA. In this report, we have removed the *Xenopus* homolog of ATR (Xatr) from egg extracts by immunodepletion. In Xatr-depleted extracts, the checkpoint-associated phosphorylation of Xchk is abolished, and the cell cycle delay induced by replication blocks is strongly compromised. Xatr from egg extracts phosphorylated recombinant Xchk1 *in vitro*, but not a mutant form of Xchk1 (Xchk1-4AQ) containing nonphosphorylatable residues in its four conserved SQ/TQ motifs. Recombinant human ATR, but not a kinase-inactive mutant, phosphorylated the same sites in Xchk1. Furthermore, the Xchk1-4AQ mutant was found to be defective in mediating a checkpoint response in egg extracts. These findings suggest that Xchk1 is a functionally important target of Xatr during a checkpoint response to unreplicated or UV-damaged DNA.

247. Claspin, a novel protein required for the activation of Chk1 during a DNA replication checkpoint response in **Xenopus** egg extracts

Akiko Kumagai, William G. Dunphy

We have identified Claspin, a novel protein that binds to *Xenopus* Chk1 (Xchk1). Binding of Claspin to Xchk1 is highly elevated in the presence of DNA templates that trigger a checkpoint arrest of the cell cycle in *Xenopus* egg extracts. Xchk1 becomes phosphorylated during a checkpoint response, and we demonstrate directly that this phosphorylation results in the activation of Xchk1. Immunodepletion of Claspin from egg extracts abolishes both the phosphorylation and activation of Xchk1. Furthermore, Claspin-depleted extracts are unable to arrest the cell cycle in response to DNA replication blocks. Taken together, these findings indicate that Claspin is an essential upstream regulator of Xchk1. We are currently

analyzing various facets of the structure and function of Claspin.

248. Repeated phosphopeptide motifs in Claspin mediate the regulated binding of Chk1
Akiko Kumagai, William G. Dunphy

In vertebrates, the checkpoint-regulatory kinase Chk1 mediates cell cycle arrest in response to DNA replication blocks and UV-damaged DNA. The activation of Chk1 depends on both the upstream regulatory kinase ATR and Claspin. Claspin is a large acidic protein that becomes phosphorylated and binds to Chk1 in the presence of checkpoint-inducing DNA templates in *Xenopus* egg extracts. Through deletion analysis, we have identified a 57 amino acid region of Claspin that is both necessary and sufficient for binding to *Xenopus* Chk1. This Chk1-binding domain (CKBD) contains two highly conserved repeats of approximately ten amino acids. A serine residue in each repeat (Ser-864 and Ser-895) undergoes phosphorylation during a checkpoint response. A mutant of Claspin containing non-phosphorylatable amino acids at positions 864 and 895 cannot bind to Chk1 and is unable to mediate its activation. These experiments indicate that two phosphopeptide motifs in Claspin are essential for checkpoint signaling.

249. Claspin, a Chk1-regulatory protein, monitors DNA replication on chromatin independently of RPA, ATR, and Rad17

Joon Lee, Akiko Kumagai, William G. Dunphy

Claspin is required for the ATR-dependent activation of Chk1 in *Xenopus* egg extracts containing incompletely replicated DNA. We show here that Claspin associates with chromatin in a regulated manner during S-phase. Binding of Claspin to chromatin depends on the pre-replication complex (pre-RC) and Cdc45 but not on replication protein A (RPA). These dependencies suggest that binding of Claspin occurs around the time of initial DNA unwinding at replication origins. By contrast, both ATR and Rad17 require RPA for association with DNA. Claspin, ATR, and Rad17 all bind to chromatin independently. These findings suggest that Claspin plays a role in monitoring DNA replication during S-phase. Claspin, ATR, and Rad17 may collaborate in checkpoint regulation by detecting different aspects of a DNA replication fork.

250. **Xenopus** Drf1, a regulator of Cdc7, accumulates on chromatin in a checkpoint-regulated manner during an S-phase arrest
Stephanie K. Yanow, Daniel A. Gold, Hae Yong Yoo, William G. Dunphy

We have cloned a *Xenopus* Dbf4-related factor named Drf1 and characterized this protein by using *Xenopus* egg extracts. Drf1 forms an active complex with the kinase Cdc7. However, most of the Cdc7 in egg extracts is not associated with Drf1, which raises the possibility that some or all of the remaining Cdc7 is bound to another Dbf4-related protein. Immunodepletion of Drf1 does not prevent DNA replication in egg extracts. Consistent with this observation, Cdc45 can still associate with chromatin in Drf1-depleted extracts, albeit at

significantly reduced levels. Nonetheless, Drf1 displays highly regulated binding to replicating chromatin. Treatment of egg extracts with aphidicolin results in a substantial accumulation of Drf1 on chromatin. This accumulation is blocked by addition of caffeine and by immunodepletion of either ATR or Claspin. These observations suggest that the increased binding of Drf1 to aphidicolin-treated chromatin is an active process that is mediated by a caffeine-sensitive checkpoint pathway containing ATR and Claspin. Abrogation of this pathway also leads to a large increase in the binding of Cdc45 to chromatin. This increase is substantially reduced in the absence of Drf1, which suggests that regulation of Drf1 might be involved in the suppression of Cdc45 loading during replication arrest. We also provide evidence that elimination of this checkpoint causes resumed initiation of DNA replication in both *Xenopus* tissue culture cells and egg extracts. Taken together, these observations argue that Drf1 is regulated by an intra-S phase checkpoint mechanism that downregulates the loading of Cdc45 onto chromatin containing DNA replication blocks.

251. Phosphorylated Claspin interacts with a phosphate-binding site in the kinase domain of Chk1 during ATR-mediated activation
Seong-Yun Jeong, Akiko Kumagai, Joon Lee, William G. Dunphy

Claspin is essential for the ATR-dependent activation of Chk1 in *Xenopus* egg extracts containing incompletely replicated or UV-damaged DNA. The activated form of Claspin contains two repeated phosphopeptide motifs that mediate its binding to Chk1. We show that these phosphopeptide motifs bind to Chk1 by means of its N-terminal kinase domain. The binding site on Chk1 involves a positively charged cluster of amino acids that contains lysine 54, arginine 129, threonine 153, and arginine 162. Mutagenesis of these residues strongly compromises the ability of Chk1 to interact with Claspin. These amino acids lie within regions of Chk1 that are involved in various aspects of its catalytic function. The predicted position on Chk1 of the phosphate group from Claspin corresponds to the location of activation-loop phosphorylation in various kinases. In addition, we have obtained evidence that the C-terminal regulatory domain of Chk1, which does not form a stable complex with Chk1 under our assay conditions, nonetheless has some role in Claspin-dependent activation. Overall, these results indicate that Claspin docks with a phosphate binding site in the catalytic domain of Chk1 during activation by ATR. Phosphorylated Claspin may mimic an activating phosphorylation of Chk1 during this process.

252. Adaptation of a DNA replication checkpoint response depends upon inactivation of Claspin by the Polo-like kinase
Hae Yong Yoo, Akiko Kumagai, Anna Shevchenko, Andrej Shevchenko, William G. Dunphy

The checkpoint mediator protein Claspin is essential for the ATR-dependent activation of Chk1 in *Xenopus* egg extracts containing aphidicolin-induced DNA replication blocks. We show that during this checkpoint

response Claspin becomes phosphorylated on threonine-906 (T906), which creates a docking site for Plx1, the *Xenopus* Polo-like kinase. This interaction promotes the phosphorylation of Claspin on a nearby serine (S934) by Plx1. After a prolonged interphase arrest, aphidicolin-treated egg extracts typically undergo adaptation and enter into mitosis despite the presence of incompletely replicated DNA. In this process, Claspin dissociates from chromatin and Chk1 undergoes inactivation. By contrast, aphidicolin-treated extracts containing mutants of Claspin with alanine substitutions at positions 906 or 934 (T906A or S934A) are unable to undergo adaptation. Under such adaptation-defective conditions, Claspin accumulates on chromatin at high levels and Chk1 does not decrease in activity. These results indicate that the Plx1-dependent inactivation of Claspin results in termination of a DNA replication checkpoint response.

253. Absence of BLM leads to accumulation of chromosomal DNA breaks during both unperturbed and disrupted S-phases
Wenhui Li, Soo-Mi Kim, Joon Lee, William G. Dunphy

Bloom's syndrome (BS), a disorder associated with genomic instability and cancer predisposition, results from defects in the BLM protein. In BS cells, chromosomal abnormalities such as sister chromatid exchanges occur at highly elevated rates. Using *Xenopus* egg extracts, we have studied *Xenopus* BLM (Xblm) during both unperturbed and disrupted DNA replication cycles. Xblm binds to replicating chromatin and becomes highly phosphorylated in the presence of DNA replication blocks. This phosphorylation depends upon *Xenopus* ATR (Xatr) and Rad17 (Xrad17), but not Claspin. Xblm and *Xenopus* topoisomerase III α (Xtop3 α) interact in a regulated manner and associate with replicating chromatin interdependently. Immunodepletion of Xblm from egg extracts results in accumulation of chromosomal DNA breaks during both normal and perturbed DNA replication cycles. Disruption of the interaction between Xblm and Xtop3 α has similar effects. The occurrence of DNA damage in the absence of Xblm, even without any exogenous insult to the DNA, may help to explain the genesis of chromosomal defects in BS cells.

254. Mcm2 is a direct substrate of ATM and ATR during DNA damage and DNA replication checkpoint responses

Hae Yong Yoo, Anna Shevchenko, Andrej Shevchenko, William G. Dunphy

In vertebrates, ATM and ATR are critical regulators of checkpoint responses to damaged and incompletely replicated DNA. These checkpoint responses involve the activation of signaling pathways that inhibit the replication of chromosomes with DNA lesions. In this report, we describe isolation of a cDNA encoding a full-length version of *Xenopus* ATM. Using antibodies against the regulatory domain of ATM, we have identified the essential replication protein Mcm2 as an ATM-binding protein in *Xenopus* egg extracts. *Xenopus* Mcm2 undergoes phosphorylation on serine 92 (S92) in response to the presence of double-stranded DNA breaks or DNA

replication blocks in egg extracts. This phosphorylation involves both ATM and ATR, but the relative contribution of each kinase depends upon the checkpoint-inducing DNA signal. Furthermore, both ATM and ATR phosphorylate Mcm2 directly on S92 in cell-free kinase assays. Immunodepletion of both ATM and ATR from egg extracts abrogates the checkpoint response that blocks chromosomal DNA replication in egg extracts containing double-stranded DNA breaks. These experiments indicate that ATM and ATR phosphorylate the functionally critical replication protein Mcm2 during checkpoint responses that prevent the replication of abnormal chromosomes.

Publications

- Dunphy, W.G. (2003) Properties of the Cdc25 family of cell-cycle regulatory phosphatases. In: Handbook of Cell Signaling, Bradshaw, R.A. and Dennis, E.A. (eds), Elsevier Academic Press, Chapter 115, pp. 693-696.
- Jeong, S.-Y., Kumagai, A., Lee, J. and Dunphy, W.G. (2003) Phosphorylated Claspin interacts with a phosphate-binding site in the kinase domain of Chk1 during ATR-mediated activation. *J. Biol. Chem.* 278:46782-46788.
- Kumagai, A. and Dunphy, W.G. (2003) Repeated phosphopeptide motifs in Claspin mediate the regulated binding of Chk1. *Nature Cell Biol.* 5:161-165.
- Kumagai, A., Kim, S.-M. and Dunphy, W.G. (2004) Claspin and the activated form of ATR-ATRIP collaborate in the activation of Chk1. *J. Biol. Chem.* In press.
- Lee, J., Kumagai, A. and Dunphy, W.G. (2003) Claspin, a Chk1-regulatory protein, monitors DNA replication on chromatin independently of RPA, ATR, and Rad17. *Mol. Cell* 11:329-340.
- Li, W., Kim, S.-M., Lee, J. and Dunphy, W.G. (2004) Absence of BLM leads to accumulation of chromosomal DNA breaks during both unperturbed and disrupted S-phases. *J. Cell Biol.* 165:801-812.
- Yanow, S.K., Gold, D.A., Yoo, H.Y. and Dunphy, W.G. (2003) Xenopus Drf1, a regulator of Cdc7, displays checkpoint-dependent accumulation on chromatin during an S-phase arrest. *J. Biol. Chem.* 278:41083-41092.
- Yoo, H.Y., Kumagai, A., Shevchenko, A., Shevchenko, A. and Dunphy, W.G. (2004) Adaptation of a DNA replication checkpoint response depends upon inactivation of Claspin by the Polo-like kinase. *Cell* 117:575-588.
- Yoo, H.Y., Shevchenko, A., Shevchenko, A., and Dunphy, W.G. (2004). Mcm2 is a direct substrate of ATM and ATR during DNA damage and DNA replication checkpoint responses. *J. Biol. Chem.* In press.

Assistant Professor of Biology: Grant J. Jensen
 Postdoctoral Scholars: Cristina Iancu, Elizabeth Wright
 Graduate Students: Jordan Benjamin, Greg Henderson,
 Peter Leong, Dylan Morris, Gavin Murphy
 Research Staff: Prabha Dias, Jane Ding, Bernard
 Heymann, Bill Tivol
 Undergraduates: Tim Barnes, Bingni Wen

Support: The work described in the following reports has been supported by:

Agouron Foundation
 DOE
 Gordon and Betty Moore Foundation
 NIH
 Searle Foundations

Summary: If we could simply look inside a cell and see its molecular components in all their complexes and conformations, cell biology would be all but finished. We are developing cryoelectron microscopy-based technologies to do this for at least the largest macromolecular complexes, hoping to show both how individual proteins work together as large "machines" and how those machines are organized into "assembly lines" within living cells. In addition, we have now begun simulation projects to understand how such spatial relationships affect cellular processes. Our cryoelectron microscopy projects range from imaging individual macromolecules to complex biochemical reactions to organelles and even to intact cells. We use two basic data collection strategies. The first, called "tomography," involves imaging a single unique object (such as a cell) from multiple directions and then merging those projections into a three-dimensional reconstruction. The second, called "single particle analysis," involves imaging a large number of identical copies of a target object (such as a purifiable protein complex), and again merging the images to produce a three-dimensional reconstruction. Both techniques are in their infancy, but together hold the promise of completing what could be called the "structural biology continuum" in a step-wise fashion by showing first how individual proteins (visible by X-ray crystallography and NMR spectroscopy) come together to form complexes (visible by single particle analysis), and how those complexes are organized within living cells (visible by electron tomography). This structural data, in turn, informs whole-cell models of the interactions of all the cell's molecular components.

Both single particle analysis and tomography begin by spreading the sample in a thin film (~300 nm) across an electron microscope grid and then plunging it into liquid ethane, which causes the water to form vitreous, rather than crystalline, ice, and preserves the sample in a native state without any unnatural fixatives, resins, or stains. For tomography, the sample is imaged from a series of angles by incrementally tilting a goniometer through ~140 degrees. For single particle analysis, each copy of the sample ("particle") structure freezes with a random orientation with respect to the plane of the grid so

that tilting is not necessary. Instead, images of hundreds of thousands of individual particles are recorded and then aligned and averaged in three-dimensions computationally. The target resolution for single particle analysis is 4-10Å, where the secondary structure of a particle can be seen and fitting atomic models of components is possible. The target resolution for tomography is 3-6 nm, where the identity, location, and orientation of individual macromolecules can be seen in their cellular contexts.

This year's milestones include completing the installation and trouble-shooting of our state-of-the-art, 300 kV, helium-cooled, FEG "Polaris" TEM. We have also now assessed the advantages/disadvantages of helium cooling, "predictive" tomography software, and the "flip-flop" dual-axis-tilting cryostage. We have applied these technical advances to several biological targets including HIV, a "minimal" bacterial cell, and a small-cell model of asymmetric cell division.

255. Comparison of helium and nitrogen as cryogens for tomography of purified protein complexes

Cristina Iancu, Bernard Heymann, Grant Jensen

EM as a technique is capable of revealing structures at atomic-level detail. Biological samples, however, are particularly sensitive to radiation damage, so their structures as solved by "cryo"-EM are routinely of only medium resolution. Helium cooling may allow the use of 3-6 times higher doses than those employed at liquid nitrogen temperature. We set out to do a systematic study to assess the effects that dose and temperature of data collection have on the resolution (quality) of reconstructions obtained by either tomography or single particle analysis techniques, for large protein structures.

For tomography, we use as a model system hemocyanin, an 8 MDa protein complex, whose structure is known to ~11Å resolution by EM single particle analysis. Tomograms of hemocyanin in solution were collected at seven different doses ranging from 10 to 350 e/Å², at both helium and liquid nitrogen temperatures. Hemocyanin molecules extracted from the tomographic reconstructions were compared to the reference map and the average cross-correlation coefficient was used as a measure of the tomogram quality. We also collected dose series in which successive images were collected of the same field of particles, in steps of 5 or 10 e/Å². Single particle analysis reconstructions were done for each image in the dose series and the dependence of the Fourier shell correlation coefficient (FSC) of the reconstructions with respect to the dose was analyzed. From these studies we determined that the rate of radiation damage is the same for both temperatures, for the resolution range that tomography can render (up to 35-40 Å). We also found optimal dose conditions for which tomographic reconstructions of hemocyanin most closely match the reference map. These dose conditions can now be used for the tomography of other protein complexes. Additionally, we determined that radiation damage is expressed differently at the two temperatures: at 80 K, as the dose

increases, the crisp shape of hemocyanin molecules becomes gradually smeared, but their contrast is retained, while at 10 K there is a progressive loss of contrast up to $\sim 200 \text{ e}/\text{\AA}^2$, and after $\sim 250 \text{ e}/\text{\AA}^2$, white bubbles appear in place of the initially dark hemocyanin subunits. We conclude that the optimal dose for tomography of purified protein complexes is $\sim 120 \text{ e}/\text{\AA}^2$, and the best results are obtained when the sample is cooled with liquid nitrogen.

256. Reducing charging effects at helium temperatures

Bill Tivol, Tim Barnes, Grant Jensen

When a high-voltage electron beam passes through a vitrified biological sample, covalent bonds are broken, secondary electrons escape, and the structure is gradually destroyed. Past experience has shown that cooling the sample to liquid nitrogen ($\sim 90\text{K}$) or even liquid helium temperatures ($\sim 10\text{K}$) seems to slow this radiation damage, perhaps by constraining molecular fragments and reactive intermediates. Unfortunately, such cooling also dramatically reduces the conductivity of the underlying carbon support film and exacerbates the problem of having temporary unmatched positive charges that cause the sample to move and distort.

We are testing whether thin films of titanium on our samples can alleviate this charging problem at liquid helium temperatures ($\sim 10\text{K}$). Among the metals that have high conductivity near absolute zero, titanium is relatively light (thus producing less background signal) and attractive for this purpose. This year we have produced thin, perforated, titanium films suitable for cryoEM specimen support and have begun to compare their charging characteristics at under liquid nitrogen and liquid helium cooling.

257. Development of dual-axis cryoelectron tomography

Bill Tivol, Bernard Heymann, Grant Jensen

In electron tomography, the sample is prepared as a thin sheet of material and imaged throughout a range of tilt angles. This range is limited, however, to approximately ± 70 degrees because the path length through the sample becomes exponentially large as the tilt angle approaches 90 degrees. Following the projection theorem, the Fourier transform of each projection is a central slice of the object's three-dimensional transform. Thus if the projection angles are limited, there arises a "wedge" of missing data in the three-dimensional transform of the object that gives rise to an anisotropic resolution degradation in the reconstruction. One way to alleviate the problem is to collect tilt series along two orthogonal axes. We have pioneered the use of a new, prototype-stage that allows dual-axis tilting, and have documented significant improvements in the quality of resulting reconstructions.

With dual-axis tilting, the missing "pyramid" of data can be reduced to just $\sim 16\%$ of the total information in reciprocal space. There are two physical laws that constrain the scattering phenomena which may allow us to

extrapolate much of that missing information: unitarity, which means that the sum of the scattering in all directions must be equal to the incident beam, and analyticity, which means that the scattering amplitudes and all their derivatives must be continuous. We are designing algorithms to use these constraints to extrapolate data into the missing pyramid and improve the quality of our tomographic reconstructions.

258. Tomography of HIV at various stages of maturation

Jordan Benjamin, Bill Tivol, Grant Jensen

HIV is perhaps the most extensively studied "organism" in terms of structural biology. It has three layers: an outer lipid membrane, the protein shell known as the matrix, and the capsid, an inner protein shell housing the genome. The structures of nearly every component of HIV have been determined in isolation, some in many different conformations and with various inhibitors, but it is still unclear how individual subunits come together to form the intact virion. Furthermore, the virus goes through multiple stages of maturation wherein the structures of these shells change in poorly understood ways. We are working to determine the three-dimensional structure of HIV at various stages of maturation by cryoelectron tomography. The structures that we obtain will allow us to confirm or refute various models that have been proposed about the organization of the protein shells and the changes underlying maturation.

In the mature form of the virus, the capsid can have numerous morphologies, with the most common being a somewhat asymmetrical cone. We are interested in understanding the mechanisms allowing such structural diversity, as well as the actual variety of morphologies and their possible functional importance. We have collected a number of dual-axis tilt series of frozen-hydrated HIV virions and produced tomographic reconstructions from them. Some of the challenges of this project include developing computational methods for classifying and measuring the morphologies of observed structures, three-dimensional alignment and averaging of repetitive structures within each unique virion, and improvements in imaging protocols to achieve higher-resolution reconstructions. Our eventual goal is to have tomographic reconstructions of HIV virions at all stages of maturation at high enough resolution to allow fitting of atomic models from X-ray and NMR data.

259. Cryoelectron tomography of a minimal cell, **Mesoplasma florum**

Elizabeth R. Wright, Grant J. Jensen

Mesoplasma florum, which inhabits citrus plants, is a simple gram-positive bacterial descendent of the class Mollicutes. The bacteria of this class have generally been termed some of the simplest free-living organisms because they lack a cell wall, outer membrane, and periplasmic space; and do not have many of the complex biosynthetic and intermediate metabolic pathways. *M. florum* has a very small genome of approximately 793 Kbp, in which

~685 proteins have been identified. *M. florum* also ranges in size from 200 to 800 nm. The simplicity and small size of *M. florum* make it an ideal specimen for whole cell cryoelectron tomography.

The wild-type strain of *M. florum* (ATCC 33453) was grown in Mycoplasma medium (ATCC 243) with the addition of phenol red as a growth indicator. Cell suspensions were flash frozen onto lacey or Quantifoil carbon grids in liquid ethane with a Vitrobot using predetermined conditions. The frozen grids were stored under liquid nitrogen until transfer to the microscope for imaging. All images of *M. florum* were recorded on our 300 kV "G2 Polara" TEM with the samples cooled by liquid nitrogen. Tilt series were collected from ~ -65° to ~ +65° with a 1° tilt step, and then the grid was rotated ~90° about the Z-axis and a second tilt series was collected from ~ -65° to ~ +65°.

As a starting point for the collection and analysis of data, two variables, the defocus and the dose, were varied to determine the optimal imaging protocol. The defocus was varied between -8 and -15 μm in order to enhance certain features of the cells such as the cell membrane or internal features like ribosomes. The total dose was varied between 30 $\text{e}^-/\text{\AA}^2$ and 120 $\text{e}^-/\text{\AA}^2$. This was done to determine not only what was tolerable for the cells, but also what would provide the greatest contrast for the cellular features. Through the analysis of the data, it has become apparent that a higher defocus provides better definition of the cell membrane, whereas a lower defocus enhanced the macromolecules contained within the cells. The total dose to which the cells were exposed impacts our ability to identify macromolecules within the cells. It appears as though the higher the dose that the cells were able to withstand, the better defined the cell contents. Current efforts are being devoted to refining the computational methods that will be employed to identify the large protein complexes within the cells.

260. Electron tomography of *Mycoplasma genitalium*

Greg Henderson, Grant Jensen

Mycoplasma genitalium is the smallest and genetically simplest living cell, but that simplicity is unlikely to be reflected in its ultrastructural organization. Electron tomography of frozen hydrated cells is a new, noninvasive, imaging technique ideally suited to study the supramolecular organization of the cytoplasm. We will use cryoelectron tomography to identify and localize large macromolecular protein complexes inside *M. genitalium* to ask the following questions: do cellular processes such as translation, glucose metabolism, and ATP generation occur in a spatially random manner, or is there a discernable underlying organization, and does *M. genitalium* have a cytoskeleton? Characterization of the attachment organelle, which is used by the cell to adhere to the host's epithelium, has revealed a detergent-insoluble component referred to as a cytoskeleton. Many of the proteins involved are known, but it is not understood how these proteins interact. A three-dimensional macromolecular

model of the attachment organelle will reveal the structure of any cytoskeleton and show the macromolecular structural basis of the attachment organelle's functions. Furthermore, our structural studies of the replication and segregation of the attachment organelle may reveal the fundamental mechanisms of bacterial genome segregation.

261. Electron tomography of *E. coli*

Gavin Murphy, Grant Jensen

Molecular biology, genetics and biochemistry have combined to approach a comprehensive understanding of the classic model cell, *E. coli*. There is now a need to compile the data in mathematical models and observe an entire cell in its natural, complete state. Cryoelectron tomography has advanced to the point where it might now reveal the number and location of the largest macromolecules in *E. coli* in their natural environment. Such information would allow spatially explicit, structure-based mathematical models of *E. coli* metabolism and physiology to be developed. This will be essential for accurate modeling, because, for instance, if a component is found to be located only in certain areas, the mathematical assumption that the component is well-mixed in the cell would be false. Accurately describing and simulating such spatially restrained components and systems is the long-term goal of structure-based systems biology.

The goal of the project is to determine the structure of many, whole *E. coli* cells to approximately 4 nm resolution using cryoelectron tomography of unfixed, unsectioned and unstained cells and to computationally identify macromolecular complexes and filaments. A resolution of 4 nm will probably be detailed enough to recognize protein complexes larger than ~1 Megadalton – including the ribosome, the pyruvate dehydrogenase multienzyme complex and the 2-oxoglutarate dehydrogenase multienzyme complex – and recently discovered cytoplasmic filaments like MreB, ParM, MinD, MinE and FtsZ. Larger features like the nucleoid might also be visible. The assumption that the prokaryotic cell is merely a "bag of enzymes" will be tested by locating these complexes in the cell and discovering any relevant distribution patterns. So far, lower resolution tomograms have been created of an *E. coli* strain, and though particular densities were visible in them, the resolution was not good enough to warrant a computationally-intensive, global cross-correlation of the tomogram with previously-determined structure templates.

262. Electron tomography of a model cell demonstrating asymmetric cell division, *Caulobacter crescentus*

Prabha Dias, Achilleas Frangakis, Grant Jensen

The structural study of the aquatic proteobacterium *Caulobacter crescentus* provides us the opportunity to make significant contributions not only to basic cell biology, but also to medicine, agriculture and applied environmental science. From a cell biological perspective, one of the reasons that the crescent-shaped *Caulobacter* is fascinating is because it is a prokaryote that

undergoes asymmetric cell division (mostly the province of eukaryotes). Its cell cycle is highly regulated both temporally and spatially. The daughter cell always arises from the tip of the crescent opposite that of the mother cell's "stalk" appendage, and the daughter cell's flagellum is at the opposite end from the site of cell division. The crescent shape of the cell almost certainly depends on some type of structural restraints within the cell, and asymmetric cell division is likely to be achieved through arranging the cell cycle components on some type of internal structure, that is, a cytoskeleton of some kind. Until relatively recently, it was thought that bacteria had very little regular internal structure and were basically a "bag of enzymes." There is now mounting evidence that this is not the case, including the discovery of bacterial homologs to eukaryotic cytoskeletal proteins such as tubulin and actin. The sequencing of *Caulobacter*'s genome revealed the presence of homologs to a third type of cytoskeletal element, intermediate filaments. This bacterium is thus an excellent place to look for a bacterial version of the eukaryotic cytoskeleton.

From a medical and agricultural perspective, *Caulobacter* is of interest because it is closely related to the human pathogens *Rickettsia prowazekii* and *Brucella abortus*, and also to the plant pathogen *Agrobacterium tumefaciens*. A better understanding of *Caulobacter*'s cell cycle could thus lead to ways to fight these pathogens. *Caulobacter* are already able to thrive in nutrient-poor environments and are known to convert toxic compounds such as heavy metals into biologically inert forms. A better understanding of how these bacteria are able to function as microbial "garbage disposals" may lead to improved methods of bioremediation of water pollution.

Until now, our knowledge of the internal structure of bacteria has been severely limited by the methods available. Bacteria in general are too small for their internal structures to be resolved by light microscopy, and *Caulobacter* is no exception. Although electron microscopy (EM) has more than enough resolving power, the difficulty associated with properly preserving bacteria for EM (i.e., chemical fixation and plastic embedding) had retarded progress. Furthermore, the heterogeneous nature of bacterial cells make them unsuitable for study by methods requiring averaging over multiple cells, like single particle analysis.

Cryoelectron tomography overcomes both the limitations of conventional fixation and of the averaging requirement. We freeze individual bacteria so rapidly that no ice crystals have time to form, and the result is a bacterium "embedded" in vitreous (amorphous) ice. We can determine the three-dimensional structure of the frozen bacterium by taking images of the bacterium tilted at various degrees in the electron beam. The information in the series of tilted images can then be combined computationally using image-processing algorithms. The result is a three-dimensional map of the electron density distribution in the bacterium. We expect to achieve resolutions high enough to locate cytoskeletal filaments in

the cell, as well as find clues as to how this cell manages asymmetric division.

263. Identification of large macromolecular complexes with cryoelectron tomograms of whole cells

Jane Ding, Bingni Wen, Grant Jensen

In our tomographic reconstructions of whole cells, individual protein complexes appear as clusters of voxels with densities higher than the mean. Our goal is to identify as many of these complexes as we can by cross-correlating their three-dimensional shapes and internal density distributions against known higher resolution structures, thereby producing a map of cellular ultrastructure at the macromolecular level. Such calculations are computationally demanding, and this year we have begun implementing parallel algorithms to execute these searches on Caltech's new 168-cpu IBM cluster for structural biology. Briefly, high-resolution structures from X-ray crystallography, NMR spectroscopy, or electron microscopy are low-pass filtered and convoluted with a contrast transfer function comparable to that governing the tomographic data collection and reconstruction process to produce "templates." Next these templates are cross-correlated against large three-dimensional reconstructions of whole cells. Eventually we will implement peak searches and local, higher resolution refinement searches.

264. Spatially-explicit models of whole cells

Dylan Morris, Grant Jensen

This year we have begun a project that complements our tomographic analysis of whole cells by simulating how various spatial relationships that we believe exist in cells regulates metabolism. The ultimate goal of this work will be to create a whole-cell model of a minimal organism. Previous efforts towards this goal have relied on either continuous, ODE-based, flux balance equations, or on discrete, stochastic simulation techniques. Neither of these approaches takes into account the spatial characteristics of the processes being modeled. They treat the bacterial cell as a well-mixed bag of enzymes, despite clear evidence that in many cases they are not.

An explicit simulation will track not simply the kinds of molecular species present within the cell, but the individual instances of each such species. We will model each molecule as it diffuses about the cell, playing its specified roles within the interactome. This approach will allow us to model the structural heterogeneity of a living cell and create new avenues for *in silico* experimentation. It will allow us to study the effects of spatial fluctuations in the concentrations of molecular reactants. The first stage will be to determine if such a model is computationally feasible. If so, we will consider specific test systems to explore the advantages and disadvantages of spatially explicit simulation as compared to the traditional stochastic or continuous models.

265. Peach, an efficient distributed computational system
Peter Leong, Bernard Heymann, Cristina Iancu, Grant Jensen

As larger particles are studied at higher resolutions in structural biology, the size of data files that store this information increases dramatically. Processing large numbers of data files by a user on a single processor machine is a huge problem, as it would take months to complete due to the sheer size of the data. At the same time, the average CPU usage of any computer in the lab, averaged over weeks, is an embarrassingly small percentage of the available processing time. An alternative to buying a super computer for processing is to efficiently use all of the available CPU processing time in the lab.

We have developed a novel distributed computation system called "Peach" that allows users to easily share and take advantage of the available processing power of all the CPUs in the lab. Basically, a user of Peach queues up processing jobs with the system and awaits email notification of the completion of the jobs. The jobs are automatically distributed throughout the network and processed on CPUs that are judged idle, without interrupting any users who might be sitting at a terminal. For example, if there are 30 processors available on the network and a user has 120 jobs which each take an hour to complete, then if 50% of the computers are free, the jobs could be over in 8 hours as compared to the five days it would have taken on a single computer used 100% of the time.

The Peach system has already been tested in the Jensen lab on 18 computers that have a total of 31 processors and has been used for processing a couple of major projects.

266. Near-atomic resolution protein structure determination without crystals
Cristina Iancu, Grant Jensen

The proteasome is a large (~800 kDa) protein complex that proteolyzes ubiquitinated substrates. The structure of its 20S core is known by X-ray crystallography, but the structures of the multi-component regulatory "base" and "lid" are unknown. We are imaging the 20S core alone as part of an attempt to understand and expand the resolution limitations of the "single particle" cryoEM technique. For this the core particle is ideal in that it is commercially available in highly purified form, its structure is known, and it is large and rigid. We are preparing to record on the order of 1 million particle images and average them to determine a near-atomic resolution (4-8 Å) structure. In a complementary study we are also imaging full 26S proteasomes to determine the structure of the base and lid components.

This year we have explored the novel and potentially advantageous imaging strategies our new instrument provides, including the use of liquid helium for sample cooling. At both liquid nitrogen (~80K) and liquid helium (~10K) temperatures, we have recorded images with a range of doses from 10 to 60 e/Å² on standard film.

Each data set contains the equivalent of about 10,000 asymmetric units. We plan to produce reconstructions from each data set and compare the results to the known atomic structure from X-ray crystallography. This will identify the optimal imaging conditions to use for the upcoming, large-scale data collection and processing phases.

267. Computer simulations of image formation and three-dimensional reconstruction
Bernard Heymann, Grant Jensen

Cryoelectron microscopy of "single" particles holds the promise of determining near-atomic resolution structures of large macromolecules without any need for crystallization. Imaging biological specimens with an electron beam, however, is a destructive process, so that the total useful exposure is limited to just ~10-20 electrons/Å². The consequence is that the signal-to-noise ratio in the electron micrographs is extremely poor, and extensive image processing is required to extract correct structural information. One method to increase image contrast is to deliberately defocus the beam, which introduces a complex contrast transfer function (CTF) that must be corrected during image processing. In addition, the beam focus changes as it interacts with different layers of the specimen, complicating CTF correction. The combination of all these challenges limits the achievable resolution.

The practical question is whether we can expect to achieve near-atomic resolution with our new, state-of-the-art microscope. We are approaching this question by simulating realistic single particle images and using these images to calculate reconstructions. This artificial approach allows control over every parameter, and reveals relationships that are difficult to elucidate from micrographs of real biological molecules. A multi-slice image simulation algorithm was implemented to reflect the passage of the electron beam through the specimen. The 20S proteasome was selected as the test molecule, because its structure is known by X-ray crystallography, and we have obtained experimental images for comparison with the simulated images. To improve the realism of the simulation, the 20S proteasome was embedded in a block of water. A data set of 10000 particle images with shot noise applied was generated of the 20S proteasome randomly oriented and shifted. These particle images were used to calculate reconstructions of the 20S structure, and to test the effect of errors in CTF correction, particle translation and particle orientation. The results show that with correct particle shifts and orientations, and with accurate CTF parameters, a resolution of ~3Å can be achieved with a pixel size of 1Å/pixel. It has also been shown that with a particle the size of the 20S proteasome, the focus change through the specimen does not pose a significant barrier to achieving near-atomic resolution. Certainly, for thicker specimens, the change in focus will be more extensive and limit the achievable resolution. Errors in CTF correction up to 500Å decrease resolution to ~5Å, with severe defects appearing at larger errors. With

errors in translation or orientation, the resolution decreases linearly, but near-atomic resolution should be achievable by single particle analysis. The challenge is to improve the microscopy and image processing to the level where this can be accomplished routinely. Next we will be testing various ideas for new and improved algorithms for these tasks through application to simulated images.

Professor: Stephen L. Mayo
 Research Fellows: Karin Crowhurst, Peter Oelschlaeger, Julia M. Shifman, Thomas P. Treynor
 Graduate Students: Benjamin D. Allen, Oscar Alvizo, Eun Jung Choi, Mary Devlin, Geoffrey K. Hom, Possu Huang, Jennifer R. Keefe, Kyle Lassila, Jessica Mao, Heidi K. Privett, Premal S. Shah, Christina Vizcarra, Eric Zollars
 Research and Laboratory Staff: Marie L. Ary, Cynthia L. Carlson, Rhonda K. Digiusto, Sarah E. Hamilton

Support: The work described in the following research report has been supported by:

Army Research Office (ARO)
 DARPA
 Howard Hughes Medical Institute
 National Institutes of Health
 Ralph M. Parson's Foundation
 Yuen Grubstake Fund

Summary: The focus of the lab has been the coupling of theoretical, computational, and experimental approaches for the study of structural biology. In particular, we have placed a major emphasis on developing quantitative methods for protein design with the goal of developing a fully systematic design strategy that we call "protein design automation." Our design approach has been captured in a suite of software programs called ORBIT (Optimization of Rotamers By Iterative Techniques) and has been applied to a variety of problems ranging from protein fold stabilization to enzyme design.

268. Exploration of the neutral sequence space between pairs of proteins

Benjamin D. Allen^{*}, Stephen L. Mayo

In protein evolution, mutations in the genetic code are subject to selection based on the proteins encoded by the affected genes. Although many different protein sequences map to each folded structure, the mechanism by which natural selection generates these varied sequences remains an open problem. It is widely believed that one sequence may evolve from another through a series of single amino acid mutations that maintain the overall folded structure at every step. In this way, each 3D structure is associated with a network of sequences that are connected to each other by energetically neutral point mutations. This neutral network hypothesis is backed by experimental data for folded RNA structures, but evidence for the neutral evolution of proteins remains elusive. A method to find neutral pathways between sequences that fold to the same structure could provide information about the evolutionary relationships between proteins. Furthermore, the determination of neutral trajectories through mutation space may shed light on the biophysical ramifications of specific mutations, and might suggest potential improvements to existing protein design strategies. We have developed a computational procedure to find energetically favorable pathways between two proteins that have similar structures and a fixed set of amino acid mutations. Our program randomly generates amino acid mutations that lead from one sequence to the

other, and evaluates the energies of the resulting sequences using a Monte Carlo side chain placement calculation and a physical force field with continuum solvation. We are currently applying this procedure to protein G and protein L, two immunoglobulin-binding proteins displayed on the cell surfaces of certain infectious bacteria to avoid immune recognition by host organisms. These proteins share a common fold topology but less than 20% sequence identity. Our program indicates that there are a large number of potential neutral trajectories between these proteins. We are expressing several proteins along one particular trajectory to assess the extent of agreement between theory and experiment. Encouraging results will prompt further analysis of the biophysical properties of these hybrid sequences, such as the determination of their 3D structures and affinities for the biological-binding targets of the wild-type sequences.

^{*}Division of Chemistry and Chemical Engineering, Caltech

269. Evaluating a force field via fixed composition sequence design calculations

Oscar Alvizo^{*}, Stephen L. Mayo

A finely tuned force field is essential to protein design and protein folding. Proper tuning is problematic, however, due to difficulties in determining the appropriate scale factors for the force field parameters and in calculating the energy of proteins in the denatured state. ORBIT's force field was improved through iterative rounds of protein design calculations and experimental measurement of predicted sequence stabilities. In order to keep the energy of the denatured state constant, design calculations were performed under fixed amino acid composition restraints. Energy discrepancies between computational predictions and experimental results could then be attributed to flaws in the force field's ability to predict folded-state sequence energies. The accuracy of the force field was quantified in three ways: by comparing the amino acids of the predicted sequences to the wild type, by determining the sequence bias required to recover the wild-type sequence, and by comparing the experimental stabilities to the predicted sequence energies. The high native stability of the designed protein (the $\beta 1$ domain of protein G) and the reduced sequence space resulting from the fixed composition restriction make it highly unlikely that predicted sequences that are vastly different from wild type will be more stable. Therefore, if the predicted sequences are significantly different from wild type, then the force field needs improvement.

Calculations started at a wild-type sequence bias of 0.0 kcal/mol, which was increased by increments of 1.0 or 0.5 kcal/mol until the wild-type sequence was recovered. With standard parameters, a large bias of 6.0 kcal/mol was required to recover the wild-type sequence, highlighting the inaccuracies in the force field. Tuning decreased this to 1.0 kcal/mol. The following modifications improved the predictive power of the force field: using a solvent exclusion-based solvation model, eliminating hydrogen bonds at the surface, including a rotamer probability scale factor, and decreasing the hydrogen bond well depth and polar burial-scale factor.

These improvements increased the predictive power of the unbiased calculation by a factor of 4.5, 4.01 and 1.6 at core, boundary and surface positions, respectively.

*Graduate Option in Biochemistry and Molecular Biophysics, Caltech

270. Designing a high affinity peptide for TRAF6
Eun Jung Choi, Stephen L. Mayo

Tumor necrosis factor receptor-associated factors (TRAFs) are a family of cytoplasmic adaptor proteins in the TNFR superfamily. They elicit various cellular responses including proliferation, differentiation and apoptosis. Six members of this family are known to date, among which TRAF6 is unique because it also interacts with the interleukin-1/Toll-like receptor superfamily. We used the ORBIT protein design software to design a high affinity peptide for TRAF6; our starting model was a high-resolution crystal structure of TRAF6 in complex with the nine-residue peptide CD40. Employing the Dreiding force field and a discrete set of allowed conformers for each of the side chains, ORBIT uses a deterministic search algorithm called Dead End Elimination to find the global minimum energy conformation for a protein fold. Currently, we are using calorimetry and fluorescence polarization analysis to measure the affinity of our designed peptides. Our first design used default parameters and yielded a peptide with slightly higher affinity for TRAF6 than CD40. Since most of the designed residues are on the surface of the peptide, we hope to be able to tailor the parameters to produce a peptide with improved binding affinity. These techniques can be used in various applications including the discovery of novel ligands and therapeutics.

271. Improvement of protein design algorithms by incorporating dynamic backbone motions
Karin Crowhurst, Stephen L. Mayo

Protein function frequently relies on dynamic processes; proteins involved in ligand binding, enzyme catalysis and signal transduction often require structural flexibility and plasticity to function properly or interact with multiple targets. These entropic factors can also contribute to protein stability. Thus, the incorporation of dynamic motions into protein design algorithms could be crucial for improving the accuracy and consistency of stable de novo protein and enzyme prediction, and could have wide-ranging implications in medical and industrial applications. The goal of my project is to move towards integrating backbone flexibility and dynamic motion into ORBIT, our protein design software.

In the first experimental phase of the project, NMR spectroscopy is being used to measure the backbone and side-chain dynamics of several mutants of the $\beta 1$ immunoglobulin-binding domain of Streptococcal protein G ($G\beta 1$), for which structural flexibility is believed to significantly impact their respective stabilities (1). Detailed analysis of this data is expected to provide insight into the impact of these dynamic processes on the stability of each protein in comparison to the wild type. Measurement of backbone relaxation experiments on a highly stable hyperthermophilic variant ($G\beta 1$ -c3b4)

revealed some unexpected results. Spin-spin relaxation rate values indicate that the protein is probably a dimer in solution. This was not previously discovered, despite having successfully solved the solution structure by NMR (2), because the protein is likely forming a symmetric dimer, which is undetectable in NMR spectra. Analytical ultracentrifugation experiments confirmed that the variant is a dimer, with a $K_D=40\pm 5 \mu M$. NMR and crystallography are currently being used to map the interface and solve the structure. Once completed, the dynamics of the dimer will be characterized. These physical data will eventually be used in the modification of ORBIT's protein design algorithms to incorporate backbone mobility, which in turn will be used to design new protein variants with dynamic characteristics.

References

1. Su, A. and Mayo, S.L. (1997) *Protein Sci.* 6:1701-1707.
2. Malakauskas, S.M. and Mayo, S.L. (1998) *Nature Struct. Biol.* 5:470-475.

272. Design and testing of engineered IgG antibodies with increased *in vivo* half-lives

Mary Devlin*, Stephen L. Mayo

Monoclonal IgG antibodies are becoming increasingly important as clinical reagents used to combat a number of cancers. Antibodies consist of two regions: the antigen-binding Fab region, which varies between antibodies of different specificities, and the relatively constant Fc region, which is required for effector functions such as triggering the complement cascade and binding to Fc receptors. IgG antibodies have relatively long half-lives in the blood compared to other proteins because they are rescued from cellular degradation by the neonatal Fc receptor (FcRn). IgGs that bind more tightly to FcRn, and therefore have increased serum half-lives, are of potential therapeutic use. Interpretations of mutational studies using an FcRn/Fc co-crystal structure revealed that Fc substitutions at the interface with FcRn generally result in antibodies with lower affinity rather than higher affinity for FcRn. The FcRn/Fc co-crystal structure revealed an optimum angle adopted by the two Fc domains when complexed with FcRn, suggesting an alternative approach. We are using our ORBIT protein design software to design antibodies that are locked into the optimal conformation to bind FcRn. Substitutions are restricted to residues that could affect the Fc conformation, but do not affect interactions with FcRn. After calculating the optimal Fc sequences to produce Fc regions locked in the optimal FcRn-binding conformation, we express the designed Fcs, measure their affinity constants for FcRn-binding, and test their efficiencies in FcRn-mediated rescue from degradation.

*Graduate Option in Biochemistry and Molecular Biophysics, Caltech

273. Determining the crystal structure of a fully redesigned helical protein

Geoffrey K. Hom^{*}, Stephen L. Mayo

We use computational protein design to determine amino acid sequences that will adopt a target structure. Previously, we determined a novel sequence that was expected to adopt the backbone structure of a 51 amino-acid, globular alpha-helical fragment of the engrailed homeodomain (EH). The design was riskier than previous ones of EH, because no knowledge of the wild-type sequence (except for one glycine) was included in any step of the design process; i.e., EH was fully redesigned (EH-FR). Thermal and chemical denaturation experiments indicate EH-FR is very stable and unfolds cooperatively. 1D ¹H-NMR spectra indicate EH-FR is also well folded and helical, and the sharpness of the peaks is indicative of a monomer.

We were surprised, then, when we solved a 1.90 Å crystal structure of EH-FR and found that it actually forms a tetrameric four-helix bundle. However, the NMR structure of a very similar redesign of EH, EH-VF, was solved by others in the lab, and EH-VF is a monomer that adopts the target EH structure. Sedimentation velocity indicates EH-FR is 88% monomeric at ~5 mg/mL; thus, EH-FR's crystal structure seems discrepant to the other data we have on EH-FR. The crystal conditions for EH-FR included ~20% dioxane and 10 mM CdCl₂; we are currently trying to ascertain whether the tetramerization of EH-FR could be due to dioxane, cadmium, a higher protein concentration, etc. We are also still trying to determine if the EH-FR monomer adopts the target EH structure.

^{*}Graduate Option in Biochemistry and Molecular Biophysics, Caltech

274. Computational design and experimental characterization of *de novo* protein dimers

Possu Huang^{*}, Stephen L. Mayo

Previous efforts in designing protein-binding interfaces have focused on altering binding specificities. These methods fall short, however, when applied to the design of novel binding sites due to difficulties in accurately modeling protein backbones. Our goal was to create novel dimers from monomeric proteins. We developed a special docking algorithm that positions the member protein subunits to a plausible configuration with respect to each other using parameters determined from the structures of known protein complexes. The docking procedure treats the proteins as rigid bodies and uses Fourier correlation theorem and fast Fourier transform to efficiently search for dimers with the highest interfacial surface complementarities. Using the docked structures as scaffolds for protein design and employing hydrophobic surface residues to drive dimer formation, we demonstrated two successful designs, one heterodimer and one homodimer, using protein G and engrailed homeodomain, respectively, as the starting monomeric proteins. The computationally designed dimers were synthesized and characterized using circular dichroism, nuclear magnetic resonance, analytical ultracentrifugation, and X-ray crystallography methods. These proteins are the first *de*

novo dimers reported that were generated using a combination of protein docking and computational protein design tools. The results suggest that this strategy can be used to address the protein recognition problem and is generally applicable to creating novel binding sites with compatible binding partners.

^{*}Graduate Option in Biochemistry and Molecular Biophysics, Caltech

275. Computationally designed chorismate mutase active site variants

Jennifer R. Keefe^{*}, Stephen L. Mayo

The development and design of enzymes with improved or novel activities is one of the ultimate goals of protein design. In order to better understand how well our computational methods describe enzymatic active sites, we used ORBIT to optimize the active site of *E. coli* chorismate mutase (EcCM). During the calculations, an *ab initio* calculated transition state structure of the reaction (1) was positioned in the active site and allowed to rotate and translate. Eighteen residues surrounding the transition state structure and active site were allowed to vary in amino acid identity and conformation. The optimization predicted a sequence with six amino acid changes, of which four were determined to be independent and two coupled. In order to experimentally validate our results, we generated four point mutants (L7I, A32S, V35I, D48I) and the double mutant I81L/V85I.

Chorismate mutase activity of the wild-type and mutant enzymes was determined by monitoring the disappearance of chorismate spectrophotometrically at 275 nm at pH 7.8. The initial rate data are described by first order Michaelis-Menten kinetics, with the exception of the data from the D48I mutant, which exhibits first order solution reaction kinetics and was fit to a straight line. These experiments indicate that the A32S variant has a faster turnover rate than the wild-type enzyme. In this case, ORBIT predicted a new hydrogen bond between the serine side chain and glutamine 88, which hydrogen bonds to the transition state structure. To the best of our knowledge, this is the first reported EcCM mutant that exhibits increased activity over wild type at physiological pH. Two of the variants, L7I and V35I, show activities comparable to wild type, while the double mutant, I81L/V85I, exhibits approximately 50% of the wild-type activity. The D48I mutant showed no activity over background.

Although every variant is not optimally active, this study indicates that ORBIT is capable of optimizing the active site of an enzyme and predicting mutations that stabilize the transition state.

^{*}Graduate Option in Biochemistry and Molecular Biophysics, Caltech

Reference

- (1) Wiest, O. and Houk, K.N. (1994) *J. Org. Chem.* 59:7582-7584.

276. Computational design of a novel enzyme for catalysis of a pericyclic reaction

Kyle Lassila*, Stephen L. Mayo

We are working towards the goal of fully-automated enzyme design. In particular, we hope to apply computational protein design methods to the task of creating a completely novel catalyst for the Claisen rearrangement of chorismate to prephenate. Naturally catalyzed by the chorismate mutases, this reaction offers many desirable features as an early test of enzyme design methods. The reaction is a first-order sigmatropic rearrangement of a single substrate and has neither intermediate steps nor involvement of catalytic groups such as general acids or bases. The reaction has been extensively studied in many contexts—as a rare enzyme-catalyzed pericyclic process, as an essential step in the biosynthesis of aromatic compounds, and as a rare example of a reaction that occurs through identical mechanisms enzymatically and in solution. Our method of enzyme design involves identifying amino acid sequences likely to bind to an ab initio transition state structure of the chorismate-prephenate rearrangement. As a part of this process, we are testing new methods that allow translation and rotation of the transition state structure within a binding cavity while simultaneously optimizing protein side chain identity and conformation. These methods will be generally applicable to the design of ligand-binding sites and enzyme active sites. The ability to computationally design new reaction catalysts can be expected to have important implications for organic synthesis, bioremediation, and biotechnology.

*Graduate Option in Biochemistry and Molecular Biophysics, Caltech

277. Computational design of a novel aldolase

Jessica Mao*, Stephen L. Mayo

Designed enzymes are attractive industrially for their efficiency, substrate specificity, and stereoselectivity. To date, there are few enzymes used in organic synthesis. The aldol condensation is one of the most important and widely utilized carbon-carbon bond-forming reactions in synthetic chemistry. It is the reaction between two aldehyde/ketone groups, yielding a β -hydroxy-aldehyde/ketone that upon dehydration by acid or base affords an enone. While natural aldolases are efficient, they are very limited in their substrate range. Novel aldolases that catalyze reactions between desired substrates would be a powerful synthetic tool. They would expand the limited repertoire of designed enzymes and further our understanding of their structure/function relationship. We are adopting the "compute and build" design cycle that combines theory, computation, and experiment to rationally design a novel aldolase. Our initial design will catalyze the reaction between acetone and benzaldehyde via the enamine mechanism that natural class I aldolases utilize. The design is currently performed on the backbone structures of triosephosphate isomerase (TIM) and ribose-binding protein (RBP). Both proteins are interesting scaffolds for building a novel protein catalyst. We chose the $(\alpha/\beta)_8$ -barrel fold of TIM because of its prevalence. This fold accounts for ~10% of all known proteins and all but one are enzymes. The ubiquity of the fold and its ability to catalyze a wide variety of reactions make it an interesting system to study. RBP was chosen because its natural substrate bears structural resemblance to the modeled

high-energy state of the chosen aldol reaction. After the potential catalytic sites are identified, we apply positive design to increase the affinity of the protein for the substrate. This can be done by designing in noncovalent interactions that stabilize the high-energy state. A favorable design has been generated and the proteins have been expressed and purified. An enzyme assay has also been developed to monitor reaction progress. Further experiments are underway, and the results will be used to optimize our design process.

*Division of Chemistry and Chemical Engineering, Caltech

278. **In silico** prediction of metallo- β -lactamases with improved catalytic efficiency

Peter Oelschlaeger, Stephen L. Mayo

Metallo- β -lactamases (MBLs) have recently raised major concern due to their ability to hydrolyze a broad spectrum of β -lactam antibiotics and thus, confer resistance to bacteria. In contrast to serine- β -lactamases, which use a serine-dependent mechanism to cleave the amide bond of the β -lactam ring, MBLs use zinc ions to activate a hydroxide for the nucleophilic attack. Two MBLs, IMP-6 and IMP-1, differ by a single residue, but have significantly different substrate spectra, and it is assumed that IMP-1 evolved from IMP-6. Molecular dynamics (MD) simulations of IMP-6 and IMP-1 in complex with near-transition-state intermediates of different β -lactam substrates were performed using a cationic dummy atom approach to represent the zinc ions (1). Stability scores for these complexes, obtained from multiple simulations with different starting conditions and at different temperatures, correlated well with experimental data (k_{cat}/K_M 's) and provided insights into the molecular basis of substrate specificity (2).

Motivated by the observed correlation for wild-type enzymes, we selected five point mutants of IMP-6 and submitted them to MD simulations in complex with ceftazidime, a broad-spectrum cephalosporin. Mutants with high stability scores (suggesting high catalytic efficiency and improved antibiotic resistance) were selected for experimental validation: they were expressed in *E. coli*, purified, and characterized biochemically (3). Catalytic efficiencies (k_{cat}/K_M 's) toward ceftazidime and six additional β -lactam antibiotics were determined. All mutants exhibited improved activity toward at least one antibiotic compared to IMP-6. Therefore, this in silico selection method led to mutants that have not been described previously but that represent a potential clinical threat because they can easily evolve from IMP-6. However, not all mutants converted ceftazidime more efficiently, indicating that the computational predictions are not always accurate. Currently, the MD simulation procedure is being refined. In addition, we are exploring a reactive MD simulation approach in collaboration with William A. Goddard for the prediction of activation barriers of the enzyme-catalyzed β -lactam hydrolysis. Computational protein design is employed to predict stable well-folded mutants.

References

- (1) Oelschlaeger, P., Schmid, R.D. and Pleiss, J. (2003) *Protein Eng.* 16:241-50.
- (2) Oelschlaeger, P., Schmid, R.D. and Pleiss, J. (2003) *Biochemistry* 30:8945-56.
- (3) Oelschlaeger, P., Mayo, S.L. and Pleiss, J. (2004) Submitted.

279. Computational design of a novel enzyme to catalyze a kinetic resolution

Heidi K. Privett, Stephen L. Mayo

Fully automated enzyme design can be envisioned as the solution to many complex synthetic organic chemistry problems. Enzymes are ideal for catalysis of organic reactions because of their extremely high rates of catalysis and their ability to perform a wide variety of chemical transformations with extreme regio- and enantioselectivity. With an increasing demand for enantiomerically pure, complex, biologically-active compounds (i.e., drugs), synthetic chemists will have to look beyond standard chemical strategies in favor of the high yields and strict selectivity of enzymatic reactions. Designed enzymes will allow the scope of enzymatic reactions to be expanded beyond the limits of natural enzymes, broadening the range of possible substrates and products.

Kinetic resolutions are a useful method for transforming a racemic starting material into an enantiomerically pure product. Our goal is to show that an enzyme can be designed to carry out a dynamic kinetic resolution using the enantioselective ring opening of 2-phenyl-4-benzylphenyloxazolin-5-one (FOX) to produce N-benzoyl-L-phenylalanine as a model system. To this end, the binding pocket and backbone structure of multiple non-catalytic periplasmic-binding proteins from *E. coli*, including maltose-binding protein and ribose-binding protein, are being evaluated for their fitness to serve as the scaffold for a novel active site for the FOX ring opening.

We are using the ORBIT protein design software to design an optimal active site around an ab initio calculated transition state of the L-FOX reaction in each of the potential scaffolds. The transition state structure is allowed to rotate and translate concurrent with the active site variation so that the active site residues and the transition state location are optimized with respect to one another. Based on the computational results, we will choose the scaffold that permits the best packing of active site residues against the transition state, best stabilizes the transition state through electrostatic and hydrogen bonding interactions, and excludes binding of the D-FOX transition state. The best designs will be synthesized and experimentally evaluated.

280. Water-soluble membrane proteins by computational design

Premal S. Shah*, Stephen L. Mayo

Integral membrane proteins (IMP) reside in the hydrophobic environment of lipid bilayers, and thus, their amino acid composition and molecular surfaces differ from water-soluble proteins. Originally, it was hypothesized that IMPs are "inside-out" proteins with nonpolar surfaces and polar cores. This idea was deemed incorrect when it was shown that the packing density and amino acid composition of IMP cores is the same as water-soluble proteins. As a result, it is generally believed that IMPs can be stabilized in aqueous

solution by just altering their surfaces to resemble those of water-soluble proteins. There is ample motivation for obtaining water-soluble membrane proteins: it would help elucidate the forces contributing to IMP stabilization in membranes, X-ray crystallographers would benefit from the higher yields typically achieved, and drug design efforts towards IMPs would be aided by the ability to work with these proteins in detergent-free solutions.

We compared the exposed nonpolar surface areas of IMPs with water-soluble proteins and found that IMPs distributed in a narrow range centered at 93%, while the water-soluble proteins display a distribution centered at 63%. This analysis served as a guide for conversion of the IMP bacteriorhodopsin (BR) to a water-soluble protein; we designed the surface of BR so that its nonpolar surface area decreased into the range of water-soluble proteins. BR is a 249-residue plasma membrane protein of the archaeon *Halobacterium salinarum*. It has a covalently attached chromophore, retinal, whose isomerization assists in BR's proton pump functionality. In our design, 58 residues were mutated to form WSBRO_HT.

WSBRO_HT contains an N-terminal His6 tag and is expressed in *E. coli* as inclusion bodies. Following purification on a Ni²⁺ affinity column under denaturing conditions, the protein is folded by rapid dilution and then concentrated to a final working concentration. The protein is soluble in 1.5 M NaCl, 50 mM phosphate, pH 7.5 up to concentrations of at least 12.5 mg/ml. Gel filtration and analytical ultracentrifugation indicate that the protein exists in an equilibrium between monomer, trimer, and higher order oligomeric states. Far-UV circular dichroism spectroscopy suggests it has mostly helical character. Further physical and structural studies are ongoing.

*Graduate Option in Biochemistry and Molecular Biophysics, Caltech

281. Computational design of Ca²⁺-deficient calmodulin: Interactions with protein kinase II

Julia M. Shifman, Mee H. Choi*, Mary B. Kennedy**, Stephen L. Mayo

Interactions of a Ca²⁺ sensor calmodulin (CaM) with a calmodulin-dependent protein kinase II (CaMKII) are central to the Ca²⁺ signaling pathways implicated in learning and memory. Ca²⁺ signals of different magnitude and duration are sensed by CaM that can bind up to four Ca²⁺ ions. Ca²⁺ binding to CaM induces a conformational change within the protein that is essential for recognition and activation of many CaM-regulated proteins including CaMKII. CaMKII activated by Ca²⁺/CaM phosphorylates a number of downstream protein targets in synapses. Traditionally, it was believed that binding of all four Ca²⁺ ions to CaM is a prerequisite for CaM-induced activation of CaMKII. However, the observed Ca²⁺ concentrations even during the periods of Ca²⁺ influx into the spine are too low to be consistent with this hypothesis. To investigate whether CaM can activate CaMKII with only two bound Ca²⁺ ions, we constructed two CaM mutants: one that binds Ca²⁺ ions only at the C-terminal domain (N^{MUT}C^{WT}), and one that binds only at the N-terminal domain (N^{WT}C^{MUT}). Both mutants were designed

computationally using our ORBIT protein design software. In each CaM mutant, the inactivated domain was designed by stabilizing it in the "closed" Ca^{2+} -free conformation, while the other domain was kept intact. Ionization mass spectrometry confirmed the 2:1 Ca^{2+} /CaM stoichiometry for the designed mutants. Both mutants were able to interact with and activate CaMKII at a Ca^{2+} concentration of 300 μM . Moreover, $\text{N}^{\text{MUT}}\text{C}^{\text{WT}}$ could activate CaMKII at lower Ca^{2+} concentrations of 5-10 μM and at a CaM concentration of 3 μM , the concentrations believed to occur in postsynaptic density in spines. Our findings show that differential activation of signaling enzymes by partially saturated CaM may contribute to synaptic plasticity's sensitivity to the timing and magnitude of postsynaptic Ca^{2+} flux. Our work suggests the need to reevaluate the sensitivity of other postsynaptic signaling enzymes to CaM containing less than four bound Ca^{2+} ions.

*Postdoctoral Scholar, Mary Kennedy's Lab, Division of Biology, Caltech

**Professor of Biology, Caltech

282. Improved continuum electrostatic solvation for protein design

Christina Vizcarra*, Stephen L. Mayo

Until now, damped Coulombic potentials, as well as empirical surface area and volume scaling functions, have been used to include electrostatic solvation energy in computational protein design. These methods have allowed for the successful design of stable proteins but have been a limiting factor in the rational design of enzymatic activity and molecular recognition, for which polar and charged amino acids are key. To bring protein design energy functions up to date with these new challenges, we are investigating more sophisticated continuum models for electrostatic solvation. Two related obstacles to improving electrostatic solvation energy functions are the combinatorial explosion in protein design, which requires energy scores for many side-chains and pairs of side-chains and therefore a very fast energy solver, and the need to calculate energies in one-body (single side-chain) and two-body (pairs of side-chains) terms without any knowledge of the rest of the structure. We are first interested in using fast perturbation methods for two-body terms, allowing for the computationally lengthy numerical solution to the Poisson equation for a large number of side-chain pairs. We are also testing the speed and accuracy of various analytical Generalized Born methods. Coupled with strategies for approximating a molecular surface during the design calculation, both of these approaches allow us to more accurately describe the energy of a protein's charge distribution in the context of its molecular geometry and surrounding solvent. Such improvements in the electrostatic solvation energy model for protein design will have a significant impact in the areas of enzyme design and molecular recognition.

*Division of Chemistry and Chemical Engineering, Caltech

283. Force field development for protein design

Eric Zollars*, Stephen L. Mayo

Protein design is an exceptionally difficult problem characterized by unique complications. Necessary restrictions such as a fixed backbone and discrete side-chain conformations require different considerations of structure-energy relationships than other fields of protein simulation. This

structure-energy relationship is the focus of our recent research, which strives to address issues including the identity of the forces that lead to protein stability and the relative strengths of these forces. Additionally, the mathematical representation of these forces must be relatively simple to allow for tractable calculations.

To this end, we developed a database of protein mutations with known thermodynamic stabilities. The gain or loss of stability of these mutants should allow for a structural characterization of free energy change based upon the identity of the mutated position. However, this is a non-trivial problem, as the forces that lead to a stable, folded protein are not quantitatively known. Thus, we hope for a "sum of terms" that will adequately represent the variety of forces contributing to protein stability. These terms include classical physical terms such as dispersion and electrostatic forces as well as terms that describe the hydrophobic effect and side-chain conformational energy. As the "sum of terms" approaches quantitative agreement with observed results taken from the database, we assume a more accurate representation of the forces involved in protein stability.

*Graduate Option in Biochemistry and Molecular Biophysics, Caltech

Reference

Mooers, B.H.M., Datta, D., Baase, W.A., Zollars, E.S., Mayo, S.L. and Matthews, B.W. (2003) *J. Mol. Biol.* 332(3):741-756.

Publications

Anderson, M.J. and Mayo, S.L. (2004) Protein solvent-accessible surface areas by pairwise decomposition. Submitted.

Bolon, D.N., Marcus, J.S., Ross, S.A. and Mayo, S.L. (2003) Prudent modeling of core polar residues in computational protein design. *J. Mol. Biol.* 329(3):611-622.

Choi, E.J. and Mayo, S.L. (2004) Generation and analysis of proline mutants in protein G. Submitted.

Gillespie, B., Vu, D.M., Shah, P.S., Marshall, S.A., Dyer, R.B., Mayo, S.L. and Plaxco, K.W. (2003) NMR and temperature-jump measurements of de novo designed proteins demonstrate rapid folding in the absence of explicit selection for kinetics. *J. Mol. Biol.* 330:813-819.

Gordon, D.B., Hom, G.K., Mayo, S.L. and Pierce, N.A. (2003) Exact rotamer optimization for protein design. *J. Comp. Chem.* 24(2):232-243.

Lazar, G.A., Marshall, S.A., Plecs, J.J., Mayo, S.L. and Desjarlais, J.R. (2003) Designing proteins for therapeutic applications. *Curr. Opin. Struct. Biol.* 13(4):513-518.

Love, J.J., Huang, P. and Mayo, S.L. (2004) A de novo designed protein/protein interface. Submitted.

Marshall, S.A., Vizcarra, C. and Mayo, S.L. (2004) Electrostatic models for protein design calculations II: One and two body decomposable Poisson-Boltzmann methods. Submitted.

Meyer, M.M., Silberg, J.J., Voigt, C.A., Endelman, J., Mayo, S.L., Wang, Z.G. and Arnold, F.H. (2003)

- Library analysis of SCHEMA-guided protein recombination. *Protein Sci.* 12(8):1686-1693.
- Moers, B.H.M., Datta, D., Baase, W.A., Zollars, E., Mayo, S.L. and Matthews, B.W. (2003) Repacking the core of T4 lysozyme by automated design. *J. Mol. Biol.* 332(3):741-756.
- Oelschlaeger, P., Mayo, S.L. and Pleiss, J. (2004) Impact of remote mutations on metallo- β -lactamase substrate specificity: Implications for the evolution of antibiotic resistance. Submitted.
- Offredi, F., Dubail, F., Kischel, P., Karinski, K. Stern, A.S., Van de Weerd, C., Hoch, J.C., Prospero, C. Francois, J.M., Mayo, S.L. and Martial, J.A. (2003) De novo backbone and sequence design of an idealized α/β -barrel protein: Evidence of stable tertiary structure. *J. Mol. Biol.* 325(1):163-174.
- Shah, P.S., Hom, G.K. and Mayo, S.L. (2004) Preprocessing of rotamers for protein design calculations. *J. Comp. Chem.* 25(14):1797-1800.
- Shifman, J.M. and Mayo, S.L. (2003) Exploring the origins of binding specificity through the computational redesign of calmodulin. *Proc. Natl. Acad. Sci. USA* 100(23):13274-13279.

Ethel Wilson and Robert Bowles Professor of Biology:
James H. Strauss
Senior Research Associate: Ellen G. Strauss
Visiting Associate: Yukio Shirako
Postdoctoral Scholar: Marlene Biller, Pritsana
Chomchan
Graduate Student: Jannigje Siebenga
Undergraduate Student: Oran Kremen
Research Laboratory Staff: Maria Farkas, Edith Lenches

Support: The work described in the following research reports has been supported by:

Ethel Wilson and Robert Bowles Professorship in
Biology
Gosney Fellowship to M.B.
National Institutes of Health

Summary: We are interested in two groups of animal viruses, the alphaviruses and the flaviviruses. These viruses contain an RNA genome of about 11,000 nucleotides and are enveloped, having a lipid envelope that surrounds an icosahedral nucleocapsid. Both alphaviruses and flaviviruses are vectored by mosquitoes and infect both mosquitoes and a wide range of vertebrates. We wish to understand the replication of alphaviruses and flaviviruses at a molecular level and to study the evolution of these two virus groups and more broadly the evolution of all RNA viruses.

The flaviviruses contain about 70 members, most of which are important human pathogens causing hundreds of millions of cases of human disease annually. Diseases caused by the flaviviruses include yellow fever, dengue fever, and encephalitis. West Nile virus, which first appeared in the Americas five years ago in New York State and then spread rapidly over most of the United States, is a member of this family. The genome RNA of about 10,700 nucleotides is the only viral message RNA and is translated into a long polyprotein that is cleaved to give both structural proteins required for virus assembly and nonstructural proteins required for RNA replication.

The alphaviruses contain about 28 members and many cause febrile illness in humans that in some cases may progress to encephalitis or polyarthritis. The genome organization of alphaviruses differs from that of flaviviruses in that the genome of 11,700 nucleotides is translated into a long nonstructural polyprotein, whereas the structural proteins are translated as a distinct polyprotein from a subgenomic RNA. Remarkably, however, the structures of the virions in the two groups have been found recently to be related. One of the two glycoproteins present on the exterior of the virions is called E in the case of flaviviruses and E1 in alphaviruses. E and E1 have been shown to be structurally identical. There are other similarities in the structures of the virions in the two groups, including the formation of a heterodimer between E or E1 and the second external glycoprotein that functions in an equivalent fashion. It seems clear that the virus structures, although they differ in important ways, are derived from a common ancestral source. We have suggested that this common structure may be important in the life of these viruses as

arboviruses, i.e., capable of infecting both hematophagous arthropods and vertebrates.

We have started an ambitious collaboration with structural biologists at Purdue University to determine the structures of alphaviruses and flaviviruses to high resolution, and to determine the structures of all of the proteins encoded by the viruses to atomic resolution. We have now determined the structure of dengue virus to 9.5 Å and the structure of immature dengue virus that contains uncleaved prM to 11 Å. This resolution is high enough that the glycoproteins can be positioned with confidence in the virus particle, that carbohydrate side chains on the glycoproteins can be seen, and even the membrane spanning domains that anchor the glycoproteins can be identified and traced. One interesting result from such analysis is that protein E has a different bend in the virion from that found in the immature virus, and that this bend also differs in the crystallized forms of E. Of even greater interest is the fact that E undergoes large structural rearrangements upon conversion of the immature virus to the mature form and again upon conversion of the mature virus to the fusion-competent form.

We are also continuing a program to obtain atomic structures of a number of other virus-encoded proteins, both structural and nonstructural, and to construct and test mutants of the viruses in order to understand the details of virus replication and assembly.

284. Flexibility of the yellow fever virus E protein Marlene Biller

The flavivirus E protein adopts three different conformations in its immature, mature, and fusion-competent states respectively. The E protein of yellow fever requires a second protein, prM, to form a complex stabilizing the fusion apparatus. prM forms a 1:1 complex with E intracellularly and protects it from being prematurely activated by low pH during transport through the acidic compartments and vesicles of the trans-Golgi network. During the transformation from the prM/E heterodimer in immature virions to the E homodimer in mature virus a large rearrangement of the E-protein must occur. The same is true for the transformation from the mature state to fusion-competent state. Flexibility of the E protein is apparently a functional requirement for assembly and infection of flaviviruses. By comparing three different crystal structures, namely dengue sE (the soluble fragment of E containing amino acids 1-395), the E monomer as fitted into the mature virion and immature virion cryo-EM envelopes, Zhang et al. (Zhang et al., manuscript in preparation) showed that the E molecule can bend at a "hinge" between domain II (DII) and domains I and III (DI+DIII). They found that during maturation, DI+DIII reorients with respect to the viral membrane and that during this reorientation, the angle between DII and DI+DIII changes by 27°. From E protein in mature virus to E protein in the fusion-competent state there is a hinge movement of 37°. Zhang et al., also noted that there are conserved glycines in the hinge region, between domain I and domain II and that these are important for maintaining the flexibility of E. We are currently mutating these glycines and alanines to amino acids that could affect flexibility of the E protein but perhaps not completely

destroy its conformation, using the Quick Change mutagenesis kit from Stratagene. These include changing the Ala at amino acid 54 to isoleucine and to lysine, the Ala at amino acid 187 to isoleucine and lysine, and the glycine at amino acid 279 to isoleucine, lysine, and threonine. Once these changes are incorporated into the full-length clone of yellow fever virus, we can transfect BHK cells, measure RNA replication by immunofluorescence and the titer of released virions by plaque assay. If the mutant viruses are alive, we can send them to Purdue for cryo-electron microscopic reconstruction.

285. The function of flavivirus E protein in virus assembly

Marlene Biller, Maria Farkas

The E protein of flaviviruses has several major functions, including receptor attachment and membrane fusion, and it also carries the major antigenic epitopes leading to a protective immune response. E proteins in mature virions form 90 head-to-tail dimers that lie parallel to and completely cover the viral membrane. Dimers of E protein have also been fitted into the cryoelectron density envelope of dengue virus and there has been interest in determining how important dimer formation by E protein is for the overall configuration (and perhaps the stability) of flaviviruses. The ectodomain of the E protein has an elongated shape and is composed of three major parts: a central domain that contains the N-terminal region (domain I), the fusion and dimerization domain (domain II), and a C-terminal putative receptor-binding domain (domain III). In mature virions the fusion peptide is probably protected by the domain III of the opposite E protein in the dimer. A set of mutants has been made to investigate dimer formation. The mutated residues are in contact regions of the homodimer and are generally conserved among flaviviruses. The first experiments will be conducted in YFV, for which we have a full-length clone in a pACNR vector.

We have eight mutations to the current time. Three are in domain II: F1 with amino acid E251->K, F2 with the same amino acid changed to glutamine, F3 with aa S253->P to insert a helix breaker. There are 4 in domain III: F4 has amino acids 313 and 314 deleted, F5 has a deletion of amino acids 313-316, F7 has the mutation aa T311->A and F8 mutates aa V319->D. F6 consists of an insertion of 3 Ala residues at residue 155 in domain I.

Following RNA transfection, mutants F1, F4, F7 and F8 grew to titers comparable to wild type YF, and have not been further characterized. Mutant F3 was not alive in preliminary experiments. Mutant F6 was less infectious than wild-type and gave plaques that were significantly smaller. We plan to determine whether mutant F6 forms dimers by examining the proteins on native gels or treating them with cross-linking reagents, since the reduced infectivity can also be caused by other things. If dimerization is reduced or abolished, we will know that domain I is important for dimerization and additional mutations in this domain can be devised.

286. Production and **in vitro** reactivation of immature yellow fever virus particles containing prM

Pritsana Chomchan

Immature flavivirus particles contain prM and E in their envelopes. Furin, a protease found in late Golgi compartments, is thought to cleave prM to generate mature particles containing M protein. Cryoelectron microscopic reconstructions of immature, prM-containing, particles of yellow fever and dengue viruses have shown that the immature forms of the two viruses are quite similar. Two potential furin cleavage sites of the form Arg-X-Arg-Arg are found in YF prM between amino acids 86-87 and 89-90 in the amino acid sequence ⁸³Arg-Ser-Arg-Arg-Ser-Arg-Arg-Ala⁹⁰. In order to generate immature particles we have constructed mutant YFV viruses from the full-length cDNA clone which contain killed furin cleavage sites either by deleting the Arg residues at amino acids 85 and 86 or by mutating ⁸⁵Arg-Arg⁸⁶ to Ser-Ala. RNA transcripts were prepared from these mutated constructs and transfected by electroporation into BHK-21 cells. At 48 hr post-transfection, the culture fluid was harvested and titred for infectivity. Transfectivity of the mutants was assayed by an immunofluorescence assay using an antibody to YF E protein. Individual cells were positive, indicating that viral RNA was replicating but viruses did not spread from cell to cell. However, no infectious virus could be detected in the culture fluid by plaque assay. Mutant virus particles were precipitated from the culture fluid with polyethylene glycol and the viral envelope proteins were detected by Western blot analysis after PAGE electrophoresis. This confirmed the fact that non-infectious prM-containing particles of yellow fever had been released from infected cells.

A similar result has been reported showing that immature particles of tick-borne encephalitis virus are not infectious, but that it was possible to reactivate infectivity of the immature TBE virus by treatment *in vitro* with trypsin. We have treated immature yellow fever virus and wild type yellow virus *in vitro* with various concentrations of trypsin and measured the infectivity of the treated virus on BHK cells. Reactivity could not be observed for YF virus, since the infectivity of both wild type and mutants decreased after trypsin treatment. We need to develop a different method of *in vitro* reactivation.

287. RNA replication and viral assembly of chimeras between yellow fever virus and dengue 2 virus

Pritsana Chomchan

Previously, we have shown that full-length yellow fever virus (YF) containing prM and E from dengue 2 virus (DEN) replicated as well as wild type YF, but that a full-length YF with all three structural proteins (capsid, prM, and E) from DEN did not replicate due to the loss of the cyclization sequence. Complementary sequences in the 5' end of the capsid protein and in the 3' non-translated region (NTR) cause flavivirus viral RNA to cyclize, and this cyclization is required for viral RNA replication. We have made two constructs of full-length YF containing CP, prM and E from DEN in which the cyclization sequences were restored. In the first construct the 5'

cyclization sequence in DEN capsid was changed to that of YF (nt 125-144 of DEN replaced by nt 147-165 of YF), and named "5' changes YFV/DEN chimera and in the second the 3' NTR of YF was changed to that of DEN (nt 10748-10766 of YF to nt 10598-10616 of DEN), named 3' changes YFV/DEN chimera." RNA replication for the two YFV/DEN chimeras with changes could be detected by an immunofluorescence assay using anti-DEN antiserum, but at levels that were extremely low compared to that of wild type YF. Both YFV/DEN chimeras are very unstable and deletions arise rapidly, and must be reconstructed often. Infectious virus is released from both RNA replicating chimeras, but at much lower levels than for wild type yellow fever at 48 hr post-transfection (2.6×10^4 for the chimera with 5' changes, 1.5×10^4 for the chimera with 3' changes compared to 1.2×10^7 for wild type YF). We hope to be able to prepare sufficient chimeric virus particles for a cryo-EM reconstruction.

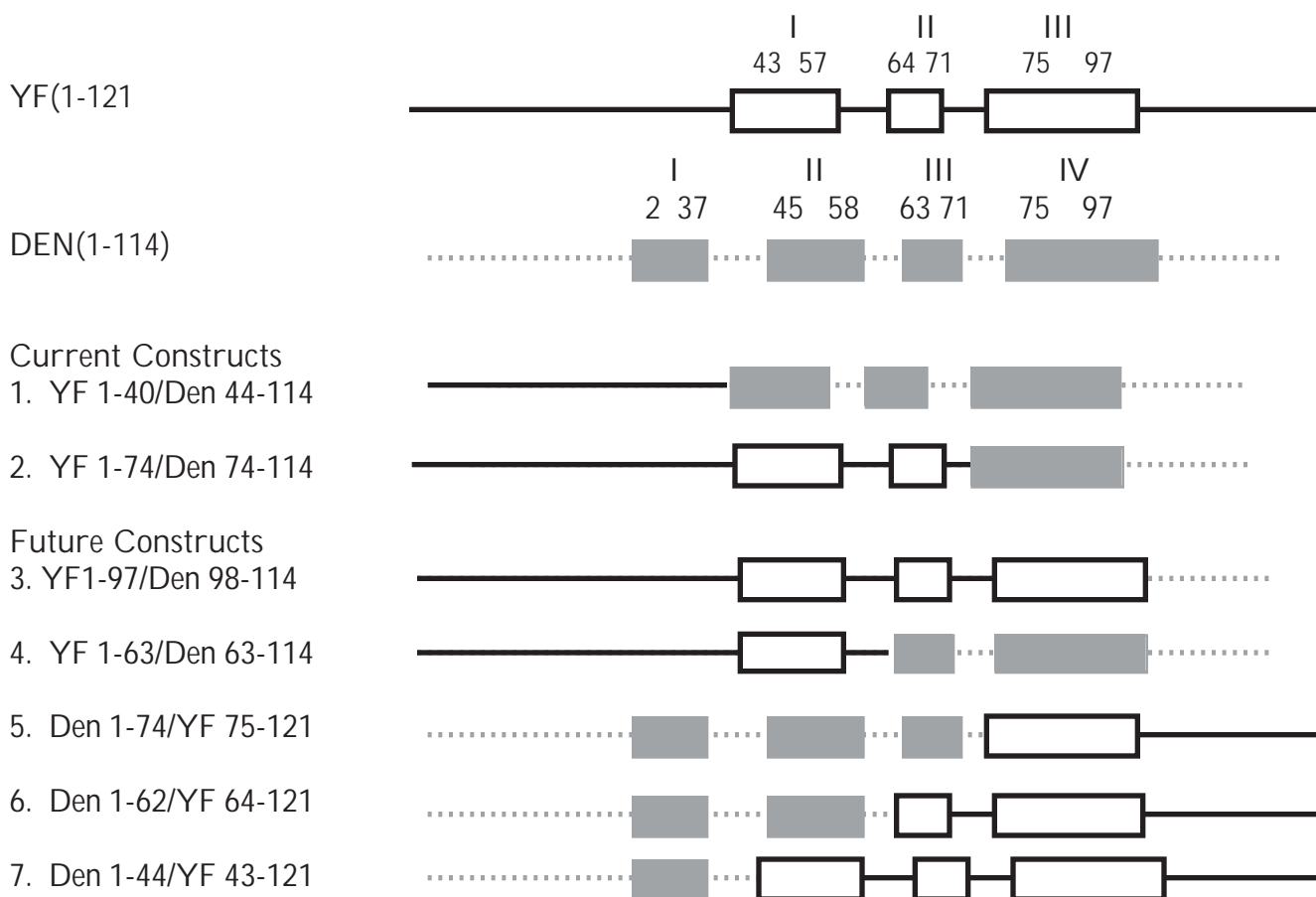
288. Capsid chimeras between YF and DEN
Pritsana Chomchan, Christopher T. Jones*

The structures of the capsid proteins of YFV and DEN have been examined by NMR spectroscopy and both proteins were found to contain a number of alpha-helical domains. The three helices of YF capsid protein were

found to correspond to alpha-helical domains 2, 3, and 4 of DEN capsid protein (open and filled boxes respectively in Figure 1). Cyclization of viral RNA through complementary sequences found in capsid and in the 3'NTR has been shown to be essential for initiation of RNA replication (see the previous abstract) but the role of capsid protein in assembly of flaviviruses has not yet been determined. In order to study the relationship between capsid protein and viral assembly, we are producing full-length yellow fever virus (YF) containing prM and E from dengue 2 virus (DEN) in which various combinations of alpha-helical domains from YFV and DEN are switched within the capsid protein. These are illustrated schematically in Figure 1. With the N-terminal 40 amino acids from YFV (construct #1) or aa 1-74 from YFV and the rest from DEN (construct #2), the level of RNA replication level is higher that we found for the two RNA replicating YFV/DEN structural protein chimeras with repaired cyclization sequences (see the previous abstract). Unfortunately, we have not yet obtained a construct that is sufficiently stable (i.e., does not delete spontaneously) for further studies of flaviviral assembly.

*Biological Sciences, Purdue University, W. Lafayette, IN

Figure 1. Capsid Chimeras between YF and DEN



289. Generation of alphaviruses containing uncleaved pE2 glycoprotein
Pritsana Chomchan

The structural proteins of alphaviruses are translated from the 26S subgenomic RNA as a polyprotein. This polyprotein is cleaved by the viral capsid autoprotease to release the capsid protein, and further processed by host signalase to generate pE2, the 6K protein, and glycoprotein E1. pE2 is the precursor to the alphavirus attachment protein, E2, and is cleaved in a late maturation step close to its amino terminus by furin to form E2 and E3. The last four amino acids of E3 contain the furin recognition sequence (Arg-X-Arg-Arg or Arg-X-Lys-Arg) in almost all alphaviruses. When the cleavage between E3 and E2 is blocked, either by changing the furin recognition sequence or introducing a glycosylation site at the N-terminus of E2, virions are produced containing pE2 in place of E2. Such pE2-containing particles have been produced for Semliki Forest virus and shown to be non-infectious. We are interested in determining the structure of alphavirions containing pE2 and therefore we are removing the furin cleavage sites between E3 and E2 in full-length cDNA clones of Sindbis virus, Ross River virus, and Aura virus.

290. Antisera against YF helicase and DEN capsid protein

Pritsana Chomchan, Christopher T. Jones¹, Susan T. Ou²

For various studies in our collaborative project with Purdue University, we need antisera against particular flavivirus proteins. cDNAs encoding the helicase domain of YFV NS3 protein and DEN capsid protein were cloned into expression vectors and expressed in *E. coli*. The proteins were purified at Purdue University and sent to Caltech to be injected into mice at the Caltech animal facility. Sensitivity and specificity of the antisera against their respective antigens were analyzed by Western blot. The titer of the antiserum against the YFV helicase was quite high; the titer of the anti-DEN capsid protein was lower. Both antiserum will be used for immunofluorescence and immunoprecipitation assays.

¹Biological Sciences, Purdue University, W. Lafayette, Indiana

²Monoclonal Antibody Facility, Division of Biology, Caltech

291. Expression and purification of alpha virus non-structural and structural proteins
M.T. Farkas, J.J. Siebenga

We have been continuing a collaborative project with structural biologists at Purdue University to determine the crystal structures of different alpha virus nonstructural proteins. Previously we have cloned and purified the N-terminal domain of Sindbis virus nsP2 protein.

The nonstructural nsP2 proteins of all alpha viruses are bifunctional proteins playing a vital role in viral RNA replication. After viral infection the RNA is translated into a polyprotein, P1234, which is cleaved by the C-terminal protease domain of nsP2 into functional enzymes. There is no structural information available for

any of the alphavirus nonstructural proteins yet. Determination of the crystal structures of all the nonstructural proteins will help us understand the RNA replication process of alphaviruses.

Full-length cDNA clones of Sindbis, Aura, Ross River, Sagiyama, and Semliki Forest viruses were acquired or cloned in our lab and used to clone all the nonstructural proteins into the pET28 bacterial expression system. The target genes are cloned downstream of a T7 promoter and upstream of a six-His tag. This system enables highly efficient expression under the right conditions. We tried a variety of induction conditions, using different temperatures (22°C, 25°C, 30°C, 37°C), different inducing agents (IPTG, salt, arabinose), different concentrations of inducing agents, and different inducible cell lines (BL21SI, BL21AI, BL21DE3 and RosettaDE3).

We were only able to express few of the targeted proteins (the Aura protease domain of nsP2, Aura nsP3, Sagiyama protease domain of nsP2, and the Sagiyama nsP3) in soluble form in small cultures. We are currently trying to optimize induction conditions for scaled up cultures that could yield sufficient soluble protein for crystallographic studies. Sagiyama nsP1, nsP4, the Sindbis N-terminal helicase domain of nsP2 and full-length Sindbis nsP2, and Aura nsP4 were also expressed but are largely present in the insoluble fraction. We will try to use denaturing conditions to purify these proteins, and then try to refold them by using serial dilution techniques.

The alphavirus structural protein E2 is a glycoprotein, which is located in the viral envelope as a heterodimer with E1. Previous attempts in our lab to purify Ross River Virus and Sindbis E2 have not worked due to poor solubility of the proteins. Currently, we are attempting to produce soluble Sagiyama and Aura E2 proteins. Because these proteins are glycosylated, they cannot be correctly produced in bacterial expression systems. The pACgp67b vector containing the extracellular portion of E2 will be used to express these glycoproteins in insect cells.

Publications

Kim, K.H., Rumenapf, T., Strauss, J.H. (2004) Regulation of Semliki Forest virus RNA replication: A model for the control of alphavirus pathogenesis in invertebrate hosts. *Virology* 323:153-163.

Kuhn, R.J. and Strauss, J.H. (2003) Enveloped viruses. *Adv. Prot. Chem.* 64:363-377.

Zhang, W., Chipman, P.R., Corver, J., Johnson, P.R., Zhang, Y., Mukhopadhyay, S., Baker, T.S., Strauss, J.H., Rossmann, M.G. and Kuhn, R.J. (2003) Visualization of membrane protein domains by cryo-electron microscopy of dengue virus. *Nature Struct. Biol.* 10:907-912.

Zhang, Y., Zhang, W., Ogata, S., Clements, D., Strauss, J.H., Baker, T.S., Kuhn, R.J. and Rossmann, M.G. (2004) Conformal changes of the flavivirus E glycoprotein. *Structure* 12:1607-1618.

Smits Professor of Cell Biology: Alexander Varshavsky
 Postdoctoral Scholars: Christopher Brower, Emmanuelle Graciet, Cheol-Sang Hwang, Rong-Gui (Cory) Hu, Konstantin Piatkov, Jun Sheng, Zanzian Xia, Zhenming (Jack) Xu, Jianmin Zhou
 Laboratory Manager: Janet Dyste

Support: The work described in the following research reports has been supported by:

Howard and Gwen Laurie Smits Professorship in Cell Biology
 Human Frontiers Science Program (HFSP)
 National Institutes of Health, USPHS

Summary: Our main subject is the ubiquitin (Ub) system. In the 1980's, my colleagues and I produced the first evidence that Ub-protein conjugation is required for protein degradation in living cells and for cell viability, discovered the first physiological functions of Ub conjugation (in the cell cycle, DNA repair, protein synthesis, transcriptional regulation, and stress responses), deciphered the first degradation signals in short-lived proteins, and identified critical mechanistic attributes of the Ub system, particularly the poly-Ub chain and subunit selectivity of protein degradation. Our work continues to focus on Ub-dependent circuits.

The effect of an intracellular protein on the rest of the cell depends on the protein's concentration. The latter is determined by the rate of synthesis and/or import of the protein in relation to the rates of its degradation, inactivation by other means, or export from the compartment. The *in vivo* half-lives of intracellular proteins range from a few seconds to many days. Over the last decade, a vast number of biological circuits were shown to contain either constitutively or conditionally short-lived proteins. In addition, damaged or otherwise abnormal intracellular proteins tend to be recognized as such and selectively degraded, largely by the same Ub-proteasome system that mediates the controlled proteolysis of short-lived regulatory proteins. The metabolic instability of a regulator provides a way to generate its spatial gradients and allows for rapid adjustments of its concentration (or subunit composition) through changes in the rate of its synthesis or degradation.

Ubiquitin (Ub) is a 76-residue protein that exists in cells either free or conjugated to many other proteins. Degradation of intracellular proteins by the Ub-proteasome system regulates a multitude of processes: cell growth, cell division and differentiation, signal transduction, responses to stress, and a broad range of metacellular (organismal) processes as well, from embryonic development to immunity and the functions of the nervous system. Ub-dependent proteolysis involves the "marking" of a substrate through covalent conjugation of Ub to a substrate's internal Lys residue. Ub conjugation is mediated by the E1-E2-E3 enzymatic cascade. E1, the ATP-dependent Ub-activating enzyme, forms a thioester bond between the C-terminal Gly of Ub and a specific Cys residue of E1. In the second step, activated Ub is

transesterified to a Cys residue of a Ub-conjugating (E2) enzyme. Thereafter a complex of E2 and another enzyme, E3, conjugates Ub to a Lys residue of a substrate. The functions of E3 include the recognition of a substrate's degradation signal (degron). The numerous proteolytic pathways of the Ub system have in common their dependence on Ub conjugation and the 26S proteasome (which processively degrades Ub-protein conjugates), and differ largely through their utilization of distinct E2-E3 complexes. Specific E3s recognize (bind to) specific degrons of their substrates. The diversity of E3s and E2s underlies the enormous range of substrates that are recognized and destroyed by the Ub system, in ways that are regulated both temporally and spatially.

One pathway of the Ub system is the N-end rule pathway (Fig. 1). The N-end rule, which relates the *in vivo* half-life of a protein to the identity of its N-terminal residue, was discovered by this laboratory in 1986, in experiments that explored the fate of a fusion between Ub and a reporter protein such as *E. coli* β -galactosidase (β -gal) in the yeast (fungus) *S. cerevisiae*. In eukaryotes, Ub-X- β gal is cleaved, cotranslationally or nearly so, by deubiquitylating enzymes (DUBs) at the Ub- β gal junction. This cleavage takes place regardless of the identity of the residue X, proline being the single exception. By allowing a bypass of the normal N-terminal processing of a newly formed protein, this result yielded an *in vivo* method (the Ub fusion technique) for generating different residues at the N-termini of otherwise identical proteins, a technical advance that led to the finding of the N-end rule. The *in vivo* half-lives of resulting X- β gal proteins were shown to range from ~2 min (e.g., Arg- β gal or Leu- β gal) to longer than 20 hr (e.g., Met- β gal or Gly- β) (Fig. 1). The N-end rule-based degradation signal, called the N-degron, consists of a destabilizing N-terminal residue and an internal lysine (or lysines) of a substrate, the Lys residue being the site of formation of a substrate-linked poly-Ub chain. The ubiquitylated substrate is degraded by the 26S proteasome.

The N-end rule pathway is present in all organisms examined, from mammals and plants to fungi and prokaryotes. The currently known functions of the N-end rule pathway include the regulation of peptide import in yeast, through the conditional (modulated by peptides) degradation of the repressor CUP9 that down-regulates a peptide transporter; the maintenance of chromosome stability, through the degradation of a separase-produced fragment of SCC1 (a subunit of cohesin) at the metaphase-anaphase transition; the regulation of meiosis in yeast and mammals; an essential role in the mammalian cardiovascular development; the regulation of apoptosis in *Drosophila*, through the degradation of DIAP1, an inhibitor of apoptosis, and a role in the leaf senescence in plants.

Functional and mechanistic studies of the N-end rule pathway in yeast and mammals are a major theme of our current work.

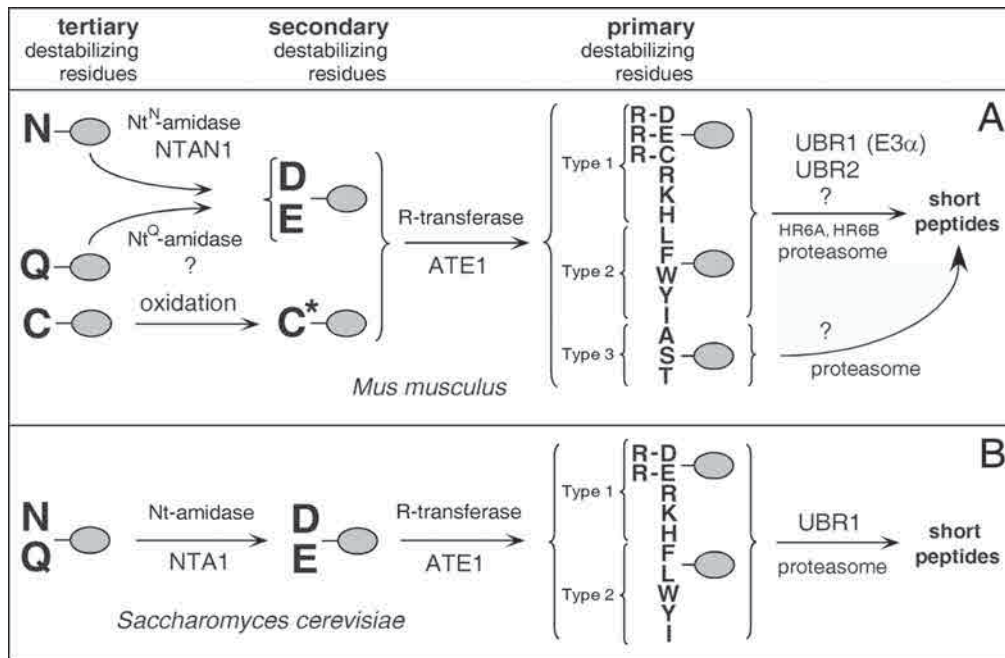


Fig. 1. The N-end rule pathway in mammals (A) and yeast (B).

292. Mechanistic and functional studies of N-terminal arginylation

Christopher Brower, Cory Hu, Jun Sheng, Jack Xu, Jianmin Zhou, Alexander Varshavsky

The N-end rule has a hierarchic structure. Specifically, N-terminal Asn and Gln are tertiary destabilizing residues in that they function through their deamidation, by N-terminal amidohydrolases, to yield the secondary destabilizing residues Asp and Glu, whose activity requires their conjugation, by ATE1-encoded Arg-tRNA-protein transferases (R-transferases), to Arg, one of the primary destabilizing residues. The latter are recognized by the Ub ligases (E3 enzymes) of the N-end rule pathway. In vertebrates, the set of secondary destabilizing residues contains not only Asp and Glu but also Cys, the latter being a stabilizing residue in the yeast N-end rule.

The two previously characterized species of mammalian Arg-tRNA R-transferases (R-transferases), ATE1-1 and ATE1-2, are produced through alternative splicing of ATE1 pre-mRNA (Kwon et al., 1999). The ratio of ATE1-1 to ATE1-2 mRNA varies greatly among the mouse tissues: it is ~0.1 in the skeletal muscle, ~0.25 in the spleen, ~3.3 in the liver and brain, and ~10 in the testis, suggesting that the two R-transferases are functionally distinct. However, the substrate specificities of ATE1-1 and ATE1-2 are similar to that of the ATE1-encoded R-transferase of *S. cerevisiae*, in that they can arginylate N-terminal Asp and Glu, but cannot arginylate N-terminal Cys (Kwon et al., 1999). Earlier work has shown that mouse ATE1(-/-) cells, which lacked ATE1-encoded R-transferases, are incapable of arginylating all three of the secondary destabilizing N-terminal residues, Asp, Glu and Cys, and that

N-terminal Cys, in contrast to N-terminal Asp and Glu, is oxidized prior to its arginylation by R-transferase. These findings suggested that the arginylation branch of the N-end rule pathway may function as an oxygen sensor. ATE1(-/-) embryos die in utero around day E15. ATE1(-/-) embryos exhibit defective cardiogenesis and defective angiogenic remodeling of the early vascular plexus. Thus, ATE1 is required for cardiovascular development, a new set of functions of the N-end rule pathway (Kwon et al., 2002).

Several mechanistic and functional studies of N-terminal arginylation in mammals and yeast are currently under way, following the advances described above.

(i) Dissection of the substrate specificity of ATE1-encoded R-transferases in *S. cerevisiae* and the mouse, including analyses of the mechanism of selective oxidation of N-terminal Cys (Cory Hu). One of our aims is to understand physiological significance of the differences in the activity of R-transferases toward N-terminal Cys versus its oxidized derivatives such as the cysteic acid residue.

(ii) Construction and functional analyses of mouse strains (and cells derived from them) in which the expression of ATE1-encoded Arg-tRNA-protein transferases (R-transferases) is selectively and conditionally abolished in specific cell lineages during embryogenesis, or postnatally (Christopher Brower). This set of projects should make it possible, among other things, a functional dissection of N-terminal arginylation in specific organ systems and cell types of adult mice. (A nonconditional ATE1^{-/-} genotype is embryonic lethal (see above).)

(iii) Construction and functional analysis of knock-in mouse strains that contain a doxycycline-inducible allele of ATE1, and thus can overproduce R-transferases, in a controllable manner, in specific cell types during embryogenesis, or postnatally (Jianmin Zhou, Christopher Brower).

(iv) Identification and analysis of new isoforms of mouse R-transferase (Cory Hu).

(v) Analysis of chromosome stability and regulation of apoptosis in mouse ATE1^{-/-} cells (Jianmin Zhou, Jun Sheng, Cory Hu, and Christopher Brower). These projects stem from the discovery of the function of the *S. cerevisiae* N-end rule pathway in the maintenance of chromosome stability (Rao et al., 2001), from the conjecture that an analogous function in mammalian cells involves the (ATE1-dependent) arginylation branch of the N-end rule pathway, and from the recent finding that in mammals the putative DNA helicase RECQL4 is physically associated with UBR1 and UBR2, two Ub ligases of the mammalian N-end rule pathway (Yin et al., 2004). Recent work (Jianmin Zhou) indicated that N-terminal arginylation is essential for the *in vivo* degradation of the separase-produced fragment of SCC1, a subunit of mouse cohesin. ATE1^{-/-} EFs are phenotypically unstable as established cell lines, in that independently produced ATE1^{-/-} cell lines tend to differ in the sets of proteins they overproduce, relative to +/+ EFs (Jun Sheng, Jianmin Zhou).

(vi) Identification of ATE1-dependent circuits (i.e., circuits that involve N-terminal arginylation) through the identification of mouse genes whose expression is significantly altered during embryonic development in ATE1^{-/-} embryos, using microarray techniques, differential display and analogous methods with ATE1^{-/-} and congenic +/+ embryos or EF cells (Cory Hu, Jun Sheng, Jianmin Zhou).

(vii) Identification of physiological substrates of R-transferases, through the testing of putative substrates of caspases and calpains that bear secondary or tertiary destabilizing N-terminal residues (Jianmin Zhou). We are also developing generally applicable methods for discovery of the physiological substrates of R-transferases (Jack Xu and Cory Hu).

References

- Kwon, Y.T., Kashina, A.S. and Varshavsky, A. (1999) *Mol. Cell. Biol.* 19:182-193.
 Kwon, Y.T., Kashina, A.S., Davydov, I.V., Hu, R.-G., An, J.Y., Seo, J.W., Du, F. and Varshavsky, A. (2002) *Science* 297:96-99.
 Rao, H., Uhlmann, F., Nasmyth, K. and Varshavsky, A. (2001) *Nature* 410:955-959.
 Varshavsky, A. (2004) *Curr. Biol.* 14:R181-R183.
 Yin, J., Kwon, Y.T., Varshavsky, A. and Wang, W. (2004) *Human Mol. Genet.* 13:2421-2430.

293. Mechanistic, structural, and functional studies of bacterial Leu/Phe-tRNA-protein transferases

Emmanuelle Graciet, Konstantin Piatkov, Cory Hu, Alexander Varshavsky

While the N-end rule pathway also exists in prokaryotes, it differs from its eukaryotic counterpart both in the N-end rule's set of destabilizing residues and in mechanisms involved. As in eukaryotes, N-terminal Phe, Leu, Trp and Tyr are primary destabilizing residues in the prokaryotic N-end rule pathway in that they are recognized directly by ClpAP, an ATP-dependent, proteasome-like protease. (Prokaryotes lack Ub and Ub ligases.) However, whereas N-terminal Asp and Glu are secondary destabilizing residues in eukaryotes (in that their function requires their preliminary conjugation to Arg by the ATE1-encoded R-transferase), in prokaryotes the secondary destabilizing residues are Arg and Lys (Tobias et al., 1991; Shrader et al., 1993). These N-terminal residues are conjugated to either Phe or Leu (largely Leu in *E. coli*) by the *aat*-encoded Leu/Phe-tRNA-protein transferase (L/F-transferase).

Prokaryotic N-end rule pathways remain largely unexplored, particularly in regard to their functions. Most gram-negative prokaryotes contain Aat sequelogs (see Abstract 299 for a description of the recently introduced sequelog/spalog terminology (Varshavsky, 2004)), but their physiological substrates and functions remain unknown. Remarkably, some prokaryotes contain sequelogs of eukaryotic ATE1 as well. The substrate specificity of these putative prokaryotic R-transferases remains to be determined. The projects mentioned below aim to address some of the issues above.

(i) Enzymological dissection of Aat (Leu/Phe-tRNA-protein transferase). The residues of *E. coli* Aat involved in substrate binding and/or catalysis are unknown. To address the mechanism of Aat, we are using extensive site-directed mutagenesis, focusing on residues highly conserved amongst Aat sequelogs. To increase the power of such analyses, we are also developing better, more efficacious enzymatic assays for L/F-transferase. Yet another line of these studies involves binding assays to measure the physical affinity of purified Aat to either one of its two co-substrates: a polypeptide bearing N-terminal Arg or Lys, and Leu (or Phe)-tRNA.

(ii) Structural studies of Aat. Overexpressed and purified *E. coli* Aat (26 kD) and Aat from the thermophilic gram-negative eubacteria *Thermosynechococcus elongatus* are being used to crystallize Aat and determine its atomic structure. Among the approaches being employed are crystallization of either untagged Aat or fusions of Aat, via a rigid linker, to maltose-binding protein (MBP).

References

- Tobias, J.W., Shrader, T.E., Rocap, G. and Varshavsky, A. (1991) *Science* 254:1374-1377
 Shrader, T.E., Tobias, J.W. and Varshavsky, A. (1993) *J. Bact.* 175:4364-4374.

294. Female lethality and apoptosis of spermatocytes in mice lacking the UBR2 ubiquitin ligase of the N-end rule pathway
Yong Tae Kwon¹, Zanzian Xia, Jee Young An¹, Takafumi Tasaki¹, Ilia Davydov², Jai Wha Seo¹, Jun Sheng, Youming Xie³, Alexander Varshavsky
The absence of gross defects in UBR1(-/-) mice (Kwon et al., 2001) suggested that the E3 function of the mouse N-end rule pathway is mediated by at least two functionally overlapping genes, one of which is UBR1. The previously identified mouse gene, termed UBR2, encodes a 200 kD protein highly similar to UBR1 (Kwon et al., 1998). UBR2(-/-) mouse strains were recently constructed and characterized, revealing a sex-specific phenotype: male infertility and female lethality (Kwon et al., 2003). The relative frequency of UBR2(-/-) males produced from heterozygous (+/- x +/-) matings was similar to that of +/+ males. Adult UBR2(-/-) males were outwardly normal, but exhibited severe defects in spermatogenesis and were sterile. Until 4 weeks after birth, the size of their testes was close to that of congenic +/+ mice. However, during the 5th and 6th weeks, the mass of UBR2(-/-) testes decreased by ~2-fold. The degeneration of testes in UBR2(-/-) mice was caused by massive apoptosis of spermatocytes and their progeny, round spermatids. The number of apoptotic germ line cells in the mutant testes dramatically increased 5 weeks after birth. The first detectable abnormality of germ cell differentiation in the UBR2(-/-) testes was a much lower number of early meiotic spermatocytes at week 2. At week 3, when meiotic divisions of spermatocytes produce round spermatids, ~2,800 round spermatids per 100 seminiferous tubules were observed in the +/+ testes, but virtually no round spermatids could be detected in the mutant testes. This and related data suggested that defective meiosis in UBR2(-/-) male mice was the primary cause of their sterility. Despite the meiotic defect, a small number of cells that appeared to be round spermatids could be detected in the UBR2(-/-) testes after week 4. However, most of these cells did not continue to differentiate, and died through apoptosis, together with meiotic spermatocytes, after week 6. The testes of 2 months old UBR2(-/-) males were severely shrunk and vacuolized; they nearly completely lacked spermatids and spermatozoa. In contrast, the spermatogonia, Sertoli cells, and Leydig cells remained apparently intact in the UBR2(-/-) testes. Thus, the absence of UBR2 (but not of its close homolog UBR1) leads to a severe defect in spermatogenesis that stems primarily, if not exclusively, from a meiotic defect. Further analysis of this phenotype showed that UBR2(-/-) spermatocytes are arrested largely at the pachytene stage of meiosis, and fail to form the synaptonemal complex that holds together the homologous chromosomes and is essential for meiotic recombination. GST-pulldown binding assays with purified N-end rule substrates and extracts from *S. cerevisiae* overexpressing mouse UBR2 have shown that UBR2 can recognize N-degrons *in vitro*. Thus, mouse UBR2 functions *in vivo* as an E3 component of the N-end rule pathway that

functionally overlaps with UBR1 (E3 α), the previously known E3 of this pathway (Kwon et al., 2003).

Yet another feature of the UBR2 (-/-) phenotype was extremely low frequency of the UBR2(-/-) female progeny from heterozygous (+/- x +/-) matings, in contrast to the normal (mendelian) frequency of UBR2(-/-) males. Strikingly, the rare UBR2(-/-) females that were born were fertile and apparently normal otherwise. This phenotype is being analyzed. It might be caused by perturbed X-chromosome inactivation in early UBR2(-/-) female embryos.

To investigate the functional interaction of UBR1 and its close homolog UBR2, we used [UBR1(+/-)UBR2(+/-)] mice to produce [UBR1(-/-)UBR2(-/-)] double-mutant mouse strains. Disruption of both UBR1 and UBR2 was lethal: none of the [UBR1(-/-)UBR2(-/-)] embryos survived beyond day E12 (Y.T. Kwon and J.W. Seo, unpublished data). Whereas most of the double-mutant male embryos died at ~E9.5, most of their female counterparts died significantly earlier. Remarkably, UBR1(-/-)UBR2(-/-) embryonic fibroblasts did contain the N-end rule pathway, albeit of significantly lower activity, indicating the presence of at least one other (third) E3 of this pathway

¹Present address: Dept. of Pharmaceutical Sciences, University of Pittsburgh, Pittsburgh, PA 15213

²Present address: Meso-Scale Discovery, Inc., 16020 Industrial Drive, Gaithersburg, MD 20877

³Present address: Dept. of Pathology, Wayne State University School of Medicine, Detroit, MI 48201

References

- Kwon, Y.T., Reiss, Y., Fried, V.A., Hershko, A., Yoon, J.K., Gonda, D.K., Sangan, K., Copeland, N.C., Jenkins, N.A. and Varshavsky, A. (1998) Proc. Natl. Acad. Sci. USA 95:7898-7903.
- Kwon, Y.T., Xia, Z.-X., Xia, Davydov, I.V., Lecker, S.H. and Varshavsky, A. (2001) Mol. Cell. Biol. 21:8007-8021.
- Kwon, Y.T., Xia, Z.X., An, J.Y., Tasaki, T., Davydov, I.V., Seo, J.W., Sheng, J., Xie, Y.M. and Varshavsky, A. (2003) Mol. Cell. Biol. 23(22):8255-8271.
295. Construction and analysis of mouse strains lacking the UBR3 ubiquitin ligase
Takafumi Tasaki¹, Yong Tae Kwon¹, Alexander Varshavsky
Kwon et al. (1998) identified two distinct mouse (and human) genes, termed UBR2 and UBR3, which encode proteins that are similar to mouse UBR1 (E3 α), the previously characterized E3 of the N-end rule pathway. In contrast to the highly similar mouse UBR1 and UBR2 proteins (47% identity and 68% similarity), the mouse UBR3 protein, while clearly a member of the UBR family, is less similar to UBR1 (25% identity and 51% similarity) and UBR2 (25% identity and 48% similarity). In addition, mouse UBR3 lacks some of the residues in its N-terminal region that have been shown to be essential for the function of yeast UBR1, and are also present in the mouse (and

human) UBR1 and UBR2 proteins. We mapped and partially sequenced the mouse UBR3 gene, and more recently constructed UBR3(-/-) mouse strains. UBR3(-/-) mice are viable, and are being characterized.

¹Present address: Dept. of Pharmaceutical Sciences, University of Pittsburgh, Pittsburgh, PA 15213

Reference

Kwon, Y.T., Reiss, Y., Fried, V.A., Hershko, A., Yoon, J.K., Gonda, D.K., Sangan, K., Copeland, N.C., Jenkins, N.A. and Varshavsky, A. (1998) Proc. Natl. Acad. Sci. USA 95:7898-7903.

296. Quantitative analyses of interactions between components of the N-end rule pathway and their substrates or effectors

Zanxian Xia, Alexander Varshavsky

Detailed understanding of the N-end rule pathway requires, among other things, the knowledge of equilibrium binding constants for the reversible interactions between UBR1 and its effectors or substrates. (With some interactions, it would be desirable to know the corresponding rate constants as well.) We are carrying out these measurements using the fluorescence polarization (FP) technique, with purified *S. cerevisiae* UBR1 (or its fragments) and a variety of UBR1 ligands, including peptides with destabilizing N-terminal residues. These analyses will be expanded to include other physiological ligands of UBR1 such as the RAD6 Ub-conjugating enzyme, and CUP9, a homeodomain repressor recognized through its C-terminal degron by a distinct (third) substrate-binding site of UBR1.

297. Phosphorylation of UBR1: Its regulation and functions

Cheol-Sang Hwang, Zanxian Xia, Alexander Varshavsky

S. cerevisiae UBR1, the E3 of the yeast N-end rule pathway, is phosphorylated *in vivo*, but the role(s) of this UBR1 modification in the multiple functions of the N-end rule pathway is unknown. Phosphorylation sites on UBR1 and the kinases/phosphatases involved remain to be identified as well. We are using biochemical and genetic approaches to understand, in functional and mechanistic detail, this modification of UBR1.

298. RECQL4, mutated in the Rothmund-Thomson and RAPADILINO syndromes, interacts with ubiquitin ligases UBR1 and UBR2 of the N-end rule pathway

Jinhu Yin¹, Yong Tae Kwon², Alexander Varshavsky, Weidong Wang¹

Helicases are ATP-dependent RNA- or DNA-unwinding enzymes. Humans and other mammals contain at least five distinct helicases of the RecQ family, named after the single RecQ gene of *E. coli*. A malfunction or absence of specific RecQ-family helicases causes several human diseases: the Bloom syndrome (BS; mutations in the BLM helicase), the Werner syndrome (WS; mutations

in the WRN helicase), and the Rothmund-Thomson syndrome (RTS; mutations in the RECQL4 helicase). One common property of these syndromes is predisposition to cancer. Clinical features of the Rothmund-Thomson syndrome (RTS) include postnatal growth retardation, skeletal abnormalities, skin and nail abnormalities, some aspects of premature aging, and predisposition to cancer, especially osteosarcoma. In the latter and several other respects, the phenotype of RTS differs from that of the Bloom syndrome, which predisposes to a large variety of cancers, and from the Werner syndrome, in which the pattern of cancer predisposition is also broader than in RTS, with a prevalence of various sarcomas.

Most (but apparently not all) cases of RTS are caused by autosomal recessive null or hypomorphic mutations in the RECQL4 gene. An RTS-related disease, termed the RAPADILINO syndrome, with a lower predisposition to cancer, was found to be also caused by mutations in the RECQL4 gene. The null phenotype of RECQL4 in mice is death in early embryogenesis. While several lines of evidence suggest that cells from RTS patients are genetically unstable, the understanding of these phenotypes in RTS cells is far from advanced. One difference between RTS and, for example, BS is a near-normal frequency of sister chromatid exchanges (SCEs) in RTS cells, in contrast to high frequency of SCEs in BS cells. Human RECQL4 encodes a 1,208-residue (133-kD) protein that contains characteristic sequences of the RecQ-family's helicase domain, but lacks other significant similarities to known proteins. RECQL4 has not been shown, thus far, to actually possess an RNA- or DNA-helicase activity, in contrast to the BLM and WRN DNA-helicases, whose enzymatic properties have been extensively characterized. No RECQL4-binding proteins have been identified so far, also in contrast to the BLM and WRN helicases, which are known to interact with each other and to function as components of large multiprotein complexes.

We have recently discovered (Yin et al., 2004) that RECQL4 isolated from HeLa cells occurs as a stable complex with UBR1 and UBR2. These highly similar 200-kD proteins are the E3 components of Ub ligases of the N-end rule pathway. Although the known function of UBR1 and UBR2 is to mediate polyubiquitylation (and subsequent degradation) of their substrates, the UBR1/2-bound RECQL4 was not ubiquitylated *in vivo*, and was a long-lived protein. We discuss ramifications of these results, possible functions of RECQL4, and the involvement of the N-end rule pathway. These findings opened up new vistas in studies of both RECQL4 and the N-end rule pathway.

¹Laboratory of Genetics, National Institute on Aging, National Institutes of Health, 333 Cassell Drive, TRIAD Center Room 3000, Baltimore, MD 21224

²Center for Pharmacogenetics and Department of Pharmaceutical Sciences, School of Pharmacy, University of Pittsburgh, Pittsburgh, PA 15261

Reference

Yin, J., Kwon, Y.T., Varshavsky, A. and Wang, W. (2004) RECQL4, mutated in the Rothmund-Thomson and RAPADILINO syndromes, interacts with ubiquitin ligases UBR1 and UBR2 of the N-end rule pathway. *Human Mol. Genet.* 13:2421-2430.

299. Spalog and sequelog: Neutral terms for spatial and sequence similarity
Alexander Varshavsky

Similarities amongst the sequences or three-dimensional (3-D) structures, and the conjectures based on similarities are a major part of molecular biology and related fields. It is therefore striking that there are no terms, at present, to denote a sequence or a 3-D structure that is similar to another sequence or 3-D structure while implying nothing at all about evolutionary relatedness or biological functions. The absence of neutral terms for denoting similarity is one reason for the widespread use of "homologs," "orthologs" and "paralogs." The former term (more than a century old) and the other two were proposed long before the advent of extensive sequence comparisons. To state that a gene or protein A is a homolog of B implies the relatedness of A and B through a common descent, a proposition to prove in most cases. In addition, two sequences can be 37% identical, but they cannot be 37% homologous: they are either homologous or not. The frequent unsuitability of the term "homolog" in the context of similarity comparisons was pointed out repeatedly, but the literature is still rife with this misuse, in part because the proper, neutral terms simply do not exist.

The disposition can be also difficult with "orthologs" and "paralogs." The former are two homologous sequences that diverged following speciation, so that the common precursor of two sequences lies in an organism that was their nearest common ancestor. "Paralogs," in contrast, are two homologous sequences that diverged after gene duplication. Besides the initial ambiguity in assigning "homology" (two orthologs are homologous, and two paralogs are homologous as well), the use of "ortholog" and "paralog" implies additional probabilistic inferences about the evolution of two sequences being compared. Yet further ambiguities often accrue, because the "ortholog-paralog" terms are also used, throughout the literature, to denote functional similarities between orthologous genes (e.g., similar enzymatic activities of protein products), and functional differences between paralogous genes. Neither of these relationships (often presumed, not proven) are implied by the definitions of ortholog and paralog. To observe that the current usage of "homologs," "orthologs" and "paralogs" is complicated and often less than rigorous would be to understate the case. A statistically significant similarity is an experimental fact, whereas "homology," "orthology" and "paralogy" are, in most cases, hypotheses. There is, at present, a striking disconnect between (generally) high rigor of statistical methods used to compare sequences or structures and the often cavalier, assumptions-laden

attitude in the use of "homolog," "ortholog" and "paralogs."

To remedy this, I recently proposed two terms, "sequelog" and "spalog" (Varshavsky, 2004). They meet the requirement of evolutionary and functional neutrality, are helpful mnemonically, and possess yet another advantage of making it possible to distinguish, through single words, between the realms of similar sequences and similar 3-D structures.

The term "sequelog" denotes a nucleotide or amino acid sequence that is similar, to a specified extent, to another sequence.

The term "spalog" (pronounced [spailog]) denotes a 3-D structure that is spatially similar, to a specified extent, to another 3-D structure.

These terms are strictly about similarity: they imply nothing about evolutionary relatedness and functional properties of the sequences or structures.

In comparing nucleotide or amino acid sequences, the extent of similarity is conveyed by a numerical score, % nucleotide or amino acid positional identity. Alternatively, the extent of similarity of two sequences can be conveyed by the probability of an identical score for a randomly chosen pair of sequences of the same length. In comparing amino acid sequences, one can also measure % similarity (as distinguished from % identity), which includes both the identities and the residues that are scored as "similar" to corresponding residues of the second sequence, according to a "similarity matrix."

When 3-D structures of two proteins or nucleic acids are compared, a standard measure of similarity is the root-mean-square deviation (r.m.s.d.) between compared atomic positions. One could, in principle, introduce the term "similog" to denote either a sequence or a 3-D structure that is similar to another sequence or 3-D structure. Note, however, the considerable advantage of "sequelog" and "spalog," vis-à-vis an all-encompassing term such as "similog," in that the former terms instantly define the nature of similarity (a sequence or a spatial one), thus obviating further clarifications.

In a typical usage of the proposed terms, one can state, for example, that protein A is a sequelog of protein B (X% identity over Y residues), or that protein C is a spalog of protein D (r.m.s.d. of X Å for Y equivalent C α atoms). Related measures of spatial similarity include a Z-score computed with the program DALI. To add qualitative, shorthand distinctions, one can state, for example, that protein A is a weak but significant sequelog of protein B (e.g., 24% identity over 165 residues), or that protein C is a strong spalog of protein D (e.g., r.m.s.d. of 2.3 Å for 120 equivalent C α atoms), or that protein E is a strong sequelog of protein F (e.g., 60% identity over 372 residues). In using the sequelog terminology, it would be best to invoke just the % identity of two sequences and its (straightforwardly computable) statistical significance, avoiding an influence by any other information, for example, similarity matrices or 3-D structures. The central idea, yet again, is to minimize "interpretational" aspects of

sequelog, spallog and the derivative terms such as, for example, sequelogy, sequelogous, spallogous, and so forth.

A strong sequelog of a given protein is very likely to be its spallog as well, but the converse is not true, in that a strong spallog of a given protein may not be its sequelog. For example, the 66-residue *E. coli* protein ThiS, the sulfur carrier in the pathway of thiamine biosynthesis, is a strong spallog of the 76-residue eukaryotic ubiquitin (r.m.s.d. of 2.4 Å over 63 equivalent C α atoms, and high Z-score of 5.2), but is not a sequelog of ubiquitin, since the sequence similarity between the two proteins (14%) is statistically insignificant, in the absence of additional information from 3-D structures. Such comparisons can also employ the adjectives "sequelogenous" or "spallogous." For example, "spallogous" can be used to denote similar local 3-D folds in otherwise dissimilar proteins. Thus: "Although protein A is not a sequelog of protein B, the 23-127 region of A is strongly spallogous to the 769-875 region of B (r.m.s.d. of 2.2 Å over 101 equivalent C α atoms, and Z-score of 5.6)."

To describe a comparison of sequences or 3-D structures, one can begin by using "sequelog," "spallog" or their derivatives in stating (and specifying numerically) the facts of similarity, as described above. After that, and only after that, one can conjecture (if necessary), based on additional evidence, that the two sequelogs or spalogs are likely to be "homologs," "orthologs," "paralogs," or whatever. This way, the rigorous, numerically explicit statements about similarities of specific sequences or 3-D structures won't be conjoined, at birth, with often unproven inferences that the latter three terms inherently imply.

Spallog, sequelog and terms derived from them fill an overt lacuna in the existing terminology. These terms would clarify and streamline discourses about similarity.

Reference

Varshavsky, A. (2004) *Curr. Biol.* 14:R181-R183.

Publications

Finley, D., Ciechanover, A. and Varshavsky, A. (2004) Ubiquitin as a central cellular regulator. *Cell* 116:S29-S32.

Kwon, Y.T., Xia, Z.-X., Davydov, I.V., An, J.Y., Seo, J.W., Sheng, J., Xie, Y. and Varshavsky, A. (2003) Female lethality and apoptosis of spermatocytes in mice lacking the UBR2 ubiquitin ligase of the N-end rule pathway. *Mol. Cell. Biol.* 23:8255-8271.

Xia, Z., Turner, G.C., Byrd, C., Hwang, C.S. and Varshavsky, A. (2004) Amino acids induce the import of peptides by accelerating degradation of the import's repressor CUP9. Manuscript in preparation.

Varshavsky, A. (2003) The N-end rule and regulation of apoptosis. *Nature Cell Biol.* 5:373-376.

Varshavsky, A. (2004) Spallog and sequelog: Neutral terms for spatial and sequence similarity. *Curr. Biol.* 14:R181-R183.

Varshavsky, A. (2004) The physiological functions of the ubiquitin system. In: *Great Experiments, Ergito*, by Virtual Text (<http://www.ergito.com/index.jsp>).

Varshavsky, A. (2004) N-end rule. *Encyclopedia of Biological Chemistry*, Acad. Press, NY. In press.

Yin, J., Kwon, Y.T., Varshavsky, A. and Wang, W. (2004) RECQL4, mutated in the Rothmund-Thomson and RAPADILINO syndromes, interacts with ubiquitin ligases UBR1 and UBR2 of the N-end rule pathway. *Human Mol. Genet.* 13:2421-2430.

Developmental and Regulatory Biology

José Alberola-Ila, M.D., Ph.D.
Marianne Bronner-Fraser, Ph.D.
Eric H. Davidson, Ph.D.
Michael H. Dickinson, Ph.D.
Michael Elowitz, Ph.D.
Scott E. Fraser, Ph.D.
Bruce A. Hay, Ph.D.
Elliot M. Meyerowitz, Ph.D.
Ellen V. Rothenberg, Ph.D.
Melvin I. Simon, Ph.D.
Paul W. Sternberg, Ph.D.
Barbara J. Wold, Ph.D.

Assistant Professor of Biology: José Alberola-Ila
 Research Fellows: Gabriela Hernandez-Hoyos, Micheline Laurent
 Graduate students: Susannah Barbee, Harry Green, Eric Tse
 Undergraduates: Danny Maria Ramirez (MURF, La Verne)
 Research and Laboratory Staff: Christie Beel, Chi Wang

Support: The work described in the following research reports has been supported by:

Cancer Research Institute
 Keck Discovery Fund
 Leukemia Society of America
 National Institutes of Health, USPHS

Summary: The main interest of my laboratory to understand how developing T cells interpret the myriad of signals they receive through their surface receptors to make decisions regarding their fate and/or functional responses. Most of the research is focused in a particular stage during T cell development, when immature CD4⁺ CD8⁺ thymocytes (Double Positive) first express a complete $\alpha\beta$ T cell receptor (TCR). Signals from this TCR determine whether immature precursors survive and differentiate into immunocompetent cells, and establish the functional program of these mature cells. The majority of thymocytes bear TCRs that do not recognize the repertoire of MHC + peptide molecules present in the thymus and die relatively rapidly (3-4 days). Those cells bearing a TCR able to interact with self-MHC can receive signals that induce either differentiation into mature T cells (positive selection) or apoptosis (negative selection). During positive selection, DP thymocytes differentiate into CD8⁺ or CD4⁺ single positive (SP) T cells, depending on the specificity of their TCR for MHC class I or class II molecules, respectively. CD4 cells are programmed to exert helper activity while CD8 cells are programmed to elicit cytotoxic functions. Thus positive selection couples TCR specificity with differentiation into the lineage expressing the corresponding coreceptor and effector function. The correct undertaking of these selection and programming events plays a central role in the homeostasis of the immune system, and in its ability to successfully control infections while maintaining self-tolerance.

The actual time of commitment and the molecular profile of cells committed to the CD4 or CD8 lineage remain unclear. After commitment, the thymocyte still requires signals for both its continued survival and the completion of maturation. The research conducted in my laboratory aims for a molecular understanding of the signals and genetic networks that regulate these cell fate decisions. The following is a summary of the projects we have pursued, as well as the future directions of these projects.

300. Lck directs CD4/CD8 lineage commitment

The mechanisms that regulate CD4/CD8 lineage commitment have been the object of intense study during the last decade. Two main models, stochastic and instructional, have been proposed to explain how MHC specificity and coreceptor expression are linked during development. The instructional model proposes that recognition and coengagement of TCR/CD8 by class I MHC or of TCR/CD4 by class II MHC will instruct the cells to follow a CD8 or a CD4 developmental pathway, respectively. It has been proposed that the distinct instructional signal would be delivered through the coreceptor. Strong support for this model came from experiments where a CD8 extracellular/CD4 intracellular chimeric receptor was shown to direct differentiation of a significant number of T cells with a MHC class I restricted TCR into the CD4 lineage. The instructional model was subsequently modified to include the notion that the difference between the signals that induce generation of CD4 T cells or CD8 T cells is a quantitative one, either in terms of the intensity or the duration of the signals. In experiments described below, we identified the tyrosine kinase Lck as the critical component that interprets differences in the signals induced by class I or class II-restricted TCRs and directs development of the DP thymocytes into the CD4 or CD8 lineages.

300a. Alterations in Lck activity can change cell fate determination

G. Hernandez-Hoyos

Lck is a src family tyrosine kinase that associates non-covalently with the cytoplasmic tails of both CD4 and CD8 and becomes catalytically activated when the coreceptors are crosslinked. On DP cells, 25-50% of surface CD4 but only 2% of surface CD8 molecules are found associated with Lck. Therefore, recognition of class II molecules by TCR/CD4 leads to induction of a strong Lck signal, whereas recognition of class I molecules by TCR/CD8 leads to a weaker Lck signal. Some experiments that created chimeric CD4/CD8 coreceptor molecules indicated that the cytosolic tail of the coreceptor played an important role in determining lineage commitment, and suggested that Lck may play a role in this decision. However, the experimental approach to test this possibility was not straightforward, because early studies that altered function of Lck, either by expression of a dominant negative mutant of this kinase or by gene disruption resulted in developmental arrest at the β -checkpoint, in the transition between DN and DP thymocytes, precluding the analysis of Lck function during positive selection and CD4/CD8 lineage commitment. To address this problem, we took advantage of an alternative set of transgenic mice that used the Lck distal promoter to express either catalytically inactive (dLGKR) or constitutively active (dLGF) Lck in thymocytes. This promoter is turned on after β -selection, therefore bypassing the early developmental block. dLGKR and dLGF mice expressing low levels of the transgene appear mostly normal, although a weak effect in both positive and

negative selection can be detected. However, when we bred these mice into transgenic TCR lines the results were remarkable. Forcing a stronger Lck signal in developing thymocytes expressing the class I restricted TCR OT-I results in their development into CD4 T cells. Conversely, a weak Lck signal induced class II restricted AND thymocytes to develop into CD8 T cells. This lineage change results in the generation of mismatched peripheral T cells that respond to their cognate antigen as their surface phenotype would predict. Class II-restricted CD8 AND/dLgKR splenocytes generate cytotoxic effector T cells when activated, and class I restricted CD4 OT-I/dLgF splenocytes respond to TCR stimulation as a bona fide helper T cells. Therefore, alterations in Lck kinase activity change lineage commitment and the complete maturation process. These results strongly support a quantitative-instructive model of lineage commitment, although they can also be made compatible with a kinetic model. We are currently trying to set the experimental system to discern between these two possibilities.

Reference

Hernandez-Hoyos, G., Sohn, S.J., Rothenberg, E.V. and Alberola-Ila, J. (2000) *Immunity* 12:313-322.

300b. Development of a tunable Lck system to directly test purely quantitative vs. kinetic models of lineage commitment

D. Leopoldt

Although Lck activity influences CD4/CD8 lineage commitment, it is not completely clear whether the cell interprets quantitative differences in Lck kinase activity or differences in the duration of the signal, as proposed by the Singer group. Furthermore, it is not clear when commitment becomes irreversible. To address these questions we are implementing a chemical-genetic approach recently developed by the Shokat group. All known protein kinases possess a bulky side chain in their ATP binding pocket. A functionally silent mutation to amino acids with small side chains at this residue creates an enlarged binding pocket that is not present in any wild-type kinase. The Shokat group has designed low-molecular-weight inhibitors derived from the kinase inhibitor PP1 that contains a bulky chemical group. These modified inhibitors bind to the mutated active site, but not to the wild-type ATP pocket, resulting in an exquisitely specific inhibition of the mutant kinase. This approach was first tested with v-src, and has been extended to other kinase families. This chemical-genetic approach holds a number of advantages compared to other strategies for altering protein kinase activity. In contrast to conventional and conditional gene targeting approaches, it is fast, tunable, and reversible, allowing for the observation of reversible effects of partial as well as total inhibition of the target kinase and thus a quantitative analysis. Furthermore, the inhibitors are exquisitely specific for the mutated kinase, as opposed to most conventional protein kinase inhibitors. We have generated ES cells with the appropriate mutation in the Lck locus, and are currently in

the process of generating Lck knock-in mice. These mice will allow us to directly address questions of intensity versus duration, timing of commitment, etc., besides being very useful tools for a wide variety of studies that address the role of Lck at different stages of T cell development and function.

301. Role of GATA-3 in CD4/CD8 lineage commitment

GATA-3 is the only member of the GATA family of zinc finger transcription factors expressed in the T lineage, from the common lymphoid precursors in the bone marrow to mature SP thymocytes. Gene disruption and antisense experiments had shown that GATA-3 is essential at the earliest stages of T-cell development. GATA-3 also has a crucial role directing mature CD4 SP T cells to differentiate as effector cells, by regulating the transcription and chromatin configuration of cytokine genes. Our experiments showed for the first time that GATA-3 is also a central component of the program that directs development of CD4 T cells in the thymus. The main focus of my laboratory at the moment is to understand how GATA-3 controls this lineage decision. To that intent, we are trying to: a) determine the signal transduction elements that regulate GATA-3 expression during CD4/CD8 lineage commitment connecting it to the Lck signals at this stage; b) to analyze the mechanism of action of GATA-3 using structure-function analyses, and c) to identify GATA-3 targets during CD4 lineage differentiation in the thymus.

301a. GATA-3 is important for CD4/CD8 development

G. Hernandez-Hoyos

We first became interested in GATA-3 because of expression data obtained in a GATA-3-lacZ knock-in that showed an upregulation of GATA-3 in CD4 SP, but not CD8 SP thymocytes. We confirmed these results using Western blot and, by sorting intermediate populations in MHC I^{-/-} and MHC II^{-/-} mice, we showed that GATA-3 upregulation occurs very early during positive selection, and exclusively in cells that develop into the CD4 lineage. Our results showed also that upregulation of GATA-3 expression in DP thymocytes responds directly to TCR signals, and the extent of upregulation correlates with the strength of the TCR signal.

These results suggested that GATA-3 induction could be one of the downstream effects that help discriminate between signals that direct DPs to become either CD4 or CD8 cells, so we tested the role of GATA-3 during positive selection and CD4/CD8 differentiation using retroviral infection of T cell precursors and reaggregate fetal thymic organ culture (RTOC). Overexpression of GATA-3 or the partial agonist KRRm during positive selection inhibits CD8 SP cell development. Conversely, repression of GATA-3 function/expression, either through the expression of the GATA-3 antagonist ROG or of a GATA-3 siRNA hairpin, markedly enhances development of CD8 SP cells and

reduces CD4 SP development. These results were recently confirmed by the Ho group using an inducible knockout of GATA-3 in double positive thymocytes. Based on these results, we think that GATA-3 is a component of a novel thymic regulatory network that helps interpret quantitative differences TCR signal during CD4/CD8 lineage decision, although it is not clear yet whether alteration in its expression is enough to redirect development of class II-restricted thymocytes to the CD8 lineage or vice versa. In fact, results from the Ho group suggest that GATA-3 may be required for CD4 development, but its absence is not enough to redirect these cells to the CD8 lineage.

References

Hernandez-Hoyos, G., Anderson, M.K., Rothenberg, E.V. and Alberola-Ila, J. (2003) *Immunity* 19:83-94.
 Hernandez-Hoyos, G. and Alberola-Ila, J. (2004) *Meths. Enzymol.* In press.

301b. Signals that control GATA-3 expression in the thymus

Chi Wang, G. Hernandez-Hoyos

Although the regulation of GATA-3 expression has been studied in detail in peripheral CD4 T cells, it is likely that different mechanisms apply in the thymus. In peripheral T cells GATA-3 upregulation seems to be mainly controlled by IL-4, through the activation of Stat-6, and then by a GATA-3 autoregulatory loop. TCR signals in isolation are not sufficient for this process. In contrast, TCR crosslinking in DP thymocytes induces upregulation of GATA-3 expression, and sustained high levels of expression are only achieved by strong TCR signals. We are analyzing in detail the biochemical mechanisms that regulate GATA-3 induction downstream the TCR using loss- and gain-of-function approaches to dissect the signal transduction pathways that contribute to GATA-3 upregulation downstream the TCR in DP thymocytes. To perform these experiments in normal DP thymocytes, we have optimized retroviral transfection and intracellular staining techniques. We use adult MHC^{-/-} thymocytes, infect them ex vivo with retroviruses expressing gain- or loss-of-function mutants in different signal transduction pathways and analyze GATA-3 induction after TCR stimulation by intracellular staining. Our results so far suggest that none of the tested pathways (Ras, calcium, NFκB) is completely required, or sufficient, to control GATA-3 expression in DP thymocytes. We think that the detailed dissection of the signal transduction pathways that control GATA-3 expression downstream the TCR in DP thymocytes is necessary to understand the regulation of lineage differentiation in the thymus, and will help us understand how the developing thymocytes integrate subtle differences in Lck activity to make fate decisions.

301c. Structure-function analysis of the GATA-3 domains important for CD4 lineage commitment

The regulation of CD4/CD8 development by GATA-3 is reminiscent of the role of GATA-3 in Th1/Th2 development. GATA-3 is upregulated early in Th2 development and is expressed at high levels in Th2 committed cells while its expression drops during Th1 development. Expression of GATA-3 is necessary for differentiation and commitment into the Th2 lineage and for inhibition of Th1 development. GATA-3 has been shown to regulate expression of cytokine genes by direct transactivation and by chromatin remodeling, and different domains mediate these different activities. Since GATA-3 could regulate CD4/CD8 development through direct transcriptional gene regulation, chromatin remodeling and/or interaction with other transcription factors we will perform a systematic structure-function analysis of GATA-3 in CD4/CD8 development to identify the domains of GATA-3 necessary for this process. This analysis will provide information as to the nature of the function of GATA-3 (i.e., transactivation vs. chromatin remodeling) and may suggest interaction partners required during this developmental process. We will determine if various GATA-3 deletion or mutant constructs can rescue the block in CD4 development observed in a GATA-3 inducible knockout. We have obtained floxed GATA-3/CD4-cre mice (FF/CD4-cre) from Dr. Ho and we are using lentiviral technology to express a number of GATA-3 deletions and point mutants in DP thymocytes.

302. Novel genes involved in CD4/CD8 lineage commitment

J. Alberola-Ila, K. Sauer*, M. Cooke*, G. Hernandez-Hoyos

Recent experiments have started to identify transcription factors responsible for implementing the genetic program that underlies CD4/CD8 lineage commitment and differentiation. We, and others, have shown that GATA-3 is necessary for CD4 development, and that its induction requires strong and/or sustained TCR signals. Similarly, Runx-3 has been identified as the transcription factor responsible for shutting off CD4 expression in CD8-lineage cells although it is not known how its activity is regulated. Our next goal is to build a broader picture of the various genes involved at different stages of CD4 and CD8 development (commitment, maturation or survival), as well as the interactions between them. We have taken a first step towards this goal by performing a wide screen for genes differentially expressed between developing CD4 and CD8 thymocytes. Our previous work demonstrated that during positive selection GATA-3 is upregulated in early CD4-lineage intermediate cells (CD4^{hi}CD8^{lo}CD69⁺ cells from MHC I^{-/-}) but not in the equivalent CD8-lineage intermediate cells (CD4^{hi} CD8^{lo} CD69⁺ cells from MHC II^{-/-}) thymocytes. Therefore, although these cells display similar surface phenotype, they are already expressing different gene programs. To identify genes expressed early on during CD4 or CD8

development we have compared the gene expression profiles of CD4^{hi}CD8^{lo}CD69⁺ cells derived from MHC I^{-/-} or MHC II^{-/-} mice, respectively. The microarray analysis was performed by our collaborators at the Genomics Institute of The Novartis Research Foundation (GNF, San Diego).

To determine the validity the results obtained, we focused on two sets of comparisons. First we compared the gene expression of the MHC I^{-/-} (or MHC II^{-/-}) population B vs. that of the DP MHC population. Among the genes with the highest changes in intensity were those known to be upregulated during positive selection; i.e., the surface antigens CD2, CD5, CD69, the transcription factors Tox, Egr-1, and Schlafen, and the survival protein Bcl-2. The TDT, Rag-1 and Rag-2 genes involved in TCR gene rearrangement were among those with the highest negative change in intensity, as expected since these genes are downregulated at the onset of positive selection. Subsequently we compared the gene expression profiles of populations B of MHC I vs. MHC II thymocytes. Setting a twofold increase and $p < 0.001$ confidence threshold this comparison yielded approximately 246 and 56 genes preferentially expressed in the CD4- and CD8-lineage cells, respectively. Interestingly, many of the genes known to be important for positive selection (Tox, Egr-1, Schlafen) are not differentially expressed. However GATA-3 was easily scored in the CD4 lineage cells. Similarly genes that should be present only in the CD8 population (CD8 α , CD8 β) or CD4 population (CD4) were also scored. These results confirm that populations B are both enriched for genes upregulated during positive selection and simultaneously include differentially expressed genes. Furthermore the ability to detect GATA-3 mRNA upregulation in the CD4-lineage cells with respect to the CD8 lineage cells (only a 5-fold upregulation in a not very abundant gene) highlights the sensitivity of this experimental approach. We are currently validating a number of the identified genes by quantitative PCR, and will test them functionally for a role in CD4/CD8 lineage differentiation using overexpression or knockdowns in RTOC, using the techniques we have implemented in the lab in the last few years.

*Genomics Institute of The Novartis Research Foundation (GNF), San Diego, CA

303. Ras/MAPK pathway and the control of positive selection

As a postdoctoral fellow in Dr. R.M. Perlmutter's laboratory, I showed that interference with the Ras-Erk pathway using dominant negative Ras (dnRas) and catalytically inactive MAPK Erk Kinase 1 (dMek) transgenes under the control of the Ick proximal promoter selectively inhibits positive selection without altering negative selection. These results showed for the first time that activation of the Ras-Erk pathway is necessary for positive selection, and that the TCR uses different signal transduction pathways to direct the cells towards further development (positive selection) and apoptosis (negative selection). After these original experiments were

published, additional evidence has accumulated showing a central role for Ras and Erk in positive selection. Since then I have been interested in understanding in more detail how Ras controls positive selection, and to explore whether this pathway plays also a role in CD4/CD8 lineage commitment. To understand better how activation of this cascade is regulated during positive selection at a single cell level, we are trying to develop Erk activity sensors based on fluorescence activated energy transfer (FRET).

303a. MAPK is not the only Ras effector involved in positive selection

The original experiments discussed above demonstrated that the Ras/Erk cascade is necessary for positive selection of T cells. Since in other developmental models, such as vulva in *C. elegans* and R7 photoreceptor in *D. melanogaster*, the Erk MAPK cascade is the only Ras effector required to direct cell fate determination processes, we decided to test whether Erk was the only downstream effector of Ras involved in positive selection. Our results showed that overexpressing constitutively active Raf (Raf-CAAX) or Mek (Mek-1_{S118,122E}) cannot rescue positive selection in dnRas mice, although the activated Mek could rescue a dMek phenotype. Therefore the Erk cascade is not the only downstream effector of Ras necessary for positive selection. We are trying to identify signaling pathways involved in positive selection downstream of Ras using two different approaches. Genetic rescue of a dnRas phenotype using Ras effector mutants, and gene profiling of different mutations in the Ras/MAPK pathways to identify genes dependent on Ras but not MAPK.

Reference

Alberola-Ila, J. and Hernandez-Hoyos, G. (2003) *Immunol. Rev.* 193:79-97.

303b. Analysis of Ras effector mutants M. Laurent

To identify other effectors we are utilizing a series of Ras effector mutants that contain point mutations made within the effector loop region of a constitutively active form of Ras. These mutants stimulate overlapping subsets of pathways downstream of Ras. Using retroviral-mediated gene transfer and RTOCs, we have introduced these mutants into dnRas thymocytes, and determined that only one of the five Ras effector mutants tested (RasV12E38) can rescue positive selection in dnRas thymocytes. This mutant is known to activate at least MAPK and RalGDS, so we are currently testing whether alterations in Ral GDS affect positive selection using conventional transgenesis and RTOCs. Of course, there may be other effectors not yet characterized, so we are also pursuing the gene profiling experiments described in the following abstract.

Reference

Laurent, M. and Alberola-Ila, J. Manuscript in preparation.

303c. Using microarrays to dissect the genetic networks that control positive selection downstream Ras

J. Alberola-Ila, K. Sauer*, M. Cooke*

To understand the process of positive selection we need a global view of the genetic program that TCR signals induce. To start dissecting this complex network we plan to concentrate in trying to identify the genes important for this process downstream of Ras. We have decided to attack this problem using a 'divide and conquer' approach, using a panel of mutations that block positive selection at different branching points in the Ras pathway to identify genes regulated downstream Ras, Egr, and Id3. dnRas transgenes, RasGRP^{-/-}, Egr-1^{-/-} and Id3^{-/-} mice are being bred in a MHC^{-/-} background to gain access to a homogeneous population of DP that have not received signals through the TCR. We will then stimulate purified DP from these mice in vitro, using CD3/CD4 or CD3/CD3 bi-bodies that drive full maturation in an RTOC, so that all the cells receive the same signal, at the same time. At different time points we will analyze the gene profile of these stimulated DP populations using Affymetrix chips, in collaboration with the Cooke and Sauer groups at the Genomics Institute of the Novartis Foundation (GNF). The hypothesis is that, by comparing the genes expressed by normal DP thymocytes and the different mutants after TCR triggering, we will be able to divide the total pattern into subsets that are, for example, Ras-dependent but Egr-independent.

This analysis would complement our current approach to identify additional Ras effector pathways important for positive selection, since it should be possible from the analysis of genes that are Ras-dependent, but Erk-independent to walk upstream to identify other Ras effectors activated during positive selection. Furthermore, the analysis of the results will also be informed from our profiling experiments with ex vivo sorted intermediates in the CD4 and CD8 lineage. We will test the functional relevance of those genes that seem the most interesting using retroviral infection of fetal thymocytes and RTOCs, or lentiviral transgenesis in vivo.

*Genomics Institute of The Novartis Research Foundation (GNF), San Diego, CA

303d. Ksr is required to link Ras to the MAPK cascade during positive selection

M. Laurent, D.M. Ramirez

Another not well-understood aspect of the regulation of Ras/Erk activation is the role played by scaffolding molecules. Genetic screens in *C. elegans* and *D. melanogaster* have identified a number of scaffolds that contribute to the regulation of the Ras/Erk pathway, including Ksr, Sur-8 and CNK. Not much is known about their physiological roles in mammalian cells, but from a theoretical point of view they have the potential to change the character of the Erk cascade signal depending on their concentration in a cell. A recent report on a Ksr-1 KO did not show an effect on T cell development, although the existence of an additional Ksr gene indicates that there is

redundancy built in the system. In our hands, overexpression of Ksr reproduces the dnRas phenotype, and this effect requires interaction of Ksr with Mek. These results suggest that Ksr plays a pivotal role in connecting Ras to the Erk cascade during positive selection.

References

- Laurent, M.N., Ramirez, D.M. and Alberola-Ila, J. (2004) *J. Immunol.* 173:986-992.
Sternberg, P.W. and Alberola-Ila, J. (1998) *Cell* 95:447.

303e. Development of ERK activity sensors to monitor MAPK activation
H. Green

An interesting aspect of the Erk cascade is its ability to function as an all-or-none switch under certain circumstances, as shown by the Ferrell group in *Xenopus* oocytes. This property of the Erk cascade is only evident at the single cell level, and because of technical problems in assessing activation of Erk in a cell-by-cell basis in mammalian cells, it is unclear whether this model applies during positive selection. Alternatively, in this process the Erk cascade could behave more like a rheostat, transmitting differences in TCR signal intensity to the nucleus. This question is specially relevant to address the possible role of the Ras/Erk cascade in determining CD4/CD8 lineage commitment, and its resolution will require the development of new tools. Some success has been achieved using intracellular staining and flow cytometry to detect the levels of activated Erk in single cells, although the limitation in these experiments is that there is no temporal information for an individual cell. The development of FRET-based sensors to detect activation of multiple signaling molecules is a promising new way to investigate signal transduction pathways at a single cell level, and may allow the direct determination of Erk activation during positive selection. We have developed a series of FRET-based Erk activation sensors (EAS) by coupling YFP and CFP with a peptide linker derived from Elk, a natural Erk substrate. Our results show that this construct changes FRET in response to phosphorylation, and is specific for the Erk MAPKs. Unfortunately at this point its use in vivo is precluded by its sensitivity to intracellular phosphatases. We are currently improving these sensors by adding a phospho-Elk binding domain to stabilize and protect the sensor. In collaboration with the Robert's lab at Caltech we have constructed a library for in vitro selection using mRNA display. The library is based in the 10th fibronectin type III domain, a stable protein scaffold, easy to produce in large scale and well expressed intracellularly. This domain is structurally analogous to the immunoglobulin VH domain. We have randomized two loop regions that correspond to the VH CDR1 and CDR3 hypervariable regions and generated a 10¹³ library. We will use a phospho-Elk peptide to select high affinity binders, and add the resulting 10FnIII domain to our sensors. This should result in a stabilization of the conformational change induced by phosphorylation, and also in protection against fast dephosphorylation in vivo.

This second generation EAS, coupled with confocal microscopy, should therefore allow us to follow Erk activation in thymocytes in RTOCs.

Reference

Green, H.M. and Alberola-Ila, J. Submitted for publication.

303f. Does the Ras/MAPK cascade play a role in CD4/CD8 determination?

H. Green, J. Alberola-Ila

The role of the Ras/Erk cascade in regulating CD4/CD8 lineage commitment is unclear at this point. In our original studies using dominant negative Ras and Mek in transgenic mice, positive selection was inhibited for both the CD4 and CD8 lineages, and no significant alteration in the CD4/CD8 ratios was observed at different levels of Mek inhibition. Similarly both dnRas and dMek blocked positive selection of thymocytes expressing class I and class II restricted tg TCRs, without inducing the generation of class II restricted CD8 cells in the class II restricted TCR systems analyzed (AND TCR, Tea TCR). A caveat in these experiments is that they were performed only with the highest expressing lines of dMek and dnRas, where Erk activation downstream the TCR is >90% blocked, so we may have missed more subtle effects. Other genetic alterations in the Ras/Erk pathway (i.e., a RasGRP KO) result in defects in positive selection of both CD4 and CD8 cells.

Most of the evidence supporting a role for the Ras/Erk cascade in determining CD4/CD8 development has been obtained using pharmacological inhibitors in FTOC systems. These experiments led the Zamoyska group to propose that activation of the Erk cascade is necessary for the generation of CD4 but not CD8 T cells. However, gene disruption experiments have shown that Egr-1 induction, and therefore Erk activation, is important for CD8 lineage commitment as well. A third type of experiments that address the role of Erk in CD4/CD8 lineage commitment uses low doses of phorbol esters and ionomycin to generate single positive cells from pre-selection DPs in suspension. In this system both CD4 and CD8 SP cells can be generated, but CD4 development requires longer and/or more intense activation than CD8 development.

Despite the uncertainties, the Erk cascade remains a good candidate to direct lineage commitment, besides being necessary for positive selection of both CD4 and CD8 T cells. Alterations in the duration of Erk signaling after stimulation have been shown to direct different cell fates in other systems, most famously in PC12 cells, where stimulation with EGF induces cell proliferation, while NGF induces differentiation. It is tempting to speculate that the Erk cascade instructs developing thymocytes in a similar way, since sustained activation could be used as a mechanism to set a threshold for the affinity of the interactions that would drive positive selection, and maybe also to distinguish signals generated by TCRs bound to MHC class II and those bound to MHC class I. In fact, as

recently shown, T cells may have the ability to integrate signals that surpass a certain threshold across time.

If Ras/MAPK are involved in the CD4/CD8 lineage differentiation, one would predict that partially inhibiting their function in class II-restricted thymocytes would, at some point in a dose titration, divert them towards the CD8 lineage, in a manner analogous to the effect of the dLGKR transgene on AND thymocytes. We are testing this hypothesis by generating transgenic mice that express AND and different levels of dMek in a RAG null background. To expedite the generation of the transgenic mice we are using lentiviral transgenesis, recently established at by the Baltimore lab at Caltech. The system is based on the use of self-inactivating lentiviral constructs and allows expression from tissue specific promoters such as the T-cell specific Ick distal promoter. This strategy allows the efficient generation of mice bearing different numbers of transgene copies, utilizing embryos of any inbred mouse strain, in our case AND/RAG. We also plan to extend this analysis to other class II-restricted TCRs.

Reference

Alberola-Ila, J. and Hernandez-Hoyos, G. (2003) *Immunol. Rev.* 193:79-97.

304. PI3-K controls thymic exit

S.D. Barbee

We first became interested in the possible role of Phosphatidylinositol 3-kinase (PI3K) in positive selection because it was identified as a Ras effector pathway in other systems. We generated transgenic mice expressing p110_{ABD}, the domain of the class I_API3K p110 α that mediates binding to the adaptor subunit, under the control of the Ick proximal promoter. Expression of p110_{ABD} sequesters the regulatory adaptor subunit p85, thus endogenous p110 exists as a highly unstable but catalytically active monomer. As a result, there is a constitutive PI3K activity in p110_{ABD} thymocytes. Phenotypically, the thymii of p110_{ABD} show an increase in the percentages and numbers the mature single positive thymocyte subsets. Experiments with the AND TCR transgenic line suggests that positive selection is specifically improved, although the interpretation of the experimental results is complicated by the migration phenotype described below. We do not observe any alterations in the life span of DP thymocytes nor defects in negative selection, as assayed both in vitro (using OT-1 deletion assays) and in vivo (superantigens). However, PI3K modulates more than just positive selection in thymocyte development. By competitively transferring a mixture of p110_{ABD} bone marrow and wild-type bone marrow into lethally irradiated host animals, we observe that despite parallel recolonization of the thymus and B cell compartments, p110_{ABD}-derived T cells take much longer to appear in the periphery. These results are confirmed by a delayed appearance of peripheral T cells in neonatal p110_{ABD} mice compared to NLC. This suggests that our disruption of class IA PI3K signaling has had an effect

upon the activity of class I_B PI3K downstream of the chemokine GPCRs that are involved in the final stages of thymocyte maturation.

305. Role of Notch during the DN to DP transition

G. Hernandez-Hoyos, Chi Wang

Work from the Robey, Bevan, Pear and Fowlkes groups suggested that the Notch cascade is involved in regulating many aspects of T cell development, including the T/B, $\alpha\beta/\gamma\delta$ and CD4/CD8 lineage decisions. Nevertheless, the mechanisms by which Notch exerts its effects are not well understood, and in some cases the physiologic role is unclear. We became interested in Notch function during positive selection because it has been shown to act as a negative regulator of the Ras/MAPK cascade in *C. elegans*, where it induces expression of a MAPK phosphatase, and the results of the Pear group suggested that it could block signals from the TCR. Using bicistronic retroviral vectors co-expressing GFP and Notch and primary DP thymocytes as well as a DP cell line, we determined that overexpression of activated Notch does not affect activation of the MAPK cascade in these cells, although induction of some activation markers, such as CD69 is affected by activated Notch. We concluded that Notch does not significantly inhibit activation of the MAPK pathway and that the block in positive selection observed by Pear, and reproduced by us must be induced by other factors.

In fact, further analyses using RTOCs and the OP9-delta system for in vitro differentiation of T cell precursors suggest that overexpression of active Notch enhances proliferation following pre-TCR selection so much that cells enter the DP cell stage (normally a quiescent stage) as blasts. We think that the inefficient selection results, at least in part, from the abnormally activated state of the DP cells. Using RNA interference, we have also shown that this proliferation is dependent on CSL, as recently shown by the Honjo group using a conditional knockout. We also plan to address molecular aspects of the Notch-induced proliferation by determining if Notch alters the expression of cell cycle regulators.

Reference

Hernandez-Hoyos, G., Wang, Chi and Alberola-Ila, J.
Manuscript in preparation.

Publications

Alberola-Ila, J. and Hernandez-Hoyos, G. (2003) The Ras/MAPK cascade and the control of positive selection. *Immunologic. Rev.* 193:79-97.

Hernandez-Hoyos, G. and Alberola-Ila, J. (2003) A notch so simple role in T cell development. *Sem. Cell Dev. Biol.* 14:121-127.

Hernandez-Hoyos, G. and Alberola-Ila, J. (2004) Analysis of T-cell development using siRNA to knockdown protein expression. *Meth. Enzymol.* In press.

Hernandez-Hoyos, G., Anderson, M.K., Rothenberg E.V. and Alberola-Ila, J. (2003) GATA-3 expression is controlled by TcR signals and regulates CD4/CD8 differentiation. *Immunity* 19:83-94.

Laurent, M.N., Ramirez D.M. and Alberola-Ila, J. (2004) KSR couples ras to the Erk MAPK cascade during T cell development. *J. Immunol.* 173:986-992.

Starck S.R., Green H.M., Alberola-Ila, J. and Roberts R.W. (2004) A general approach to detect protein expression in vivo using fluorescent Puromycin conjugates. *Chem. & Biol.* 11:1-20.

Albert Billings Ruddock Professor of Biology:
 Marianne Bronner-Fraser
 Visiting Associates: Andrew Groves, Mark Selleck
 Senior Research Fellows: Laura Gammill, Martin Garcia-Castro, David McCauley
 Postdoctoral Fellows: Meyer Barembaum, Ed Coles, Maria Elena deBellard, Maxellende Ezin, Yun Kee, Vivian Lee, Peter Lwigale, Katherine McCabe, Daniel Meulemans, Tatjana Sauka-Spengler, Lisa Ziemer
 Graduate Students: Meghan Adams, Martin Basch, Sujata Bhattacharyya, Houman Hemmati
 Research and Laboratory Staff: David Arce, Mary Flowers, Constanza Gonzalez, Matthew Jones, Samuel Ki, Anitha Rao, Nephi Santos, Johanna Tan-Cabugao

Support: The work described in the following research reports has been supported by:
 American Heart Association
 Howard Hughes Medical Institute
 National Institutes of Health (NINDS, DE)
 NASA

Summary: This laboratory's research centers on the early formation of the nervous system in vertebrate embryos. The peripheral nervous system forms from two cell types that are unique to vertebrates: neural crest cells and ectodermal placodes. We study the cellular and molecular events underlying the formation, cell lineage decisions and migration of these two cell types. The neural crest is comprised of multipotent stem-cell-like precursor cells that migrate extensively and give rise to an amazingly diverse set of derivatives. In addition to their specific neuronal and glial derivatives, neural crest cells can also form melanocytes, craniofacial bone and cartilage and smooth muscle. Placodes are discrete regions of thickened epithelium that give rise to portions of the cranial sensory ganglia, as well as form the paired sense organs (lens, nose, ears). Placodes and neural crest cells share several properties including the ability to migrate and to undergo an epithelial to mesenchymal transition. Their progeny are also similar: sensory neurons, glia, neuroendocrine cells, and cells that can secrete special extracellular matrices.

Our laboratory concentrates on studying the cellular and molecular mechanisms underlying the induction, early development and evolution of the neural crest and placodes. This research addresses fundamental questions concerning cell commitment, migration and differentiation using a combination of techniques ranging from experimental embryology to genomic approaches for novel gene discovery. These studies shed important light on the mechanisms of neural crest and placode formation, migration and differentiation. In addition, the neural crest and placodes are unique to vertebrates. In studying the evolution of these traits, we hope to better understand the origin of vertebrates.

Because these cell types are involved in a variety of birth defects and cancers such as neurofibromatosis, melanoma, and neuroblastoma, the results on the normal mechanisms of neural crest development provide

important clues regarding the mistakes that may lead to abnormal development or loss of the differentiated state.

306. A novel chicken **spalt** gene expressed in branchial arches reduces neurogenic potential of the cranial neural crest
 Meyer Barembaum, Marianne Bronner-Fraser
 Cranial neural crest cells differentiate into diverse derivatives including neurons and glia of the cranial ganglia and cartilage and bone of the facial skeleton. Here, we explore the function of a novel transcription factor of the spalt family that may be involved in early cell lineage decisions of the avian neural crest. The chicken spalt4 gene is expressed in the neural tube, migrating neural crest, branchial arches and transiently in the cranial ectoderm. Later, it is expressed in the mesectodermal but not neuronal or glial derivatives of midbrain and hindbrain neural crest. After over-expression by electroporation into the cranial neural tube and neural crest, we observed a marked redistribution of electroporated neural crest cells in the vicinity of the trigeminal ganglion. In control-electroporated embryos, numerous labeled neural crest cells (~80% of the population) entered the ganglion and differentiated into neurons and glia. In contrast, few (>30% of the population) spalt-electroporated neural crest cells entered the trigeminal ganglion. Instead, they localized in the mesenchyme around the ganglionic periphery or continued further ventrally to the branchial arches. Interestingly, little or no expression of neuronal markers was observed in spalt-electroporated neural crest cells. The results suggest that spalt negatively biases the ability of neural crest cells to populate peripheral ganglia and to adopt a neuronal fate.

307. Cancerous stem cells can arise from pediatric brain tumors
 Houman Hemmati, Harley Kornblum*, Marianne Bronner-Fraser
 Pediatric brain tumors are significant causes of morbidity and mortality. Often arising in the midline and of unknown cellular origin, and intriguing possibility that they derive from self-renewing, multipotent neural stem cells. Here, we tested whether different pediatric brain tumors, including medulloblastomas and gliomas, contain cells with properties similar to neural stem cells. We find that tumor-derived progenitors form neurospheres that can be passaged at clonal density and are able to self-renew. Under differentiative conditions, individual cells are multipotent, giving rise to both neurons and glia in proportions that reflect the tumor of origin. Unlike normal neural stem cells, however, tumor-derived progenitors have an unusual capacity to proliferate and sometimes differentiate into abnormal cells with multiple differentiation markers. Gene expression analysis reveals that both whole tumors and tumor-derived neurospheres express many genes characteristic of neural and other stem cells, including CD133, Sox2, musashi-1, and bmi-1, with variation from tumor to tumor. After grafting to neonatal rat brains, tumor-derived neurosphere cells migrate,

produce neurons and glia, and continue to proliferate for more than four weeks. The results show that pediatric brain tumors contain neural stem-like cells with altered characteristics that may contribute to tumorigenesis. This may have important implications for treatment via specific targeting of stem-like cells within brain tumors.

*Associate Professor, Depts. of Pharmacology and Pediatrics, UCLA Geffen School of Medicine

308. **Id** gene expression in amphioxus and lamprey highlights the role of genetic cooption during neural crest evolution

Daniel Meulemans, David McCauley, Marianne Bronner-Fraser

Neural crest cells are unique to vertebrates and generate many of the adult structures that differentiate them from their closest invertebrate relatives, the cephalochordates. *Id* genes are robust markers of neural crest cells at all stages of development. We compared *Id* gene expression in amphioxus and lamprey asked if cephalochordates deploy *Id* genes at the neural plate border and dorsal neural tube in a manner similar to vertebrates. Furthermore, we examined whether *Id* expression in these cells is a basal vertebrate trait or a derived feature of gnathostomes. We found that while expression of *Id* genes in the mesoderm and endoderm is conserved between amphioxus and vertebrates, expression in the lateral neural plate border and dorsal neural tube is a vertebrate novelty. Furthermore, expression of lamprey *Id* implies that recruitment of *Id* genes to these cells occurred very early in the vertebrate lineage. Based on expression in amphioxus we postulate that *Id* cooption conferred sensory cell progenitor-like properties upon the lateral neurectoderm, and pharyngeal mesoderm-like properties upon cranial neural crest. Amphioxus *Id* expression also supports an evolutionary relationship between the anterior neurectoderm of amphioxus and the presumptive placodal ectoderm of vertebrates. We relate these observations to previous studies and propose that neural crest evolution was driven in large part by cooption of multi-purpose transcriptional regulators from other tissues and cell types.

309. Combined intrinsic and extrinsic influences pattern cranial neural crest migration and pharyngeal arch morphogenesis in axolotl

Robert Cerny¹, Daniel Meulemans, Marianne Bronner-Fraser, Hans-Henning Epperlein²

Cranial neural crest cells migrate in a precisely segmented manner to form cranial ganglia, facial skeleton and other derivatives. Here, we investigate the mechanisms underlying this patterning in the axolotl embryo using a combination of tissue culture, molecular markers, scanning electron microscopy and vital dye analysis. In vitro experiments reveal an intrinsic component to segmental migration; neural crest cells from the hindbrain segregate into distinct streams even in the absence of neighboring tissue. In vivo, separation between neural crest streams is further reinforced by tight juxtapositions that arise during early migration between

epidermis and neural tube, mesoderm and endoderm. The neural crest streams are dense and compact, with the cells migrating under the epidermis and outside the paraxial and branchial arch mesoderm with which they do not mix. After entering the branchial arches, neural crest cells conduct an "outside-in" movement, which subsequently brings them medially around the arch core such that they gradually ensheath the arch mesoderm in a manner that has been hypothesized but not documented in zebrafish. This study, which represents the most comprehensive analysis of cranial neural crest migratory pathways in any vertebrate, suggests a dual process for patterning the cranial neural crest. Together with an intrinsic tendency to form separate streams, neural crest cells are further constrained into channels by close tissue apposition and sorting out from neighboring tissues.

¹Dept. of Zoology, Charles University, Prague, Czech Republic

²Dept. of Anatomy, TU Dresden, Dresden, Germany

310. Graded potential of neural crest to form cornea, sensory neurons and cartilage along the rostrocaudal axis

Peter Lwigale, Gary Conrad*, Marianne Bronner-Fraser

Neural crest cells arising from different rostrocaudal axial levels form different sets of derivatives: cranial neural crest forms cartilage, cornea and cranial ganglia; cardiac neural crest forms the outflow tract of the heart; trunk crest forms sympathetic and dorsal root ganglia. Here, we test whether these differences in derivatives are due to differences in developmental potential by challenging cardiac and trunk neural crest cells by transplanting them into the midbrain environment and examining their long-term differentiation into cornea, trigeminal ganglion and branchial arch cartilage. Although both cardiac and trunk neural crest migrate to the periocular region, they do not contribute appropriately to the cornea. Cardiac neural crest cells make only a small contribution to the stroma or endothelial cell layers, and often form ectopic-pigmented masses on the dorsal corneal surface. Trunk neural crest cells only differentiate into melanocytes after transplantation to the midbrain regardless of their site of localization in the cornea. After both cardiac and trunk grafts, a trigeminal ganglion of reduced size forms, apparently due to a significant decrease in somatosensory neurons, most pronounced for truncal grafts. Those few neurons that differentiate, do, however, make appropriate connections to their peripheral targets in the cornea. In the first branchial arch, cardiac neural crest contributes to the quadrate, but only nominally to Meckle's cartilage. Trunk neural crest cells form no cartilage after transplantation, even when grafted directly into the first branchial arch. These results suggest a graded rostrocaudal loss in neural crest populations with respect to their ability to form somatosensory neurons and cartilage even after transplantation to a permissive environment.

*Kansas State University, Manhattan, Kansas

311. Segregation of lens and olfactory precursors from a common territory

Sujata Bhattacharyya, Andrew Bailey*, Marianne Bronner-Fraser, Andrea Streit*

Cranial placodes are focal regions of columnar epithelium next to the neural tube that contribute to sensory ganglia and organs in the vertebrate head, including the olfactory epithelium and the crystalline lens of the eye. Using focal dye labeling within the presumptive placode domain, we show that lens and nasal precursors arise from a common territory surrounding the anterior neural plate. They then segregate over time and converge to their final positions in discrete placodes by apparently directed movements. Since these events closely parallel the separation of eye and antennal primordia (containing olfactory sensory cells) from a common imaginal disc in *Drosophila*, we investigated whether the vertebrate homologues of *Distalless* and *Eyeless*, which determine antennal and eye identity in the fly, play a role in segregation of lens and nasal precursors in the chick. *Dlx5* and *Pax6* are initially co-expressed by future lens and olfactory cells. As soon as presumptive lens cells acquire columnar morphology all *Dlx* family members are down-regulated in the placode, while *Pax6* is lost in the olfactory region. Lens cells that express ectopic *Dlx5* never acquire lens-specific gene expression and are excluded from the lens placode to cluster in the head ectoderm. These results suggest that the loss of *Dlx5* is required for cells to adopt a lens fate and that the balance of *Pax6* and *Dlx* expression regulates cell sorting into appropriate placodal domains.

*Dept. of Craniofacial Development, King's College London, Guy's Campus, London, UK

312. Developmental origins and evolution of jaws: New interpretation of "maxillary" and "mandibular"

Robert Cerny, Daniel Meulemans, Hans-Henning Epperlein, Marianne Bronner-Fraser

Cartilage of the vertebrate jaw is derived from cranial neural crest cells that migrate to the first pharyngeal arch and form a dorsal "maxillary" and a ventral "mandibular" condensation. It has been assumed that the former gives rise to palatoquadrate and the latter to Meckel's (mandibular) cartilage. In anamniotes, these condensations have been thought to form the framework for the bones of the adult jaw and, in amniotes, appear to prefigure the maxillary and mandibular facial prominences. Here, we directly test the contributions of these neural crest condensations in axolotl and chick embryos, as representatives of anamniote and amniote vertebrate groups, using molecular and morphological markers in combination with vital dye labeling of late-migrating cranial neural crest cells. Surprisingly, we find that both palatoquadrate and Meckel's cartilage derive solely from the ventral "mandibular" condensation. In contrast, the dorsal "maxillary" condensation contributes to trabecular cartilage of the neurocranium and forms a part of the frontonasal process but does not contribute to the jaw joint as previously assumed. These studies are the first

to reveal the morphogenetic processes of cranial neural crest cells within the first arch that build the primordia of jaw cartilages and of the anterior cranium.

313. Discover of genes involved in placode formation

Katy McCabe, Andrea Manzo, Laura Gammill, Marianne Bronner-Fraser

The peripheral nervous system of the head is derived from cranial ectodermal placodes and neural crest cells. Placodes arise from thickenings in the cranial ectoderm that invaginate or ingress to form sensory ganglia and the paired sense organs. We have combined embryological techniques with array technology to identify genes that are expressed as a consequence of placode induction. As a secondary screen, we used whole mount *in situ* hybridization to determine the expression of candidate genes in various placodal domains. The results reveal 52 genes that are found in one or more placodes, including the olfactory, trigeminal and otic placodes. Expression of some of these genes is retained in placodal derivatives. Furthermore, several genes are common to both neural crest and ectodermal placodes. This study presents the first array of candidate genes implicated in placode development, providing numerous new molecular markers for various stages of placode formation. Importantly, the results uncover previously unknown commonalities in genes expressed by multiple placodes and shared properties between placodes and other migratory cells, like neural crest cells.

Publications

Ahlgren, S., Vogt, P. and Bronner-Fraser, M. (2003) Excess *FoxG1* causes overgrowth of the neural tube. *J. Neurobiology* 57:337-349.

Barembaum, M. and Bronner-Fraser, M. (2004) A novel chicken spalt gene expressed in branchial arches reduces neurogenic potential of the cranial neural crest. *Neuron Glia* 1:57-63.

Bhattacharyya, S., Bailey, A.P., Bronner-Fraser, M. and Streit, A. (2004) *Pax6*, *Dlx5* and cell sorting during olfactory and lens placode development: Parallels between vertebrates and *Drosophila*. *Dev. Biol.* 271:403-414.

Cerny, R. Meulemans, M., Berger, J., Wilsch-Brauminger, M., Kurth, T., Bronner-Fraser, M. and Epperlein, H.H. (2004) Cranial neural crest migration and pharyngeal arch morphogenesis in axolotl. *Dev. Biol.* 266:252-269.

Cerny, R., Lwigale, P., Ericsson, R., Meulemans, D., Epperlein, H.H. and Bronner-Fraser, M. (2004) Developmental origins and evolution of jaws: New interpretation of "maxillary" and "mandibular." *Dev. Biol.* In press.

Chen, Y., Gutmann, C., Haipek, B., Martinsen, B., Bronner-Fraser, M. and Krull, C. (2004) Characterization of chicken *Nf2/merlin* indicates potential roles in growth regulation and cell migration. *Dev. Dynam.* 229:541-554.

- DeBellard, M., Rao, Y. and Bronner-Fraser, M. (2003) Dual function of Slit2 in repulsion and enhanced migration of trunk neural crest cells. *J. Cell Biol.* 162:269-280.
- Gamill, L. and Bronner-Fraser, M. (2003) Neural crest specification: Migrating into genomics. *Nature Rev. Neurosci.* 4:795-805.
- Hemmati, H.D., Nakano, I., Lazareff, J.A., Masterman-Smith, M., Geschwind, D.H., Bronner-Fraser, M. and Kornblum, H.I. (2003) Cancerous stem cells can arise from human pediatric brain tumors. *Proc. Natl. Acad. Sci. USA* 100:15178-15183.
- Lee, V., Sechrist, J., Luetolf, S. and Bronner-Fraser, M. (2003) Both neural crest and placode contribute to the ciliary ganglion and oculomotor nerve. *Dev. Biol.* 263:176-190.
- Lwigale, P.Y., Conrad, G. and Bronner-Fraser, M. (2004) Graded potential of neural crest to form cornea, sensory neurons and cartilage along the rostrocaudal axis. *Development* 131:1979-1991.
- McCabe, K., Manzo, A., Gamill, L. and Bronner-Fraser, M. (2004) Discovery of genes implicated in placode formation. *Dev. Biol.* In press.
- McCauley, D. and Bronner-Fraser, M. (2003) Neural crest contributions to the lamprey head. *Development* 130:2317-1227.
- Meulemans, D., McCauley, D. and Bronner-Fraser, M. (2003) Id gene expression in amphioxus and lamprey highlights the role of genetic co-option during neural crest evolution. *Dev. Biol.* 264:430-42.
- Peters, J., Sechrist, J., Luetolf, S., Lored, G. and Bronner-Fraser, M. (2003) Spatial expression of the alternatively spliced E11B and E11A segments of fibronectin in the early chicken embryo. *Cell Comm. Adhes.* 9:221-238.
- Venters, S.J., Argent, R.E., Deegan, F.M., Wong, T.S., Tidyman, W.E., Marcelle, C., Bronner-Fraser, M. and Ordahl, C.P. (2004) Limb muscle precursor cells do not undergo precocious terminal differentiation when isolated from lateral inhibitory signals. *Dev. Dynam.* 229:591-599.

Norman Chandler Professor of Cell Biology: Eric H. Davidson
 Distinguished Carnegie Senior Research Associate Emeritus: Roy J. Britten
 Visiting Associates: Hamid Bolouri¹, Lee Hood¹, Gary Wessel²
 Senior Research Associate: R. Andrew Cameron
 Senior Research Fellow: Paola Oliveri
 Member of the Professional Staff: Andrew Ransick, Chiou-Hwa Yuh
 Research Fellows: Gabriele Amore, Cristina Calestani, Lili Chen, Feng Gao, Veronica Hinman, Takuya Minokawa, Ochan Otim, Qiang Tu
 Graduate Students: Sagar Damle, C. Titus Brown, Meredith L. Howard, Pei Yun Lee, Carolina B. Livi, Stefan Materna, Roger Revilla
 Undergraduates: Elizabeth Dorman, Meng-meng Fu, Katherine Gora, Charlotte Guo, Maria K. Ho, Kelly Lin, Gwendolyn Ong
 Research and Laboratory Staff: Carlzen Balagot, Barbara Barth, Kevin Berney, Ted Biondi, William Chiu, Elly Chow, Ping Dong, Jessica Gamboa, Rachel Gray, Julie Hahn, Eve Helguero, Patrick S. Leahy, Ian Lipsky, Harrison Luu, Albert Nguyen, Jane Rigg, Deanna Thomas, Leah Vega, John Williams, Jane Wyllie, Qiu-Autumn Yuan, Jina Yun, Miki Yun

¹Institute for Systems Biology, Seattle, WA

²Brown University

Support: The work described in the following research reports has been supported by:

Applied Biosystems
 Beckman Institute
 Caltech President's Fund
 Department of Energy
 Lucille P. Markey Charitable Trust
 NASA/Ames
 National Institutes of Health, USPHS
 National Science Foundation
 Norman Chandler Professorship in Cell Biology

Key outside collaborators in many of these projects include:

George Weinstock and Richard Gibbs, Human Genome Sequencing Center, Baylor College of Medicine
 Lee Hood and Hamid Bolouri, Institute for Systems Biology
 Sorin Istrail, Applied Biosystems
 David J. Bottjer, University of Southern California
 Jun-Yuan Chen, Early Life Research Center, Chengjiang, Yunnan, China

Summary: The major focus of research in our laboratory is on gene regulatory networks (GRNs) that control development, and the evolution of these networks. Most of our research is done on sea urchin embryos, which provide key experimental advantages. Among these are: an easy gene transfer technology, which makes this a system of choice for studying the genomic regulatory

code; availability of embryonic material at all seasons of the year; an optically clear, easily handled embryo that is remarkably able to withstand micromanipulations, injections and blastomere recombination and disaggregation procedures; a very well understood and relatively simple embryonic process; and in-house egg-to-egg culture of the species we work with, *Strongylocentrotus purpuratus* (in a special culture system we have developed, located at Caltech's Kerckhoff Marine Laboratory). There is also a rich collection of arrayed cDNA and BAC libraries for sea urchins. The genome of *S. purpuratus* is being sequenced at HGSC (Baylor) and this project is expected to be finished in the first half of 2005. A very extensive repertoire of effective molecular technologies for experimentation on sea urchin gene regulatory systems has evolved. The experimental model that we utilize for evolutionary GRN comparisons is another echinoderm, also of local provenance, the starfish *Asterina miniata*. The embryo of this animal proves to be as excellent a subject for gene regulation molecular biology as is that of the sea urchin.

We pursue an integrated, "vertical" mode of experimental analysis, in that our experiments are directed at all levels of biological organization, extending from the transcription factor-DNA interactions that control spatial and temporal expression of specific genes to the system-level analysis of large regulatory networks. It has become apparent that the only level of analysis from which explanations of major developmental phenomena directly emerge, is the system level represented by the sea urchin GRN.

The main initiatives at the present time are as follows: **i. Analysis of the gene regulatory network underlying endomesoderm specification in *S. purpuratus* embryos:** At present about 50 genes have been linked into this GRN. The architecture of the network is emerging from an interdisciplinary approach in which computational analysis is applied to perturbation data obtained by gene expression knockouts and other methods, combined with experimental embryology. Regulatory and downstream genes required for skeletogenesis and for territorial specification have been isolated utilizing high-density arrayed cDNA libraries. A predictive model of the GRN has emerged which indicates the inputs and outputs of the cis-regulatory elements at its key nodes. Most of the individual projects reported below are contributing to understanding of this network. **ii. Testing the cis-regulatory predictions of the GRN:** The GRN has been constructed essentially by integrating the results of a massive perturbation analysis of expression of individual genes with spatial and temporal expression data for these genes. It predicts the required specific regulatory inputs and outputs linking the genes within the GRN. These predictions are subject to direct experimental cis-regulatory test, and correction, if need be. At present we have in hand the cis-regulatory elements that control the following important genes of the regulatory network, all of which play important and unique roles: *wnt8*, *gatae*, *krox1*, *foxa*, *delta*, *otx* (several cis-regulatory modules),

gcm, brachury. We are determining at the DNA level the inputs into these cis-regulatory elements, and their response to the relevant upstream perturbations. We will soon have similar data regarding cyclophylin, pmar1, alx1, tbr. For some regions of the GRN the analysis is approaching maturity, in that it extends convincingly from maternal inputs to cell-type differentiation. The best example is the GRN subregion determining skeletogenic micromere specification. The subnetwork determining the stability of the endodermal specification state is also among the regions of the GRN that are well established at the cis-regulatory level. Overall, the results of these experiments promise to convert the GRN into a map of the hard-wired genomic control logic for this portion of development.

iii. Completion of the repertoire of regulatory genes engaged in the endomesoderm GRN:

We are using the data emerging from the genome sequence project to identify and assemble computationally all gene sequences that encode transcription factors. The temporal patterns of expression of these genes are determined, and for those possibly relevant to the GRN, the spatial patterns as well. Those genes that evidently play a role in endomesoderm specification will then be linked into the GRN by perturbation and cis-regulatory analysis.

iv. Computational representation of core GRN linkages:

A mathematical representation of the transcription factor target site preferences for key regulatory genes of the GRN will depend on accurate knowledge of these preferences, and these are being measured *in vitro*. Methods can then be developed for "reading" the GRN architecture from the genomic sequence, using the established GRN as a test bed.

v. Evolution, viewed as a process of change in GRN architecture:

Starfish and sea urchins shared a last common ancestor about 500 million years ago. Thus, analysis of the GRN controlling endomesoderm specification events in the starfish embryo will reveal both the nature of functional change in the GRN, and conservation of features that are so essential that they have resisted alteration for half a billion years. We have already seen examples of both. The underlying processes are of course change, or alternatively, conservation, of functional cis-regulatory features. To study this we are examining starfish/sea urchin GRN differences at the cis-regulatory level. In a separate, large-scale effort, we have nearly completed the isolation of BACs containing 12 genes the cis-regulatory elements of which are known in *S. purpuratus*, from genomic libraries of five different sea urchin species ranging from 15 to 250 million years since divergence from the lineage leading to *S. purpuratus*. These will afford the opportunity of studying by computational and experimental methods the process of cis-regulatory evolution, which is very poorly understood.

vi. Oral ectoderm GRN: We have begun work on the GRN that controls oral ectoderm specification. Three parts of this process can be distinguished, initial specification, maintenance of oral ectoderm state, and oral ectoderm regionalization (i.e., into the neurogenic ciliary band and apical plate, and the central columnar epithelium). The GRN so far concerns only the maintenance parts of the

process. Nonetheless, maintenance alone involves complex feedback loops and repression, as also seen in the endomesodermal GRN.

vii. Computational and experimental kinetic cis-regulatory model:

To build a logic model of the information processing functions of a cis-regulatory element that relates the input kinetics (i.e., the temporal changes in relevant transcription factor levels) to its output, we have returned to the *cyllia* gene. The logic model of the regulatory system of this gene is being completed by additional mutational gene transfer experiments, and input kinetics are being measured.

viii. Various explorations by new methods and approaches:

As always, we are trying to expand knowledge by use of novel technologies for analysis of the GRN and the genome. Current initiatives include first attempts to "reengineer" the process of embryonic development, by installing regulatory subcircuits in novel spatial domains; tests of new reagents for perturbing gene expression; utilization of a new technology for FACS sorting GFP-expressing embryos to the goal of obtaining quantitative cis-regulatory measurements; use of BAC GFP recombinants for analysis of genomic regulatory apparatus; application of quantitative imaging methods to assessment of expression construct function; and a project to obtain a physical map of the sea urchin genome, using the inbred lines in our system to measure assortment of microsatellite markers.

xi. Computational approaches to regulatory gene network analysis:

Regulatory gene networks for development cannot be informatively treated as equilibrium or steady-state systems. With Hamid Bolouri of the Institute for Systems Biology, Seattle, WA, a new approach to mathematical description of these developmental regulatory systems describes its unidirectional progression through successive spatial regulatory states. In addition, several genome analysis tools are being developed, and a new project to build probability models of target sites for all known transcription factors in the endomesoderm network is under way. With Sorin Istrail of Applied Biosystems an effort is also being made to categorize cis-regulatory logic functions as a first step to interpretation of the genomic regulatory code underlying development. Many additional computational genomics and other projects are summarized below.

The Center for Computational Regulatory Genomics CCRG

The goal of the Center for Computational Regulatory Biology is to develop, refine and test computational approaches in genomics broadly and cis-regulatory analysis specifically. The primary focus for the latter is the elucidation of gene regulatory networks in development. The Center interacts with the wider research community in several ways: it provides open source software for use by academic research groups; it provides web-based servers for genomic analysis using software developed locally; and it maintains databases fundamental to the Sea Urchin Genome Project, an initiative that began in the Davidson laboratory and at the Genomics

Technology Facility. The Facility provides to the Caltech and external scientific community upon request services and materials stemming from the macroarray libraries and arraying equipment that we maintain. The Center and the Facility are both under the direction of R. Andrew Cameron. Oversight for the Genomics Technology Facility is shared by the PI of this Center (Eric Davidson) and the PI of the Genomics Research Center (Mel Simon).

Genomics Technology Facility

The operation of the Facility centers on the Genetix Arraying Robot, a large flatbed robotic arm with video camera used to produce bacterial macro-array libraries and filters. This year we upgraded our robot to the latest design. Ancillary equipment in support of robot library construction, including automated medium handling equipment and an automated DNA preparation unit, are also housed in the Facility. An additional robotic DNA preparation machine is situated in the PI's laboratory and is available for Facility high-throughput use. We currently maintain in -80°C freezers 27 different echinoderm libraries comprising a total of approximately three million arrayed clones. In addition to providing these materials to academic research groups, we also offer the opportunity for outside groups from Caltech and elsewhere to array and spot their own libraries.

Our robot utilization for the past year was quite consistent and efficient. We arrayed a total of 1.28 million library clones and printed a total of 285 filters. The in-house jobs consisted of reprinting filters from four existing libraries and both arraying and printing of four new libraries. We also re-arrayed our *S. purpuratus* BAC library for use by the sequencing effort. The four new libraries extended the comparative genomics aspect of the Facility by adding a new sea star genomic BAC library and both cDNA and BAC libraries for the related sea urchin species, *Arbacia punctulata*. In support of the Sea Urchin Genome Project, we produced an extension of our original genomic BAC library using a different restriction enzyme for cloning. This will reduce any unevenness in the representation of particular genomic regions by reducing cloning bias. For outside users, we trained and supervised two off-campus groups and four on-campus groups. One of the groups associated with the Southwest Medical Branch, San Antonio, Texas came to us through our connection to the National Center for Research Resources, the agency that provides a large portion of Facility support. Personnel: The staff for the facility are Eve Helguero and Autumn Yuan.

Research Center

Computational aspects of gene regulatory network project. The description and simulation of gene regulatory networks can only be accomplished with computational tools specific to the task. We have locally developed several software tools that are in constant use by our laboratory investigating sea urchin development, as well as over 110 users working in a variety of other systems. These tools were specifically designed to aid the

experimentalist working at the bench and using iterative cycles of experimentation and computation. The software tools include: BioArray, a program that uses macroarray spot data from phosphoimagers to manage intensity and position information; SUGAR, a system to perform, display and correlate large-BAC sequence analyses to aid the experimentalist with the functional analysis of cis-regulatory elements in genomic DNA; SeqComp and FamilyRelations, programs for comparative sequence analysis; and NetBuilder, an environment for creating and analyzing models of gene networks.

In order to make the sequence analysis programs convenient we have installed a web-based facility, the Cartwheel Project, that allow the user to have complete control over the process. Within the circumscribed domain of genomic sequence-based information, Cartwheel provides facilities to organize, analyze, and curate information on the level of individual labs. The analyses are then viewable by programs such as FamilyRelations. The Cartwheel Project is the umbrella term for a bioinformatics infrastructure first developed by Titus Brown and now maintained and extended by the computational staff of the Center. As the genome data has expanded, we have found it necessary to install another queuing package, Parasol, to facilitate bulk jobs not covered by Cartwheel.

The equipment that supports the computational efforts of the Center includes two 18-unit Beowulf clusters, a web server for the Sea Urchin Genome Project (SUGP) and several dual processor-development machines used by the staff for software construction, testing and maintenance. In the past year we have decommissioned one obsolete Beowulf cluster and installed a new one.

The utility of these comparative sequence analysis facilities is reflected in the user population. At present, the Caltech Cartwheel server, Woodward, has 249 total registered users in 40 lab groups. A total of 22181 jobs have run in the last year for a total of 123 CPU days. The majority of these are Seqcomp and Blast analyses.

The sea urchin genome project web site. The Sea Urchin Genome Project web site (<http://sugp.caltech.edu/>) is the distribution center for laboratory-specific sequence and annotation information related to the sea urchin genome and our macroarray libraries. We have continued to rework this part of the facility as new data from the sequencing project is made available from Baylor College of Medicine, Human Genome Sequencing Center and the Mapping Group at the Genome Sciences Center of the British Columbia Cancer Agency. We are working with the NCBI Computational Branch to produce a specific sea urchin genome page at http://www.ncbi.nlm.nih.gov/genome/guide/sea_urchin/. This includes at NCBI a set of well-curated purple sea urchin reference sequences representing all known genes.

As genomic BAC sequence from the *S. purpuratus*, *L. variegatus*, *Arbacia punctulata* and other echinoderm genomes accumulates, it is annotated using the software package SUGAR, which operates through the

Cartwheel queueing system. These programs also reside on the SUGP machines and efficiently interdigitate with the existing packages. The static annotations are posted on the web site.

The Sea Urchin Genome Project Web site is the database for macroarray filter information. Since all of our libraries are arrayed and catalogued, all new sequence and gene annotation information collected in the process of screening these library filters, for whatever purpose, is stored by location. This includes sequence collections from complex probes screens such as those used for the identification of genes in the endomesoderm specification pathway; the results of homology screening strategies, and random EST projects. Because the data is coupled to a filter location that contains an individual clone from the library, the clone is immediately recoverable. As more clones are characterized in a library, that library becomes more valuable. Eventually, the several well-characterized libraries can be used to confirm *ab initio* gene predictions and confirm gene catalogs for the sea urchin.

Personnel: The staff who support the computational aspects of the Center are: Kevin Berney, C. Titus Brown, and Ian Lipsky.

314. Computational analysis of the emerging sea urchin genome sequence

R. Andrew Cameron, Kevin Berney, C. Titus Brown, Ian Lipsky

The posted whole genome shotgun sequence for the purple sea urchin produced by the Baylor College of Medicine, Human Genome Sequencing Center with support from HGRI has reached eight million traces. The Sea Urchin Genome Project housed in the Center for Computational Regulatory Genomics provided the materials including libraries for this project. The sequences are being assembled currently and the result is expected to average sequence scaffolds of 20-30,000 bp. The computational arm of the Center will continue to provide simple analyses in order to facilitate gene discovery and future annotation of the genomic sequences for the broader sea urchin community. We have developed a data pipeline to collect, assemble and analyze trace sequences collected from searches against small candidate gene databases. In addition to the transcription factor gene collection produced in a parallel effort, we have produced gene lists for putative innate immunity genes and sex determination genes. The computational staff of the Center is continuously conducting other sorts of analyses on the available trace sequences as well. Quality control and distribution measurements of the trace collection are derived from comparison to other data sets of sequences collected in the past, viz., the BAC-end STC sequences determined at the High-throughput Sequencing Center at the University of Washington and posted on the website. The Sea Urchin Genome Project web site (<http://sugp.caltech.edu/>) serves as the information exchange site for these projects.

315. The conservation of *cis*-regulatory information in lower deuterostomes

R. Andrew Cameron, Jonathan P. Rast, Ping Dong, Julie Hahn, Jane Wyllie

Sequences conserved between the genomes of two species can be presumed to reflect a functional significance. The evolutionary distances at which informative conserved elements emerge from the background are poorly understood. We have shown that in sea urchins a divergence of 50 million years provides adequate change for conservation of sequence to be visible in many of the examples so far examined. Often these conserved sequence regions possess *cis*-regulatory function and current results show that this approach may yield a more than ten-fold increase in rate of experimental *cis*-regulatory element discovery, compared to the most efficient "blind" search methods. We have launched a project to explore the rules for efficient *cis*-regulatory sequence prediction by interspecific sequence analysis. The work is focused on 20 different gene candidates whose expression pattern, regulatory inputs and downstream targets are well characterized in the purple sea urchin. The orthologous genes come from several different echinoderm species that display a range of phylogenetic relatedness. We have constructed BAC libraries for four species of sea urchins, and for more distant comparisons, a sea star and a hemichordate. We are currently screening the libraries to obtain BACs containing the candidate genes. As the BACs are identified they are put in the pipeline for sequencing. The BACs are characterized and a reporter-coding region inserted into the gene using a bacterial recombination system. Gene transfer is used to determine the spatial and temporal expression pattern compared to the endogenous expression. Using the BAC sequences putative *cis*-regulatory regions indicated by interspecific sequence comparison at diverse distances are identified. The BAC reporter construct is then manipulated in order to test the function of these regions by gene transfer. A method that uses the BAC reporter for sequencing is under investigation as well. This will shortcut the sequencing procedure since only the immediate, useful gene region will be sequenced. We expect that this approach will reveal rules for computational *cis*-regulatory analysis while extending the current repertoire of BAC libraries, improving computational tools, and generating more efficient laboratory methods for this essential research area.

316. A microsatellite-based physical map of the purple sea urchin genome

R. Andrew Cameron, Kevin Berney, Elly Chow, Autumn Yuan, Eve Helguero, Ochan Otim

The sea urchin genome is the first large animal genome to be sequenced for which no physical map is available. However, mapping data are going to be required in order to enhance the quality of the genome sequence assembly. To produce a linkage map, we will extend our previously published microsatellite mapping strategy using animals of known relationship from our inbred lines.

Genotyping by microsatellite markers will yield two kinds of evidence that address two related problems: clustering markers in linkage groups, i.e., chromosomes; and determining the order of the markers within each chromosome. In preparation for the genotyping of single embryos resulting from crosses in the pedigreed lines, we have scaled down the PCR reactions to use extracts of single embryos at about 200-300 cells or less than one nanogram of template DNA. In practice, the steps of this project are: 1) Design primer pairs computationally. Using the more than 8 million purple sea urchin whole genome traces we have pursued a computational strategy to identify useful primer sets taking into account sequence quality and primer frequency. We have tested this algorithm and demonstrated that it produces effective primers that amplify efficiently under standard conditions. 2) Test each primer pair using unlabeled primers and three genomes: two from the inbred animals and a third from the animal being sequenced. Considering the high degree of genomic polymorphism (4-5%) present in purple sea urchins, these latter tests are crucial to the design of a useful panel of micro-satellite markers. Indeed, about one-third of the primers sets display polymorphism in this screen. 3) Measure the fragment size on an AB 3730 Sequencer, using GeneMapper software. There are 27 DNA samples from the pedigreed animals that will total about 120, 96-well plates of reactions for this phase of the analysis. Segregation behavior of these polymorphic variants will define linkage groups. 4) Generate crosses among the pedigreed lines to genotype with linkage group markers in order to define the order of markers in each group. About 1600 embryos from each cross should produce sufficient recombination to determine order. At this density of observation we will have a fair chance of detecting as little as 5-10% recombination, since both the reciprocals will be present. This will suffice to provide at least ordered groups of markers within each chromosome.

317. Understanding gene regulation through motif analysis
Meredith Howard

The genetic program directing the development of a single-cell fertilized egg into a sea urchin embryo is encoded in the organism's genomic DNA. The essence of this program is a network of genes encoding transcription factors and the cis-regulatory modules controlling the expression of those genes. Each module can receive multiple inputs at multiple sequence-specific target sites for other transcription factors in the network, and these signals are integrated into a single output resulting in the gene being turned on or off in different areas of the developing organism at different points in time. Understanding the developmental process therefore requires finding the functional linkages of the network – connecting the output of regulatory genes to the genomic target sites to which those products bind to activate further rounds of specification. This task is made challenging by our incomplete understanding of how transcription factors discern functional target sites from the vast population of

non-functional sites with the same sequence in the genome.

In order to study how functional target sites within cis-regulatory modules differ from non-functional sites scattered throughout the genome, we propose assembling a target site database of transcription factors known to be active in the gene regulatory network (GRN) that controls early development of the sea urchin. This data will then be incorporated into a cis-regulatory prediction algorithm that maps onto a sequence the most probable positions of binding sites and background. Possible cis-regulatory modules can then be identified by choosing a window size and threshold of binding sites per window.

Since the quality of data available on transcription factor binding sites in the literature is highly variable, the SELEX method (systematic evolution of ligands by exponential enrichment) will be used to generate libraries of sequences that bind specifically to *S. purpuratus* endomesodermal transcription factors. To this purpose, a set of proteins have been cloned fused to both a polyhistidine tag for purification purposes, and a V5 epitope to allow SELEX immunoprecipitation. The proteins SpOtx, SpEve, SpGataE, SpFoxA, SpFoxB, SpBra, SpGataC, SpTbr, SpGcm, and SpPmar1 have all been successfully cloned and purified. Once the SELEX methodology has been verified using the well-characterized sea urchin protein SpP3A2, we will experimentally determine the binding sites for these ten proteins. This data will not only to deepen our understanding of the current model, but also help us extend the model by identifying co-regulated genes among the set of transcription factors recently identified from the sea urchin genome and characterized by expression pattern.

318. A genome-wide survey of sea urchin transcription factors
Meredith Howard, Lili Chen, Stefan Materna, C. Titus Brown, R. Andrew Cameron

The sea urchin genome-sequencing project now underway has given us the opportunity to do a definitive survey of transcription factors involved in the organism's development. The goal is to characterize when and where these genes are expressed so that they may be incorporated into the current *Strongylocentrotus purpuratus* endomesodermal gene regulatory network (GRN), filling in any missing connections and rendering the model complete.

The project has proceeded in several phases. The first step was to obtain a non-redundant set of sea urchin transcription factors from among the unassembled traces of the genome. This was accomplished by BLASTX of a set of known transcription factors against the collection of genome traces to fish out any putative transcription factor sequence. The resulting traces were then sorted into bins by the reverse BLASTX such that each trace was associated with its most likely homolog. Finally, small-scale assembly was done within each bin to limit redundancy among merges. In all, more than 250

previously unknown sea urchin proteins were identified, including members of the homeobox, sox, ets, zinc-finger, nuclear receptor, forkhead, bHLH, and bzipper, families. The zinc-finger family presented a particular challenge in that the inherent similarity of all zinc fingers made it nearly impossible to unambiguously assemble individual traces into merges or associate the various exons of individual proteins. Hence to date, only the most easily distinguishable zinc-finger proteins have been studied, though work is underway to resolve this problem.

In the next stage, QPCR time-courses were obtained to map the expression of each gene from the unfertilized egg up to 48 hours of development. From the data, it is apparent that the vast majority of transcription factors, 86%, are used at least once during these 48 hours. In addition, new transcription factors are activated at a nearly steady rate throughout this time period irrespective of gene family, indicating that the spatial complexity of the embryo is being steadily elaborated through rounds of specification even before visible morphological evidence of this appears. In addition, the data indicate that 99.6% of maternally-expressed genes are later expressed by the embryo, further illustrating the economical usage of regulatory proteins in development.

Currently, whole mount in situ hybridization (WMISH) studies are underway to identify the spatial expression domains of transcription factors during development. To date, we have located the expression of previously unknown genes to all territories of the embryo, including the vegetal plate, primary mesenchyme cells, the archenteron, and both the oral and aboral ectoderm. This information, along with perturbation analyses of currently known genes, will facilitate placing the newly found transcription factors into the endomesodermal GRN being constructed in the lab.

319. Transcriptional control of the sea urchin **brachyury** gene

R. Andrew Cameron, William Chiu, Jane Wyllie, Elly Chow

The brachyury gene is a participant in the endomesoderm specification pathway and the founding member of T-box family of transcription factors. Gene expression is localized to the vegetal plate as seen by in situ hybridization in the blastula stage. By the gastrula stage transcripts are present in the oral ectoderm and in the region of the blastopore. Expression then subsides and increases again during the larval stage. Previously we had identified two sequence fragments that recapitulate the temporal and spatial extent of this pattern: a 4 kb region just 5' of and including the transcription start site and a region about 1800 bp that occupies most of the intron between the 6th and 7th exons of this transcription unit. In the process of analyzing these two sub regions we identified another sequence tract that lies 5' of the ubiquitous enhancer near the transcription start site and that contains a sequence identical to the Smad inhibiting protein (SIP) binding site found in the upstream region of the Xenopus 'blimp' gene, a ortholog of sea urchin

brachyury. The activity of this site is under investigation. Now we have narrowed the basal promoter of the brachyury gene to a 50 bp sequence containing a TATA box and lying just 5' of the start of transcription. An artificial construct containing these two elements, the intron sequence and the basal promoter, is being used to test the inputs to brachyury identified by Q-PCR experiments with other members of the endomesoderm specification gene regulatory network.

320. **cis**-Regulation of Spgcm

Andrew Ransick

Using a variety of experimental approaches, work continues toward defining the cis-regulatory architecture and critical 'trans' inputs of Spgcm, the echinoderm ortholog of the transcription factor glial cells missing. GFP-reporter constructs microinjected into fertilized eggs and assayed in embryos demonstrated that the regulatory sequences that promote expression of this gene in the secondary mesenchyme domain at the mesenchyme blastula are distributed across ~15 kilobases of sequence upstream of Spgcm coding exons, but are concentrated into a proximal (P) and distal (D) module working in concert with a relatively short but indispensable enhancer (E) element. Specification of the secondary mesenchyme cells is known to require a functional ligand/receptor interaction between Delta (D) and Notch (N), and suggests a role in regulating this gene via Suppressor of Hairless (Su(H)), a transcription factor known to be an effector of D/N signaling. Interestingly, while D/N signalling can lead to activation of specific target gene expression via a Su(H)/Notch interaction, this factor will also apparently repress transcription of those same target genes when D/N signalling is absent via Su(H) interactions with prevalent co-repressor proteins. Six binding sites for Su(H) occur in Spgcm regulatory sequences, including a pair of sites in the E-element that resemble a characterized and broadly distributed paired Su(H) site. Inserting point mutations in all six Su(H) sites in the combined E+D+P GFP-constructs produces significant defects in spatial expression patterns, although the E-module paired Su(H) site still functions at about 30% efficiency. Additional alterations intended to completely disable that element are in progress. Microinjection of dominant-negative (dn) Su(H) mRNA results in strong down-regulation of Spgcm. Q-PCR on cDNA harvested from injected embryos shows a 5-10 fold lower amounts of Spgcm message, while WMISH signals range from staining in a few cells relative down to completely undetectable. All embryos injected with dnSu(H) mRNA develop with pigment cell defects – many with an albino phenotype similar to that obtained after microinjection of GCM morpholinos, or dnD or dnN mRNAs. The spatial distribution of Spgcm expression is also known to be limited by the forkhead domain factor, foxa, and work is just beginning to discern the critical sites for this factor in Spgcm regulatory sequences.

321. **cis-Regulatory analysis of SpWnt8**

Takuya Minokawa, Athula Wikramanayake*

SpWnt8 is a signaling molecule that is involved in the early specification of endomesoderm in the sea urchin embryo. The goal of this project is to understand the regulatory mechanisms responsible for SpWnt8 expression in the context of the endomesodermal gene regulatory network (GRN). Our GRN studies predict that there are at least two positive inputs in the cis-regulatory region for SpWnt8. These are mediated by the transcription factors (TF), TCF and Krox. This prediction is being tested by cis-regulatory analysis using gene transfer.

We already identified two DNA regions in the flanking regions of SpWnt8 exons (Fragment A and C) that are responsible for correct SpWnt8 expression at cleavage stage. These regions were cloned into CAT reporter constructs. Some putative TCF-binding sites in both A and C fragments and a putative Krox binding site in C fragment have been found by the sequence analysis. To test whether these fragments contain functional TF binding sites, perturbation experiments have been done. Synthetic mRNA of Cadherin intracellular domain (Cad) and morpholino-substituted antisense oligonucleotide (MASO) for Krox have been used to block the TCF and Krox inputs, respectively. Each of these inhibitors has been co-injected in the embryos with one of the CAT expression constructs. As a result, the transcription of CAT mRNA from both A- and C-CAT was strongly suppressed by the overexpression of Cad mRNA, indicating that at least one of the TCF binding sites in both Fragments A and C is functional. Inhibition of CAT mRNA transcription from C-CAT by Krox MASO has also been observed, indicating that the putative binding site for Krox in fragment C is functional. A series of mutagenesis experiments on these putative TF binding sites is scheduled to determine the real functional binding sites for both TCF and Krox.

*University of Hawaii

322. **cis-Regulatory analysis of SpFoxb**

Takuya Minokawa, Gwendolyn Giok Bwee Ong

Forkhead-class transcription factors are known for their multiple roles in the differentiation of endoderm and axial mesoderm in vertebrates. A forkhead transcription factor, SpFoxb, is expressed dynamically during the early embryogenesis of *Strongylocentrotus purpuratus*, suggesting that SpFoxb plays multiple roles in the sea urchin development, too. SpFoxb is exclusively expressed in the PMCs (which are micromere descendants) at mesenchyme blastula stage. This PMC-restricted expression is diminished at early gastrula stage. Following the diminishing PMC expression, the oral part of both endoderm and ectoderm start to express SpFoxb.

Our extensive studies of the PMC gene regulatory network, suggests that SpFoxb is downstream of the SpPmar1 subnetwork system, and receives positive inputs from SpAix, SpTbr and SpEts1 (see our website: <http://sugp.caltech.edu/endomes/>; Oliveri et al., 2003). The purpose of this project is to understand the regulatory

mechanisms responsible for SpFoxb expression, especially in the context of PMC gene regulatory sub-network. The identification of a DNA region responsible for PMC expression and testing of the predicted inputs are the immediate focus of this project.

A software analysis tool "FamilyRelations" was used to find candidate cis-regulatory elements. We identified in the region flanking the coding sequence more than ten tracts highly conserved between *Strongylocentrotus purpuratus* and *L. variegatus*. Using CAT-reporter vector system, we examined the function of these conserved regions. One of the expression construct, which contains a 5' DNA region next to the transcription start site of SpFoxb, exclusively expresses in the PMCs at 24 hr mesenchyme blastula stage, indicating that this DNA region contains cis-regulatory element(s) responsible for correct PMC expression. Detailed sequence analysis followed by mutagenesis experiments targeted to putative transcription factor binding sites in this fragment are scheduled in near future to test the prediction from our PMC gene regulatory network study.

Reference

Oliveri, P., McClay, D.R. and Davidson, E.H. (2003) *Dev. Biol.* 258:32-43.

323. Transposition of the "regulatory module"—from the study of the negative modules in the **Endo16** promoter

Chiou-Hwa Yuh, Sagar Damle

Across different phyla, members belonging to particular classes show a high degree of sequence similarity, and in some cases, a striking degree of conservation in expression domains and functions. These features bestow transcription factor genes with unique advantages for studying the evolution of development and the origin and diversification of body plans. Not only is the protein itself conserved, the regulatory region is also much conserved. A hypothesis that explains evolutionary diversity of gene regulation is that pre-existing regulatory modules, rather than being created by novel mechanisms, can move in different position of the genome by transposition. As a consequence, the diversification of the gene expression pattern arises from the combination of these transposable regulatory modules. We have found a perfect tool to test this important evolutionary question.

The Endo16 promoter contains a very unique-negative module (EF module), which is surrounded by repeat sequences. Our previous work showed that 5' serial deletion of the Endo16 regulatory region had a very minor effect on endoderm-specific expression. Instead, on an intact Endo16 promoter, mutation of putative transcription factor binding sites on the EF module resulted in a dramatic increase in ectopic expression.

The sea urchin genome is highly polymorphic. Dr. Wray's lab recently sequenced the Endo16 regulatory region from ten *S. purpuratus* individuals, and found that only one has the whole EF module. The remaining nine individuals either lacked the EF module, or contained a

different DNA sequence. For instance, the individual SpuLA29 is missing the EF module, whereas SpuSB68U is missing EF, but also contains a long insertion in its G module. SpuSB68L is also missing EF, and SpuSB49 is similar to the original isolated clone. On the other hand, SpuR1 has a totally different sequence in place of the EF module. To test the function of each allele, we used fusion PCR to replace the 5' Endo16 regulatory region with regulatory modules from different alleles and detected CAT mRNA localization by *in situ* hybridization. The *in situ* pattern showed that the SpuR1 has a restricted expression pattern identical to that of the published Endo16 sequence. This implies that two unrelated insertions at approximately the same location both have a similar functional impact on repression in the ectoderm. Fusion constructs from individuals lacking the EF module released repression toward ectoderm and the CAT mRNA expression domain expanded slightly toward the ectoderm border. This result is consistent with those from the *in vitro* mutagenesis experiment.

We have searched the sea urchin genome traces, and discovered 242 matches to EF modules. We also found 154 matches to the SpuR1-specific repression domain, but only three that matched the BA module. At the time of the search, the sea urchin genome had been sequenced to 3X coverage. This result implies that the genome has about 81 sites that contain the original EF module, and 52 sites containing the SpuR1-specific repression allele, but only one site (which is in front of Endo16) that contains the BA module. This evidence strongly suggests that the EF module is a transposable regulatory module. It will be interesting to find out which other genes are regulated by the EF modules. This may solve a fundamental mystery of evolution, where recombination among modular regulatory regions results in novel patterns of developmental gene expression. The interesting evolutionary hypothesis is that the EF module must transpose from somewhere else in the genome. It was accidentally transposed into 5' end of the Endo16 gene.

324. Identified, proving and cloning UI, a protein involved in the sea urchin developmental regulatory gene network
Chiou-Hwa Yuh, Elizabeth R. Dorman, Titus C. Brown

The study of the transcriptional regulation of Endo16, which is an early vegetal plate marker gene, can help us understand endomesoderm specification. Detailed analyses have been carried out in the positive modules (A, B and G) of the Endo16 promoter. Module B is responsible for late stomach expression. The mutation of UI site on the module B absolutely shut off this module's activity as shown by *in situ* hybridization on the mutated construct. Therefore, the UI site has been identified as a spatial controller of module B. Experimental and computational analysis of Endo16 module A and B has revealed aspects of cis-regulatory organization that are of great importance.

Nuclear extracts from 20 hr embryos were prepared from a large-scale embryo culture. After affinity column purification, proteins were separated on SDS-PAGE and Coomassie blue stained bands were cut from the gel. In-gel digestion of the protein and amino-acid sequencing were then performed by an amino acid sequencer. Then, degenerate oligos deduced from the peptide sequences were designed to hybridize to cDNA clones from an arrayed library. Since the sea urchin genome has been sequenced, we also used the peptide sequences for UI to computationally mine the genome for UI candidate genes.

We found two cDNA clones by screening the cDNA library with degenerate oligos: one belongs to a zinc-finger binding protein, and the other is an octamer binding protein. Computational searching identified five different genomic sequences that align to the UI-peptide sequences. We named them Merge 0 to Merge 4. Q-PCR primers were made according to the cDNA sequences predicted by BLAST search. Preliminary real-time RT-PCR results show that there is a class 3, POU domain transcription factor (Merge 0) that has very low expression at an early stage, and starts to be expressed after 30 hr post-fertilization. It reaches a peak at 60 hr post-fertilization, which correlates to the late expression peak of endogenous Endo16. We also found the two cDNA clones obtained from cDNA library screening have similar expression time courses: they are expressed at the 20 to 30 hr stage and show pretty low expression at later stages.

The endogenous expression patterns of Merge 0 were obtained by *in situ* hybridization. This novel POU-domain transcription factor expresses at midgut region of post-gastrulate embryo. Its localization at midgut region mimics the expression pattern of Endo16. As we proposed at the beginning, the UI site has been identified as the spatial controller of module B, which is responsible for the midgut expression at the post-gastrulated stage. It is very likely that we found the UI candidate from this search. We are currently trying to get full-length cDNA clones by either RACE library or additional screening of the cDNA library. Once full-length cDNAs have been obtained, antisense morpholinos against these genes will be tested on the expression of the Endo16 gene, as well as other genes in the endomesoderm network.

325. Develop a high-throughput way to identify the interrelationship between regulatory modules and finding the non-conserved repression modules in the *Otx* locus
Chiou-Hwa Yuh

Analysis of cis-regulatory systems of territorially expressed genes is one of the main focuses in our laboratory. Traditionally, we are using *in vitro* mutagenesis and reconstruction of regulatory systems with synthetic DNA fragments in order to unravel the cis-regulatory "information processing system." With the help of "FamilyRelations," we are able to find highly conserved genomic DNA sequences between two species of sea urchin, *S. purpuratus* and *L. variegatus*. Linking these

conserved elements into reporter genes has been the most straight forward way to test for functionality. There are several problems with using this method. First of all, the interrelationship between modules is difficult to identify by this strategy. Secondly, the negative functional modules usually are evolutionary non-conserved, so they can be missed by searching only for conserved modules. Thirdly, the Endo16 basal promoter which we use in the expression constructs may not universally interact with regulatory elements from other genes. Fourthly, this method is time consuming and requires a great deal of effort.

We have invented several new methods for high-throughput gene expression analysis. With homologous recombination, we can very easily replace an endogenous gene's small exon with a GFP reporter gene. Using PCR amplification, we can make GFP expression fragments containing different portions of genomic DNA. By fusion PCR, we can fuse conserved DNA fragments together, and test their effect in combination. With the help of a newly purchased cell-sorting machine, COPAS (Complex Object Parametric Analysis and Sorting), we can detect GFP activity quantitatively within minutes. Furthermore, by gel shift assay, in which we use a bait regulatory DNA as a probe and add a different sequence of unlabeled putative regulatory DNA to the reaction, we can find out which DNA fragments physically interact with each other through protein-protein contacts mediated by bound transcription factors. We can further test their function directly by fusing them to the bait and a CAT reporter system through fusion PCR.

To understand the regulatory mechanism, the locus containing the Otx gene has been discovered by screening a BAC library from two different species of sea urchin. Using the newly developed program "FamilyRelations," we were able to find 17 partially conserved regions. Among them, the element 15 locates immediately upstream of Otx-beta1/2 and element 17 locates immediately upstream of Otx-alpha. Four elements (11, 14, 15 and 17) had been shown to express in endomesoderm when linked individually to the CAT reporter system. We used the homologous recombination technique to replace exon 6 with GFP. This construct was therefore designed to detect the transcriptional activity of the Otx-alpha promoter. We also replaced exon 4 and 5 with GFP to detect the transcriptional activity of the Otx-beta1/2 promoter. Five PCR fragments surrounding the Otx-alpha transcription start site and ten different PCR fragments surrounding the Otx-beta1/2 transcription start site were made within a few days, and their activity identified quantitatively by the COPAS. We found the conserved region number 16 has a strong up-regulatory effect, a 9.2-fold increase compared to element 17 alone on Otx-alpha transcription. We also discovered a 3.23-fold increase compared to element 15 alone on Otx-beta1/2 transcription. Furthermore, element 17 can enhance the expression of Otx-beta1/2 by two-fold, and the element 15 will repress the expression of Otx-alpha by two-fold. An interesting finding was that the nonconserved DNA

fragment in between element 14 and 15 has a repressive effect.

To test the repressor, we carried out a gel shift assay to detect the negatively nonconserved interactive modules. We used PCR amplification to perform a non-biased screen for interactive modules that can interact with the Otx bait fragment. The bait fragment contains three Otx binding sites and a GATA4,5 binding site that have been shown to be important for expression in endomesodermal territory but that can still express in ectoderm. By gel shift assay, we identified a few DNA fragments that can compete the DNA-protein complex formation on the bait. We tested their function by linking these domains to the bait DNA using fusion PCR and joining this construct to a CAT reporter. Interestingly, two fragments suppressed oral ectoderm expression, and one fragment suppressed aboral ectoderm expression. Upon further examination of the DNA sequence, we found that the two oral ectoderm suppression modules had classical CREB binding sites and oral ectoderm repressor contained binding sites identified from the Spec2a promoter study.

The purpose of the project is to develop a high throughput way of identifying not only the positive modules, and the interrelationship between modules, but also to help to identify the functional but nonconserved negative modules.

326. **Trans**-specification of primary mesenchyme cells through genetic rewiring of the mesoderm specification network

Sagar Damle

In the sea urchin *Strongylocentrotus purpuratus*, the identity and regulatory relationship of a number of transcription factors involved in endomesoderm development have been well characterized. However, the ultimate demonstration of intellectual control of the causal moving parts of a system is to reengineer it. The goal of my project is to determine whether SpGcm is sufficient to trans-specify primary mesenchyme cells (PMC) into a secondary mesenchyme cell (SMC) fate. This will be done by placing the SpGcm coding sequence under the control of a promoter that directs PMC-specific gene expression. The Davidson lab has developed a system whereby BAC-sized DNA fragments can be introduced into fertilized sea urchin eggs through microinjection and integrated into the genome as early as the two-cell stage. With this system, it should be possible to explore the effects of creating novel connections between regulatory pathways.

SpGcm is thought to play two roles in development. Its early expression in all presumptive mesoderm suggests it is capable of setting up a mesodermal transcriptional state. This state gives cells a competency to respond to signals that specify various SMC or mesodermal cell lineages. Some evidence for this theory already exists. For example, embryos injected with antisense morpholino against SpGcm do not correctly express SpGataC in the oral arch of veg2 mesoderm (A. Ransick, unpublished data). The later role of SpGcm

in pigment cell specification is perhaps more difficult to characterize through morpholino analysis. However, in situ hybridization shows late Gcm expression exclusively in pigment cells.

The T-box transcription factor Tbrain is expressed in the large micromeres at swimming blastula stage. Its expression persists through gastrulation as micromeres differentiate into PMCs and arrange themselves within the blastocoel. I will replace the first exon of SpTbrain with the SpGcm coding sequence. This recombinant BAC construct will have the SpGcm coding sequence under control of SpTbrain's regulatory system, which induces expression in PMCs.

The degree to which Gcm can both override the skeletogenic program of PMCs and specify either pigment cell or mesodermal cell fate will be determined by measuring the spatial distribution transcripts of a number of well-known molecular markers. SpGata-C is a mesoderm-specific transcription factor controlled by SpGcm, whereas SpPks, SpSult and SpFmo are all thought to play roles in the biosynthesis of the pigment echinochrome in pigment cells. Whole mount in situ hybridization with probes for these genes will be used to identify the extent of Gcm respecification. While both PMCs and SMCs have the ability to migrate, their final positions in the embryo are different. The location of Gcm-expressing PMCs and their degree of pigmentation will therefore also be useful in characterizing Gcm's role in mesoderm specification.

327. **cis-Regulatory analysis of the sea urchin *delta* gene**

Roger Revilla

The *delta* gene plays two different roles in the specification of the endomesoderm of the sea urchin embryo. Each one of these roles requires Delta to be localized in a specific territory of the embryo. It is first required in the micromeres to serve as a signal that is necessary to segregate the mesodermal and endodermal fates of the surrounding cells. It is later localized in the prospective SMCs, where it signals the endodermal cells and is required for gastrulation to occur. The goal of this project is to analyze the cis-regulatory system that localizes the expression of Delta in the right place and the right time to serve its roles in the specification of the endomesoderm. It has already been shown that the early localization of Delta in the micromeres depends on activator(s) that are present ubiquitously, and a repressor that is present everywhere except in the micromeres. Comparison of genomic DNA sequences of *Strongylocentrotus purpuratus* containing *delta* gene with the orthologous region of *Lytechinus variegatus* genome has been used to identify conserved patches of sequence that might contain cis-regulatory elements. Two sequence elements have been identified that are able to recapitulate the two phases of expression of the *delta* gene. The element that recapitulates its early phase of expression has been shown to contain binding sites for activator(s) ubiquitously present and binding sites for the repressor that

localizes *delta* in the micromeres. Future work will identify the sites in the DNA that bind these factors, and it will also elucidate the binding sites of the key factors that are responsible for localizing Delta in the prospective SMCs. Finally, we also hope to be able to identify the transcription factor that acts as a repressor of *delta* everywhere in the embryo except the micromeres, which has been suggested to play a key role in the installation of the skeletogenic program of gene expression.

328. **A cis-regulatory analysis of *SpGata-e***

Pei Yun Lee, Kelly Lin

SpGata-e is the *S. purpuratus* ortholog to vertebrate Gata genes 4/5/6. The expression of *SpGata-e* is first detected in presumptive secondary mesenchyme cells (SMCs) during the hatching blastula stage. Its expression expands to include both future SMCs and endoderm in the mesenchyme blastula. In the gastrula, *SpGata-e* is expressed in at the tip of the archenteron and hindgut. By the end of embryogenesis, *SpGata-e* is expressed in the midgut and coelomic pouches.

A 600 bp DNA sequence in the first intron is the only cis-regulatory element discovered thus far that is active during embryogenesis. It is responsible for directing *SpGata-e* expression in the vegetal plate from the onset of zygotic *SpGata-e* expression in the 15 hr blastula. This element also maintains expression in mesoderm cells at the tip of the invaginating archenteron and endoderm cells until mid-gastrulation. After gastrulation, this element loses its specificity in directing expression; instead it controls ubiquitous low-level expression. Current ongoing cis-regulatory analysis includes cloning overlapping 5 kb fragments of the *SpGata-e* genomic region into reporter vectors to identify the element(s) responsible for regulating post-gastrulation expression of *SpGata-e*.

A search in the sequence of the 600 bp cis-regulatory element for putative DNA-binding sites of transcription factors known to be upstream of *SpGata-e* identified three putative SpOtx-binding sites. Co-injection of mRNA of an Otx-engrailed fusion or a morpholino to the Otx-b transcript abolished the expression of GFP RNA molecules as assayed by quantitative real-time PCR. Gel shift analysis has shown that the Otx transcription factor binds cooperatively to a pair of Otx binding sites in the cis-regulatory element.

329. **Constitution of transcription complexes at the C-element of *sm50* gene**

Ochan Otim

The complexity of interactions in embryonic nuclear extracts associated with the functions of the 25 bp C-element of the cis-regulatory region of the sea urchin *Strongylocentrotus purpuratus sm50* was examined by extensive mutation and gel shift analyses. The C-element exercises the primary spatial control function for accurate expression of the SM50 protein in the skeletogenic lineages. Six nuclear extract preparations representing the early stages of development ranging from 6 (32-cell stage)

to 26 hr (mesenchyme blastula stage) were employed to visualize radiologically the binding activities at the element. At least eight uniquely identifiable transcription complexes are formed as a consequence of direct or indirect transcription factors interaction with the C-element. Site-specific mutagenesis of the C-element has revealed a cluster of at least three distinct target sites within the 25 bp, all of which are utilized in varying combinatorial arrangements depending on the embryonic developmental age; one of these sites (also recognized by SpHnf6) is required constitutively. Attempts to identify the complexes are under way.

330. Understanding the transcriptional control of **cyiia**

C. Titus Brown

CyIIIa is a cytoskeletal actin expressed at high levels throughout development in the aboral ectoderm of *S. purpuratus*. The 2.3 kb of genomic DNA immediately adjacent to the transcription start site is sufficient to direct correct spatiotemporal expression of a CAT reporter gene, and contains binding sites for nine distinct proteins present in 22 hr crude nuclear extract (Calzone et al., 1988). Eight of these nine proteins have been characterized to some extent, but one protein remains unidentified, and several proteins play roles that have not been fully examined.

I am continuing to expand our understanding of the CyIIIa cis-regulatory region in several ways. First, I have used the results of the whole genome transcription factor catalog (Howard et al., unpublished) to screen for candidates for the remaining unidentified transcription factor, and have found a strong candidate in a zic/odd-paired transcription factor ortholog. I have also expressed the TEF-1 transcription factor in vitro and shown via gel shift that it binds to the P5 binding site. Finally, I am using Q/RT-PCR on cDNA from embryos staged at every 6 hr through 60 hr to determine the time-courses of the eight known proteins.

The ultimate goal of the cyiia project is to build a complete understanding of its transcriptional regulation by showing that the spatiotemporal expression patterns of its regulators are sufficient to explain, both quantitatively and spatially, the expression pattern of cyiia itself. In addition to the above work, we are building a cis-regulatory "wiring diagram" (Yuh et al., 1998) for CyIIIa that will put the individual binding sites into a combined functional context.

References

- Calzone, F.J., Theze, N., Thiebaud, P., Hill, R.L., Britten, R.J. and Davidson, E.H. (1988) *Genes Dev.* 2(9):1074-1088.
 Yuh, C.H., Bolouri, H. and Davidson, E.H. (1998) 279(5358):1896-1902.

331. cis-Regulation of the early and late forms of **SpKrox1**

Carolina Becker Livi

The sea urchin zinc-finger transcription factor SpKrox1 is an important early regulator in the endomesoderm network. Previously we have characterized some of the downstream functions of SpKrox1 and established a subset of its downstream connections. More recently, we have made progress characterizing its cis-regulatory region in an effort to test the predictions made by the network model regarding upstream regulators of SpKrox1.

SpKrox1a and b are two splice forms expressed in different temporal patterns in the sea urchin embryo. Their respective regulatory regions have been found by both computational and experimental means. First we compared the sequences 5' and 3' of the exon (including introns) of *Strongylocentrotus purpuratus* and *Lytechinus variegatus* using "FamilyRelations." Patches indicating significant levels of conservation were selected for further experimental work. An analysis of the distribution of putative binding sites for TFs was also performed, more specifically searching for binding sites for those TFs thought to regulate SpKrox1 expression by perturbation analysis. Fragments far upstream of the exons were also tested, but none yielded expression when using Endo16 basal promoter. We believe that the endogenous basal promoter is necessary for the appropriate expression of promoter constructs.

We used fusion PCR to attach genomic DNA fragments containing the putative cis-regulatory elements and basal promoter to the coding region of green fluorescent protein (GFP). A construct containing a 900 bp fragment together with exon 1a recapitulates the expression pattern of the late form driving expression in the gut in 95% of the embryos with GFP expression. This fragment contains several Otx binding sites, but we do not yet know if they mediate SpKrox1 expression.

We used the homologous recombination technique to replace the coding region of exon 1b with GFP in the BAC clone of SpKrox1. This construct was therefore designed to detect the transcriptional activity of the SpKrox1b promoter under its own basal promoter control. Using PCR amplification, we made 10 or so GFP expression fragments containing different portions of genomic DNA. A 600 bp fragment located 5' of exon 1b recapitulates the expression pattern of the early form driving expression in the vegetal plate endoderm in 85% of the embryos with GFP expression. This fragment also contains several otx sites and preliminary experiments show that injecting antisense morpholino oligos against SpOtx does reduce the number of embryos expressing this construct. In similar experiments we have found that inhibiting the β -catenin pathway by injecting the intracellular domain of Cadherin also reduces the percentage of embryos that express constructs driving GFP.

Now we will further test whether or not mutating binding sites within these fragments will affect GFP

expression and therefore confirm the inputs predicted by the endomesoderm network.

332. Delta expression in starfish and sea urchin embryo after 500 my divergence

Feng Gao, Veronica F. Hinman, Kirsten Welge

Delta expression is required for normal endomesodermal specification in starfish and sea urchin embryogenesis, the two of which last shared a common ancestor around 500 mya.

Three phases of Delta expression were identified in sea urchin embryos as a part of the *S. purpuratus* GRN project. It is first expressed in the micromere descendant cells around 6 hr after fertilization, which serves as the Delta-notch signalling targeted at mesodermal Gcm to segregate the mesodermal and endodermal fates of veg2 descendant cells. By mesenchyme blastula stage, its expression is extinguished in the ingressed PMCs, while is activated in SMCs which results in an upregulation of GataE in precursive endomesodermal cells required for gastrulation to occur. During gastrulation, expression is seen in the apical plate of the embryo while disappearing in the vegetal plate.

As a part of a comparative network analysis project undertaken between *S. purpuratus* and *A. miniata*, the following work was done with the AmDelta gene: 1) a full-length AmDelta cDNA was isolated by cDNA library screening; 2) a time-course of Delta expression was determined by real-time QPCR; 3) WMISH was performed on post-hatching embryos; 4) 25 BAC clones positive to AmDelta were found through BAC library screening; 5) homologous recombination was used to insert the GFP reporter just in place of the first exon of AmDelta BAC DNA; 6) AmDelta-BAC-GFP and antisense morpholinos against AmDelta were microinjected into fertilized starfish eggs. Two phases of Delta expression were identified in starfish embryos based on WMISH and AmDelta-BAC-GFP microinjection. Its first phase was found in the center of the vegetal plate at blastula stage, where Delta is required for normal endomesodermal specification and acts as an input into AmGataE from AmDelta morpholino microinjection. After gastrulation, expression is seen around the blastopore and in the oral ectoderm, with a strikingly similar pattern to that of the brachyury gene. In the context of timing, spatial pattern, gene expression and developmental fate, we speculate the 1st phase of Delta expression in starfish embryo is homologous to the 2nd phase expression in sea urchin, and probably represents the most basal function of the Delta gene in echinoderms. The 1st phase of expression individually in sea urchins is late-derived and lineage-specific to echinoderms as an accessory to the invention micromere. The 2nd phase of expression in starfish and 3rd phase in sea urchin are distantly divergent as a result of their 500 my divergence.

Identification of the cis-regulatory regions of Delta in starfish and sea urchin holds the answer to the inferences above. Two cis-regulatory elements of SpDelta have been identified which are respectively responsible for the first two phases of expression in the sea urchin embryo.

A new experimental method is underway to locate cis-regulatory regions of starfish AmDelta given that the genomic sequence of starfish delta gene is still unknown. This involves the following steps: 1) PCR walking outward from both ends of the Delta coding sequence along AmDelta-BAC-GFP; 2) PCR products sequencing; 3) designing primers from two distal ends of the AmDelta sequence; 4) PCR again; 5) microinjection with PCR products to locate the regions regulating the two phases of AmDelta expression.

333. Regulatory gene network evolution: A comparison of endomesoderm specification in starfish and sea urchins

Veronica F. Hinman, Albert Nguyen

We are undertaking an evolutionary comparison of the gene regulatory network (GRN) of transcription factors underlying the specification of endomesoderm in sea urchins and starfish. The extensive analysis of this network in sea urchins has provided a unique opportunity for a comparative investigation to elucidate mechanism of evolution at this level. We would like to answer questions such as, which components of such a regulatory system are conserved, how are changes incorporated into a GRN, and how do these changes relate to the evolution of morphology? The starfish *Asterina miniata* has been developed as an ideal experimental model for this analysis. Gametes are readily available and gene transfer and perturbation of gene products have been performed. Starfish last shared a common ancestor with sea urchins around 500 million years ago and they appear to be at an ideal evolutionary distance for meaningful comparisons; they share many conserved aspects in their development and yet there exist specific morphological differences.

We have previously shown that a common developmental feature of starfish and sea urchin GRNs is the use of an orthologous three gene-positive regulatory feedback loop that serves to 'lock down' gene expression required for the specification of the endoderm and thus, to drive development forward. The conservation of this feature across the immense period of evolutionary time such as separates these echinoderms demonstrates the indispensable nature of such a process in their development. Several differences were also noted in the GRN architecture. We have noted that *tbrain* (*tbr*) is incorporated into the endomesoderm-specification network in starfish while it is involved in primary mesenchyme cell specification in sea urchins. Also, the starfish *gatae* gene is repressed from the mesoderm by *foxa* while this is not the case in sea urchins.

We are continuing these GRN architecture comparisons, principally by examining the specification of the mesoderm. Certain differences were already noted between this process in starfish and sea urchins e.g., the different usage of *tbr* and *gatae* genes (see above). We have cloned several starfish regulatory genes that are expressed in the mesoderm, viz the transcription factors AmGcm and AmGataC and the signalling ligand AmDelta. Unlike in sea urchins, the starfish *gcm* gene is not

expressed in the vegetal plate but is expressed in a patch of cells in the pre-blastula that appear to migrate throughout the aboral ectoderm. The delta gene of sea urchins has two phases of expression, firstly in the micromeres where it is required for the expression of the mesodermal factors *gatac* and *gcm*, and secondly in the vegetal plate where it is needed for the specification of the endoderm. It appears that the second phase of expression and function is conserved in the starfish, but Delta is not required at all for the expression of the mesoderm factors AmGcm and AmGataC. Significant differences may thus, have occurred in the specification of mesoderm in these two taxa that is related to the novel acquisition of the micromeres by sea urchins.

We are further expanding this work to identify and analyze the cis-regulatory elements of several genes of the starfish GRN. The regulatory relationships underlying the architecture of the GRN are inherited as the coding sequence of the transcription factor and the DNA sequence of its binding site. Binding site modifications are likely to provide the greatest potential for evolution.

We know from the comparative GRN analysis that the brachyury (*bra*), orthodenticle (*otx*) and *gatae* genes in starfish and sea urchins are similarly regulated, yet comparative sequence analyses using "FamilyRelations" fail to find any significant patches of sequence conservation in the surrounding 100-150 Kbp of DNA. In order to understand how the sequence of a cis-regulatory region has evolved, we are analyzing, in detail, the cis-regulatory region of the starfish *bra*, *otx* and *gatae* genes and are comparing these to the regulatory regions of orthologous sea urchin genes. We have used several methods to identify the regulatory regions. We currently have an approximately 500 bp region including the 5' UTR of AmBra DNA that drives correct reporter gene expression in pregastrular starfish embryos. Expression of this regulatory element is enhanced by fusing it with either of two genomic regions downstream of the coding region. We also have identified an approximately 500 bp region of DNA downstream of the *otx* coding region that drives correct reporter gene expression. This region was identified using the "Cluster Buster" software that searched for a statistical over representation of consensus-binding motifs for the Otx, Krox and Gatae transcription factors, all of which are known to regulate *otx* expression. The arrangement of these binding sites in the cis-regulatory elements of the starfish and sea urchin *otx* genes was found to be remarkably similar suggesting that some functional constraint must exist in their relative arrangement.

We are also collaborating with Christophe Battail and Hamid Bolouri to use a bioinformatics approach to search for over-represented "words" in the genomic regions surrounding coding sequence as a method to identify regulatory elements. Testing is underway on potential regions.

334. Regulatory aspects of sea urchin biomineralization

Gabriele Amore

In echinoderms larval skeletogenesis is observed only in two of the five classes of the phylum, echinoids and ophiuroids. It is considered a derived feature in these groups. In sea urchins (echinoids) the skeletal matrix (*sm*) genes involved in the making of the larval skeletal spicules, are believed to be the same that are used in adult spines and tests. A cooption of the *sm*-genes from the adult to the larval life phase is hypothesized. Studying the regulation of the expression of sea urchin *sm*-genes provides an opportunity to approach the more general problem of the evolution of the regulation of gene expression.

To reveal the genomic organization of *sm*-genes, BAC libraries were screened with probes obtained from *sm*-cDNAs and BLAST analysis were performed. The four *sm*-genes *pm27*, *sm37*, *sm50* and *sm32* were found in a cluster. The presence in the same cluster of *pm27* and *sm32* is a new finding. Also, the *sm50* and *sm32* genes share the same first exon, so they represent splice variants. The same arrangement for these genes was found in two closely-related sea urchin species, *S. purpuratus* and *L. variegatus*, although little conservation was observed in the non-coding sequences. To determine if all the *sm*-genes are clustered in the sea urchin genome, more BAC clones will be isolated and characterized.

The cluster arrangement of the *sm*-genes is suggestive of a common mechanism responsible for their coordinated expression, maybe via a locus control region (LCR). Recombination techniques that allow the knock-in of the green fluorescent protein (GFP) coding sequence into *sm*-genes in the BAC clones will be employed. In these constructs, GFP expression will be driven by the promoter of only one of the four *sm*-genes. Sequences far upstream or downstream from each gene will then be modified. The short- and long-range effects of these mutations will then be tested by microinjecting the whole BAC clones into sea urchin zygotes and analyzing GFP expression.

335. Discovery of a Precambrian bilaterian microfossil

Jun-Yuan Chen¹, Paola Oliveri, Feng Gao, Chia-Wei Li², David J. Bottjer³

Bilaterian animals cannot have suddenly sprung forth fully blown in the Lower Cambrian (the Lower Cambrian boundary is at 543 mya), when the fossils of most major phyla and superphyla appear in the geological record. The Precambrian fossil record has, however, been almost entirely uninformative with respect to bilaterian origins prior to its very final phase. Deposits that sample the period shortly before the Cambrian boundary have revealed some enigmatic small shelly fossils; many tracks and trails or trace fossils; and at least a few apparently genuine macroscopic bilaterian forms (e.g., the late Ediacaran *Kimberella*). Forty to fifty million years earlier, at about 600 mya, a long period of intermittent world-wide

glaciation and very anoxic ocean conditions came to an end ("Snowball Earth"). Both this geological scenario and recent molecular phylogeny strongly indicate that the divergence of the modern bilaterian superphyla, i.e., the deuterostomes, the ecdysozoans, and the animals lumped in the (probably paraphyletic) lophotrochozoans, should be sought in the period following Snowball Earth and preceding the late Ediacaran. For several years, a consortium of paleontologists and evolutionary biologists from USC, Caltech, Taiwan, and the Early Life Research Center, Yunnan, China has been scanning a Precambrian microfossil assemblage discovered in Guizhou Province for evidence of bilaterian origins. This material, from the Doushantuo Formation, has been preserved in phosphate mineral inclusions with unprecedented resolution of detail, given its age, which extends for several million years through exactly the period of interest following the termination of Snowball Earth. Viewed and digitally imaged in section under the microscope, Doushantuo eggs, embryos, and various sponge and cnidarian forms have been reported previously (including some reports from our consortium, and other reports displaying a subset of this material in three dimensions by scanning EM). Strikingly, all animal forms of this vintage so far seen are microscopic in dimension (<1 mm). Now ten specimens of a remarkable, similarly small, bilaterian-grade fossil have come to light. Named Vernanimalcula (small "spring" animal, following the "winter" of Snowball Earth), fossils of this animal appear only once in every several thousand fossilized organisms observed. It is only about 200 microns in its longer dimension, but some beautifully well-preserved specimens show clearly that it was a triploblastic, bilaterally symmetric organism with paired coeloms, a through gut, a muscular pharynx, and an unmistakable anterior/posterior organization. It was apparently a benthic surface grazer as its mouth is oriented downward toward what we interpret as the ventral surface. As further specimens are revealed, its three-dimensional structure will become less speculative than it is at present. The results are certain to illuminate the early course and pathways of bilaterian evolution.

¹Early Life Research Center, Yunnan, China

²National Tsing Hua University, Taiwan

³University of Southern California

Publications

- Britten, R.J., Rowen, L., Williams, J. and Cameron, R.A. (2003) Majority of divergence between closely related DNA samples is due to indels. *Proc. Natl. Acad. Sci. USA* 100:4661-4665.
- Cameron, R.A., Oliveri, P., Wyllie, J. and Davidson, E.H. (2004) cis-Regulatory activity of randomly chosen genomic fragments from the sea urchin. *Gene Exp. Patt.* 4:205-213.
- Cameron, R.A., Rast, J.P. and Brown, C.T. Experimental analysis of the development of sea urchins and other non-vertebrate deuterostomes. *Meth. Cell Biol.* In press.

- Chen, J.-Y., Bottjer, D.J., Oliveri, P., Dornbos, S.Q., Gao, F., Ruffins, S., Chi, H., Li, C.-W. and Davidson, E.H. (2004) Small bilaterian fossils from 40 to 55 million years before the Cambrian. *Science* 305:218-222.
- Ettensohn, C.A., Illies, M.R., Oliveri, P. and De Jong, D.L. (2003) Alx1, a member of the Cart1/Alx3/Alx4 subfamily of paired-class homeodomain proteins, is an essential component of the gene network controlling skeletogenic fate specification in the sea urchin embryo. *Development* 130:2917-2928.
- Hinman, V. and Davidson, E.H. (2003) Expression and function of a starfish Otx ortholog, AmOtx: A conserved role for Otx proteins in endoderm development that predates divergence of the eleutherozoa. *Mech. Dev.* 120:1165-1176.
- Hinman, V.F., Nguyen, A., Cameron, R.A. and Davidson, E.H. (2003) Developmental gene regulatory network architecture across 500 million years of echinoderm evolution. *Proc. Natl. Acad. Sci. USA* 100:13356-13361.
- Hinman, V.F. and Davidson, E.H. System-level properties revealed by a gene regulatory network analysis of pregastrular specification in sea urchins. (2004) In: *Gastrulation*, Stern, C.D. (ed.), Cold Spring Harbor Press, NY, pp 643-652.
- Howard, M.L. and Davidson, E.H. (2004) cis-Regulatory control circuits in development. *Dev. Biol.* 271:109-118.
- Lee, P.Y. and Davidson, E.H. Expression of Spgatae, the Strongylocentrotus purpuratus ortholog of vertebrate GATA4/5/6 factors. *Gene Exp. Patt.* In press.
- Minokawa, T., Rast, J.P., Arenas-Mena, C., Franco, C.B., and Davidson, E.H. (2004) Expression patterns of four different regulatory genes that function during sea urchin development. *Gene Exp. Patt.* 4:449-456.
- Oliveri, P. and Davidson, E.H. Gene regulatory network analysis in sea urchin embryos. *Meth. Cell Biol.* In press.
- Oliveri, P. and Davidson, E.H. Gene regulatory network controlling embryonic specification in the sea urchin. *Curr. Opin. Genet. Dev.* 14:351-360.
- Otim, O., Amore, G., Minokawa, T., McClay, D.R. and Davidson, E.H. SpHnf6, a transcription factor that executes multiple functions in sea urchin embryogenesis. *Dev. Biol.* In press.
- Ransick, A. Detection of mRNA by in situ hybridization and RT-PCR. *Meth. Cell Biol.* In press.
- Revilla-i-Domingo, R. and Davidson, E.H. (2003) Developmental gene network analysis. *Int. J. Dev. Biol.* 47:695-703.
- Revilla-i-Domingo, R., Minokawa, T. and Davidson, E. H. R11: A cis-regulatory element that controls expression of SpDelta and responds to the Pmar1 repression system. *Dev. Biol.* In press.
- Takacs, C.M., Amore, G., Oliveri, P., Poustka, A.J., Wang, D., Burke, R.D. and Peterson, K.J. (2004) Expression of an NK2 homeodomain gene in the apical ectoderm defines a new territory in the early sea urchin embryo. *Dev. Biol.* 269:152-164.

Yuh, C.-H. Dorman, E. R., Howard, M. L. and Davidson, E. H. (2004) An *otx* cis-regulatory module: A key node in the sea urchin endomesoderm gene regulatory network. *Dev. Biol.* 269:536-551.

Esther and Abe Zarem Professor of Biology: Michael H. Dickinson
 Postdoctoral Scholars: Doug Altshuler, William Dickson, Mark Frye, Clare Hayward, Andrew Straw
 Graduate Students: John Bender, Seth Budick, Gwyneth Card, Mary Dunlop, Sean Humbert, Michael Reiser, Alice Robie, Jasper Simon
 Undergraduate Students: Robert Bailey, Qing Liu, Martin Peek, Hans Scholze
 Research and Laboratory Staff: Rosalyn Sayaman, Amber Steele

Support: The work described in the following research report has been supported by:

Air Force Office of Scientific Research
 Jet Propulsion Lab
 National Science Foundation
 Office of Naval Research
 The Packard Foundation

Summary:

1. We have constructed and tested a prototype MEMS-based flight balance for fruit flies that will have use in many future experiments.
2. We have been able to map the aerodynamic consequence of the several key steering muscles.
3. We have demonstrated the changes in flow structure and force production around the wing as a function of Reynolds number.
4. We have succeeded preliminary in vivo measurements of changes in the calcium concentration within power muscles during flight.
5. We have characterized the interaction between olfactory and visual reflexes during flight, and have mapped the spatial tuning of visual motion reflexes.
6. We have characterized the interaction between visual and mechanosensory stabilization reflexes.
7. We have developed a control theory model that replicates the salient features of a male's tracking behavior during courtship.

336. Neural control of hummingbird flight
 Doug Altshuler

Many flying insects exhibit remarkable flight agility owing in part to high wing beat frequencies and hovering ability. Thus, insects have for decades served as models for the neuromuscular control of high performance motor behavior. Similarly, hummingbirds are unique among vertebrates for their ability to sustain both hovering posture and relatively high wing beat frequency during flight. The combination of experimentally tractable and highly complex flight behavior in hummingbirds makes them an ideal model for examining mechanisms of neuromuscular control in a vertebrate. We have studied hummingbird wingbeat kinematics and muscle activity during hovering and maneuvering flight using synchronized high-speed digital video and EMG recordings from the flight power muscles. Wingbeat kinematics can be described as the time-course of three

wing angles, defined with respect to body: stroke position, stroke deviation, and kinematic angle of attack. Throughout the wing beat cycle, the time-course of stroke deviation and angle of attack is strikingly similar to those found in fruit flies and bees, indicating that hovering is achieved using almost identical kinematics despite vast differences in the structure and function of the sensorimotor and musculoskeletal systems. EMG recordings were made from the downstroke and upstroke power muscles, which are the largest muscles in hummingbirds, representing 17% and 8% of the body mass, respectively. Unlike most vertebrate EMG recordings, which display compound wave forms representing the activation of multiple motor units, hummingbird EMGs display relatively simple wave forms reminiscent of insect flight muscle activation patterns. The temporal structure of the hummingbird EMGs suggests that they comprise either very few individual motor units or, the tightly synchronized activation of a larger group of motor units. Thus, the neuromuscular control of hummingbird flight appears to be highly insect-like in that muscles are activated very briefly and produce highly complex patterns of wing kinematics.

337. Analysis of odor localization in walking **Drosophila**
 Alice Robie

Multimodal sensory feedback experiments have indicated *Drosophila* use a linear sum of olfactory and vision in the control of flight. However, *Drosophila* perform interesting and complex behaviors such as courtship and mating, resource localization and utilization while walking. It has been demonstrated that a different set of visual feedback cues are used to control walking than to control flight. We hypothesize that in this lower dynamic range the integration of olfactory and visual information will also be different than in flight. In order to study the multimodal sensory control of walking we are developing an automated tracking arena for walking flies. Flies with clipped wings are able to walk freely in the 25 cm diameter arena. A two-dimensional tracking system using an IR video camera records the orientation and X,Y position of the walking fly, allowing us to do quantitative analysis on the search trajectory of flies as they explore the arena. The IR recording set up also allows the separation of recording and stimuli light, as the flies are not reactive to the long-wave length light used to illuminate the floor of the arena. Experiments in apparent darkness and a variety of visual conditions will allow us to determine the important visual cues used by the flies in order to localize a resource. Change in this search trajectory in the presence or absence of an olfactory point-source stimulus will give insight into the type of multimodal sensory integration the flies uses in order to localize a food resource.

338. Kinematics and steering-muscle control of saccades in flying **Drosophila**

Rosalyn Sayaman

In flight, flies search their sensory landscape using a series of straight flight sequences interspersed with rapid changes in heading termed saccade, during which the fly changes course by approximately 90 deg in less than 100 ms. These rapid maneuvers are elicited by rapid expansion flow fields located peripherally across the fly's visual field. Our previous study of the kinematics of free-flight saccades illustrated how subtle changes in stroke position, deviation and angle of attack differentially affected the magnitude and direction of the aerodynamic forces acting on the wings to sufficiently produce the necessary torque for the maneuver.

To further understand the control system involved in the changes in wing kinematics, we studied saccades in the context of tethered-flight. Flies are glued to a fine pin from the thorax and are placed in a flight-simulation arena. An expanding pattern stimulus located 90 deg either to right or left of the fly is used to trigger a saccade. As with the free-flight experiments, three high-speed video cameras positioned orthogonally from each other are used to capture the stroke cycles prior to and during a saccade at a rate of 5000 fps. Custom software is used for the digitization and extraction of kinematic parameters from the high-speed video images. Aerodynamic forces are measured by replaying the wing kinematics through a dynamically-scaled flapping robot. Additional measurements were also obtained using a lab-designed wing-beat analyzer and torque sensor.

The results of the tethered-flight experiments show similar kinematic trends as those of the free-flight experiments: 1) An increase in stroke amplitude of the outside wing and/or decrease in stroke amplitude of the inside wing; 2) A slight increase in stroke deviation of the inside wing; and 3) A slight advance in the ventral flip of the outside wing. As such, these factors act to tilt the stroke plane angle of the inside wing relative to the outside wing.

I am currently conducting EMG recordings in different steering-muscle groups that connect structurally to the wing hinges. Whereas the large flight muscles are responsible for the continuous downward and upward flapping of the wings, the differing activities of populations of steering muscles determine the changes in wing amplitude, deviation and angle of attack. The goal is to correlate firing frequency of different steering-muscle groups to the observed changes in wing kinematics during the triggered saccades.

339. Biomechanics and neurobiology of flight initiation in **Drosophila**

Gwyneth Card

Before a fly can begin to search for food or mates, it must get itself airborne. In under 33 ms, *Drosophila melanogaster* is able to launch itself from a standstill into controlled flight. Relatively little is known about how this complicated maneuver is achieved given the extreme

rapidity of the movement and the limited video technology previously available. Older work using high-speed film cameras distinguished two different "types" of flight initiation. In Type 1 takeoffs, the fly first elevates and rotates its wings in preparation for flight initiation. The wings are then depressed simultaneously with extension of the mesothoracic legs. In Type 2 takeoffs, the fly jumps with its legs before the wings are elevated, so wing motion does not begin until the fly is airborne. Trimarchi and Schneiderman correlated Type 2 takeoffs with visually elicited escape responses and Type 1 takeoffs with "voluntary" (non-stimulated) flight initiation.

The advance of video technology has enabled us to look at flight initiation in more detail than possible previously. We film jumping flies in three dimensions at 6 kHz with a 512 X 512 pixel resolution. Both voluntary (Figure 1) and visually-stimulated takeoffs are recorded and analyzed. Ethogram analysis of the video sequences (Figure 2) confirm that there are mechanistic differences between voluntary and visually-stimulated takeoffs. As previously observed, visually-stimulated takeoffs are more stereotyped than voluntary takeoffs, due to the large variance in the timing of voluntary wing raising. Our higher time resolution analysis, however, also shows that in all of the 12 visually-stimulated takeoffs analyzed, flies do begin to raise their wings before starting to jump. This may explain why stimulation of the escape response giant fiber pathway first triggers the wing depressors before exciting the tibia-extensor muscles to start the escape jump.

Further mechanistic differences occur in the first several wing beats of flight. Whereas visually-stimulated flies flap with upstrokes and downstrokes of roughly the same period, the first three-four strokes of voluntary takeoffs are performed with a downstroke 1.5 times longer than the upstroke. We presume this difference is the result of different partitioning of lift force generation between legs and wings in voluntary versus visually-stimulated takeoffs. Current work includes the construction of a force platform to measure the vertical force generated by a fly during takeoff. Combined with kinematic video analysis, this will allow us to determine the relative contributions legs and wings make to getting the fly airborne.

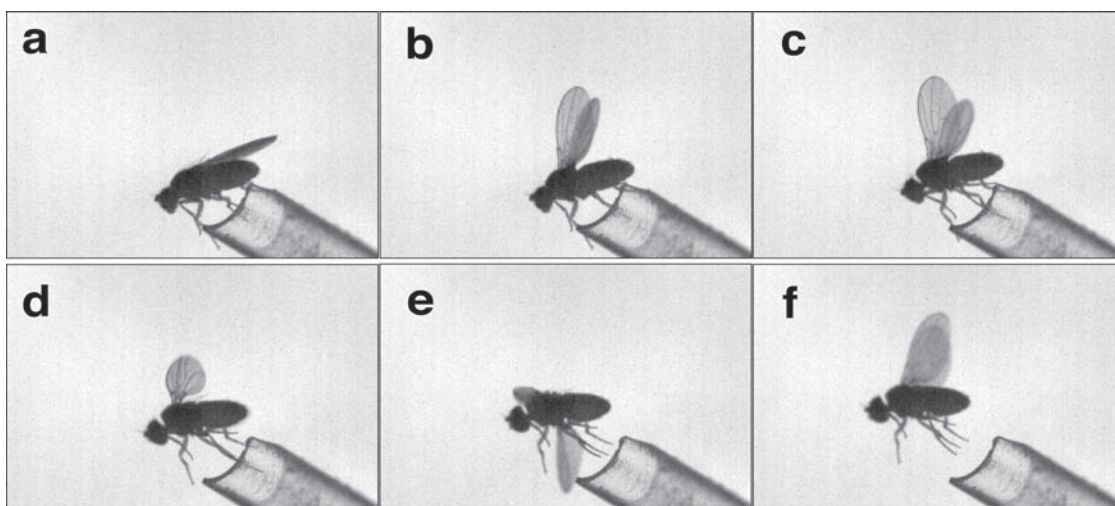


Figure 1. Images from high-speed video sequence of a typical voluntary takeoff (a-f show key events of the takeoff; the time between each frame shown is not the same).

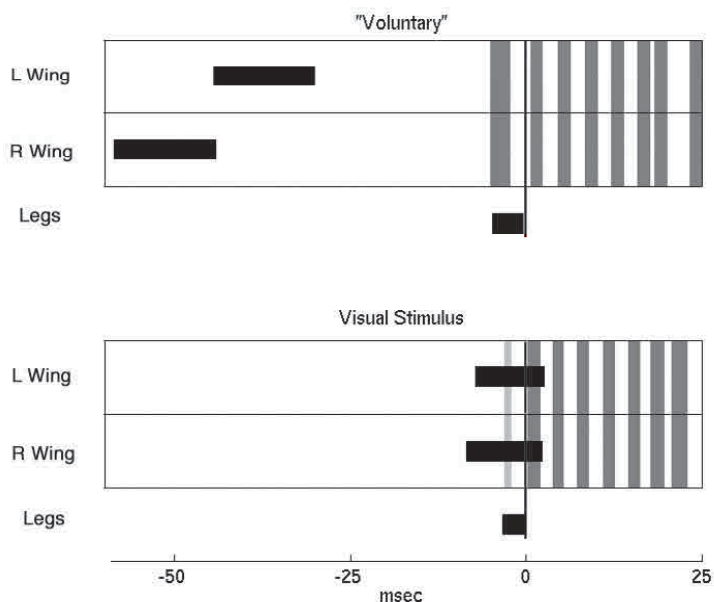


Figure 2. Averaged ethogram for events in voluntary and visually-stimulated takeoffs. Black horizontal bars represent the duration of left wing raising, right wing raising, and leg extension as labeled. Gray vertical bars represent downstroke period. The bars represent time from takeoff (0 ms, legs leave the ground, black line) and are mean values for 14 voluntary takeoffs and 12 visual takeoffs.

340. Odor localization in flying *Drosophila*

Seth Budick

Localization of feeding and oviposition sites is essential in the life cycle of any insect, including the fruit fly, *Drosophila melanogaster*. In the case of *D. melanogaster*, such sites are typically associated with fermenting vegetable matter resulting in conspicuous olfactory targets. Though odor localization in insects has been studied relatively extensively, those studies have been phylogenetically limited in scope, pertaining almost exclusively to pheromone localization in Lepidoptera.

Recent work in our laboratory has described odor localization by *D. melanogaster* flying in still air.

Unfortunately, it can be difficult to relate behavior to short-term olfactory experience in a still air environment where the precise dimensions of the olfactory stimulus must remain somewhat obscure. Similarly, odor localization in real life conditions may occur largely in moving air, possibly requiring a different behavioral strategy from that manifested in still air. To further study olfactory search in *D. melanogaster*, we have recently obtained a low velocity wind tunnel in which we can characterize the three-dimensional flight trajectories of *D. melanogaster* while precisely controlling the visual and olfactory environment.

For many insects, localizing the source of an attractive odorant involves odor-initiated upwind flight, but little was known of how *D. melanogaster* individuals alter their flight trajectories after encountering a plume of an attractive odorant. We have shown that flies respond to contact with a narrow plume of an attractive odorant by reducing their crosswind velocity while flying faster upwind, resulting in an upwind surge toward the odor source. In response to a tonic olfactory stimulus, a homogeneous odor cloud, flies fly fast headed straight upwind. With intermittent olfactory stimulation, fly trajectories are sometimes characterized by counterturns, as well as cross wind casts on apparent odor loss. There are, thus, both important similarities and differences between the odor-mediated behavior of *D. melanogaster* and that of male moths responding to pheromone plumes, implying possible differences in underlying neural mechanisms.

341. Modular displays for rapid development of programmable visual stimuli
Michael Reiser

Whereas flying insects make use of many sensory modalities, most of the behaviors we observe are dominated by visual control. For this reason, presenting a controlled visual environment to tethered insects continues to be a powerful experimental paradigm. Conventional display technologies (LCDs, CRTs, etc.) are not well-suited for use as stimuli for insect experiments, because their refresh rates are typically several times slower than the flicker fusion rate of insect visual systems. LEDs are used because they can be rapidly refreshed, which is necessary to maintain the illusion of motion. We have designed modular panels of 64 LEDs each, which can be connected to 'tile' an experimental environment with controllable displays (Figure 1). Patterns to be displayed are designed using custom software, downloaded to a controller board, and displayed on the individually addressed panels via a rapid serial interface. The panels have been designed to be extremely bright, with the added flexibility of individual pixel programmable brightness control, allowing experimentation over a broad range of behaviorally-relevant stimuli conditions. The panels are controlled via a microprocessor controller which, for most experiments, will not require a computer in the loop, greatly reducing the experimental infrastructure. This technology allows an experimenter to build and program a visual arena with a customized geometry in a matter of hours. This system is currently being used in several experiments with tethered *Drosophila*.

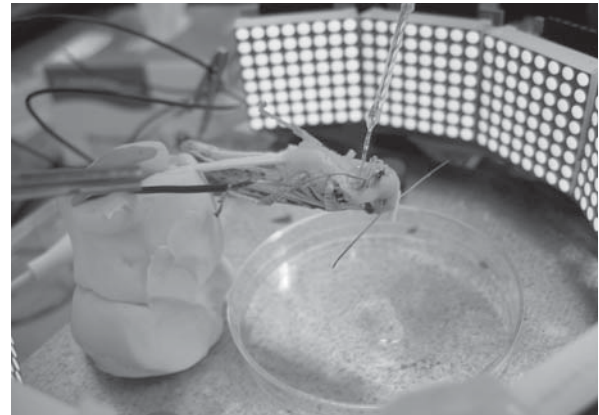
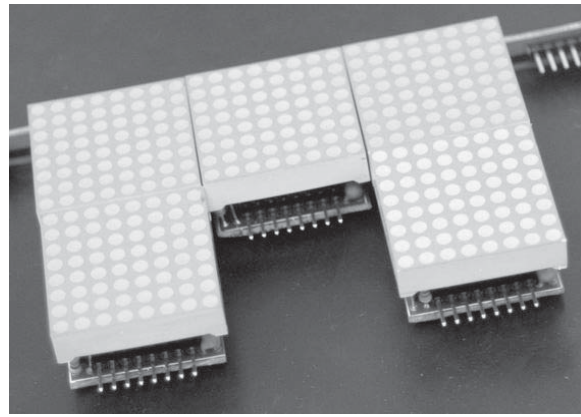


Figure 1. Visual display tiles and example use in electrophysiological experiment.

342. Vision as a compensatory mechanism for disturbance rejection in upwind flight
Michael Reiser

Recent experimental results demonstrate that flies possess a robust tendency to orient towards the frontally-centered focus of the visual motion field that typically occurs during upwind flight. We have developed a closed loop flight model (Figure 1), with a control algorithm based on feedback of the location of the visual focus of contraction, which is affected by changes in wind direction. We have demonstrated the feasibility of visually guided upwind orientation with a model derived from current understanding of the biomechanics and sensorimotor computation of insects. The matched filter approach used to model the visual system computations compares extremely well with open-loop experimental data. To test the ability of the closed loop system to orient the fly in the upwind direction, we presented 'step inputs' to the control system, where the fly was given an initial velocity and orientation and the wind was set at a fixed magnitude and direction (Figure 2). It is clear from the step responses that the tracking works, in the sense that the steady-state error is driven to zero, resulting in upwind orientation. Closed-loop simulations show stable upwind orientation behavior over the range of behaviorally-relevant wind speeds and sensitivity only to very low frequency disturbances. In future work we expect to

extend this simulation to three dimensions and six degrees of freedom, and investigate vision algorithms that take advantage of global optic flow cues. Also of immediate interest is the velocity control problem associated with transition from backwards to forward flight in the upwind direction.

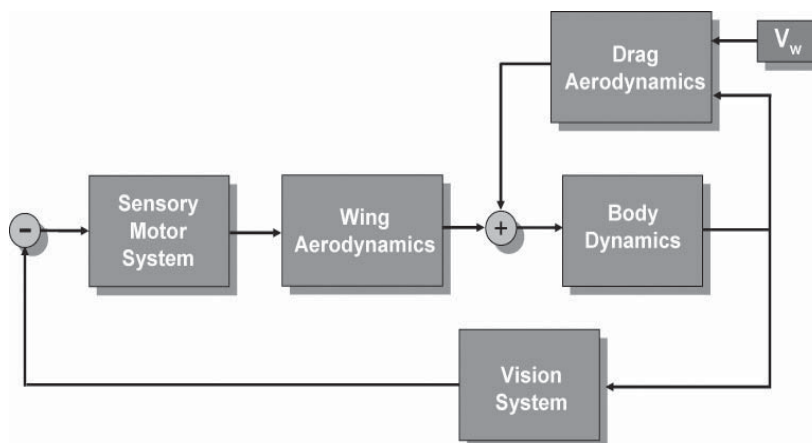


Figure 1. Closed loop model of upwind flight with wind disturbances.

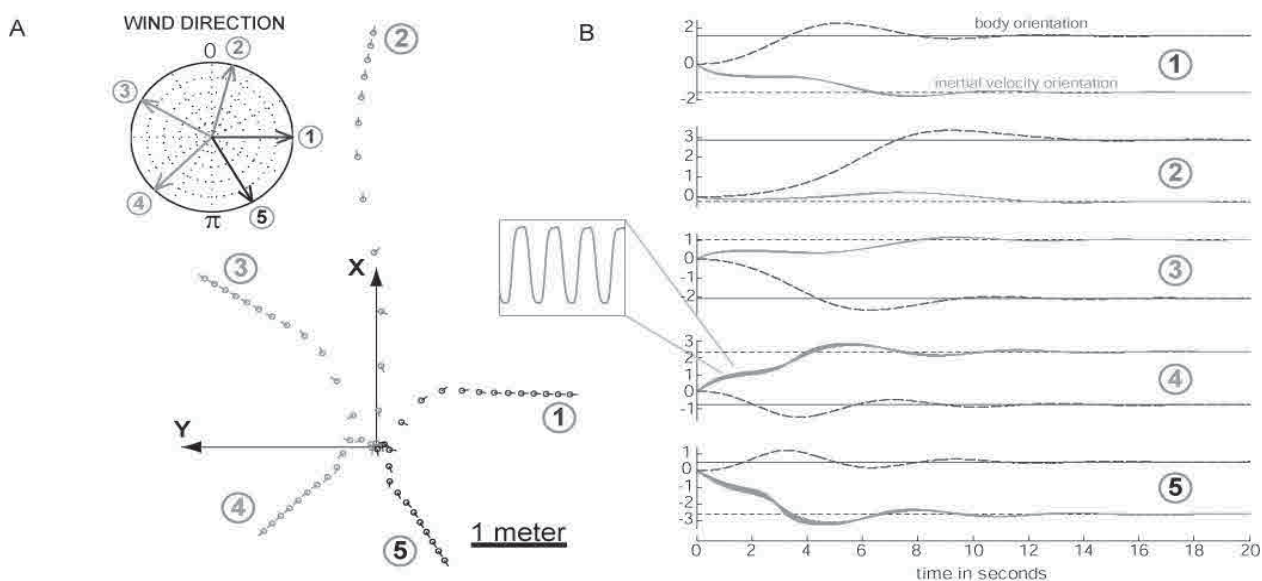


Figure 2. Closed-loop simulation results show the robustness of the tracking behavior. (A) Simulated 20 second flight trajectories, with fly positions plotted every 1.5 seconds. (B) Step responses in wind direction, showing zero steady-state error.

343. Visual-olfactory sensory fusion in fruit flies Mark Frye

Fruit flies make their living seeking the sources of attractive odors in widely varying and complex visual environments. My research has focused on two components of sensory-mediated flight behavior: the organization of visuo-motor reflexes and visual-olfactory integration. To examine the visual equilibrium reflexes that enable flies to fly straight and avoid collisions I used a computerized flight simulator in which a tethered fly responds to controlled motion of the visual panorama by

steering back and forth. Flies produce much greater torque to patterns of visual expansion than rotation. Furthermore, the rotation responses represent the linear sum of opposite signed expansion responses (Figure 1).

Armed with a better understanding of visual reflexes in *Drosophila*, I examined the influence of odor on expansion triggered turning responses. Presenting combinations of attractive odor and visual expansion stimuli indicate that visual responses are linearly superimposed upon odor responses, suggesting that there is no synergistic effect of multimodal stimulation. This

result indicates that the two sensory signals are likely processed along functionally-independent sensorimotor pathways.

Taken together, the results suggest a simple model that may explain how vision and olfaction are integrated for flight control in fruit flies. Rapid visual reflexes are organized by spatially varying inputs from elementary motion detectors in the brain, and these signals project selectively to small muscles of the wing hinge that coordinate steering maneuvers. Consequently, when animals encounter, for example, an expanding visual stimulus such as when flying toward an object, a collision avoidance response is orchestrated by asymmetric input to the steering muscles, evoking a turn. By contrast, olfactory signals project to the muscles that control the amplitude, frequency, and mechanical power production required to sustain flight. When the animal encounters an odor plume, a forward surge is orchestrated by symmetric input to the power muscles that results in increased wingbeat amplitude, frequency and forward thrust.

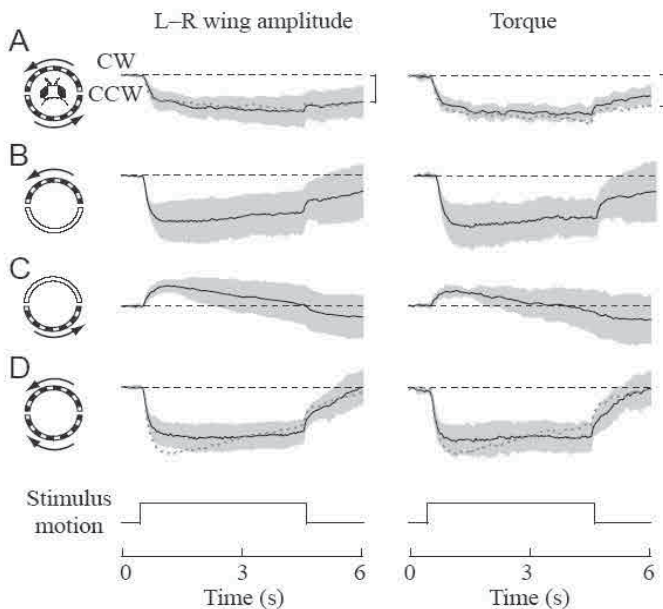


Figure 1. Responses of tethered flies to patterns of image motion on the front or rear half of the visual field. Flies were tethered within an electronic visual display and their wing motions or torque were monitored as the display was moved according to the icons on the left. A-counter-clockwise image rotation. Red indicates B+C. B-stimulation of the front field of view. C- stimulation of the rear field of view. D- image expansion. Red indicates B-C. Dark lines indicate mean, grey envelope indicates standard deviation

344. Advanced numerical simulation model of free flight behavior in insects

Titus Neumann

Flying insects exhibit a multitude of highly robust and effective behaviors, such as three-dimensional flight stabilization and drift compensation, obstacle avoidance, tracking, and odor localization. Many of these behaviors are based on complex interactions of the insect sensorimotor system with the physical environment. They often require the simultaneous evaluation and integration of multiple sensory channels, and the control of a motor system with multiple degrees of freedom. Various elementary control mechanisms for specific behavioral components have been characterized over the past decades, and a number of recent studies demonstrate the effects of the proposed control models using computer simulations. However, most of these models and simulations are restricted to a single degree of freedom. Furthermore, they are often based on the assumption of heavily simplified and idealized models of the input stimulus, force generation, body dynamics, and physical environment.

In this project, an advanced computer simulation model of the fruit fly *Drosophila* has been developed. The model integrates multiple key components of the sensorimotor system of the fly into a common framework, including highly accurate numerical models of the visual system, the motor system, and the physical environment.

In particular, a highly accurate simulation model for insect compound eyes has been included into the system. It allows the specification of the optical axis and spatial sensitivity distribution of each individual light receptor unit in a spherical field of view. It is capable of accurately reproducing the optical sampling and filtering properties of the *Drosophila* eye which comprises approximately 700 ommatidia with an average angular distance of 5° and Gaussian-shaped receptive fields. This model can be used to reconstruct the visual stimulus received by an insect eye with sub-pixel acuity. Further, a numerical model for the homogeneous computation and representation of local image motion in a spherical field of view has been added to the system. This model is based on the correlation-type elementary motion detector after Hasenstein and Reichardt, and allows to reconstruct the neural activation patterns in the retinotopic processing layers immediately preceding the wide field integration units in the lobula plate.

A highly realistic model of the fly motor system has also been developed and integrated into the simulation framework. It is based on a quasi-steady aerodynamic model for the generation of flight forces by flapping wings. The force coefficients used to calculate the lift and drag components of each wing have been determined from a dynamically-scaled robotic model reproducing wing kinematics recorded from real flies during free flight. Although force production by the flapping wings is an unsteady process, the quasi-steady model provides a good approximation of the average forces and torques acting on the body of the fly during each wing stroke. Together with

the body dynamics, these forces ultimately determine the changes in position and orientation of the fly.

In its entirety, the simulation framework developed in this project provides a unique and powerful tool for the analysis of experimental data and the assessment of control models derived from experimental work. Furthermore, it allows to develop and test novel, biomimetic control algorithms for artificial systems such as autonomous ground-based or aerial robots.

345. Ethological studies on resource-emigration in *Drosophila*

Jasper Simon

The distribution, abundance, and quality of natural food resources for *Drosophila* are unpredictable—at times quite scarce. Consequently, it seems flies should stay indefinitely on an established resource, but casual observation proves this false. What might influence the probability of a fly to stay or leave? To address the aforementioned behavior, this past year we built an experimental biosphere (Figure 1). FlyWorld incorporates commercially available environmental incubators capable of creating various ambient temperatures, photoperiods, and monitoring humidity to

house isolated chambers connected together by tubing. Automated, solenoid-driven doors and infra-red sensors together control and quantify locomotor behavior between these chambers. Our general, modular design allows the experimenter the flexibility for a variety of behavioral studies that include parallel configurations necessary for anticipated, high-throughput neuro-genetic studies. Finally, computer software and dedicated microprocessors incorporated in circuit boards all of our laboratory's own design allow a single computer the capacity to run over 900 modules. Currently, we perform experiments to address the influence of food depletion, food deprivation, and genetic variability between several natural isolates of *Drosophila melanogaster* on resource emigration behavior.

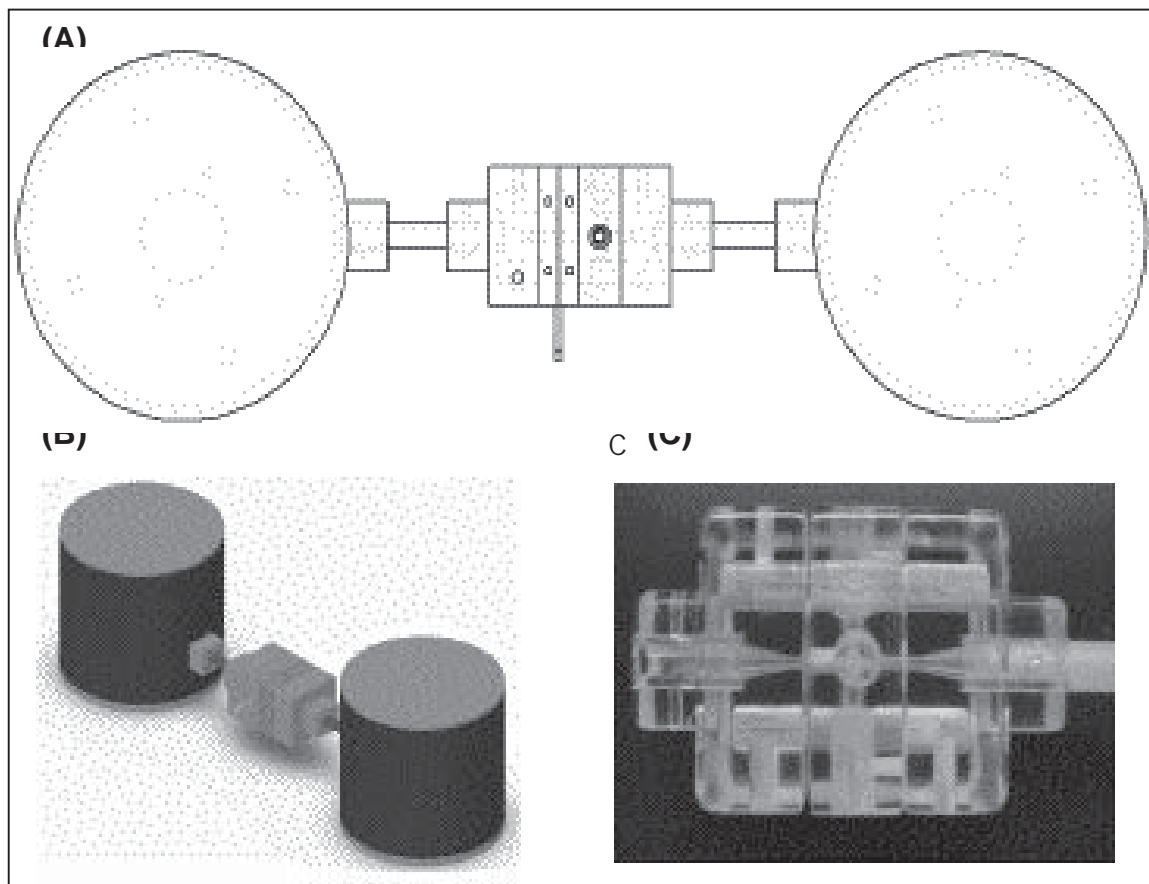


Figure 1. Prototype components of the FlyWorld apparatus. (A) Top schematic view of simple configuration consisting of two canisters, tubing, detector, and gate. (B) CAD-rendered view of configuration drawn in A. (C) Photograph of prototype detector block fabrication from stereo lithography.

346. Aerodynamics of forward flight in **Drosophila**
Will Dickson

Recent studies have demonstrated that a quasi-steady model closely matches the instantaneous force produced by an insect wing during hovering flight. It is not clear, however, if such methods extend to forward flight. In this study we use a dynamically-scaled robotic model of the fruit fly *Drosophila melanogaster* to investigate the forces produced by a wing revolving at constant angular velocity while simultaneously translating at velocities appropriate for forward flight. Because the forward and angular velocities were constant wing inertia was negligible and the measured forces can be attributed to fluid dynamic phenomena. The combined forward and revolving motions of the wing produce a time-dependent free-stream velocity profile that suggests that added mass forces make a contribution to the measured forces. We find that the forces due added mass make a small, but measurable, component of the of the total force and are in excellent agreement with theoretical values. Lift and drag coefficients are calculated from the forces traces after subtracting the contributions due to added mass. The lift and drag coefficients, for fixed angle of attack, are not constant for nonzero advance ratios, but rather vary in magnitude throughout the stroke. This observation implies that modifications of the quasi-steady model are required in order to accurately predict the instantaneous forces produced during forward flight. We show that the dependence of the lift and drag coefficients upon advance ratio and stroke position can be characterized effectively in terms of the tip velocity ratio - the ratio of the chordwise components of flow velocity at the wing tip due to translation and revolution. On this basis we develop a modified quasi-steady model which can account for the varying magnitudes of the lift and drag coefficients. Our model may also resolve discrepancies in past measurements of wing performance based on translational and revolving motion.

Publications

- Balint, C.N. and M.H. Dickinson (2004) Neuromuscular control of aerodynamic forces and moments in the blowfly, *Calliphora vicina*. *J. Exp. Biol.* In press.
- Birch, J. and Dickinson, M.H. (2003) The influence of wing-wake interactions on the production of aerodynamic forces in flapping flight. *J. Exp. Biol.* 206:2257-2272.
- Birch, J., Dickson, W. and Dickinson, M.H. (2004) Force production and flow structure of the leading edge vortex at high and low Reynolds numbers. *J. Exp. Biol.* 207:1063-1072.
- Dickinson, M.H. (2004) The initiation and control of rapid flight maneuvers in fruit flies. *Int. Biol.* In press.
- Dickinson, M.H. and Dudley, R. (2003) Flight. In: *Encyclopedia of Insects*, V.H. Resh and R. Carde, eds., Elsevier, New York, p 900.
- Dickinson, M.H. (2003) How to walk on water. *Nature* 424:621-622.

- Dickson, W. and M.H. Dickinson (2004) The effect of advance ratio on the aerodynamics of revolving wings. *J. Exp. Biol.* In review.
- Fry, S.N., Sayaman, R. and Dickinson, M.H. (2003) The aerodynamics of free-flight maneuvers in *Drosophila*. *Science* 300:495-498.
- Frye, M.A., Tarsitano, M. and Dickinson, M.H. (2003) Odor localization requires visual feedback during free flight in *Drosophila melanogaster*. *J. Exp. Biol.* 206:843-855.
- Frye, M.A. and Dickinson, M.H. (2003) A signature of salience in the *Drosophila* brain. *Nature Neurosci.* 6:544-546.
- Frye, M.A. and Dickinson, M.H. (2004) Closing the loop between neurobiology and flight behavior in *Drosophila*. *Curr. Op. Neurobiol.* In press.
- Frye, M.A. and Dickinson, M.H. (2004) Motor output reflects the linear superposition of visual and olfactory inputs in *Drosophila*. *J. Exp. Biol.* 207:123-131.
- Reiser, M.B. and Dickinson, M.H. (2003) A test bed for insect-inspired robotic control. *Proc. Roy. Soc. Lond. A* 361:2267-2285.
- Sherman, A. and Dickinson, M.H. (2003) A comparison of visual and haltere-mediated equilibrium reflexes in the fruit fly, *Drosophila melanogaster*. *J. Exp. Biol.* 206:295-302.
- Sherman, A. and Dickinson, M.H. (2004) Summation of visual and mechanosensory feedback in *Drosophila* flight control. *J. Exp. Biol.* 207:133-142.
- Tammero, L.F., Frye, M.A. and Dickinson, M.H. (2004) Spatial organization of visuomotor reflexes in *Drosophila*. *J. Exp. Biol.* 207:113-122.
- Wang, J., Birch, J.M. and Dickinson, M.H. (2004) Unsteady forces and flows in low Reynolds number hovering flight: Two-dimensional computations vs. robotic wing experiments. *J. Exp. Biol.* 207:449-460.

Assistant Professor of Biology and Applied Physics:
Michael Elowitz
Postdoctoral Scholars: David Sprinzak, Gurol Süel
Graduate Students: Robert Sidney Cox III, Chiraj Dalal
Technician: Jonathan Young

Support: The work described in the following research reports has been supported by:

Burroughs-Wellcome Career Awards at the Scientific Interface
Human Frontiers Collaborative Grant (with Uri Alon, Weizmann Institute)
NIH (Collaborative Grant with the Harvard Center for Genomic Research)
Searle Scholars Award

Summary: The lab is interested in how cellular functions are implemented using networks of interacting genes and proteins. We are equally interested in the complementary question of how novel networks can be engineered within cells to implement alternative cellular behaviors. We address these two problems together using a combination of experimental and theoretical techniques.

Recently, we have focused on a number of specific issues that are crucial for a quantitative understanding of the behavior of both natural and synthetic gene regulation networks. These include: (a) dynamics of feedback and other regulatory structures on cellular behavior; (b) effects of stochasticity, or 'noise' in gene regulation; and (c) mechanisms for engineering synthetic 'replicas' of natural genetic circuits. The lab is developing general methods for the analysis of gene expression over time in individual cells and cell lineages, primarily using fluorescent proteins, automated time-lapse microscopy, and image analysis.

347. Gene regulation at the single cell level
Nitzan Rosenfeld¹, Uri Alon¹, Peter Swain²
Jonathan Young, Michael Elowitz

Genetic networks are based on regulation of gene expression by transcription factors. Their function often depends critically on the quantitative relationship between transcription factor concentrations and downstream promoter activity. This Gene Regulation Function (GRF) cannot be inferred from either in vitro or population average measurements. We are currently determining the GRF of a repressor-promoter interaction measured in individual living cells of *Escherichia coli*. These measurements are based on dynamic, time-lapse fluorescence tracking of single cells expressing fluorescent protein fusions to well-characterized transcription factors. A fluctuation-based technique involving protein segregation errors enables calibration of the GRF in molecular units. That is, even though we can't detect single molecules of Green Fluorescent Protein, we are nevertheless able to calibrate in these units. This in vivo approach to biochemistry allows characterization of genetic elements and circuits within their cellular context. It thus provides elusive biochemical parameters that are

essential for designing and analyzing genetic circuits. We have further observed that protein production rates in individual cell lineages show a long correlation time, on the order of the cell cycle. This non-genetic 'memory' helps explain the observed population variance in protein content and has implications for dynamic responses of genetic networks.

¹Weizmann Institute, Rehovot, Israel

²McGill University, Montreal, Canada

348. Probabilistic decision-making in *Bacillus subtilis* starvation response

Gurol Süel

Due to their small size and low copy numbers of important molecules (e.g., DNA, transcription factors), bacterial cells can act in a stochastic, or 'noisy' manner. In previous work, we established the relative importance of stochastic effects in gene expression. Now we are exploring its relevance for a natural pathway of microbial development. Although potentially problematic for homeostatic processes, noise may be exploited for probabilistic decision-making. In the bacteria *Bacillus subtilis*, genetically identical cells in a homogeneous environment exhibit a variety of alternative responses. In response to starvation, for example, individual cells may sporulate or become competent for DNA uptake (other responses are also possible). The 'decision' between these outputs involves both an intracellular gene regulation network and extensive intercellular signaling. Using fluorescent protein reporters and time-lapse assays, we are investigating the dynamic events involved in this process to understand how probabilistic decision-making can be genetically programmed (and manipulated).

349. Synthetic transcriptional network motifs
Robert Sidney Cox III

Transcription regulatory networks, composed of interacting genes and proteins, were recently found to be built of recurring circuit elements termed "network motifs," which can be thought of as elementary gene circuit building blocks. In order to gain a fundamental understanding of network function, we examine the behavior of these motifs at the level of cell populations and individual cells. We will work in parallel with natural systems and analogous synthetic circuits constructed from well-characterized components. Studies of these networks at the individual cell level will allow us to identify sources of variability in the timing and amplitude of network responses, and highlight circuit architectures that amplify or attenuate this "noise." The experiments will be compared to mathematical models of these circuits, on both the population and stochastic individual cell levels. The results of these studies will serve as a foundation for future studies of more complicated network designs in diverse cell types.

350. Framework for the construction of synthetic transcriptional networks

Robert Sidney Cox III

Recently, it has become possible to design and build genetic circuits 'from scratch,' using well-characterized genetic elements. This allows the possibility of creating arbitrary new behaviors within cells and analyzing alternative circuit designs. However, a number of difficulties hinder the assembly and analysis of genetic circuits. Here we describe the use of kilobase DNA synthesis to create a synthetic "scaffold" within which a range of transcriptional networks can be created. The scaffold contains three distinguishable fluorescent reporter genes. It is engineered to allow convenient insertion of regulatory genes, rearrangement of promoters, alteration of ribosome binding sites, addition of protein degradation tags to reporter genes, and creation of reporter fusion proteins. Cre/loxP recombination sites at each end allow the construct to be transferred to other DNA molecules. Multiple terminators between each operon protect against transcriptional read-through, and codon optimization of the reporters improves the sensitivity of detection. We anticipate that the scaffold will be useful in a wide range of synthetic biology applications.

Publications

- Garcia-Ojalvo, J., Elowitz, M.B. and Strogatz, S.H. (2004) Modeling a synthetic multicellular clock: Repressilators coupled by quorum sensing. *Proc. Natl. Acad. Sci. USA* 101(30):10955-10960.
- Lahav, G., Rosenfeld, N., Sigal, A., Geva-Zatorsky, N., Levine, A.J., Elowitz, M.B. and Alon, U. (2004) Dynamics of the p53-Mdm2 feedback loop in individual cells. *Nat. Genet.* 36(2):147-150.
- Overholtzer, M., Rao, P.H., Favis, R., Lu, X.Y., Elowitz, M.B., Barany, F., Ladanyi, M., Gorlick, R. and Levine, A.J. (2003) The presence of p53 mutations in human osteosarcomas correlates with high levels of genomic instability. *Proc. Natl. Acad. Sci. USA* 100(24):14511.

Anna L. Rosen Professor of Biology: Scott E. Fraser
 Members of the Beckman Institute: Russell E. Jacobs,
 Jerry Solomon

Members of the Professional Staff and Senior Staff:
 Gary Belford, Benoit Boulat, Mary Dickinson, David
 Kremers, Russell D. Lansford, P.T. "Jim" Narasimhan,
 Carol Readhead, Seth Ruffins, Peter Siegel, Stephen
 Speicher, J. Michael Tyszka, Chang-Jun Yu, Xiaowei
 Zhang

Visitors and Visiting Associates: Elaine Bearer, Andres
 Collazo, John Faiz Kayyem, Francoise Marga, John
 Wallingford

Collaborators: Gabriel Acevedo-Bolton, Caleb Behrand,
 Titus Brown, Arian Forouhar, Mory Gharib, Richard
 Harland, David Laidlaw, Rex Moats, Marysia Placzek,
 Eduardo Rosa-Molinar, Michael Roukes, Changhui Yang
 Postdoctoral Research Fellows: Andrew Ewald,
 Maxellende Ezin, Bridget Hanser, David Koos, Michael
 Liebling, Melanie Martin, Helen McBride, Sean Megason,
 Cyrus Papan

Graduate Students: Magdalena Bak, Christie Canaria,
 Joe Duimstra, Jeffrey Fingler, Ying Gong, Sean Gordon,
 Elizabeth Jones, Reinhard Köster, Rajan Kulkarni, Carole
 Lu, James Maloney, David Van Velan

Research and Laboratory Staff: John Carpenter, Sonia
 Collazo, Mary Flowers, Kristy Hilands, Tim Hiltner, Aura
 Keeter, Edriss Merchant, Jeff Smith, Chris Waters, Jon
 Williams

Staff of the Caltech Brain Imaging Center: Andrey
 Demyanenko, Steve Flaherty, K. Craig Goodrich, Martha
 Henderson, Mary Munoz, Lauren Somma

Undergraduates: John Oh, Jonathan So

Support: The work described in the following research
 reports has been supported by:

- American Heart Association
- Anna L. Rosen Professorship
- Beckman Institute
- Carl Zeiss Jena
- Defense Advanced Research Projects Agency
- House Ear Institute
- Human Brain Project
- Human Frontier Science Program
- Jet Propulsion Laboratory
- Moore Foundation
- National Aeronautics and Space Administration
- National Institute for Biomedical Imaging and
 Bioengineering
- National Institute of Child Health and Human
 Development
- National Institute of Mental Health
- National Institute on Drug Abuse
- National Institutes of Health
- National Science Foundation
- PhRMA Foundation
- That Man May See

Summary: Our laboratory has dedicated itself to
 performing tests of the cell and molecular basis of
 developmental patterning, using in vivo imaging tools.
 The explosion of data from molecular approaches and the
 dramatic progress from in vitro culture assays have
 resulted in a rich set of proposals for the mechanisms that
 underlie developmental patterning. Our goal is to test these
 proposed mechanisms in the intact embryo, with the hope
 of moving forward from what might happen to what does
 happen in the natural biological context. There are many
 challenges to such tests, including the tagging of cells or
 molecules so that they can be followed in the intact
 system, the visualization of the tagged structures, and the
 interpretation of the time-varying events these images
 represent. Solutions to these challenges require the
 coordinated efforts of researchers spanning the life and
 physical sciences.

In the past year we have made significant
 advances in understanding the motions of cells in the
 gastrulating vertebrate embryo using techniques ranging
 from experimental embryology to microscopic MRI (e.g.,
 abstracts by Ewald, Gong, Papan). The molecular control
 of the processes that elongate the body axis of fish and
 frog embryos appears to have many common elements,
 although the basic processes that are under control can
 range from medio-lateral intercalation motions to oriented
 cell divisions. By combining imaging and molecular
 approaches, we obtain findings with implications for both
 the embryology and the molecular biology of early
 development.

Parallel improvements in imaging hardware and
 software have advanced our knowledge of the events that
 build embryos. New, faster microscope designs permit
 dynamic events to be followed with greater clarity.
 Multispectral laser-scanning microscopes permit large
 numbers of distinctly labeled cells to be followed over
 time. Software for following such multidimensional data
 make it more straightforward to extract understanding
 from the imaging data, and improvements in image atlases
 make it possible to share the data broadly with the research
 community. Our hope is that the sum product of these
 advances will be better research design and interpretation
 in many different laboratories.

An exciting recent development has been the
 establishment of the Caltech Brain Imaging Center, which
 builds upon the successes both here and elsewhere to
 create a center with the ability to image both human and
 animal subjects. The Center, an outgrowth of the interest
 of faculty in at least four different Divisions at Caltech, has
 become fully functional in a very short period of time.
 The staff of our laboratory and the rest of the campus
 should take pride in the parts they have played in this
 emerging success story.

351. Cranial neural crest migration in the avian embryo

Carole Lu, Scott E. Fraser

Cranial neural crest cells are a migratory multipotent population of cells that form craniofacial structures and some PNS derivatives in the vertebrate embryo. In the chick hindbrain, these cells migrate out from the dorsal neural tube in three discrete streams from rhombomere(r) 2, r4, and r6 and fill up ectodermal pouches known as the branchial arches. Previous work in our lab has been directed at understanding the migratory behavior and pathways of these cells *in vivo*. In order to visualize the migrating neural crest cells, we pressure inject lipophilic dyes or electroporate reporter constructs expressing GFP or RFP. By using an explant culture system developed in the lab we can watch the migration process on an inverted confocal microscope for up to 24 hrs. We are currently studying the importance of cell-cell

interactions and the role of members of the ephrin/Eph family of adhesion and guidance molecules in migration.

The discrete streams of migrating cranial neural crest show individualistic characteristics. At the level of r4, the neural crest cells migrate in a tight lateral stream directly from the neural tube to branchial arch 2. This stream is separated from other neural crest cells by crest-free regions adjacent to r3 and r5. In the posterior hindbrain, the neural crest cells first form a field of cells that are then segregated amongst branchial arches 3 and 4. This is similar to what occurs in *Xenopus*, where the cranial crest cells first migrate as a wave and then segregate to the different arches. Differences in the r4 and r6 streams of neural crest cells suggest the mechanisms that guide their migration are also different. We are studying the effect of genetic perturbations upon the migration and the segregation of neural crest cells that populate branchial arches 3 and 4 and correlating it with the formation of the branchial arches.

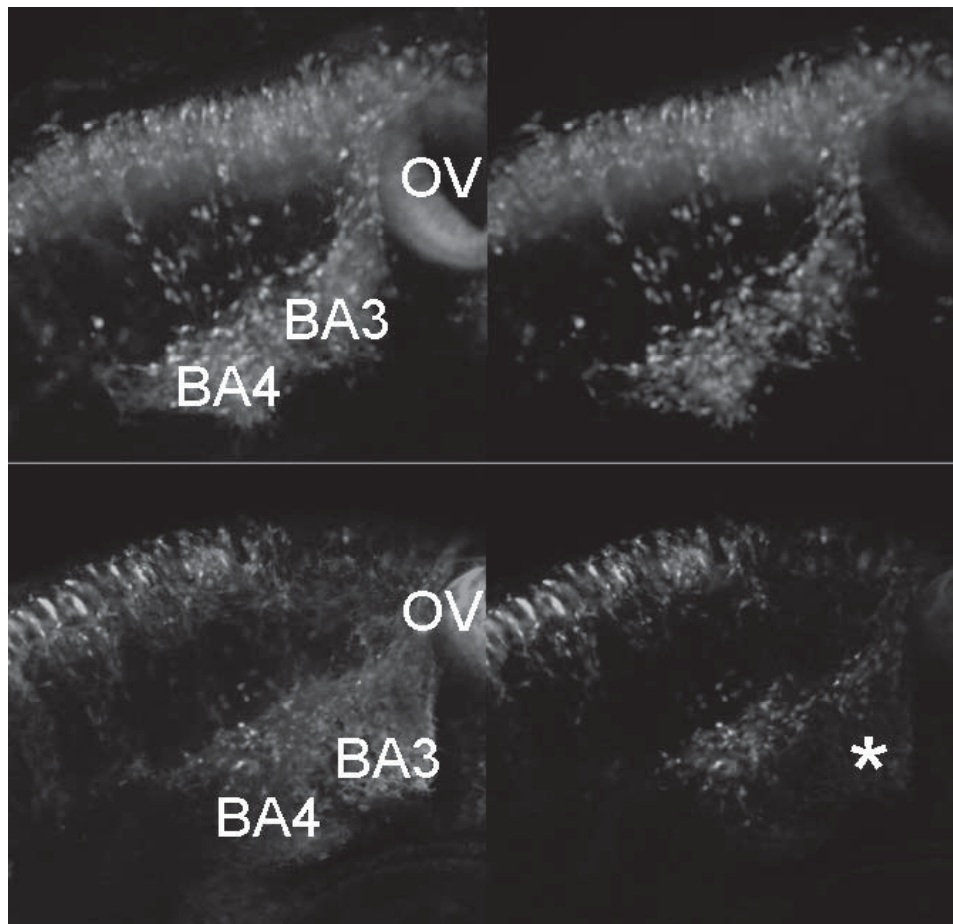


Figure 1. Top panel shows neural crest cells expressing a GFP reporter migrating to BA3 and BA4. In the bottom panel, the ectopic expression of Ephrin A5 leads to fewer GFP-positive cells migrating to BA 3, asterisk. BA branchial arch, OV otic vesicle.

352. Organization and development of genetically-defined olfactory glomeruli

David S. Koos, Scott E. Fraser

A primary step in the development of olfaction sense is the formation of precise connections between olfactory sensory neurons (OSNs) and their appropriate second-order targets within the first relay station of the olfactory nerve, the olfactory bulb (OB). These axonal connections into the OB are organized such that all neurons expressing the same odorant receptor (OR) converge their axons onto common glomeruli that are located at similar positions in all individuals from a species. The ultimate goal of this research program is to understand the cellular mechanisms underlying the establishment and elaboration of this precise and complex innervation pattern and to explore how axo-axonic interactions are involved.

In order to address this question, I have been using two-photon laser scanning microscopy (TPLSM) and transgenic mice in order to characterize the organization and behaviors of genetically-defined olfactory axons as they innervate their glomerular targets in the olfactory bulb. In collaboration with Dr. Peter Mombaerts at the Rockefeller University, novel strains of mice were constructed in which the subset of OSNs that express a specific OR gene, M72, also produce a fusion of tau with a fluorescent protein (GFP). As a result, in these engineered mice, all of the OSNs that express M72 are also fluorescently labeled and, therefore, can be visualized in vivo either at specific time points or chronically over long periods of time. The superior depth penetration into light scattering tissue obtained by TPLSM combined with its low degree of photo toxicity and bleaching allows us to generate high-resolution three-dimensional reconstructions of both mature and developing glomeruli that are innervated by M72 expressing axons. These studies are providing an unprecedented view of the axonal behaviors that underlie olfactory glomerulus stabilization and will be useful for understanding the mechanisms involved in the formation of neural connections in general.

353. Becoming a new neuron in the adult olfactory bulb

A. Carleton¹, L.T. Petreanu², R. Lansford, A. Alvarez-Buylla², P.M. Lledo¹

New neurons are continually recruited throughout adulthood in certain regions of the adult mammalian brain. How these cells mature and integrate into preexisting functional circuits remains unknown. Here we describe the physiological properties of newborn olfactory bulb interneurons at five different stages of their maturation in adult mice. Patch-clamp recordings were obtained from tangentially and radially migrating young neurons and from neurons in three subsequent maturation stages. Tangentially migrating neurons expressed extrasynaptic GABA(A) receptors and then AMPA receptors, before NMDA receptors appeared in radially migrating neurons. Spontaneous synaptic activity emerged soon after migration was complete, and spiking activity was the last

characteristic to be acquired. This delayed excitability is unique to cells born in the adult and may protect circuits from uncontrolled neurotransmitter release and neural network disruption. Our results show that newly born cells recruited into the olfactory bulb become neurons, and a unique sequence of events leads to their functional integration.

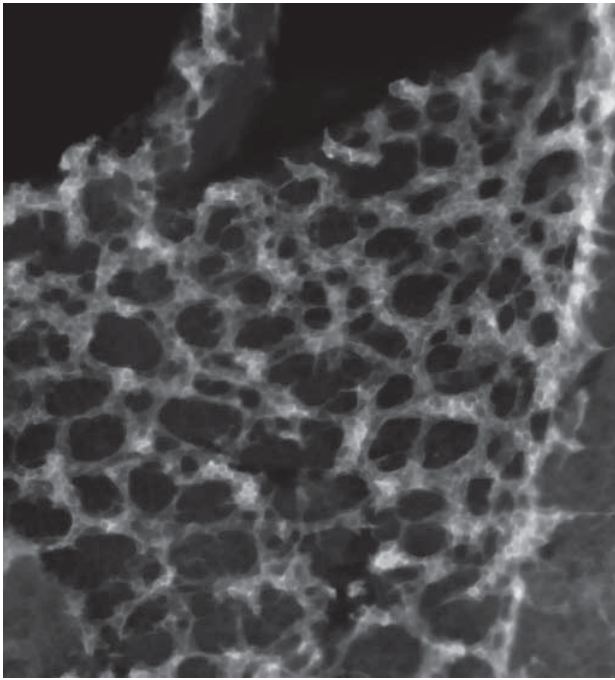
¹Pasteur Institute

²U.C., San Francisco

354. Imaging the enteric nervous system in development and in disease

Helen McBride

My goal is to examine the enteric nervous system (ENS) using various imaging modalities during development and in the case of motility disorders in order to better understand the dynamics underlying these processes. During development of the ENS, neural crest cells migrate from their entry point in the stomach caudally to the end of the colon. As they migrate, these cells proliferate and differentiate into all of the neurons and glia of the intrinsic ENS, literally millions of cells in an adult animal. How does migration stall and what does this tell us about the signaling events necessary for migration and it's associated behaviors to proceed normally? By using confocal time-lapse imaging of neural crest cells migrating through both chicken and mouse explanted gut tissue, I am characterizing both normal and perturbed migration in a search for new signaling pathways involved in these events. In adult mice, I use uMRI as a method to examine the gut motility in live transgenic and knockout mice to identify new mouse models of dysmotility. When coupled with traditional methods for examining the adult ENS including electrophysiology, epithelial secretion and tension recording, the uMRI provides a non-invasive and rapid method to identify candidate mouse lines for a lengthy characterization process. The first mouse line I examined, DBH::Galanin has constipation associated with high amplitude intestinal contractions and visceral hypersensitivity. These mice are proving to be a good model for irritable bowel syndrome (IBS), a disease that affects millions of individuals around the world and for which there have been no good mouse models demonstrating perturbed bowel function as well as the pain reported by human patients. By using the uMRI to screen other candidate mouse lines, I can quickly identify animals with dysmotility with the goal of using these models to better understand human ENS disease states.



355. Planar cell polarity signaling controls orientation of oriented cell divisions during zebrafish gastrulation

Ying Gong, Chunhui Mo, Scott E. Fraser

Oriented cell division is an integral part of pattern development in processes ranging from asymmetric segregation of cell-fate determinants to the shaping of tissues. Despite the many proposals that it can play an important role in tissue elongation, the mechanisms regulating division orientation have been little studied outside of the invertebrates *Caenorhabditis elegans* and *Drosophila melanogaster*. Here, we have analyzed mitotic divisions during zebrafish gastrulation using *in vivo* confocal imaging and found that cells in dorsal tissues preferentially divide along the animal-vegetal axis of the embryo. Establishment of this animal-vegetal polarity requires the Wnt pathway components Silberblick/Wnt11, Dishevelled and Strabismus. Our findings demonstrate an important role for non-canonical Wnt signalling in oriented cell division during zebrafish gastrulation and indicate that oriented cell division is a driving force for axis elongation. Our results suggest that non-canonical Wnt signalling plays a conserved role in vertebrate axis elongation, orienting both cell intercalation and mitotic division.

356. Convergent extension and **Xenopus** gastrulation: Convergent extension is required for blastopore closure, archenteron elongation and archenteron inflation, but is dispensable for mesoderm internalization

Andrew J. Ewald, J. Michael Tyszka, Sara Peyrot¹, John B. Wallingford², Scott E. Fraser

Two main goals of vertebrate gastrulation are to close the blastopore and to initiate and elongate the archenteron, or future gut, of the animal. It has been

proposed that both processes are largely driven by convergent extension in the overlying mesoderm.

Convergent extension has been hypothesized to be the primary motor driving blastopore closure and mesendoderm internalization during gastrulation in the frog, *Xenopus laevis*. We directly test this relationship by quantitatively examining the progress of blastopore closure in embryos with varying disruptions in Dishevelled (XDsh) mediated convergent extension. We demonstrate that blastopore closure requires XDsh function in the dorsal and lateral/ventral regions. By following blastopore closure over time in living embryos, we further observe that mesoderm internalization is driven by a coordinated movement of surface material around the dorsal lip of the blastopore and by reciprocal movements within the yolk plug. We conclude that these internalization movements can be uncoupled from convergent extension as they can proceed normally in the near absence of either convergent extension or blastopore closure. We propose that convergent extension is the primary motor of blastopore closure, but is largely dispensable for mesoderm internalization.

We then explore the correlation between archenteron elongation and convergent extension and test for a coupling between the two by blocking convergent extension through interference with Dishevelled (XDsh) signaling. We observe shorter archenterons in embryos in which convergent extension is blocked in the dorsal tissues. However, archenteron development proceeds surprisingly well even in severely affected embryos. Furthermore, the defect seems specific to the elongation, not to the expansion of the archenteron. We propose a model for archenteron development whereby it initiates through apical constriction of bottle cells, elongates due to a coordinate involution of yolk plug and marginal zone material, and then inflates due to a transfer of blastocoelar fluid to the archenteron. We identify a role for convergent extension in ensuring the correct tissue alignments prior to involution so that the archenteron can effectively elongate.

¹University of California, Berkeley, CA

²University of Texas, Austin, Texas

357. Quantitative imaging of the sea urchin genetic regulatory network

Bridget Hanser

The goal of this project is to develop approaches for quantitative imaging of components of the genomic regulatory network in early sea urchin embryos. In particular, I propose to study the temporal and spatial variation of specific components of the genetic regulatory network, in collaboration with the Professor Eric Davidson's laboratory at Caltech. The sea urchin was selected because of the significant amount of known regulatory information for the early embryo, the ease of producing large numbers of embryos, and the strong need for quantitative measurements of the transcription and degradation rates for key regulatory components in various parts of the developing embryo.

This project requires tools for quantitatively assessing the amount of fluorescent reporter gene activation *in vivo*. This will necessitate the development of correction methods for quantitative imaging of living samples for confocal and two-photon microscopy. Using information gathered from other microscopy techniques, such as brightfield, Nomarski differential interference contrast (DIC) and reflection imaging, I propose to develop a computational scheme to use this information to either correct these aberrations during imaging using an adaptive optics scheme or to apply computational corrections after data collection.

358. Assessing the role of microvascular blood flow during mammalian development

Elizabeth A.V. Jones, Chris W. Waters, Margaret H. Baron*, Scott E. Fraser, Mary E. Dickinson

Hemodynamics, or blood fluid dynamics, is of great importance in vascular biology, both in normal angiogenesis as well as in wound healing and disease. Its role during embryonic development, however, is less well understood. Many genes that appear to be regulated by shear stress are also important for developmental angiogenesis. In mice, several mutations have been isolated that effect angiogenesis. Some defects are caused by mutations in genes that have required functions in endothelial cells (e.g., Carmeliet, 1996; Ferrara, 1996; Goumans, 1999; Lindahl, 1997; Suri, 1996) whereas others occur in genes required for heart function, but have secondary defects in the vasculature (e.g., Huang, 2003; Wakimoto, 2000). Unfortunately, a precise understanding of how flow disruptions in flow lead to secondary defects in the vasculature has been hampered by the inadequacy of existing analytical tools.

To permit the measurement of blood flow rates in early mouse embryos, we have established a model system to directly image and measure circulation using fluorescence microscopy (Jones et al., 2002; Jones et al., 2004). A transgenic mouse line in which green fluorescent protein is expressed under the control of epsilon-globin is used to visualize primitive erythroblasts (Dyer et al., 2001). Using a method based on continuous laser line scanning, we are capable of measuring flow rates that are too fast for conventional whole-field fluorescence. The resulting line scan images encode the speed of the red blood cell because the erythrocyte is imaged by more consecutive line scans the slower it is moving. Furthermore, these measurements, combined with measurements of hematocrit have been used to calculate the shear stress that endothelial cells are exposed to at different times during development and vascular remodeling.

In order to understand how hemodynamic signals regulate vascular remodeling, we have begun to investigate changes in angiogenesis induced by increasing or decreasing shear stress during development. We relate these alterations to cellular processes, including peripheral cell recruitment and protein expression. These studies establish a link between the pattern of blood flow within

the vasculature and the stage of cardiovascular development and enable analysis of the influence of mechanical forces during development.

*Department of Cell and Developmental Biology, Mt. Sinai Medical School, New York, NY, 10029

References

- Carmeliet, P., Ferreira, V., Breier, G., Pollefeyt, S., Kieckens, L., Gertsenshtein, M., Fahrig, M., Vandenhoek, A., Harpal, K., Eberhardt, C., Declercq, C., Pawling, J., Moons, L., Collen, D., Risau, W. and Nagy, A. (1996) *Nature* 380:435-439.
- Dyer, M.A., Farrington, S.M., Mohn, D., Munday, J.R. and Baron, M.H. (2001) *Development* 128:1717-1730.
- Ferrara, N., Carver-Moore, K., Chen, H., Dowd, M., Lu, L., O'Shea, K.S., Powell-Braxton, L., Hillan, K.J. and Moore, M.W. (1996) *Nature* 380:439-442.
- Goumans, M.J., Zwijsen, A., van Rooijen, M.A., Huylebroeck, D., Roelen, B.A. and Mummery, C.L. (1999) *Development* 126:3473-3483.
- Huang, C., Sheikh, F., Hollander, M., Cai, C., Becker, D., Chu, P.H., Evans, S. and Chen, J. (2003) *Development* 130(24):6111-6119.
- Jones, E.A., Baron, M.H., Fraser, S.E. and Dickinson, M.E. (2004) *Am. J. Physiol. Heart Circ. Physiol.* In press.
- Lindahl, P., Johansson, B.R., Leveen, P. and Betsholtz, C. (1997) *Science* 277:242-245.
- Suri, C., Jones, P.F., Patan, S., Bartunkova, S., Maisonpierre, P.C., Davis, S., Sato, T.N. and Yancopoulos, G.D. (1996) *Cell* 87:1171-1180.
- Wakimoto, K., Kobayashi, K., Kuro, O.M., Yao, A., Iwamoto, T., Yanaka, N., Kita, S., Nishida, A., Azuma, S., Toyoda, Y., Omori, K., Imahie, H., Oka, T., Kudoh, S., Kohmoto, O., Yazaki, Y., Shigekawa, M., Imai, Y., Nabeshima, Y. and Komuro, I. (2000) *J. Biol. Chem.* 275:36991-36998.

359. Circulating blood island-derived cells contribute to vasculogenesis in the embryo proper

A.C. LaRue*, R. Lansford, C.J. Drake*

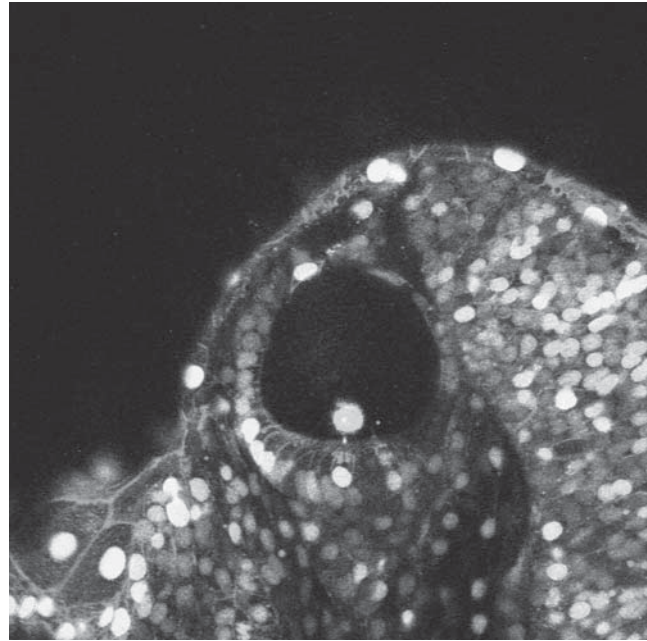
While recent findings have established that cells derived from the bone marrow can contribute to vasculogenesis in the adult, it is unclear whether an analogous population of cells in the embryo can also contribute to vasculogenesis. Using a retroviral labeling strategy, we demonstrate that circulating blood island-derived cells contribute to the genesis of both extra- and intraembryonic blood vessels in the early quail embryo. This finding establishes that vasculogenesis in the embryo is a composite of two processes: the direct *in situ* formation of blood vessels from mesodermally derived angioblasts and the incorporation and differentiation of circulating endothelial cell progenitors into forming embryonic blood vessels.

*Medical University of South Carolina

360. **In toto** imaging of zebrafish development

Sean Megason, Scott E. Fraser

We are interested studying zebrafish development using in toto imaging, a novel technology we are developing. Advances in both laser-scanning microscopy and GFP technology are combining to make possible imaging-based approaches for studying developmental mechanisms that were previously impossible. Modern confocal and multi-photon microscopes are pushing the envelope of speed, sensitivity, spectral resolution, and depth resolution to allow in vivo imaging of whole, live embryos at cellular resolution over extended periods of time. In toto imaging, in which nearly every cell in a developing embryo or tissue can be tracked through space and time, may become a standard technique for small transparent embryos such as zebrafish, *C. elegans*, and early-stage chick and mouse embryos. There are several technical challenges that must be met in order to permit in toto imaging. Firstly, embryos must be labeled in such a way to allow all of the cells in the region of interest to be individually distinguishable so they can be segmented. We have developed a labeling method using Histone2B-EGFP and membrane localized mRFP1 to label all the nuclei green and cell membranes red. This labeling technique allows each cell in a tissue to be segmented and reveals cellular morphology very nicely. The next technical challenge that must be met for in toto imaging, is that embryos must be imaged at sufficient spatial and temporal resolution to allow every cell to be tracked during development without damaging the embryo. We have developed mounting, confocal imaging, and data storage techniques that make it possible to continuously image a zebrafish embryo at very high spatial and temporal resolution for 48 hours and to successfully archive the gigabytes of images. The final and most difficult challenge for in toto imaging is to actually segment and track the cells in the image set. I have developed a software package called GoFigure for this purpose. GoFigure can automatically segment cells in image sets and connect the segmented cells to form cell tracks and cell lineages. I am first applying in toto imaging for determining the full lineage of the inner ear of zebrafish, but we would like to extend these methods to the whole embryo.



A representative image from an in toto image set of the developing inner ear of the zebrafish. Nuclei are marked green using Histone2B-EGFP and cell membranes are marked red using a membrane-localized mRFP1. We are trying to determine the complete lineage of the inner ear.

361. Automatic registration of 3D time-periodic confocal images

Michael Liebling, Arian S. Forouhar, Scott E. Fraser, Morteza Gharib, Mary E. Dickinson

Being able to acquire, visualize and analyze three-dimensional time-series (4D) data from living embryos makes it possible to understand complex dynamic movements at early stages of the embryonic development. However, current state-of-the-art confocal microscopes can be quite slow at capturing 4-D data at a sufficient resolution. However, when the studied motion is periodic, such as for a beating heart, a way to circumvent this problem is to acquire, successively, sets of 2D+time data at increasing depths over at least one time period and later rearrange them to recover a 3D+time sequence. Manual registration is tedious, error-prone, and difficult to reproduce consistently. We have, therefore, developed an automatic procedure to align the stacks at different depths. This registration algorithm is based on the minimization (in the least-squares sense) of an objective criterion that measures the similarity between the data from neighboring depths. Working at different resolutions (multiresolution approach) ensures both fast execution and robust, noise-independent, results.

362. Analysis of intracellular non-viral vector motion using correlation spectroscopy
Rajan Kulkarni, Scott E. Fraser

Recently, there has been much interest in developing alternatives to viral-based gene therapy due to safety and efficacy concerns. Non-viral gene vectors hold the promise of delivering DNA to cells in a more controllable fashion than through traditional viral vectors. However, less is known about the intracellular dynamics and kinetics of such novel vectors. Of particular interest are a group of synthetic cyclodextrin vectors that have been previously shown to be taken up by different cell lines. By fluorescently labeling DNA and complexing it with cyclodextrin vectors, these particles can be tracked within the cell upon internalization. Once inside the cells, these vectors display varied dynamic behavior ranging from subdiffusion through directed transport. This latter behavior is the most interesting, because it suggests that the particles might be able to engage the intracellular transport machinery (microtubules and motor proteins). The mechanism for this is still unclear, but likely involves transport of the particles while they are enclosed in endosomes. Image correlation spectroscopy (ICS), which uses spatial and temporal information encoded within an image series, was used to analyze the fluorescence fluctuations of the particles to determine biophysical parameters of the system. ICS relies on correlating the fluctuation of the signal between different temporal and spatial points with the average intensity of the system. Diffusion coefficients for entire cells, as well as for subsets, were measured using ICS and were compared to theoretical Stokes-Einstein diffusion values. However, such analyses give ensemble average measurements and do not yield information on individual entities. Both single particle tracking analysis and higher order autocorrelation are being explored to address the stochasticity and dynamics of individual particle motion.

363. Biofunctionalization of self-assembled monolayers on Au substrates

Christie A. Canaria, James R. Maloney, Jeffrey O. Smith, C.J. Yu, Rusty Lansford, Scott E. Fraser

An understanding of the interactions of proteins and other biological molecules with solid supports is vital for the development of detection systems and assay platforms. These relationships are frequently quite complex, involving hydrophobic interactions, electrostatic interactions, van der Waals forces and covalent chemical bonds. Employing self-assembled monolayers (SAMs) on substrates allows for the flexibility of tuning the chemical properties on the surface. In particular, alkane thiols form very good SAMs on gold surfaces and can be designed so that the monolayer presents the chemical moiety of choice. The goal of this research is to set up the platforms necessary to carry out sensitive studies on surface-mediated biochemical reactions. In order to demonstrate that substrates can be modified to capture specific analytes, we currently study the classic streptavidin-biotin pair. Biotin-terminated SAMs bind fluorescently labeled

streptavidin while SAMs presenting poly(ethyleneglycol)-terminated groups (PEG) help reduce non-specific binding of proteins to the surface. The functionality of these biologically modified monolayers is assayed using fluorescent microscopy.

Furthermore, hydroquinone (HQ)-terminated SAMs are investigated as a method for functionalization of pre-assembled monolayers with biotinylated cyclic disulfides and subsequent binding of fluorescently labeled streptavidin.

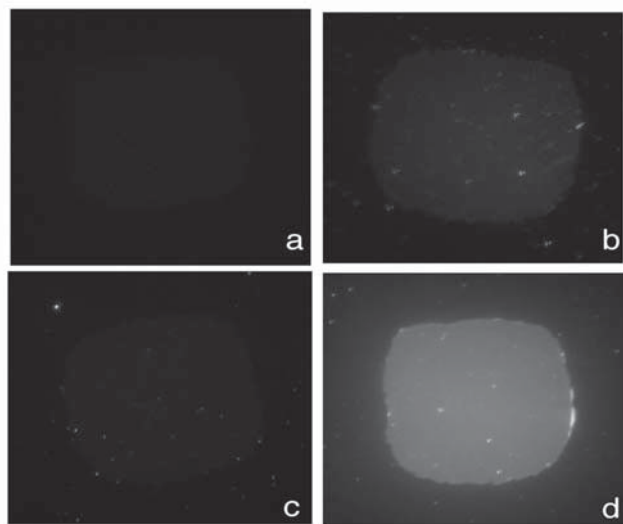


Figure 1: Fluorescence images of Au pads on Si substrates. Each pad is 150 μm wide. Images were taken in the Cy3 channel. a) Negative control sample, no exposure to Cy3-streptavidin. b) No SAM formation on Au, incubated with Cy3-streptavidin. c) PEG SAM on Au, incubated with Cy3-streptavidin. d) Mixed biotin/PEG SAM on Au, incubated with Cy3-streptavidin.

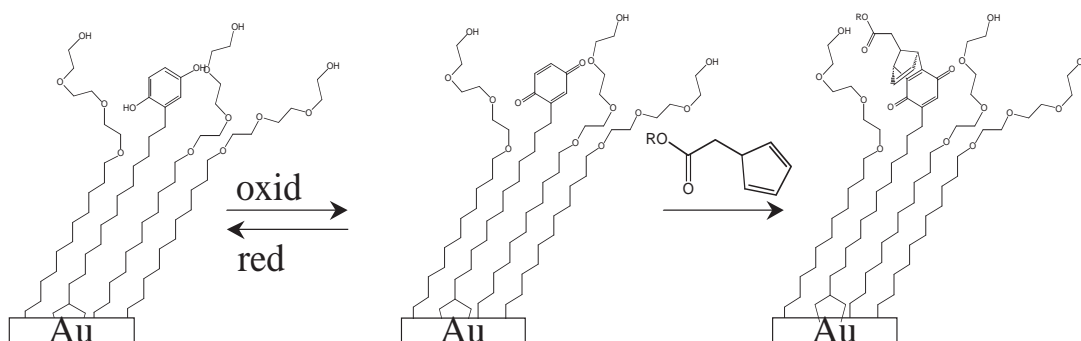


Figure 2: A mixed monolayer of HQ and PEG-modified alkane thiolates on gold is depicted. The hydroquinone is reversibly oxidized and reduced. While in the oxidized state, the benzoquinone may undergo a Diels-Alder adduct in the presence of a diene.

364. Biofunctionalized nano-electromechanical systems (BioNEMS)

James Maloney, Scott E. Fraser, Michael Roukes

The Biofunctionalized Nano-electromechanical Systems (BioNEMS) project applies ultra-sensitive force spectroscopy to the detection and interrogation of biological systems on the single-cell or single-molecule scale. The sensors couple passivated silicon sensors to a microfluidic casing capable of manipulating picoliter volumes of fluid. To characterize the process of biofunctionalizing semiconductor materials we have used electrochemical techniques such as cyclic-voltammetry and electrical impedance spectroscopy (EIS) to monitor, in solution, the deposition of organic molecules cross-linking the sensors to their target analytes. The synthesized organic molecules incorporate alkanethiol chemistry and form a self-assembled monolayer (SAM) on gold-plated surfaces. Substrates are fabricated using photolithography, thermal evaporation, and electron beam evaporation. Imaging functionalized substrates after exposure to fluorescently labeled target molecules measures the extent of specific binding to the thin film electrodes. Microfluidics will allow studies of these chemical interactions with picoliter volume control and mixing capabilities. The complete detection system is amenable to large-scale integration; requiring small amounts of fluids and capable of highly sensitive parallel detection of label-free analytes.

365. Applications of terahertz imaging to medical diagnostics

Peter H. Siegel, Scott E. Fraser

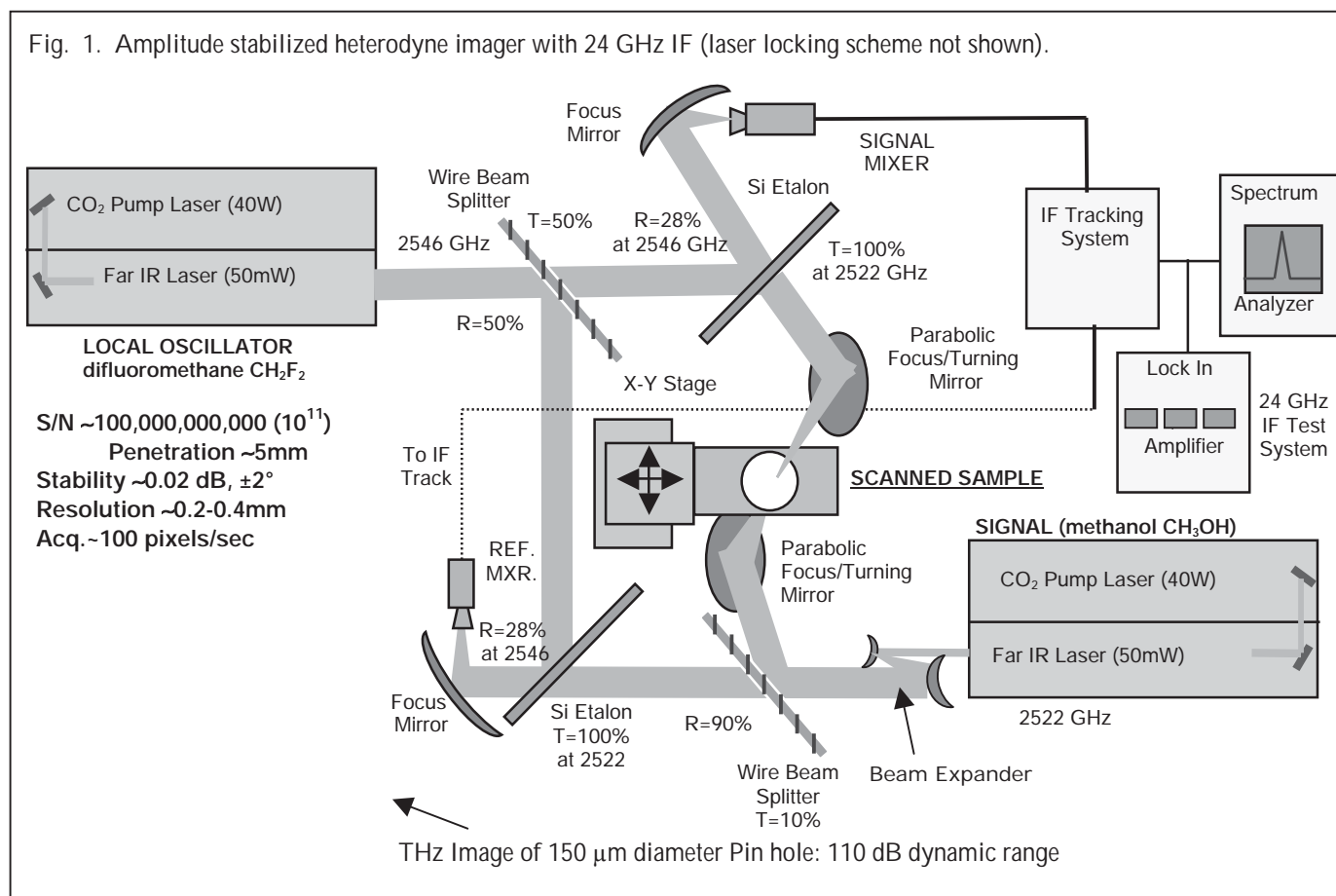
Terahertz (THz) imaging represents a new and extremely exciting modality that is just beginning to be exploited in fields as diverse as space and planetary science, defense and security, materials screening, chemical and biological spectroscopy and diagnostic medicine [1,2]. Government, university and commercial interest in this unique, long wavelength regime (spanning 1 mm to 30 microns – 300 GHz to 10 THz) has exploded in recent years, due in large measure to the advent of fast-pulse time domain spectrometry (TDS) [3] and ultra-wide dynamic range RF heterodyne techniques [4]. The unusual

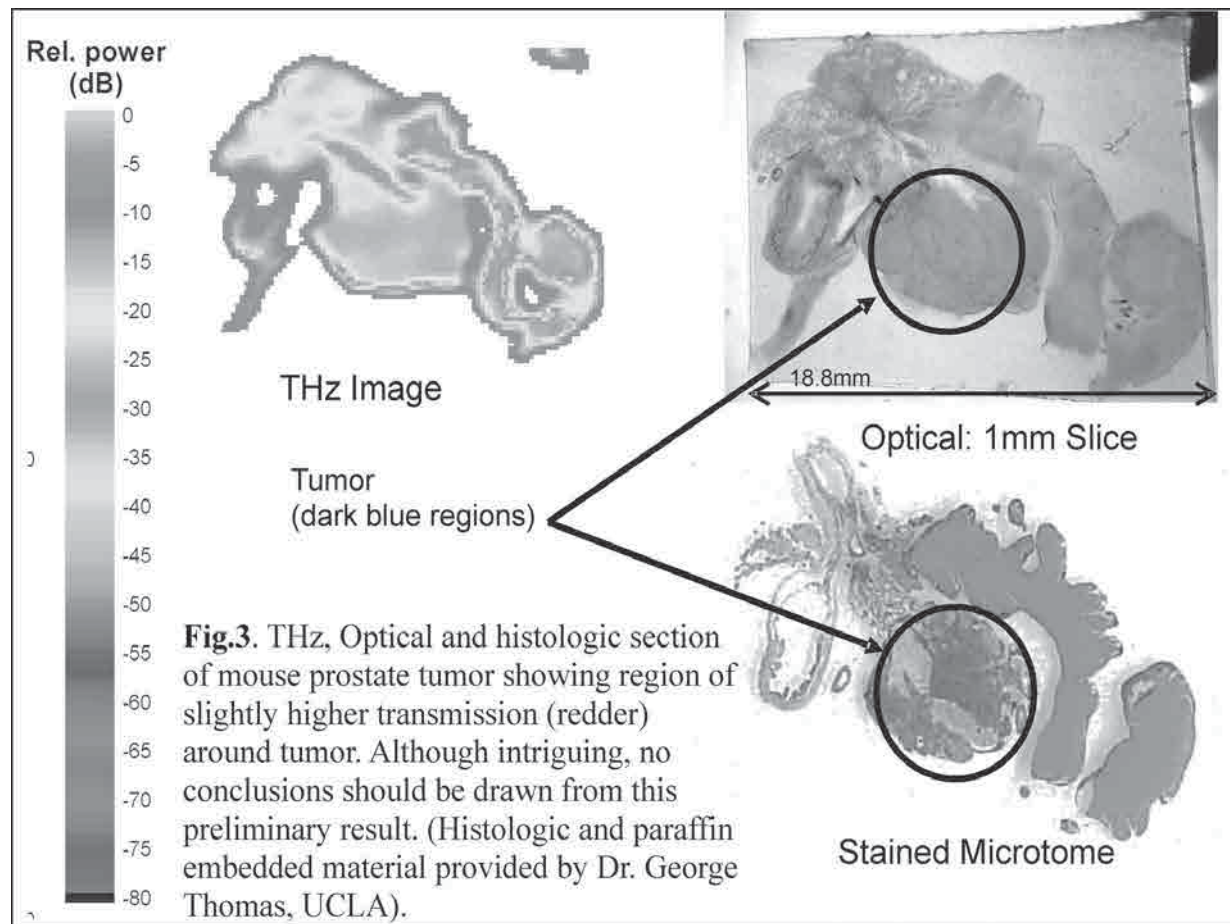
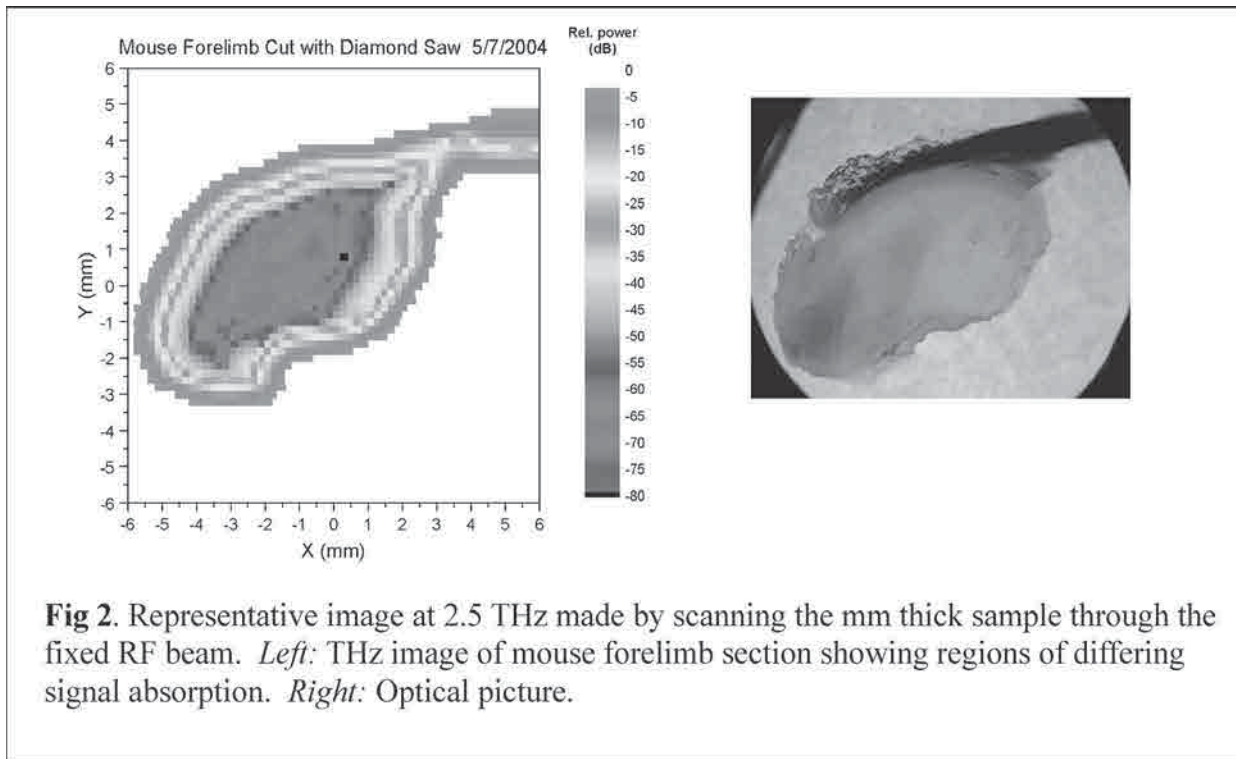
reflection, transmission and scattering properties of materials in the THz frequency range allow some unique imaging modalities not available at shorter wavelengths, and unlike longer wavelength microwave imaging, the high frequencies permit diffraction limited resolution at the submillimeter scale and imaging at a distance with modest-sized optical focusing elements. In a collaboration between the Biological Imaging Center (BIC) at the Caltech Beckman Institute and the Submillimeter Wave Advanced Technology (SWAT) group at JPL, component and instrument technologies developed for space sensor systems are being applied towards passive and active THz imaging of biological samples to investigate new contrast mechanisms and the potential for disease diagnosis. Unlike infrared and optical signals, THz penetration in tissue is dominated by absorption, not scattering, making the contrast mechanisms very different than those that are already being exploited for back scattered subcutaneous imaging. Water absorption is extremely high ($I=I_0e^{-\alpha x}$, I =input signal intensity, x =penetration in cm, α =100-500 cm^{-1}) which has the disadvantage that very strong THz signal sources are required for significant tissue penetration, but the advantage that very subtle changes in fluid content will be detectable. The first successful THz imaging systems have been based on femtosecond pulsed-laser time domain spectroscopy (TDS) techniques. These instruments offer unique spectral and time resolved information content but have limited penetration depth (tens of microns in tissue) and only modest signal-to-noise ratio (100-1000 thus far). This program seeks to increase the signal-to-noise of a THz imaging system by more than one hundred million times (heterodyne noise equivalent power, NEP_H , of 10^{-19} W/Hz) and increase the penetration depth in tissue by more than one hundred times to at least 5 mm using strong CW THz sources (CO_2 pumped far IR gas lasers) and novel heterodyne downconverter techniques. During the first year of the program a very wide dynamic range ($S/N > 10^{10}$) amplitude stabilized heterodyne instrument (Figure 1) was developed and is being operated at 2.5 THz to investigate the properties of normal and disease bearing tissue from both animals (mice) and human donors (UCLA tissue bank). New techniques for preparing and fixing the samples that

accommodate the longer wavelength imaging (thick, flat and parallel slices) have been developed. Unfixed, frozen, formalin, paraffin, PBS and epoxy-embedded samples have been evaluated (Figures 2-3). The high sensitivity to water absorption has enabled spin-off applications for materials evaluation such as the density variation and water content of aerogel (Figure 4), that link back to JPL space science missions. In the biomedical area, contrast between normal and tumor-containing tissue has been confirmed by TDS systems [5] and subcutaneous imaging has been used to determine the boundaries of diseased tissue. Of great interest in the current program are the manifestations and diagnosis of Alzheimer's disease through developing a quantitative measure of A β (beta-amyloid) plaque, LB (Lewy Body) and NFT (neurofibrillary tangles) in brain tissues; subcutaneous boundaries between normal and diseased tissue on a macroscopic scale; skin hydration levels and the impact on wound healing, cutaneous drug uptake and disease condition; subsurface radiometry (thermography); and ultimately in vivo imaging of disease state via endoscopes, catheters or needle probes. The impact of THz radiation on cellular and subcellular interactions is also of great interest. The work is being funded by an NIH K25 training grant and is at a very early stage. Since terahertz imaging is very sensitive to water concentration there is a natural link with MRI work at BIC, which the investigators hope to exploit in the coming year.

References

- [1] Siegel, P.H. (2003) Terahertz technology. In: Terahertz Sensing Technology, Vol. 1, editors, D.L. Woolard, et. al. World Scientific Publishing Co. Pte., Ltd., Singapore.
- [2] Siegel, P.H. (2004) Thz technology in Biology and Medicine. To appear in: IEEE Transactions on Microwave Theory and Techniques.
- [3] Mittleman, D. ed., (2003) Sensing with terahertz radiation. In: Springer Series in Optical Sciences, Springer-Verlag, Berlin.
- [4] Siegel, P.H. and Dengler, R.J. (2004) SPIE, Vol. 5354.
- [5] Woodward, R.M., Wallace, V.P. and Pye, R.J. (2003) J. Invest. Dermatol. 120:72-78.





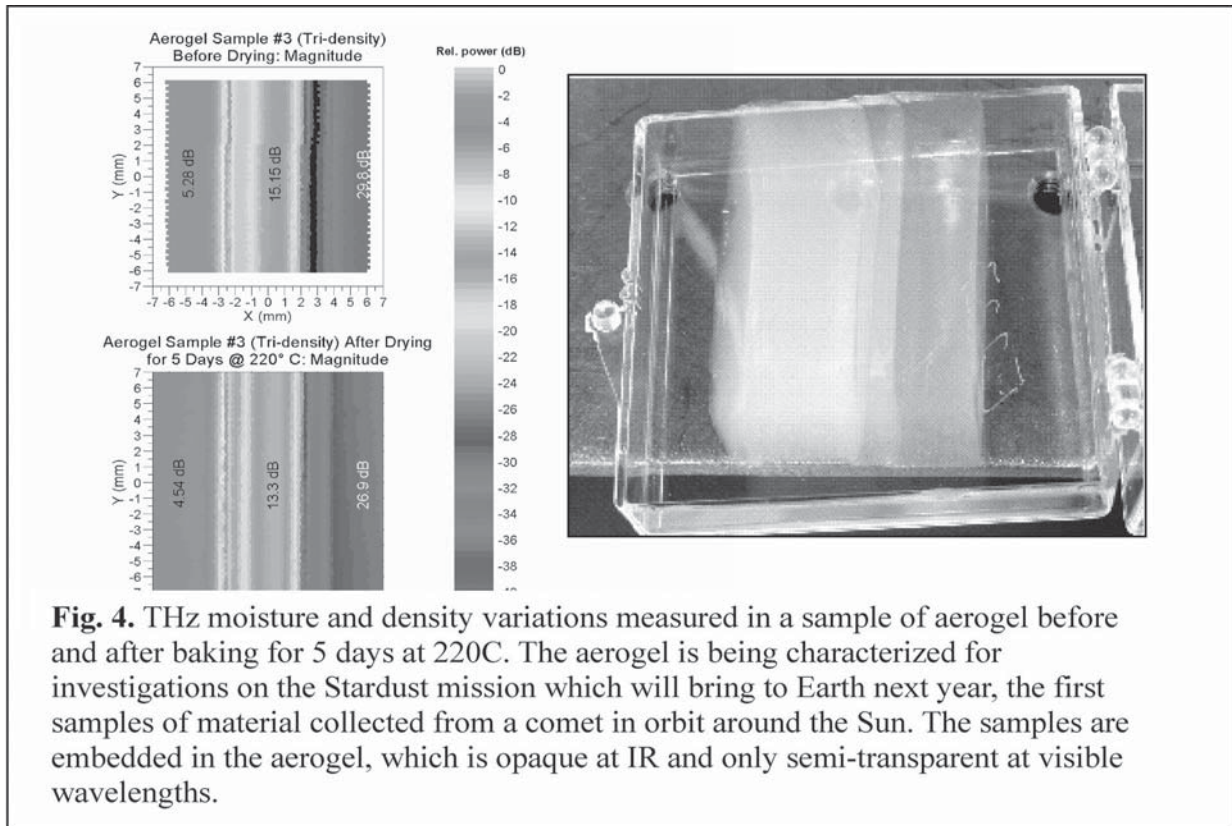


Fig. 4. THz moisture and density variations measured in a sample of aerogel before and after baking for 5 days at 220C. The aerogel is being characterized for investigations on the Stardust mission which will bring to Earth next year, the first samples of material collected from a comet in orbit around the Sun. The samples are embedded in the aerogel, which is opaque at IR and only semi-transparent at visible wavelengths.

366. MRI of quail embryogenesis
Russell Lansford, Melanie Martin, Seth Ruffins,
Russell E. Jacobs

Numerous experiments have been carried out with an 11.7 Tesla magnetic resonance imager (MRI) to determine which parameters are the most useful to optimize image contrast in developing avian and mouse embryos. In MRI, signal intensity is obtained from water protons and is a function of the concentration/environment of water. MRI contrast results from variations in the environment that changes the characteristics of proton relaxation times. The T2-weighted 3D multi-spin echo routine used to collect images of murine embryos at different developmental stages (Dhenain et al., 2001) has also worked for quail embryos. Currently, the acquired 3D quail datasets have 20-50 μm voxel resolution. We are able to take images of quail embryos in ovo and in vitro.

Current atlases of embryonic avians are composed of micrographs of specimens processed by histological techniques, which is problematic due to problems of tissue warping and image alignment. We are using an MRI microscope for the acquisition of multi-modal volumetric data of live avian embryos in ovo. In brief, we are building and populating a software atlas for storing, viewing, searching, and sharing gene expression and cell migration patterns in the context of time-space collected images of quail embryos. This avian atlas can then be interactively rotated, computationally sliced, and then analyzed from any direction. This approach does not

suffer from the warping and image alignment problems of all known histological approaches.

An important feature of the digital quail atlas is the ability to integrate other data types, such as gene expression patterns and cell migration routes, into the anatomical models. There are several modes to input and integrate other data types. For example, we can superimposed or 'paint' gene expression derived from histological sections onto the models (Dhenain et al., 2001), we can assimilate cell migration data by overlaying images acquired using two-photon microscopy, or we can integrate gene expression patterns obtained in vivo using MRI by synthesizing an MRI contrast agent that is inactive until cleaved by beta-galactosidase (Louie et al., 2000).

367. 3D time-lapse analysis of early **Xenopus** development using μMRI
Cyrus Papan, Benoit Boulat, Scott E. Fraser,
Russell E. Jacobs

To directly examine the early development of the live frog embryo, we are using microscopic magnetic resonance imaging (μMRI). Tissue-specific image contrast allows to distinguish the vegetal cell mass, the animal cap tissue, the blastocoel, the archenteron and the cleft of Brachet in 3D image volumes at a spatial resolution of $(39 \mu\text{m})^3$ and an imaging time of 55 min and in 2D slice images at a in-plane resolution of $23 \mu\text{m}$ with an imaging time of < 7 min. Time series of unlabeled embryos shows the timing of morphogenetic movements like pregastrula epiboly, blastocoel floor elevation and

expansion, blastocoel roof thinning, morphogenesis of the vegetal cell mass, archenteron invagination and formation of the cleft of Brachet. Time-lapse analysis of embryos in which the B1 or C1-blastomere was labeled with NMR contrast agents we enabled us to more specifically characterized the tissue movements and the spatial and temporal relationship between the germ layers during blastula and gastrula stages. Currently we are conducting experiments aimed at perturbing genes involved in early morphogenetic movements and analyze the effect of the perturbations in vivo by 2D and 3D MR time lapse imaging.

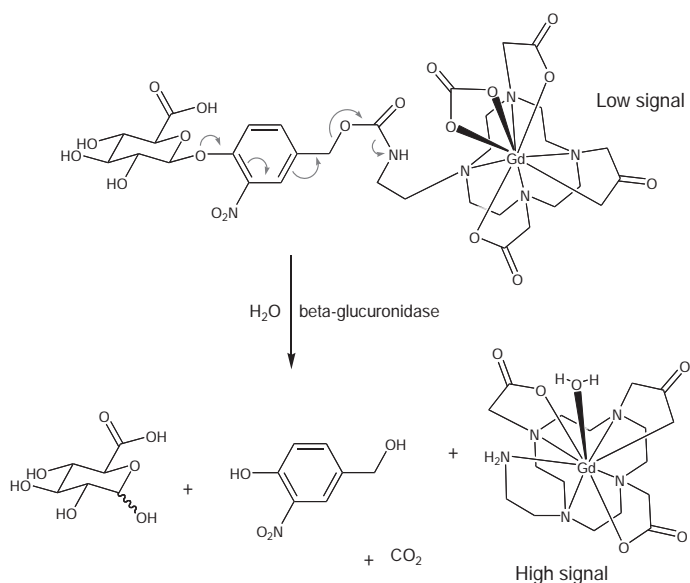
In summary, our results show the following: beginning at stage 9, pregastrula epiboly moves tissue from the animal cap into the dorsal, but not the ventral marginal zone. Simultaneously the animal cap thins and the vegetal cell mass extends upward by about 20%. With the upward-extending vegetal cell mass blastocoel floor expands from $5 \times 10^5 \text{ mm}^2$ at blastula to $2 \times 10^6 \text{ mm}^2$ after gastrulation. Expansion begins towards the dorsal side, then towards ventral side and begins to contact the animal cap forming the anterior part of the cleft of Brachet. Shortly after the dorsal blastoporal lip becomes visible. About 30 min later the mesendodermal leading edge begins to curve upwards and by stage 10.5 the archenteron begins to invaginate. Cell labeling of the B1 and the C1 blastomere shows that animal cap tissue moves into the superficial dorsal marginal zone where it comes into vertical contact with the deep dorsal marginal zone tissue prior to gastrulation and forms the posterior part of the cleft of Brachet by epiboly. Mesendodermal tissue is not internalized by involution but is rather already mostly deeply located. Only the small fraction of the mesendodermal tissue located in the suprablastoporal region is internalized by involution.

368. Enzyme responsive MRI contrast agents for cancer imaging Joseph Duimstra

The ability to non-invasively detect the onset of cancer in patients would be a boon to medical science. This type of diagnosis requires a marker for cancer, which is readily visualized. The combined use of magnetic resonance imaging (MRI) and a drug or contrast agent-sensitive to cancerous tissue presents an excellent solution to this problem. Towards this end, I have designed and synthesized a molecule, which is sensitive to the enzyme beta-glucuronidase and is MRI responsive. The body's immune system responds to necrotic tumor masses by secretion of beta-glucuronidase via macrophages. Researchers have taken advantage of the localized high enzyme level by creating chemotherapeutics whose toxicity is masked by conjugation to the enzyme's substrate. In this fashion, the toxicity of the drug is only unleashed where there is high beta-glucuronidase levels, allowing healthy tissue to remain less affected. My MRI contrast agent extends this methodology to the modulation of an MRI signal. This is accomplished by varying the

degree to which the agent interacts with the surrounding water molecules.

I am currently examining several of the contrast agent's key parameters. First, I've shown that the relaxivity of the agent, that is, how much the agent affects the MRI signal, is very dependent on the nature of the medium in which the agent is dissolved. I have also shown that the agent is processed by the enzyme as desired. The rate of cleavage and resulting change in MRI signal has yet to be quantified. I would like the rate to be as fast as possible and the change in signal to be as large as possible so that the agent would be quite sensitive. Further mechanistic and in vivo studies of the contrast agent will lay the groundwork for future generations of optimized contrast agents. These in turn will move us closer to the goal of non-invasive cancer diagnostics.



369. Contrast enhanced magnetic resonance microscopy of diffusion anisotropy in biological tissues

J. Michael Tysza, Carol Readhead, Scott E. Fraser, Russell E. Jacobs

Magnetic resonance imaging estimation of the water diffusion tensor within biological tissues (Diffusion Tensor Imaging or DTI) is a well-established technique for determining subvoxel organization of membranes and other restrictions to diffusion. MR microscopy, particularly at high resolution can be extremely time-consuming with typical 3D experiments lasting several hours. In order to estimate the apparent diffusion tensor, at least seven MR images with different diffusion direction encodings are required, which further constrains the spatial resolution and signal-to-noise ratio that can be obtained in a practical time frame. Although several MR pulse sequence variants (EPI, RARE and U-FLARE) allow significant reductions in total imaging time, they are typically associated with increased image artifact levels which typically increase in severity at higher fields. Since

much of the high-resolution DTI in the Biological Imaging Center is performed on fixed tissue samples (MR histology) we have focused on reducing the total imaging time by reducing the longitudinal relaxation time (T_1) of water within the sample using low molecular-weight contrast agents such as gadoteridol (Prohance®, Bracco Diagnostics Inc., Princeton, NJ). The reduced T_1 allows for much shorter pulse repetition times with lower saturation effects, and removes the need for rapid sequence variants and their associated artifacts.

Following perfusion fixation with 4% paraformaldehyde (PFA), mouse brains were soaked or

rocked first in saline for at least one week, then transferred to 4-20 mM gadoteridol for at least one week prior to DTI at 4°C or 15°C. Residual PFA in both the intracellular and interstitial tissue compartments is first replaced with saline, then contrast agent, significantly reducing T_1 relaxation time of the brain parenchyma by approximately one order of magnitude. Non-invasive cytoarchitectural and white-matter connectivity studies are now possible with isotropic 75-micron resolution, compared to 140 microns using previous protocols without contrast enhancement in a comparable time-frame (15 hours).

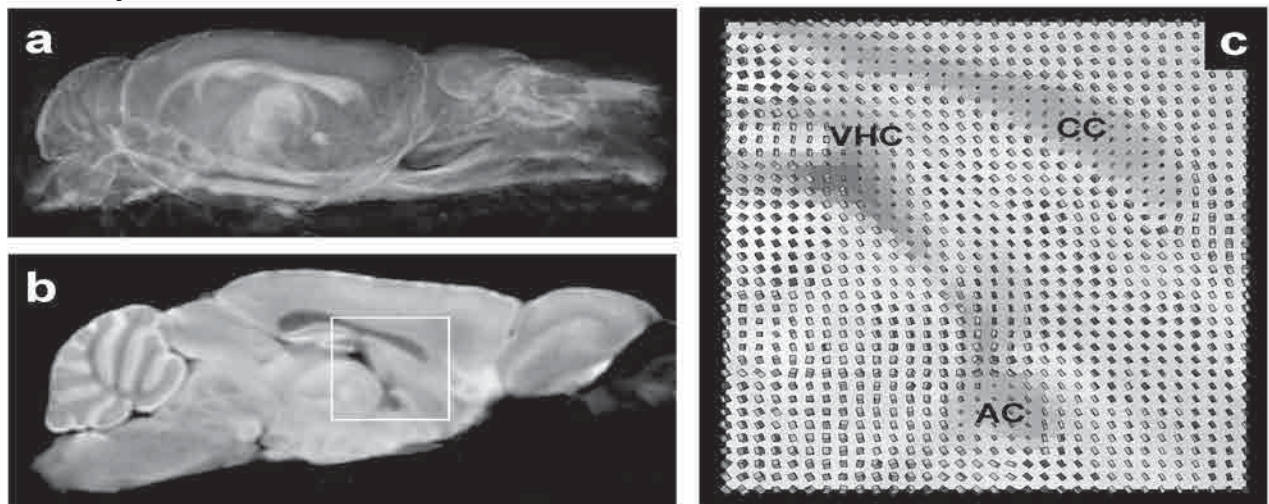


Figure 1: Contrast enhanced diffusion tensor microscopy of a fixed PM114 shiverer mutant brain with a nominal isotropic resolution of 75 microns. (a) A volume rendering of the linear shape factor (CL) derived from the tensor reveals the major white matter tracts and fascicles of the brain, including the internal and external capsules, optic tract, corpus callosum, trigeminal and optic nerves. (b) Approximately midsagittal section through the 3D associated isotropic diffusion-weighted image reveals high contrast-to-noise anatomic features. (c) Diffusion tensor cuboids for the normalized principle tensor eigenvector reveal tissue organization within and around the corpus callosum (CC), anterior commissure (AC) and ventral hippocampal commissure (VHC).

370. **In vivo** assessment of brain function in transgenic mice using manganese enhanced MRI

Xiaowei Zhang, Russell E. Jacobs

Manganese (Mn^{2+}) is an effective T_1 MRI contrast agent providing local hyperintense regions. Further, it is believed to be taken up by neuronal cells via voltage activated calcium channels, transported along microtubules to the presynaptic terminal, ejected, and taken up by next neuron in the circuit [1]. The application of Mn^{2+} -enhanced MRI (MEMRI) to delineate active neurons was demonstrated to be valuable for the studies of neural circuit tracking in the olfactory, visual, and vocal pathways [2-4]. We evaluated the brain enhancement patterns of Mn^{2+} with three groups of mice: transgenic mice engineered to produce excess amounts of β -amyloid (Tg2576), a catechol-O-methyltransferase knockout mouse (COMT-KO) and wide-type C57BL/6 mice (WT). In our experimental approach 20 nL of 200 mM $MnCl_2$ was injected via pulled glass capillary into the third ventricle. MR images were acquired using 11.7T MRI scanner with a

20 mm birdcage coil at 30 min, 8 hr and 24 hr post-injection. A 3D UFLARE sequence was used for MRI data collection. The dynamics of Mn^{2+} transports (as indicated by hyperintensity in the MR images) was determined by measuring intensity changes in identical small regions. The enhancements of the selected regions were calculated as compared with the baseline images obtained before Mn^{2+} injection.

Results and Discussion

Third ventricle application of Mn^{2+} bypasses the blood-brain barrier and provides direct access to the brain parenchyma. Early time point (30 minutes post injection) enhancement observed in the CSF of the ventricles, ventricle walls, choroid plexus, and adjacent parenchyma is likely the result of simple diffusion of Mn^{2+} ion.

Spatially distinct enhancements seen in the cortico-hippocampal region for all three groups of animals at all time point image (Figure 1) are likely due to active transport from choroids plexus and ventricle walls to the regions of enhancement. Hyperintensity at short times (30

minutes and 8 hours) in the Tg2576 and WT animals is seen in subfields of the hippocampus (the dentate gyrus, CA1, and CA3), while significantly less hyperintensity, which arises at later times, is observed in the COMT-KO animals (Figure 1). At all time points the COMT-KO has significantly less enhancement in CA1 than the other two groups.

Figure 2 summarizes the results of quantitative measurement of MR intensities in several regions. MR intensities differed among three groups at the different imaging times. The WT animals intensity increased to $29 \pm 3\%$ compared to the COMT-KO animals at $19 \pm 2.5\%$ enhancement at 30 minutes post-injection. Both WT and COMT-KO animals' enhancement increased at the 8-hour time point, but was relatively unchanged at 24 hours. In contrast, the Tg2576 animal's enhancement increased monotonically from 30 minutes to 24 hrs ($54 \pm 3.8\%$).

The interpretation of these results is complicated as the transgenic and KO mice are themselves' complicated

and not completely characterized. Catechol-O-methyltransferase (COMT) is one of the major mammalian enzymes involved in the metabolic degradation of catecholamines [5]. However, under normal conditions, COMT deficiency does not appear to affect significantly brain dopamine and noradrenaline levels in spite of relevant changes in their metabolites [6]. Tg2576 mice express the Swedish mutation of the human amyloid precursor protein and develop age-related Alzheimer-like β -amyloid deposits. Brain transgenic APP is 5.6 times more than endogenous APP and in older mice (12 months) a 5-fold increase in $A\beta$ (1-40) and a 14-fold increase in $A\beta$ (1-42/43) is observed over levels measured in young, unimpaired transgenic mice [7]. It is clear that the functional states of the brains of the transgenic and KO mice are different than the normal mouse and different from each other.

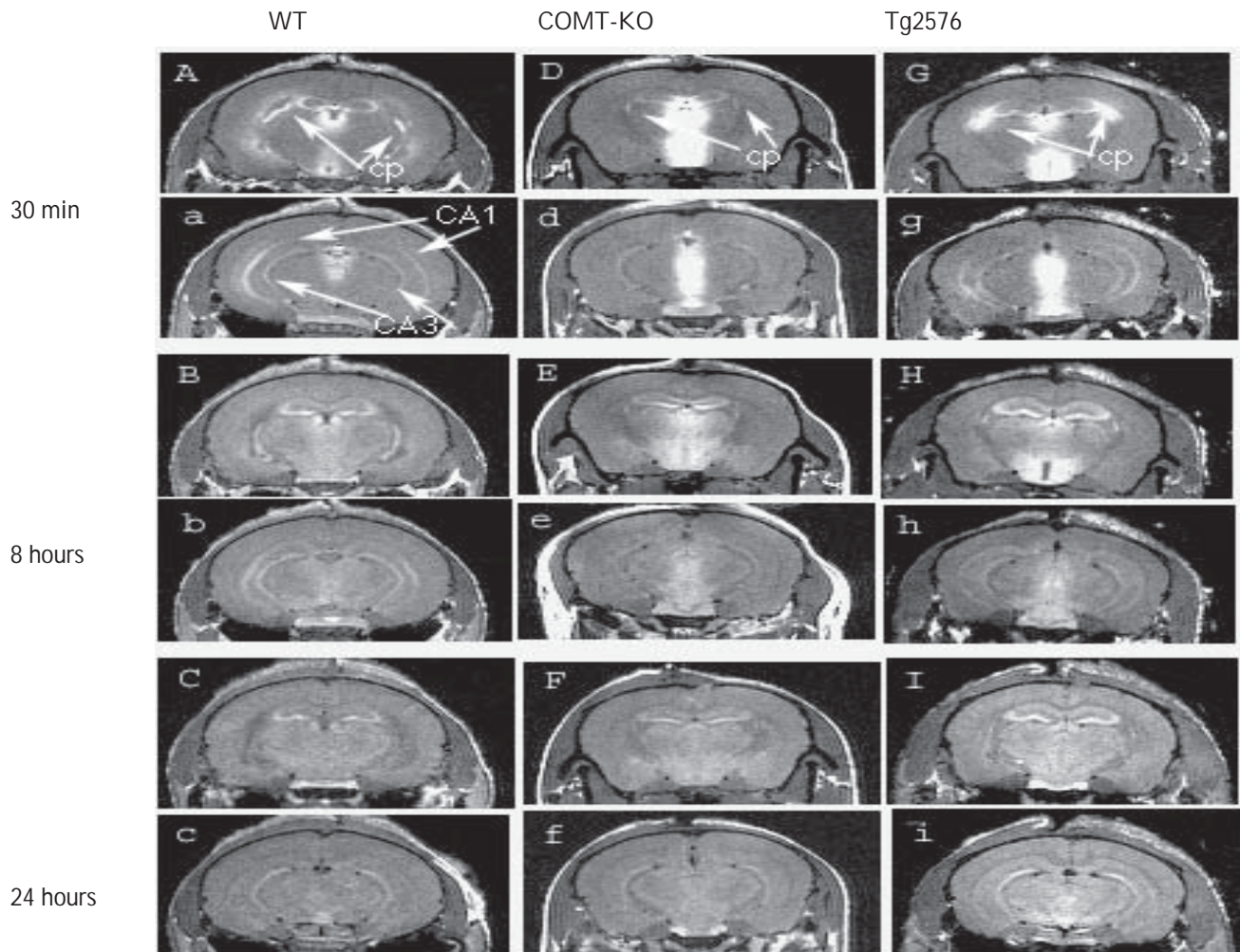


Figure 1. 3D UFLARE MRI of the mouse brains. A&a, B&b and C&c are WT animals imaged at 30 minutes, 8 and 24 hours after third ventricle injection of $MnCl_2$, D&d, E&e and F&f are COMT, and G&g, H&h and I&i are Tg2576 animals, respectively. Lower case characters indicate different slice locations in same 3D image. cp: chorioid plexus.

Conclusion

These data demonstrate the feasibility of administering Mn^{2+} into the third ventricle of mice to assess the functional state of the brain using MEMRI. Interpretation of the data at the cellular and molecular levels awaits additional MEMRI experiments (age dependence of MEMRI in the Tg2576 system and MEMRI response of COMT-KO to challenge with L-dihydroxyphenylalanine) and correlation of MEMRI with histological examinations.

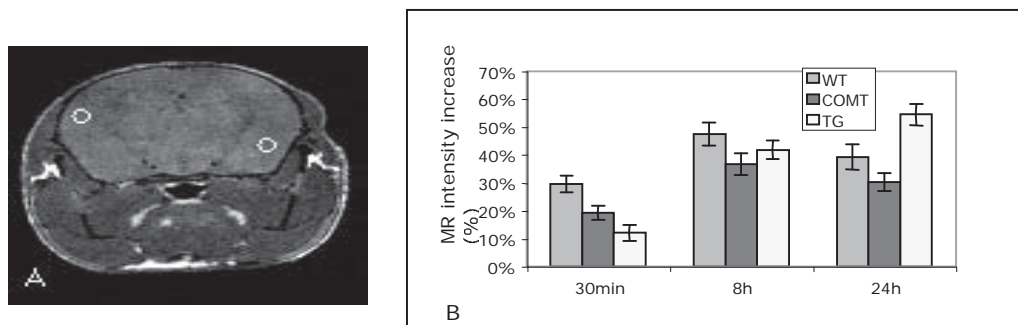


Figure 0. A shows a typical baseline image. The signal intensities were acquired with defined regions of interest (two slices per image and two per slice) using ImageJ at the same location of cortex in three group animals. B shows the mean value of three animals in each group. WT, wide-type C57LB/6; COMT, catechol-O-methyl transferase-KO; TG, transgenic β -amyloid overproducing mice

References

1. Lin, Y.J. and Koretsky, A.P. (1997) *Magn. Reson. Med.* 38(3):378-388.
2. Lin, C.P., Wedeen, V.J., Chen, J.H., Yao, C. and Tseng, W.Y.I. (2003) *Neuroimage* 19(3):482-495.
3. Pautler, R.G. and Koretsky, A.P. (2002) *Neuroimage* 16(2):441-448.
4. Van der Linden, A., Verhoye, M., Van Meir, V., Tindemans, I., Eens, M., Absil, P. and Balthazart, J. (2002) *Neuroscience* 112(2):467-474.
5. Carson, R.P. and Robertson, D. (2002) *J. Pharmacol. Exp. Ther.* 301(2):410-417.
6. Huotari, M., Gogos, J.A., Karayiorgou, M., Koponen, O., Forsberg, M., Raasmaja, A., Hyttinen, J. and Mannisto, P.T. (2002) *Eur. J. Neurosci.* 15(2):246-256.
7. Hsiao, K., Chapman, P., Nilsen, S., Eckman, C., Harigaya, Y., Younkin, S., Yang, F. and Cole, G. (1996) *Science* 274(5284):99-102.

371. Fast imaging at high fields with intermolecular multiple quantum coherences
P.T. Narasimhan, Benoit Boulat, Russell E. Jacobs

Magnetic resonance (MR) signals arising from intermolecular multiple quantum coherences (i-MQC) are weaker (~10%) than the conventional single quantum (SQ) spin or gradient echo signals [1]. Consequently, the MR imaging time with i-MQC's is much longer. To shorten it the gradient echo version of the echo planar imaging (GE-EPI) scheme has been generally used for the acquisition part of the i-MQC sequences. Even though i-MQC signals

increase with field strength, at high fields the GE-EPI scheme suffers from chemical shift and susceptibility artifacts. To avoid these problems we have developed imaging sequences in which the "front end" is typically one of the i-MQC pulse sequences, followed by a fast spin echo (FSE) module for acquisition. The RARE version [2] of FSE was adapted in our work [3]. We employed broadband refocusing 180° pulses known as REBURP pulses [4] in the RARE train. Particular attention was paid to choosing the various parameters in our imaging pulse sequences in order to satisfy the so-called "CPMG condition" [5]. This enabled us to minimize artifacts and ensured a smooth variation in the intensity of the echoes over the echo train.

We have successfully implemented i-ZQRARE and i-DQRARE imaging sequences suitable for intermolecular zero-quantum (i-ZQC) and double-quantum (i-DQC) coherence imaging of biological samples with our high field (11.7T) MR imaging system (Bruker Avance DRX500). This system is equipped with an actively shielded gradient set (Micro 2.5). A 20 mm birdcage coil was employed.

2D images with i-ZQC and i-DQC of a fixed mouse brain can be obtained in less than 4 minutes (matrix size 128×128). 3D images (matrix size $128 \times 128 \times 32$) can be obtained in about 20 minutes. We have been able to measure the SQ and i-DQ transverse spin relaxation times T_2 and T_{2D} , respectively, in different regions of the fixed mouse brain (see Figure 1 and Table 1). While contralateral sides exhibit similar values, the T_2 and T_{2D} values are in the approximate ratio of 2:1. The variation in

the relaxation time values from region to region in the mouse brain reflects the different environments of the water molecule in the tissues. A comparative study of the merits and demerits of i-ZQC and i-DQC images is currently in progress.

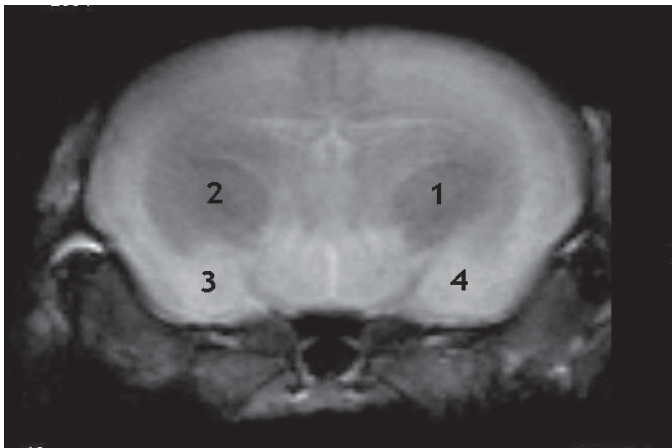


Table 1: T_2 & T_{2D} for the mouse brain

	T_2 [MS]	T_{2D} [MS]
REGION 1	68.93 ± 3.94	30.74 ± 0.44
REGION 2	66.90 ± 0.62	30.76 ± 1.42
REGION 3	64.05 ± 2.38	32.10 ± 0.42
REGION 4	70.07 ± 0.65	33.60 ± 1.25

References

- [1] Warren, W.S. et al. (1998) *Science* 281:247.
- [2] Hennig, J., Nauerth A. and Friedburg, H. (1986) *Magn. Reson. Med.* 3:823.
- [3] Narasimhan, P.T., Boulat, B. and Jacobs, R.E. (2004) 45th ENC, April 18-23, Asilomar.
- [4] Geen, H. and Freeman, R. (1991) *J. Magn. Reson.* 93:93.
- [5] See for ex. G. Liu et al. (1996) *Magn. Reson. Med.* 35:671.

372. Design and development of RF micro-surface coil for NMR microscopy

Andrey V. Demyanenko, J. Michael Tyszka, Russell E. Jacobs

In achieving high spatial resolution in MR microscopy an important issue is the development of highly sensitive RF receiving coils.

It has long been recognized that reducing the size of the coil increases its sensitivity (1). While, the reducing of whole body (volume) coils is limited by the sample size, for many applications it is enough to get signal from a small region of interest. In this case, it is advantageous to use a surface coil which could be adapted in size to the desired field of view (2). A surface coil receives larger signal amplitude from the region of interest than a volume coil due to the smaller coil diameter and the small distance between coil and the region of interest. Additionally, the coil is only loaded by a restricted sub-volume of a sample, hence the signal to noise is improved also by reduced sample noise (3).

A 1.5 mm diameter RF surface coil was designed and fabricated for specific application to MR microscopy of the *Xenopus laevis* frog embryo (approximately 1.0 to 1.5 mm diameter). The coil size is chosen from consideration of trade off between sensitivity and penetration depth. The conducting structure was made by etching in double-sided copper clad laminate (POLYFLON 1 mil Teflon substrate, 5 mil copper on both sides). The etched structure was mounted on a Teflon block (10x10x20 mm) with 2x2 mm groove milled on one of its longer sides. The block with outer circuitry for fine tuning and matching was mounted on a plastic flange (Figure 1).

The coil was tested with a fixed embryo in the 12 Tesla MR microscope in the Biological Imaging Center (Figure 2) and demonstrated high sensitivity, large penetration depth of RF magnetic field, and high quality factor ($Q=190$). Future development will concentrate on optimization of the coil diameter for improving SNR.

References

- (1) Hoult, I. and Richards, R.E. (1976) *J. Magn. Reson.* 24:71.
- (2) Ackerman, J.J.H., Grove, T.H., Wong, G.G., Gadian, D.G. and Radda, G.K. (1980) *Nature* 130:283.
- (3) Kneeland, J.B. and Hyde, J.S. (1989) *Radiology* 171:1.

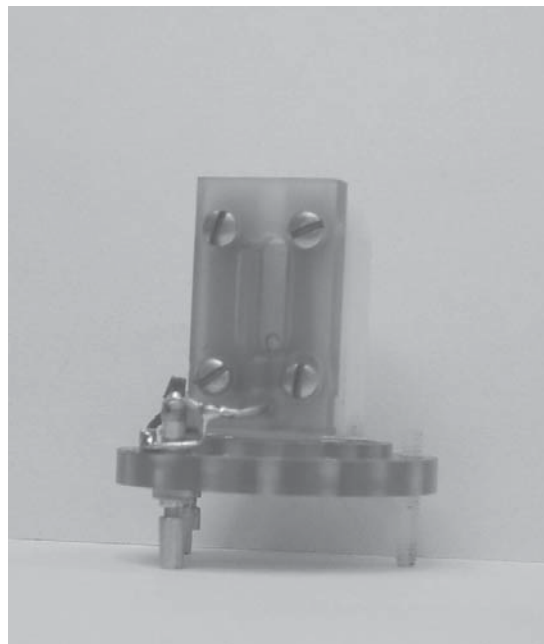


Figure 1: 1.5 mm surface MR microscopy coil and frame. Tuning elements are visible in the foreground and the fixed embryo is mounted within the sample well.

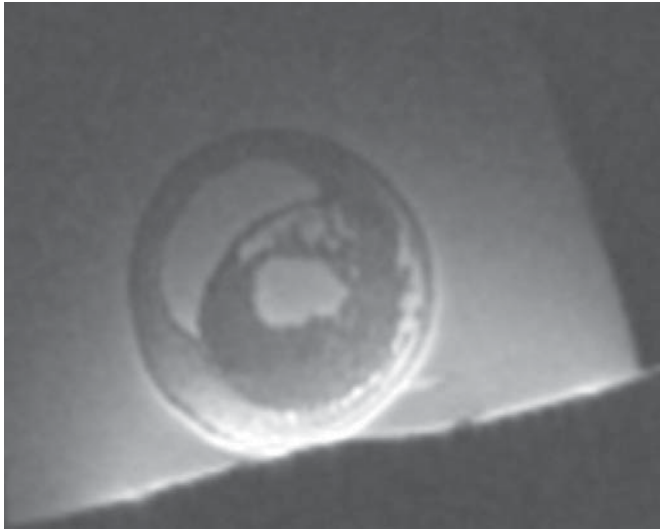


Figure 2: Coronal MR projection image of the approximately 1.25 mm diameter fixed embryo within the RF coil (in-plane resolution 20 μ m).

373. Neuronal circuitry by magnetic resonance imaging in living animals

Elaine L. Bearer, Xiaowei Zhang, Tim Hiltner, J.M. Tyszka, Russell E. Jacobs

Recently, my laboratory at Brown University discovered that human Herpes Simplex Virus Type 1 (HSV) physically interacts with the amyloid precursor protein (APP) implicated in Alzheimer's disease (Satpute-Krishnan, DeGiorgis et al., 2003). We further showed that a peptide domain of APP is sufficient to recruit anterograde motors and mediate the transport of cargo to the synapse in neurons. These discoveries raise the alarming possibility that HSV, cause of the common cold sore, might be a risk factor for Alzheimer's disease. HSV DNA has been found in the brain, but how it gets there is an open question. One project to explore this is to discover whether HSV enters the brain by intraneuronal transport from sites of infection at the body surface. At Caltech during a mini-sabbatical this spring, I explored whether magnetic resonance imaging (MRI) could be used to study intraneuronal transport in living animals. Development of this technology will not only allow a focused study on HSV transport but also provide a new approach to discover the circuitry of the living brain that is expected to produce insights in thought, behavior, emotion, and pathological neurological states.

To develop this novel technique, we used the visual system because it is relatively simple and the neuronal tracts and the rates of anterograde transport are well known in normal animals. For an MR contrast agent to reveal neuronal pathways we used the divalent metal ion, manganese (Mn^{++}), which increases the relaxation of water and appears as a high intensity signal by MRI. This MR contrast agent is being developed in the lab of Dr. Russell E. Jacobs at Caltech (Pautler, Mongeau et al., 2003). Mn^{++} appears to be a general tracer interacting

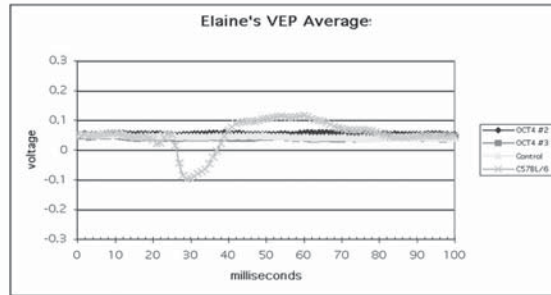
with many different transportation systems inside cells. It may preferentially enter neurons that are active.

We injected Mn^{++} into three locations along the visual system: the eye, the optic chiasm and the visual cortex. We used two different strains of mice, one that is sighted (c57b6) and the other blind (OCT4/CBA). We confirmed by PCR genotyping that the OCT4 and CBA mice are blind due to insertion of a transposable element into exon 1 of the Pde6b gene that encodes the beta subunit of the G-protein-linked phosphodiesterase required for light detection by rod cells (Gimenez and Montoliu 2001). This mouse is a model for retinal degeneration, a major cause of blindness in humans. Rod cells die at 3 weeks of age.

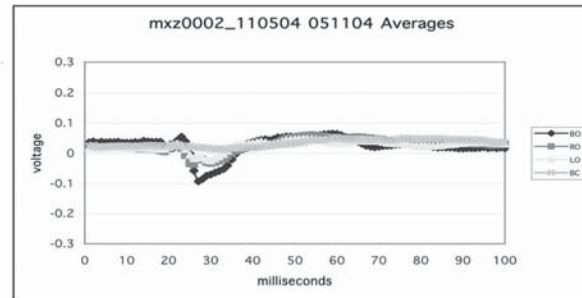
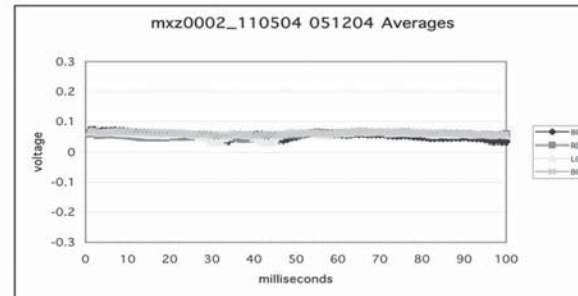
We tested mice before Mn^{++} injection for visual-evoked potentials (VEP), electrical changes in the occipital lobe of the cortex in response to light activation of the retina, a standard measure of light perception. As expected, c57b6 had robust VEPs while OCT4/CBAs had no VEPs (Figure 1A). After injecting the minimal amount of Mn^{++} required to detect a signal in the MRI into the eye, sighted mice had a reversible loss of VEP (Figure 1B-D). Parallel injections of saline had no such effect. This indicates that any transport observed after Mn^{++} injection by MRI is not dependent on electrical signaling, and that no permanent toxic injury to the visual system occurs with this amount of Mn^{++} injection.

Fig. 1

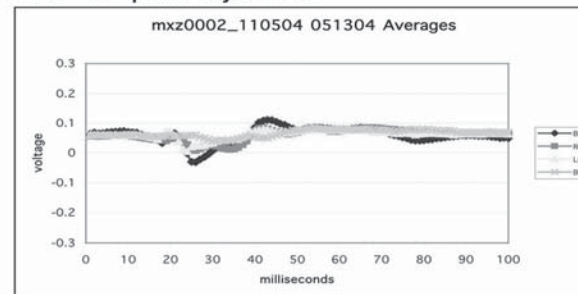
A. VEP of Oct4 (blind) and c57b6 (sighted)



B. Preinjection, c57b6

C. 4 hr post Mn⁺⁺ 0.25 μ l of 200 mM Mn⁺⁺

D. 24 hr post injection



After Mn⁺⁺ injection, the anesthetized mouse was immediately placed in the 11.7T Bruker micro-MRI and the success of the Mn⁺⁺ injection confirmed by capturing a low resolution image quickly. To monitor movement of the Mn⁺⁺ along the optic tract, a time series (5 min intervals for 2 hr) of restricted 16 mm-thick 3D slab images composed of 32 slices were captured that encompass the pathway of the optic nerve from the eye through the chiasm to the brain. Imaging typically began 30 min after injection. Resultant images are transported to the image analysis program Amira and intensities correlated.

Injection into the eye of sighted mice (c57b6) resulted in the rapid appearance of contrast along the optic tract to the chiasm ($\sim 0.5 \mu\text{m/s}$) while in blind mice this transport was significantly slower ($\sim 0.05 \mu\text{m/s}$) (Figure 2). In contrast, transport in the opposite direction, from chiasm to retina, was slower in sighted mice ($\sim 0.2 \mu\text{m/s}$) and ten times faster in some blind mice ($2.0 \mu\text{m/s}$) (Figure 3).

Increased contrast was detected in the brain - the optic tectum and the visual cortex - after eye injection but not after chiasm injection in sighted mice. Thus, the entry

point of the Mn⁺⁺ may determine its ultimate distribution in the axonal circuit. This result also demonstrates that the Mn⁺⁺ ions that modulate the water MRI signal are not freely diffusing in the axoplasm, as diffusion would produce hyperintensity in both directions from the entry point.

This is the first time that transport has been imaged in an intact living brain of an adult animal. In order to quantify these results, there remain many technical challenges. These include: 1) more precise delivery of the contrast agent in the chiasm; 2) internal standards of intensity measures; and 3) warping of images to overlay anatomical structures across many individual mice. In the visual system, the rates of anterograde transport from eye to brain of a wide variety of interneuronal components have been carefully studied over many years, but retrograde transport from brain to eye are less well characterized, nor has the effect of retinal degeneration and decreased electrical stimulation been evaluated in terms of transport activity. The Mn⁺⁺ injections into the chiasm and the visual cortex coupled with microMR imaging are likely to provide insights into how intraneuronal transport is linked to synaptic activity and neuronal survival. These

studies can be extended to transport in tracts within the brain, such as hippocampal projections, and to include more specific contrast agents that label one or the other of the many intraneuronal cargo routes.

Figure 2: Mn⁺⁺ injection into the eye imaged by time-lapse microMRI

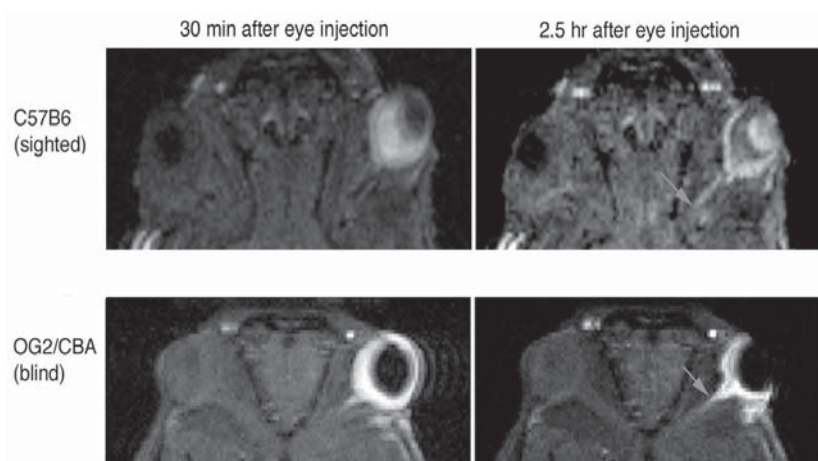
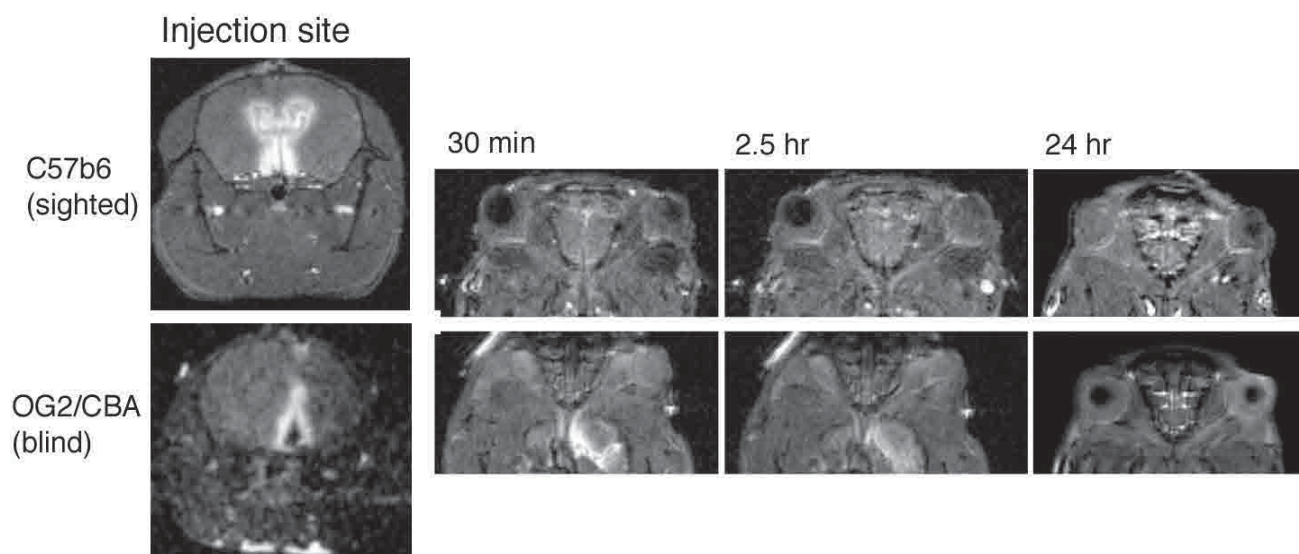


Figure 3: Mn⁺⁺ injection into the optic chiasm imaged by time-lapse micro-MRI



References

- (1) Gimenez, E. and Montoliu, L. (2001) *Lab Anim.* 35(2):153-156.
- (2) Pautler, R.G., Mongeau, R. et al. (2003) *Magn. Reson. Med.* 50(1):33-39.
- (3) Satpute-Krishnan, P., DeGiorgis, J.A. et al. (2003) *Aging Cell* 2(6):305-318.

Publications

- Bak, M. and Fraser, S.E. (2003) Axon fasciculation and differences in midline kinetics between pioneer and follower axons within commissural fascicles. *Development* 130(20):4999-5008.
- Chen, H., Detmer, S.A., Ewald, A.J., Griffin, E.E., Fraser, S.E. and Chan, D.C. (2003) Mitofusins Mfn1 and Mfn2 coordinately regulate mitochondrial fusion and are essential for embryonic development. *J. Cell Biol.* 160(2):189-200.
- Dickinson, M.E. (2004) Multiphoton, multispectral laser scanning microscopy. In: *Live Cell Imaging: A Laboratory Manual*, Cold Spring Harbor Laboratory Press, Cold Spring Harbor, NY, USA. In press.
- Dickinson, M.E., Simbuerger, E., Zimmermann, B., Waters, C.W. and Fraser, S.E. (2003) Multiphoton excitation spectra in biological samples. *J. Biomed. Optics* 8:329-338.
- Dorman, J.B., James, K.E., Fraser, S.E., Kiehart, D.P. and Berg, C.A. (2004) Bullwinkle is required for epithelial morphogenesis during *Drosophila* oogenesis. *Dev. Biol.* 267:320-341.
- Fraser, S.E. (2003) Crystal gazing in optical microscopy. *Nature Biotech.* 21(11):4-5.
- Fraser, S.E. and Stern, C. (2004) Early rostrocaudal patterning of the mesoderm and neural plate. In: *Gastrulation: From Cells to Embryo*, Claudio Stern, ed., Cold Spring Harbor Laboratory Press, Cold Spring Harbor, NY, USA. In press.
- Gong, Y., Mo, C. and Fraser, S.E. (2004) Planar cell polarity signaling controls orientation of cell divisions during zebrafish gastrulation. *Nature*. In press.
- Hadjantonakis, A.K., Dickinson, M.E., Fraser, S.E. and Papaioannou, V.E. (2003) Technicolour transgenics: Imaging tools for functional genomics in the mouse. *Nature Rev. Genet.* 4:613-625.
- Hove, J.R., Köster, R.W., Forouhar, A.S., Acevedo-Bolton, G., Zarandi, M.M., Fraser, S.E. and Gharib, M. (2003) Intracardiac fluid forces are an essential epigenetic factor for embryonic cardiogenesis. *Nature* 421:172-177.
- Jacobs, R.E., Papan, C., Ruffins, S., Tyszka, J.M. and Fraser, S.E. (2003) MRI: Volumetric imaging for vital imaging and atlas construction. *Nature Rev. Mol. Cell Biol.* 4:SS10-SS16.
- Jones, E.A.V., Baron, M.H., Fraser, S.E. and Dickinson, M.E. (2004) Hemodynamic changes during the development of the mammalian vasculature. *Am. J. Physiol. Heart Circulation*. In press.
- Jones, E.A.V., Crotty, D., Baron, M.H., Fraser, S.E. and Dickinson, M.E. (2004) Dynamic in vivo imaging of mammalian hemato-vascular development using whole embryo culture. In: *Developmental Regulation of Hematopoiesis: Methods and Protocols*, M.H. Baron, ed., *Methods in Molecular Medicine* series, Humana Press, New York, N.Y., USA. In press.
- Jones, E.A.V., Hadjantonakis, A-K. and Dickinson, M.E. (2004) Imaging mouse embryonic development. In: *Imaging in Neuroscience and Development: A Laboratory Manual*, Cold Spring Harbor Laboratory Press, Cold Spring Harbor, NY, USA. In press.
- Kasemeier, J.C., Lefcort, F., Fraser, S.E. and Kulesa, P.M. (2004) A novel sagittal slice explant technique for time-lapse imaging of the formation of the chick peripheral nervous system. In: *Imaging in Neuroscience and Development*, R. Yuste, A. Konnerth, eds., Cold Spring Harbor Laboratory Press, Cold Spring Harbor, NY, USA. In press.
- Kaur, D., Yuantiri, F., Rajagopalan, S., Kumar, J., Mo, J.O., Boonplueang, R., Viswanath, V., Jacobs, R., Yang, L., Beal, M.F., DiMonte, D., Volitaskis, I., Ellerby, L., Cherny, R.A., Bush, A.I. and Andersen, J.K. (2003) Genetic or pharmacological iron chelation prevents MPTP-induced neurotoxicity in vivo: A novel therapy for Parkinson's disease. *Neuron* 37:899-909.
- Köster, R.W. and Fraser, S.E. (2004) Time-lapse microscopy of brain development. In: *The Zebrafish - Cellular and Developmental Biology*, William Detrich, Monte Westerfield, Leonard Zon, eds., Elsevier Press, San Diego, CA, USA. In press.
- Kulesa, P.M. and Fraser, S.E. (2004) In ovo imaging of avian embryogenesis. In: *Imaging in Neuroscience and Development*, R. Yuste, A. Konnerth, editors, Cold Spring Harbor Laboratory Press, Cold Spring Harbor, NY, USA. In press.
- McBride, H.J., Fatke, B. and Fraser, S.E. (2003) Wnt signaling components in the chicken intestinal tract. *Dev. Biol.* 256(1):18-33.
- Megason S.G., Amsterdam A., Hopkins N. and Lin S. (2004) Uses of GFP in transgenic vertebrates. In: *Green Fluorescent Protein: Properties, Applications and Protocols*, Second Edition, Steven R. Kain and Martin Chalfie, eds., Wiley Press, Hoboken, NJ, USA.
- Megason, S.G. and Fraser, S.E. (2003) Digitizing life at the level of the cell: High-performance laser-scanning microscopy and image analysis for in toto imaging of development. *Mech. Dev.* 120:1407-1420.
- Modo, M., Mellowdew, K., Cash, D., Fraser, S.E., Meade, T., Price, J. and Williams, S.C. (2003) Mapping transplanted stem cells after a stroke: A serial, in vivo magnetic resonance imaging study. *NeuroImage* 21(1):311-317.
- Nashmi, R., Dickinson, M.E., McKinney, S., Jareb, M., Labarca, C., Fraser, S.E. and Lester, H.A. (2003) Localization, trafficking and resonance energy transfer in functional fluorescently-labeled alpha-4 beta-2 nicotinic acetylcholine receptors. *J. Neurosci.* 23:11554-11567.
- Patten, I., Kulesa, P., Shen, M., Fraser, S.E. and Placzek, M. (2003) Distinct modes of floor plate induction in the chick embryo. *Development* 130(20):4809-4821.
- Pautler, R.G. and Fraser, S.E. (2003) The year(s) of the contrast agent – micro-MRI in the new millennium. *Curr. Op. Immunol.* 15(4):385-392.

- Pautler, R.G., Mongeau, R. and Jacobs, R.E. (2003) In vivo trans-synaptic tract tracing from the murine striatum and amygdala utilizing manganese enhanced MRI. *Magnet. Reson. Med.* 50(1):33-39.
- Redwine, J.M., Kosofsky, B., Jacobs, R.E., Games, D., Reilly, R.F., Morrison, J.H., Young, W.G. and Bloom, F.E. (2003) Dentate gyrus volume is reduced before onset of plaque formation in PDAPP mice: A magnetic resonance microscopy and stereologic analysis. *Proc. Natl. Acad. Sci. USA* 100(3):381-1386.
- Wood J.C., Tyszka J.M., Carson S., Nelson M.D. and Coates, T.D. (2004) Myocardial iron loading in transfusion-dependent thalassemia and sickle cell disease. *Blood* 103(5):1934-1936.

Associate Professor: Bruce A. Hay
 Research Fellows: Chun Hong Chen, Israel Muro,
 Peizhang Xu, Soon Ji Yoo
 Graduate Students: Jeffrey Copeland, Jun R. Huh
 Collaborators: Rollie Clem³, M. Guo², H.-A.J. Müller¹,
 Yigong Shi⁴
 Research Staff: Hong Yu
¹Heinrich-Heine Universität, Düsseldorf, Germany
²Department of Neurology, UCLA
³Kansas State University, Manhattan, KS
⁴Princeton University, Princeton, NJ

Support: The work described in the following research report has been supported by:

The Ellison Medical Research Foundation
 Lawrence L. and Audrey W. Ferguson
 Margaret Early Trust
 National Institutes of Health

Summary: We are interested in how cell fate choice is regulated and carried out. For further information on Hay lab research consult our web page (<http://www.its.caltech.edu/~haylab/>). A large focus of our work is directed towards understanding the genetic and molecular mechanisms that regulate and bring about cell death. Specifically, we are using *Drosophila melanogaster* as a model system to identify genes that function to regulate cell death, and to identify important roles that cell death plays in normal development. Important cellular regulatory pathways are evolutionarily conserved; thus, molecules identified as important regulators of cell death in *Drosophila* are likely to have homologs in vertebrates and the pathways that link these molecules are likely to be regulated similarly. A second set of goals is to take the molecules and pathways uncovered in *Drosophila* and apply this information to the study of cell death in vertebrates, with the ultimate goal of determining the role that aberrations in this process play in human pathologies. In this context we see *Drosophila* as a powerful tool for uncovering conserved components and modes of death regulation.

374. Yeast and fly-based screens for proteases that can cleave in a transmembrane environment
 Ming Guo, Hong Yu, Bruce A. Hay

Alzheimer's disease is genetically heterogeneous, but it is invariably associated with the accumulation in the brains of affected individuals of senile plaques consisting largely of amyloid beta peptide (A-beta), which is derived by proteolytic processing from the amyloid precursor protein (APP). A large body of evidence suggests that A-beta deposition is a cause rather than a consequence of Alzheimer's disease. Thus, blocking A-beta deposition is an important therapeutic goal. APP is initially translated as a type 1 transmembrane protein, but it can be processed by different pathways. In the major pathway, alpha secretase releases the APP N-terminal ectodomain into the luminal and extracellular space. Alpha secretase cleaves in the middle of the sequence that could give rise to the A-

beta peptide, thus precluding its formation. In an alternative pathway A-beta peptides are formed through the action of beta and gamma secretases. Gamma secretase activity (which may consist of distinct proteases) cleaves in the transmembrane region of APP to generate, in conjunction with beta secretase, two major A-beta species of 40 or 42-43 residues in length, differing in the length of their C-termini. The longer forms of A-beta aggregate and are thought to seed the formation of amyloid plaques. The molecular nature of the gamma secretase(s) is unknown.

We have developed two screens to search for proteins that either are gamma secretase activity, or that regulate its activity. The first screen, is a simple variant of the caspase reporter system in yeast, in which lacZ expression is the readout. We generated a form of APP in which a cleavable signal sequence lies just N-terminal to the APP beta secretase cleavage site. APP C-terminal sequences are then followed by the transcription factor LexA-B42. We are using yeast expressing this construct, as well as one of the presenilins, as a background in which to screen for proteins that show potential gamma secretase activity: cleavage-dependent reporter activation.

We have also set up a related screen in *Drosophila*, in which a similar APP fusion protein (in which the transcription factor is GAL4) is expressed in the eye in flies that carry a UAS-rpr construct (Guo et al., 2003). In this system release of GAL4 from the membrane, as a result of gamma secretase activity, creates a cell death signal, and thus, flies with small eyes. This readout is very convenient for us because we can compare modifiers identified in GMR-rpr screens with those identified in GMR-APP-GAL4 screens. Those modifiers that are specific for GMR-APP-GAL4 are potentially interesting in terms of identifying genes that regulate APP cleavage. At this point we have carried out several large screens for enhancers and suppressors and have identified a modest number of interesting loci that are being pursued. Importantly, mutations that alter the levels of components of gamma secretase - presenilin and nicastrin - alter the reporter eye phenotype in the expected way. These observations give us confidence that the screen is likely to be pulling out interesting loci.

Doing a screen for modifiers of gamma secretase activity in a higher eukaryote is also important for the following reason. While gamma secretase is of course critical for cleavage of APP, it is also likely to be important for the cleavage of other transmembrane signaling proteins such as Notch. Thus, drugs targeted directly at gamma secretase may have pleiotropic effects. A genetic approach that focuses more generally on identifying modifiers of this activity may point towards new ways of modifying its activity or specificity in ways that more specifically affect APP processing.

Reference

Guo, M., Hong, E.J., Fernandes, J., Zipursky, S.L. and Hay, B.A. (2003) *Human Molec. Genet.* 12:2669-2678.

375. Gene activation screens for cell death regulators: MicroRNAs, small non-coding RNAs, define a new family of cell death regulator

Peizhang Xu, Chun Hong Chen

The GMREP vector contains an eye-specific promoter near one P-element end, as well as sequences sufficient for plasmid rescue of genomic DNA flanking the site of P-element insertion. When this P element inserts near the 5' end of a gene it causes the gene to be misexpressed at high levels in the developing eye (Hay *et al.*, 1997). We have mobilized this P element throughout the genome and are characterizing the insertions that act as cell death regulators. We first score the lines for dominant phenotypes that may be due to increased cell death (a small eye) or decreased cell death (a large, rough eye). We then cross these insertions to lines of flies that express the cell death activators REAPER, HID or GRIM specifically in the eye (GMR-rpr, GMR-hid, or GMR-grim flies), and that thus have small eyes. The progeny of these crosses are then scored for the ability of the GMREP insertion to alter the GMR-rpr-, GMR-hid- or GMR-grim-dependent small eye phenotype. These modifiers identify new cell death regulators. Genomic DNA that is likely to contain a portion of the gene being overexpressed can be quickly isolated using plasmid rescue. The *Drosophila* genome is now finished. Thus, a small sequence tag from the end of the P element serves to tell us exactly where in the genome our insertion is. Because GMREP-dependent phenotypes are primarily due to insertions near the transcription start site, and because GMREP carries the dominant eye-color marker *white*, imprecise P-element excision using a genomic source of transposase or X-rays can be carried out to rapidly generate deletions that create loss-of-function phenotypes for the overexpressed gene.

We generated and screened 8,000 transposon insertions for their ability to suppress *rpr*-, *hid*-, or *grim*-dependent cell death and identified a modest number of new loci (about ten) that specifically suppress death due to overexpression of one or the other, or all of these genes in the eye. We are in the process of characterizing some of these lines. One death suppressor encodes the large ubiquitin conjugation protein Bruce (Vernooy *et al.*, 2002) (we didn't name it), while four others encode cell death-inhibiting microRNAs (Xu *et al.*, 2003).

References

- Hay, B.A., Maile, R. and Rubin, G.M. (1997) *Proc. Natl. Acad. Sci. USA* 94:5195-5200.
 Vernooy, S.Y., Chow, V., Su, J., Verbrugghe, K., Yang, J., Cole, S., Olson, M.R. and Hay, B.A. (2002) *Curr. Biol.* 12:1164-1168.
 Xu, P., Vernooy, S.Y., Guo, M. and Hay, B.A. (2003) *Curr. Biol.* 13:790-795.

376. IAPs, cell death and ubiquitination
Soon Ji Yoo, Jun Huh, H. Arno J. Müller

DIAP1, as with many IAPs, also shows E3 ubiquitin-protein ligase activity. The function of this

activity *in vivo* is unclear. One possibility is that this activity simply constitutes a mechanism for conferring a short half-life to the IAP, thus serving a proapoptotic function. Alternatively, ubiquitination of IAP-bound proapoptotic proteins may provide a prosurvival mechanism by which IAPs can catalytically remove these molecules. IAPs may also engage in substrate choice, preferentially degrading themselves when not bound to proapoptotic molecules, but degrading-binding partners when the opportunity arises. In this way IAPs could serve to create, through a posttranscriptional mechanism, a relative balance between pro- and antiapoptotic proteins, at different levels of proapoptotic proteins. Finally, binding of proapoptotic proteins to DIAP1 may promote DIAP1 degradation, thereby promoting apoptosis. Over the last year we have obtained evidence for all of these activities. An important goal for the future is to understand how these diverse activities of DIAP1 are regulated in the contexts of developmental cues and environmental stresses.

References

- Chai, J., Yan, N., Huh, J.R., Wu, J-W., Li, W., Hay, B.A. and Shi, Y. (2003) *Nature Struct. Biol.* 10:892-898.
 Muro, I., Hay, B.A. and Clem, R.J. (2002) *J. Biol. Chem.* 278:4028-4034.
 Olson, M.R., Holley, C.L., Yoo, S.J., Huh, J.R., Hay, B.A. and Kornbluth, S. (2003) *J. Biol. Chem.* 278:4028-4034.
 Yoo, S.J., Huh, J.R., Muro, I., Yu, H., Wang, L., Wang, S.L., Feldman, R.M.R., Clem, R.J., Müller, H.-A.J. and Hay, B.A. (2002) *Nature Cell Biol.* 4:416-424.

377. Identification of DIAP1-interacting proteins

Soon Ji Yoo, Hong Yu, Jeff Copeland

DIAP1 is required for cell survival in *Drosophila*.

This suggests that its activity is likely to be regulated through interactions with other proteins. Genetic screens for cell death regulators provide one approach to identifying proteins that may interact with DIAP1. However, a more direct approach to identifying proteins that regulate DIAP1 function involves identifying proteins that physically bind DIAP1 in living *Drosophila*. We are using multiply-tagged versions of DIAP1 as bait to immunoprecipitate, identify and characterize associated proteins from healthy cells, as well as from cells exposed to various death stimuli.

378. How does *Drosophila* activate caspase-dependent cell death?

Soon Ji Yoo, H.-A.J. Müller, Jun Huh

An important set of questions is how different cell death signals, which in many cases are initiated through distinct signal transduction pathways, converge to activate a set of common downstream effector pathways. In *Drosophila* many different death signals lead to the transcriptional activation of one or more of three genes, *reaper* (*rpr*), *hid* and *grim*. The function of these genes is required for most normally occurring and induced cell death in *Drosophila*. Thus, their transcriptional activation acts as a point of death signaling convergence. One of our

primary goals has been to identify mechanisms by which these different proteins activate cell death. Three important facts are known about these proteins that suggested testable mechanisms of action. These are: 1) that death induced by their expression requires caspase activity; 2) that their death-promoting activity is suppressed in a dose-dependent manner by DIAP1; and 3) that REAPER (RPR), HID and GRIM bind to DIAP1 in insect cells. These results have suggested several models of how DIAP1, caspases and RPR, HID and GRIM might interact to regulate cell death. In one model, death-activating proteins such as REAPER, HID or GRIM activate caspases through an IAP-independent pathway. This model postulates that *Drosophila* IAPs act at two different points to suppress apoptosis: by acting as a sink for death activators such as REAPER, HID or GRIM, preventing them from interacting with their normal targets; and by inhibiting the caspase activity initiated by their action. In a second model, DIAP1 is proposed to function primarily as a caspase inhibitor, and REAPER, HID and/or GRIM initiate caspase-dependent cell death by preventing IAPs from productively interacting with caspases, thereby promoting their activity, and ultimately cell death.

Susan Wang, a former graduate student, and Christine Hawkins, a former postdoc, carried out experiments in *Drosophila*, yeast and *in vitro* to test the idea that RPR, HID and GRIM promote apoptosis by blocking DIAP1's ability to inhibit caspase activity (Wang *et al.*, 1999). They found that all three proteins, while nontoxic on their own, killed yeast coexpressing DCP-1 or drICE, and DIAP1, suggesting that they were blocking DIAP1's ability to function as a caspase inhibitor. They pursued the basis for this activity further with HID and found, both in yeast and *in vitro*, that proteins containing the N-terminal 37 residues of HID, which are sufficient to induce apoptosis in insect cells, suppressed DIAP1's ability to inhibit DCP-1 activity.

These results are consistent with a model in which RPR, HID and GRIM act through DIAP1 to promote death-inducing caspase activity. This model predicts that DIAP1 should be essential for cell survival, and that a loss of DIAP1 function should result in an increase in DIAP1-inhibitable caspase activity. To test this idea they carried out a second set of experiments in which we characterized the phenotype of a DIAP1 loss-of-function mutation, as well as the phenotype of a double mutant that removed DIAP1, as well as *rpr*, *hid* and *grim*. They found that the DIAP1 loss-of-function phenotype consists of an embryo-wide set of cellular changes reminiscent of apoptotic cell death, and that these were associated with the activation of DIAP1-inhibitable caspase activity. Furthermore, double mutants that remove zygotic *rpr*, *hid*, *grim*, and DIAP1 function showed phenotypes similar to those of the DIAP1 loss-of-function mutant alone (Wang *et al.*, 1999).

Together, the above observations suggest that a principal function of DIAP1 is to promote cell survival by blocking caspase activity, and that at least one mechanism by which REAPER, HID and GRIM promote apoptosis is

by disrupting IAP-caspase interactions. These early studies left several important questions unanswered: 1) How does RPR, HID or GRIM binding to DIAP1 suppress DIAP1's ability to inhibit caspase activity? 2) Do RPR, HID and GRIM regulate DIAP1 function through other mechanisms? Domain analysis of RPR and GRIM suggests that these proteins have apoptotic domains distinct from their N-terminal DIAP1-binding motifs. One question we are interested in is whether these other domains regulate DIAP1 through other mechanisms. 3) Finally, it is interesting to ask if there exist other proteins that function similarly to RPR, HID and GRIM. However, the yeast survival-based assay we used to show that these proteins disrupt IAP-caspase interactions provides a straightforward approach to screening for such molecules. Importantly, because such a screen is a function-based screen, and does not rely on identifying candidates based on sequence homology, we may identify proteins that disrupt IAP-caspase interactions even if they have only minimal homology to RPR, HID or GRIM.

Finally, the DIAP1 loss-of-function phenotype, the caspase-dependent death of all cells in the embryo, raises an important question. What is the source of the activity DIAP1 fights against to maintain cell survival? The generation of double mutants in cell culture using RNAi of Dronc or Ark, and DIAP1 (Muro *et al.*, 2002), provides a clear answer - Ark and Dronc-dependent caspase activation. An important implication of these observations is that cells that normally live experience a chronic Ark-activating death signal. This promotes the continuous activation of Dronc. DIAP1 promotes cell survival, at least in part, by suppressing this Dronc activity. An important unsolved question is the source of the signal that activates Ark. In mammals Apaf-1 is activated by cytochrome *c*, released from mitochondria, and ATP or dATP. The role of mitochondria and cytochrome *c* release in *Drosophila* is still unclear. Exposure of apoptosis-specific cytochrome *c* epitopes has been observed by the Abrams lab, and cytochrome *c* can be found associated with a high molecular weight apoptosome-like complex in cell extracts (Dorstyn *et al.*, 2002). However, depletion of cytochrome *c* in cell culture using RNAi has failed to demonstrate any involvement of this protein in Ark-dependent cell death [Zimmermann *et al.* (2002) *J. Cell Biol.* 156:1077]. This latter observation raises the intriguing possibility that Ark activation in flies (and by implication perhaps in other organisms, as well) can be regulated through associations with other molecules. We have designed several screens and biochemical approaches to address this question.

379. Bruce, cell death, caspases and spermatogenesis
Jun Huh

As mentioned above, one of the potent cell death suppressors we identified is the Bruce gene. Bruce mutants are viable, but they are male sterile. In examining this we discovered several interesting facts: 1) Bruce mutants are blocked in a late aspect of spermatogenesis

known as individualization, in which spermatids (which develop in a common cytoplasm) eventually become enclosed in individual plasma membranes; 2) During the process of individualization spermatids have very high levels of active caspases. But these cells do not die. Together these observations suggest that spermatids use caspase activity for nonapoptotic purposes during differentiation. We have found that multiple caspases, acting through distinct pathways, and at distinct points in time and space, are required for spermatid individualization (Huh *et al.*, 2004a). Spermatid individualization is an evolutionarily conserved process, about which little is known. Several questions are of interest to us: 1) What are the sources of the caspase activity (what are the upstream signals); 2) What are the nonapoptotic targets that facilitate differentiation; 3) How is cell death prevented in the face of high levels of caspase activity that would normally be associated with cell death; 4) Do caspases play similar roles in promoting spermatid differentiation in mammals.

Reference

Huh, J.R., Vernooy, S.Y., Yu, H., Yan, N., Shi, Y., Guo, M. and Hay, B.A. (2004) *PLoS Biol.* 2:43-53.

380. Maintaining tissue size: The role of death-induced compensatory proliferation
Jun Huh

Achieving proper organ size requires a balance between proliferation and cell death. Tissues often experience stresses that lead to ectopic death. In order for normal development to occur, this death must be followed by compensatory proliferation that fills in the gaps. We were interested in exploring the idea that it is the dying cell itself that sends a signal to neighbors, driving their proliferation. We tested this hypothesis in several ways. In brief, we found that activation of the apical caspase Dronc, activity of which is required for many cell deaths in the fly, is both necessary and sufficient to drive compensatory proliferation in neighboring cells (Huh *et al.*, 2004b). Interesting questions for the future include: 1) What are the targets Dronc acts on to promote proliferation in neighbors; 2) Are there other contexts in which caspases function in a sense non-autonomously to alter cell fate or behavior.

Reference

Huh, J.R. Guo, M. and Hay, B.A. (2004) *Curr. Biol.* 14:1262-1266.

381. Autophagic cell death, caspase inhibition in *C. elegans*, and the *echinus* mutant
Jeffrey Copeland

While much cell death is apoptotic, a number of cell deaths share features with a process known as autophagy, which has been described in some molecular detail in yeast. In yeast, starvation leads to a cellular response in which double membrane-bound vesicles are formed that take up and hydrolyze organelles, as well as

bulk cytoplasm. This process of autodigestion provides the cell with nutrients, allowing survival under starvation conditions. It has been clear for some time that there are a number of situations in which cell death in animals shows morphological features similar to those of autophagy rather than apoptosis. However, the molecular mechanisms that mediate these deaths has remained unexplored. *Drosophila* homologs are available for many of the yeast proteins involved in autophagy. The goal of my project is to explore the molecular mechanisms underlying autophagic cell death in *Drosophila*.

In *C. elegans*, in contrast to the situation in flies and mammals, caspase inhibitors have not been identified. I used the yeast screens described above to identify several potential *C. elegans* caspase inhibitors. One of these is highly evolutionarily conserved. We are currently focusing our characterization on the *Drosophila* counterpart of this gene.

Echinus is a *Drosophila* mutant that lacks normally occurring cell death in the eye. I have generated multiple new alleles of *echinus* and cloned the gene. Characterization of its activities is in progress.

Publications

Chai, J., Yan, N., Huh, J.R., Wu, J-W., Li, W., Hay, B.A. and Shi, Y. (2003) Molecular mechanism of Reaper/Grim/Hid-mediated suppression of DIAP1-dependent Dronc ubiquitination. *Nature Struct. Biol.* 10:892-898.

Guo, M., Hong, E.J., Fernandez, J., Zipursky, S.L. and Hay, B.A. (2003) A reporter for amyloid precursor protein gamma-secretase in *Drosophila*. *Human Mol. Gen.* 12:2669-2678

Hay, B.A. and Guo, M. (2003) Coupling cell growth, proliferation and death: Hippo weighs in. *Dev. Cell.* 5:361-363.

Huh, J.R., Vernooy, S.Y., Yu, H., Yan, N., Shi, Y., Guo, M. and Hay, B.A. (2004a) Multiple apoptotic caspases are required in nonapoptotic roles for *Drosophila* spermatid individualization. *PLoS Biol.* 2:43-53.

Huh, J.R., Guo, M. and Hay, B.A. (2004b) Compensatory proliferation induced by cell death in the *Drosophila* wing disc requires activity of the apical cell death caspase Dronc in a nonapoptotic role. *Curr. Biol.* 14:1262-1266.

Olson, M.R., Holley, C.L., Yoo, S.J., Huh, J.R., Hay, B.A. and Kornbluth, S. (2003) Reaper is regulated by IAP-mediated ubiquitination. *J. Biol. Chem.* 278:4028-4034.

Xu, P., Vernooy, S.Y., Guo, M. and Hay, B.A. (2003) The *Drosophila* microRNA mir-14 suppresses cell death and is required for normal fat metabolism. *Curr. Biol.* 13:790-795.

George W. Beadle Professor of Biology: Elliot M. Meyerowitz

Senior Research Associate: Jose Luis Riechmann

Moore Distinguished Visiting Scholars: Ottoline Leyser, Ioan Negrutiu

Postdoctoral Scholars: Catherine Baker, Pradeep Das, Annick Dubois, Venugopala Gonehal, Elizabeth Haswell, Marcus Heisler, Toshiro Ito, Nicole Kubat, Patrick Sieber, Frank Wellmer, Hao Yu, Yuanxiang Zhao

Visiting Associates: Marcio Alves Ferreira, James P. Folsom

Undergraduate Students: Noelle de la Rosa, Mai Le, David McKinney, Amar Patel, Kim Ridley, Jean Sun, Emma Thomas

Research and Laboratory Staff: Arnavaz Garda, Carolyn Ohno, Maral B. Robinson

Support: The work described in the following research report has been supported by:

Colvin Fund for Research Initiative in Biomedical Science

DOE

EMBO

Helen Hay Whitney Memorial Fund

Jane Coffins Childs Memorial Fund

NIH

NSF

Summary: Our laboratory is trying to understand how plants grow, by studying a variety of different growth phenomena in the small mustard *Arabidopsis thaliana*, or mouse-ear cress. We choose this plant because its small size and rapid growth, as well as other properties, make it well suited for work in a laboratory. One aspect of development in which we have been interested for many years is flower development. Flowers in general have four types of organs, which from the outside to the inside of the flower are sepals, petals, stamens, and the carpels that constitute the ovary. The flowers originate in groups of a few dozen cells called floral primordia, in which all of the cells look the same. Over the course of two weeks in *Arabidopsis*, the cells of the floral primordium divide in precise patterns so as to produce organs of the right shape, and change into the variety of twenty or so cell types that characterize the mature floral organs, with each organ comprised of different types of cells. How do the cells know where they are in the primordium, so as to turn into the proper organ-specific cell types? How are their patterns and amounts of cell division controlled, so that the organs end up the right size and shape? To find out we have over many years isolated mutant plants, which are changed in the function of one or a few genes, and which do not have normal numbers or types of floral organs. From this work we have established a model of floral organ specification called the ABC model, that relates how the function of three groups of regulatory genes act together to direct organ development. In the past year we have advanced our understanding of how these genes work in several ways, as described below. One way is based on

the fact that the regulatory genes acting in floral organ specification code for proteins that are transcription factors, that is, proteins that bind to other genes and turn on or off their ability to produce proteins. The application of microarray technology is now giving us the list of genes regulated by the ABC genes, and thereby teaching us how these genes lead cells from an unstructured primordium to a mature flower.

We are also studying similar processes in the shoot apical meristems, which are the small groups of cells at the tip of each shoot, and which provide for shoot growth as well as the formation of leaves or of floral primordia. We have a number of mutations that affect the behavior of shoot apical meristem cells, and as a result lead to shoots different from normal. Some of the genes whose malfunction gives these abnormal shoots are described below, and the analysis of some of them at the molecular level is also reported. As the effects of changes in gene function on the meristem is often at the level of cell division, and of changes in the expression of other genes, we have also developed a suite of new methods for the detailed study of shoot apical meristems. These methods have three aspects: following the complete set of cell divisions in the entire shoot apical meristem over several days by use of laser scanning confocal microscopy and novel image processing methods; following in real time the changes in the cellular domains of expression of the genes that regulate shoot growth by the use of fluorescently-tagged versions of the proteins coded by these genes; and control in space and time of the activation or inactivation of the genes that regulate shoot growth, so that the effect of changing their activities can be followed at the level of individual cells in the meristem. The development of these methods and their application is also recounted below.

382. A gene expression map for **Arabidopsis** flower development

Frank Wellmer, Márcio Alves-Ferreira, José Luis Riechmann, Elliot M. Meyerowitz

We have used oligonucleotide-based 'whole genome' microarrays to identify genes whose expression is restricted to certain floral organs and/or to certain stages of *Arabidopsis* flower development. For the analysis of organ-specific gene expression, we have compared the gene expression profiles of wild-type inflorescences with those of the floral homeotic mutants *apetala1*, *apetala2*, *apetala3*, *pistillata*, and *agamous*. In these homeotic mutants, certain types of floral organs are absent or are replaced by other types of organs. By combining the data sets obtained from these experiments, groups of genes were identified that are predicted to be specifically expressed or strongly enriched in one type of floral organ. For the analysis of temporal gene expression during early flower development, we have generated transgenic plants that allow a specific induction of the floral meristem identity factor *APETALA1* (*AP1*) in an *ap1* cauliflower mutant background. In this double mutant, flower formation is significantly delayed leading to an

accumulation of apical meristems. Activation of AP1 in this background causes a simultaneous transformation of these meristems into floral buds, which undergo the early steps of flower development in a synchronized manner. Thus, this system greatly facilitates the collection of a large number of floral buds that are at about the same developmental stage. By comparing the gene expression patterns of samples from these plants that were collected at different times after AP1 activation, genes whose expression is stage-specific were identified. The combination of the data from the analyses of temporal and spatial gene expression will help to generate a comprehensive gene expression map for Arabidopsis flower development.

383. Cell behavior and gene expression dynamics in SAMs

G. Venugopala Reddy, Elliot M. Meyerowitz

The shoot apical meristem (SAM) is a collection of distinct cell types located in specific positions with specialized functions. The central zone (CZ) cells harbor initials or stem cells, while the cells at specialized regions in the peripheral zone (PZ) differentiate into organ primordia. The cells in rib zone are incorporated into the developing stem. The SAM retains a nearly constant size from germination to senescence, despite a constant flux of cells from the meristem to newly established lateral organs and underlying stem. Thus the SAM has to coordinate two independent but related functions, firstly to ensure a constant cell number in different regions of the SAM, and at the same time to allow cells in defined locations to differentiate and become part of primordia. A tight coordination between cell division and displacement of the progeny both within and across clonally distinct layers of the SAM has been proposed to be a major factor in regulating the size of the SAM and in generating the radial pattern of the shoot apex. These cell types are located in a dynamic environment and hence they have to constantly assess their position in order to retain their identity. The dynamics of cell fate specification can be best studied by combining cell type-specific markers and cell behavior in a single study.

Earlier work has revealed dynamics of cell division patterns in the SAM (Reddy et al., in press). The main aim of the current study is to monitor gene expression dynamics in relation to cell division patterns. This project involves defining cell type specific markers for the CZ, PZ, and the RZ. Thus far we have generated transgenic plants expressing GFP tags under the influence of promoters for the genes CLAVATA3 (CLV3), CLAVATA1 (CLV1), WUSCHEL (WUS), UNUSUAL FLORAL ORGANS (UFO) and LEAFY (LFY). Currently we are combining individual promoters driving different spectral variants of fluorescent proteins and brighter versions of these variants in a single plant so that two or more of these cell types could be followed in real time. Efforts aimed at following individual cell types in relation to cell division patterns would involve combining one or more of these expression domains with ubiquitously

expressing cell division markers. We have employed strategies to boost the expression levels of cell division markers so that they can be excited with minimum amount of laser with an ultimate aim of increasing the imaging duration. From this analysis, we hope to derive the following information: 1) Which cell types make contact with each other? 2) How do the expression domains match with meristem compartments? 3) Are the dynamics of expression patterns in any way related to cell division patterns? 4) A subset of genes used to mark different cell types have been implicated in intercellular signaling and meristem maintenance and this study hopes to visualize such a signaling process at a descriptive level.

Reference

Reddy, G.V., Heisler, M.G., Ehrhardt, D.W. and Meyerowitz, E.M. Development. In press.

384. Transient perturbation of signaling and meristem maintenance

G. Venugopala Reddy, Elliot M. Meyerowitz

Genetic studies have revealed signaling mechanisms involved in meristem maintenance. Mutations in CLAVATA (CLV) genes (CLV1, CLV2 and CLV3) result in larger meristems, while mutations in WUSCHEL (WUS) result in a failure to maintain a functional meristem. Several studies have contributed to a model involving positive and negative feedback loops to maintain meristem size; as the CLV genes code for cell-cell communication proteins, the models involve signaling within the meristem. The function of SHOOT MERISTEMLESS (STM) adds another layer of regulation in SAM establishment and/or maintenance as the stm mutants fail to develop a functional SAM. These studies demonstrate a role for short-range signaling between adjacent groups of cells both within and across clonally distinct layers of cells. Understanding how these signaling mechanisms interface with cell division patterns is central to understanding meristem maintenance and morphogenesis. However, the studies aimed at understanding the cell behavior and analyzing cell types in these mutant contexts are restricted to single time-point observations and mostly restricted to the inflorescence meristem, which represents a terminal phenotype. The function of these gene products can be best understood by analyzing the effects of their transient dysfunction, in real time, both on cell type and on cell behavior.

We have employed a hormone-inducible system to interfere with signaling events in meristem maintenance, either through over expression or double-stranded RNAi (dsRNAi)-mediated transient gene silencing. We have analyzed the effect of WUS over expression on CLV3, UFO and LFY promoters by monitoring the changes in their expression patterns in live imaging. This analysis has revealed that WUS over expression results in expansion of CLV3 domain and a dramatic increase in CLV3 expression levels. At the same time the PZ cells fail to maintain UFO expression and fail to express LFY, which is a marker for organ differentiation. We have also noticed that the lateral

expansion of the CLV3 domain is not due to the additional cell divisions within the native CLV3-expressing cells. This study demonstrates that the expansion of the CZ after WUS activation is due to the re-specification of cell types. We hope to extend these studies to transient gene silencing mediated by dsRNAi. The analysis of dsRNAi directed towards silencing CLV3 is in progress. Constructs required at silencing WUS and STM are being made.

385. Regulation of **WUSCHEL** expression and **WUSCHEL** activity

G. Venugopala Reddy, Elliot M. Meyerowitz

WUS is a critical regulator of meristem maintenance. WUS encodes a homeodomain transcription factor, whose transcripts are mainly localized to central region of the corpus and are excluded from the tunica layers where CLV3 transcripts are localized. Based on genetic evidence, it has been proposed that the spatial regulation of WUS expression is achieved through an inhibitory signal mediated by a CLV signaling cascade involving CLV3, a secreted protein and CLV1, a cell surface receptor. However, the nature of this regulation is unclear. We are attempting to gain further insights by analyzing the effect of CLV signaling on regulation of WUS activity. This involves analyzing WUS transcription and WUS protein in response to transient activation or inactivation of CLV signaling. We have generated constructs that can report WUS transcription and WUS levels in vivo. We aim to impair CLV signaling by following methods: 1) Hormone-induced overexpression or transient silencing of CLV3; 2) Hormone-induced selective activation of diphtheria toxin in CLV3-expressing cells; and 3) Selective laser ablation of CLV3-expressing cells. The transgenic plants required for carrying out these experiments are being obtained.

386. Analysis of post-transcriptional regulation of **MODIFIER OF B FUNCTION**

Carolyn Ohno, Marcus Heisler

The **MODIFIER OF B FUNCTION** (MOB) gene encodes a plant-specific putative transcription factor and is a negative regulator of the floral homeotic B function gene **PISTILLATA** (PI) that is involved in specification of petal and stamen identity. **UNUSUAL FLORAL ORGANS** (UFO) encodes an F-box protein that has been shown to directly interact with components of an SCF-type E3 ubiquitin ligase complex in Arabidopsis. Since ufo loss-of-function mutants display reduced petal and stamen formation (B function activity), one possibility is that UFO targets a negative regulator of B function activity for proteolytic degradation. Strikingly, mutation at the MOB locus suppresses the Ufo mutant phenotype in mob ufo double mutant flowers that produce more petals and stamens in comparison with ufo single mutants.

To test the possibility that MOB is the target of UFO-mediated proteolytic degradation, we have expressed myc- and HA-tagged versions of MOB and UFO in plants for biochemical pull-down assays and analysis of MOB protein levels. In addition we are monitoring a

MOB::CFP translational fusion under the control of the MOB promoter regulatory sequences in plants that also express a developmentally regulated, spatially restricted pUFO::GFP reporter gene to determine if MOB protein levels are influenced in the domain of UFO expression. A transgene has been constructed that will function as a reporter of MOB protein and RNA expression to demonstrate if MOB is post-transcriptionally regulated in vivo. The pMOB::MOB::CFP::IRES::DsRED transgene contains an Internal Ribosomal Entry Sequence (IRES) such that the MOB promoter also directs expression of a DsRED fluorescent marker. A third reporter gene pPI::YFP is used to monitor the petal-and stamen- specific expression of PI, that is transcriptionally regulated by MOB. Confocal laser scanning microscopy will be used to localize RNA and protein expression patterns in living meristems and flowers in order to test our hypothesis that MOB could be post-transcriptionally regulated by UFO.

387. Identifying genes involved in leaf identity as downstream transcriptional targets of **JAGGED** and investigating upstream regulators

Carolyn Ohno

Constitutive expression of the **JAGGED** (JAG) gene is sufficient to cause ectopic growth of leaf tissues. JAG encodes a putative transcription factor with a single C2H2 zinc-finger domain and a EAR transcriptional repressor motif (C. Ohno et al., 2004). It is expressed in all growing lateral organs and loss-of-function jag alleles result in narrow vegetative and floral organs. Clearly factors in addition to JAG promote growth of lateral organs since jag mutants do develop relatively normal albeit narrow lateral organs. Nevertheless, one hypothesis is that JAG may function as a transcriptional repressor of genes that negatively regulate the specification of leaf cell identity. Transcriptional profiling with Arabidopsis whole genome oligonucleotide microarrays will be used to identify the genes that are altered upon inducible constitutive expression of JAG. Transgenic lines that result in dexamethasone hormone-inducible JAG expression have been constructed using a two-component expression system (LhG4; OP). Changes in the mRNA transcriptome from transgenic seedlings overexpressing JAG will be compared to that of jag-2 loss-of-function mutant seedlings using microarray technology to discover genes that are up- or down-regulated. Parallel studies in the presence of the protein synthesis inhibitor cyclohexamide will identify immediate and/or direct JAG transcriptional targets.

In order to identify additional components of the JAG pathway upstream of JAG transcription, regulatory sequences that have previously been shown to be sufficient for genomic complementation have been fused to a GFP-GUS reporter gene. A series of N-terminal and C-terminal truncations of these sequences has been generated in order to identify important cis-regulatory sequences. Dissection of the JAG promoter may help to uncover the trans-acting

factors that activate JAG expression in all lateral organs but that prevent JAG expression in the cryptic bract.

388. Improving an **in vivo** experimental system for studying **Arabidopsis** meristem development
 Marcus Heisler, Pradeep Das, Carolyn Ohno, G. Venugopala Reddy

In order to understand the temporal and spatial dynamics of development in the *Arabidopsis* meristem, an *in vivo* imaging system based on confocal microscopy and 3D volume registration has been developed that allows 4D fluorescence data to be analyzed from imaging over several days of growth. Recently this system has been used to follow the division patterns of clonally related cells in order to start to characterize the overall dynamics of cell behavior in the meristem (Reddy et al., 2003). Our objective in this project is to optimize this system and to expand its role from being purely observational to being a tool for manipulation at cellular resolution.

Although our system is capable of imaging some GFP reporters for up to several days, our imaging ability is limited by the requirement that laser exposure must be kept to a minimum. To increase signal-to-noise ratios we have pursued a strategy of generating reporter constructs consisting of multimerized GFPs. This approach is both relatively simple and cheap. So far both CFP and YFP variants have been multimerized (3X) and fused to nuclear and plasma membrane localization tags. We are also enhancing their expression levels in two-component systems based on LhG4; 6XOP and GAL4;UAS. Imaging of 3XYFP controlled by the CUC2 promoter has indeed confirmed that this approach is a powerful way of generating extremely bright reporter fluorescence levels.

We have also begun to test our ability to image two or more GFP variants simultaneously. So far 1XdsRED and GFP markers have been successfully imaged together over a period of 30 hr with stacks taken every three hr. Triple labeling with dsRED, GFP and YFP has also worked over a shorter period. Such efforts will be enhanced greatly through the use of the GFP multimer markers described above.

389. **In vivo** manipulation of **Arabidopsis** gene expression at the cellular level
 Marcus Heisler, Pradeep Das, Carolyn Ohno, G. Venugopala Reddy

Existing techniques for the *in vivo* manipulation of gene expression in *Arabidopsis* rely on the use of hormone or chemical treatments that, at best, are used in conjunction with specific promoters in order to express a gene in a particular pattern with temporal resolution. However, this control is not at cellular resolution and requires the time consuming cloning of promoters. We are developing the use of laser-activated heat shock to achieve complete control over where and when a transgene is expressed. At present, we are testing a 440 nm micropoint laser in conjunction with the promoter of HSP18.2 driving nuclear localized dsRED and 3XCFP. This laser produces a diffraction-limited beam that has sub cellular resolution.

Preliminary experiments suggest that cell-specific ablation can be achieved and testing for heat shock-induced expression is in progress. We are also assessing the ability of a two-photon (2P) IR laser to induce heat shock and ablation. A potential advantage of 2P induction is that targeting may be achieved simply by defining any arbitrary region of interest using the regular Zeiss imaging software. The expression of induced transgenes will be monitored through the use of an Internal Ribosomal Entry Sequence (IRES) between the gene of interest and a reporter GFP. Lastly, we are making these constructs Gateway compatible to allow their rapid construction.

The ability to combine live imaging with cellular perturbation techniques should facilitate *in vivo* experimentation at new temporal and spatial resolution limits. When also combined with computer-assisted segmentation and modeling, this system should provide a uniquely powerful resource able to test causal connections and reveal the dynamics of plant meristem growth and pattern formation.

390. Auxin and phyllotaxis
 Marcus Heisler, Henrik Jönsson¹, Bruce Shapiro², Eric Mjolsness³

Plants mutant for the auxin efflux carrier PIN1 fail to produce primordia on the meristem flanks. It has been established in our lab as well as in others that the efflux carrier polarity in the meristem is consistent with the hypothesis that auxin is transported directly to sites of primordium formation. Previously we found that PIN1 is regulated rapidly by auxin and this has been confirmed using live imaging techniques. Furthermore, we have found that in the wild type, PIN1 expression spreads when auxin transport is disrupted or exogenous auxin is applied. These data support the proposal that there is a zone of auxin depletion surrounding primordia as they develop. However, the patterning mechanism that governs PIN1 polarity is still not understood. We are combining live imaging techniques with computer modeling to investigate several theories to explain PIN1 polarity and phyllotaxis.

Our simplest model consistent with the available data and capable of generating phyllotactic patterning is based on the polarization of PIN1 by auxin gradients. By polarizing PIN1 up auxin concentration gradients, peaks of high auxin concentration can be generated with regular spacing. When such spacing is superimposed in a growing meristem the familiar spiral pattern of primordia emerges with PIN1 polarized towards these primordia, as seen in the real plant. A second model is based on polarization by an intermediate diffusive factor X that is produced by primordia once they are initiated by high concentrations of auxin. Lastly, a model based on a cell's internal gradient of auxin (a more biological equivalent of the pure flux model of Mitchison) is being developed that includes cytoplasmic, membrane and wall compartments.

These models are simulated on a meristem template generated from real cell position and shape data. Thus, the theories can be used to try and predict the position of future primordia and then the results compared

with the actual future primordium position. Furthermore, extracted PIN1 protein expression data can also be used to set the initial conditions for these simulations.

To test these models more directly, experiments are in progress to examine the response of PIN1GFP to localized sources of auxin placed on the meristem. The results of these experiments will be checked against predictions made by the simulations.

¹Lund University, Lund, Sweden

²Jet Propulsion Lab (JPL) La Canada, CA

³University of California, Irvine, CA, USA

391. Spatio-temporal dynamics of primordial gene expression, growth and signaling

Marcus Heisler, Carolyn Ohno, Henrik Jonsson¹, Victoria Gor², Bruce Shapiro², Eric Mjolsness³

Once primordial position is specified, primordium development involves changes to the direction of growth and cell differentiation events. This project aims to investigate these processes using our live imaging system. An initial application of our imaging is simply to establish the temporal and spatial dynamics of known genes involved in primordial specification. Initially, a set of ten markers has been chosen for detailed study including polarity genes, boundary genes and others involved in primordium specification. So far, the PIN1 gene encoding an auxin efflux transporter appears to be the first gene localized in regions predicted to form primordia, consistent with its proposed role in specifying primordium position. A REV reporter appears approximately one plastochron later and FIL, one plastochron later than REV. The characterization of many other genes is in progress. The aspects of cellular behavior we are particularly interested in are the changes in division rate/orientation and expansion that result in primordial outgrowth and how these features may be influenced by auxin and gene activity.

In order to gather accurate data regarding cell division orientations, expansion rates and expansion directions, multimerized GFPs (3X) tagged to the membrane and nucleus have been put under a set of promoters identified as promoting high expression. These are being used to develop automated segmentation methods to extract cell position and shape from the confocal data. The proposed overall process is outlined below:

Collection of time lapse image stacks ⇒ Z correction based on nucleus shape ⇒ automated volume registration using Multimodality Image Registration Using Information Theory (MIRIT) limited to rigid transformations ⇒ automated extraction of nuclear position, cell shape and expression data ⇒ correspondence established between cells at different time points ⇒ calculation of division rates, division orientations, cell expansion vectors and correlation statistics.

Finally the use of laser ablation and possibly laser activated gene expression should enable us to dissect signaling events between different primordia or parts of primordia and possibly the meristem. For instance, we

could investigate the proposed inhibitory effect of one primordium on the position of subsequent adjacent primordia by ablating primordia or the cells between primordia at different stages and monitor the effects on PIN1 and the other GFP markers. We should also be able to investigate the competitive interaction between the flower and cryptic bract that has been revealed by previous work using the diphtheria toxin.

Cell-specific activation of genes using a heat-shock system may also enable many interesting experiments, including examining the effects of STM, WUS, expansin, MP, PID, as well as RNAi for these genes on the development of primordia. In case heat-shock activation is not possible, the activation of some of these genes through an inducible two-component system is also being pursued.

¹Lund University, Lund, Sweden

²Jet Propulsion Lab (JPL) La Canada, CA

³University of California, Irvine, CA, USA

392. Microarray analysis of auxin induced genes

Marcus Heisler

An ongoing study is the analysis of genes identified by microarray analysis to be induced by auxin in the pin1 meristem. Approximately 150 genes were identified to be altered more than two-fold after 30 min. of treatment. After this first burst of activity little change is observed for the next 6 hr.

In situ hybridization experiments have revealed that the expression patterns of many of these genes can be classified into just a few different pattern types. An interesting dichotomy is between those expressed in the tunica vs. those expressed in the corpus. Most of the genes expressed in the corpus appear to be localized to the developing vascular tissue. In the tunica some genes are expressed in the developing primordia, while others appear to be expressed at their borders. Presently, a number of transcription factors are under investigation through overexpression and knock-out analysis.

Initially, it had been thought that many known genes that are expressed in primordia would be identified by this microarray approach. However, so far few such genes appear up regulated in the first 6 hr. Two possible explanations for this are being investigated. Firstly, known genes may act later than 6 hr after auxin application. Secondly, many of these genes may be already on at such levels that further up-regulation is marginal. From our live imaging data we now know that genes such as REV and FIL become expressed in primordia at least 12 hr later than when PIN1 is first up-regulated suggesting that extending the microarray analysis over 24 hr may be fruitful.

393. HANABA TARANU is a GATA transcription factor that regulates shoot apical meristem and flower development in **Arabidopsis**

Yuanxiang Zhao, Leonard Medrano¹, Kazuaki Ohashi², Jennifer C. Fletcher³, Hao Yu, Hajime Sakai⁴, Elliot M. Meyerowitz

We have isolated a new mutant, hanaba taranu (han), which affects both flower and shoot apical meristem (SAM) development in *Arabidopsis thaliana*. Mutants have fused sepals, and reduced organ numbers in all four whorls, especially in the 2nd (petal) and 3rd (stamen) whorls. han meristems can become flatter or smaller than in wild type. HAN encodes a GATA-3-like transcription factor with a single zinc-finger domain. HAN is transcribed at the boundaries between the meristem and its newly initiated organ primordia, and at the boundaries between different floral whorls. It is also expressed in vascular tissues, developing ovules and stamens, and in the embryo. han interacts strongly with *clavata* (*clv*) mutations (*clv1*, *clv2* and *clv3*), resulting in highly fasciated SAMs, and we find that *WUS* expression is altered in han mutants from early embryogenesis. In addition, HAN is ectopically expressed both in *clv1* and *clv3* mutants. We propose that HAN is normally required for establishing organ boundaries in shoots and flowers, and for controlling the number and position of *WUS*-expressing cells. Ectopic HAN expression causes growth retardation, aberrant cell division pattern and loss of meristem activity, suggesting that HAN is involved in controlling cell proliferation and differentiation.

¹Ceres, Inc., Thousand Oaks, CA

²Tohoku University, Sendai, Japan

³USDA Plant Gene Expression Center, Albany, CA

⁴E.I. Dupont and Co., Newark, DE

394. Interactions between HAN and CUC proteins in setting up organ boundaries in **Arabidopsis**

Yuanxiang Zhao, Patrick Sieber, Pradeep Das, Elliot M. Meyerowitz

HAN (HANABA TARANU) is a GATA-like transcription factor involved in both shoot apical meristem (SAM) and flower development. The *Arabidopsis* flower is initiated as a buttress of undifferentiated cells (floral meristem) at the flanks of the SAM, which gradually gives rise to four whorls of organs from the outer to the inner whorls. Both the loss-of-function han mutant phenotype and the expression pattern of HAN in the flower suggests that HAN is required for setting up boundaries between the floral meristem and floral organs, as well as between organs in the same whorl. CUC (CUP-SHAPED COTYLEDONS) proteins (CUC1, 2 & 3) belong to a family of NAC-domain containing plant specific proteins that are also involved in SAM and flower development. Similar to han mutants, cuc mutants also show floral organ boundary defects, and CUC genes are expressed in similar domains as HAN. To investigate the roles of HAN and CUC in setting up organ boundaries, we generated han cuc double mutants, which show more dramatic organ fusion and organ number reduction defects than in either single

mutant. In addition, while the han mutation is recessive in a wild-type background, a single han null allele enhances both single homozygous cuc mutant phenotypes and double heterozygous cuc mutant phenotypes. This suggests that HAN and CUC proteins could either interact in the same protein machinery, or that they act in different genetic modules that converge into the same biological event (boundary set up). The expression pattern of each gene in the other mutant is being determined in order to examine whether the genes cross-regulate on a transcriptional level. A GFP reporter gene driven under the HAN promoter is being introduced into an already established transgenic line carrying the VENUS reporter gene driven by the CUC2 promoter, and observation of the two labels by confocal microscopy will reveal the degree of overlap between the HAN and CUC2 expression domains at a single-cell resolution. In addition, to test whether the two proteins physically interact, we will apply BRET (Bioluminescence Resonance Energy Transfer) by tagging HAN with blue light-emitting luciferase (LUC) and CUC2 with yellow light-emitting YFP. Close physical proximity of LUC and YFP due to protein interactions will result in an increase in the yellow-to-blue luminescence ratio, which can be detected in live plant cells. Furthermore, it has been shown that CUC is required for STM expression during normal SAM development, and ectopic expression of CUC using a 35S constitutive promoter induces ectopic STM expression as well as ectopic meristematic cells in cotyledons, weakly mimicking the effect of ectopic expression of STM. We have initial evidence indicating that in 35S::HAN plants, KNAT1/2, two known downstream effectors of the STM protein, were ectopically induced, though no apparent ectopic meristems are formed in these plants. To find if HAN and CUC functionally converge on the regulation of STM or its downstream effectors, double transgenic plants carrying 35S::HAN and 35S::CUC will be generated; synergistic effects on STM or its downstream effectors would be reflected by enhanced ectopic expression of STM and/or KNAT1/2, as well as enhanced ectopic meristem formation.

395. Probing the cellular function and downstream targets of HANABA TARANU, a GATA transcription factor essential for **Arabidopsis** development

Yuanxiang Zhao, Elliot M. Meyerowitz

HANABA TARANU (HAN) plays important roles in the development of both the shoot apical meristem (SAM) and the floral meristem in *Arabidopsis*, and it has an interesting expression pattern in these structures, at the boundary between the meristem region and the early initiating organ primordia. The meristem structure encompasses a group of stem cells whose descendants will give rise to all the lateral organs. In the absence of HAN function, the expression of *WUS*, a meristematic cell marker gene in the center zone of the meristem, becomes less centered, while ectopic overexpression of HAN causes growth retardation, elimination of *WUS*-expressing cells,

and termination of the meristem structure. To further test whether HAN normally delimits WUS expression domain during meristem development, we have expressed HAN in wild-type plants or plants that have excessive WUS-expressing cells and a fasciated meristem (such as a *clv3* mutant plant), under the control of the WUS promoter as well as other meristems-specific promoters. If the hypothesis is true, ectopic expression of HAN should rescue in some degree or even suppress the fasciation phenotype of *clv3* mutants. Furthermore, the cellular effect of ectopic HAN upon WUS-expressing cells could be visualized in live plants by expressing a dexamethasone-inducible HAN-GR fusion protein under the above promoter(s) in transgenic plants carrying a pWUS::GFP transgene. Potential HAN effects on cell division could also be explored in parallel by comparing cell proliferation rates between *han-1* mutant and wild-type inflorescences, as well as between DEX-treated and mock-treated 35S::HAN-GR plants by using BrdU staining, which labels mitotic cells in S phase. And lastly, we have made a construct expressing HAN-GR fusion protein under the control of the HAN promoter, which provides full rescue of *han* mutant phenotypes when driving HAN expression. This construct will be introduced into *han* mutants, and the differential RNAs from steroid-treated and mock-treated plants will be examined using a microarray that represents RNAs normally expressed in wild-type plants. Comparison between the two groups of expression profiles will lead us to potential target genes of HAN.

396. Functional analysis of two close homologs of HANABA TARANU in **Arabidopsis** development

Yuanxiang Zhao, Elliot M. Meyerowitz

HANABA TARANU (HAN) encodes a GATA-like transcription factor and plays an important role in shoot apical meristem and flower development in *Arabidopsis*. There are an estimated 25 GATA-like transcription factors in *Arabidopsis* genome, but their functions are still mostly unknown. Among these, there are two close HAN homologs we have named HANL1 and HANL2, sharing 96% or 100% identity within the zinc-finger domain, and 40% or 44% total amino acid sequence identity when compared to the HAN protein, respectively. Expression patterns of both genes have been examined by RNA in situ hybridization. Both genes are expressed in all vascular tissues, in the stamen and petal primordia of young flowers, but absent from the meristem. Two *han2* alleles, both with single amino acid change mutations, have been identified (by Dr. Wolfgang Lukowitz of the Carnegie Institution, Stanford). The *han2* mutation by itself does not cause a mutant phenotype, but it enhances the floral phenotypes of the weak *han-2* mutant. The enhancing effect is less noticeable when combined with a *han-1* loss-of-function mutation. Double-stranded RNAi constructs that target specific coding region of HANL1 or the complete coding region of HANL2 have been introduced separately into wild-type plants, in order to obtain loss-of-function phenotypes for each gene. In

case that single knock-out of each gene function does not result in any visible phenotypes due to functional redundancy, both RNAi constructs are also being introduced into the *han-2* mutant background, as well as a *cuc* mutant background.

Overexpression of either HANL1 or HANL2 results in small plants with serrated leaves and short siliques with a wavy surface. Strong ectopic induction of either gene during germination also results in stalled growth of the seedling and in aberrant cell division. While all three HAN subfamily genes cause similar overexpression phenotypes, it has been shown that only HANL2, but not HANL1, could fully complement HAN function when expressed under the control of the endogenous HAN promoter (by Dr. Wolfgang Lukowitz's, personal communication), indicating that HAN and HANL2 have functional redundancy. Potential homodimerization or heterodimerization interactions will be addressed using biochemical and/or biomolecular fluorescence complementation approaches.

397. A semidominant mutation of **HANABA TARANU** causes fasciated shoot apical meristem in **Arabidopsis**

Yuanxiang Zhao, Kazuaki Ohashi, Elliot M. Meyerowitz

HANABA TARANU (HAN) is involved in both shoot apical meristem (SAM) and flower development. Four different mutant alleles, named *han-1*, *-2*, *-3* & *-4*, have been isolated, and all are recessive except for *han-3*. Besides sharing similar flower defects including reduced floral organ numbers and organ fusion defects with the other mutants, *han-3* mutants have a fasciated SAM and stem, which becomes acropetally more severe. The fasciation phenotype is caused at least partially by the overexpression of WUS, as WUS is ectopically expressed in the SAM of *han-3* mutants, and lack of one functional copy of WUS partially rescues the *han-3* phenotype. The *han-3* mutation appears slightly semi-dominant in the wild-type L-er background, with a weak silique phenotype, but in a *cuc* heterozygous mutant background, a single *han-3* allele causes strong dominant effects on flower development, while other *han* alleles cause only a very weak effect. The *han-3* mutation was caused by multiple copies of a T-DNA inserted in the first exon of HAN, N-terminal to the zinc-finger motif. The HAN-3 5' coding sequences are prematurely terminated after 8 aas in-frame reading (YIHRQMGA) into the T-DNA sequences, and RT-PCR shows that HAN coding sequences on both sides of the T-DNA insertion are transcribed. A PCR screen indicates that there is no gene deletion within a 20 kb range on either side of the *han-3* mutation. A genomic fragment spanning the whole HAN gene that provides full rescue to other *han* mutations can only partially rescue *han-3* mutant phenotypes, resulting in *clv1* mutant like plants with fasciated SAMs and floral meristems. To test the hypothesis that the fasciated SAM phenotype in *han-3* mutants is caused by the transcribed truncated regions of HAN-3, constructs expressing the truncated regions under

the control of a constitutively active CaMV 35S promoter or of the endogenous HAN promoter, have been introduced into han-1/+ plants (han homozygous plants are sterile). In addition, double-stranded RNAi constructs targeting both of the transcribed regions have been introduced into han-3/+ plants.

398. The homeotic protein AGAMOUS controls microsporogenesis by regulation of **SPOROCTELESS**

Toshiro Ito, Frank Wellmer, Hao Yu, Pradeep Das, Natsuko Ito*, Marcio Alves Ferreira, Jose Luis Reichmann

The *Arabidopsis* homeotic selector gene AGAMOUS (AG) is necessary for the specification of reproductive organs (stamens and carpels) during the early steps of flower development. AG encodes a transcription factor of the MADS-box family. However, the developmental processes that AG might control and the genes that are controlled by this factor during reproductive organ development are largely unknown.

We produced a strain with inducible AG activity (Ito et al., 2004). This strain is homozygous for the ag-1-null mutation and transgenic for 35S::AG-GR, a constitutive promoter-driven AG gene with a carboxy-terminal fusion to the steroid-binding domain of the rat glucocorticoid receptor. Continuous treatment with the steroid hormone dexamethasone (DEX)—which leads to a translocation of the fusion protein from the cytoplasm to the nucleus—completely rescues the ag-1 mutant phenotype, showing that AG-GR is functional in a DEX-dependent manner.

We have performed cDNA and full-genome microarray screening using ag-1 35S::AG-GR plants and identified several AG-responsive genes. One of the AG-inducible genes, SPOROCTELESS/NOZZLE (SPL/NZZ), encodes a putative transcription factor implicated in ovule pattern formation and early microsporogenesis (Schiefthaler et al., 1999; Yang, et al., 1999). We showed that AG directly regulates SPL/NZZ based on five lines of evidence (Ito et al., 2004). Firstly, SPL/NZZ expression increases very rapidly after activation of AG-GR. Secondly, this induction occurs even in the presence of a protein synthesis inhibitor. Thirdly, the expression patterns of AG and SPL/NZZ correlate well during the reproductive organ development. Fourthly, AG binds to the CArG box-like sequence in the 3' region of the SPL/NZZ gene in vitro. Lastly, mutation of this site strongly affects the expression of SPL/NZZ in vivo. Furthermore, we demonstrated that SPL/NZZ can induce microsporogenesis in the absence of AG function, suggesting that SPL/NZZ is a central mediator for the microsporogenesis function of AG. These results show that AG controls a specific process during organogenesis by activating another regulator that performs a subset of its functions.

*Volunteer

References

- Ito, T., Wellmer, F., Yu, H., Das, P., Ito, N., Ferreira, M.A., Reichmann, J. and Meyerowitz, E.M. (2004) Nature. In press. (doi:10.1038/nature02733)
- Schiefthaler, U., Balasubramanian, S., Sieber, P., Chevalier, D., Wisman, E. and Schneitz, K. (1999) Proc. Natl. Acad. Sci. USA 96:11664-11669.
- Yang, W.C., Ye, D., Xu, J. and Sundaresan, V. (1999) Genes Dev. 13:2108-2117.

399. Downstream functions of the homeotic protein AGAMOUS during stamen development

Toshiro Ito, Hao Yu

In developmental biology, the term "selector gene" has been used to describe genes that are able to trigger an entire developmental pathway. The floral homeotic selector gene AGAMOUS (AG), together with other members of the same class of floral homeotic genes, is sufficient to trigger male and female reproductive organ (stamen and carpel) development. Although AG is the most studied example of a floral homeotic gene, the mechanisms by which the floral organ primordia of whorls 3 and 4 respond to the genetic activities initiated by AG, and thereby differentiate into stamens and carpels, are largely unknown. There are two extreme hypotheses about how AG functions. One is that AG triggers a few genes at the top of a hierarchy to determine reproductive organ identity, and in turn, these AG targets regulate other genes. The second possibility is that AG directly regulates the expression of many genes with different functions acting throughout stamen and carpel development. The continued expression pattern of AG throughout flower development might suggest the latter case.

To find if either of these hypotheses describes AG action in flower development, a strain with DEX-inducible AG activity was used for temporal induction experiments. By performing a series of timed-induction experiments we showed that AG has various different functions throughout stamen development in microsporogenesis, filament elongation and dehiscence of four-loculed anthers. The direct measurement of active AG-GR protein in these plants showed that the prolonged AG activity which extends 8-9 days from stage 3 floral buds—is necessary to produce normal stamens of *Arabidopsis*. These results indicate that AG expressed throughout stamen development directly regulates the expression of various genes with different functions. To reveal target genes of AG during late stamen development, expression profiling following whole stamen development has been initiated using lines with the inducible AG activity.

400. Evolutionarily function of homeotic gene AG during stamen development

Toshiro Ito

The floral homeotic selector genes are conserved throughout angiosperms (for review see Ma and dePamphilis, 2000). In the basal angiosperm ANITA plants, flowers have thick connective and often leaf-shaped laminar stamens (Endress, 2001). To examine the

functions of the floral homeotic gene *AGAMOUS* (*AG*) in stamen morphology of the basal angiosperms, the expression of *AG* orthologs was examined in *ANITA* plants. In *Magnolia* species, which show laminar stamens, the expression of the *AG* ortholog is initiated in the entire stamen primordium, as in *Arabidopsis*. However, in contrast to *Arabidopsis*, where *AG* keeps being expressed in anthers and filaments of developing stamens, continued expression was not observed in presumptive connectives or filaments of developing stamens in the *ANITA* plant. The expression was localized to lateral edges where locules are induced. These results, together with our timed-induction experiments using *Arabidopsis* (see above), permits a speculation that the morphological change of stamen form from a laminar to a filamentous structure might be dependent on the duration of *AG* activity (perhaps along with other *MADS*-box floral homeotic proteins). Morphological changes of laminar stamens to filamentous stamens and vice versa are suggested to have occurred several times independently during angiosperm evolution (Hufford, 1996). This simple possible mechanism (a change of *AG* expression caused by mutations in cis-elements and/or transacting factors) might have facilitated the multiple evolutionary origin and reversals of the laminar-filament transformation. The in situ hybridization analysis using other *ANITA* plants, *Nymphaea tetragona*, which shows petal-stamen intermediate structures between whorls of petals and stamens, and *Cabomba caroliniana*, which has filamentous stamens, are underway to obtain independent corroborations to our hypothesis.

This work is in collaboration with Dr. Mitsuyasu Hasebe's group (National Institute of Basic Biology, Japan)

References

Endress, P.K. (2001) *Int. J. Plant Sci.* 162:1111-1140.

Hufford, L. (1996) The origin and early evolution of angiosperm stamens. In: The origin and early evolution of angiosperm stamens, W.G. Darcy and R.C. Keating, eds., Cambridge/New York, Cambridge University Press, pp. 58-91.

Ma, H. and dePamphilis, C. (2000) *Cell* 101:5-8.

401. cis-Element analysis of the **AGT2ATH** gene, a putative target of *AGAMOUS* involved in polarity establishment in **Arabidopsis** carpels
Toshiro Ito

We have identified the *AGT2ATH* gene based on bioinformatics approaches. The gene contains a putative binding site of *AG* in the 3' downstream region. The *AGT2ATH* gene encodes a member of the AT hook-type DNA binding protein family and shows *AG*-dependent expression after stage 5 in flower development. *AGT2ATH* is expressed throughout wild-type floral primordia during stages 1-5. From stage 6, *AGT2ATH* expression is localized to the stamen and carpel primordia, and the expression continues at the adaxial side of the pistil. In a loss-of-function *ag-1* mutant background, *AGT2ATH* expression is only detected in the early-stage floral buds,

and the late-stage expression after stage 5 disappears gradually. In *ag-1 35S::AG-GR* plants, *AGT2ATH* was induced shortly after *DEX* treatments in the presence of a protein synthesis inhibitor. By functional analyses, *AGT2ATH* has been shown to be a negative transcriptional regulator of *ETT*, which controls the polarity of the gynoecium (Sessions et al., 1997; Nemhauser et al., 2000). The strong overexpression of *AGT2ATH* in the wild-type plants mimicked the *ettin* (*ett*) mutant phenotypes. Consistent with this observation, *ETT* expression was reduced significantly in the overexpression line of *AGT2ATH*. Furthermore, the expression patterns of *AGT2ATH* and *ETT* were mutually exclusive in stamen, carpel and ovule primordia. The overexpression of *AGT2ATH* in *ag-1* and RNA silencing experiments also suggested that *AGT2ATH* is involved in ovule and anther development in addition to negative regulation of *ETT* under the *AG* cascades.

To obtain independent evidence that *AG* directly regulates *AGT2ATH*, we produced promoter constructs containing the 7.3 kb flanking sequences of the *AGT2ATH* gene and examined the cis-activity of the putative binding site of *AG*. However, the wild-type construct did not confer the early-middle stage expression patterns, as observed by in situ hybridization experiments. After anthesis, *GUS* staining was observed in valve margins where highly homologous genes with *AG*, *SHATTERPROOF 1* and *2* are expressed (Liljegren et al., 2000; Pinyopich et al., 2003). In the plants with a mutated *GUS* construct in the putative binding site of *AG*, weaker *GUS* staining was observed in these valve margins. Currently we are working on why our constructs did not show the early stage *GUS* expression and also testing whether *SHP1* and *SHP2* could regulate *AGT2ATH*.

References

Liljegren, S.J., Ditta, G.S., Eshed, Y., Savidge, B., Bowman, J.L. and Yanofsky, M.F. (2000) *Nature* 404:766-770.

Nemhauser, J.L., Feldman, L.J. and Zambryski, P.C. (2000) *Development* 127:3877-3888.

Pinyopich, A., Ditta, G.S., Savidge, B., Liljegren, S.J., Baumann, E., Wisman, E. and Yanofsky, M.F. (2003) *Nature* 424:85-88.

Sessions, A., Nemhauser, J.L., McColl, A., Roe, J.L., Feldmann, K.A. and Zambryski, P.C. (1997) *Development* 124:4481-4491.

402. Systematic analyses of transcriptional networks during reproductive organ development in **Arabidopsis**

Toshiro Ito, Annick Dubois, Pradeep Das, Frank Wellmer

Reproductive organ development presumably involves temporally- and spatially-specific expression of thousands of genes. One of our goals is to understand molecular mechanisms that orchestrate a large number of genes, leading to elaborate functions and shapes of reproductive organs during the flower development. For

that purpose, we have been working on the downstream genes of two key regulators, AGAMOUS and SUPERMAN, in stamen and carpel development, using microarray technology and transgenic lines with inducible gene function. To increase robustness of the datasets and also determine the hierarchy of downstream genes, we have modified the sample preparation methods and also started working on downstream genes of other key regulators of reproductive organ development.

AGAMOUS (AG) acts as an organ identity gene and is required for providing determinacy in the center of the floral meristem. Our timed-induction experiments (see abstract 399) showed that the meristem determinacy function is achieved by AG at stage 3-4, before stamen identity is established. SUPERMAN (SUP) acts to prevent cell proliferation in floral primordia of whorl 3 and to promote differentiation of the whorl 4 floral meristem at stages 3-5 (Sakai et al., 1995; Ito et al., unpublished results). Previously, floral samples were collected by the naked eye containing floral buds from stage 1 through stage 10 or 11. The dataset obtained from these experiments seems to be biased for genes that are dominantly expressed at middle-late stages. Based on the volume calculation of floral buds at each stage, we reasoned that genes that are expressed only at early stages were likely to be under-represented. In inflorescence samples containing stage 1-10 floral buds, the ratio of stage 3-5 floral buds is estimated to stand at only a few percent. To identify the early-stage targets of AG and SUP, which might be involved in floral meristem control and early organogenesis steps, we have started to collect floral samples from stages 1-5 under the dissecting microscope. This time-consuming step greatly enhanced the ratio of stage 3-4 floral buds to ~30 % (V/V), which would make it possible to detect the up- or down-regulation of early targets. By correcting 30 inflorescences, we could obtain a few micrograms of total RNA, which is barely sufficient for probe synthesis. Repeated sample preparation and microarray hybridization are underway.

We also established transgenic lines with inducible activity for SUPERMAN-like proteins, SPOROCTELESS/NOZZLE, AGT2ATH, ETTIN, and SPATULA (Heisler et al., 2001; and see abstract 398 and 401). These lines contain protein fusions of a transcription factor and the steroid-binding domain of the rat glucocorticoid receptor followed by epitope tags, which allow us to control the activity of transcription factors post-translationally. Microarray analysis using these lines would help us to categorize the current datasets and also determine the hierarchy of the downstream network leading to stamens and carpels.

Reference

Heisler, M.G., Atkinson, A., Bylstra, Y.H., Walsh, R. and Smyth, D.R. (2001) *Development* 128:1089-1098.

403. Genome-wide binding site analysis of AG by chromatin immunoprecipitation (ChIP) in **Arabidopsis**

Toshiro Ito, Nicole J. Kubat

For our analysis of the transcriptional network during reproductive organ development, it is important to distinguish between direct interactions and secondary downstream effects. To analyze the robust dataset of expression profiles obtained from microarrays, we have been performing chromatin immunoprecipitation (ChIP) analysis for genome-wide binding sites of a transcription factor. Although this method has been successfully applied to a single-celled eukaryote and cultured mammalian cells, it has technical limitations in sensitivity in a multicellular organism with a relatively large genome size. In order to overcome the limits of the application of ChIP to a multicellular plant system, we originally used homogeneous populations of cultured cells with both inducible gene activity and efficient epitope tags. We generated transgenic plants in which GR-epitope (HA or c-myc) fusion proteins with AG, SEP3, AP3 or PI are ectopically expressed. We first produced callus culture overexpressing AG and SEP3, which are sufficient to induce carpel identity. Although we found that one of the AG targets, AGT4HOX, was induced after DEX treatment in the callus tissue, some other targets of AG, including SPL/NZZ, were not significantly induced. Therefore, we have decided to use floral buds of ag-1 35S::AG-GR-epitope for ChIP experiments. We prepared two independent lines transgenic for ag-1 35S::AG-GR-HA and ag-135S::AG-GR-myc. With the help of the other lab members, we obtained approximately 1 ml of floral buds in 10 min. They were fixed for 10-20 min with 1% paraformaldehyde solution and frozen with liquid nitrogen. Following the ChIP experiments, we are going to test the enrichment of promoter regions for the putative AG direct targets, SPL/NZZ, AGT2ATH and AGT4HOX. Then we will amplify the DNA by the effective DNA amplification methods reported in last year's annual report, and use full genome tiling array (NimbleGen, WI USA) to detect the genome-wide binding sites of AG.

404. Exploring floral organ number patterning Pradeep Das

While much is known about the processes that regulate certain aspects of floral development, such as meristem or organ identity, others, such as organ number specification, remain largely unexplored. The PERIANTHIA (PAN) gene, which encodes a bZIP transcription factor, is one of the few genes known to affect floral organ number without altering meristem size and meristem identity. While wild type *Arabidopsis* flowers are tetramerous (four sepals and four petals), flowers of pan mutant plants are largely pentamerous (five sepals and five petals). To determine how PAN impacts organ number patterning, we are following two lines of investigation – microarray analyses to identify downstream targets of PAN and misexpression studies to explore its mechanism of action.

We are carrying out two types whole-genome microarray analyses. Firstly, we are comparing the gene expression profiles of pan mutants and wild-type floral buds of stages 1-5, when the earliest organ primordia are being laid down. Secondly, we are using a dexamethasone-inducible form of PAN (by fusing it to a portion of the rat glucocorticoid receptor). Time-course experiments determining the expression profiles of inflorescences 0, 4 or 8 hr after activation with dexamethasone are expected to yield both genes that are directly activated by PAN as well as targets of those genes. Analysis of these loci should shed some light on the processes downstream of PAN.

In a separate effort, we are using directed expression studies to determine the minimum domain of expression required for PAN to fulfill its normal functions in floral development. This is achieved by placing PAN or a PAN-GFP fusion downstream of various heterologous promoters with specific expression patterns (e.g., AP1, AP3, AtML1, etc.), introducing these into pan mutants and assaying their ability to rescue the mutant phenotype. In addition, we are using laser-driven heat shock to activate expression of PAN or PAN-GFP in very small groups of cells lacking functional PAN protein and monitoring the effects on floral organ number. Such clones of cells will help further narrow the requirement for PAN activity and provide a way to explore certain aspects of primordium initiation, such as the influence of organ number in one whorl on organ number in an adjacent whorl.

405. Identifying genetic partners of **PAN**
Pradeep Das, Antha Mack*

Wild-type Arabidopsis flowers have four sepals, four petals, six stamens and two carpels. In mutants of the PERIANTHIA (PAN) gene, the number of perianth organs is increased to five sepals and five petals. PAN is one of the few genes known to impact organ spacing (and hence organ number) without also increasing the field of cells from which their primordia are patterned. Little is known about the mechanism of PAN function: the developmental pathways it might impinge on or the processes it might help shape.

The phenotype of pan mutants is both incompletely penetrant (a small percentage of mutant flowers are morphologically wild type) as well as variable (sepal and petal numbers range from six-seven), suggesting that PAN may function redundantly with other genes, possibly some that share sequence homology with it. BLAST searches suggest that there are several genes with over 65% similarity to PAN. Mutants for most of these genes are not publicly available.

One way to identify the loci with which PAN may interact to specify organ number is by performing genetic modifier screens for second-site mutations that enhance or suppress the pan-3 phenotype. Thus far, we have screened approximately 1000 lines and identified several enhancers but no suppressors. These include mutants resembling known loci such as apetala1, apetala2, unusual floral organs and leafy. Additionally, we have identified some

mutants with novel phenotypes. One of these, designated E159, is a dramatic enhancer of pan-3 petal number, with double mutants displaying up to 12 petals. Single mutants of this line display two-to-three petals with normal numbers of the other floral organs.

We are currently in the process of genetically mapping the locus with the aim of cloning it molecularly. We are also characterizing its phenotypes in greater detail and determining its genetic interactions with other loci involved in floral development. Such characterization should shed light on how primordium initiation and organ spacing are patterned.

*Volunteer

406. Identification of LFY and AP1 downstream genes in **Arabidopsis** using microarrays
Annick Dubois, Frank Wellmer, Toshiro Ito, David McKinney, Arnavaz Garda

Flowering in higher plants involves the transition of a vegetative meristem, producing leaves and stems, into a floral meristem, producing flowers. LEAFY (LFY) and APETALA1 (AP1) are transcriptional regulators that play a key role in the initiation of floral development in the plant Arabidopsis thaliana. The LFY gene and its direct target AP1 are primarily expressed in the whole meristem and act as a molecular switch to floral development, activating floral homeotic genes in a whorl-specific pattern. To identify genes that are downstream of LFY or AP1, we are using post-translational activation of the transcription factors in planta, using different mutant backgrounds and different tissues. The transcription factors are fused to the hormone-binding domain of the rat glucocorticoid receptor, and these fusions can be activated in planta by treating with dexamethasone. We use whole-genome microarray analysis at different time points after this induction, to find genes that are differentially expressed upon induction of LFY or AP1.

Following the identification of LFY and AP1 downstream genes using microarray analysis, we will perform chromatin immunoprecipitation (ChIP) experiments coupled to promoter-array analysis to identify the direct target genes. To provide an inducible activity of the transcription factors, we will use plants expressing 35S : LHG4-GR ; 6XOP : AP1 (or LFY)-Tag constructs. To enhance the sensitivity of the assay, the ChIP experiments will be coupled to promoter-array hybridization. Together with the transcriptional analysis, these experiments should lead to a better view of the genetic networks acting downstream of LFY and AP1. The genes that have been identified using the microarrays will be confirmed by quantitative PCR, and their expression patterns will be determined by in situ hybridization. They will be grouped according to their expression pattern for promoter analysis. Furthermore, some of them will be chosen for functional characterization, to study their role in the LFY/AP1 genetic pathways.

407. Looking for genes involved in the AP1 pathway

Annick Dubois, Carolyn Ohno, Patrick Sieber

We are interested in understanding how AP1 functions in the determination of floral organ identity and meristem identity. A very weak recessive allele of AP1 (ap1-511) has been identified that does not resemble any previously characterized alleles of the gene. The mutant plants have an enlarged inflorescence, petaloid sepals, and extra petals in the first 12 to 15 flowers. In contrast to ap1-511, strong loss-of-function ap1 alleles produce bract-like sepals in the first whorl, reduced petal number in the second whorl of the flower, and secondary flowers that initiate in the axils of the first whorl organs. Similar to other ap1 alleles, the ap1-511 allele also interacts with leafy alleles. The ap1-511 EMS-induced mutation results in an amino-acid substitution in the K domain of AP1, a domain which was shown to be involved in the interaction with the SEP3 transcription factor, and the B function transcription factors AP3 and PI. To better understand the AP1 pathway, and to identify potential partners of AP1, we have done an EMS mutagenesis screen to identify enhancers of this weak mutant phenotype. Three groups of enhancers have been identified in the first group, plants have a phenotype resembling more severe alleles of AP1. Most of these plants have an extra mutation in the coding region of the AP1 gene responsible for the phenotype. Some of them that are not mutated in the AP1 coding region are currently being analyzed. In the second group, the petaloid sepal phenotype is enhanced. These lines are currently being outcrossed and the single mutant phenotypes are being characterized. Finally, two families of enhancers have more petals than the initial mutant, and are currently being outcrossed and mapped.

408. **EEP1** microRNA regulates organ number during flower development in **Arabidopsis thaliana**

Catherine Baker*, Patrick Sieber, Frank Wellmer, Elliot Meyerowitz

Flowers of *Arabidopsis* are normally composed of a nearly invariant number of organs (i.e., four sepals, four petals, six stamens and two fused carpels from the outermost whorl to the center). We have detailed knowledge of how floral organs adopt their specific identity by the combinatorial action of floral homeotic genes. However, the mechanisms by which the number of organs and their location within a specific whorl are specified, is less understood. Plants homozygous for a mutation affecting the EARLY EXTRA PETALS 1 (EEP1) locus have extra petals in the first 10 to 15 flowers, with normal petal number in subsequent flowers. Neither meristem size nor organ numbers of other whorls are affected in eep1. We identified the EEP1 locus by map-based cloning. The eep1 mutant phenotype co-segregates as a recessive trait with a naturally occurring TAG1 transposon insertion approximately 160 base pairs upstream of a previously un-annotated microRNA on chromosome V. Reintroducing a 3 kb genomic fragment

into eep1 mutant plants rescues the mutant phenotype. EEP1 is related to two sister microRNAs in the *Arabidopsis* genome, and at least six *Arabidopsis* genes contain a putative target sequence with high complementarity to EEP1. All putative targets belong to the NAC family of transcription factors. Quantitative real-time PCR and in situ hybridization analysis showed that transcription of two targets, cup-shaped cotyledon1 (cuc1) and cuc2, is up-regulated in eep1 when compared to wild type. The phenotype of the cuc1 cuc2 eep1 triple mutant is consistent with the hypothesis that the eep1 phenotype is the result of up-regulated CUC1 and CUC2 expression. No loss-of-function in a plant microRNA showing a phenotype distinct from wild type has been reported thus far. This makes eep1 mutant plants a valuable tool to address questions like as to what extent EEP1 and its sister microRNAs are functionally redundant. Complementation tests showed that only one of EEP1's two sister microRNAs is able to rescue the eep1 mutant phenotype, indicating that they can be functionally distinct. The phenotypic defects observed in eep1 occur in a sub-population of EEP1-expressing cells. This might be due to redundancy with its sister microRNAs. We have identified a knock-out mutant in two of the sister microRNAs. Analysis of the triple mutant might reveal redundant functions among the related microRNAs during flower development.

*Current Address: Stanford University, Stanford, CA

409. Identification of additional factors in the **EEP1** microRNA regulated pathway of organ boundary formation in **Arabidopsis thaliana**

Patrick Sieber, Catherine Baker*, Frank Wellmer, Elliot Meyerowitz

Floral organ arrangement in *Arabidopsis* follows a nearly invariant pattern. Organs initiate in four concentric whorls, each whorl occupied by a single class of organs, e.g., four sepals, four petals, six stamens and two fused carpels from the periphery to the center. Flowers of early extra petals 1 (eep1) loss-of-function mutants make more petals in the first 10 to 15 flowers. Petal primordia initiate at the correct position in eep1 mutants, but often additional primordia form very close to the initial petal primordia and split primordia are frequently observed. In addition eep1 mutant plants show a mild carpel fusion defect during gynoecium development. EEP1 "encodes" a microRNA, which negatively regulates the transcription of members of the NAC family of transcription factors and that way prevents the formation of ectopic boundaries in the second whorl of the flower.

In order to identify additional factors with a role in organ boundary formation, we transformed eep1 mutant plants with the plasmid vector pSKI015. The inserted T-DNA contains four copies of an enhancer element from a strong viral promoter pointing outwards. This enhancer can increase transcription of flanking genes and thus allows screening for dominant "activation-tagged" traits in the T1 generation and in addition permits the identification

of homozygous recessive loss-of-function phenotypes in the T2 generation. We screened 1664 transgenic lines for enhancers and/or suppressors of the *eep1* mutant phenotype and have identified 19 mutants awaiting further characterization. We categorized the mutants into five categories according to morphological criteria, where numbers in brackets indicates numbers of mutants falling into a distinct class: extra late petals (1); large and fused petals (1); apetala-like (5); over-proliferation of gynoecium marginal tissue (5); and various (7). Over-expression of a microRNA-resistant version of one of the EEP1 targets from a strong and constitutive promoter leads to overproduction of gynoecium marginal tissue. EEP1 is expressed in the carpel margins and also necessary for proper carpel fusion thus some of the affected genes might encode functions either upstream of EEP1 or downstream of the EEP1 target genes in the process of postgenital carpel fusion. Identification of genomic sequences flanking the T-DNA insertions by using thermal asymmetric interlaced-PCR (TAIL-PCR) is in progress.

*Current Address: Stanford University, Stanford, CA

410. A family of putative mechanosensitive ion channels in *Arabidopsis thaliana*

Elizabeth S. Haswell, Elliot M. Meyerowitz

Little is known about the process by which mechanical signals such as gravity, vibration, touch or osmotic cues are sensed and transduced into the appropriate cellular responses (1). The bacterial mechanosensitive ion channels MscS and MscL are required to maintain cell integrity during extreme osmotic downshock, and are thought to be gated by deformation of the membrane in which they are imbedded (2). Genes with homology to MscS and MscL were recently identified in Archaea and cell-walled eukaryotes (3). We identified a ten-member family of putative mechanosensitive ion channels in *Arabidopsis thaliana*, termed AtMS1-10, and have initiated the characterization of these genes and the proteins they encode. Insertional mutants for eight of the ten AtMS genes were collected, and their phenotypes are being assessed along with transgenic plants that overexpress each AtMS gene. We have also characterized the expression pattern of six AtMS genes using reporter transgenes. These six genes are expressed in various tissues that are likely to be engaged in turgor-driven processes, such as the root vasculature, the guard cells of the stomata (Figure 1), the chalazal endosperm, and young tissues undergoing cell expansion. Further characterization of the expression pattern of these genes, as well as expression analysis of the other four AtMS genes are underway, should provide clues to the function of the AtMS gene family in plant growth and development. AtMS-GFP fusion proteins are localized to various cellular membranes, including mitochondria, the plasma membrane, and probable inclusion bodies. We anticipate that further characterization of the AtMS genes and gene products will provide insight into the mechanism and physiological relevance of mechanosensation in plants.

References

- (1) Garcia-Anoveros, J. and Corey, D.P. (1997) *Annu. Rev. Neurosci.* 20:567-594.
- (2) Perozo, E. and Rees, D.C. (2003) *Curr. Opin. Struct. Biol.* 13:432-442.
- (3) Martinac, B. and Kloda, A. (2003) *Prog. Biophys. Mol. Biol.* 82:11-24.

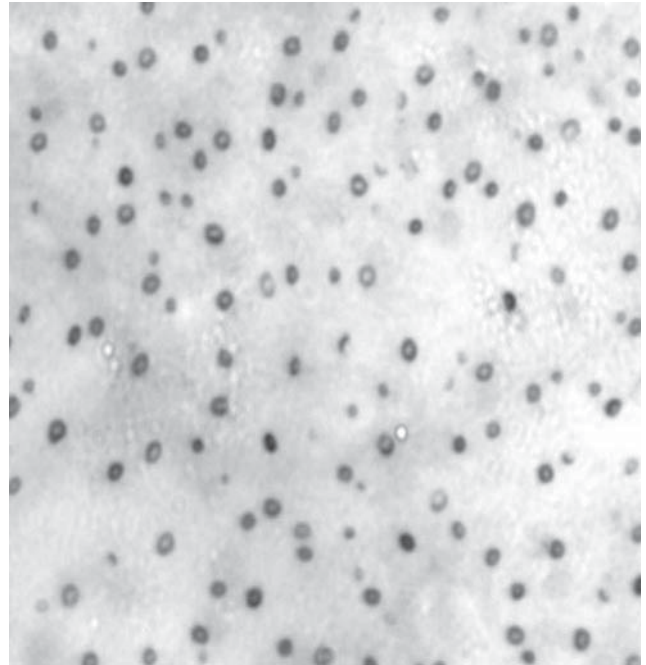


Figure 1

The AtMS4 promoter drives reporter gene expression (visualized as a blue precipitate) in the guard cells of the stomata.

Publications

- Ito, T., Sakai, H. and Meyerowitz, E.M. (2003) Whorl-specific expression of the SUPERMAN gene of *Arabidopsis* is mediated by cis elements in the transcribed region. *Curr. Biol.* 13:1524-1530.
- Ito, T., Wellmer, F., Yu, H., Das, P., Ito, N., Alves-Ferreira, M., Riechmann, J.L. and Meyerowitz, E.M. (2004) The *Arabidopsis* homeotic selector protein AGAMOUS directly controls a gene involved in microsporogenesis. *Nature*. In press.
- Jönsson, H., Shapiro, B.E., Meyerowitz, E.M. and Mjolsness, E. (2003) Signaling in multicellular models of plant development. In: *On Growth, Form, and Computers*, Kumar, S. and Bentley, P.J. (eds.), Academic Press, London, UK, pp. 156-161.
- Jönsson, H., Shapiro, B.E., Meyerowitz, E.M. and Mjolsness, E. (2004) Modeling plant development with gene regulation networks including signaling and cell division. In: *Bioinformatics of Genome Regulation and Structure*, R. Hofstaedt and N. Kolchanov (eds.), Kluwer, Boston, pp. 311-318.

- Ohno, C., Reddy, G.V., Heisler, M. and Meyerowitz, E.M. (2004) The Arabidopsis JAGGED gene encodes a zinc finger protein that promotes leaf tissue development. *Development* 131:1111-1122.
- Reddy, G.V., Heisler, M.G., Ehrhardt, D.W. and Meyerowitz, E.M. (2004) Real-time analysis reveals oriented cell divisions associated with morphogenesis at the shoot apex of Arabidopsis thaliana. *Development*. In press.
- Wagner, D., Wellmer, F., Dilks, K., William, D., Smith, M.R., Kumar, P.P., Riechmann, J.L., Greenland, A.J. and Meyerowitz, E.M. (2004) Floral induction in tissue culture: A system for the analysis of LEAFY-dependent gene regulation. *Plant J.* In press.
- Wellmer, F., Riechmann, J.L., Alves-Ferreira, M. and Meyerowitz, E.M. (2004) Genome-wide analysis of spatial gene expression in Arabidopsis flowers. *Plant Cell* 16:1314-1326.
- Yu, H., Ito, T., Wellmer, F. and Meyerowitz, E.M. (2004) Repression of AGAMOUS-LIKE 24 promotes floral meristem identity in flower development. *Nature Gen.* 36:157-161.
- Yu, H., Ito, T., Zhao, Y., Peng, J., Kumar, P. and Meyerowitz, E.M. (2004) Floral homeotic genes are targets of gibberellin signaling in flower development. *Proc. Natl. Acad. Sci USA* 101:7827-7832.
- Zhao, Y., Medrano, L., Ohashi, K., Fletcher, J.C., Yu, H., Sakai, H. and Meyerowitz, E.M. (2004) HANABA TARANU is a GATA transcription factor that regulates shoot apical meristem and flower development. *Plant Cell*. In press.

Professor of Biology: Ellen V. Rothenberg
 Members of the Professional Staff: Rochelle Diamond, Mary Yui
 Senior Postdoctoral Scholar: C. Chace Tydell
 Postdoctoral Scholars: Satoko Adachi, Deirdre Scripture-Adams, Elizabeth-Sharon David Fung, Tom Taghon, Angela Weiss
 Graduate Students: Christopher Dionne, Luigi Warren, Mark Zarnegar
 Undergraduate Student: Christopher Franco
 Research and Laboratory Staff: Stephanie Adams, Alexandra Arias, Ruben Bayon, Parvin Hartsteen, Rashmi Pant

Support: The work described in the following research reports has been supported by:

- DNA Sequencer Patent Royalty Funds
- Elizabeth Ross Endowment
- NASA
- National Institutes of Health

Summary: The Rothenberg group seeks to define the molecular mechanisms that control commitment of hematopoietic precursors to develop into T lymphocytes. Lineage choice in hematopoiesis is a combinatorial function of the activities of multiple transcription factors. At the same time, the set of permitted outcomes available to a given precursor is restricted by inputs from signaling molecules in the microenvironment. Thus, whereas any particular lineage choice (e.g., "T vs. B lymphocyte") can be seen to be controlled by one of these factors, an understanding of the full lineage commitment process ("T vs. anything else") must take into account the activities of multiple factors, and also the timing and microenvironmental contexts of their actions. In the past several years, new cellular and molecular approaches have begun to make such an undertaking approachable. Individual projects in this lab dissect particular components of the process, addressing the gene expression changes associated with each stage of the commitment process and the regulatory influences that control them.

T-lineage commitment is a protracted process that can remain inconclusive for up to ten rounds of cell division, even while T-lineage associated gene expression begins. The most persistent alternatives to T-lineage fate are development into B cells, into natural killer cells (NK), or into non-lymphoid components of the innate immune system known as dendritic cells (DC). The transcription factors PU.1 (or its close relative Spi-B), Id2 in opposition to bHLH type I factors (e.g., E2A and HEB), and GATA-3, together with microenvironmental stimuli from Notch/Delta interactions and cytokine receptors, have been identified as potent influences in these choices throughout the period of cell fate "negotiation." Over the past several years, we have carried out gain-of-function perturbation experiments with several of these factors, assessing the immediate dose-dependent changes in gene expression and the developmental effects that result in the longer term. In current work, we are optimizing ways to complement these

gain-of-function experiments with methods of causing loss of regulatory function. Many germline gene knockouts are available in the mouse system. However, the effects of these transcription factors are exquisitely stage-dependent, even in terms of their effects on the same target genes. To understand the process through which these factors collaborate to bring about T-lineage specification, perturbation studies must be focused on very specific time windows and developmental states. Thus, one major issue that our group has tackled in the past year has been to define the exact time course of regulatory changes during the approach to T-lineage commitment, both *in vivo* and *in vitro*. Using a new stromal co-culture system, we have been able to dissect the kinetics of this process in detail and determine the degree to which each step is reversible.

A paradoxical feature of T-cell specification is that none of the factors required for this process appears to be a simple, instructive positive regulator: none of them appears to enhance the number of cells developing as T cells when it is overexpressed in multipotent progenitors. This could be explained by a need to maintain a delicate balance of factors at all steps, or because some key rate-limiting regulator has not yet been identified. In a gene discovery project, we have characterized the broad set of transcription factors, cofactors, chromatin remodeling factors, and other potential regulatory players expressed in the earliest stages of T-cell development, and using a subtractive hybridization analysis we have identified a subset of these genes that appears to be specifically upregulated in early T as opposed to early B or early myeloid cell development. While this work continues, the factors are being screened to determine which are expressed in a tight correlation with particular phases of T-cell specification, using the *in vitro* stromal coculture system just described.

The prospects of explaining how these factors work in development depend on being able to show how they alter the expression of functionally important genes. This is difficult to do in primary hematopoietic precursors. However, in one project in the lab, we have established subclones from an immature T cell-like lymphoma cell line which differ sharply in their developmental plasticity under perturbation. These clones constitute a valuable tool for studying the commitment phase of the T-cell development process, and provide a convenient and resilient system in which to carry out perturbation analyses and molecular biological characterization of transcription factor/target gene interactions. We are taking advantage of this resource to investigate the interaction between endogenous transcription factors and activation of signaling pathways during T-lineage commitment, to define the quantitative effects of mutations in protein-interaction domains of a transcription factor, and to examine the chromatin configurations associated with different states of permissiveness for expression of important genes.

T-lineage commitment is apparently complete only when the cells pause before the β -selection checkpoint. This is when, for the first time, the cells are

tested for success in undergoing a productive T-cell receptor gene rearrangement. The enforcement of the checkpoint could be linked, directly or indirectly, with the mechanisms that complete commitment. It is therefore interesting to examine the rare cases in which cells can bypass the β -selection checkpoint without a rearranged T-cell receptor gene. One of these cases is found in the autoimmunity-prone NOD mouse. We have found that the NOD precursors are deranged in their developmental control of the checkpoint and have determined a unique pattern of gene expression perturbations that are correlated with the NOD-specific form of checkpoint violation. Genetic mapping studies are being undertaken to assess whether this checkpoint breakthrough depends on a locus that has been associated previously with autoimmunity.

T and B lymphocytes appear to have emerged as definite cell types only at the base of the vertebrate radiation. The cartilaginous fish, the most anciently divergent group of jawed vertebrates, have well-defined B and T lymphocytes and lymphoid organs with properties similar to those of birds and mammals. In contrast, there are lymphoid-like cells in the jawless vertebrates, the lampreys, which have recently been shown to use a somatic gene rearrangement program to generate diverse recognition specificities, but acting on a totally different gene family than the one that encodes the lymphocyte receptors in jawed vertebrates. For the past several years, therefore, we have examined the transcriptional regulatory profiles of hematopoietic tissues in cartilaginous fish and have begun to compare them with those of lampreys. The skate, a cartilaginous fish, demonstrates that the transcription factor usage seen in mammals is strikingly well conserved in skate hematopoietic cells, with a few alterations in detail. The lamprey possesses representatives of most of the same transcription factor families as those used in lymphocytes of jawed vertebrates, but our initial results indicate that they may be used differently and may differ substantially in structure outside of the DNA-binding domains. The lamprey poses an excellent test case of a general evolutionary question: whether transcription factor combinations may be conserved for particular developmental programs, even when those programs have diverged so as to activate different target genes.

411. Transcriptional changes induced by Notch signaling and a transcriptional and kinetic analysis of B- and T-cell development
Tom Taghon

B and T lymphocytes are blood cells that belong to the adaptive immune system and are characterized by receptors on the cell surface that are responsible for recognizing pathogens and eventually for their elimination from the body. Besides these similar characteristics, B and T lymphocytes have many different features, one of them being the place in the body where they originate. While B cells, like other blood cell types, develop in the bone marrow, T lymphocytes require a specific niche for their maturation, provided by an organ that is called the thymus.

As a result of this specific requirement, studying the development of T lymphocytes has been seriously hampered. B cells can easily be generated *in vitro* by culturing hematopoietic progenitor cells on OP9 cells, a bone marrow derived stromal cell line. Recently, a cell culture system was reported by a Canadian research group (1) that also allows T-cell development in the absence of the thymus. To accomplish this, they stably introduced Delta-like ligand, which interacts with Notch, into OP9 cells. Notch signaling is critical for T-cell development and continuous activation of this pathway inhibits B-cell differentiation. As a result, developing hematopoietic cells can no longer develop into B cells on the OP9 stromal cells that express the Delta-like ligand but instead differentiate along the T-cell pathway. We used this tool to carefully monitor the kinetics and transcriptional effects of the development of hematopoietic progenitor cells into B and T cells, starting from the same progenitor cells, to understand more clearly the instructive signals provided by Notch signaling.

Notch-specific target genes are already upregulated after 24 h of culture in progenitor cells cultured on OP9 cells that express Delta-like ligand. These genes, however, are not necessarily the T-cell specific genes that would indicate that the cells have become specified towards the T-cell lineage. Known genes for both T- and B- cell specification seem to be induced only after 72 h of culture, in parallel with the identification by FACS analysis of the first cells with B or T cell committed progenitor phenotypes in these cultures. Remarkably, clonal analysis shows a high variability in the responses of hematopoietic progenitor cells to the instructive Notch signals, as some single cells can still give rise to B cells after 1 week of continuous Notch signaling. This shows a high degree of plasticity in lymphoid progenitors to respond to Notch signaling and indicates that continuous activation of the Notch signaling pathway is required to sustain T-cell development.

Reference

Schmitt, T.M. and Zúñiga-Pflücker, J.C. (2002) *Immunity* 6:749-756.

412. Notch target genes and their roles in T-cell development

Tom Taghon

Notch receptor signaling results in expression of downstream target genes which clearly must have important roles during T-cell development. However, it is still not clear which of those genes are responsible for the induction of T-cell development at the expense of B-cell development. Among the Notch target genes are members of the HES and HERP families of transcription factors. Using the OP9 coculture system with fetal liver cells as input, we know that HES-1, HERP-1 and HERP-2 are upregulated within 24 h of Notch signaling. It is known that HES-1 alone is not capable of completely replacing Notch signaling, however, little is known about the role of HERP-1 and HERP-2. Besides being expressed in fetal

liver cells after induction of the Notch signaling pathway, we observed expression of both genes at the DN3 stage of T-cell development, correlating with the highest levels of Notch signaling during early T-cell development. Overexpression of HERP-1 or HERP-2 results in inhibition of both B- and T-cell development, indicating also that HERP proteins alone are not sufficient to mimic Notch signaling. Therefore, our current approach is to perform a double infection to overexpress both HES and HERP in the same cells since it is known from other developmental systems that they can form heterodimers.

413. Using retroviral expression of siRNAs to test the requirement for GATA-3 at the DN3 stage of thymopoiesis

Deirdre D. Scripture-Adams

The development of the cells in the blood is a complex, controlled process, requiring precise regulation of gene transcription at each stage of development. Progression and survival is dependent upon a correctly regulated procession of changes in the nuclear complement of transcription regulators. Transcription factors control both increases and decreases in expression of developmentally important genes, and which factors are present changes as the cells progress along the T-cell developmental pathway. This ebb and flow of transcription factors is incompletely understood.

Retroviral infection has been used extensively in our group to evaluate the effects of experimentally inducing high levels of different transcription factors within developing T cells and has allowed us to identify several stages in T cell-development which require down regulation of these factors in order survive and/or progress through the T-cell developmental program. These experiments cannot tell us which factors are essential at a given T cell developmental stage, however, nor can they help us discover whether alternative fates are available to developing cells in the absence of certain putatively required transcription factors.

To identify a requirement for a particular transcription factor at a certain developmental stage, we are using retrovirally delivered siRNA transcripts which can prevent protein synthesis of our transcription factors of interest in infected cells. Small interfering RNAs (siRNA) interact with mRNA within the cell, and through the action of an enzyme called DICER, destroy the mRNA, eliminating production of protein from the relevant gene. These viruses also expresses a green fluorescent protein tag, which allows easy identification of infected cells with decreased levels of a transcription factor of interest.

We have first used this virus system to study the role of GATA-3 in early T development. GATA-3 is essential for T-cell development from the earliest stages, but it is mostly maintained at low levels and can block T-cell development if overexpressed (see next abstract). Thus, a stage-specific loss-of-function approach is needed to reveal its roles. These experiments can be done in the adh.2C2 system (a DN3-like cell line), in fetal liver derived haematopoietic precursors grown on OP9 or

OP9-DL1 stromal cell layers (suitable for promoting B or T cell development, respectively), and in primary early thymocytes. Reduced expression of the gene of interest is monitored by quantitative PCR after reverse transcription of cellular RNA. Flow cytometry is used in these experiments to monitor developmental changes as assessed by changes in surface expression of key developmental marker proteins. Preliminary data suggest that loss of GATA-3 is catastrophic for the DN3 stage T cell: Although initial levels of retroviral infection are comparable between the siRNA containing vector and the control virus, cells containing the siRNA (and thus losing GATA-3 protein) quickly disappear from cultures, suggesting either death or lack of competitive advantage. This is accompanied by increasing levels of CD25 and CD8, both important developmental markers. Initial studies in primary cells suggest that the loss of GATA-3 is lethal: Cells infected with the GATA-3 siRNA producing virus have not been observed to survive with levels of infection comparable to control infections, suggesting that GATA-3 might be critical for survival in these early stage cells. These experiments will be expanded upon with the development of additional siRNA producing viral vectors to knock down other important transcriptional regulators in the T and B cell developmental pathways, and with the use of additional culture systems currently under development in the lab.

414. A developmentally regulated upper limit for GATA-3 activity in T-lineage differentiation

Tom Taghon, Alexandra Arias

Like Notch1, GATA-3 is essential for T cell development. GATA-3 is one of the first genes turned on during T-lineage differentiation in response to Notch/Delta signaling, and accumulated data from several labs show that T-lineage differentiation cannot begin without it. However, studies that tested the effects of overexpression of this transcription factor have shown that it is important to upregulate GATA-3 at precise stages of T cell development. Paradoxically, overexpression of GATA-3 in mouse fetal liver progenitors results in a drastic loss of GATA-3 infected cells and an almost complete arrest of T cell development at the earliest stage. However, in a few experiments some cells apparently escaped this developmental block, and these were apparently able to differentiate further. Cells transduced with GATA-3 at later stages in the thymus show much more selective effects. These data, combined with evidence from overexpression studies with human thymocytes, suggest that the developing T lymphocytes show different sensitivities to high level GATA-3 expression at different stages of their development.

Two kinds of approaches are being used to investigate the mechanisms that confer GATA-3 tolerance on developing T cells. First, we are testing the effects of overexpressing wild-type GATA-3 and a hypomorphic form of GATA-3, the GATA-3 KRR mutant, which has previously been found to allow more proliferation than the wild-type form of GATA-3. After retroviral transduction,

the transduced cells are assayed for T and non-T lineage differentiation on OP9-control and OP9-DL1 stromal monolayers. The results appear very different depending on the source of the precursor cells. The GATA-3 KRR mutant had identical effects with wild-type GATA-3 in prethymic fetal liver cells, blocking B and myeloid development as well as T-cell development. However, effects of the mutant form sharply diverged from those of wild-type GATA-3 when expressed in fetal thymocytes, in which the mutant permitted extensive, almost-normal T-cell differentiation in contrast to the inhibitory effects of the wild-type gene. Wild-type GATA-3 appeared to foster the development of an abnormal, c-kit⁺ population from both prethymic and thymic precursors. This abnormal differentiation could also occur in stromal-free culture, supported by cytokines alone.

A second approach has been to construct a GATA-3/Estrogen Receptor chimeric protein that allows for the conditional activation of GATA-3. This allows GATA-3 overexpression to be quantitatively and temporally controlled. Overexpression of this chimeric protein results in effects like those of wild-type GATA-3 in the presence of tamoxifen, and greatly attenuated effects in the absence of tamoxifen. The correlation of these developmental effects with actual intranuclear protein levels is still being investigated. However, both the inhibitory effects of GATA-3 on lymphoid and myeloid differentiation and the promotion of the unusual c-kit⁺ cells are duplicated by the GATA-3/ER chimera.

A central question is how the combined effects of Notch and properly titrated GATA-3 activity result in the blockade of this abnormal differentiation pathway as well as fostering the T-cell pathway. We will further investigate this by retroviral overexpression in precisely defined cells at different stages of T-cell differentiation and by eliminating GATA-3 expression using RNAi constructs as described in the previous abstract. The kinetic framework established in the studies described in abstract 411 now enables us to design experiments to pinpoint the critical durations of Notch/Delta signaling, affected subpopulations, and gene expression requirements for the shifting effects of GATA-3.

415. Functional analysis of the hematopoiesis-specific transcription factor PU.1 in the development of T lymphocytes
Angela Weiss, Christopher Franco, Rochelle Diamond

PU.1 is a hematopoietic-specific, Ets family transcription factor which is necessary for the development of a variety of hematopoietic lineages, including T lymphocytes. It is known that PU.1 expression is downregulated during T-cell commitment and that constitutive expression of PU.1 blocks all T-cell development. Using retroviral transduction into murine fetal liver cells, fetal thymus cells, and SCID.adh cell line derivatives (see next abstract), followed by quantitative gene expression analyses, we are resolving the effects of PU.1 overexpression on T-cell development. These

experiments have shown that sustained expression of PU.1 can inhibit the T-cell program at several different points. Overexpression can block entry into the lymphoid precursor pathway, as shown by a rapid inhibitory effect on the emergence of c-Kit⁺ CD27⁺ Lin⁻ fetal liver progenitors in short-term culture. This effect probably reflects the ability of high-level PU.1 to block lymphocyte development of multipotent progenitors while allowing myeloid development. Once precursor cells are already established in the fetal thymus, and no longer multipotent, PU.1 transduction still blocks development in the T-cell lineage, but now without promoting myeloid development. Although PU.1 can inhibit RAG gene expression, this inhibitory effect does not depend on an inhibition of TCR gene rearrangement, since PU.1 even inhibits T-cell development of precursors from TCR-transgenic mice. These results show that continued expression of PU.1 is incompatible with T-cell development even when it cannot divert the cells to an alternative developmental fate (see next abstract).

The gene expression effects of PU.1 are context dependent, and there are different effects on the same target genes when measured in PU.1-overexpressing fetal liver precursors or in thymocytes. This is presumably the result of interactions with different sets of cooperating and competing transcription factors in these two developmental states. Thus, a full explanation of the developmental effects of PU.1 in terms of gene expression will need further work.

We are also in the process of localizing the effects of PU.1 overexpression to particular functional domains of the transcription factor with the use of specific functional domain mutants. By expressing these deletion mutants in primary cells and cell lines, we have found that the Ets DNA-binding domain is required for the block in T-cell development, but that the Q-rich transactivation and PEST domains are not. It still remains to be determined whether the DNA-binding domain is sufficient to block T-cell development. To do so, we must determine what role, if any, the N-terminal acidic transactivation domain of PU.1 plays in the development of T cells.

416. Subversion of T-lineage commitment by PU.1 in a clonal cell line system
Christopher J. Dionne, Kevin Tse*

The lack of a cell line representative of stages in early thymocyte development has limited probes into the mechanism of T-lineage commitment. As described in last year's Annual Report, we have recently developed a panel of clones from the SCID.adh murine thymic lymphoma line that appear to fill this niche. The subcloned cell lines adh.2C2 and adh.6D4 have similar, committed pre-T-like phenotypes but markedly divergent responses to forced expression of the Ets family transcription factor PU.1, which thymocytes normally express before commitment. PU.1 induces a large fraction of adh.2C2 cells to undergo diversion to a myeloid-like phenotype with multiple coordinate gene expression changes, whereas many adh.6D4 cells commit suicide while preserving T-lineage

gene expression in the survivors. Stimulation via phorbol ester or type I interferon relieves the block to lineage diversion in adh.6D4 cells without enhancing survival. The results show distinct roles for regulated cell death and for another discrete, MAP kinase-sensitive function establishing a threshold for competence to undergo diversion. The SCID.adh subclones reproduce features of normal T-cell development, for Bcl2-transgenic primary pre-T cells can also be diverted to a Mac-1⁺ phenotype when transduced with PU.1 in short-term culture. The adh.2C2 and adh.6D4 clonal cell lines thus provide an attractive, accessible system in which to define mechanisms controlling developmental plasticity in early T cell development.

*Undergraduate, Caltech; present address: University of California San Diego Medical School

417. Identifying the potential regulatory elements controlling PU.1 expression
Mark Zarnegar

The Ets family transcription factor PU.1 is restricted to hematopoietic cells and is differentially expressed in the various blood lineages. The transcription factors controlling PU.1 transcription and the regulatory elements through which they function have yet to be determined. We are particularly interested in understanding how PU.1 is turned off in developing T cells. Early thymic precursors (DN1 and DN2) express PU.1 but cease to express it by the time they become committed to the T-cell lineage (DN3). Failure to turn off expression prevents further T-cell development (see abstracts 415 and 416). By comparing the sequences of the mouse and human loci, we have identified several pockets of Conserved Elements (CE1-9) upstream of exon 1 that may function to regulate PU.1 transcription.

DNase hypersensitivity (DHS) and chromatin immunoprecipitation assays (ChIP) were used to characterize the accessibility of the conserved upstream regions. The DHS assays revealed regions of chromatin that are open in both PU.1-expressing myeloid cells and in non-expressing T cells, at -14 kb near CE8-9. ChIP assays were used to examine the acetylation patterns of histones 3 and 4, and of methylated histone 3 at lysine 4. These histone modifications are correlated with gene expression. Using quantitative real-time PCR to analyze the ChIP assays, several distinct patterns emerged. Myeloid cells (express high levels of PU.1) showed a high degree of acetylated H3 and H4 across regions CE1-CE9. Early B cells (moderately express PU.1) showed high levels of acetylation at only CE1, CE8, and CE9. While committed T cells (do not express PU.1) also have elevated levels of H3 and H4 acetylation at CE8 and CE9 relative to CE1-7, the degree of histone modification is much less than in the PU.1 expressing lineages. The data suggests CE3-7 may contain a myeloid-specific enhancer, while CE8-9 may be nonspecific but critical to all PU.1 expressing cells. The conserved element that may be involved in turning off PU.1 in T-cells remains unclear.

Much effort has gone into identifying the transcription factors that bind and thus control the activity of the potential regulatory elements. Previous electrophoretic mobility shift assays implicated two important transcription factor families, Ets and Runx, which may contribute to the regulated expression of PU.1. Members of these families bind CE8 in vitro. In vivo footprinting also suggests CE8 is bound by Runx and/or Ets proteins. The footprinting analysis also indicates that CE8 is occupied by different factors in T cells, B cells, and myeloid cells, perhaps contributing to the different PU.1 expression patterns in these lineages. Gel shifts are currently being performed across CE3-CE7. Early results indicate several potential cell type-specific complexes.

418. Functional characterization of PU.1 regulatory elements
Mark Zarnegar

We are developing several systems to examine the regulatory functions of CE1-9. Standard transient transfections and production of cell lines with stably integrated PU.1 regulatory constructs is underway. We are creating reporter constructs under the control of various combinations of CE1-9. Transient transfections of PU.1 expressing and non-expressing cells with our luciferase and/or GFP reporters will indicate potential functional activity of the different elements. The stable integrants may provide insight into the requirement of chromatin regulation for proper PU.1 expression.

In order to discern the normal in vivo PU.1 expression pattern, will utilize transgenic animals. By creating a "knock-in" mouse, with an IRES-GFP inserted into the PU.1 3' UTR, we hope to be able to follow GFP expression patterns in a developing embryo as controlled by normal PU.1 regulatory elements. Once the normal expression of PU.1 is fully known, we will use the knock-in animal as a background for perturbations in PU.1 regulatory domains. We are constructing PU.1-BAC constructs with deletions of particular conserved elements. The BAC clones will harbor luciferase-IRES-DsRed2 in place of PU.1. By examining GFP vs. DsRed2 using flow cytometry, we hope to determine how the conserved elements contribute to the overall expression pattern of PU.1 in hematopoietic cells. We will also be able to use cell sorting to isolate GFP and/or DsRed2 cells and look at luciferase levels to more quantitatively examine the effects of our deletions.

Transgenic animal studies are time consuming and expensive. An alternative to mouse studies could be the in vitro differentiation of ES cells into T cells. It has previously been shown that ES cells can be cultured to give rise to PU.1-expressing myeloid and B cells, but producing T cells has proven difficult. A tissue culture system has recently been developed that may provide a quicker and more efficient means of studying T-cell development without animals. In terms of development, the thymic environment is most important for providing Notch stimulation of progenitors to allow T-cell development while inhibiting B cells. A bone marrow

stromal cell line, OP9, stably transduced with the Notch ligand Delta-like-1, has been shown to give rise to T cells when co-cultured with embryonic stem cells (1). We are attempting to develop this system for use in studying PU.1 expression. This system would allow us to transfect ES cells with BAC constructs and follow reporter expression. From the same ES cell, we could observe how our deletions affect PU.1 expression in myeloid, B cells, T cells, and non-hematopoietic lineages. This will allow us to perform a much greater range of experiments on a significantly smaller time-scale. The *in vitro* differentiation system may also make it possible to perform RNAi and overexpression analysis with transcription factors thought to affect T-cell development.

Reference

1. Schmitt, T.M. et al. (2004) *Nat. Immunol.* 5:410-417.

419. A regulatory "parts list" for early T-cell development

Elizabeth-Sharon D. (David) Fung, Lee Rowen*

In an attempt to determine the participants in the changing transcriptional state and networks of developing thymic pro-T cells, a series of screens were devised to identify cDNAs encoding putative transcription factor and signaling mediators. A cDNA library from SCID thymocytes, representing T-cell precursors up to the stage of commitment, was arrayed and screened with transcription factor conserved-domain probes (Michele Anderson and E.-S. David) and from it a smaller, transcription factor-enriched re-array was constructed. By using mRNA from mouse thymi and from cell lines that represent different stages of stem- and T-cell development as probe on the re-array, clones with a relatively up-regulated expression in pro-T development were identified.

The re-array clones have been completely sequenced, the clones encoding likely regulatory factors have been selected, and quantitative expression studies have now been carried out using quantitative real-time RT-PCR. The genes of interest were first assayed for expression in a panoply of adult mouse tissues. Transcriptional regulators detected more highly in haematopoietic tissues, and especially in thymi (T cell specific) more strongly than in bone marrow (B cell- or myeloid-specific), were then studied in sorted subsets of mouse cells to determine whether they were indeed pro-T cell-specific, lymphoid in character or pan-haematopoietic. Of the pro-T-cell-specific genes, as well as a few lymphoid genes, all expression patterns were assayed in the early stages of pro-T development, viz. DN1 through DN4. Here, several interesting patterns of expression were identified and activators as well as repressors of transcription were seen to be developmentally regulated. Finally, levels of factors that were found to be especially concentrated in the DN1 and DN2 stages were again determined by quantitative PCR, but this time in sorted subsets of the DN1 and DN2 stages of development of mutant B6 Rag2^{-/-} thymocytes, which are known to be free

of more mature contaminants and are enriched for pre-NK cells.

Our results show that several transcription factors have very interesting patterns of expression in specific sublineages or particular stages. Gata3 is slightly upregulated in TCR $\gamma\delta$ T cells, while T-bet is highest in mutant pre-natural killer cells, but also quite high in wild-type DN4 cells. Several transcription factors rise steadily from the wild-type DN1 to DN3 stages of expression, decreasing in DN4, post- β -selection (FoxP4, STAT5b, Tle3, Mta3, and to a certain extent KIAA1115, HKR3 and Period).

Armed with these detailed expression data, we are now using cluster analyses to define linked patterns of expression among the different regulatory genes. Mta3, STAT5b and Tle3 cluster in their expression patterns, as do Pou6f1 with Ets1 and PU.1 with Fli-1. Meanwhile, the Ets transcription factors Fli-1 and PU.1 have a diametrically opposing pattern of expression to that of Ets1 and Pou6f1. These results give us a basis for setting up detailed and networked circuits of transcription factor gene expression at changing stages of early, adult mouse T-cell development.

*Institute for Systems Biology, Seattle, WA

420. Genes upregulated specifically in pro-T cells as compared to pre-myeloid cells

C. Chace Tydell, Elizabeth-Sharon D. (David) Fung, Lee Rowen

To explore the mechanisms guiding hematopoietic precursor cells to a T lymphocyte-fate we have employed a gene discovery technique that allows us to compare transcript abundance in two closely-related cell populations. Traditional genetic methods have only identified two transcription factors that are specifically upregulated in T-cell precursors as compared to other hematopoietic precursors, and the roles of these factors, GATA-3 and TCF-1, do not seem to explain the onset of the T-lineage differentiation program. The arrayed cDNA library from SCID thymocytes (see previous abstract) is likely to contain many genes encoding regulatory proteins that could collaborate in the T-cell program. Therefore we have screened this library for those genes that are specifically upregulated in pro-T cells vs. pre-myeloid cells (also see next abstract for pro-T vs. pro-B). Pro-T cells and pre-myeloid cells were obtained from B6-Rag2 knockout mice through a combination of cell sorting and tissue culture techniques. Subtracting pre-myeloid from pro-T transcripts enriched the resulting probe for sequences that were upregulated in pro-T cells relative to their expression in pre-myeloid cells. The probe was used to hybridize to our macroarray library of more than 70,000 clones generated from thymocytes in the stages immediately preceding commitment. Upregulated clones selected by the pro-T minus pre-M subtraction will include both T-specific and generally lymphocyte-specific transcripts.

Our first approximation of success for the pro-T minus pre-M subtraction was identifying sequences known

to be upregulated in the pro-T population among our enriched clones. Among the 1% most enriched clones, more than 1/3 of the sequences were already reported to be found in pro-T and not in pre-myeloid cells. Among the upregulated clones, we identified several transcription factor candidates not previously linked to T-cell development, by using the BLAST and Ensembl databases. qRT-PCR was used to verify that each of these candidates is indeed upregulated in pro-T relative to pre-myeloid RNA. Rbik (RB-associated KRAB repressor), proThymosin- α (a CBP interacting co-regulator) and Pigen/FUS (a nuclear protein with a zinc-finger motif and putative transcription activation domain) are lymphocyte-specific transcription factors not previously associated with T-cell development. TRIM44, a tripartite motif (or Ring-finger B-box coiled-coil) factor with potential regulatory function, is also expressed in a lymphoid-biased way. ERF (ETS2 repressor factor), BRD4 (bromodomain-containing factor) and RW1 (an uncharacterized protein with a putative AT hook) are candidate transcription factors or transcriptional modulators, identified in the pro-T minus pre-M screen, that are not only enriched in lymphocytes but are specific to the T lineage.

FUS, Rbik, ERF and RW1 have subsequently been verified to be equally upregulated in the pro-T cells of wild-type mice. The impact of each of these genes on development will be explored in overexpression and expression inhibition assays.

*Institute for Systems Biology, Seattle, WA

421. Genes upregulated in pro-T cells as compared to pro-B cells
Elizabeth-Sharon D. (David) Fung, C. Chace Tydell, Lee Rowen*

Early in adult haematopoiesis, daughters of stem cells begin to differentiate down pathways to form functionally different immune cells. Two of these pathways are the lymphoid and the myeloid, and the lymphoid arm of immune development in adults involves the formation of T and B cells. While both cell types originate in the bone marrow, T cells migrate to the thymus early on where, as pro-T cells, they phenotypically change over several weeks until they rearrange T-cell receptor genes successfully and go through β -selection. After this they exhibit newly rearranged T-cell receptor genes, before developing into mature T cells. B cells, however, continue developing in the bone marrow, where in a similar manner they undergo somatic mutation to acquire different clonal recognition properties that then mark them through development into mature, functioning B cells. Our aim has been to isolate genes for transcription factors that are present or up-regulated in developing pro-T-cells over pro-B-cells. This will not only give us an insight into causes of the differences in the two arms of lymphoid development, but also identifies a set of T cell-specific transcription factors – whether activators or repressors of transcription.

Subtractive hybridization was used between two cell populations of mouse B6 Rag2^{-/-} thymic pro-T cells and bone-marrow CD19+ pro-B cells. The subtractate

mRNA species (pro-T minus pro-B as well as pro-B minus pro-T) were used to probe different sets of macroarray filters from the SCID thymocyte pro-T arrayed cDNA libraries. Clones that were calculated to have an up-regulated expression level were sequenced and blasted to NCBI or Ensembl genome servers, for identification.

Our results show that several known, and unknown or putative transcription factors are up-regulated in the pro-T minus pro-B cells. Rbik (RB-associated KRAB repressor) again appeared among the specifically enriched clones. Other interesting T cell-specific clones that we identified were ERF (Ets-2-related factor) and NCor2 (Nuclear Co-receptor 2), both of which we have analyzed by quantitative PCR and shown to be T-cell specific. A startling result was the presence of a large number of mitochondrial DNA clones that seemed most highly expressed in pro-T-cells. The functional relevance of this mitochondrial activation is now being investigated.

Genes that we short-list as being T cell-specific will be tested by over-expression and knock-down studies to ascertain their function and role in specification of pro-T cell development.

*Institute for Systems Biology, Seattle, WA

422. Exploring the state-space of transcriptional regulatory networks

Luigi A. Warren, Josh Marcus, Steven P. Quake*

In hematopoiesis, the state of a small network of regulatory genes dictates the phenotype and lineage potential of developing blood cells. This network can be modeled as a 'state machine' inasmuch as its future time evolution is constrained by the current state at any given point in development. To a first approximation, cell phenotype is an effect of regulatory network state: the transcription of differentiation genes is controlled by the expression of transcription factors, yet the regulatory networks are not themselves regulated by their downstream targets. How does an hematopoietic stem cell produce daughter cells of differing phenotype and potential? The diversity of outcomes within such a clone is due to both external and internal contingencies: the microenvironmental signals the individual cells encounter in their wanderings, and the stochastic nature of gene expression. The relative significance of these two factors is an open question in developmental biology. To investigate, we need a way to probe the activity of regulatory networks in individual cells. Given that, we could explore how network states are distributed within progenitor cell populations and how internal states correlate with phenotype and lineage potential.

The technical challenge is to assay multiple mRNA targets at low copy number (<100 transcripts) in single-cell lysates. To this end, we are developing a sensitive "digital RT-PCR" assay. The effort involves integrating multiplexed qPCR, microfluidics, and microarray scanner technology. To date, we have identified and characterized a suitable lysis/RT-PCR reaction, and we have made considerable progress on the development of the PCR chip. In the near term our efforts

will be focused on proving out multiplex PCR in the chip and on mass-producing the chips. Our ultimate goal is to gather quantitative single-cell regulatory network state data from hundreds of exemplars of the canonical precursor populations known in early T-cell development.

Professor of Applied Physics, Caltech

423. Evolution of transcriptional regulatory ensembles that support lymphocyte development

Rashmi Pant, Stephanie Adams

Previous studies have shown that the signature transcription factors required in T- and B- cell development were available in the genome at least as early as the emergence of chordates (e.g., ascidians) and therefore were not the rate limiting feature for the evolution of lymphocyte development. However, cells with the canonical properties of mammalian lymphocytes appear only in jawed vertebrates. To understand how older regulatory components might have been assembled into the "new" lymphocyte developmental program, it is necessary to look at the deployment of these factors in chordates that lack lymphocytes. Lampreys are jawless fish that seem to be ideal for insights into lymphocyte origins, for they possess cells that morphologically resemble lymphocytes, but without apparent sign of Ig, TCR, or MHC genes that are used for immune recognition by lymphocytes of jawed vertebrates.

The cell and molecular biology of lamprey hematopoiesis have begun a dramatic advancement in the past few years through the application of flow cytometry to isolate these cells and genomic techniques to characterize their gene expression profiles. These cells express homologues of cell adhesion activation molecules, highly diverse receptors with variable leucine rich repeats and some signaling pathway linker molecules that have been deployed for T- and B- cell signaling cascades in jawed vertebrates. New evidence also shows that they use somatic mutation mechanism for clonal receptor diversification, confirming their homology with lymphocytes in jawed vertebrates, even though the receptors used are unrelated to Ig genes. This result shows that the clonal diversification strategy is older than the use of any particular recognition structure.

Building on this evidence from our own and other labs, we are in the process of looking for previously unreported transcription factor genes in the lamprey that are known to play pivotal roles in lymphocyte development, using techniques such as degenerate PCR and library screening. It is also imperative to us to determine whether the transcription factors that collaborate for mammalian lymphocyte developmental programs are co-expressed in the same cells in the lamprey. To this end, our lab is also looking at the gene expression profiles of these purified "lymphocyte like" cells. In the near future we also intend to look at the regulatory sequences of lamprey receptor genes which undoubtedly will provide a rich source of evidence on the conservation of function of specific ensembles of lymphocyte transcription factors.

One lamprey regulatory gene is particularly interesting to study for structure-function relationships with its jawed vertebrate counterparts. The lamprey spi gene encodes a member of the Ets family of transcription factors and has only recently been isolated. The mouse relative of this gene, PU.1, plays regulatory roles in hematopoiesis (see abstracts 415, 416, 417 and 418). The DNA binding domains show great amounts of conservation between the two genes while the rest of the domains, which mediate interactions with other transcription factor genes, show just a hint of similarity. The lamprey spi is found in sites of hematopoiesis in the lamprey but it is not known if its functions in these cells are similar to those of mammalian PU.1. Over the past six months the actual coding portion of the lamprey spi gene was isolated, cloned into an intermediate vector and then transferred to a retroviral vector. It is now awaiting packaging by Phoenix cells, to be used for comparison with mammalian PU.1 in functional studies in mouse cell lines. The exploration of lamprey Spi and other factors in these lymphocyte-like cells may shed light on how the functions and the immune system itself were formed.

424. Developmental potentials of early thymocyte subsets

Tom Taghon, Rashmi Pant

Developing T cells progress through a series of developmental stages in the thymus that can be identified through their expression of cell surface markers. The most immature subsets, called double-negative (DN) thymocytes because they lack the expression of both CD4 and CD8, are classically subdivided into four stages by the use of the markers CD44 and CD25. The most immature thymocytes (DN1) start off with a CD44+ CD25- phenotype. First the cells acquire CD25 to become CD44+CD25+ thymocytes (DN2) and then they downregulate the expression of CD44 (CD44-CD25+). These DN3 thymocytes are undergoing extensive rearrangements of the T-cell receptor β chain genes and if successful, the cells will progress through a process called β -selection to become CD44-CD25- (DN4) thymocytes. These different subsets are still heterogeneous, and recently, the expression of c-kit has been useful as an additional marker to identify the 'true' cells with precursor activity in the DN1 and DN2 subsets. We have investigated the use of CD27 as an additional marker to provide another functionally important distinction. Characterization of these different DN subsets was performed by gene expression analysis and OP9 stromal coculture to identify their developmental potentials.

DN1 cells that express c-kit virtually all express relatively high levels of CD27 and as the cells progress, the expression of this marker is slightly reduced. At the DN3 stage, most of the cells express low levels of CD27. These cells are still in the process of rearranging their T-cell receptor genes, as seen by the high levels of RAG-1 and pT α expression and their failure to express TCR- β chains intracellularly. The small fraction of DN3 cells that express high levels of CD27 do express the TCR- β chain

intracellularly and thus have progressed beyond the β -selection check point. This correlates with a much faster differentiation of the CD27+ cells towards the DP stage of T-cell development, as compared to their CD27 low expressing DN3 counterpart. Thus, CD27 enables us for the first time to phenotypically subdivide the DN3 subset into two different cell populations before and after β -selection. This allows us to precisely characterize the molecular changes that occur at this important stage of T-cell development. However, a very small fraction of the DN3 thymocytes with high levels of CD27 did not express a TCR- β chain intracellularly, suggesting that they may have received a β -selection-like signal by means of a different receptor. One possibility is that these are TCR- $\gamma\delta$ cells. To investigate this further, we also analyzed these DN thymocytes subsets in TCR- β -deficient mice. Interestingly, CD27^{high} DN3 thymocytes were also present in these mice and upon culture, were able to generate TCR- $\gamma\delta$ T cells. Thus, this seems to suggest that TCR- $\alpha\beta$ and TCR- $\gamma\delta$ T cells can follow similar pathways of development. Analysis of transcription factor expression in the different DN subsets of wild-type and TCR- β deficient mice shows few significant differences thus far, further demonstrating this similarity.

425. Deranged early T-cell development in immunodeficient strains of non-obese diabetic mice

Mary Yui

Non-obese diabetic (NOD) mice exhibit defects in T-cell functions, which have been postulated to contribute to diabetes susceptibility in this strain. However, early T-cell development in NOD mice has been largely unexplored. NOD mice with the scid mutation and Rag1 deficiency were examined for a detailed analysis of pre-T cell development in the NOD genetic background. These strains reveal an age-dependent, programmed breakdown in β -selection checkpoint enforcement. At 5-8 weeks, even in the absence of TCR- β expression, CD4⁺ and CD4⁺CD8⁺ blasts appear spontaneously. However, these breakthrough cells fail to restore normal thymic cellularity. The breakthrough phenotype is recessive in hybrid (NOD X B6)F1-scid and -Rag1^{null} mice. The breakthrough cells show a mosaic phenotype with respect to components of the β -selection program. They mimic normal β -selection by upregulating germline TCR-C α transcripts, CD2, and BclX_L, and downregulating Bcl-2. However, they fail to downregulate transcription factors HEB-alt and Hes1 and initially express aberrantly high levels of Spi-B, c-kit (CD117), and IL7R α . Other genes examined distinguish this form of breakthrough from previously reported models. Some of the abnormalities appear first in a cohort of postnatal thymocytes from one of the earliest T-cell precursor populations, the DN2 stage. Thus, our results reveal an NOD genetic defect in T-cell developmental programming and checkpoint control, which permits a subset of the normal outcomes of pre-TCR signaling to proceed even in the absence of TCR β rearrangement.

Furthermore, this breakthrough may initiate thymic lymphomagenesis that occurs with high frequency in both NOD-scid and -Rag1^{null} mice.

426. Genetic mapping of the pre-T cell checkpoint breakthrough in NOD-scid/scid mice

Mary Yui, Rachel Cota, Jeffrey Longmate*

The genetics and pathogenesis of diabetes are very complex, with over 20 genes known contribute to diabetes in this mouse strain. However, only a few of the genes involved in disease have yet been identified. Autoimmunity in the non-obese diabetic (NOD) mouse appears to be dependent upon a balance between pathogenic and regulatory T cells. Various defects have been reported in the immature and mature $\alpha\beta$ -TCR⁺ cells, NKT and NK cells of NOD mice, all of which share common T cell precursors. We previously found that immunodeficient NOD-scid and -Rag1^{null} mice, which cannot rearrange a T-cell receptor, spontaneously break through the β -selection checkpoint, at which the cells should arrest. This checkpoint violation demonstrates a defect in early T-cell differentiation programming in NOD mice. As a fairly simple trait, which possibly contributes to diabetes, the cell breakthrough should be amenable to genetic analysis. This is a recessive trait, as F1 (NOD X B6)-scid and -Rag1^{null} animals do not exhibit this breakthrough phenotype. To determine whether the defective gene(s) leading to this trait is (are) linked to one of the previously identified genetic intervals leading to diabetes susceptibility, and to begin to understand its molecular basis, we are performing a linkage analysis using PCR-based microsatellite repeat polymorphisms to map the gene(s) responsible for the trait. This is being done in a genetic backcross of (NOD X B6) XNOD-scid/scid animals. So far 58 backcross mice have been phenotyped and then genotyped in the genomic regions including 17 diabetogenic loci found on seven chromosomes. In a preliminary analysis of the results, using quantitative trait locus (QTL) mapping and other statistical methods, we found two suggestive genomic regions mapping within the genetic intervals on chromosomes 2 and 4 containing diabetes susceptibility loci. Furthermore, a possible genetic interaction between the genetic interval on chromosome 2 and a region of chromosome 1 was detected. Additional backcross animals and more complete genome-wide genetic coverage should allow us to map the NOD T-cell defect more precisely.

*Professor of Biostatistics, City of Hope

427. Preferential expression of an IL-2 regulatory sequence transgene in TCR $\gamma\delta$ and NKT cells

Mary A. Yui

A transgene with 8.4 kb of regulatory sequence from the murine IL-2 gene drives consistent expression of a green fluorescent protein (GFP) reporter gene in all cell types that normally express IL-2. However, quantitative analysis of this expression shows that different T-cell subsets within the same mouse show divergent abilities to

express the transgene as compared to endogenous IL-2 genes. TCR $\gamma\delta$ cells, as well as $\alpha\beta$ TCR-NKT cells, exhibit higher *in vivo* transgene expression levels than TCR $\alpha\beta$ cells. This deviates from patterns of normal IL-2 expression and from expression of an IL-2-GFP knock-in. Peripheral TCR $\gamma\delta$ cells accumulate GFP RNA faster than endogenous IL-2 RNA upon stimulation, whereas TCR $\alpha\beta$ cells express more IL-2 than GFP RNA. In TCR $\gamma\delta$ cells, IL-2-producing cells are a subset of the GFP-expressing cells, whereas in TCR $\alpha\beta$ cells, endogenous IL-2 is more likely to be expressed without GFP. These results are seen in multiple independent transgenic lines and thus reflect functional properties of the transgene sequences, rather than copy number or integration site effects. The high ratio of GFP to endogenous IL-2 gene expression in transgenic TCR $\gamma\delta$ cells may be explained by subset-specific IL-2 gene regulatory elements mapping outside of the 8.4-kb transgene regulatory sequence, as well as accelerated kinetics of endogenous IL-2 RNA degradation in TCR $\gamma\delta$ cells. The high levels and percentages of transgene expression in thymic and splenic TCR $\gamma\delta$ and NKT cells, as well as skin $\gamma\delta$ -DETC cells, indicate that the IL-2-GFP transgenic mice may provide valuable tracers for detecting developmental and activation events in these lineages.

428. Epigenetic marking of the IL-2 locus without transcription in IL-2-inducible T-lineage cells
Satoko Adachi

IL-2 is subject to cell-type-specific regulation as well as activation-specific regulation, and this has raised the possibility that the IL-2 gene might be held in a specifically inducible conformation in T-lineage cells even when they have not been induced to transcribe the gene. Transgenic assays have shown previously that a region from -2.0 to -8.4 kb relative to the promoter of the IL-2 gene is important for position-independent activity of an IL-2 regulatory sequence transgene, even though this region does not act as a conventional enhancer in transient assays. We have therefore been interested in the possibility that the sequences needed for efficient access of transcriptional machinery to these transgenes may also play a role in the normal establishment of a permissive chromatin configuration of the endogenous gene as a specific outcome of T-cell development. By using chromatin immunoprecipitation (ChIP) assays, we previously showed that acetylation of histone H3 and H4 is increased by PMA/A23187 stimulation from -8.4 through -2.0 kb region in EL4 T-lineage cells. We analyzed further upstream (-10.2 to -10.0 and -8.9 to -8.7 kb) and downstream regions (-2.0 kb through + 0.25 kb). The acetylation in stimulated EL4 cells was greatly elevated (ten-fold more than unstimulated cells at some points) from -4.6 through +0.25 kb except for proximal promoter (-0.24 to -0.05 kb). At the proximal promoter, acetylation looked slightly decreased after stimulation. Since this is a core region of IL-2 promoter, huge protein complexes are assembled there after stimulation. They

might mask epitopes of acetylated histone and lower precipitation efficiency. Acetylation was not increased through the locus in NIH/3T3 non-T cells, whether unstimulated or stimulated.

Histone methylation is another important modification for gene regulation. Like acetylation, histone H3 methylation at lysine 4 (MeH3/K4) has been known as an epigenetic marker of an active locus, and in most cases, these two histone modifications show similar patterns. To support the result of acetylation, we looked at MeH3/K4 at the same regions of the IL-2 locus in EL4 cells. Methylation was increased from -4.6 through +0.25 kb in accordance with acetylation. Surprisingly, this increase was observed in unstimulated EL4 cells too, and was not observed in unstimulated or stimulated NIH/3T3 cells. MeH3/K4 at the proximal promoter (-0.24 to -0.05 kb) was also elevated in unstimulated EL4 cells, although it looked somewhat decreased after stimulation, probably due to the same reason as acetylation.

These results show that MeH3/K4 is observed in association with a locus which is potentially active, regardless of whether transcription itself is active or inactive. In contrast, Ach3 and Ach4 are observed at a locus which is actively being transcribed. How these histone modifications regulate gene expression is still unknown. As we reported last year, addition of histone deacetylase inhibitor Trichostatin A (TSA) decreases IL-2 gene expression in EL4 cells. We looked at how histone acetylation changes when TSA is added. TSA increased both Ach3 and Ach4, but increase of Ach4 was higher extent than that of Ach3. This result showed that increase of histone acetylation does not solely facilitate transcription. There may be an optimal level of acetylation, or the balance of Ach3 and Ach4 is critical.

Since IL-2 is a T cell-specific gene, it is interesting to determine whether all T-lineage cells have MeH3/K4 associated with the IL-2 locus, even those that are incompetent to produce IL-2. At least in SCID.adh which is a non-IL-2 producing immature T-cell lymphoma line (abstract 416), neither Ach3, Ach4, nor MeH3/K4 was detected, suggesting that the epigenetic marking is linked with functional competence to express IL-2 on induction, and not simply a marker of all T-lineage cells. However, because the SCID.adh line is an abnormal lymphoma, further study is required for this subject.

All these results were obtained from transformed cell lines. Therefore, we cannot exclude the possibility that they maintain the IL-2 gene in an abnormal chromatin state. To determine whether this histone modification is also seen in normal T cells, we isolated B220⁺ splenocytes from C57BL/6 mice and performed ChIP assays. The results showed significant methylated H3K4 in the presence and absence of stimulation, in the same pattern as in EL4 cells. However, in these primary cells stimulation induced histone acetylation to a much lower in extent than in EL4 (four-fold was maximum), probably due to a lower percentage of IL-2 producing cells in the whole B220⁺ population.

In conclusion, these results show that T cells competent to express IL-2 on induction maintain a cell type-specific histone modification over the sequences from the IL-2 promoter to -4.5 kb even when they are not induced and the locus is not being transcribed. This modification establishes the limits of the region which undergoes histone acetylation when the cells are stimulated and IL-2 transcription is allowed to begin.

Publications

- Anderson, M.K., Pant, R., Miracle, A.L., Sun, X., Luer, C.A., Walsh, C.J., Telfer, J.C., Litman, G.W. and Rothenberg, E.V. (2004) Evolutionary origins of lymphocytes: Ensembles of T-cell and B-cell transcriptional regulators in a cartilaginous fish. *J. Immunol.* 172:5851-5860.
- Hernández-Hoyos, G., Anderson, M.K., Wang, C., Rothenberg, E.V. and Alberola-Ila, J. (2003) GATA-3 expression is controlled by TCR signals and regulates CD4/CD8 differentiation. *Immunity* 19:83-94.
- Rothenberg, E.V. (2004) From totipotency to T in a dish. *Nature Immunol.* 5:359-360.
- Rothenberg, E.V. and Pant, R. (2004) Origins of lymphocyte developmental programs: Transcription factor evidence. *Semin. Immunol.* In press.
- Rothenberg, E.V. and Taghon, T. Molecular genetics of T-cell development. *Annu. Rev. Immunol.* 23: In press.
- Telfer, J.C., Hedblom, E.E., Anderson, M.K., Laurent, M.N. and Rothenberg, E.V. (2004) Localization of the domains in Runx transcription factors required for the repression of CD4 in thymocytes. *J. Immunol.* 172:4359-4370.
- Yui, M.A. and Rothenberg, E.V. (2004) Deranged early T-cell development in immunodeficient strains of non-obese diabetic (NOD) mice. *J.Immunol.* 173: In press.
- Yui, M.A., Sharp, L.L., Havran, W.L. and Rothenberg, E.V. (2004) Preferential activation of an Interleukin-2 (IL-2) regulatory sequence transgene in TCR $\gamma\delta$ and NKT cells: Subset-specific differences in IL-2 regulation. *J. Immunol.* 172:4691-4699.

Anne P. and Benjamin F. Biaggini Professor of Biological Sciences: Melvin I. Simon
 Member of the Professional Staff: Sangdun Choi, Pamela Eversole-Cire
 Senior Research Associate: Iain D.C. Fraser
 Postdoctoral Scholars: Bryan Beel, Lingjie Gu, Kum-Joo Shin, Sang-Kyou Han, Jong-Ik Hwang
 Visiting Associate: Tracy L. Johnson
 Visitors: Ung-Jin Kim, Ana Mendez
 Research and Laboratory Staff: Anna Cao, Mi Sook Chang, Joyce Kato, Santiago Laparra, Sun Young Lee, Jamie Liu, Josephine Macenka, Valeria Mancino, Blanca Mariana, Ji Young Park, Leah Tager Santat, Estelle Wall, Mei Wang, Joelle Zavzavadjian, Shu Zhen (Jaclyn) Zhou, Xiaocui Zhu

Support: The work described in the following research reports has been supported by:

Anne P. and Benjamin F. Biaggini Professorship of Biology
 Beckman Institute
 German Government Fellowship
 Grubstake Presidents Fund
 National Institutes of Health, USPHS

Summary: During this past year we made progress in the Alliance for Cellular Signaling. The Alliance is a joint research project that coordinates research on the mechanisms involved in signal transduction in six different laboratories and involves more than 40 Ph.D. scientists. The Alliance switched from using primary B-cells to working with the RAW macrophage cell line. We have developed approaches using RNAi to generate lentiviral vectors that are then able to be introduced into the RAW cells and eliminate specific gene expression. Thus far we have developed over 65 vectors and cell lines that result in specific gene knockdown or elimination. We plan to complete 100 vectors by the end of the year. The Alliance is studying the effects of these perturbations on signaling systems in RAW cells, with a specific focus on calcium-mediated responses. In addition we continue to work on the yeast two-hybrid system with Myriad Genetics and to develop new vector systems for expressing specific protein fusions and other constructs that can be used in the study of the RAW cell signaling system. In addition, we have extended microarray analysis to the RAW system. We have been looking at the effects of specific ligands on transcription events. The RAW cell is wonderfully suited to these experiments. We see very large changes and co-regulation of groups of genes in response to the activation of Toll receptors. In time series studies we can define cascades of gene expression that correspond to different times of exposure to ligand activation. Some of these coexpressed genes have been found previously to be induced by the activation of Toll receptors, others are interesting new sub-groups of genes. Furthermore, we have also been able to detect changes in gene expression very early after ligand addition. We have used the microarray experiments to examine transcriptional control

in double ligand experiments where LPS is used together with gamma interferon or with 2MA. The double ligand effects point to interaction between signaling pathways and regulatory systems.

We have continued to push the use of RNAi in a model system built around the J774 monocyte cell line. In addition to generating knockdowns of single genes we have used this cell line to develop methods for doing double gene knockdown. This is very useful, particularly if we want to turn off gene expression regulated by a specific pathway where multiple overlapping genes might function.

We are also continuing our collaboration with Dr. David Anderson working on the Mrg-GPCR receptors found to be expressed in dorsal root ganglion derived cells. These receptors are found in cells that innervate the skin. They are transduced by the Gq family of G proteins and activate the phospholipase, PLC β 3. We have mouse mutants that were generated in David Anderson's laboratory that lack specific Mrg genes and we have mutants generated in our laboratory that are deficient for specific G proteins and for specific phospholipases. We are now generating double mutants by the appropriate crosses and we will examine the effects of the double deficiency on nociception and other functions that might be related to the Mrg receptors.

In the visual system we have stopped our experiments on the photoreceptors and are concentrating primarily on retinal ganglion cells. These cells include a variety of different subsets that are morphologically and functionally distinguishable. We are trying to develop specific molecular markers for each of these subsets so that we can study their individual function in greater detail.

429. Molecular Biology Laboratory of the Alliance for Cellular Signaling (AfCS): RNAi project
 Iain D.C. Fraser, Joelle R. Zavzavadjian, Jamie Liu, Leah Santat, Estelle Wall, Kavitha Dhandapani, Melvin I. Simon

We reported last year the development of a sophisticated vector system for the application of RNAi to the AfCS project. The refractoriness of the WEHI231 B cell line to RNAi precipitated a change in the AfCS model system to the RAW264.7 mouse macrophage cell line, and this system has proved much more tractable to RNAi. We have implemented a reagent development program with the capacity to produce validated siRNAs and shRNAs for four genes/week. The issue of rational siRNA sequence selection has been addressed by collaboration with Dharmacon to acquire siRNAs designed by their SMARTpool algorithm at a significantly reduced cost. For each gene, four chemically synthesized siRNAs designed by Dharmacon's SMARTpool algorithm are tested against the endogenous target in RAW cells. The best siRNA is converted to an shRNA and tested again to confirm that the sequence retains inhibitory activity in the shRNA context. Validated shRNAs are subcloned to lentiviral vectors for virus generation and RAW cell infection in the

AfCS Macrophage laboratory (UCSF). This approach has, thus far, led to the creation of more than 40 stable RAW264.7 cell lines depleted in specific target genes with a further 40+ genes in progress (http://www.signaling-gateway.org/aboutus/supplement/AM2004/19_Fraser.ppt). The phenotypes exhibited by these lines in response to stimulation of the C5a, UDP/UTP and Fc gamma receptors suggest some intriguing interplay between the Ca²⁺ and PIP3 signaling pathways (http://www.signaling-gateway.org/aboutus/supplement/AM2004/21_Seaman.ppt). We believe that the ability to knockdown multiple target genes will be essential to address the hypotheses arising from this single knockdown data. To this end, we have developed lentiviral vectors containing a variety of cell surface markers and drug selection genes to permit the creation of lines expressing more than one shRNA. In addition to continuing RNAi reagent development for AfCS target genes, we are using a variety of approaches to establish the specificity of target gene knockdown in the existing cell lines, including microarray analysis to assess the frequency of 'off-target' effects. We are also developing methods to improve the efficacy of shRNAs and are investigating approaches to regulate shRNA expression from inducible promoters.

430. Molecular Biology Laboratory of the Alliance for Cellular Signaling (AfCS): cDNA cloning projects

Joelle R. Zavzavadjian, Estelle Wall, Kavitha Dhandapani, Jamie Liu, Leah Santat, Melvin I. Simon, Iain D.C. Fraser

The Molecular Biology Laboratory was proposed to be a resource for the preparation and dissemination of essentially all nucleic acid-based materials required by the AfCS Laboratories. To meet this requirement, we felt it necessary at the outset of the project to establish a technical infrastructure that would facilitate the cloning and subcloning of DNA sequences into a wide range of expression vector platforms. Gateway Cloning Technology (Invitrogen) has been invaluable in this respect and we have adopted this platform for almost all of our plasmid work. We have established robust protocols for PCR-based cloning of full-length mouse sequences from a mixture of cDNA sources. In the early stages of the project we encountered issues with discrepancies between our cloned sequences and those deposited in Genbank. We now independently isolate two forms of every cDNA (+/- termination codon) which, in addition to the practical necessity of expressing various 'tags' at either C- or N-terminus, allows us to differentiate between base changes introduced by PCR versus genuine differences with a Genbank record. We perform full-length double-stranded sequencing of every gene and use a sophisticated assembly program (Paracel Genome Assembler) to produce sequence contigs. Although we have developed relatively high-throughput protocols for isolation of candidate cDNAs, sequence analysis of clone candidates remains rate limiting. Sequences verified by both our lab

and the AfCS Microscopy lab (Stanford) currently number almost 1500. In addition to full-length cDNAs this number includes shRNAs cloned by linker ligation. The cDNAs cover a wide range of signaling proteins with protein kinases representing the predominant gene family. We have also cloned a comprehensive set of subcellular markers which are used routinely by the Microscopy lab in their localization analyses (<http://www.signaling-gateway.org/reports/v1/DA0002/DA0002.pdf>).

Over 200 Gateway-compatible expression vectors (termed 'parent' vectors) have been generated, ranging from vectors for tagging genes with GFP variants and epitopes, to lentiviral vectors used for expression of shRNAs. From the 1500 cloned gene sequences and 200 parent vectors we have generated over 5000 constructs. All sequence validated clones, parent vectors and resulting constructs are recorded in a web-based plasmid database developed with the AfCS Bioinformatics and Microscopy labs. This database is mirrored in a publicly accessible site (<http://www.signaling-gateway.org/data/plasmid/>) which displays those constructs that are available to the research community (currently almost 3000) through the ATCC. The plasmid database also facilitates the distribution of plasmids and recording of lab specific details at multiple AfCS sites. The development and generation of nucleic acid-based reagents continues to be an important contribution of our lab to the AfCS program.

431. Molecular Biology Laboratory of the Alliance for Cellular Signaling (AfCS): Yeast two-hybrid project

Iain D.C. Fraser, Melvin I. Simon

Of the techniques available to detect protein-protein interactions, the AfCS selected yeast two-hybrid (Y2H) as the main approach due to its relatively high throughput. We proposed to collaborate on this project with Myriad Genetics, who have established a refined Y2H platform using proprietary strains and techniques to significantly increase the reliability of the interaction data. Prior to the initiation of the screens, mRNA derived from various B-cell and myocyte sources was provided to Myriad for synthesis of screening libraries specific to these cell types. Proteins known or suspected to transduce signals in these cells, and considered likely to participate in multiple interactions, were selected as 'bait' candidates. A brief communication on the general approach to the Y2H project has been published online (<http://www.signaling-gateway.org/reports/v1/DA0004.pdf>). 163 bait proteins were screened against the B-cell and myocyte libraries and to date these screens have produced over 1000 interactions. A dedicated website in the AfCS data center provides free access to this data (<http://www.signaling-gateway.org/data/Y2H/cgi-bin/y2h.cgi>). In addition to the tabular presentation of bait proteins with links to their interacting preys, the website provides links to download the complete data set in formats compatible with freely available interaction mapping software and also

provides a function to 'build' interaction networks directly on the website starting with a bait of interest.

Since the AfCS focus changed to the mouse macrophage, a new activation domain library has been generated from a mixture of three macrophage sources; resting RAW cells, LPS/g-interferon stimulated RAW cells and primary bone marrow-derived macrophages. Our criteria for selecting Y2H baits during the last year have focused on capturing interactions that are likely to occur in this new cell model. We selected primarily, but not exclusively, cytosolic signaling proteins that are known to be activated by ligands acting on macrophage receptors such as Toll receptors, Fc receptors and selected GPCRs. 28 of the 74 bait proteins selected for macrophage library screening have previously been screened using the B-cell and cardiac myocyte libraries, but were considered high enough priorities in macrophage signaling to warrant re-analysis. Details of these baits, for which data is close to release, are included in the poster at the following weblink (http://www.signaling-gateway.org/aboutus/supplement/A_M2004/P07.ppt).

432. Inhibition of gene expression in the macrophage-like cell line RAW264.7
 Pamela Eversole-Cire¹, Joseph Johnston², Iain D. C. Fraser¹, Melvin I. Simon¹

The ability to selectively inhibit gene expression is necessary to elucidate cellular signaling pathways in a spatial and temporal context. Nucleic acid based methods, such as the use of antisense oligonucleotides (ASOs) and siRNA duplex molecules to inhibit gene expression, are particularly useful in cell culture systems. Therefore, the effectiveness of ASOs, alone and in combination with siRNA duplexes, at inhibiting the expression of various genes involved in cellular signaling pathways in the macrophage-like cell line RAW264.7 was assessed. Phosphorothioate oligonucleotides with 2'-O-methoxyethyl modifications at the 5' and 3' ends, synthesized and validated as effective ASO reagents at inhibiting the expression of target genes in cultured cell lines by ISIS Pharmaceuticals, were used. Gene-specific knockdown of BLNK, PTEN, Syk, Akt2, and Gi alpha two messages using ASO targeted to respective mRNA sequences was found to be dose-dependent in the RAW264.7 cell line.

Simultaneous inhibition of different genes could also be achieved via co-transfection of different ASOs. While ASOs and siRNAs individually inhibited gene expression, siRNA did not significantly enhance the antisense inhibitory effect upon co-transfection of the two nucleic acids. Since optimal delivery of ASOs and siRNAs require different transfection reagents, gene inhibition using a combination of ASO and siRNA may be accomplished by transfecting ASOs into lentiviral stable cell lines expressing shRNA. Although the effect of a given ASO on the expression of at least one additional non-specific gene was assessed for every experiment and was found to be negative in all cases, microarray analyses of cells treated with ASOs are currently being performed

to assess global non-specific effects on gene expression. In addition, functional assays will be performed to determine if phenotypes produced in lentiviral cell lines expressing shRNAs can be reproduced in cells transfected with ASOs. Antisense technology may, therefore, be used to complement studies using siRNAs to inhibit the expression of specific genes involved in macrophage signaling pathways.

¹Alliance for Cellular Signaling, Molecular Biology Laboratory, California Institute of Technology, Pasadena, CA

²ISIS Pharmaceuticals, Carlsbad, CA

433. Transcriptional ligand screen of mouse B cell and macrophage reveals signaling pathways
 Sangdun Choi, Xiaocui Zhu, Mi Sook Chang, Sun Young Lee, Ji Young Park, Shu Z. Zhou, Yun Anna Cao, Melvin I. Simon

We developed the capacity to fabricate high-quality cDNA and oligonucleotide microarrays as a part of the AfCS (Alliance for Cellular Signaling: <http://www.signaling-gateway.org>) project. Comparisons of the Agilent inkjet-deposited cDNA and oligo arrays with Affymetrix GeneChips and quantitative RT-PCR showed good correlation with a high degree of array quality and accuracy (<http://www.signaling-gateway.org/reports/v1/DA0010.pdf>; accepted by Journal of Biotechnology). Transcriptional analysis of the B-cell single ligand screen was carried out using the cDNA arrays. Primary B cells stimulated with 33 single ligands were harvested at four time points (0.5, 1, 2 and 4 hr) and compared to a spleen cell standard and to B cells cultured for the same period in the absence of ligand. Large-scale and highly significant transcriptional changes were observed with anti-IgM, anti-CD40, LPS, IL-4 and CpG-oligodeoxynucleotide, and smaller subtle changes in gene expression were found with BLC, IFN β , IL-10, PAF, and SDF1 (submitted to The Journal of Immunology). Based on the results from the B cell single ligand screen, a subset of ligands was chosen for transcript analysis of double ligand stimulation. The data suggested interesting crosstalk in the signaling pathways downstream of the proliferative ligands anti-IgM, anti-CD40 and LPS (manuscript in preparation). In addition to the analysis of wild-type splenic B cells, a study was carried out on B cells derived from human Bcl2 transgenic mice. B cells from these mice have sustained survival in culture and their transcript profile was found to be sufficiently similar to wild-type cells to support their use as a stable, long-term culture system for splenic B cell study (<http://www.signaling-gateway.org/reports/v2/BC0013/BC0013.pdf>). The B-cell data remain a valuable resource and a good basis for further exploration of the regulatory mechanisms that are engaged in "activated" B cells.

We have analyzed transcriptional changes that occur after the addition of ligands that are known to induce specific responses in the macrophage cell line RAW264.7. A time series was done to examine the effects of adding LPS. A cascade of induced gene expression was observed

where responses could be clearly subdivided into Early (0.5-2 hr), Intermediate (2-6 hr), and Late (6-24 hr) phases. Based on cytokine release data, LPS/IFN γ and LPS/2MA sets were also chosen for transcriptional analysis from the addition of single or double ligands in RAW and identification of signal pathways that cross-talk between two ligands. Concurrently, we have begun a series of transcriptional analysis to examine the target-specific and off-target effects on lentiviral shRNA cell lines. The cell lines harboring Gi2, G β 2, or SHIP1 shRNA are being tested to assess both the effectiveness of RNAi gene knockdown and the extent of off-target effects.

434. Isotype-specific roles of G β subunits in chemokine-dependent cellular responses
Jong-Ik Hwang, Iain D.C. Fraser, Melvin I. Simon

Upon ligand binding, heterotrimeric G protein-coupled receptors (GPCRs) trigger various cellular responses by stimulating GTP exchange of G α subunits. The G α subunits are localized in plasma membrane, forming protein complexes with G $\beta\gamma$ subunits. The specific roles of G α subunits in the GPCR-mediated cellular responses have been largely established. On the other hand, the β and γ subunits composed of 5 and 12 isotypes each was thought to be accessory molecules in signal transduction. Recently the subunits have been understood as signal transduction molecules with their own functions; regulation of various intracellular molecules, including ion channels, adenylate cyclases, phospholipase C, and PI3 kinase.

G β in a lower eukaryote, *Dictyostelium* ameba which contains unique G β subunit, is known to be involved in migration to chemotactic stimulants and phagocytosis. In mammals, specific roles for G β are not well defined. Using the small interfering RNA technique, we developed lentivirus containing specific hairpin sequences of each G β subunit, GFP, and different antibiotics resistant gene - puromycin or hygromycin. As a model system, we used J774A.1 cell, a mouse monocytic cell line which express G β 1, G β 2, and trace amount of G β 4. After two cycles of virus infection and selection with antibiotics, the cells lacking G β 1 and G β 2 were established. Upon stimulation with C5 α , a chemokine, migration activity, Akt phosphorylation, and Ca $^{2+}$ mobilization were abolished in the absence of G β subunits. When the cells were treated with C5a to determine the effect of G β on G α 12 family-mediated signaling by chemokine receptors, actin polymerization was detected in control cells but not in the cell lacking G β subunits. When we treated the cell with UTP, an agonist of P2Y receptors which induce G α q-dependent signaling, Ca $^{2+}$ mobilization was not observed. These results suggest that G β regulates G α -dependent signaling pathways as well as directly activates downstream signaling events. However, phagocytic activity was normal in the absence of G β ,

suggesting that G β is not involved in phagocytosis-related signaling pathway in mammalian immune cells.

435. Identification of retinal ganglion cell subset-specific genes

Kum-Joo Shin, Melvin I. Simon

Retinal ganglion cells (RGCs) are the output neurons that transmit visual information to the brain. Intensive anatomic and physiological studies have shown that there are more than 12-15 subsets of RGCs that have distinct morphologies and functions. However, the underlying molecular mechanisms and functions of these differentiated cells are not known yet. Therefore, we are investigating specific genes of subsets of RGCs. RGCs were isolated from postnatal mice using antibody for thy-1, an RGC marker, conjugated with magnetic beads. We applied the RNA from purified RGCs and RGC-depleted retinal cells to microarray analysis to compare the expression of genes and search for RGC-specific expression. The results were confirmed with quantitative RT-PCR. Through in situ hybridization of selected genes, we found that several candidate genes such as protein kinase C theta, sox 6 and protocadherin α 1 were expressed in subsets of RGCs. Their specific roles on the subset of RGCs will be investigated.

Publications

- Bastiani, C.A., Gharib, S., Simon, M.I. and Sternberg, P.W. (2003) *C. elegans* G α q regulates egg-laying behavior via a PLCb-independent and serotonin-dependent signaling pathway, and likely functions in both the nervous system and in muscle. *Genetics* 165:1805-1822.
- Hwang, J.I., Fraser, I.D.C., Choi, S., Qin, X.-F. and Simon, M.I. (2004) Analysis of C5a-mediated chemotaxis by lentiviral delivery of small interfering RNA. *Proc. Natl. Acad. Sci. USA* 101:488-493.
- Krispel, C.M., Chen, C.-K., Simon, M.I. and Burns, M.E. (2003) Prolonged photoresponses and defective adaptation in rods of G β 5 $^{-/-}$ mice. *J. Neurosci.* 23:6965-6971.
- Krispel, C.M., Chen, C.-K., Simon, M.I. and Burns, M.E. (2003) Novel form of adaptation in mouse retinal rods speeds recovery of phototransduction. *J. Gen. Phys.* 122:703-712.
- Makino, C.L., Dodd, R.L., Chen, J., Burns, M.E., Roca, A., Simon, M.I. and Baylor, D.A. (2004) Recoverin regulates light-dependent phosphodiesterase activity in retinal rods. *J. Gen. Physiol.* 123:729-741.
- Marinissen, M.J., Servitja, J.M., Offermanns, S., Simon, M.I. and Gutkind, J.S. (2003) Thrombin protease-activated receptor-1 signals through Gq- and G13-initiated MAPK cascades regulating c-Jun expression to induce cell transformation. *J. Biol. Chem.* 278:46814-46825.

- Moers, A., Nieswandt, B., Massberg, S., Wettschreck, N., Grüner, S., Konrad, I., Schulte, V., Gratacap, M.-P., Simon, M.I., Gawaz, M. and Offermanns, S. (2003) G₁₃ is an essential mediator of platelet activation in haemostasis and thrombosis. *Nat. Med.* 9:1418-1422.
- Park, S.-Y., Beel, B.D., Simon, M.I., Bilwes, A.M. and Crane, B.R. In different organisms, the mode of interaction between two signaling proteins is not necessarily conserved. *Proc. Natl. Acad. Sci. USA*. In press.
- Quezada, C.M., Gradinaru, C., Simon, M.I., Bilwes, A.M. and Crane, B.R. Helical shifts generate two distinct conformers in the atomic resolution structure of the CheA phosphotransferase domain from *Thermotoga maritima*. *J. Mol. Biol.* In press.
- Waters, E., Hohn, M.J., Ahel, I., Graham, D.E., Adams, M.D., Barnstead, M., Beeson, K.Y., Bibbs, L., Bolanos, R., Keller, M., Kretz, K., Lin, X.Y., Mathur, E., Ni, J.W., Podar, M., Richardson, T., Sutton, G.G., Simon, M.I., Söll, D., Stetter, K.O., Short, J.M. and Noordewier, M. (2003) The genome of *Nanoarchaeum equitans*: Insights into early archaeal evolution and derived parasitism. *Proc. Natl. Acad. Sci. USA* 100:12984-12988.
- Yi, T.-M., Kitano, H. and Simon, M.I. (2003) A quantitative characterization of the yeast heterotrimeric G protein cycle. *Proc. Natl. Acad. Sci. USA* 100:10764-10769.
- Zhu, X., Hart, R., Kim, J.-W., Lee, S.Y., Chang, M.S., Cao, Y.A., Mock, D., Ke, E., Saunders, B., Alexander, A., Grosseohme, J., Yan, Z., Hsueh, R., Fruman, D., Subramaniam, S., Sternweis, P., Simon, M.I. and Choi, S. Analysis of the major patterns of B cell gene expression changes in response to short-term stimulation with 33 single ligands. *J. Immun.* In press.

Thomas Hunt Morgan Professor: Paul W. Sternberg
 Senior Research Fellow: Jane E. Mendel
 Research Fellows: Todd Ciche, Bhagwati Gupta, Byung Hwang, Takao Inoué, Jan Karbowski, Mihoko Kato, Nadeem Moghal, Hans-Michael Müller, Gary Schindelman, Alok Saldanha, David Sherwood, Jagan Srinivasan, Cheryl Van Buskirk, Allyson Whittaker, Xian-Zhong Xu, Weiwei Zhong
 Graduate Students: Jolene Fernandes, Ted Ririe, Jennifer Sanders, Adeline Seah, Hui Yu
 Research and Laboratory Staff: Mary Alvarez, Christopher Cronin, John DeModena, Shahla Gharib, Yvonne Hajdu-Cronin, Gladys Medina, Barbara Perry
 WormBase Staff: Igor Anteshechkin, Carol Bastiani, Juancarlos Chan, Wen J. Chen, Lisa Girard, Eimear Kenny, Ranjana Kishore, Raymond Lee, Cecilia Nakamura, Andrei Petcherski, Erich Schwarz, Kimberly Van Auken, Daniel Wang
 Collaborators: Robert Stirbl, Barbara Wold

Support: The work described in the research reports has been supported by:

California Breast Cancer Research Program
 Damon Runyon Research Foundation
 Defense Advanced Research Projects Agency
 Gordon Ross Medical Foundation
 Helen Hay Whitney Foundation
 Howard Hughes Medical Institute
 National Institutes of Health, USPHS

Summary: We seek to understand how the genome controls the development and behavior of *C. elegans*. Our main foci are on signaling pathways and transcriptional regulation. Our approaches are experimental, computational and synthetic. Specifically, we use molecular genetics to understand detailed mechanisms, and functional genomics to obtain global views of development and behavior. We take computational approaches to understand signal transduction, developmental pattern formation and behavioral circuits. We are also trying to modify nematodes and their cells to test our understanding of fundamental biological principles. Moreover, we study the genomes, genetics and biology of other nematodes to help us comprehend *C. elegans*, to learn how development and behavior evolve, and to learn how to control parasitic and pestilent nematodes.

One major focus of the lab is on signal transduction. We continue to define pathway interactions and are trying to understand the determinants of signaling specificity: how does the same pathway lead to distinct outcomes in different tissues? For these studies we analyze EGF-receptor signaling, WNT signaling, TRP channels, and G protein-mediated signaling pathways. We have found that a cell can respond to distinct WNTs using different classes of receptors.

Another lab focus is on transcriptional regulation. We are trying to unravel the transcriptional network underlying vulval development, a paradigmatic case of

organogenesis. We have found one transcriptional program that specifies the ability of the gonadal anchor cell to invade the vulval epidermis.

Vulval development involves a remarkable series of intercellular signaling events that coordinate the patterning of the uterine and vulval epithelia and allow them to connect precisely. Specification of the anchor cell from the ventral uterine epithelium breaks the symmetry of the gonad. The anchor cell then produces the vulval-inducing signal, LIN-3, an epidermal growth factor-like protein that acts via *C. elegans* homologs of EGF-receptor, RAS and MAP kinase. Inductive signaling is regulated at the level of ligand production as well as the responsiveness of the receiving cells. LIN-3 is produced in a highly localized and regulator manner. After the anchor cell induces the vulva, a complex program of further pattern formation, cell type specification and morphogenesis follows. The primary (1°) vulval lineage generates an E-F-F-E pattern of cell types while the 2° vulval lineage generates an A-B-C-D pattern of cell types. We now have our hands on a number of receptor proteins, transcription factors and regulated genes; we are trying to define this regulatory network to understand how organogenesis is genetically programmed. The anchor cell recognizes one of the seven vulval cell types and invades the vulval epithelium in a process akin to tumor metastasis, and we have found genes necessary for this process. Regulation by the EGF-receptor, WNT and HOM-C pathways impinge not only on vulval development but also the neuroectoblast P12 specification and male hook development. By comparing these examples with vulval development, we seek to understand the signaling specificity and signal integration.

Our efforts in genomics are experimental and computational. Our experimental genome annotation includes finding the 5' ends of mRNAs with a new method we developed, identifying *in vitro*, binding sites for transcription factors, testing enhancer function in transgenic worms, and systematic inactivation of *C. elegans* transcription factors. We are investigating ways to compare the genomes of *Caenorhabditis* species. We are part of the consortium that is annotating three *Caenorhabditis* species whose genomes are being sequenced. We have collaborated with the Joint Genome Institute and Professor Wold's lab to pilot genomic sequence for species CB5161 and PS1010. Our computational projects involve establishing pipelines for cis-regulatory computational analysis, new programs to use orthology and known binding sites or motifs, etc.

Our bioinformatics efforts involved participation in the WormBase consortium, which develops and maintains WormBase, a web-accessible comprehensive database of the genome, genetics and biology of *C. elegans* and close relatives (www.wormbase.org). We are part of the Gene Ontology Consortium (www.geneontology.org) which seeks to annotate gene and protein function with a standardized, organized vocabulary, which the Consortium continually develops. We have developed Textpresso

(www.textpresso.org), an ontology-based search engine for full text of biological papers. Textpresso is used by *C. elegans* researchers as well as WormBase staff; it is being expanded to other organisms and fields of study. WormBase, Gene Ontology and Textpresso are part of the Generic Model Organism (GMOD) Project (www.gmod.org), a collaborative project among organism-specific databases to develop generic software.

Our behavioral studies focus on understanding male mating behavior as well as locomotion of both sexes. For specific projects we study egg-laying, feeding, chemotaxis, osmotic avoidance, among other simple behaviors. Mating behavior, with its multiple steps, is arguably the most complex of *C. elegans* behaviors; because it is not essential for reproduction, given the presence of internally self-fertilizing hermaphrodites, male mating is useful to elucidate how genes control behavior. We are studying several aspects of male mating behavior to understand the neuronal circuits that control the behavior and how they are genetically encoded. Our comparative studies include both analyzing behavioral differences among species, and genetic analysis of *C. briggsae*, *Pristionchus pacificus* (a nematode species we discovered during the 1990s), and *Heterorhabditis bacteriophora* (an insect-killing nematode).

We have developed a machine-vision system that automatically quantifies the locomotion of nematodes. We use this system to study individual genes, to measure the length of worms, and to obtain data to support a mathematical modeling effort. We are expanding this effort to analyze mating behavior of nematodes.

We are involved in efforts to model worm movement, vulval pattern formation and aspects of signal transduction. We are trying to modify *C. elegans* cells to test our understanding of signal processing by sensory neurons and of the circuits that control locomotion. We are also trying to adapt bacterial and yeast circuits for use in *C. elegans*, as tools to understand circuits.

436. A physiological role for EGFR signaling in *C. elegans* growth
Cheryl Van Buskirk

Cell-cell signaling through the Epidermal Growth Factor Receptor (EGFR/ErbB1) plays critical roles in human physiology and disease. Because of the power of genetic screens, much of our knowledge of the developmental roles of EGFR has come from studies on invertebrates, such as *C. elegans*. The single EGF receptor homolog in *C. elegans*, LET-23, has multiple functions during development. LET-23 signals through the ras/MAPK pathway to specify cell fates in the ventral cord, vulva, male tail, and excretory system. LET-23 also signals through a PLC/IP3 pathway to regulate ovulation. We have observed that overexpression of the EGFR ligand LIN-3 from a heat-shock inducible promoter, in addition to affecting the expected cell fates, also slows down growth of the animals as compared to heat-shocked controls. This growth defect, which affects time to adulthood but not the final size of the animal, occurs in response to

overexpression of LIN-3 at any developmental stage, and thus is unlikely to be due to a cell fate specification defect. The growth defect is suppressible by mutations in *let-23*, and we are currently testing known downstream targets of LET-23 for suppression to determine which pathway is involved. We are also investigating possible underlying causes of this growth phenotype in order to characterize this previously undescribed physiological role for *let-23* signaling.

437. The *Caenorhabditis elegans* fos family member **Ce-fos**, promotes cell invasive behavior
David R. Sherwood

We are interested in the cellular, genetic and molecular mechanisms that regulate the invasion of the gonadal anchor cell (AC) into the vulval epithelium of the hermaphrodite *C. elegans* larva. This process involves a secreted signal from the vulval cells that stimulates AC invasion, followed by the precise removal of the basement membrane separating both tissues directly bordering the AC, and concludes with the invasion of the AC between the central vulval cells. We have found that in *evl-5* mutants, AC invasion is either absent or is severely delayed. Visualization of the AC in mutants revealed it extends cellular processes toward the developing vulva, and thus is still attracted to its target. However, in many cases the processes flattened at the basement membrane, suggesting an inability to cross this structure.

We cloned *evl-5* and found that it encodes the *C. elegans* homologue of the proto-oncogene *fos* (*Ce-fos*), a component of the AP-1 transcription factor heterodimer. This appears to be the only *fos* family member in *C. elegans*. *Ce-fos* generates two transcripts utilizing distinct 5' exons, which encode a shorter 331 amino acid protein (*Ce-FOS-S*), and a longer 467 amino acid protein (*Ce-FOS-L*) containing an additional 136 amino acids at the N-terminus. Both proteins share the conserved DNA-binding and dimerization region, however, the longer form contains a putative transactivation domain. Sequencing the *evl-5* allele revealed a stop mutation within the unique 5' region of the *Ce-fos-L* transcript, indicating that this mutation selectively disrupts *Ce-FOS-L*. Translational fusion proteins of the Cyan Fluorescent protein (CFP) and the Yellow Fluorescent Protein (YFP) inserted into the unique 5' exons of *Ce-fos-S* and *Ce-fos-L*, respectively, revealed that *Ce-FOS-S* is expressed in many cells and tissues, but *Ce-FOS-L* is primarily confined to somatic gonad cells. Furthermore, *Ce-FOS-L* is expressed at high levels specifically in the AC during invasion, strongly suggesting it functions within the AC to control invasion. To begin to identify genes that *Ce-FOS-L* may regulate within the AC to promote invasion, the expression of several integrated reporter fusion genes in *evl-5* animals is being examined. *CDH-3::GFP* (a cadherin family member) is reduced in expression, while *hemicentin::GFP* (extracellular matrix protein) and *ZMP-1::GFP* (zinc-matrix metalloproteinase) are completely absent in the AC in *evl-5* animals. Null mutations in all of these genes individually have no AC invasion defect, suggesting

that they may function redundantly to regulate invasion. We are thus currently constructing combinatorial mutants of these genes and examining whether other members of gene families may be regulated by Ce-FOS-L and play a role in invasion.

438. Frizzled and Ryk pathways function in parallel to control P7.p lineage orientation in the **C. elegans** vulva

Takao Inoue

C. elegans is an excellent system in which to investigate organogenesis and signal transduction at the single-cell level. During the development of the *C. elegans* vulva, the P7.p cell lineage undergoes a stereotyped series of cell divisions and cell fate determination events resulting in five distinct cell types (vulA, vulB1, vulB2, vulC, vulD) arranged in an anterior-posterior series. Previous results suggested that mutations in *lin-17* (encoding Frizzled) and *lin-18* alter the development of the P7.p lineage. GFP fusion reporters suggest that *lin-18* is expressed in the vulval tissue, along with *lin-17*. Using preexisting mutations and RNAi, we found that Wnt ligands LIN-44, MOM-2 and CWN-2 redundantly control P7.p development. To place these components in a genetic pathway, we carried out analyses of mutant phenotypes using molecular markers and cell morphology. We found that *lin-17* and *lin-18* mutations reverse the anterior-posterior orientation of the P7.p lineage. This was suggested previously but not confirmed at the cellular level. We also found that *lin-17*; *lin-18* double mutants exhibit a stronger phenotype than either single mutant alone. Since mutations used are nulls, this enhancement indicates that *lin-17* can function in the absence of *lin-18* and that *lin-18* can function in the absence of *lin-17*. Moreover, we found that mutations in different Wnt ligands exhibit complementary patterns of interactions with the receptor mutations: *lin-44* mutations enhance *lin-18* but not *lin-17*; *mom-2* mutations enhance *lin-17* but not *lin-18*. Taken together, these results indicate that *lin-17* and *lin-18* function in independent (parallel) pathways that have different ligand specificities. We are currently using the system to identify components of the *lin-18* (Ryk) signaling pathway through a genetic screen.

439. The role of **cam-1** in **C. elegans** vulval development

Jennifer L. Sanders

Signaling via the Wnt pathway is known to regulate the polarity governing asymmetric cell division and cell migration. The *C. elegans* CAM-1 protein, homologous to the Ror family of RTKs, has also been shown to mediate these processes. Ror proteins are orphan RTKs characterized by an extracellular Frizzled-like cysteine-rich domain, a juxtamembrane Kringle domain, and an intracellular kinase domain. Although CAM-1 has a cysteine-rich domain associated with Wnt binding, the identity of the ligand and the mechanism of *cam-1* signaling have not been established. The development of the *C. elegans* hermaphrodite vulva serves as an excellent

model for the study of conserved signaling pathways. Vulval phenotypes due to mutations in Wnt pathway genes have been reported by others. For example, a *bar-1* (β -catenin) loss-of-function mutation results in an under-induced phenotype while activated *bar-1* results in over induction. Mutations in *lin-17* (Frizzled) manifest as a bivulva phenotype due to a disruption of asymmetric cell division. LIN-17 also mediates signaling between the inner and outer 1° VPC descendants. I am examining the genetic interactions of *cam-1* with other Wnt signaling components in the context of vulval development.

440. Cell fate patterning and/or differentiation in 2° vulval lineages

Jolene Fernandes

Vulval cell types can be distinguished by the expression of specific cell fate markers as well as traditional lineage analysis. Earlier work has demonstrated that proper patterning of the 1° VPC descendants is dependent on a short-range LIN-3 signal from the anchor cell as well as intercellular signaling between the outer and inner vulE and vulF cells. Our current goal is to determine how correct patterning and differentiation of the 2° VPC descendants is established. To provide some insight about this mechanism, we have adopted a dual strategy: the first approach is to investigate whether the *lin-12*/*glp-1* pathway is required for the proper patterning of the vulA, vulB, vulC and vulD cells. Since the 2° VPCs employ LIN-12 receptor during lateral signaling, it is possible that *lin-12* is also utilized at a later stage to mediate cell fate decisions between the 2° vulval descendants. We are testing known components of the *lin-12*/Notch pathway, and utilizing specific cell fate markers to assay for cell fate transformation. The second approach entails conducting an RNAi screen of all the known and putative transcription factors in the *C. elegans* genome in a *ceh-2::yfp* background. *ceh-2* is a marker that serves as a readout for vulB fate during the L4 stage and, consequently, can be used to screen for cell fate transformation and/or ectopic specification of vulB fate. Modifiers of *ceh-2* expression are likely candidates that are involved in facilitating accurate patterning and/or differentiation of 2° vulval descendants. Thus far, several candidate transcription factors found to be involved in proper patterning and/or differentiation of the secondary vulval lineages have been isolated and are in the process of being further characterized.

441. Heterochronic transcription factor **lin-29** and coordination of vulval morphogenesis

Ted Ririe

The *lin-29* gene encodes two isoforms of a (Cis)₂-(His)₂ zinc-finger transcription factor that are involved in several developmental events that occur at the transition from the fourth larval stage (L4) to the adult in *C. elegans*. LIN-29 has been shown to participate in coordinating the development of the hypodermal syncytium. In *lin-29* mutants the number of vulval cell divisions is normal but the vulva appears to evert

incorrectly resulting in a protruding vulva phenotype, indicating that *lin-29* may also play a role in the developmental coordination of the hermaphrodite vulva, a significantly more complex organ than the hypodermis. Several genes have been shown to be crucial for proper vulval cell fate execution. The spatial and temporal expression patterns of these marker genes in the 1° and 2° lineages of the vulva are promising tools for identifying LIN-29 functionality. The expression of the vulval cell markers *lin-11::gfp* (LIM homeodomain transcription factor) and *egl-17::gfp* (fibroblast growth factor) is either reduced or abolished in a *lin-29* mutant background. We are exploring a possible regulatory pathway involving these three genes during vulval differentiation and morphogenesis. T04B2.6 is an uncharacterized gene that is expressed in the vulB1, vulB2 and vulD cells of the adult vulva. The expression of T04B2.6::yfp commences later than that of all other cell fate markers regulated by *lin-29*; its expression, however, is unexpectedly abolished in a *lin-29* background. We speculate that *lin-29* might indirectly regulate T04B2.6. A screen using RNA interference to all the known and putative transcription factors in the *C. elegans* genome is being conducted to identify transcription factors necessary for T04B2.6 expression. Thus far, this screen has revealed five transcription factors that may interact with LIN-29 in developmental coordination of the vulva.

442. Role of Wnt and Notch signaling and Hox gene in the patterning of **C. elegans** hook sensillum competence group
Hui Yu

In *C. elegans* males, three posterior Pn.p cells, P(9-11).p, form the hook sensillum competence group (HCG). Like hermaphrodite VPCs, each of the three multipotential HCG cells choose one of three fates (1°, 2°, 3°), and LIN-12 signaling is necessary for 2° fate specification. However, there is no evidence that LET-23/RAS pathway specifies the 1° HCG fate. We examined specification of cell fates in the *C. elegans* male HCG and found that the competence of HCG depends on Wnt signaling and the Hox gene *mab-5*. The Wnt pathway also promotes the 1° fate in HCG, in contrast to the vulval development in which EGF signaling induces the 1° VPC fate. Excess Wnt signaling caused by decreased Axin alters the competence of anterior P(3-8).p cells and induces ectopic 1° HCG fates. Additional *mab-5* activity by a gain-of-function mutation plus a proliferation signal from a non-Wnt pathway such as LIN-12 or EGF signaling could mimic the effect of Wnt signaling activation to induce ectopic HCG fates in anterior P(1-8).p cells.

443. Spicule development and signal transduction specificity

Adeline Seah, Shahla Gharib, Paul Sternberg
LET-23 activates two signal transduction pathways: RAS-MAPK for P11/P12 cell fate determination, vulval development and male spicule development and IP_3 - Ca^{2+} for ovulation. It is not known

what determines the specificity among the Ras-MAPK-dependent inductions. One possibility is that signaling specificity is achieved by the integration of multiple signaling pathways. In the male tail, anterior vs posterior fate specification of the four pairs of B.a great-grand-daughter cells is partially determined by positional cues provided by other male-specific blast cells or their progeny. These four pairs are known as the ventral (aa), dorsal (pp) and two identical lateral pairs (ap/pa). Each pair of cells has an anterior (α, γ or ϵ) and a posterior (β, δ or ξ) fate that produce different cell lineages and distinct fates. *lin-3* (EGF) has been implicated as the signal provided by the male-specific blast cells, U and F. Reduced activity of some of the genes in the EGF pathway causes abnormal anterior cell lineages. Conversely, *lin-12* reduction-of-function mutations exhibit posterior-to-anterior fate transformations. A role for the WNT pathway has been observed in the development of the male tail. Prior to fate specification of the B.a progeny, the WNT pathway is used to maintain the asymmetric B-cell division. Later in development, it is required for the SPD sheath cell fate. Consequently, we are looking at fate specification of B.a progeny in WNT pathway mutants. Fate transformations in previous studies were assayed using cell division patterns. Use of cell specific markers would provide greater accuracy in determining cell fate transformation. We are looking for molecular markers of the cell cycle as well as of the B cell lineage. A genome-wide RNAi screen is also being carried out to identify genes involved in male spicule development.

444. Male linker cell migration
Mihoko Kato

The linker cell (LC) is a sex-specific cell that leads the migration of the elongating gonad in the male. This stereotypic migration begins on the ventral body wall in the anterior direction and undergoes a series of turns along the body wall to connect the proximal end of the gonad to the developing proctodeum in the posterior region of the animal. I am interested in understanding the cell biology of the migration of the LC. Experiments involving either the ablation of cells neighboring the LC or the ectopic expression of extra LCs have shown that the LC alone is capable of migrating. In order to identify genes involved in LC migration, I have performed a pilot screen of approximately 200 genes using the RNAi feeding strains to look for defects in the male gonad. One gene identified to function in the LC is R07E5.3, a homolog of SNF5/INI1, which is a component of the SWI/SNF chromatin remodeling complex in many species.

445. WormBase, database of **Caenorhabditis** genomes, genetics and biology
Igor Antoshechkin, Carol Bastiani, Juancarlos Chan, Wen J. Chen, Ranjana Kishore, Raymond Lee, Hans-Michael Müller, Cecilia Nakamura, Andrei Petcherski, Erich Schwarz, Kimberly Van Auken, Daniel Wang, Paul Sternberg, the WormBase Consortium

WormBase (www.wormbase.org) has been improved in several ways over the last year. Entirely new data sets have been added (antibody, gene regulation, interactome, microarray, protein structure, SAGE, and ORFeome) and an anatomy ontology has been devised. Preexisting data types such as gene predictions, expression patterns, and functional annotations continue to be updated and expanded. The user interface has been revised for greater clarity and efficiency, and integrated with the Textpresso literature search tool. Batch downloads of genetic and sequence data have been provided. Remote, scriptable access to WormBase and stably archived releases ("freezes") through Perl modules and ACEDB query language enable reproducible bioinformatics analyses. Finally, WormBase is being expanded to comparative genomics, with orthologies to other model organisms and the impending analysis of five *Caenorhabditis* genomes.

446. WormBook - An online review of **C. elegans** biology
Lisa Girard, Juancarlos Chan, Eimear Kenny, Lincoln Stein¹, Paul Sternberg, Martin Chalfie²

WormBook is a new online book currently under development that will be an up-to-date resource for a range of topics relevant to *C. elegans* biology. Due to the exponential growth of the field, both *The Nematode C. elegans* and *C. elegans II* are now out of date. The growing complexity and sheer number of topics can no longer be done justice by another print version. Instead, utilizing an online format for WormBook will afford numerous advantages over print. WormBook will serve as a tightly linked component of WormBase, providing a context to elaborate on the facts that WormBase provides and offer a more general treatment of the information. Chapters in WormBook will be extensively cross-referenced among themselves, as well as in and out of Worm Base. WormBook will therefore be replacing and building on the functions of the two previous print books, as well as *Worm Breeder's Gazette*. The WormBook Editorial Board has already begun soliciting contributions from authors and we plan to have it freely available by June, 2005.

¹Cold Spring Harbor Laboratory, NY

²Columbia University, NY

447. Predicting genetic interactions by multi-source data integration
Weiwei Zhong

Genome-scale molecular and genetic experiments and systematic literature curation by model organism databases have made it possible to develop new methods to infer gene functions and interactions. We have developed an approach to predict genetic interactions genome-wide in *C. elegans* based on probabilistic analysis. Our method integrates genetic data from multiple sources and cross species. For each possible *C. elegans* gene pair, we search for genetic features such as identical phenotype, co-localization of gene products, and co-expression in microarray experiments. We then search for the genetic features of its orthologous gene pair in *Drosophila* and *S. cerevisiae*. We also examine whether the two genes have orthologs that interact genetically or physically in those organisms. Finally, a weighted score is assigned to each of the above-mentioned genetic features. We combine all the genetic features the gene pair possesses and compute the overall likelihood that the two genes genetically interact. We compare several statistic models, namely voting, logistic regression and Bayesian networks, for our scoring scheme. We also validate de novo predictions by genetic experiments. Our results show that although each genetic feature by itself is not enough to indicate a genetic interaction, combining these weak predictive features gives reliable predictions of genetic interactions.

448. Experimental annotation of **C. elegans** and **C. briggsae** genomes by the TEC-RED technique
Byung Joon Hwang, Hans-Michael Müller

Current genome annotation uses several gene prediction programs, but our limited understanding about genome complexity and diversity necessitates experimental methods to verify or correct these predictions. The most commonly used experimental method to identify expressed genes is expressed sequence tag (EST) analysis, which is biased towards the identification of the 3'-end of transcripts and is of limited utility for identifying the true 5'-end of an RNA transcript. In particular, when different RNA transcripts are produced from a single gene by alternative transcriptional initiations, EST sequencing alone cannot distinguish the shorter full-length alternative transcripts from partially degraded or incompletely extended versions of the longer transcripts.

We have developed a high-throughput technique (1) that efficiently identifies 5'-RNA ends, and thus can distinguish coding regions from regulatory regions and identify genes as well as their alternative transcripts that have different 5'-ends. *Caenorhabditis elegans* mRNA was chosen to develop and test this technique, (trans-spliced exon coupled-RNA end determination [TEC-RED]), because about 70% of mRNAs in *C. elegans* have a common first exon at their 5' ends, generated by a trans-splicing reaction between spliced leader (SL) RNA and the 5'-outrons (intron-like sequences at 5'-ends of pre-mRNAs). The *C. elegans* genome is one of the most

extensively annotated by computational analysis and by ESTs, which allows the fidelity of this TEC-RED technique to be tested. Application of TEC-RED to about 10% of the *C. elegans* genome yielded tags 75% of which experimentally verified predicted 5'-RNA ends, and 25% of which provided new information about 5'-RNA ends, including the identification of 99 previously unknown genes and 32 unknown operons.

In a collaborative project with the Genome Sciences Centre at the British Columbia Cancer Agency, a large-scale DNA sequencing effort has produced over 230,000 new 5' tags derived from *C. elegans* and *C. briggsae* trans-spliced mRNAs. This collection of tag sequences corresponds to 40-45% of the 5'-ends of the mRNAs from both nematode transcriptomes. In addition to 5'-end determination, we are also comparing TEC-RED tags from the mixed-stage *C. elegans* population with the 3' tag sequences from a Serial Analysis of Gene Expression (SAGE) library prepared from a similar biological sample (2). We expect that this combinatorial approach will complement SAGE-based transcription profiling and serve as an efficient way to annotate nematode genomes by accurately determining 5' and 3' ends of transcripts.

References

- (1) Hwang, B.J., Müller, H.M., and Sternberg, P.W. (2004) Proc. Natl. Acad. Sci. USA 101:1650–1655.
- (2) Jones, S.J., Riddle, D.L., Pouzyrev, A.T., Velculescu, V.E., Hillier, L., Eddy, S.R., Stricklin, S.L., Baillie, D.L., Waterston, R. and Marra, M.A. (2001) Genome Res. 11:1346-1352

449. **cis-regulatory sequence analysis in *Caenorhabditis sensu stricto* versus *sensu lato***
Erich M. Schwarz, John A. DeModena, Tristan De Buysscher, Eunpyo Moon, Nora Mullaney¹, Hiroaki Shizuya², Barbara J. Wold³, Paul W. Sternberg

The *Caenorhabditis* genus has ten known, culturable species; of these, four are morphologically and genetically similar enough to *C. elegans* to comprise an "Elegans group" (Kiontke et al., 2004). Within the Elegans group, *C. sp.* CB5161 is intermediate between the two organisms with sequenced genomes (*C. elegans* and *C. briggsae*). Outside the Elegans group, *C. sp.* PS1010 is the most closely-related species with substantive behavioral and morphological differences to *C. elegans*. In collaboration with the Joint Genome Institute, we isolated ~500 kb of sequence data from spp. CB5161 and PS1010 apiece, comprising ~0.5% of each species' genome. We find that comparative analysis of CB5161 and PS1010 genes gives very different results. The *lin-3* and *lin-11* genes of CB5161 are structurally similar to those of *C. elegans*, and a two-step process of alignment with Mussa (mussa.caltech.edu) and local scanning with YMF/Explanators reliably yields regulatory sequence motifs in both of these genes whose functions are experimentally validated. The statistical strength of these

predictions (YMF z-scores) steadily increases as the number of species within the Elegans group being compared is increased from two to four. Conversely, neither the *lin-3* nor the *lin-11* genes of PS1010 yield these sequence motifs, and incorporating them in multiple genome comparisons simply increases statistical noise. If these results are taken at face value, a complete genomic rewiring of two genes critical for postembryonic development would seem to have occurred after the diversification of the *Caenorhabditis* genus but before that of the Elegans group. We are currently using the CB5161 sequences as a test set for development of cis-regulatory sequence annotation pipelines that should be applicable to the genomes of *Caenorhabditis* species closely resembling *C. elegans*. At the same time, we are trying to make sense of the more challenging data from PS1010 by scanning for statistically overrepresented sequences within PS1010 genes alone.

¹Caltech undergrad

²Caltech, Member of the Professional Staff

³Professor, Division of Biology, Caltech

Reference

Kiontke, K., Gavin, N.P., Raynes, Y., Roehrig, C., Piano, F. and Fitch, D.H. (2004) Proc. Natl. Acad. Sci. USA 101:9003-9008.

450. Pipeline for **cis-regulatory** sequence annotation
Alok Saldanha, Daniel Fu

We have constructed a pipeline for high throughput identification of evolutionarily constrained regions. Since an optimal solution to this task has not been determined, we have developed a modular architecture using standard interchange formats such as GFF, that can scale as new computational methods and genomes become available. This allows us to take an empirical approach, determining a "gold standard" set of enhancers, and then evaluating the ability of leading methods to find these regions on an even playing field. The output of the pipeline can be viewed in standard GFF browsers, such as Apollo, or can be used as the basis for further computation. As an optimal strategy emerges, the pipeline will likely be incorporated into WormBase, enabling rapid reannotation as new nematode sequence becomes available and making high quality estimation of evolutionarily conserved regions in the worm publicly available.

We are investigating the mechanisms that drive tissue-specific gene expression in the hypodermis using the cuticle collagens as a reference gene set. We have begun testing computationally predicted tissue-specific enhancers for their ability to recapitulate the expression of full-length flanking sequence. It is our hope that a large catalog of enhancers will allow us to computationally mine for important sequence features such as motifs and spacing and orientation constraints. We hope to build a predictive model of hypodermal enhancers and shed light on the molecular basis of cell type. Ultimately, we hope to discover a principle that will be of some use in heterologous systems.

* Caltech undergraduate

451. Functional analysis of EGL-30-mediated signaling in **C. elegans**

Carol A. Bastiani, Shahla Gharib, Wen J. Chen

egl-30 encodes the *C. elegans* ortholog of vertebrate $G\alpha_q$, and is over 80% identical to vertebrate $G\alpha_q$. It is required for the regulation of many behaviors in *C. elegans*, including egg laying and pharyngeal pumping. We have found that the pathways downstream of EGL-30 that regulate these two basic behaviors are likely to be distinct. EGL-8, the *C. elegans* ortholog of vertebrate PLC β 4, appears to be the primary effector of EGL-30 for the regulation of pharyngeal pumping, while EGL-8 plays at most a minor regulatory role downstream of EGL-30 with respect to egg laying. PLC β isoforms are the only well characterized effectors for $G\alpha_q$. We are currently mapping four independently isolated extragenic suppressor mutations of an egl-30 reduction-of-function mutation, and expect to identify genes that encode other candidate effectors or regulators for EGL-30. Based on sequence and functional conservation of EGL-30 and $G\alpha_q$, we expect that the identification of these signaling components will provide insight into signaling by vertebrate $G\alpha_q$ family members.

We are also examining functional interactions of EGL-30 with regulatory proteins and with candidate receptor proteins in human cell lines. Previous studies in the lab identified RGS proteins as key molecules for integration between the $G\alpha_o$ and $G\alpha_q$ signaling pathways in *C. elegans*. Genetic analyses, as well as physical interaction studies in human cell lines, suggest that these RGS proteins integrate signals bidirectionally between the $G\alpha_o$ and $G\alpha_q$ signaling pathways. Functional studies suggest that other components that might be required for the integration of these signaling pathways are conserved in human cell lines. We are currently examining the mechanisms for how integration between these signaling pathways is achieved.

Coexpression of vertebrate receptor proteins, which can couple to $G\alpha_q$ /EGL-30, with the effector EGL-8 has revealed that receptor-EGL-8 interactions play a role in the stable expression of EGL-8. Such receptor-effector interactions may play an important role in determining which downstream signaling pathways predominate in different cell types.

452. Sperm transfer during male mating behavior
Gary Schindelman

When attempting to mate, *C. elegans* males exhibit a seamlessly reproducible series of sub-behaviors culminating in the transfer of sperm to the hermaphrodite. These sub-behaviors are: response to hermaphrodite, backing, turning, vulval location, spicule insertion and sperm transfer. By dissecting each sub-behavior, their eventual integration as a complex series of overlapping behaviors can be understood and provide insight into sensory perception and nervous system function. One of

our foci has been on the last sub-behavior in this process, sperm transfer. Observation of wild-type sperm transfer has defined four steps in this process: initiation, release of sperm, continuation and cessation of transfer. To begin to answer fundamental questions about how sperm transfer is regulated, we performed a genetic screen designed to isolate males defective for this process and isolated two mutants. One mutant is defective in the initiation step of sperm transfer (sy671) and the other defective for sperm transfer continuation (sy672); both appear morphologically wild type.

We positionally cloned sy671 and it is an allele of unc-18, a Sec1-related protein involved in the docking of vesicles at the pre-synaptic terminal. Mutants with severe paralysis initially defined the unc-18 locus, but weaker alleles exist. Of the 12 published sequences of unc-18 alleles (weak and strong), all have molecular lesions in either exon 4 or exon 9. Interestingly, sy671 has a mutation in exon 8 and a weak uncoordinated (Unc) phenotype. UNC-18 was reported to be expressed in all the ventral cord motor neurons and some unidentified head neurons in the adult hermaphrodite. Its expression in the male has not been reported. We made a rescuing *punc-18::unc-18-YFP* transgene that shows this expression pattern, but also shows that UNC-18 is expressed in neurons in the male tail, as well as in the male gonad (a non-neuronal tissue). The expression in the male gonad is in the "valve" region where sperm are initiated to move from the seminal vesicle to the vas deferens. We expressed the unc-18-YFP transgene under different tissue-specific promoters to define the site of action for the initiation of sperm transfer. The neuronal expression, but not the gonadal expression, is necessary to rescue the defect in initiation of sperm transfer in unc-18(sy671). This rescued line however shows a defect in the continuation of sperm transfer, which can be rescued by adding back the gonadal expression. Therefore unc-18 has two sites of action in different tissue types for sperm transfer behavior.

453. Control of locomotory behavior in **C. elegans** male mating

Allyson J. Whittaker, Gary Schindelman, Shahla Gharib, Yvonne Hajdu-Cronin

We are interested in how genes encode behavior.

To address this question we are examining control of locomotory behavior and its modulation by sensory input. The *C. elegans* male is a good model for addressing this question as during male mating behavior a number of alterations occur in the normal sinusoidal movement pattern. We are particularly interested in the early steps of mating behavior, response, backing and turning as this is when the most dramatic changes in locomotory behavior occur. When a male contacts a hermaphrodite he presses the ventral side of his tail against the hermaphrodite and initiates backing behavior. If he reaches the end of the hermaphrodite without contacting the vulva, he turns around the hermaphrodite and continues backing on the other side. When the vulva is reached, the male stops

backward locomotion inserts his spicules and transfers sperm.

In an attempt to dissect the neural circuits and signaling pathways controlling response, backing and turning behavior we have performed an F2 clonal screen for mutations that disrupt mating behavior. From this screen, eight mutations were isolated that disrupt these early steps of mating behavior. We are currently focusing on one of these mutations, sy682, that disrupts response and vulva location behavior. 93% of sy682 males are defective in response and 42% for vulva location in comparison to 16.7 % response defective and 0% vulva location defective seen in wild-type males assayed on the same days. Specifically, these males touch many hermaphrodites before responding and pass the vulva more times before stopping than wild-type males. We are additionally studying cod-5, a mutant isolated in a mating efficiency screen. Of males homozygous for mutations in cod-5, 81% are disrupted in response, 62% are defective in turning and 44% are disrupted in vulva location. Specifically, cod-5 mutant males take longer than normal to respond to a hermaphrodite. Although males are able to execute a turn correctly they often fail to initiate a turn, backing off of a hermaphrodite and either swimming away or loosely making contact with the other side. Mutant males also have difficulty keeping their tails straight during backing and often briefly back along the lateral side of hermaphrodites. We are determining the genes disrupted in these two mutant lines. A more direct approach is also being taken in which the effects of the application of exogenous neurotransmitters on male tail movement and the effect of neurotransmitter synthesis mutants on mating behavior are being examined.

454. Comparative analyses of ASH-mediated behaviors

Jagan Srinivasan, Krisha Begalla*

We are taking a comparative approach to address behavioral variation among different species of nematodes. *C. elegans* has a simple nervous system consisting of 302 neurons to detect and respond to diverse environmental stimuli. Some neurons respond to a single stimulus whereas others respond to multiple (polymodal) stimuli. A question that arises is, how does a single neuron evolve multiple functions to sense different stimuli? Is polymodality necessary to circumvent some constraint or to efficiently use the small number of neurons? The goal of these studies is to understand whether polymodality evolves or is a general property of nematode nervous systems. The polymodal neuron is known to detect several different stimuli such as mechanical, osmotic and chemical stimuli and has been well characterized in *C. elegans*. The activation of the ASH neurons leads to a synaptic input to the interneurons which regulate/cause spontaneous reversals and backward locomotion. Given the prolific nature of nematodes and the availability of a good phylogenetic tree, we tested different species i) *C. elegans* (N2), ii) *C. briggsae* (AF16), iii) *Caenorhabditis* sp (CB5161), iv) *Caenorhabditis* sp. (PS1010), v) *P.*

pacificus (PS312) vi) *Cruzema* sp. (PS1351) and vii) *Panagrellus redivivus* for a) osmotic avoidance, b) response to nose touch, and c) volatile chemical repellence. Our behavioral assays indicate some differences in ASH-mediated behavior in some species of nematodes. For the osmotic avoidance assay, all species we tested avoided the high osmolarity. However, we observe differences in behavior for the nose touch and volatile repellent assays. We are using laser ablation studies to confirm that these behaviors are mediated by ASH in other species of nematodes.

*Pre-frosh, UCSD

455. An automated system for measuring parameters of nematode sinusoidal movement
Christopher Cronin, Jane E. Mendel

Nematode sinusoidal movement is a fascinating yet not well understood example of sinusoidal movement, but movement defects have been used in a large number of studies of *C. elegans* development, behavior and physiology including aging. Molecular genetic analysis depends in part on the accuracy of phenotypic analysis, and thus an enhanced capability to analyze nematode movement might help in the analysis of gene function. A few years ago, we developed with Saleem Muhktar and Shuki Bruck a system to analyze nematode movement in an automated and quantitative manner. We have made this user-friendly. In this system nematodes are automatically recognized and a computer-controlled stage ensures that the nematode is kept within the camera field of view. The images are stored to tape. In a second step, the images of the videotapes are processed to recognize the worm, and to extract information about their length, posture, etc. From this information, a variety of parameter of movement are calculated. These parameters include the velocity of worm centroid, the velocity along the worm's track, the extent and frequency of body bending and the propagation of the contraction wave along the body. We applied this system to genetic analysis and gene-toxin interactions. The system allows discrimination of distinct genotypes (activation of Gq-alpha versus loss of Go-alpha function), as well as of different mutant alleles at a single locus (null and dominant-negative alleles of the *goa-1* gene, which encodes Go-alpha). Dose-response curves for toxins arsenite and aldicarb, both of which affect motility, were determined in wild-type and several mutant strains. *cat-4* were more sensitive to arsenite but not aldicarb; P-glycoprotein mutants are more sensitive for both compounds.

456. Nematode sinusoidal movement: Theory and experiment

Jan Karbowski, Adeline Seah, Christopher J. Cronin, Jane E. Mendel

We are interested in understanding the mechanism controlling the undulatory locomotion of nematodes. We recorded movement of worms with our automated movement analysis system, focusing on genetic perturbations to potential controlling parameters, including neurons, muscle, and cuticle. We also examined the undulatory locomotion of different *Caenorhabditis* species. We constructed a theoretical model that combines neural dynamics, mechanics, and biophysics, and that can be directly-related to parameters measured experimentally. These parameters include velocity of movement, frequency, amplitude, and wavelength of undulations. The model fits the data well. For the cases we studied, the undulatory locomotion is robust. We suggest that the control mechanisms, implemented by mechano-sensory feedback, are robust as well, and optimize the velocity.

457. Quantitative analyses of nematode locomotion on different food sources

Jagan Srinivasan, Angie Shih*, Jerome Muller², Christopher Cronin

Many free living nematodes inhabit the soil, which is an ecosystem containing different food sources. An interesting question that arises is, how do nematodes move on these food sources? Since the lab has developed a machine-vision system that quantifies nematode locomotion, we are currently using this technology to quantify locomotion of different species of nematodes on different food sources. The nematode species that are being tested are: i) *C. elegans* (N2), ii) *C. briggsae* (AF16), iii) *Caenorhabditis* sp (CB5161), iv) *Caenorhabditis* sp. (PS1010), v) *P. pacificus* (PS312), vi) *Cruzema* sp. (PS1351) and vii) *Panagrellus redivivus*. We have currently chosen six different bacterial species for analyses viz. *E. coli* OP50, *Pseudomonas aeruginosa*, *Micrococcus luteus*, *Bacillus subtilis*, *Serratia marcescens* and *E. coli* HB101. Each nematode species will be tested with all the six different bacteria and various locomotory parameters will be computed. Additionally genetic screens in some species, for instance *Pristionchus pacificus*, will be carried out to isolated hyperactive mutants for comparative analyses with *C. elegans*.

¹Pre-frosh, Caltech

²Special Grad Student, Caltech

458. Beneficial and pathogenic interactions in the nematode gut: One bacterium, two interactions
Todd Ciche

Despite being dependent on bacteria for food and being immersed in a microbial world, details concerning the innate immune system of nematodes are still being elucidated. The enteric insect pathogenic bacterium, *Photorhabdus luminescens*, is an obligate symbiont of the rhabditid nematode, *Heterorhabditis bacteriophora* and pathogenic to *Caenorhabditis elegans*. The bacterium is

specifically transmitted in the gut mucosa of the dauer juvenile of *H. bacteriophora*, where it is regurgitated into the hemocoel of insects, usually resulting in insect mortality. The bacterium is normally pathogenic to *C. elegans*, producing toxic metabolites that inhibit nematode growth and reproduction. However, under low nutrient and high salt conditions the bacterium is permissive for *C. elegans* growth and reproduction. Using GFP-labeled bacteria and genetics, we are investigating how *H. bacteriophora* distinguishes between symbiotic and non-symbiotic bacteria and how *C. elegans* prevents colonization by *P. luminescens* in the adult intestine. Several *C. elegans* mutants exhibiting increased susceptibility to *P. luminescens* have been obtained and are being characterized. By taking a comparative approach, factors specific to beneficial nematode-bacterium interactions and common to nematode innate immunity can be determined.

Most animal intestines are inhabited by numerous and diverse communities of microbes some of which are beneficial to the host. Beneficial bacteria benefit their hosts by aiding digestion, biosynthesis of essential nutrients, exclusion of pathogens, tissue development and proper immune functioning. Animal intestines have the ability to discriminate between beneficial and pathogenic bacteria, facilitating colonization and growth of the former, while defending against the latter. The mechanisms by which animals distinguish beneficial (i.e., symbiotic) bacteria from non-symbiotic (or pathogenic) bacteria is being studied in the nematode *Heterorhabditis bacteriophora* because it is genetically tractable and is obligately and mutually associated with the enteric bacterium, *P. luminescens*, which the nematode selectively transmits in the gut of the infective juvenile. The nematode is a vector for the bacteria delivering it into the blood cavity of susceptible insect hosts. The bacteria are labeled with a green fluorescent protein so that they can be easily observed in the gut of the nematodes. Genetics are being employed to identify genes in the nematode required to discern symbiotic from non-symbiotic bacteria. Few symbiotic interactions are available where both the host and symbiont are genetically tractable and the result of the interaction obvious.

459. Engineering *C. elegans* cells

Jane E. Mendel, John DeModena, Weiwei Zhong, Shawn Xu, Paul Sternberg

We are starting to engineer *C. elegans* cells. One of our approaches is to express G protein coupled receptors (GPCRs; e.g., β -adrenergic receptor) in a particular sensory neuron and achieve reproducible responses to ligands. We would like to determine whether distinct GPCRs can be engineered to have distinct channels of intracellular communication. The readouts for responses include transcriptional GFP reporters, as well as direct indicators of second messenger levels. Towards this goal, we are expressing exogenous proteins in *C. elegans* cells to serve as sensors of intracellular second messengers. We are also trying to adapt bacterial and yeast proteins (e.g.,

GAL4, lacI, etc., for use in *C. elegans* so we can take advantage of other people's work on synthetic circuits. Our goal is to more efficiently probe *C. elegans* biology as well as to alter the properties of *C. elegans* to test our understanding of biological circuits.

Publications

- Bastiani, C.A., Gharib, S., Simon, M.I. and Sternberg, P.W. (2003) *C. elegans* G α q regulates egg-laying behavior via a PLC-independent signaling pathway, and likely functions in both the nervous system and in muscle. *Genetics* 165(4):1805-1822.
- Bourbon, H.M., Aguilera, A., Ansari, A.Z., Asturias, F.J., Berk, A.J., Bjorklund, S., Blackwell, T.K., Borggreffe, T., Carey, M., Carlson, M., Conaway, J.W., Conaway, R.C., Emmons, S.W., Fondell, J.D., Freedman, L.P., Fukasawa, T., Gustafsson, C.M., Han, M., He, X., Herman, P.K., Hinnebusch, A.G., Holmberg, S., Holstege, F.C., Jaehning, J.A., Kim, Y.J., Kuras, L., Leutz, A., Lis, J.T., Meisterernest, M., Naar, A.M., Nasmyth, K., Parvin, J.D., Ptashne, M., Reinberg, D., Ronne, H., Sadowski, I., Sakurai, H., Sipiczki, M., Sternberg, P.W., Stillman, D.J., Strich, R., Struhl, K., Svejstrup, J.O., Tuck, S., Winston, F., Roeder, R.G. and Kornberg, R.D. (2004) A unified nomenclature for protein subunits of mediator complexes linking transcriptional regulators to RNA polymerase II. *Mol. Cell.* 14(5):553-557.
- Gupta, B.P. and Sternberg, P.W. (2003) The draft genome sequence of the nematode *Caenorhabditis briggsae*, a companion to *C. elegans*. *Genome Biol.* 4:238.
- Hajdu-Cronin, Y.M., Chen, W.J., and Sternberg, P.W. (2004) The L-type cyclin CYL-1 and the heat-shock factor HSF-1 are required for heat-shock induced protein expression in *C. elegans*. *Genetics*. In press.
- Harris, T.W., Chen, N., Cunningham, F., Tello-Ruiz, M., Antoshechkin, I., Bastiani, C., Bieri, T., Blasiar, D., Bradnam, K., Chan, J., Chen, C.-K., Chen, W. J., Davis, P., Kenny, E., Kishore, R., Lawson, D., Lee, R., Müller, H.-M., Nakamura, C., Ozersky, P., Petcherski, A., Rogers, A., Sabo, A., Schwarz, E. M., Van Auken, K., Wang, Q., Durbin, R., Spieth, J., Sternberg, P.W. and Stein, L.D. (2004) WormBase: A multi-species resource for nematode biology and genomics. *Nucl. Acids Res.* 32:D411-D417.
- Hwang, B.J. and Sternberg, P.W. (2004) A cell-specific enhancer that specifies *lin-3* expression in the *C. elegans* anchor cell for vulval development. *Development* 131:143-151.
- Hwang, B.J., Müller, H.-M. and Sternberg, P.W. (2004) Genome annotation by high-throughput 5'-RNA end determination. *Proc. Natl. Acad. Sci. USA* 101:1650-1655.
- Inoue, T., Oz, H.S., Wiland, D., Gharib, S., Deshpande, R., Hill, R.J., Katz, W.S. and Sternberg, P.W. (2004) *C. elegans* LIN-18 is a Ryk ortholog and functions in parallel to LIN-17/frizzled in Wnt signaling. *Cell* 118:795-806.
- Kariya, K., Bui, Y.K., Gao, X., Sternberg, P.W. and Kataoka, T. (2004) Phospholipase C ϵ regulates ovulation in *Caenorhabditis elegans*. *Dev. Biol.* 274:201-210.
- Miley, G.R.K., Fantz, D., Glossip, D., Lu, X., Saito, R.M., Inoue, T., Palmer, R.A., van den Heuvel, S., Sternberg, P. W. and Kornfeld, K. (2004) Identification of residues of the *Caenorhabditis elegans* LIN-1 ETS domain that are necessary for DNA-binding and regulation of vulval cell fates. *Genetics* 167:1697-1709.
- Müller, H.-M., Kenny, E. and Sternberg, P.W. (2004) Textpresso: An ontology-based information retrieval and extraction system for *C. elegans* literature. *PLoS Biol.* In press.
- Schwarz, E.M. and Sternberg, P.W. (2004) Searching WormBase for information about *Caenorhabditis elegans*. In *Current Protocols in Bioinformatics*, A.D. Baxevanis, D.B. Davison, R.D.M. Page, G.A. Petsko, L.D. Stein, and G.D. Stormo., eds., John Wiley & Sons, New York. [Unit 1.9, Supplement 2].
- Sternberg, P.W. (2004) Developmental biology: A pattern of precision. *Science* 303(5658):637-638.
- The Gene Ontology Consortium (2004) The Gene Ontology (GO) database and informatics resource. *Nucl. Acids Res.* 32:D258-D261.
- Whittaker, A.J. and Sternberg, P.W. (2004) Sensory processing by neural circuits in *Caenorhabditis elegans*. *Curr. Op. Neurobiol.* 14:450-456. In press.

Bren Professor of Molecular Biology: Barbara J. Wold
 JPL Visiting Associate: Eric Mjolsness
 Member Professional Staff: Hiroke Shizuya
 Visitors: Liberia Berghella, Eunpyo Moon
 Postdoctoral Scholar: Brian Williams
 Graduate Students: Tristan DeBuyscher, Christopher Hart, Tony Kirilusha, Tracy Teal
 Research and Laboratory Staff: Leslie Dunipace, Richele Gwartz, Brandon King, Dee Page, Joe Roden, Diane Trout

Support: The work described in the following research reports has been supported by:

- Department of Energy
- Keck Foundation
- National Cancer Institute
- National Institute of Arthritis and Musculoskeletal and Skin Disease
- National Institutes of Health/USPHS

Summary: In the Wold group we are interested in the composition, evolution and function of gene regulatory networks and we often use muscle development as a favored model system. We are especially interested in networks that govern how cell fates are specified and executed during development and during regeneration. This theme extends to related lineages of adult stem cells for our model system and to the way in which cells of this same lineage can become tumorigenic. Approaches to these problems increasingly use genome-wide and proteome-wide assays. To do this some of our efforts now include development of new wet-bench genomic technology and computational methods, the latter developed in an on-going partnership with Professor Eric Mjolsness of JPL/University of California, Irvine. Many of the technologies, computational tools, modeling databases, etc., are first developed and tested and vetted using yeast as the model genomic system.

A key challenge is to understand the regulatory events that drive the progression from multipotential precursor cells to determined unipotential progenitors and then to fully differentiated cells. We are currently studying these cell states and transitions using microarray gene expression analysis, global protein:DNA interaction measures, mass spec-based proteomics of multiprotein complexes, and comparative genomics. The mouse is our primary experimental animal, and the focal developmental lineage arises from paraxial mesoderm to produce muscle (also bone, skin and fat, among other derivatives). Skeletal myogenesis is governed by both positive- and negative-acting regulatory factors. The MyoD family of four closely related, positive-acting transcription factors are key. Upon transfection each can drive nonmuscle recipient cells into the myogenic pathway. Given their extraordinary power to drive or redirect a cell fate decision, a central goal is to understand how the regulatory network in which they are embedded directs cell fate selection and execution of the differentiation transition. At cellular and molecular levels, it is clear that negative

regulators of skeletal myogenesis are probably just as important for regulating the outcome as are the positive regulators. The interaction between positive- and negative-acting regulators continues to be of particular interest. Multiple negative regulators of skeletal muscle are expressed in multipotential mesodermal precursors and in proliferating muscle precursors (myoblasts). It is generally believed that some of these are important for specifying and/or maintaining precursor cells in an undifferentiated state, though exactly how the system works is unknown and a subject for investigation. A new addition to our studies of myogenic development and degeneration asks what role differential translation and RNA-mediated regulatory mechanisms play at each step, and how these might mediate cell communication in the neuromuscular system.

To define protein:protein complexes in the network more comprehensively, we developed a major collaborative effort with the Deshaies lab here and the John Yates lab at Scripps to modify and apply MudPIT mass spectrometry, coupled with dual affinity epitope tagging, to characterize multiprotein complexes. New technology development projects are focused on large-scale measurements of protein:DNA interactions. To define the cis-acting regulatory elements to which these protein complexes bind, we have entered into a collaboration with Eric Greene at NIH to isolate and sequence genes from our network from ten vertebrate species each. The computational tools described below have been used to find candidate conserved regulatory elements, and these are, in turn, being subjected to functional assays via lentiviral-mediated transgenesis. These same tools are being used to analyze data from multiple species of worms related, in differing degrees, to *C. elegans*. This project is in partnership with the Sternberg lab and Hiroke Shizuya here at Caltech, and the DOE Joint Genomics Institute, where large-scale DNA sequencing is done. In this project large insert, random shear libraries were made for two new worm species, and genes from several regulatory networks, including the myogenic one are being isolated and sequenced for comparative analysis. In addition to clarifying how many and which worm genomes give us the most leverage for identifying functionally important noncoding elements in the genome, we hope to gain insights into the evolution of myogenic and cell cycle networks across large phylogenetic distances between vertebrates, worms and flies.

Our work with Dr. Timothy Triche and colleagues at Children's Hospital is showing how the myogenic developmental pathway relates to cells of the myogenic lineage when they run amok in cancer. Transcriptome analysis of over 100 rhabdomyosarcomas has given us several new insights into the nature of these tumors, plus identification of previously unappreciated signaling pathways that are candidates for causal contributions to tumor properties. Of particular interest was a surprising reclassification of one subgroup of tumors. These are, by histological criteria, of the alveolar class. However, by expression profiling and subsequent computational analysis, these tumors proved to be very different from classic

Alveolars and more similar to the other major class (embryonal). Retrospectively, we were able to relate this to the absence of a chromosomal translocation that characterizes the most alveolar tumors. This analysis also showed, surprisingly, that genes whose expression best separates conventional alveolar and embryonal types does not correlate with their histological appearance, but rather refers to other molecular differences. We postulate that these "invisible" differences may have more powerful prognostic capacity than conventional histopathology, since the two tumor classes differ significantly in outcome, than does histopathological classification. This has implications for treatment pathways and prognosis.

A new project for the lab is Tracy Teal's study of biofilm development that is joint effort with Diane Newman in the Division of Geology and Planetary Science. The goal is identify, visualize, and ultimately understand the multiple different metabolic cell states that comprise a biofilm at different stages of its development and under differing environmental stimuli. The degree to which principles and regulatory strategies used by metazoans during development are or are not employed by bacteria in creating biofilm structures is being probed by marking bacteria with multiple GFP derivatives driven by genes that will mark functional domains (aerobic vs. anaerobic, for example).

460. Analysis of transcriptional protein complexes via MudPIT mass spectrometry
Leslie Dunipace, Johannes Graumann¹, Jae Hong Seoul²

It is difficult to overestimate the usefulness of learning the *in vivo* protein associations that mediate a cellular process. This project focuses on protein complexes involved in regulating gene expression and is part of a larger collaborative effort between our lab, the Deshaies lab, and John Yates' lab at Scripps. The overall collaboration has the initial goal of modifying and then applying at relatively high throughput, a mass spectrometry-based method for mapping protein interactions *in vivo*. This approach couples MudPIT (MultiDimensional Protein Identification Technology) which originated in the Yates lab, with a dual affinity protein tagging/sample retrieval system constructed in the Deshaies group called HTM/HPM. Leslie used the tag to establish 25 yeast strains, each carrying the product of targeted recombination at a selected gene, so that the protein produced (from its normal regulatory sequences in the chromosome) carries an affinity tag at the carboxy-terminal end. This affinity tag contains two epitopes (His-9 and Myc-9) separated by a protease site. The His and Myc tags were used for sequential and rapid affinity purification. The purpose of the affinity steps is to enrich the sample for the tagged protein together with proteins associated with it, while eliminating unassociated proteins. Dual affinity is designed to eliminate the need for gel purification and "band-cutting," which has been a rate-limiting step in sample preparation in similar studies in the Deshaies lab and elsewhere in the past. The mass-spec

analysis that follows identifies peptides in the sample by reference to the known genome and its predicted proteome, using a version of the Sequest software. By increasing throughput to this level, we have now shown that a cell biology lab can perform comprehensive network-scale analyses of multiprotein complexes.

Results from this first study showed that, surprisingly, we could identify and verify new protein associations for major and well studied cellular protein "machines," including the Swi2 and GCN5 chromatin remodeling complexes.

A transcription oriented MudPIT project in mammalian systems focuses on identifying interacting proteins for MyoD and its family members. Leslie generated a family of retroviral vectors that can be used to make transgenic mice or to mediate expression in cultured mouse or human cells. Two such vectors – one placing the dual affinity HPM tag at the amino terminus of the target protein (gene) and the other at the carboxy terminus were constructed, and transgenic cell lines are now being used for protein:protein interaction measurements and for chromatin immunoprecipitation.

¹Division of Biology, Ray Deshaies Lab, Caltech

²Seoul National University, Korea

461. Developing genomic DNA as a comprehensive cohybridization standard for use in microarray gene expression measurements

Richele M. Gwartz, Brian A. Williams

Standardization of gene expression measurements on spotted microarrays is accomplished by ratiometric quantitation. This is necessary because the mass of hybridizable material deposited on each spot is not uniform. In practice, ratiometric standardization is accomplished by simultaneous co-hybridization of the array to two samples of fluorescently-labeled nucleic acid. The general form of this ratio is that the numerator measurement contains fluorescent intensity for the experimental sample, while the denominator measurement contains fluorescent intensity for a reference sample. Subsequent comparison of multiple samples is accomplished through the common denominator RNA preparation. In any given comparison of two cell populations or experimental conditions, a number of genes will be expressed in both cell types, and will yield reliable ratiometric measurements. However, ratiometric measurements are problematic for genes that are not expressed in the reference population (the denominator measurement), and also for genes that are expressed at exceedingly high levels in the reference. Thus, as the denominator measurements become increasingly small, the ratiometric values for the gene in question become disproportionately large and error riddled.

To address the various shortcomings of RNA denominators, we were able to show that genomic DNA can be a high quality, universal, low cost microarray cohybridization standard. For reproducibility and stability of ratios, we showed that DNA outperforms commercially available RNA mixtures which are the current widely used state of the art. A genomic DNA standard performs three

functions that the RNA mixes fall short of: 1) Since genomic DNA includes all genes present in the mouse genome, it provides universal coverage of the spots on the microarray, and should avoid the problem of highly unstable denominator intensity figures in computed ratios; 2) Since the vast majority of genes are represented at equimolar (single copy) concentration in genomic DNA, available sites for hybridization of labeled experimental sample are uniform and are of modest, technically desirable intensity; and 3) Genomic DNA is the same in sequence content from lab to lab and from prep to prep. This generates universality. RNA reference samples inevitably vary and cannot be identical from lab to lab and over time.

For organisms with a relatively low genomic DNA complexity, such as *Arabidopsis thaliana* or *C. elegans*, or yeast, the signal expected per gene feature is expected to be even more robust than in mouse where we did the development work. We therefore predict that this approach will work well for these model genomes as well. The final objective in the project for the coming year is to develop DNA as a "third color," such that it can be used as the reference standard in a reaction that contains two different RNA probes. See the Wold group website for the most current protocol and Williams et al. (2004) for supporting data.

462. Defining myogenic determination and differentiation on a whole-genome scale

Brian A. Williams, Richele Gwartz, Shuling Wang*

The immediate biological goal in this project is to define comprehensively the gene expression states in a model vertebrate developmental pathway. Within this goal is the aim of dissecting out responses to multiple signaling pathways that act to enhance or suppress myogenic differentiation. This pathway has three defined stable cell states linked by dynamic transitions: 1) Proliferating multipotential mesodermal precursor cells that can elect the myogenic pathway or several other possibilities; 2) These multipotential precursors can be stimulated to convert to "determined" myoblasts which are proliferating unipotential muscle precursor cells; and 3) Myoblasts can then be triggered to differentiate, at which point they express the genes and cellular properties of a mature muscle cell or myocyte.

The second goal is to use the data obtained to help evaluate our suite of different "clustering" algorithms to determine which ones are most useful in which ways for analyzing large-scale data of this kind (see entry from Chris Hart et al., in this section). A third goal is to use the data to advance our current model of the regulatory circuitry that controls this developmental pathway. Clustered expression data is one key input in defining the circuit, which is then joined by comparative genomic DNA sequence data and protein:DNA binding studies (see entry of Tristan DeBuysscher).

Fluorescently-labeled cDNA populations representing skeletal muscle cells during several time courses of differentiation have been co-hybridized to the

arrays in the presence of cDNA from each of several "reference RNAs." Biologically relevant reference RNA sets include undifferentiated proliferating myoblasts (multipotential muscle precursor cells) and multipotential mesodermal precursor cells whose possible developmental fates include muscle cells. The comparisons of muscle differentiation courses with different reference RNA sets is designed to expose groups of genes whose expression in muscle changes relative to each of the different reference cell states. Through use of various clustering methods we have identified components of a contractile apparatus regulon. Detailed kinetics reveal that this group is subdivided into kinetic classes, and the working hypothesis is that each of these groups depends differently on input signals (calcium-dependent; FGF-dependent; insulin-dependent, etc.). These suggest, in turn, differential participation by specific transcription factors activated or repressed by each signal. The regulon was also shown to contain a number of expressed sequence tags representing previously unidentified genes in the mouse genome. To internally monitor the readout of these pathways dissected from each other, we created modified myogenic cell lines that allow us to measure the activities of individual transcription factors that we know are important in our system (MyoD family sites; MEF2 sites) to assist in attributing readout at natural complex genes. This information is then used in conjunction with computational tools to identify and categorize the cis-acting regulatory domains that drive genes within the regulon. Other groups of genes that belong to novel clusters have been identified and highlighted for further study, including some whose expression precedes any previously known regulator in the myogenic differentiation pathway, making them candidates for hitherto unknown upstream regulatory functions.

*University of California, Irvine

463. Characterization of pediatric sarcomas by microarray-based gene expression studies

Sagar Damle¹, Joe Roden, Ben Bornstein², Dennis DeCoste², Eric Mjolsnes

The central model system for our lab's developmental biological studies is paraxial mesoderm with emphasis on the myogenic pathway. In cancer biology, tumors derived from these cell lineages are the sarcomas of childhood, and those in the muscle lineage are called rhabdomyosarcomas. This work begins by probing a well-defined and large set of rhabdomyosarcomas via large-scale expression analysis and ask a series of questions including: How does gene expression in the tumors relate to that seen in normal development? Can we detect groups of genes whose patterns of expression predict how aggressive a tumor will be? Can we identify patterns of genes that classify tumors into subgroups that correspond to those currently generated by pathologists? Is there a group of genes whose expression that corresponds with presence of two known chromosomal translocation events that are believed to be causal for one subtype of tumor? Is there a set of genes that can help explain the bizarre observation that a small subset of these tumors are highly metastatic, yet

essentially benign, while others that look histologically similar are rapidly fatal? We then seek to relate what is known about the identities of signature genes with signaling pathways, cell shape and migration, gene regulation, etc., to identify candidate genes or pathways for future drug treatments.

Two histopathologically different kinds of rhabdomyosarcoma (RMS), alveolar and embryonal RMS are associated with distinct clinical characteristics and different cytogenetic properties. Most alveolar class RMS are characterized by a t(2:13) or t(1:13) chromosomal translocation which results in the fusion of the DNA-binding motifs of either PAX7 or PAX3 and the carboxy-terminal activation domain of forkhead gene. Embryonal class RMS instead show allelic loss of regions of chromosome 11 thought to contain tumor suppressor genes. In a long-term collaboration with the Triche Laboratory and Children's Hospital LA, Affymetrix microarrays (U133A/B) were used to measure the gene-expression profiles of 31,728 unigene-derived features in 56 RMS tumors (35 ERMS, 21 ARMS). Statistical analysis was performed using a two-class T-test. Despite the relatively common muscle backgrounds of these two cell types, we were able to identify several hundred differentially expressed genes (with a p-value less than 0.05). Members of this subset have been identified as having roles in specific cell cycle regulatory and apoptosis-related pathways. Surprisingly, cannabinoid receptor 1, expressed normally in the hippocampus and responsible for phosphorylation of focal adhesion kinase (FAK), is overexpressed in ARMS relative to ERMS. FAK, in turn, is upstream of several signaling pathways including adhesion-dependent survival and cell motility and inhibits apoptosis through pathways that inhibit degradation of AKT. FAK activation may explain the relative severity of prognosis and incidence of metastasis seen in ARMS. Alternatively, the transcription factor FoxF1 and its upstream regulator, Shh, were repressed in many ERMS, with corresponding upregulation of antagonist and growth factor, BMP4.

Other more sophisticated analyses, including both supervised and unsupervised clustering algorithms, have been applied in further characterizing the expression patterns seen in these tumors. Artificial neural networks (Ben Bornstein, JPL), support vector machines (Dennis DeCoste, JPL) and other machine-learning algorithms are being used to identify genes whose expression differs across PAX3/PAX7 (ARMS), prognosis and metastasis boundaries in addition to the ARMS/ERMS divide. Gene subsets gathered from these lines of analysis have allowed for a finer parsing of tumor types. A two-dimensional plot of the PCA-transformed tissue space in which the gene space was restricted to these subsets (Joe Roden, JPL) has helped to provisionally reclassify translocation negative ARMS tumors on the basis of their ERMS-like gene expression patterns. The possibility that these tumors also share the more favorable ERMS prognosis and the inevitable power this will allow in the customization of

cancer treatment remains to be seen, but the prospects are encouraging.

¹Biology Graduate Student, Eric Davidson Lab, Caltech

²Jet Propulsion Laboratory, Pasadena, CA

464. Gene expression and metabolic organization in *Shewanella oneidensis* biofilms

T.K. Teal, B.J. Wold, D.K. Newman*

Bacteria have traditionally been viewed as living a primarily planktonic lifestyle. In the last decade, however, it has become more apparent that bacteria spend much of their lives as surface-attached microbial communities, i.e., biofilms. These films have considerable three-dimensional structure, meaning that the environment within different areas of the biofilm can vary markedly. These biofilms are prevalent in natural as well as man-made systems. Because of their medical and environmental importance, biofilms have recently become the subject of more intense study. We are interested in the process of biofilm formation and the metabolic organization of the biofilm. While more has become known about the biofilm lifestyle, including the existence of intercellular signaling pathways, very little is understood about the temporal and spatial metabolic states within the biofilm and how they influence further biofilm development. This collaboration between the Newman and Wold labs is particularly centered on probing similarities and differences in the strategies used in forming three-dimensional developing biofilms, comparing and contrasting the strategies used with those used in metazoan development. It is secondarily centered on implementing genomic-scale assays, as called for in the project.

To investigate these topics we will be using biofilms comprised of *Shewanella oneidensis* strain MR-1. *S. oneidensis* is an environmentally important class of bacteria. It is a facultative anaerobe with remarkable respiratory versatility. Its genome has been sequenced, and it is relatively easy to manipulate genetically. We have started by investigating which parts of *S. oneidensis* biofilms are metabolically active. To do this we have tagged the ribosomal promoter *rrnBPI* with the unstable GFP *gfp(AAV)* and cloned it into a plasmid that is stable in MR1. Fluorescence levels from this promoter/GFP system have been shown to be a good indicator of cell growth and replication. We are growing the biofilms in a flow cell system and imaging them using two-photon fluorescence microscopy. Using this technique we can correlate the level of fluorescence we see using microscopy with metabolic activity and can determine the regions of the biofilm in which cells are the most metabolically active, as well as explore how quickly this state can change in response to environmental perturbations. Additional constructs using promoters sensitive to other metabolic parameters are in progress.

To gain a better understanding of the process of biofilm formation, we are interested in the genes being expressed as the biofilm develops. We have created a test DNA microarray with 75 selected genes from MR-1 thought to be involved in different aspects of biofilm formation. We will assay *S. oneidensis* biofilms for gene

expression over time, and perhaps selected on the basis of GFP marker gene expression. We anticipate that we will see expression of genes important in biofilm attachment and growth, as well as those involved in cell-cell signaling or quorum sensing. Using this data we will then use 'classical genetics' techniques to determine the precise role of the identified genes. Ultimately we hope to develop a computational model of the key genetic networks involved in biofilm formation and cell-to-cell communication.

*Assistant Professor of Geobiology and Environmental Science and Engineering, Caltech

References

Bassler B.L. (1999) *Curr. Op. Microbiol.* 2(6):582-587.

Hernandez M.E. and Newman D.K. (2001) *Cell. Mol. Life Sci.* 58(11):1562-1571.

Whitely, M. et al (2001) *Nature* 413(6858):860-864.

465. Comparative sequence analysis in vertebrate genomes: Seqcomp, and MUSSA

Tristan DeBuysscher, Nora Mullaney*

Comparative sequence analysis in our lab is based on Seqcomp and FamilyRelations tools, developed by C. Titus Brown in Dr. Eric Davidson's lab and Tristan De Buysscher in our lab. These tools (described in detail and available for use at <http://family.caltech.edu>) were created to help identify regions of DNA that are high quality candidates to function as cis-regulatory modules for nearby genes. They are based the straightforward expectation that more highly conserved domains of DNA sequence between two genomes that are at auspicious evolutionary distance from each other are good candidates for functional importance. Specifically, we expect some conserved domains located outside RNA coding regions of genes to regulate transcription by acting as promoters, enhancers, silencers, and locus control domains. Our work focuses on mammalian and, more recently, multiple nematode species with mouse and *C. elegans* as the respective reference model organisms.

Our recent work focuses on the problem of many-genome comparisons, in contrast to the pairwise comparisons for which FR was designed. Higher genome numbers, when properly distanced evolutionarily, are expected to deliver greater further "resolving power" to help identify sequences conserved because of function rather than identical by chance. The tool developed for this purpose we call MUSSA. It uses a recursive transitivity finding algorithm to analyze multiple Seqcomp files into an arbitrary N-way analysis. A GUI has been developed to allow biologists to navigate the results of a N-sequence analysis using a histogram of region conservation, graphical overview of the links of highly conserved region in the manner of FR, plus tools for viewing the sequence of the conserved regions, performing simple DNA motif searches, and annotating results.

Current applications using MUSSA encompass both the myogenic regulatory pathway of interest to our lab and other genes for which we have sufficient (several tens of kilobases) orthologous sequence from multiple

species. At present we are focusing on vertebrate genomes for one set of studies and, in separate but conceptually similar project, we are studying genes from four species of nematode worms in a collaboration with Hiroke Shizuya and Paul Sternberg. We have now used MUSSA to ask some very basic questions about vertebrate genome comparisons with respect to noncoding regulatory sequences: How much resolving power one can get with each additional genome being compared? How does the evolutionary distance between genomes affect resolving power? What fraction of conserved features found outside RNA coding regions contribute to transcriptional regulation of nearby genes? A basic aim in the studies for which we developed MUSSA is to learn what fraction of these conserved domains, on average, govern transcription, and conversely to find out how many known cis-regulatory modules can be detected with a given suite of genomes.

*Undergraduate, Caltech

466. Identifying and testing candidate regulatory regions for genes of the myogenic regulatory circuit

Tristan DeBuysscher, Libera Berghella

Using the sequence comparisons and Family Relations tools, a dozen genes from the paraxial segmentation and myogenic regulatory circuits are being analyzed by mouse/human comparisons. Mouse BAC sequences are from sequencing performed by collaborators and the DOE Joint Genome Institute. The BACs were originally obtained from the mouse BAC library made by Hiroke Shizuya and colleagues, with screening by Mai Wang of the Mel Simon genomics group at Caltech. The conserved noncoding candidate regulatory domains are amplified by PCR and cloned into reporter vectors designed for introduction into mice by transgenesis. Because the pathways in question are active at midgestation, the transgenics can be productively assayed ~9 days after injection, giving an acceptably rapid assay compared with germline transgenesis. This project has recently been further advanced by data obtained in collaboration with Dr. Eric Green (NIH Genome Institute) which is giving us a six-genome-deep comparison of several myogenic and somitogenic pathway genes. Initial functional analysis of myogenin via multigenom sequence comparison has uncovered a highly conserved element that appears critical for expression of myogenin in adult muscle.

467. CompClust: A computational framework for machine learning and data mining

Christopher Hart, Lucas Scherenbroic¹, Ben Bornstein², Diane Trout, Joe Roden, Barbara Wold, Eric Mjolsness

Genome-scale analysis, including various genome sequence features, large-scale RNA expression analysis, protein interaction maps, tissue arrays and complex collections of in situ images collectively present us with the problem of large amounts of data of diverse types. The need to perform many different computational analyses on these large datasets and then to view and integrate results

from multiple analyses is a common problem in bioinformatics and for end-user biologists. We have therefore constructed a software architecture designed to provide easy access to many machine learning algorithms and techniques and to facilitate analysis of results derived from diverse algorithms. Using CORBA as the connection bridge, our suite of algorithms is available from several computational environments currently including mathematica, matlab, C/C++, python and Java. We have also implemented a fairly complete python application programmer interface (API), which provides a foundation for building novel analysis applications or can be used directly from the python interpreter as an interactive data analysis environment. Several of the lab's projects are now using and extending this framework.

The python API includes a powerful embeddable plotting tool, IPlot. I-PLOT provides for rapid construction of interactive 2D visualizations. In the case of microarray data analysis, it is critical to be able to quickly impose several data features onto a single plot. To accommodate this need, IPlot is designed to allow for the mapping of any data features onto any plot feature (i.e., color all points by cluster membership, size all data points by p-values, point coordinates determined by PCA projection of a data vector, etc). The other major feature of IPlot is to provide interactive "clickable" linkages to any information linked to a data vector, which is accomplished using the MLX architecture.

¹UC, Irvine

²Jet Propulsion Laboratory, Pasadena, CA

468. Comparison of clustering algorithms for use in large-scale gene expression analysis
C.E. Hart, Diane Trout, Sagar Damle¹, B. Bornstein², J. Roden, E. Mjolsness, B. Wold
DNA microarrays and other large-scale gene expression analyses generate datasets of unprecedented size and complexity. Measurements for thousands of genes across tens to hundreds of tissue types, signaling stimuli, developmental time points, genetic variants, drug doses, and the like are now routine. A pivotal step in mining large-scale gene expression data is to group genes displaying similar expression profiles and/or to group samples that are most similar to each other. A growing repertoire of clustering algorithms can be used to reveal underlying structure in other kinds of large datasets and they are rapidly being adapted and fruitfully applied to large-scale expression data. As a group, these algorithms provide the essential computational infrastructure needed to extract patterns of co-expression which are often then used, alone or in conjunction with other data, to generate hypotheses about co-regulation, biological relatedness of samples, etc. However, each algorithm makes different underlying assumptions about data structure and operates by a different mechanism. These differences are expected to and do interact with differently with data properties such as sample number, degree of sample similarity, gene number, and experimental noise. In addition, each algorithm requires the selection of distance metric and, for

many, specification of the number of clusters and selection of initialization conditions. These choices also lead to differing outcomes. The end-user biologist is usually faced with a confusing array of possibilities and little guidance about relative strengths and weaknesses.

To measure and understand effects of dataset properties and algorithm properties we constructed a framework for comparing clustering results. We then made a systematic across several major algorithms using both real and synthetic microarray data. The comparative tool framework includes a mechanism to quantitatively assess and visualize cluster overlap by generating receiver operator characteristic (ROC) curves. We also implemented modified normalized mutual information (NMI) and a linear assignment (LA) metrics to interpret the degree of agreement and disagreement between different clusterings of the same dataset. In addition to these quantitative measures, we implemented interactive visualization tools (I-PLOT) to explore how different algorithms are organizing the data space. Thus far, we have implemented and compared an Expectation Maximization (EM) algorithm searching for a mixture of Gaussians, K-means, phylogenetic clustering (Xclust) to which we have added a novel agglomeration step, and self-organizing maps (SOMs). We then used Compclust to complete a comparative study of these algorithms, using yeast cell cycle time courses as test datasets. We found that EM is most robust to added noise in the data. We also showed that even for "well behaved" datasets, the different algorithms partition vectors quite differently, and that results from two such analyses may be of similar quality. For the biology end-user, this means it is important to know which genes in a cluster – and which clusters – are robust and which ones are sensitive to algorithm.

¹Biology Graduate Student, Eric Davidson Lab, Caltech

²Jet Propulsion Laboratory, Pasadena, CA

Reference

(1) Forbes, A.D. (1995) *J. Clin. Monitor.* 3:189-206.

469. Role of a homeogene, **msx-1**, in adult muscle regeneration
Libera Berghella
Regeneration of adult skeletal muscle after an injury or disease is understood to be mediated primarily by muscle satellite cells. In an intact muscle this population of cells is composed of rare, mononucleate cells located beneath the basal lamina of the mature fiber. In healthy adult muscle the satellite cells are mitotically quiescent. Muscle injury triggers their metabolic and mitotic activation. They emerge from G₀ mitotic arrest, proliferate and concomitantly undergo a series of developmental changes. This pathway ultimately ends, for the majority satellite cell progeny, in differentiation and fusion to form new myofibers or differentiation coupled with fusion into existing fibers. However, some cells apparently have a different fate. Instead of differentiating as muscle fibers, they return to replenish the satellite pool in order to support future regeneration.

Biochemical and molecular analysis of muscle regeneration has, in the past, been hampered by the rarity of satellite cells and the absence of reliable molecular markers for these cells, especially when they are in the quiescent state. Prior work in this lab led to a method of studying gene expression in individual satellite cells over the timecourse of an activation response (Cornelison and Wold, 1997; Cornelison et al., 2000). Among the genes studied, the homeobox gene *msx-1* revealed a peculiar and interesting expression pattern, with transcripts being detectable only at extremely early timepoints (<30 minutes post-fiber isolation). This suggested that quiescent cells express *msx-1* but quickly downregulate its expression once they are activated. It is also known that forced expression of *msx-1* in cultured myoblasts inhibits differentiation and can suppress MyoD expression (Woloshin et al., 1995). Based on these and other preliminary results, our working hypothesis is that *msx-1* expression marks satellite cells that are in quiescence or are returning to it, and that it may be causal in suppressing expression of MRFs in quiescent satellite cells.

References

Cornelison, D.D.W and Wold, B.J. (1997) *Dev. Biol.* 191:270-283.

Cornelison, D.D.W., Olwin, B.B, Rudnicki, M.A. and Wold, B.J. (2000) *Dev. Biol.* 224(2):122-137.

Woloshin, P. et al. (1995) *Cell* 82:611-620.

470. Expression profiling of stem cell lines
Libera Berghella, Sagar Damle¹, Brian Williams, Giulio Cossu²

In collaboration with the lab of Giulio Cossu at the University of Roma, we have initiated a large-scale gene expression characterization of cell lines isolated from the embryonic dorsal aorta of mice. The special interest in these cells comes from their capacity to differentiate into muscle, cardiocytes, bone or other derivatives when grown under various culture conditions. This mimics the *in vivo* potential of dorsal aorta multipotential cells implanted into a host animal via transfusion into the blood. Such transplanted cells can subsequently be found in mature muscle fibers, and in other tissues as well. Thus, the isolation and initial characterization of this cell line supports the hypothesis that multipotent mesenchymal cells may be present embedded in vascular endothelium (De Angelis et al., 1999). Using cDNA microarrays, made in the lab, I have begun to analyze the transcription program of these cells in comparison with more conventional myogenic cell lines that are believed to be unipotential and myogenic (C2C12, MM14) or multipotential (10T1/2), or totipotent (embryonic stem cells). Results have revealed genes expressed in common only with 10T1/2 or with 10T1/2 and ES cells, but not myoblast lines. Other genes are novel to one or both of the aorta lines, whose developmental potentials are only partially overlapping. Among genes in common with stem-like cells is CD34, a putative marker of stem cells in several other contexts. These results are being verified by

independent methods, and the impact of the compound trichostatin (a global pharmacological modifier of chromatin access) are next to be tested and correlated with phenotypic impact.

¹Biology Graduate Student, Eric Davidson Lab, Caltech

²Stem Cell Research Institute, Milan, Italy

Reference

De Angelis et al. (1999) *J. Cell. Biol.* 147:869-877.

471. A new method for assaying gene expression
John Murphy^{*}, Barbara Wold, Brian Williams, Mark Davis^{*}

Gene microarrays are proving to be very powerful for large-scale gene expression analysis. However, they have significant shortcomings that we would like to bypass. They generally call for relatively large amounts of input RNA to achieve robust answers, and they are at their best with more abundantly expressed RNAs. They also have dynamic range limits that are considerably narrower than those of the RNA samples to be measured. In all their manifestations so far, they are semiquantitative, even under the best of circumstances. From an entirely different kind of methodology (multiplex single-cell RT-PCR) (Cornelison and Wold, 1997) we know that being able to simultaneously monitor multiple genes in single cells gives a different and illuminating view of the gene expression combinatoric "states" that one cannot achieve using pooled cell samples. However, the latter assays are thus far quite limited in simultaneous gene number (maximally seven simultaneous genes, thus far), and they also give little information about the quantity of each RNA type in an expressing cell. It is clear that in many biological settings, it would be highly desirable to get good quantitative measurements from just one or a few cells per determination for tens, hundreds, or even thousands of genes simultaneously.

To address this problem, we developed the underlying chemistry to make possible an approach that takes advantage of specifically designed families of chemical tags. Oligonucleotides, each designed to hybridize to a specific RNA species of interest, are synthesized such that each oligo carries a unique covalently attached peptoid (not peptide) tag with a unique mass. At the end of hybridization, chemical methods are used to separate hybridized oligos from those that do not react with a complementary RNA, and then tags are cleaved from their respective oligonucleotides. In these methods, the tags, rather than the RNAs or oligos, are ultimately counted. The first method of choice for analysis is mass spectrometry. We expect that this approach will permit direct RNA quantitation over several orders of magnitude, and it has the potential to begin with very small input RNA samples. A virtue of the design is that it uses hybridization in which all components are in solution phase, and these reactions are considerably better understood and more efficient than is nucleic acid hybridization in which one member is in solid phase, as is the case for microarrays. Multiple designs were tested for linking the oligonucleotide moiety to the peptoid

tag and robust strategy identified. Isotopic rationing has also been worked out to allow precise quantitation.

*Division of Chemistry and Chemical Engineering, Caltech

472. Computational analysis of Pho4 binding site presence, **in vivo** Pho4 binding, and phosphate dependent gene expression

Elena Fabrikant*, Christopher E. Hart, Leslie Dunipace, Barbara J. Wold

Transcription factor binding sites are notoriously short and degenerate, yet molecular genetic studies have shown that single transcription factors that recognize these sites direct remarkably specific changes in transcription of genes they regulate. A further observation is that most of these degenerate recognition sequences occur widely in the genome, including many occurrences near genes that are not detectably regulated by the corresponding factor. This raises questions about the mechanistic basis for discriminating the "functional" sites from the apparently nonfunctional "orphan" sites. Do the orphan sites fail to bind the factor *in vivo* entirely? Does the factor bind but fail to be active for lack of other nearby factors of other types? For lack of multiple occurrences of a given site near each other? Does the chromatin organization prevent binding interaction? With the advent of global *in vivo* protein:DNA interaction assays (chromatin immunoprecipitation assayed on microarrays), and full knowledge of expression patterns and genomic DNA sequence, one can now ask address these questions. Pho4, the key transcriptional activator of the phosphate metabolic pathway in yeast, is a bHLH class factor that has been used as a model system for transcriptional regulation for many years. A great deal is known about control of the factor by regulatory kinases, its preferred DNA binding sites, etc. Although exceedingly well-studied, we still lack a genome-scale understanding of how the binding activity of Pho4, relates to the presence and organization of the its consensus binding sites and how either of these two factors impinge on the *in vivo* activities of genes during a phosphate response. In this project we leverage measurements of global *in vivo* binding activity under phosphate stress, expression data measuring the transcriptional response of every gene, and the phylogenetic relationships of binding motifs across the seven sequenced *Saccharomyces* genomes. This allowed the derivation of a list of genes most likely to be transcriptionally regulated by Pho4, which matched well to the list of genes previously known to be so regulated. We also used this information, along with structural data from the literature, to develop a refined and more specific consensus binding site. Finally, genes with a high prevalence of the Pho4 binding site which did not show either Pho4 binding or a typical phosphate-dependent change in expression were used to investigate the presence of a new site that is a candidate for a Pho4 repressor or modulation factor.

*Undergraduate Student, Caltech

473. The Sigmoid pathway modeling system

Eric Mjolsness, Diane Trout, Barbara Wold

The Sigmoid modeling system is a generative, scalable software infrastructure for pathway bioinformatics and systems biology. It uses a three-tier software architecture comprising distributed modules that implement pathway/cell model generation and simulation (Cellerator), a pathway modeling database (Sigmoid proper), a Web service-oriented middleware, a graphical user interface, and in the future, parameter optimization and other data mining technologies. Key to the design of the infrastructure is its scalability ensured by leveraging symbolic computer algebra and self-generation of database and other code from high-level representations such as UML schema. All Sigmoid modeling software components are available through: <http://sigmoid.sourceforge.net/> and <http://www.igb.uci.edu/servers/sb.html>.

An innovative approach to coordinating the various software modules is taken in Sigmoid by using the Universal Modeling Language (UML) to diagram the most important biological objects (notably reactions and molecular reactants) and their relationships, in consultation between bioinformaticians and biologists. This UML diagram then actually becomes source code from which important parts of our system are automatically generated, in particular the actual database (implemented in PostgreSQL) and the Java persistent storage Application Programmers, Interface (API) to the database via the Object Broker object-relational mapping software used by the middleware. Also the Graphical User Interface (GUI) uses reflection% to automatically discover much of what it needs to know about the Sigmoid schema. Thus there is a guarantee that the software actually implements something quite close to the agreed-upon biological objects.

Sigmoid provides a GUI and database to access some of the simulation capabilities of Cellerator or, eventually through SBML, other back-end cell simulators. Many models of molecular interactions have been implemented in Cellerator using different formalisms, such as deterministic or stochastic differential equations and ranging from the law of mass action and simple Michaelis-Menten models to more complex models of enzyme reactions (e.g., the Monod-Wyman-Changeaux or MWC model for allosteric enzymes) and gene regulation (Segel, 1993). The list of reaction models continues to expand as along with the library of actual pathway models comprising sets of coordinated reactions with parameters derived from the literature whenever possible. Existing models that are particularly relevant, for instance, for studying signaling and cancer include: G-coupled protein receptor activation, phosphoinositol metabolism reproducing an observed peak in membrane-bound PIP3, MAPK cascade (Shapiro et al., 2002, Bardwell 2004) with feedback and possible oscillations, NFkB pathway (Hoffmann 2002) with feedback and observed oscillations, and published models of yeast cell cycle checkpoints. An extended set of enzyme mechanism models for single- and multi-substrate, positively and negatively regulated and allosteric enzymes, called kMech, has been written for Cellerator (Yang et al.,

2004). Many other models have been expressed in Cellerator as well.

Collaborators: Andre Levchenko, Johns Hopkins; Lee Bardwell and Pierre Baldi, U.C., Irvine

References

Segel, D., Mukamel, D., Krichevsky, O. and Stavans, J. (1993) *Physical Rev.* 47:812-819.

Hoffmann, A., Levchenko, A., Scott, M.L. and Baltimore, D. (2002) *Science* 298:1189-1190.

Shapiro, B. et al. (2002) In: *Foundations of Systems Biology*, H. Kitano, ed, MIT Press, pp. 145-162.

Publications

Bardwell, L. (2004) A walk-through of the yeast mating pheromone response pathway (Review). *Peptides*. In press.

Shapiro, B.E., Levchenko, A., Meyerowitz, E.M., Wold, B.J. and Mjolsness, E.D. (2003) Cellerator: Extending a computer algebra system to include biochemical arrows for signal transduction simulations. *Bioinformatics* 19(5):677-678.

Yang, C.R., Shapiro, B.E., Mjolsness, E.D. and Hatfield, G.W. (2004) Cellerator extensions for modeling the enzyme mechanisms of the branched chain amino acid biosynthetic pathways of *Escherichia coli*. Submitted for publication. Preprint available at <http://www.igb.uci.edu/servers/coli/kmech.html>.

474. Comparative genomics for somite development regulatory element identification
Steven Kuntz

During vertebrate embryonic development, the posterior region of the embryo divides into segments, or somites, at regular time intervals. The regulatory pathways involved in this segmentation are beginning to be understood in higher vertebrates, such as mammals and birds, but much progress remains to be made. It is known the sequential development of each somite corresponds to the periodicity of the certain transcription factor expression [Palmeirim, I. et al. (1997) *Cell* 91(5):639-648]. These transcription factors, hairy/enhancer of split (Hes1/Hes7), lunatic fringe (Lfng), and axis-inhibition protein (Axin2), are all expressed in a cycle of identical period, though they are expressed out of phase with one another [Rida, P.C.G. et al. (2004) *Dev. Biol.* 265:2-22]. We are interested in determining what transcription factors target these genes for regulation and do so by analyzing the enhancer elements to which these factors may bind. To search for such elements, we utilized comparative genomics to illuminate conserved sequences either upstream or downstream of the gene, or within the introns. It is believed that important regulatory elements that control somite development would be evolutionarily conserved among vertebrates, much as the coding regions of the gene are conserved. For such comparative analysis, up to seven alignable vertebrate sequences were compared with a sequence comparison program (MUSSE). With numerous conserved elements identified, genome-wide scanning for

additional occurrences of such elements, generally 15 to 30 base pairs in length, was performed with another program (Cistematic) to narrow the scope of elements from those conserved to those that may be of regulatory interest. The relation of these elements to genes throughout the genome will be compared to the relation of the same elements to genes throughout the genome of another species. This should serve as a useful tool to narrow the scope of important elements. Several elements of interest have been identified and how they control expression will be analyzed in mouse, with a simple LacZ basal reporter construct, in order to determine if or when these sites are involved in developmental regulation.

475. Optimization of the sequence comparison algorithm by the core match method
Tony Kirilusha

The standard sequence comparison (SeqComp) algorithm is applied to DNA sequences in order to locate regions consisting of n nucleotides that match the criteria of having at least $n*t$ bases matching when the regions are aligned, where t (0 – 100%) is the similarity threshold selected by the user. If $n*t$ is not a whole number, the result is always rounded up (i.e., if $n = 10$ and $t = 84\%$, then $n*t = 8.4$ which will be rounded up to 9). The ability to perform such a search is instrumental in locating regulatory elements responsible for controlling gene expression, however, the algorithm requires time proportional to the product of the lengths of the sequences being examined, and is therefore too slow to be used for comparing sequences with length greater than 100,000 base pairs. We proposed an optimization of the SeqComp algorithm that allows it to avoid a large number of unnecessary comparisons by requiring that any two windows reported as matching have a small block of contiguous matching base pairs (a core). The size of the core can be specified by the user and, in general, a larger core size leads to a greater speedup but also increases the chances that certain matching windows that would have been reported by the unoptimized algorithm will be omitted. This is especially true for lower values of t , where the distribution of mismatches between two sequence windows can have a greater variety. We then examined in some detail the combinatorial aspects of the optimization, as well as the probability of a matching pair of windows not being recognized. Finally, we evaluated the speedup resulting from this optimization. Currently, the optimized algorithm allows us to compare sequences of up to 20,000,000 base pairs within a reasonable amount of time (2 days) utilizing a standard workstation.

476. Regulation of messenger RNA translation during skeletal muscle differentiation
Richele M. Gwartz, Brian A. Williams

Assay of total cellular transcription (the "transcriptome") is a beginning step towards understanding the complex regulatory information that results in the collection of expressed proteins characteristic of cell type. We are trying to identify regulatory inputs that recruit subpopulations of mRNA from the transcriptome to

cytosolic polyribosomes during skeletal muscle differentiation. The AKT/mTOR and ras/mek signaling pathways have been shown to influence the recruitment of specific mRNAs for translation [Rajasekhar, et al. (2003) *Mol. Cell* 12:889-901]. These pathways can be manipulated in culture by small molecule antagonists, and both are active during differentiation in the C2C12 mouse skeletal muscle cell line.

Using sucrose density gradient centrifugation, we have successfully separated polyribosomal associated RNA from C2C12 cells 24 hours after differentiation, and are applying it to other stages and steps in the differentiation (and later degeneration) process. In initial studies cDNA is synthesized from the RNA using labeled nucleotide precursors and is primed with oligo dT to enrich the labeled target population for mRNA. The labeled polyribosomal fraction is then cohybridized to a mouse oligonucleotide array with a labeled genomic DNA standard, and ratiometric gene expression measurements are taken. Preliminary results indicate that a distinct group of ribosomal proteins, signaling molecules and other specific messages in the low abundance class is enriched in the polyribosomal fraction. High abundance messages for contractile protein genes are well represented in both the polyribosomal and total mRNA fractions. We are currently performing experiments with inhibitors of the AKT and ras pathways to clarify in this system the extent and sequence specificity of polysomal recruitment. If strong, gene-specific recruitment differences are identified, the next goal is to probe the mechanism in several ways, including identification of RNA motifs capable of mediating selective recruitment to polyribosomes. The fractionation system will also be used to investigate possible participation of small regulatory RNAs in this system.

477. Transcriptome changes in rat skeletal muscle in response to simulated microgravity
Brian A. Williams, Joe Roden, Richele M. Gwartz, Kayla Smith, Jose-Luis Riechmann¹, Bruce Shapiro², Eric Mjolsness

Skeletal muscle tissue is maintained in a dynamic balance between proliferation and atrophy that is affected by environmental conditions. Several different kinds of environmental and disease stimuli can shift the balance toward skeletal muscle degeneration. These stimuli include periods of disuse as in patient bedrest, microgravity, or diseases that cause cachexia (see entry from Gilberto Hernandez). We are attempting to understand transcriptional regulatory changes that accompany muscle atrophy using Affymetrix microarrays to assay RNA extracted from atrophied rat skeletal muscle, cardiac muscle and bone (which also undergoes major degenerative change in microgravity). The arrays are constructed with a new 11 μ m feature size, allowing the representation of 31,042 expressed sequences from the rat genome on a single array.

Skeletal muscle atrophy is modeled in laboratory rodents using a hindlimb unloading protocol, which results

in a reduction of the mass of all the muscles of the lower leg. At the overall physiological level, the soleus, a postural muscle comprised primarily of slow twitch fibers, is affected to a much greater extent than the gastrocnemius and the tibialis anterior, which are primarily fast twitch. Previous results indicate that the effect on the soleus is due mainly to loss of slow myosin protein. Using RNA from hindlimb unloaded muscle and bone biopsies provided by collaborators at Johnson Space Center, we found a decrease in total RNA per unit mass of soleus tissue that is significantly greater than the decrease found in medial gastrocnemius and tibialis anterior. Analysis of the global microarray data to determine how sequence specific these losses are is ongoing. In particular, singular value decomposition will be used to identify principal components of the data showing maximal variance, and multiple clustering algorithms will be applied to identify coregulated groups of genes. The goal is to use this information to construct as complete a picture of the regulatory network driving this process, at the transcriptional level as possible. These results will be analyzed in the context of cis-regulatory element studies being performed on two known causal regulators of skeletal muscle degeneration, *Mafbx* and *MURF1* (and its paralogs) being performed by Gilberto Hernandez in the lab.

This work was performed in collaboration with the Marshall Space Flight Center, Huntsville AL.

¹Millard and Muriel Jacobs Genetics and Genomics Laboratory, Caltech

²Jet Propulsion Laboratory, Pasadena, CA

478. Automation of genome-wide and cross-genome cis-regulatory element identification and assessment using Cistematic
Ali Mortazavi

Using classical experimental approaches (i.e., promoter/enhancer bashing blind mutagenesis), detection of functional cis-regulatory elements in the non-coding portions of genes continues to be a painstaking task. This process can now be informed, accelerated, and made "whole genome comprehensive" by using large-scale gene expression data to first identify groups of genes that are co-expressed under multiple conditions and/or spatial domains. Co-expression patterns, in the best and most tractable examples, reflect co-regulation by a small number of transcription factor combinations, each binding to a "specific," albeit typically short and degenerate, DNA sequence motif. In silico methods are thus used to identify within a Coexpression group, over-represented over-represented motifs that are candidates to be such cis-regulatory binding motifs. These searches are, however, prone to high levels of false positives and false negatives. The searches can be additionally constrained by seeking common motifs residing within domains of preferential evolutionary conservation (phylogenetic footprinting). We therefore started by evaluating the performance of such as Meme and AlignAce by comparing their results to those found by imposing conservation constraints by phylogenetic footprinting in a systematic and automated way.

We have expanded the resulting package, called Cistematic, to automate sequence retrieval from all currently available eukaryotic genome assemblies, to compare candidate motifs with known motifs in the literature, and to retrieve as well as characterize (using both genome annotations and the GO ontology) all other genes within a genome that share candidate motif sites within a certain radius. We then check for occurrence of the motifs in orthologous and paralogous genes in other genomes. Cross-genome homology is currently done using the HomoloGene dataset as well as custom entries for the seven *Saccharomyces* species, but we will be integrating Cistematic into the BioHub later this year to take advantage of its more advanced orthology mapping capabilities.

All data is stored transparently in relational form using the cross-platform Sqlite package. Cistematic provides several layers of abstractions, which allow users of varying levels of sophistication to customize their use of Cistematic. Thus, while most users will simply supply locus identifiers and thresholds to the Experiment classes and receive the standard analysis results, some users may wish to use and extend lower-level objects that handle Motifs, Programs, Genomes, and Hologology/Annotation mapping.

Cistematic currently, runs on Mac OS, Linux, and Solaris, and has a prototype web front-end for users wishing to run Cistematic experiment objects without writing python scripts. We intend to make Cistematic publicly available by the end of 2004.

479. Multigenome-scale analysis of **cis**-regulatory elements for specific transcription factors
Ali Mortazavi, Barbara Wold

At this point, a relatively small number of eukaryotic transcription factors have been studied much more extensively than the rest because of their key roles in various aspects of cell/organismal development and function. Some of these factors are very well characterized with respect to the regulation of a small number of "model" target genes. There are also relevant global descriptive data by analysis of microarray data, RNAi, mutational studies, and chromatin IP. These highly studied factors are the best test case to assess the performance of both in silico cis-regulatory element predictions. In particular, we are interested in assessing the performance of known cis-regulatory element descriptions (whether in degenerate consensus or position weight matrix form) in identifying genes that are both known to be regulated or that fall within the family of expected genes that would be regulated by the factor based on the known biology. We will use conservation of the motifs in orthologous genes in related genomes as a first-order approximation for functionality.

We chose NRSF/REST and p53 as the first two transcription factors. The Neuronal Restrictive Silencing Factor, first identified by the David Anderson lab, has an array of zinc fingers that bind to a 21 bp cis-regulatory element that has been repeatedly found in UTRs, introns,

and adjacent non-coding DNA of many neuronal genes (and more recently a group of immune system genes). We will be identifying and assessing candidate NRSF binding sites in all available mammalian and vertebrate genomes. Several alternative splice variants of NRSF have been reported in the literature, with different combinations of zinc fingers, and we will therefore seek possible binding sites for these variants. Refinement of the binding site consensi to discriminate different factor forms and other possible sources of variation in binding that may include RNA-mediated interactions are further related goals.

The tumor suppressor p53 is the subject of intensive studies because of its central role in the cellular response to a variety of stresses (e.g., DNA damage) by activating both a repair response, as well as initiating apoptosis of the cell is beyond repair. P53 binds as a tetramer to a binding site composed of two decamers separated by a spacer that is 0 to 13 base pairs long and is found in all vertebrates, as well as *Drosophila* and nematodes. We can thus use all vertebrate and invertebrate genomes sequenced to date to evaluate our matches for p53. Interestingly, the p53 vertebrate paralogs p63 and p73 also share a similar binding domain and are thought to bind the same target sites with different affinity, but are thought to be primarily involved in development rather than tumor suppression. Hence, we will evaluate the possibility that different PWMs will efficiently segregate developmental genes with candidate sites from known p53 target sites that are directly involved in tumor suppression.

We will verify some of our results using chromatin IP on genes of particular interest. As an additional benefit of our analyses, we should also be able to map out the evolutionary history of both cis-regulatory elements. For example, we expect to observe an expansion in NRSF binding sites in primates, while we expect a set of metazoan core of genes to be responsive to p53. Last, but not least, we are interested in comparing our results to known microarray and other large-scale gene expression data to see at what precision good, conserved sequences are predictive of gene expression for these known factors.

480. An analysis of the relationship of zinc finger structure in mammalian transcription factors and of their preferred binding sites
Ali Mortazavi

The explosive growth of sequenced genomes holds the promise of finding ways to use genomic sequence information to comprehensively predict regulatory relationships, map connectivity and ultimately understand the relationship of gene network architecture to network function. However, a number of basic properties of transcription factors and the DNA sequences they recognize make this a very substantial challenge. First, the number of transcription factors found in animal and plant genomes is large- numbering in the thousands, and many of them bind small degenerate cis-regulatory elements. Other aspects of transcriptional regulation such as competition by multiple factors for the same or overlapping binding sites, combinatorial control, alternative splicing of factors,

redundancy due to gene duplication chromatin state and tissue-specific expression, all further complicate the simplest efforts to identify "real" factor binding sites in target genes and to attribute factor identity and function correctly.

We believe that with the availability of enough genomes, we will in the next few years have identified a majority of conserved cis-regulatory modules in any given genome. Even with the advent of global in vivo assays for protein:DNA interactions (ChIP/array), and in vitro methods of site definition such as SELEX, the expense and large number of candidate factors in vertebrate genomes means that a computational approach that could predict true target sites and affinities for a given factor would be a great advance. The simplest solution would be to predict the binding site affinities of transcription factors from knowledge of the protein sequence (and implied structure) of the factor. Given our continuing inability to predict structure, this seems quite implausible.

However, there is a class of transcription factors that holds some promise. The C2H2 family of zinc fingers comprises over half of the transcription factors found in genomes such as ours. Individual residues on the alpha helix of each zinc finger specifically recognize bases along DNA (as well as RNA), such that every zinc finger recognizes 3 bp of DNA. Zinc finger transcription factors typically carry three to 30 zinc finger units that are arranged in arrays to recognize specific sequences. Following the seminal work showing the structure of zinc finger-DNA interaction for a handful of zinc fingers, much of the work in the field has focused on designing artificial zinc fingers to bind to specific sequences upstream of genes of interest for medical and commercial applications. We are instead interested in using the work done to date to understand how much of what is known can be applied to understanding existing zinc fingers in genomes.

We are cataloging zinc fingers in mammalian genomes to assess the prevalence of key finger residue combinations and to generate predictions of binding sites based on the currently known data. We are particularly interested in duplicated zinc fingers such as those found on human chromosome 19, which affords us the opportunity to study relatively recent transcription factor duplications and their potential function, as well as motif conservation/divergence. Our ultimate goal is to tie zinc finger structure to the values of its position weight matrix (or other binding site affinity descriptions) in a rational manner. A related goal, which will call for new experimental work will be to predict whether various factors also bind RNA targets and how those RNA targets are related to DNA binding and binding sites.

Publications

Graumann, J., Dunipace, L.A., Seol, J.H., McDonald, W.H., Yates, J.R., Wold, B.J. and Deshaies, R.J. (2004) Applicability of tandem affinity purification MudPIT to pathway proteomics in yeast. *Mol. Cell. Proteo.* 3(3):226-237.

Hart, C.E. et al. (2004) Framework for quantitative comparison and exploration of microarray clusterings. Submitted.

Williams, B.A., Gwartz, R.M. and Wold, B.J. (2004) Genomic DNA as a cohybridization standard for mammalian microarray measurements. *Nucl. Acids Res.* 32(10):Art. No. e81.

Facilities

Flow Cytometry and Cell Sorting Facility
Genetically Altered Mouse Production Facility
Millard and Muriel Jacobs Genetics and Genomics Laboratory
Monoclonal Antibody Facility
Nucleic Acid and Protein Sequence Analysis Computing Facility
Protein Expression Center
Protein Microanalytical Laboratory

Flow Cytometry and Cell Sorting Facility

Supervising Faculty Member: Ellen Rothenberg

Facility Manager: Rochelle Diamond

Operators/Technical Specialists: Stephanie Adams, Rochelle Diamond, Patrick Koen

The Caltech Flow Cytometry Cell Sorting Facility is a multi-user facility that has been providing flow cytometric technology on a fee-for-service basis to the Caltech community for over 20 years. Particles such as cells, beads, and micro-organisms in heterogeneous populations can be analyzed based on their scatter and fluorescent properties. These properties are correlated on a single-cell basis to reveal both qualitative and quantitative information, providing statistical population characteristics for all cells in the sample. In addition, the cells can be sterilely sorted, based on their characteristics, into tubes or multi-well plates.

The particular applications provided by the facility are user driven, defined by the needs of the Caltech research community. This technology is a useful multi-faceted tool to study many aspects of cell biology including cell cycle analysis, and defining and isolating cell populations in immunological, neurobiological, and developmental systems. Some examples are: isolation of transfectants that exhibit reporter gene expression which can be correlated with other desired properties; real-time measurements of physiological responses in cells; quantitation of cell death; isolation of populations for preparation of cDNA for qPCR and gene chip analyses; and single-cell cloning by direct deposition. This past year the facility has serviced 16 research groups encompassing 47 individual researchers from the Biology, Chemistry, and Chemical Engineering Divisions, representing and trained six new FACSCalibur users.

The facility is equipped with several sorters and analyzers. The facility has just acquired a new state-of-the-art high-speed cell sorter, the Becton Dickinson FACSAria. This sorter is capable of four-way cell sorting at 25,000 cells per second with excellent precision and recovery, and analysis of at least 11 different fluorescence parameters. Factory training for the operators has been completed and validation of the instrument is underway. The BD FACSVantage SE is a research-grade flow cytometer/cell sorter capable of sorting 3000 events per second based on the multiparameter analysis of cell size, density and fluorescence intensity of up to six colors. In addition, the facility owns an older Coulter Epics Elite optimized for three-color analysis and excellent for cell cycle work. A non-sorting FACSCalibur analyzer and a free-standing work station is available to researchers for self-service analysis around the clock provided that the investigators demonstrate competence with the analyzer or take training provided by the facility.

Recent publications utilizing the facilities services include the following:

- Davis, M.E., Pun, S.H., Bellocq, N.C., Reineke, T.M., Popielarski, S. R., Mishra, S. and Heidel, J.D. (2004) Self-assembling nucleic acid delivery vehicles via linear, water-soluble, cyclodextrin-containing polymers. *Curr. Med. Chem.* 11:179-197.
- Giannetti, A.M. and Bjorkman, P.J. (2004) HFE and transferrin directly compete for transferrin receptor in solution and at the cell surface. *J. Biol. Chem.* 279:25866-25875.
- Hernandez-Hoyos, G., Anderson, M.K., Wang, C., Rothenberg, E.V. and Alberola-Ila, J. (2003) GATA-3 expression is controlled by TCR signals and regulates CD4/CD8 differentiation. *Immunity* 19:83-94.
- Lesur, I. and Campbell, J.L. (2004) The transcriptome of prematurely aging yeast cells is similar to that of telomerase-deficient cells. *Mol. Biol. Cell* 15:1297-1312.
- Laurent M.N., Ramirez D.M. and Alberola-Ila, J. (2004) Kinase Suppressor of Ras couples ras to the ERK cascade during T-cell development. *J. Immunol.* 173:986-992.
- Link, A.J. and Tirrell, D.A. (2003) Cell surface labeling of *Escherichia coli* via Copper(1)-catalyzed [3+2] cycloaddition *J. Am. Chem. Soc.* 125:11164-11165.
- Luo, K.Q., Elsasser, S., Chang, D.C and Campbell, J.L. (2003) Regulation of the localization and stability of Cdc6 in living yeast cells. *Biochem. Biophys. Res. Comm.* 306:851-859.
- Mishra, S., Webster, P. and Davis, M.E. (2004) PEGylation significantly affects cellular uptake and trafficking of non-viral gene delivery particles. *Eur. J. Cell Biol.* 83:97-111.
- Verma, R., Oania, R., Graumann, J. and Deshaies, R.J. (2004) Multiubiquitin chain receptors define a layer of substrate selectivity in the ubiquitin-proteasome system. *Cell* 118:99-110.
- Yui, M.A., Sharp, L.L., Havran, W.L. and Rothenberg, E.V. (2004) Preferential activation of an IL-2 regulatory sequence transgene in TCR $\gamma\delta$ and NKT cells: Subset-specific differences in IL-2 regulation. *J. Immunol.* 172:4691-4699.

Genetically Altered Mouse Production Facility

Director: Shirley Pease, F.I.A.T.

Mouse Facility Manager: Bruce Kennedy, M.S., RLATG

Mouse Facility Supervisor: Jenny Arvisu, ALAT

Embryonic Stem Cell Culture: Jue Jade Wang, M.S.

Cryopreservation and Microinjection: Juan Silva, B.S., LAT

Staff: Jennifer Alex, AA, RLAT; Armando Amaya; Cirila Arteaga; Donald Campos; Hernan Granados; Carlos Hernandez; Jorge Mata, ALAT; Jose Mata; Gustavo Munoz, B.A.; John Papsys, B.S.; Lorena Sandoval; Vanessa Vargas; Charles Winters

The transgenic technique for gene addition (Gordon et al., 1980) and targeted gene modification (Zijlstra et al., 1989) have been established at Caltech since 1984 and 1993, respectively. Gene addition in the mammalian system is accomplished by injecting DNA into the pronucleus of a fertilized egg. Targeted disruption of specific genes, however, requires the manipulation of pluripotent embryonic stem (ES) cells in vitro and their subsequent return to the embryonic environment for incorporation into the developing embryo. The resulting chimeric mouse born is useful for two purposes: 1) it is comprised of tissue from two sources, the host embryo and the manipulated stem cells. More importantly, 2) it can be mated, so as to produce descendants that are entirely transgenic, resulting from the ES cell contribution to the germline of the chimeric mouse. More recently, the Facility together with the Baltimore lab, participated in the development of a new method for the introduction of DNA into early-stage embryos (Lois et al., 2002). This method makes use of non-recombinant lentivirus as a vector for the introduction of DNA into one-cell embryos. The method has proven to be highly efficient and promises to be useful for studies in mice and rats, where large numbers of constructs need to be tested. This new methodology also makes feasible the generation of transgenic animals in species that were hitherto impractical to work with, due to the very low numbers of embryos available for use.

The newly refurbished, pathogen-free barrier-operated mouse facility was opened and re-stocked with pathogen-free strains in February, 1995. In addition to 86 transgenic, knockout and knockin strains, we also maintain colonies of inbred and outbred animals, which are used to support the development of new lines, by investigators at Caltech. We also have many mouse models on both an inbred and an outbred background, plus intercrosses between two or three different but related mouse models. In total, we currently maintain 193 separate strains of mouse. Some of these strains are immune deficient and require specialized care to protect them from bacteria commonly present, (and non-pathogenic) in immune competent animals. In immune deficient animals, these hitherto harmless organisms can cause a problem. This may interfere with the well being of the animal and the extraction of reliable experimental results. Facility staff

provides a complete service to investigators. All colony management operations are carried out by staff at the request of investigators. The work of the staff and manager of the facility continues to reflect Caltech's commitment to good laboratory animal practice and our adherence to NIH guidelines. In 2001/2002, the Facility participated in the campus effort to become accredited by the International Association for the Accreditation of Laboratory Animal Care.

The facility, in collaboration with the Anderson, Baltimore, Lester, Simon, Wold and Varshavsky laboratories, has generated multiple transgenic, knockout and knockin mouse strains. Presently, twelve principal investigators and their postdoctoral fellows or graduate students use the facility.

New transgenic lines have continually been produced and in all, 69 new transgenic lines for gene addition and 59 new knockouts have been produced since February 1995. Since the lentiviral vector method was established, 76 transient or established mouse models have been generated by this means, together with one Tg rat model. Facility staff has performed all embryo manipulation involved in the production of these new lines. Microinjection equipment has been set up within the barrier facility, which operates on restricted access as part of the "barrier" itself. A room outside the facility has been allocated by the Division to be used primarily for teaching grad students, technicians and postdocs the techniques involved in transgenic mouse production. This room has been operating since July 1996. Investigators have the option of using this room to perform their own microinjection of embryos, rather than using the full technical service available from the Genetically Altered Mouse Facility.

In tissue culture and the use of embryonic stem cells, the Facility participated in the derivation of new ES cell lines derived from genetically altered mice (see Simon laboratory Annual Report, 2001). Goals for the coming year for this part of the Facility include the acquisition of new ES cell lines for general use, such as those on a C57BL/6 background and also hybrid ES cell lines. C57BL/6 ES cells provide a significant advantage in that the mutation will be established initially on this well understood genetic background, instead of undertaking a two-year breeding program to reach the same point, having initially established the mutation on a sub-optimal genetic background. Hybrid ES cells may be useful for their reported vigor. In using hybrid cells, we would also like to establish the tetraploid embryo complementation technique, for the generation of animals wholly of ES cell origin.

In the generation of mouse models involving the use of embryonic stem cells, we continue to pre-screen candidate clones for injection by the preparation of chromosome spreads. In establishing the chromosome count of each clone prior to injection, we find we are reliably able to predict which clones will generate good chimeras that will transmit through the germline. In effect,

we have been able to increase efficiency by 100% in the production of germline transmitting chimeras.

In cryopreservation, 61 mouse models are either stored or partially stored. For each line, between 200 and 500 embryos at eight-cell stage have been preserved in liquid nitrogen. There are currently 19,000 embryos frozen in total. We shall continue to preserve embryos from every single mouse strain the Core maintains. The advantages of such a resource are many. Unique and valuable mouse strains that are currently not in use may be stored economically. In the event that genetic drift should affect any strain, over time, then the option to return to the original documented genetic material is available. Lastly, in the event of a microbiological or genetic contamination occurring within the mouse facility, we have the resources to set up clean and genetically reliable mouse stocks in an alternative location.

In addition to producing a total of 204 new animal models since February 1995, we have re-derived 53 pre-existing genetically altered strains of mice. This practice is being continued by the Office of Laboratory Animal Resources.

The production of pathogen-free animals enables Caltech to exchange valuable genetically-altered mouse models with other academic groups around the world. As more and more mouse models become available and the exchange of animals more frequent, it is essential for Caltech to be in a position to deal effectively with animal lines generated in the facility and in other laboratories. To this end, the Division has funded the refurbishment of two quarantine animal holding areas. This now enables us to safely contain and "clean up" other mouse models coming in from other institutions without putting our own colony at risk.

Listed below are the names of the twelve principal investigators and their postdoctoral fellows or graduate students who are presently using the transgenic facility.

Pepe Alberola-Ila

Susannah Barbee, Christie Beel, Harry Green, Gabriela Hernandez-Hoyos, Micheline Laurent, Chi Wang

David Anderson

Gloria Choi, Ben Deneen, Xinzhong Dong, Limor Gabay, C.J. Han, Christian Hochstim, Wolf Hubensak, Walter Lerchner, Li Ching Lo, Sally Lowell, Jaesang Kim, Raymond Mongeau, Yosuke Mukoyama, Donghun Shin, Qiao Zhou, Mark Zylka

David Baltimore

Eric Brown, Rafael Casellas, Jolene Chang, Alexander Hoffman, Wange Lu, Mollie Meffert, Xiao-Feng Qin, Jeff Wiezorek, Lili Yang

Scott Fraser

Mary Dickinson, Angelique Louie, Carol Readhead, Seth Ruffins, Chris Waters

Mary Kennedy

Holly Carlisle, Jenia Khoroseva, Irene Knuesel, Pasquale Manzerra, Alan Rosenstein, Leslie Schenker, Laurie Washburn

Henry Lester

Purnima Deshpande, Carlos Fonck, Princess Imoukhuede, Joanna Jankowsky, Steven Kwoh, Cesar Labarca, Sacha Malin, Sheri McKinney, Raad Nashmi, Johannes Schwarz, Eric Slimko, Irina Sokolova, Amber Southwell, Andrew Tapper

Paul Patterson

Sylvian Bauer, Ben Deverman, Kristina Holmberg, Bradley Kerr, Ali Koshnan, Jennifer Montgomery, Amber Southwell

Ellen Rothenberg

Alexandra Arias, Elizabeth-Sharon David, Deirdre Scripture-Adams, Tom Taghon, Angela Weiss, Mary Yui

Erin Schuman

Changan Jiang

Melvin Simon

Pam Eversole-Cire, Lingjie Gu, Jong-Ik Hwang, Valeria Mancino, Kum Joo Shin

Alexander Varshavsky

Cory Hu, Jun Sheng

Barbara Wold

Jennifer Ambroggio, Libera Berghella, Leslie Dunipace, Richel Gwirtz, Brian Williams

References

- Gordon, J.W., Scangos, G.A., Plotkin, D.J., Barbosa, J.A. and Ruddle, F.H. (1980) *Proc. Natl. Acad. Sci. USA* 77:7380-7384.
- Liu, X., Wu, H., Loring, J., Hormudzi, S., Disteche, C.M., Bornstien, P. and Jaenisch, R. (1997) *Dev. Dynam.* 209:85-91.
- Overbeek, P.A., Aguilar-Cordova, E., Hanten, G., Schaffner, D.L., Patel, P., Lebovitz, R.M. and Lieberman, M.W. (1991) *Transgenic Res.* 1:31-37.
- Zijlstra, M., Li, E., Sajjadi, F., Subramani, K.S. and Jaenisch, R. (1989) *Nature (London)* 342:425-638.

Millard and Muriel Jacobs Genetics and Genomics Laboratory

Director: José Luis Riechmann

Staff: Brandon King Vijaya Rao, Kayla Smith

Support: The work at the Laboratory has been supported by:

Muriel and Millard Jacobs Fund for Genomics and Genetic Technology

Millard and Muriel Jacobs Family Foundation

Summary: The goal of the Millard and Muriel Jacobs Genetics and Genomics Laboratory (formerly known as the Gene Expression Center), in the Division of Biology, is to provide a suite of cutting-edge genomic research tools to all interested Caltech scientists, with an initial emphasis on large-scale gene expression profiling. The Laboratory performs gene expression analyses using DNA microarray technology, and is equipped with the necessary experimental and bioinformatics infrastructure that is needed to generate, store, and analyze large-scale datasets from a variety of microarray technological platforms.

The variety of commercially available platforms and reagents differs considerably among different organisms. Reagent availability and technical and cost considerations determine our choice of microarray platform for each particular project. Available equipment in the laboratory includes a QIAGEN 3000 liquid handling robot, a MicroGridII arrayer (from BioRobotics), a GenePix 4200A scanner (from Axon Instruments), a BioAnalyzer (from Agilent Technologies), and the necessary instruments to use Affymetrix GeneChips (Fluidics Station 400, Hybridization Oven 640, and GeneArray 3000 scanner). The MicroGridII arrayer allows us to generate hundreds of microarray slides in a cost effective manner, by using whole genome 70-mer oligonucleotide sets from QIAGEN. In this way, we have generated microarrays for Arabidopsis and yeast. Arabidopsis microarrays have been used in research projects related to flower development (work performed together with Professor E.M. Meyerowitz's group) and to flowering time (work performed in collaboration with Professor Rick Amasino, University of Wisconsin, Madison). Yeast microarrays prepared in the Laboratory have been used in work performed with Professor Ray Deshaies' group. The availability of the Affymetrix GeneChip 3000 scanner allows us to use the latest generation Affymetrix GeneChips. Among the research groups at Caltech that have benefited from that technology are those of Professors, David Anderson, Barbara Wold, Henry Lester, Ellen Rothenberg, Melvin Simon and, in the Division of Chemistry, Peter Dervan.

We have also assembled the basic bioinformatics infrastructure that is needed for microarray data storage and analysis, combining both commercial and in-house written software. The Laboratory uses Resolver (from Rosetta Biosoftware) as its primary gene expression data analysis system. Resolver is a robust, enterprise-scale,

gene expression system that combines a high capacity, MAGe-compliant database and advanced analysis software in a high-performance server framework. The system is accessible through client stations using a web-based interface. Resolver has been developed with a plug-in framework architecture, which allows for customization and extension, and integration with third-party products. We are extending the system with links to other public and proprietary databases, and we also plan to integrate into Caltech's customized Resolver additional analysis tools that have been developed by the groups of Barbara Wold and Eric Mjolsness. We also have at our disposal additional microarray software tools and analysis packages, both public and commercial. The hardware infrastructure of the Laboratory currently includes a Sun Fire V880 server (from Sun Microsystems), that we use for the Resolver database (Oracle) and analysis system.

Publications

- Broun, P., Pointdexter, P., Osborne, E., Jiang, C.-Z. and Riechmann, J.L. (2004) WIN1, a transcriptional activator of epidermal wax accumulation in Arabidopsis. *Proc. Natl. Acad. Sci. USA* 101(13):4706-4711.
- Ito, T., Wellmer, F., Yu, H., Das, P., Ito, N., Alves-Ferreira, M., Riechmann, J.L. and Meyerowitz, E.M. (2004) The homeotic protein AGAMOUS controls microsporogenesis by regulation of SPOROCTELESS. *Nature* 430:356-360.
- Riechmann, J.L. (2004) Arabidopsis transcription factors: Genome-wide comparative analysis. In: *Encyclopedia of Plant & Crop Science*, R.M. Goodman (ed.), Marcel Dekker, Inc., New York, pp 51-54.
- Riechmann, J.L. Genetic Analysis of Flower Development in Arabidopsis thaliana: The ABC model of floral organ identity determination. In: *Key Techniques in Practical Developmental Biology*, M. Mari-Beffa and J. Knight (eds.), Cambridge University Press, New York. In press.
- Wagner, D., Wellmer, F., Dilks, K., William, D., Smith, M.R., Kumar, P.P., Riechmann, J.L., Greenland, A.J. and Meyerowitz, E.M. (2004) Floral induction in tissue culture: A system for the analysis of LEAFY-dependent gene regulation. *The Plant Journal* 39:273-282.
- Wellmer, F., Riechmann, J.L., Alves-Ferreira, M. and Meyerowitz, E.M. (2004) Genome-wide analysis of spatial gene expression in Arabidopsis flowers. *Plant Cell* 16(5):1314-1326.

Monoclonal Antibody Facility

Supervisor: Paul H. Patterson

Director: Susan Ker-hwa Ou

Staff: Shi-Ying Kou

The Monoclonal Antibody Facility provides assistance to researchers wishing to generate monoclonal antibodies (mAbs), polyclonal ascites Abs (immunizing the mice with antigen until the serum titer is high enough then induce the mice with sarcoma cells to obtain high titer polyclonal ascites), ascites fluid or other tissue culture services. In addition to these service functions, the Facility also conducts research on the development of novel immunological techniques.

In its service capacity, the Facility produced Mabs for the following groups during the past year. The Rees lab obtained mAbs against the Vit B12 transporter and against the membrane protein ECH2. The Ou lab (USC) obtained mAbs against HCV F protein. The Benzer lab obtained mAbs against peptide sequences from Painless protein from *Drosophila*. The Zinn lab obtained mAbs against bleached (*Drosophila* protein involved in axonogenesis). The Parker lab obtained polyclonal ascites against a peptide sequence from the viral proteins V5-KLH and V5-OVA. The Rajasekaran lab (UCLA) obtained mAbs against human embryonic kidney cells. The Baltimore lab obtained polyclonal ascites against the RYK GST-fusion protein and polyclonal ascites against human B94 protein induced by cytokines. The Cho lab (Baylor) obtained polyclonal ascites against *Drosophila* GST-DLGS97. The Colicelli lab (UCLA) obtained mAbs against His-tagged human ARG.

We are currently working with the following groups: The Miller lab (USC) is looking for mAbs against a peptide from Madd (mitogen activating death domain protein). The Bjorkman lab is making mAbs against murine cytomegalovirus protein. The Baltimore lab is making polyclonal ascites against a protein from mouse brain expressed in bacteria. The Wetzel (University of Tennessee) and Patterson labs are making mAbs against calmidazolium A β protofibrils. The Schuman lab is making polyclonal ascites against GST-Ncad. The Strauss lab is making polyclonal ascites against dengue virus capsid and yellow fever virus helicase proteins. The Fong lab (USC) is making mAbs against RGR opsin.

Papers citing the Facility

Fu, G. and Shi, W. (2002) *J. Dental Res.* 81:0756.

Lee, O., Frese, K.K., James, J.S., Chadda, D., Chen, Z., Javier, R.T. and Cho, K. (2003) *Nature Cell Biol.* 10:1038-1055.

Miller, L.C., Swayne, L.A., Chen, L., Feng, Z., Wacker, J.L., Muchowski, P.J., Zamponi, G.W. and Braun, J.E.A. (2003) *J. Biol. Chem.* 278:53072-53081.

Qi, F., Chen, P., Caufield, P.W. and Shi, W. (2002) *J. Dental Res.* 81:2244.

Nucleic Acid and Protein Sequence Analysis Computing Facility

Supervisor: Stephen L. Mayo

Staff: David R. Mathog, Manager, Sequence Analysis Facility

The Sequence Analysis Facility (SAF) provides software, computers, and support for the analysis of nucleic acid and protein sequences. Currently the SAF hardware consists of a Sun Netra running Solaris (mendel.bio.caltech.edu), a small Beowulf cluster of 20 Athlon XP nodes, a file server, a 32 page per minute duplexing laser printer, and a color laser printer. The Biology Division's slidemaker, and the PCs that comprise the "structure analysis facility" are also located in our facility. The SAF has over 250 registered users distributed among 50 research groups.

Most common programs for sequence analysis are available on Mendel. These include the GCG and EMBOSS Packages, PRIMER3, Phred, Phrap, Cross_Match, Phylip, and HMMER. Many of these may be accessed through the W2H or Pise web interfaces. Users may supply their own sequences or use those in the locally maintained databases (Genbank, PIR, SwissProt, and others). Other programs, custom written programs, or special databases are available on request. The PCs boot either Linux or Windows XP and support hardware stereo in either mode. Under Linux the programs O, Molscript, XtalView, CCP4, and Delphi are available. Under Windows XP Swiss PDB Viewer, O, POVray, and various drawing and animation programs may be used. The searchable documentation for these programs is available on the SAF web server (<http://saf.bio.caltech.edu/>). The lecture notes and homework from the introductory course "Fundamentals of Sequence Analysis" are also available on the SAF web server. BLAST jobs submitted through the SAF web interface run on the SAF Beowulf cluster (in parallel) faster than they do at the NCBI server. An enhanced parallel HMMER server offers the full set of HMMER programs plus the unique ability to search any of the installed BLAST databases with an HMM.

Nucleic acid sequences from the DNA sequencing facility are distributed through the SAF web and FTP servers and may be analyzed on our servers. We also distribute site-licensed software such as DNASTAR, Gene Construction Kit, ChemSketch, and X-Win.

Publication

Mathog, D.R. (2003) Parallel BLAST on split databases. *Bioinformatics* 19(14):1865-1866.

Protein Expression Facility

Supervisor: Pamela J. Bjorkman

Director: Peter M. Snow

Staff: Cynthia Jones, Inderjit Nangiana

(<http://www.its.caltech.edu/~bjorker/pef.html>)

The Protein Expression Facility was established in 1996 to meet the needs of the Caltech community in all areas related to protein expression. The services provided include generation of recombinant DNA constructs, expression of recombinant proteins in a variety of expression systems, and purification of the expressed proteins.

Expression Facility Services and Capabilities: The Facility is equipped to perform most common techniques in molecular biology including PCR, construction and analysis of recombinant DNA vectors, and molecular cloning of DNA molecules. We also perform protein concentration, protein purification (by FPLC), and analysis using standard biochemical techniques (for example most types of electrophoresis). The tissue culture portion of the facility is equipped with an inverted phase contrast microscope designed for examination of cells, two laminar flow hoods suitable for sterile manipulations, two incubators capable of supporting the growth of mammalian cell lines, and two refrigerated incubators housing eight spinner plates that are used for the growth of insect cells. A 15-liter bioreactor that is suitable for larger-scale production of proteins expressed in baculovirus-infected insect cells or mammalian cells is also available. A second fermenter gives us the capability to grow both bacteria and yeast in volumes up to ten liters. Smaller quantities of both bacteria and yeast may be grown in our shaking incubator. We are also capable of growing mammalian cell lines on a more limited basis. The facility also has a Cell Pharm, a hollow-fiber bioreactor designed for high-level expression of secreted proteins in mammalian cells, which gives the facility additional versatility with respect to the variety of expression systems we are capable of exploring and utilizing.

Expression Systems: We have chosen to focus primarily on a eukaryotic expression system to preserve glycosylation and other post-translational modifications that can be important for protein function. To date, the majority of recombinant proteins that have been produced at the Facility have been expressed in the baculovirus system, which is the most widely used and versatile eukaryotic system for the generation of recombinant proteins. Since its inception the Facility has generated over 800 recombinant viruses and has generated an average of 300 liters of infected viral cells per year. The recombinant DNA used for the generation of a significant number of these viruses was also constructed by the staff of the Facility. A more limited number of proteins have been expressed in bacterial cells and mammalian cells. The use of an additional eukaryotic expression system (the

methylotropic yeast *Pichia pastorius*) has also been explored, although this system is not yet in routine use.

Protein Expression, Purification, and Applications Involving Recombinant Proteins: A significant number of the recombinant proteins that have been expressed have also been purified by the Facility staff. The purification methodology has ranged from affinity chromatography to more standard techniques, such as ion exchange or size exclusion chromatography, or a combination of these. The proteins that have been expressed and purified are as diverse in their biochemical and functional characteristics, ranging from nuclear proteins involved in DNA replication to cell surface proteins mediating cell-cell interactions.

Proteins expressed and/or purified by the Expression Facility have been used for a variety of experiments or applications. Some have been used as immunogens for the generation of antibodies, or to study or utilize their functional activity. In other projects, we have generated up to 30 different variants of a protein in order to allow investigators to do an exhaustive site-directed mutagenesis study to map a binding site. Many other proteins have been used in crystallization trials to solve their three-dimensional structures, resulting in the determination of several crystal structures by the Bjorkman laboratory. To aid in crystallographic efforts, we have developed the ability to express selenomethionine-substituted proteins in baculovirus-infected insect cells, which allows determination of crystal structures by multiwavelength anomalous dispersion (MAD) methods.

Protein-Protein Interactions: In one of the more interesting applications, which we would like to pursue more extensively in the future, recombinant fusion proteins have been expressed for use in attempts to identify interacting proteins. These experiments by the Zinn and Anderson laboratories have involved using the fusion proteins as "bait" to bind their putative ligands in a variation on affinity chromatography. The putative ligands have subsequently been analyzed by mass spectroscopy at the PPMAL facility, allowing their identification. While these experiments have thus far yielded results which are inconclusive, the strategy shows promise, and we will continue to refine it in the future.

Utilization of Facilities: During the past year, the Facility has expressed more than 140 different proteins in varying quantities (requiring the generation of more than 350 liters of baculovirus-infected insect cells and 45 liters of bacterial cells) for a number of investigators both at Caltech and outside of the Institute. During this period, we have made 115 new recombinant viruses, with the recombinant DNA used for the generation of 23 of these viruses being constructed at the Center. Fifty-five viruses have been titered, and 17 viruses have been plaque-purified. In addition, 31 of the expressed proteins were concentrated and at least partially purified by Facility personnel for the investigators. We have also expressed

three recombinant proteins in bacteria, and purified one of the expressed proteins.

The Facility has provided services for the following investigators at Caltech: David Anderson, Pamela Bjorkman, Jacqueline Barton, Judith Campbell, David Chan, Peter Dervan, Ray Deshaies, Grant Jensen, Mary Kennedy, Stephen Mayo, Paul Patterson, Douglas Rees, Richard Roberts, Paul Sternberg, James Strauss, Alexander Varshavsky, Linda Hsieh-Wilson, and Kai Zinn.

We have also provided services to Harald Althaus, Dade Behring Marburg GmbH, Marburg, Germany; David Carmichael, Xencor; Jue Chen, Department of Biological Sciences, Purdue University; Dr. James Cook and Dr. Mark Worwood, University of Kansas Medical Center; Martine Coue, Texas Tech University; Balazs Gereben at the Institute of Experimental Medicine, Hungarian Academy of Sciences, Budapest, Hungary; I. Kaltashov, University of Massachusetts; Robert Kriwacki, Department of Structural Biology, St. Jude Children's Research Hospital, Memphis, Tennessee; Chih-Pin Liu at City of Hope Hospital; Anne Mason at the University of Vermont College of Medicine; Scott Rajski at the University of Wisconsin School of Pharmacy; Michael Stallcup at USC School of Medicine; Brian Thoma, University of Texas; and Larry Zipursky, UCLA.

Publication

Giannetti, A.M., Snow, P.M., Zak, O. and Bjorkman, P.J. (2003) Mechanism for multiple ligand recognition by the human transferrin receptor. *Public Library of Science (PloS)* 1:341-350.

Publications Acknowledging the Expression Facility

Delker, S.L., West, Jr., A.P., McDermott, L., Kennedy, M.W. and Bjorkman, P.J. (2004) Crystallographic studies of ligand binding by Zn-alpha2-glycoprotein. *J. Struct. Biol.* In press.

Giannetti, A.M. and Bjorkman, P.J. (2004) HFE and transferrin directly compete for transferrin receptor in solution and at the cell surface. *J. Biol. Chem.* 279:25866-25875.

Herr, A.B., Ballister, E.R. and Bjorkman, P.J. (2003) Insights into IgA-mediated immune responses from the crystal structures of human Fc α RI and its complex with IgA1-Fc. *Nature* 423:614-620.

Herr, A.H., White, C.L., Milburn, C., Wu, C. and Bjorkman, P.J. (2003) Bivalent binding of IgA1 to Fc α RI suggests a mechanism for cytokine activation of IgA phagocytosis. *J. Mol. Biol.* 327:645-657.

Hwan-Ching, T., Khidekel, N., Ficarro, S.B., Peters, E.C. and Hsieh-Wilson, L.C. (2004) Parallel approach to accelerate the identification of O-GlcNAc modified proteins from cells. *J. Am. Chem. Soc.* In press.

Khidekel, N., Arndt, S., Lamarre-Vincent, N., Lippert, A., Poulin-Kerstien, K.G., Ramakrishnan, B., Qasba, P.K. and Hsieh-Wilson, L.C. (2003) A chemoenzymatic approach toward the rapid and sensitive detection of O-GlcNAc posttranslational modifications. *J. Am. Chem. Soc.* 125:16162-16163.

Sprague, E.R., Martin, W.L. and Bjorkman, P.J. (2004) pH-dependence and stoichiometry of binding to the Fc region of IgG by the herpes simplex virus Fc receptor gE-gI. *J. Biol. Chem.* 279:14184-14193.

West, Jr., A.P., Herr, A.B. and Bjorkman, P.J. (2004) The chicken yolk sac IgY receptor, a functional equivalent of the mammalian MHC-related Fc receptor, is a phospholipase A2 receptor homolog. *Immunity* 20:601-610.

Protein Micro Analytical Laboratory
 Director: Gary M. Hathaway, Ph.D.
 Associate Biologist: Felicia Rusnak, B.S.
 Senior Research Assistant and MPS: Jie Zhou, Ph.D.
 Faculty Advisor: Kai Zinn, Ph.D.
<http://www.its.caltech.edu/~ppmal>, or
<http://www.caltech.edu/subpages/analyt.html> or
<http://www.its.caltech.edu/~bi/bicatalog.html#ppmal>

The Protein Micro Analytical Laboratory Facility (PPMAL) performs consultation and structure analysis on proteins, peptides and other biopolymers. The laboratory develops new techniques for analyzing biopolymers. Cost recovery is from charge-back with support from the Beckman Institute.

Activity Centers

Biopolymer Mass Spectrometry and Proteomics

- Tandem mass spectrometry (MS/MS) peptide sequencing.
- LC-MS/MS for detecting post translational and chemical modifications.
- Capillary liquid chromatography coupled MS and MS/MS.
- MALDI-TOF MS.
- In-gel digestion for mass mapping and sequencing by MS.
- Fragmentation analysis and database search for protein identification.

Edman Sequencing

- Subpicomole, aminoterminal sequence analysis of proteins and peptides by Edman degradation.

High Performance Liquid Chromatography

- Submillimeter and capillary HPLC for analysis and purification.

Specialty Analyses

- De novo sequence analysis of MS/MS derived data.
- Chemical modification of proteins and peptides for mass spectrometry. Including acetylation, O-methylisourea conversion of lysine residues, chemical modification of phospho- and glyco-peptides for mass and chemical sequence analysis.
- Consultation on sample preparation and error analysis including dissemination of information including the maintenance of our web site.
- Database search and analysis.

SPECIFICS

Mass spectrometry of biopolymers: The facility houses three mass spectrometers: A triple-quadrupole, tandem mass spectrometer, MALDI time-of-flight mass spectrometer and a new electrospray quadrupole time-of-flight mass spectrometer. The liquid chromatography (LC/MS) interface is coupled to a technique for gradient elution using static mini-gradients. We construct the reverse phase columns for use within the electrosprayer of

our design. MS/MS fragmentation spectra can be achieved with as little as ten femtomoles of peptides.

Protein/peptide chemical sequence analysis by Edman degradation: A dual reaction cartridge, capillary microsequencer with subpicomole sensitivity is used. The instrument extends the use of the technology for combined chemical and MS sequencing projects. Our modified chemistry is used to improve performance.

Chemical modification of proteins and peptides: Chemical conversions of native peptides: In particular, those with post-translational modifications are carried out to facilitate analysis. The facility also publishes its original research efforts in this area and applies the new technology.

Database search and analysis: The laboratory maintains access to database search via the web with programs such as MASCOT, BLAST, and others using information obtained from mass and chemical sequencing.

Collaborations and accomplishments: During the course of the year the lab interacted with 25 Caltech laboratories. Mass analyses were performed for the Divisions of Biology and Chemistry. Additional faculty was supported through our efforts on behalf of the Biopolymer Synthesis and Protein Expression Facilities. The facility published improvements it has made in the chemical identification of post-translationally modified residues (CTID) chemistry it first introduced in 2002.

Future expectations and directions: Our laboratory continuously strives to develop new procedures that will permit high throughput analysis while maintaining high sensitivity. With the acquisition of the new hybrid mass spectrometer, we will be upgrading the liquid chromatography capabilities to include state-of-the-art two-dimensional separation for proteomic studies. Other improvements in the facility's capability for handling high-sensitivity, high mass accuracy demanding projects will be instituted as time and availability permits.

Publication

Rusnak, F., Zhou, J. and Hathaway, G.M. Determination of multiple phosphorylation sites in β -casein by chemically targeted identification (CTID). Submitted.

Graduates

Doctor of Philosophy - 2004 Division of Biology

Ramzi I. Azzam, Ph.D.

Biology

B.S., University of California, Santa Barbara, 1996

M.A., University of California, Santa Barbara, 1997

Thesis: The Role of Net1 Phosphorylation in Regulating CDC14 Release During Mitotic Exit.

Catherine Craig Baker, Ph.D.

Biology

B.A., Princeton University, 1997

Thesis: Genetic and Genomic Studies of Shoot and Flower Growth in *Arabidopsis*.

Martín Leandro Basch, Ph.D.

Biology

Licenciado, Universidad de Buenos Aires, 1996

Thesis: Early Neural Crest Specification, Induction and Competence.

Kyle Alan Bernheim, Ph.D.

Biology

B.S., Pennsylvania State University, 1998

Thesis: Functional and Structural Magnetic Resonance Imaging of Humans and Macaques.

Eliot Christen Bush, Ph.D.

Biology

A.B., Harvard College, 1997

M.S., California Institute of Technology

Thesis: Evolution and Scaling in Mammalian Brains.

Anthony Michael Giannetti, Ph.D.

Biochemistry and Molecular Biophysics

B.S., University of California, Santa Barbara, 1998

Thesis: Biochemical, Biophysical, and Cellular Investigations of the Interactions of Transferrin Receptor with Transferrin and the Hereditary Protein, HFE.

Ying Gong, Ph.D.

Biochemistry and Molecular Biophysics

B.S., Peking University, 1996

M.A., Smith College, 1998

Thesis: Cell Polarity and Morphogenesis: Functions and Mechanisms of Cell Divisions in Vertebrate Gastrulation.

Po-Ssu Huang, Ph.D.

Biochemistry and Molecular Biophysics

B.A., University of California, Berkeley, 1998

Thesis: Computational Design and Experimental Characterization of Protein Oligomers.

Daniel Keith Meulemans, Ph.D.

Biology

B.S., University of Hawaii at Manoa, 1996

M.S., California Institute of Technology, 1999

Thesis: Genetic Correlates of Neural Crest Evolution.

Javier Perez-Orive, Ph.D.

Computational and Neural Systems

B.S., Universidad Iberoamericana, 1995

M.S., Case Western Reserve University, 1998

Thesis: Neural Oscillations and the Decoding of Sensory Information.

Robert J. Peters, Ph.D.

Computation and Neural Systems

B.S., University of Wisconsin, Madison, 1995

Thesis: Visual, Attention and Object Categorization: From Psychophysics to Computational Models.

Kathleen Miho Sakamoto, Ph.D.

Biology

B.A., Williams College, 1979

M.S., University of Cincinnati College of Medicine, 1982

Thesis: Targeting Proteins for Ubiquitination and Degradation in the Treatment of Human Disease.

W. Bryan Smith, Ph.D.

Cellular and Molecular Neurobiology

B.S., University of Southern California, 1998

M.S., California Institute of Technology, 2000

Thesis: Local Control of Synaptic Strength: Neurotrophic and Dopaminergic Modulation of Dendritic Protein Synthesis.

Luis E. Vázquez, Ph.D.

Biology

B.S., University of Puerto Rico, Mayaguez, 1998

M.S., California Institute of Technology, 2000

Thesis: SynGAP Controls Synapse Formation by Regulating Spine Development and Morphology.

Lili Yang, Ph.D.

Biology

B.S., University of Science and Technology of China, 1997

M.S., University of California, Riverside, 1999

Thesis: Towards Engineering Immunity

2004 – Master of Science, Biology

Charles Walter Bugg (Biochemistry and Molecular Biophysics)

Surelys Galeno (Biology)

Toby Abraham Rosen (Biology)

Terry Torao Takahashi (Biochemistry and Molecular Biophysics)

Eric H. Tse (Biology)

2004 - Bachelor of Science, Biology

Neda Afsarmanesh (Biology)

Kamilee Willow Christenson (Biology)

Patrick James Codd* (Biology)

Robin Christine Deis* (Biology)

Yile Ding* (Biology)

Peter Louis Freddolino* (Biology)

Katherine Ann Homann (Biology)

Andrew Lee Hsieh (Biology)

Di Hu* (Biology)

Cristian Sandel Jitianu* (Biology and Chemistry)

Greta Susan Jo (Biology)

Robert Lin Li* (Biology and Computer Science)

Elinor Yen-Ru Lin (Biology)

Charlene Sow-Lin Mak* (Biology and Business Economics and Management)

Andrea Valenzuela Manzo (Biology)

Benjamin John Matthews (Biology)

Andrea Elizabeth McColl (Biology)

Jong Oh (Biology)

Melinda Tsaoying Owens* (Biology)

Anna Katherine Sczaniecka (Biology)

Francy Yi-Hsuan Shu (Biology)

Christopher Tao-Kai Sung* (Biology and Chemistry)

Jian Yuan Thum* (Biology)

Theresa Kay Tiefenbrunn* (Biology)

*Students whose names are followed by an asterisk are being graduated with honor in accordance with a vote of the faculty.

Financial Support

Financial Support

The financial support available for the work of the Division of Biology comes from many sources: The Institute's General Budget and Endowment and special endowment funds; from gifts, grants or contracts from individuals, corporations, foundations, associations, and U.S. government agencies.

Agouron Institute
 Air Force Office of Scientific Research
 Alfred P. Sloan Foundation (Sloan Center for Theoretical Neuroscience)
 American Cancer Society
 American Federation for Aging Research
 American Foundation for Alzheimer's Research
 American Heart Association
 American Liver Foundation
 Amgen, Inc.
 Andy Lou and Hugh Colvin Postdoctoral Fellowship
 Anonymous and personal donations also made
 Applied Biosystems
 Army Research Office (ARO)
 Arnold and Mabel Beckman Foundation
 Association for the Cure of Cancer of the Prostrate CaPCURE

George Beadle Professorship in Biology
 Beckman Institute
 Beschorman Memorial Fund
 Anne P. and Benjamin F. Biaggini Professorship of Biology
 Bing Professorship in Behavioral Biology
 Biological Sciences Initiative
 James G. Boswell Foundation
 James G. Boswell Professorship of Neuroscience
 Ethel Wilson and Robert Bowles Professorship of Biology
 Donald Bren Foundation
 Bren Professorship of Biology
 Mr. Donald L. Bren, Bren Scholars Program
 Bristol-Myers Squibb
 Mr. Eli Broad, Broad Center for the Biological Sciences
 Burroughs-Wellcome Career Awards at the Scientific Interface
 Burroughs Wellcome Fund

California Breast Cancer Research Program
 California Tobacco-Related Disease Research Program
 Callie McGrath Charitable Trust
 Caltech President's Fund
 Cancer Research Fund of the Walter Winchell-Damon Runyon Foundation
 Cancer Research Institute
 Cancer Research Institute Postdoctoral Fellowship
 Norman Chandler Professorship in Cell Biology
 Charles B. Corser Fund
 Christopher Reeve Paralysis Foundation
 Cline Neuroscience Discovery Grant
 Colvin Fund for Research Initiatives in Biomedical Sciences
 Croucher Foundation
 Albert and Kate Page Crutcher
 Cure Autism Now Foundation

Damon Runyon-Walter Winchell Cancer Fund
 David & Lucile Packard Foundation
 Allen and Lenabelle Davis Professorship of Biology
 Defense Advanced Research Projects Agency (DARPA)
 Della Martin Foundation
 Department of Defense, Prostate Cancer Research
 Department of Energy (DOE)
 Department of Navy, Office of Naval Research (ONR)
 DNA Sequencer Patent Royalty Funds
 Donald E. and Delia B. Baxter Foundation

Elizabeth Ross Fellowship
 Ellison Medical Research Foundation
 EMBO
 Engineering Research Center for Neuromorphic Systems (ERC-NSF)
 European Molecular Biology Organization
 Evelyn Sharp Fellowship

John and Ellamae Fehrer Endowed Biomedical Discovery Fund
 Ferguson Fellowship
 Ferguson Fund for Biology
 Lawrence L. and Audrey W. Ferguson Prize
 Fletcher Jones Foundation
 Fling Charitable Trust
 Frank P. Hixon Fund
 French Foundation for Alzheimer Research

Gates Grubstake Fund
 The German Academy of National Scientists Leopoldina
 German Government Fellowship
 William T. Gimbel Discovery Fund in Neuroscience
 Ginger and Ted Jenkins
 Gordon E. and Betty I. Moore Foundation
 Gordon Ross Fellowship
 Gordon Ross Medical Foundation
 Gosney Fellowship Fund
 Grubstake Presidents Fund

William D. Hacker Trust
 Lawrence A. Hanson, Jr. Professorship of Biology
 The Helen Hay Whitney Memorial Fund
 The Helen Hay Whitney Foundation
 Hereditary Disease Foundation
 Hicks Fund for Alzheimer Research
 HiQ Foundation
 Hixon Professorship of Psychobiology
 Dr. Norman Horowitz
 House Ear Institute
 Howard Hughes Medical Institute
 Human Brain Project
 Human Frontiers Collaborative Grant
 Human Frontiers in Science Program (HFSP)

Huntington Hospital Research Institute
Huntington's Disease Society of America

Instituto Gulbenkian de Ciência

James S. McDonnell Foundation
Jane Coffin Childs Memorial Fund for Medical Research
Japan Society for the Promotion of Science (JSPS)
Jet Propulsion Lab
Josephine V. Dumke Fund
Joyce Charitable Fund
Joyce Fund for Alzheimer's Disease Research

Keck Discovery Fund
W.M. Keck Foundation for Discovery in Basic Medical
Research
Kroc Foundation

L.A. Hanson Foundation
Leonard B. Edelman Discovery Fund
Leukemia and Lymphoma Society
Life Science Research Foundation
Lucille P. Markey Charitable Trust

Margaret E. Early Medical Research Trust
Max Planck Research Award for International Cooperation
Helen and Arthur McCallum Foundation
McGrath Foundation
McKnight Endowment Fund for Neuroscience
McKnight Foundation
McKnight Neuroscience of Brain Disorders Award
Merck & Co., Inc.
Mettler Fund for Autism
The Millard and Muriel Jacobs Family Foundation
Mind Science Foundation
The Betty and Gordon Moore Fellowship
Moore Discovery Grant Program
Moore Foundation
Muscular Dystrophy Association

NASA/AMES
National Aeronautics and Space Administration
National Cancer Institute
National Eye Institute
National Geospatial Intelligence Agency
National Heart, Lung and Blood Institute
National Institute for Biomedical Imaging and
Bioengineering
National Institute of Allergy and Infectious Diseases
National Institute of Arthritis and Musculoskeletal and
Skin Disease
National Institute of Child Health and Human Development
National Institute of General Medical Science
National Institute of Mental Health, USPHS
National Institute of Neurological Diseases and Stroke
National Institute on Aging
National Institute on Deafness and Other Communication
Disorders
National Institute on Drug Abuse
National Institutes of Health, USPHS

National Parkinson Foundation
National Science Foundation (NSF)
Norman & Annemarie Davidson Fund for Research in Biology
Norman Chandler Professorship in Cell Biology
Norman Davidson Lectureship
Norman W. Church Fund

Office of Naval Research

The Packard Foundation
Ralph M. Parsons Foundation
Pasadena Neurological Fellowship
Passano Foundation
PhRMA Foundation
Pritzker Neurogenesis Research Consortium

Research Management Corporation
Retina Research Foundation
Rita Allen Foundation
Rockefeller Foundation
Roman Reed Spinal Cord Injury Research Fund of California
Ronald and Maxine Linde Alumni Challenge
Rosalind W. Alcott Scholarship Fund
Anna L. Rosen Professorship
Benjamin Rosen Family Foundation
William E. Ross Memorial Student Fund
Albert Billings Ruddock Professorship
Damon Runyon Fellowship

Sandia National Laboratories
Warren and Katherine Schlinger Foundation
Edwin H. Schneider Fund
Searle Foundation
Searle Scholarship Award
The Skirball Foundation
Alfred P. Sloan Research Fellowship
Alfred P. Sloan Foundation
Howard and Gwen Smits Professorship of Cell Biology
Stanley Medical Research Institute
Grace C. Steele Professorship in Molecular Biology
Swartz Foundation
Swiss National Science Foundation

Technology Transfer Gates Grubstake Fund
That Man May See, Inc.
Walter and Sylvia Treadway Funds
Lois and Victor Troendle Professorship
Troendle Trust
TRDRP

United Mitochondrial Disease Foundation

Wiersma Visiting Professorship of Biology Program
Robert E. and May R. Wright Foundation Fund

Yuen Grubstake Fund

Ernest D. Zanetti Fund
Carl Zeiss Microimaging

Index of Names

Index of Names

- Abelson, John N. – 13
 Acevedo-Bolton, Gabriel – 211
 Adachi, Satoko – 250, 259
 Adams, Megan – 182
 Adams, Stephanie – 250, 257, 291
 Adolphs, Ralph – 26
 Afsarmanish, Neda – 91
 Akutagawa, Eugene – 60
 Al-Anzi, Bader – 39, 40
 Alberola-Ila, José – 14, 175, 177, 179, 180
 Alex, Jennifer – 292
 Alexandru, Gabriela – 137, 138
 Allen, Benjamin D. – 154
 Allman, John M. – 13, 25, 26
 Alon, Uri – 209
 Altomare, Katia – 107, 110
 Alvarez, Mary – 266
 Alvarez-Buylla, A. – 213
 Alvizo, Oscar – 154
 Amaya, Armando – 292
 Ambroggio, Xavier – 137, 139
 Amore, Gabriele – 186, 198
 An, Jee Young – 168
 Andersen, Richard A. – 6, 13, 27, 28, 29, 30, 94
 Anderson, David J. – 13, 32, 33, 34, 35, 36, 37, 38, 40
 Anderson, Kristen – 27
 Anteshechkin, Igor – 266, 270
 Arce, David – 182
 Arias, Alexandra – 250, 252
 Armand, Elena – 98
 Arteaga, Cirilia – 292
 Arvizu, Jenny – 292
 Ary, Mary L. – 154
 Atshuler, Doug – 201
 Attardi, Giuseppi – 13, 107, 108, 111
 Auyeung, Vincent C. – 71, 128
 Axe, Richard – 40
 Axel, Richard – 37
 Ayala, Elizabeth – 21
 Azzam, Ramzi – 137, 141, 303
- Bäcker, Alex – 48
 Bae, Esther – 144
 Baer, Janet F. – 21
 Bailey, Andrew – 184
 Bailey, Robert – 201
 Bak, Magdalena – 211
 Baker, Catherine – 236, 247, 303
 Balagot, Carlzen – 186
 Ballister, Darcy – 117
 Ballister, Edward – 117
 Baltimore, David – 13, 113, 114, 115
 Barbee, Susannah – 175, 180
 Barembaum, Meyer – 182
- Barnes, Tim – 148, 149
 Baron, Margaret H. – 215
 Barth, Barbara – 186
 Basch, Martin – 182, 303
 Bastiani, Carol – 266, 270, 272
 Bauer, Sylvian – 80, 82
 Bayon, Ruben – 250
 Beale, Beale – 44
 Bearer, Elaine – 211, 227
 Becker, Christian F.W. – 77
 Beel, Bryan – 261
 Beel, Christie – 175
 Beene, Darren L. – 67, 68
 Begalla, Krisha – 273
 Behrand, Caleb – 211
 Belford, Gary – 211
 Bender, John – 201
 Benjamin, Jordan – 148, 149
 Bennett, Melanie J. – 123
 Ben-Shaul, Y. – 51
 Benzer, Seymour – 6, 13, 37, 39, 40, 41, 42
 Berghella, Liberia – 276, 280, 282
 Berk, Arnold J. – 74
 Berney, Kevin – 186, 189
 Bernheim, Kyle – 27, 303
 Bernstein, Lynne E. – 91
 Bertani, Elizabeth – 127, 128, 131
 Bezanilla, Francisco – 71
 Bhattacharya, Joydeep – 91, 93, 94
 Bhattacharyya, Rajan – 27
 Bhattacharyya, Sujata – 182, 184
 Biller, Marlene – 161, 162
 Bingol, Baris – 86, 89
 Biondi, Ted – 186
 Bjorkman, Pamela J. – 6, 13, 41, 117, 297
 Blue, Peggy – 21
 Bogen, Joseph – 48
 Boldin, Mark – 113
 Bolouri, Hamid – 186
 Boone, Charles – 127
 Bornstein, Ben – 278, 280, 281
 Boronat, Susanna – 127, 129, 130
 Bottjer, David J. – 198
 Boulat, Benoit – 211, 221, 225
 Bower, Kiowa – 67, 69
 Bowser, David N. – 72
 Branchaud, Eddie – 27
 Breznen, Boris – 27, 28
 Brieu, Philippe P. – 48
 Britten, Roy J. – 13, 186
 Brokaw, Charles J. – 13, 126
 Bronner-Fraser, Marianne – 6, 13, 182, 183, 184
 Broome, Bede M. – 62, 63
 Brower, Christopher – 165, 166
- Brown, C. Titus – 186, 189, 190, 193, 196, 211
 Brozovic, Marina – 27, 28
 Brummel, Ted – 39, 41
 Budd, Martin – 127, 128, 131, 132
 Budick, Seth – 201, 203
 Bugg, Walter – 80, 305
 Bugga, Lakshmi V. – 98, 99,
 Buneo, Chris – 27, 30
 Burt, Michael – 21
 Bush, Eliot C. – 25, 303
 Buzsaki, G. – 50
- Calestani, Cristina – 186
 Cameron, R. Andrew – 186, 189, 190, 191
 Campbell, Judith L. – 13, 127, 128, 129, 130, 131, 132
 Campos, Donaldo – 292
 Campos, Michael – 27, 28
 Canada, Stephanie – 21
 Canaria, Christie – 211, 217
 Cao, Anna – 261, 263
 Card, Gwyneth – 201, 202
 Carleton, A. – 213
 Carlisle, Holly – 44
 Carlisle, Roxanne – 21
 Carlson, Cynthia L. – 154
 Carpenter, John – 211
 Carter, Ronald McKell – 48, 57
 Carvalho, Gil – 39, 42
 Cashin, Amanda L. – 67
 Cassenaer, Stijn – 62, 64
 Caton, William L. – 27
 Cerny, Robert – 183, 184
 Cesare, Tony – 108
 Chalfie, Martin – 270
 Cham, Jorge – 27
 Chan, David C. – 14, 133
 Chan, JuanCarlos – 266, 270
 Chanda, Baron – 71
 Chang, Jung Sook – 32
 Chang, Mi Sook – 261, 263
 Changizi, Mark A. – 91
 Chawla, Aman – 94
 Chee-Ruiter, Christine – 91, 95
 Chen, Chun Hong – 232, 233
 Chen, Hsiuchen – 133, 134, 135
 Chen, Jun-Yuan – 198
 Chen, Lili – 186, 190
 Chen, Wen J. – 266, 270, 272
 Cheung, Evelyn – 117
 Chik, Mabel – 21
 Ching, Alisa – 41
 Chiu, William – 186, 191
 Cho, Jaehyoung – 107, 108, 109
 Choi, Eun Jung – 154, 155, 158

- Choi, Gloria – 32, 33
 Choi, Mee-Hyang – 44, 45, 46
 Choi, Sangdun – 261, 263
 Chomchan, Pritsana – 161, 162, 163, 164
 Chomyn, Anne – 107, 110, 111
 Chow, Elly – 186, 189, 191
 Christianson, Bjorn – 60
 Ciche, Todd – 266, 274
 Clayton, Daniel – 67, 77
 Clem, Rollie – 232
 Cohen, Bruce – 67, 73, 74
 Coles, Ed – 182
 Collazo, Andres – 211
 Collazo, Sonia – 211
 Collins, Allan C. – 73, 74
 Connolly, Jason – 27
 Conrad, Gary – 183
 Cooke, M. – 177, 179
 Cope, Gregory – 137, 139
 Copeland, Jeffrey – 232, 233, 235
 Corneil, Brian – 27, 29
 Cornelison, Stephanie – 39
 Cossu, Guilio – 282
 Cota, Rachel – 258
 Covert, Markus – 113, 115
 Cox III, Robert Sidney – 209, 210
 Cronin, Christopher – 266, 273, 274
 Crowhurst, Karin – 154, 155
 Cui, He – 27
- Dahan, David – 67, 71
 Dalal, Chiraj – 209
 Damle, Sagar – 186, 192, 194, 278, 281, 282
 Dao, Susan – 91
 Das, Pradeep – 236, 239, 241, 243, 244, 245, 246
 Davidson, Eric H. – 13, 186
 Davidson, Norman – 77
 Davis, Mark – 282
 Davis, Mindy – 117, 123
 Davydov, Ilia – 168
 De Bellard, Maria Elena – 182
 De Coste, Dennis – 278
 De Guzman, Frances – 27
 De la Rose, Noelle – 236
 De la Torre, Manny – 21
 DeBuysscher, Tristan – 271, 276, 280
 Deis, Robin – 117, 121
 Delker, Silvia – 117, 122
 DeModena, John – 266, 271, 274
 Demyanenko, Andrey V. – 211, 226
 Deneen, Benjamin – 32, 34
 Denny, Elissa – 113
 Deshaies, Raymond J. – 6, 14, 137
 Deshpande, Purnima – 67, 72, 73, 74, 75
 Detmer, Scott – 133, 134, 135
- Deverman, Benjamin – 80, 81
 Devlin, Mary – 154, 155
 Dhandapani, Kavitha – 261, 262
 Diamond, Rochelle – 250, 253, 291
 Dias, Prabha – 148, 150
 Diba, Kamran – 48, 49
 Dibas, Mohammed – 67, 71, 72
 Dickinson, Mary – 120
 Dickinson, Mary – 120, 211, 215, 216
 Dickinson, Michel H. – 13, 201
 Dickson, William – 201, 208
 Dieterich, Daniela – 86, 88
 DiGiusto, Rhonda K. – 154
 Ding, Jane – 148, 151
 Dionne, Christopher – 250, 253
 Do, Giao K. – 21
 Dong, Ping – 186, 189
 Dong, Xinzhong – 32
 Dorigo, Oliver – 74
 Dorman, Elizabeth – 186, 193
 Dougherty, Dennis A. – 67, 68, 69, 71, 78
 Douglas, R. – 58
 Drake, C.J. – 215
 Dubois, Annick – 236, 244, 246, 247
 Duimstra, Joe – 211, 222
 Dunipace, Leslie – 276, 277, 283
 Dunlop, Mary – 201
 Dunphy, William G. – 13, 144, 145, 146
 Duron, Yolanda – 21
 Dyste, Janet – 165
- Ebert, Jana – 75
 Edgington, D.R. – 58
 Edwards, Jessica – 86
 Edwards, Shaune – 127, 129
 Elliot, Abigail – 44, 45
 Elowitz, Michael – 6, 14, 209
 Ennis, Caroline A. – 123
 Epperlein, Hans-Henning – 183, 184
 Eversole-Cire, Pamela – 261, 263
 Ewald, Andrew – 211, 214
 Ezin, Maxellende – 182, 211
- Fabrikant, Elena – 283
 Fann, Ming-ji – 80, 82
 Farivar, Sarah – 62, 64
 Farkas, Maria – 161, 162, 164
 Fernandez, Jolene – 266, 268
 Ferreira, Marcio A. – 236, 243
 Feuerabendt, Andreas – 21
 Fineman, Igor – 27, 30
 Fingler, Jeffrey – 211
 Fish, Jennifer – 107
 Fisher, James – 72
 Flaherty, Steve – 211
 Fletcher, Jennifer C. – 241
 Flores, Jesse E. – 21
- Flowers, Mary – 182, 211
 Folsom, James P. – 236
 Fonck, Carlos – 67, 74
 Fong, Pamela – 67
 Ford, William – 44, 67
 Forouhar, Arian S. – 211, 216
 Fox, Nicki – 100
 Franco, Christopher – 250, 253
 Frangakis, Achilleas – 150
 Fraser, Iain D.C. – 261, 262, 263, 264
 Fraser, Scott E. – 13, 211, 212, 213, 214, 215, 216, 217, 218, 221, 222
 Freddolino, Peter – 128
 Fried, I. – 51, 52
 Frye, Mark – 201, 205
 Fu, Daniel – 271
 Fu, Meng-meng – 186
 Fuller, Margaret T. – 111
 Fung, Elizabeth-Sharon David – 250, 255, 256
- Gail, Alexander – 27
 Gamboa, Jessica – 186
 Gammill, Laura – 182, 184
 Gao, Feng – 186, 197, 198
 Garcia, H. – 51
 Garcia-Castro, Martin – 182
 Garda, Arnavaz – 236, 246
 Gaston, Jahlionais – 113
 Gause, Cheryl – 44
 Gehre, Sabine – 74
 Ghaboosi, Nazli – 137, 139
 Gharib, Morteza – 211, 216
 Gharib, Shahla – 266, 269, 272
 Giannetti, Anthony – 117, 122, 303
 Gil, Jose S. – 74
 Girard, Lisa – 266, 270
 Glidden, Hilary – 27, 30
 Goard, Michael – 86
 Gold, Carl – 48, 50
 Gold, Daniel – 144, 145
 Gonehal, Venugopala Reddy – 236, 237, 238, 239
 Gong, Ying – 211, 214, 301
 Gonzalez, Constanza – 182
 Gonzalez, Jose – 21
 Goodale, Mel – 27
 Goodrich, K. Craig – 211
 Gor, Victoria – 240
 Gora, Katherine – 186
 Gordon, Sean – 211
 Gourlie, Noah – 86, 87
 Graciet, Emmanuelle – 165, 167
 Gradinaru, Viviana – 80, 83
 Granados, Hernan – 292
 Graumann, Johannes – 88, 137, 140, 277
 Gray, Harry B. – 124
 Gray, Rachel – 186

- Green, Harry – 175, 179, 180
 Greger, Bradley – 27, 29
 Gregg, Jeff – 80
 Griffin, Erik E. – 133, 135
 Griffith, Jack – 108
 Groves, Andrew – 182
 Gu, Lingjie – 261
 Gu, Ming – 49, 96
 Guo, Charlotte – 186
 Guo, Huatao – 113
 Guo, Ming – 232
 Guo, Zijian – 145
 Gupta, Bhagwati – 266
 Gwartz, Richele – 276, 277, 278, 284, 285
- Hadju-Cronin, Yvonne – 266, 272
 Hahn, Julie – 186, 189
 Hainline, Margaret – 44, 45
 Hájek, Petr – 107, 111
 Hakeem, Atiya – 25
 Halbrooks, Peter J. – 122
 Hamburger, Agnes – 117, 121, 124
 Hamilton, Kathleen – 67
 Hamilton, Sarah E. – 154
 Hamker, Fred – 48, 52
 Han, C.J. – 48
 Han, Sang-Kyou – 261
 Hanser, Bridget – 211, 214
 Hao, Shengli – 113, 115
 Harland, Richard – 211
 Hart, Christopher – 276, 280, 281, 283
 Hartstein, Parvin – 250
 Haswell, Elizabeth – 236, 248
 Hathaway, Gary M. – 299
 Haubensak, Wulf Eckhard – 32, 34
 Hay, Bruce A. – 14, 232
 Hayashi, Ryusuke – 91, 94
 Hayashi, Yuichiro – 60
 Hayward, Clare – 201
 He, Wanzhong – 117, 119
 He, Yongning – 117, 120
 Heisler, Marcus – 236, 238, 239, 240
 Heitzman, Tim – 21
 Helguero, Eve – 186, 189
 Hemmati, Houman – 182
 Henderson, Greg – 148, 150
 Henderson, Martha – 211
 Henze, D. – 50
 Hergarden, Anne – 32, 34, 37, 40
 Hernandez, Carlos – 292
 Hernandez-Hoyos, Gabriela – 175, 176, 177, 181
 Herr, Andrew – 120
 Heymann, Bernard – 148, 149, 152
 Hilands, Kristy – 211
 Hiltner, Tim – 211, 227
 Hinman, Veronica – 186, 197
 Ho, Maria K. – 186
- Hochstim, Christian – 32, 35
 Hofstoetter, Constanze – 48, 53, 54
 Holmberg, Kristina – 80, 83
 Hom, Geoffrey K. – 154, 156
 Hood, Lee – 186
 Hopfield, John J. – 13
 Horowitz, Norman H. – 13
 Howard, Meredith L. – 186, 190
 Hu, Rong-Gui – 165, 166, 167
 Huang, Possu – 154, 156, 303
 Huang, Stephanie – 67
 Huey-Tubman, Kathryn (Beth) – 117, 121, 124
 Huh, Jun R. – 232, 233, 234, 235
 Humbert, Sean – 201
 Hwang, Byung – 266, 270
 Hwang, Cheol-Sang – 165, 169
 Hwang, Jong-Ik – 261, 264
- Iancu, Cristina – 148, 152
 Ilicheva, Aleksandra – 27
 Imoukhuede, Princess – 67, 77
 Inoué, Takao – 266, 268
 Irwin, Carol – 21
 Ito, Hiroshi – 96
 Ito, Toshiro – 236, 243, 244, 245, 246
 Itti, Laurent – 54
 Iyer, Asha – 48, 54, 55
- Ja, William W. – 41
 Jacobs, Russell E. – 211, 221, 222, 223, 225, 226, 227
 Jacobson, Gilad – 49
 Jankowsky, Joanna – 67, 76
 Jayaraman, Vivek – 62, 63, 65
 Jensen, Grant J. – 6, 14, 119, 148, 149, 150, 151, 152
 Jeon, Mili – 98, 100
 Jeong, Seong-Yun – 144, 146
 Jiang, Changan – 86, 87
 Johnson, Tracy L. – 261
 Johnston, Joseph – 263
 Jones, Christopher T. – 163, 164
 Jones, Cynthia – 297
 Jones, Elizabeth A.V. – 211, 215
 Jones, Matthew – 182
 Jönsson, Henrik – 239, 240
 Jortner, Ron A. – 62, 64
 Jungnitsch, Maja – 75
- Kagan, Igor – 27
 Kanai, R. – 92
 Kapahi, Pankaj – 39, 41, 42
 Karbowski, Jan – 266, 274
 Karplus, Valerie – 117, 123
 Kato, Joyce – 261
 Kato, Mihoko – 266, 269
 Kayyem, John F. – 211
 Kee, Yun – 182
- Keeffe, Jennifer R. – 154, 156
 Keeter, Aura – 211
 Kennedy, Bruce – 292
 Kennedy, Malcolm W. – 122
 Kennedy, Mary B. – 13, 44, 158
 Kenny, Eimear – 266, 270
 Kerr, Bradley – 80, 82
 Kewley, David – 48
 Khakh, Baljit S. – 72
 Khorosheva, Eugenia – 44
 Khoshnan, Ali – 80, 83, 84
 Ki, Samuel – 182
 Kim, Soo-Mi – 144, 146
 Kim, Ung-Jin – 261
 King, Brandon – 276, 294
 Kiper, Daniel C. – 54
 Kirilusha, Tony – 276, 284
 Kirschvink, Joseph L. – 131
 Kishore, Ranjana – 266, 270
 Kleiger, Gary – 137, 140
 Knoblich, Ulf – 50
 Knuesel, Irene – 44, 45
 Ko, Jan – 80, 83
 Koceski, Sandra – 21
 Koch, Christof – 13, 29, 48, 49, 50, 51, 52, 53, 54, 55, 56, 57, 58
 Kochendoerfer, Gerd G. – 77
 Koen, Patrick – 291
 Konishi, Masakazu – 6, 13, 60, 61
 Koos, David – 14, 211, 213
 Kornblum, Harley – 182
 Koshiba, Takumi – 133, 135
 Köster, Reinhard – 211
 Kou, Shi-Ying – 295
 Kovalchik, Stephanie – 25
 Kraskov, Alexander – 48, 52
 Kreiman, G. – 51
 Kremen, Oran – 161
 Kremers, David – 211
 Kubat, Nicole – 236, 245
 Kulkarni, Rajan – 211, 217
 Kumagai, Akiko – 144, 145, 146
 Kuntz, Steven – 284
 Kurusu, Mitsuhiko – 98, 101
 Kwoh, Steven – 67
 Kwon, Yong Tae – 168, 169
- Labarca, Cesar – 67, 72, 73, 74, 75
 Laidlaw, David – 211
 Lamb, Leroy – 21
 Lansford, Russell D. – 211, 213, 215, 217, 221
 Laparra, Santiago – 261
 LaRue, A.C. – 215
 Lassila, Kyle – 154, 157
 Laurent, Gilles – 14, 62, 63, 64, 65
 Laurent, Micheline – 175, 178, 179
 Lawrence, Nick – 39
 Le, Mai – 236

- Leahy, Patrick S. – 186
 Lease, William F. – 21
 Lebestky, Tim – 32, 35
 Lee, Brian – 27, 28
 Lee, Jennifer – 124
 Lee, Joon – 144, 145, 146
 Lee, Lori – 67, 78
 Lee, Pei Yun – 186, 195
 Lee, Raymond – 266, 270
 Lee, Sun Young – 261, 263
 Lee, Vivian – 182
 Leite, John – 67
 Lenches, Edith – 161
 Leong, Peter – 148, 152
 Leopoldt, D.M. – 176,
 Lerchner, Walter – 32, 35
 Lester, Henry A. – 14, 49, 67, 68, 74,
 75, 78
 Lesur, Isabelle – 127, 128
 Leung, Thomas – 113
 Lewis, Edward B. - 13
 Lewkowicz, David J. – 95
 Leyser, Ottoline – 236
 Li, Caroline – 127, 129
 Li, Chia-Wei – 198
 Li, Fei Fei – 55
 Li, Jennifer – 80, 82
 Li, Pingwei – 117, 122, 124
 Li, Wenhui – 144, 146
 Liebling, Michael – 211, 216
 Lin, Alice – 91
 Lin, Catherine – 107, 111
 Lin, Kelly – 186, 195
 Lin, Yen-Ru – 91
 Lindsell, Claire – 21
 Link, A. James – 88
 Lipford, Rusty – 137, 140
 Lipsky, Ian – 186, 189
 Liu, Jamie – 261, 262
 Liu, Lilyn – 127
 Liu, Qing – 201
 Livi, Carolina B. – 186, 196
 Llamas, Lynda – 117
 Lledo, P.M. – 213
 Lo, Liching – 32, 36
 Longmate, Jeffrey – 258
 Lu, Carole – 211, 212
 Lu, Wange – 113, 114
 Lubenov, Evgueniy – 96
 Lucic, Vladan – 45
 Lummis, Sarah C.R. – 68
 Luong, Tinh – 44
 Lust, Ana Maria – 86
 Luu, Harrison – 186
 Lwigale, Peter – 182, 183
 Lynham, Rain – 67
 Lyttle, Lloyd – 133
 Ma, Wei Ji – 52
 Ma, Whee Ky – 48
 Ma, Vincent – 21
 Macenka, Josephina – 261
 Mack, Antha – 246
 Maeda, Fumiko – 91
 Mah, Angie – 137, 141
 Malkova, Natalia – 80, 81, 82
 Malone, Janie – 21
 Maloney, James – 211, 217, 218
 Mamelak, Adam – 86, 90
 Mancino, Valeria – 261
 Mancuso, Gina – 32
 Manzerra, Pat – 44, 45
 Manzo, Andrea – 184
 Mao, Jessica – 154, 157
 Marcora, Edoardo – 44
 Marcus, Josh – 256
 Marga, Francoise – 211
 Mariona, Blanca – 261
 Marks, Michael J. – 73, 74
 Marsh, Mary – 21
 Martel, Lea – 27
 Martin, Melanie – 211, 221
 Martin, W. Lance – 121
 Martinez, Monica – 32
 Martin-Hernandez, Miguel – 107, 108,
 109
 Mason, Anne B. – 122
 Mata, Jorge – 292
 Mata, Jose – 292
 Materna, Stefan – 186, 190
 Mathog, David R. – 296
 Matthews, Ben – 25
 Matthews, Benjamin – 91
 Mayo, Stephen L. – 6, 14, 154, 155,
 156, 157, 158, 159, 296
 Mayor, Thibault – 137, 141
 Mays, Laura L. Hoopes – 132
 Mazor, Ofer – 62, 64
 McBride, Helen – 211, 213
 McCabe, Katherine – 182, 184
 McCauley, David – 182, 183
 McDermott, Lindsay - 122
 McDowell, Doreen – 80
 McKinney, David – 236, 246
 McKinney, Sheri – 67, 72, 73, 74
 McMenimen, Kathryn – 67
 Medina, Gladys – 266
 Medina-Marino, Andrew – 44
 Medrano, Leonard – 241
 Meeker, Daniella – 27, 29
 Meffert, Mollie – 113
 Megason, Sean – 211, 216
 Meister, Markus – 62
 Mendel, Jane E. – 266, 273, 274
 Mendez, Ana – 261
 Mendez, Jane E. – 14
 Menon, Kaushiki – 98, 101
 Merchant, Edriss – 211
 Meulemans, Daniel – 182, 183, 184,
 303
 Meyerowitz, Elliot – 5, 6, 13, 14, 236,
 237, 238, 241, 242, 247
 Mihalas, Anca – 113
 Mihalas, Stefan – 44, 46
 Miller, Carol A. – 39
 Mindorff, Patricia – 21
 Minokawa, Takuya – 186, 192, 192
 Mitra, Partha - 27
 Mitros, Ania – 48
 Mjolsness, Eric – 239, 240, 271, 276,
 278, 280, 281, 283, 285
 Mo, Chunhui – 48, 49, 214
 Moats, Rex – 211
 Moghal, Nadeem – 266
 Mohl, Dane – 137, 141
 Monahan, Sarah – 67
 Montgomery, Jennifer – 80, 84
 Moon, Eunpyo – 271, 276
 Moradi, Farshad – 48, 53, 91, 92
 Morales-Castro, Janie – 21
 Moreaux, Laurent – 62
 Morris, Dylan – 148, 151
 Mortazavi, Ali – 285, 286
 Mosconi, Gabriele – 32
 Moss, Fraser – 67, 70, 76
 Mosser, Eric – 86, 88
 Mu, Tingwei – 67, 68
 Muffat, Julien – 39, 41
 Mukoyama, Yosuke – 32, 36
 Mullaney, Nora – 271, 280
 Müller, H.-A.J. – 232, 233
 Müller, Hans-Michael – 266, 270
 Muller, Jerome – 274
 Mulliken, Grant – 27, 29
 Munoz, Gustavo – 292
 Munoz, Jose – 67
 Munoz, Mary – 211
 Murdock, Gwen – 21
 Muro, Israel – 232
 Murphy, Gavin – 148, 150
 Murphy, John – 282
 Murphy, Marta – 117
 Musallam, Sam – 27, 29
 Mysore, Shreesh – 86
 Nadasdy, Zoltan – 27, 28, 29, 51
 Nakamura, Cecilia – 266, 270
 Nangiana, Inderjit – 297
 Narasimhan, P.T. Jim – 211, 225
 Nash, Cody Z. – 131
 Nashmi, Raad – 67, 72, 73, 74, 75
 Negrutiu, Ioan – 236
 Neil, Patricia – 91, 94, 95
 Nelson, Matthew – 27
 Nenadic, Zoran – 27
 Nesterova, Violana – 98

- Neumann, Titus – 206
 Newman, D.K. – 279
 Ng, Lydia – 67
 Nguyen, Albert – 186, 197
 Nick, Theresa – 60
 Nieman, Dylan – 91
 Norton, Scot – 21
- Oania, Robert – 137, 142
 O'Dell, Shannon M. – 48
 Oelschlaeger, Peter – 154, 157
 Oh, Jeong – 44, 46
 Oh, John – 211
 Ohashi, Kazuaki – 241, 242
 Ohno, Carolyn – 236, 238, 239, 240, 247
 Oliveri, Paola – 186, 198
 Olson, Rich – 117, 121
 Ong, Gwendolyn – 186, 192
 Orimoto, Kenji – 32, 36
 Otim, Ochan – 186, 189, 195
 O'Tuathaigh, Colm – 48
 Ou, Susan Ker-hwa – 164, 295
 Owen, Ray D. – 13
 Owens, Melinda – 86
 Oz, Yasmin – 49
- Page, Dee – 276
 Pant, Rashmi – 250, 257
 Pantoja, Rigo – 67, 70
 Papadopoulou, Maria – 62, 66
 Papan, Cyrus – 211, 221
 Papan, Rachel (Kraut) – 98, 102
 Papsys, John – 292
 Park, Ji Young – 261, 263
 Park-Lee, Sungmin – 133, 135
 Patel, Amar – 236
 Patrick, Gentry – 86, 89
 Patterson, Paul H. – 6, 14, 80, 81, 82, 83, 84, 295
 Pease, Shirley – 292
 Peek, Martin – 201
 Pejsa, Kelsie – 27
 Peña, José Luis – 60, 61
 Pérez, Maria Lucia – 60, 61
 Perez, Myra – 32
 Perez-Orive, Javier – 62, 304
 Perona, Pietro – 55, 56, 58
 Perrone, Pat – 21
 Perry, Barbara – 266
 Pesaran, Bijan – 27, 28, 29, 30
 Petcherski, Andrei – 266, 270
 Peters, Robert – 48, 54, 304
 Petersson, E. James – 67, 68, 70, 71
 Petreanu, L.T. – 213
 Petroski, Matthew – 137, 142
 Peyrot, Sara – 214
 Piatkov, Konstantin – 165, 167
 Pierce, James R. – 14
- Pinguet, Thierry J. – 73
 Placzek, Marysia – 211
 Pogodin, Timur – 144
 Polaczek, Piotr – 127
 Price, Kerry L. – 68
 Privett, Heidi K. – 154, 158
 Puig, Parlène – 91
- Qi, Yan – 117, 121
 Quake, Steven P. – 256
 Quian Quiroga, Rodrigo – 27, 48, 51, 52
- Ramirez, Danny M. – 175, 179
 Ramirez-Lugo, Juan – 144
 Ransick, Andrew – 186, 191
 Rao, Anitha – 182
 Rao, Vijaya – 294
 Rast, Jonathan P. – 189
 Rathbun, Alana – 86
 Ratnaparkhi, Anuradha – 98, 101
 Raub, Chris – 130
 Raule, Nicola – 107, 108, 110
 Readhead, Carol – 211, 222
 Reddy, Lavanya – 48, 51, 56, 56
 Reddy, Leila – 48, 53
 Rees, Douglas C. – 123
 Reis, Clara – 127, 131
 Reiser, Michael – 201, 204
 Remondes, Armando M. – 86, 90
 Revel, Jean-Paul – 14
 Revie, Julian – 73
 Revilla, Roger – 186, 195
 Rice, Adrian – 117, 123
 Richard, Renaud – 62
 Ridley, Kim – 236
 Riechmann, Jose Luis – 236, 243, 285, 294
 Rigg, Jane – 186
 Ririe, Ted – 266, 268
 Rizzuto, Dan – 27, 30,
 Roberts, Richard W. – 41, 89
 Robie, Alice – 201
 Robinson, Maral B. – 236
 Roden, Joe – 276, 278, 280, 281, 285
 Rodrigues-Pinguet, Nivalda – 67, 73, 74
 Rodriguez, Erik – 67
 Roldan-Ortiz, Maria – 107
 Rolfe, Jason – 96
 Rosales, Maria C. – 107
 Rosa-Molinar, Eduardo – 211
 Rosen, Tobias – 133, 305
 Rosenfeld, Nitzan – 209
 Rosenstein, Alan – 44
 Rothenberg, Ellen V. – 6, 14, 250, 291
 Roukes, Michael – 211, 218
 Rowan, Lee – 255, 256
- Rubin, Ben – 62, 63
 Ruffins, Seth – 211, 221
 Rusnak, Felicia – 299
 Rutishauser, Ueli – 58, 86, 90
- Saenz, M. – 29
 Saenz, Melissa – 48, 55
 Sakai, Hajime – 241
 Sakamoto, Kathy – 137, 142, 304
 Salazar, Anna – 98, 102
 Saldanha, Alok – 266, 271
 Sanders, Jennifer – 266, 268
 Sandoval, Lorena – 292
 Santat, Leah Tager – 261, 262
 Santel, Ansgar – 111
 Santiestevan, Eric – 113
 Santos, Nephi – 182
 Sapin, Viveca – 39
 Sauka-Spengler, Tatjana – 182
 Sayaman Rosalyn – 201, 202
 Scheier, Christian – 95
 Schenker, Leslie T. – 44
 Scherberger, Hans – 27, 29
 Scherenbroic, Lucas – 280
 Scherer, Stewart – 14
 Schindelman, Gary – 266, 272
 Schmid, Alice – 100
 Scholze, Hans – 201
 Schuman, Erin – 5, 13, 14, 86, 89
 Schwarz, Erich – 266, 270, 271
 Schwarz, Johannes – 67, 73, 74, 75
 Schwarz, Sigrid – 67, 74
 Scripture-Adams, Deirdre – 250, 252
 Seah, Adeline – 266, 269, 274
 Segev, Idan – 49
 Selleck, Mark – 182
 Seo, Jai Wha – 168
 Seoul, Jae Hong – 276
 Seroude, Laurent – 41
 Seyffarth, Petra – 75
 Shah, Premal S. – 154, 158
 Shams, Ladan – 52, 91
 Shanbhag, Sharad – 60, 61
 Shapiro, Bruce – 239, 240, 285
 Shapovalov, George – 67, 77, 78
 Shcherbatyuk, Viktor – 27
 Shen, Kai – 62, 65
 Sheng, Jun – 165, 166, 168
 Sherwood, David – 266, 267
 Sherwood, Nina – 98, 102
 Sheth, Bhavin – 91
 Shevchenko, Andrej – 146
 Shevchenko, Anna – 146
 Shi, Limin – 80, 82
 Shi, Yigong – 232
 Shiau, Celia – 44
 Shifman, Julia – 46, 154, 158
 Shih, Angie – 274
 Shimoda, Daphne – 137

- Shimojo, Shinsuke – 14, 53, 91, 92, 93, 94, 95
 Shin, Donghun – 32, 37
 Shin, Kum-Joo – 261, 264
 Shirako, Yukio – 161
 Shizuya, Hiroaki – 271, 276
 Siapas, Athanassios G. – 14, 96
 Siebenga, Jannigje – 161
 Sieber, Patrick – 236, 241, 247
 Siegel, Peter – 211, 218
 Silva, Juan – 292
 Silverlake, John – 39
 Simion, Claudiu – 91, 92, 93
 Simon, Anne – 41
 Simon, Jasper – 201, 207
 Simon, Melvin I. – 14, 75, 261, 262, 263, 264
 Slimko, Eric – 67
 Smith, Geoff – 88, 137, 140
 Smith, Jeffrey O. – 211, 217
 Smith, Kayla – 285, 294
 Smith, Stephen – 80, 81, 82
 Smith, W. Bryan – 5, 86, 89, 304
 Snow, Peter – 129, 297
 So, Jonathan – 211
 Sokolova, Irina – 67, 75, 77
 Solomon, Jerry – 211
 Solyom, Anthony – 21
 Somma, Lauren – 211
 Southwell, Amber – 80, 84
 Speicher, Stephen – 211
 Sprague, Elizabeth – 117, 121
 Sprinzak, David – 209
 Spronk, Steve A. – 67, 78
 Srinivasan, Jagan – 266, 273, 274
 Starck, Shelly R. – 89
 Steele, Amber – 201
 Stein, Lincoln – 270
 Sternberg, Paul W. – 14, 266, 269, 270, 271, 274
 Stirbl, Robert – 266
 Stopfer, Mark – 62
 Strauss, Ellen G. – 161
 Strauss, James H. – 14, 161
 Straw, Andrew – 201
 Streit, Andrea – 184
 Stuetzer, Alexandra – 74
 Süel, Gurol – 209
 Suer, K. – 177, 179
 Suh, Gregory S.B. – 32, 37, 40
 Sun, Jean – 236
 Sung, Christopher – 128
 Suntoke, Tara – 133, 136
 Sutton, Michael – 86, 87
 Swain, Peter – 209
 Taganov, Konstantin – 113, 115
 Taghon, tom – 250, 251, 252, 257
 Tai, Chin-Yin – 86
 Tan-Cabugao, Johanna – 182
 Tapper, Andrew – 67, 73
 Tasaki, Takafumi – 168, 168
 Teal, Tracy – 276, 279
 Tesar, Devin – 117, 119, 120
 Tetreault, Nicole – 25
 Thomas, Deanna – 186
 Thomas, Emma – 236
 Thomas, Leonard – 117, 123
 Tiangco, Noreen – 117, 119
 Tiefenbrunn, Theresa – 128
 Tirrell, David A. – 88
 Tivol, Bill – 148, 149
 Tognazzini, Cynthia – 21
 Tong, Amy – 127, 128
 Torres, Elizabeth – 27, 30
 Torrice, Michael – 67, 69
 Tracey, W. Dan – 39
 Treynor, Thomas P. – 154
 Trindler, J. – 58
 Trout, Diane – 276, 280, 281, 283
 Tse, Eric – 175, 253, 305
 Tsuchiya, Naotsugu – 48, 57
 Tu, Nora – 80
 Tu, Qiang – 186
 Tubman, Tom – 21
 Turner, Glenn C. – 62
 Tydell, C. Chase – 250, 255, 256
 Tyszka, J. Michael – 211, 214, 222, 226, 227
 Valerio, Roberto – 50
 Van Auken, Kimberly – 266
 Van Buskirk, Cheryl – 266, 267, 270
 Van Rullen, Rufin – 48, 55, 56
 Van Trigt, Laurent – 32, 35
 Van Velan, David – 211
 Vargas, Vanessa – 292
 Varshavsky, Alexander – 6, 14, 165, 166, 167, 168, 169, 170
 Vasconcellos, Andrea – 80, 82
 Vavra, Candace – 48
 Vázquez, Luis – 44, 45, 304
 Vega, Leah – 186
 Verma, Rati – 137, 142
 Verstraten, R.A.J. – 92
 Vizcarra, Christina – 154, 159
 Walker, David W. – 39, 40, 41, 42
 Wall, Estelle – 261, 262
 Wall, Nick – 86, 87
 Wallingford, John – 211, 214
 Walsh, Michael P. – 21
 Walther, Dirk – 48, 58, 58
 Wang, Chi – 175, 177, 181
 Wang, Daniel – 266, 270
 Wang, Horng-Dar – 39, 42
 Wang, Jing – 37
 Wang, Jue Jude – 292
 Wang, Mei – 261
 Wang, Shuling – 278
 Wang, Sophie X. – 145
 Wang, Weidong – 169
 Warren, Luigi – 250, 256
 Washburn, Lori – 44
 Watanabe, Dai – 60
 Watanabe, Masataka – 91
 Waters, Chris – 211, 215
 Watkin, Erin – 80, 83
 Watson, Karli – 25, 26
 Wawrousek, Karen – 144
 Wei, Ching-Hua – 39
 Wei, Tao – 127
 Weiss, Angela – 250, 253
 Weitao, Tao – 132
 Weld, Holli – 86
 Welge, Kirsten – 197
 Wellmer, Frank – 236, 243, 244, 246, 247
 Wen, Bingni – 148, 151
 Wessel, Gary – 186
 West, Jr., Anthony – 41, 117, 120, 121, 122, 124
 West, Randall – 21
 Westcott, Samantha – 21
 Westman, Mattias – 62
 Whiteaker, Paul – 73, 74
 Whittaker, Allyson – 266, 272
 Wierzynski, Casimir – 51, 96
 Wiezorek, Jeff – 113, 114
 Wikramanayake, Athula – 192
 Wilken, Patrick – 48, 52
 Williams, Brian – 276, 277, 278, 282, 284, 285
 Williams, John – 186
 Williams, Jon – 211
 Wilson, Rachel I. – 62
 Winkler, Jay – 124
 Winters, Charles – 292
 Wold, Barbara J. – 266, 271, 276, 279, 280, 281, 282, 283, 286
 Wong, Allan – 37, 40
 Worra, Carole – 21
 Wright, Ashley – 98, 102
 Wright, Elizabeth – 148, 149
 Wu, Daw-An – 91, 93
 Wu, Shau-Ming – 27
 Wyllie, Jane – 186, 189, 191
 Xia, Zanxian – 165, 168, 169
 Xie, Youming – 168
 Xiu, Joanne – 67, 69
 Xu, Peizhang – 232, 233
 Xu, Shawn – 274
 Xu, Wendy – 80, 81
 Xu, Xian-Zhong – 266
 Xu, Zhenming – 165, 166

Yamamoto, Vicky – 113
Yang, Changhui – 211
Yang, Lili – 113, 114, 304
Yang, Zhiru – 117, 121
Yanow, Stephanie K. – 145
Yao, Tessa – 27
Yarom, Yosef – 49
Yaron-Jakoubovitch, Anat – 49
Yin, Jinhu – 169
Yoo, Hae Yong – 144, 145, 146
Yoo, Soon Ji – 232, 233
Young, Jonathan – 209
Young, Rosalind – 39
Yu, Chang-Jun – 211, 217
Yu, Hao – 236, 241, 243
Yu, Hong – 232, 233
Yu, Hui – 266, 269
Yuan, Qiu-Autumn – 186, 189
Yuh, Chiou-Hwa – 186, 192, 193, 193
Yui, Mary – 250, 258
Yun, Jina – 186
Yun, Miki – 186

Zacharias, Niki – 67
Zarnegar, Mark – 250, 254
Zavzavadjian, Joelle – 261, 262
Zedan, Rosie – 107
Zhang, Jin – 107, 108
Zhang, Xiaowei – 211, 223, 227
Zhao, Yuanxiang – 236, 241, 241, 242
Zhigulin, Valentin – 62
Zhong, Weiwei – 266, 270, 274
Zhou, Jianmin – 165, 166
Zhou, Jie – 299
Zhou, Shu Zhen – 261, 263
Zhu, Xiaocui – 261, 263
Zid, Brian – 39, 41
Ziemer, Lisa – 182
Zinn, Kai – 14, 98, 100, 299
Zollars, Eric – 154, 159
Zygourakis, Corinna - 26
Zylka, Mark – 32, 38

